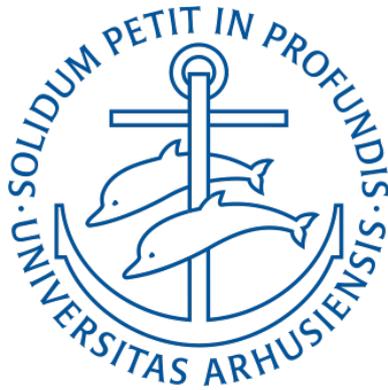# Stochastic Models
# of Higher-Order Networks

Stochastic Models
of Higher-Order Networks

Point Processes and Topological Data Analysis

PhD Thesis

Péter Juhász

Supervised by Christian Hirsch

Stochastic Models of Higher-Order Networks
Point Processes and Topological Data Analysis

PhD Dissertation by
Péter Juhász

Department of Mathematics, Aarhus University
Ny Munkegade 118, 8000 Aarhus C, Denmark

Supervised by
Associate Professor Christian Hirsch, Aarhus University
Professor Claudia Strauch, Heidelberg University

This PhD thesis was typeset using LATEX
with the `memoir` document class.

Abstract

Higher-order networks, which model interactions among groups of entities of an arbitrary number, emerged as a generalization of simple networks with pairwise interactions. Their analysis requires the development of stochastic models that can capture complex spatial, topological, and temporal dependencies. This thesis presents new probabilistic frameworks for modeling such networks grounded in point process theory.

The first contribution establishes a Poisson approximation result for the number of degree-k nodes in weighted random connection models. Nodes are embedded in $\mathbb{R}^d$ via a weighted Poisson point process, and edges are formed based on both spatial proximity and node weights. We identify scaling regimes under which the spatial distribution of degree-k nodes converges in Kantorovich–Rubinstein distance to a homogeneous Poisson point process.

In the second part, we analyze the age-dependent random connection model, a spatial network model viewed as a higher-order network. Limit theorems are shown for higher-order degree distributions, Betti numbers, and edge counts. Then, the model is fitted to a real-world collaboration network, and hypothesis tests are conducted to assess how well the model captures the topological features of the network.

Next, the framework is extended to hypergraphs. Both network nodes and hyperedges are modeled as weighted Poisson point processes, and hyperedges are formed based on joint connections to points representing the hyperedges. In this model, we prove normal and stable limit theorems for simplex counts, Betti numbers, and edge statistics. We also present a simulation study and an application to a collaboration network extracted from the arXiv dataset, comparing the model with real-world hypergraphs.

Finally, a dynamic version of the hypergraph model is proposed, where we equip the vertices with birth-death dynamics. We establish two functional limit theorems for the edge-count process in the model: for light-tailed degree distributions, it converges to a Gaussian process with Matérn-type covariance. In heavy-tailed regimes, the edge count process converges to a non-Markovian, non-Lévy stable process. These results constitute the first dynamic limit theorems for spatial higher-order networks.

Resumé

Højereordens netværk, som modellerer interaktioner mellem grupper af et vilkårligt antal enheder, er opstået som en generalisering af simple netværk med parvise interaktioner. Deres analyse kræver udvikling af stokastiske modeller, der kan indfange rumlige, topologiske og tidsmæssige afhængigheder. Denne afhandling præsenterer nye sandsynlighedsteoretiske rammer for modellering af sådanne netværk, baseret på punktproces-teori.

Det første bidrag etablerer et Poisson-approksimationresultat for antallet af noder med grad-k i vægtede tilfældige forbindelsesmodeller. Noderne placeres i $\mathbb{R}^d$ via en vægtet Poisson-punktproces, og kanter dannes ud fra både rumlig nærhed og nodernes vægte. Vi identificerer skaleringsregimer, hvorunder den rumlige fordeling af grad-k-noder konvergerer i Kantorovich–Rubinstein-afstand til en homogen Poisson-punktproces.

I den anden del analyserer vi den aldersafhængige tilfældige forbindelsesmodel, en rumlig netværksmodel, der betragtes som et højereordens netværk. Grænsesætninger vises for højereordens gradfordelinger, Betti-tal og antallet af kanter. Herefter tilpasses modellen til et reelt samarbejdsnetværk, og hypotesetest udføres for at undersøge, hvor godt modellen fanger de topologiske træk i netværket.

Dernæst udvides rammen til hypergrafer. Både netværksnoder og hyperkanter modelleres som vægtede Poisson-punktprocesser, og hyperkanter dannes på baggrund af fælles forbindelser til punkter, der repræsenterer hyperkanterne. I denne model beviser vi normale og stabile grænsesætninger for antallet af simplekser, Betti-tal og kantstatistikker. Vi præsenterer også en simuleringsundersøgelse og en anvendelse på et samarbejdsnetværk udtrukket fra arXiv-datasættet for at sammenligne modellen med virkelige hypergrafer.

Afslutningsvis foreslås en dynamisk version af hypergrafmodellen, hvor vi udstyrer toppunkterne med fødsels-døds-dynamik. Vi opstiller to funktionelle grænsesætninger for kanttællingsprocessen i modellen: for letthalegradfordelinger konvergerer den mod en Gaussisk proces med Matérn-lignende kovarians. I tunghaleregimer konvergerer kanttællingsprocessen mod en ikke-Markovsk, ikke-Lévy stabil proces. Disse resultater udgør de første dynamiske grænsesætninger for rumlige højereordens netværk.

To my wife, Linda

Preface

With this thesis, I conclude my PhD studies at the Department of Mathematics, Aarhus University, which spanned from November 2022 to October 2025.

Coming from a background in physics and having spent several years working in industry before my PhD, the transition into mathematics research was initially a significant challenge. Adjusting to the level of abstraction, the rigor of proofs, and the patience required for long-term academic projects was not an easy task. However, these challenges proved to be rewarding—I managed to develop new ways of thinking and to approach problems with greater precision. Looking back, the difficulties at the beginning served as the foundation for this steep learning curve that shaped both my research and a deeper understanding of mathematics.

The research presented in this thesis is the result of a collaboration with my coauthors. Although there was no strict division of work, I contributed extensively to all aspects of the research, including theoretical results, computational methods, implementation, data analysis, and manuscript writing.

* * *

<div align="right">

Péter Juhász

Aarhus, October 2025

</div>

Contents

Introduction

My PhD thesis presents the results of the research conducted under the project entitled "Stochastic models for higher-order networks: Point processes and topological data analysis", which was financed by the Danish Data Science Academy (DDSA) PhD Fellowship grant with grant number *DDSA-PhD-2022-008*.

This thesis investigates stochastic point processes and topological structures in random networks. The research focuses on both theoretical and applied aspects, addressing the following major topics.

- We study spatially embedded random graphs, with particular emphasis on weighted and age-dependent random connection models. Our analysis covers generalized degree distributions, edge and simplex counts, and Betti numbers. In particular, we investigate the influence of heavy-tailed distributions on these network characteristics.

- We apply tools from topological data analysis (TDA), such as Betti numbers and simplicial complexes, to capture higher-order connectivity of random networks.

- The theoretical results are complemented by simulations and empirical studies on collaboration networks, demonstrating the practical relevance of the models developed.

The thesis is based on the following four papers:

Paper A Poisson approximation of fixed-degree nodes in weighted random connection models. Published in *Stochastic Processes and their Applications* [51].

Paper B On the topology of higher-order age-dependent random connection models. Published in *Methodology and Computing in Applied Probability* [49].

Paper C Random connection hypergraphs. Preprint available at *arXiv* [19].

Paper D Functional limit theorems for edge counts in dynamic random connection hypergraphs. Preprint available at *arXiv* [52].

These research papers have been included in this thesis without significant modifications compared to their published versions. The specific changes, apart from minor typographical corrections and formatting adjustments made to the papers, are listed in Section Errata.

The thesis is organized as follows.

- The Introduction introduces the overall topic, and establishes the main mathematical framework necessary for understanding the results presented in this thesis. Then, the included papers are summarized, highlighting their main contributions and findings. This part of the thesis intentionally overlaps with the included papers as they address the same model, results, and background material. Next, an overview of the computational framework is provided, which was developed for simulating random connection models and simplicial complexes. The last part of the Introduction discusses the Boolean model, which serves as a simple model to demonstrate the proof techniques applied throughout several of the included papers.

- Paper A presents the paper titled *Poisson approximation of fixed-degree nodes in weighted random connection models* [51], a joint work with Christian Hirsch, Benedikt Jahnel, and Sanjoy K. Jhawar. In this paper, we investigate the Poisson approximation of degree-k vertices in weighted random connection networks.

- Paper B contains the paper titled *On the topology of higher-order age-dependent random connection models* [49], in which we study the age-dependent random connection model viewed as a higher-order network. This paper is a joint work with Christian Hirsch.

- Paper C comprises the paper *Random connection hypergraphs* [19], which was written jointly with Christian Hirsch, Moritz Otto, and Morten Brun. This paper presents a novel hypergraph model that incorporates both theoretical and computational results.

- Finally, Paper D consists of the paper *Functional limit theorems for edge counts in random connection hypergraphs* [52], which is a result of collaboration with Christian Hirsch and Benedikt Jahnel. The primary focus of this paper is on a functional normal and a functional stable limit theorem derived for random connection hypergraphs.

1 Motivation

Complex systems are characterized by behaviors that cannot be directly inferred from their components' properties, i.e., the relationships between their components are crucial for their understanding. Simple networks are mathematical models to represent these relationships, where vertices represent components and the interactions between them are modeled by edges. Although these traditional network models have been successful in explaining properties emerging from pairwise interactions, they fall short in helping to understand group interactions seen in, among others, neural networks, scientific collaborations, and chemical reactions. This drawback is visualized in Figure 1, which illustrates a collaboration network where multibody interactions naturally arise.

(a) Three pairwise collabo-
rations

(b) A single three-way col-
laboration
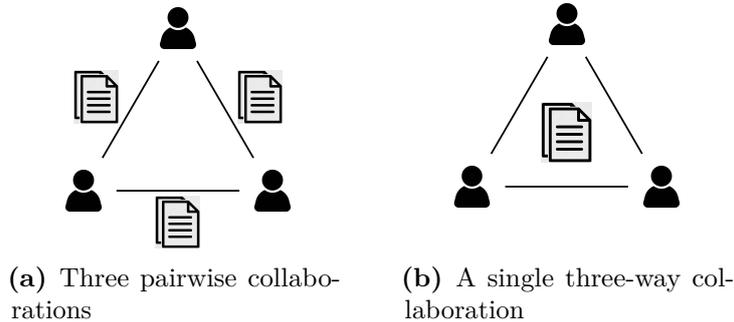
Figure 1: In a collaboration network, vertices represent scientists or authors, and there is a connection between them whenever they have a common publication together. The system can be modeled using the same graphical representation if the three authors have three publications, each written by a pair of authors (left), or if the three authors have a single, common publication (right). In this case, the simple graphical representation leads to information loss.

To overcome this limitation, two related concepts have been introduced: *hypergraphs* and *higher-order networks*, the latter being a subset of the former. Hypergraphs are generalizations of simple networks, where edges, called *hyperedges* can connect more than two vertices. Higher-order networks are a special case of hypergraphs in which each subset of vertices in a hyperedge is itself connected by a hyperedge. This means that higher-order networks are represented as *simplicial complexes*, which are combinatorial structures that generalize graphs to higher dimensions, and will be defined in Section 2.

Although higher-order networks have been studied for many years [25, 53], only a few papers discuss the higher-order structure of these systems using simplicial complex models. Despite a range of studies in this field, the structure and dynamics of higher-order interactions are still not well understood. The aim of this thesis is to develop, describe, and simulate stochastic higher-order network models. The modeling phase relies on the theory of stochastic point processes and random simplicial complexes, described in [76, 106], and [11]. Due to the complexity of the mathematics involved, most of our results are proved in the large network limit.

In two of the papers included in this thesis, Papers B and C, we relate our models to real-world collaboration networks, where higher-order relationships naturally arise [6]. In these networks, nodes represent scientists, while their higher-order interactions can be inferred from common publications they authored [65]. The dataset used for this research is the *arXiv database* [1], which at the time of the study contained a diverse set of approximately 2.5 million published and unpublished documents in various disciplines. To compare our models with these data, we first conducted simulation studies of our model to examine whether our results derived in the large network limit are valid in finite-size networks. As simulating large networks is computationally expensive, efficient algorithms had to be developed, which are detailed in Section 4. After fitting the model parameters to the data, we applied statistical tests to examine how well our model describes the various datasets.

2 Mathematical framework

This section provides an overview of the main mathematical concepts and tools used throughout this thesis. It covers the theory of point processes, higher-order networks, stable distributions, and functional convergence of stochastic processes. These topics form the foundation for understanding the models and results presented in the included papers.

Poisson point processes

The definitions and properties presented in this section are based on [66].

A point process is a random collection of points in a mathematical space, often used to model random events. In our context, point processes provide the probabilistic foundation for our network models. Vertices are sampled as random points, and edges are drawn based on their locations and the marks assigned to them. Let $(\Omega, \mathcal{F}, \mathbb{P})$ be a probability space and $(\mathbb{S}, \mathcal{S})$ a measurable space. We denote by $\mathbf{N}_{<\infty}$ the set of all $\mathbb{N}_0$-valued measures on $\mathbb{S}$, i.e., for all measures $\xi \in \mathbf{N}_{<\infty}$ and all bounded subsets $A \in \mathcal{S}$, we have $\xi(A) \in \mathbb{N}_0$. Let $\mathbf{N}$ be the set of measures that can be written as a countable sum of measures from $\mathbf{N}_{<\infty}$, i.e., for all $\xi \in \mathbf{N}$, there exist $\xi_1, \xi_2, \ldots \in \mathbf{N}_{<\infty}$ such that $\xi = \sum_{i=1}^{\infty} \xi_i$. Furthermore, let $\mathcal{N}$ be the σ-algebra generated by subsets of $\mathbf{N}$ of the form

$$\{\xi \in \mathbf{N} \colon \xi(A) = k\}, \qquad A \in \mathcal{S}, k \in \mathbb{N}_0,$$

i.e., $\xi \mapsto \xi(A)$ is measurable for all $A \in \mathcal{S}$.

Definition 2.1 (Point process). *A point process ξ on $\mathbb{S}$ is a measurable map $\xi \colon (\Omega, \mathcal{F}) \to (\mathbf{N}, \mathcal{N})$.*

Let ξ be a point process on $\mathbb{S}$, and let $A \in \mathcal{S}$ be an arbitrary measurable set. Then, $\xi(A)$ is a random variable representing the number of points of the process in the set A. For all $k \in \mathbb{N}_0$, the event that there are exactly k points in A is given by $\{\xi(A) = k\}$, which is an element of $\mathcal{F}$ due to the measurability of ξ.

Remark 2.2. *If $\mathbb{S}$ is a complete separable metric space, then any locally finite point process on $\mathbb{S}$ can be represented as a countable sum of Dirac measures, i.e., there exist points $x_1, x_2, \ldots \in \mathbb{S}$ such that $\xi = \sum_{i=1}^{\infty} \delta_{x_i}$, where δ_x is the Dirac measure at point $x \in \mathbb{S}$.*

To compute expectations with respect to a point process, we need the notion of intensity measure, which gives the mean number of points in a given measurable set.

Definition 2.3 (Intensity measure). *The intensity measure λ of a point process ξ on $\mathbb{S}$ gives the mean number of points in a given measurable set $A \in \mathcal{S}$, and is defined by $\lambda(A) = \mathbb{E}[\xi(A)]$.*

Campbell's formula provides a way to compute expectations of functionals of point processes.

Proposition 2.4 (Campbell's formula). *Let ξ be a point process on $\mathbb{S}$ with intensity measure λ, and let $f \colon \mathbb{S} \to [-\infty, \infty]$ be a measurable function. If $\int_{\mathbb{S}} |f(x)| \, \lambda(\mathrm{d}x) < \infty$, then*

$$\mathbb{E}\Big[\sum_{x \in \xi} f(x)\Big] = \int_{\mathbb{S}} f(x) \, \lambda(\mathrm{d}x),$$

where the sum is over all points x in the point process ξ.

The distribution of a point process is characterized by its finite-dimensional distributions, which describe the joint distribution of the number of points in a finite collection of measurable sets.

Definition 2.5 (Finite-dimensional distributions). *Let ξ be a point process on $\mathbb{S}$. The finite-dimensional distributions of ξ are the joint distributions of the random variables $\xi(A_1), \ldots, \xi(A_n)$ for any finite collection of disjoint measurable sets $A_1, \ldots, A_n \in \mathcal{S}$.*

A point process is called stationary if its distribution is invariant under translations. Next, we define the Poisson point process, a fundamental example of a point process, which will serve as the underlying model for vertex locations in each of the papers included in this thesis. Before doing so, recall that a measure μ on $(\mathbb{S}, \mathcal{S})$ is called *s-finite* if there exist finite measures $\mu_1, \mu_2, \ldots$ such that $\mu = \sum_{i=1}^{\infty} \mu_i$.

Definition 2.6 (Poisson point process). *A point process $\mathcal{P}$ on $\mathbb{S}$ is a Poisson point process with intensity measure λ if λ is s-finite, and for all disjoint bounded sets $A_1, \ldots, A_n \in \mathcal{S}$, the random variables $\mathcal{P}(A_1), \ldots, \mathcal{P}(A_n)$ are independent and Poisson distributed with parameters $\lambda(A_1), \ldots, \lambda(A_n)$, respectively.*

Remark 2.7. *The symbol $\mathcal{P}$ for a Poisson point process will be used in two ways throughout this thesis. Specifically, $\mathcal{P}$ will either denote the Poisson point process as a random closed set of points, or the associated random counting measure, $\mathcal{P} = \sum_{p \in \mathcal{P}} \delta_p$. The intended meaning will always be clear from the context.*

In the following, we introduce the Mecke formula, which is a powerful tool for computing expectations involving Poisson point processes.

Proposition 2.8 (Multivariate Mecke formula). *Let $\mathcal{P}$ be a Poisson process on $\mathbb{S}$ with intensity measure λ, and let $f \colon \mathbb{S}^m \times \mathbf{N} \to [0, \infty]$ be a measurable function with $m \in \mathbb{N}_0$. Then,*

$$\mathbb{E}\Big[\sum_{\boldsymbol{p}_m \in \mathcal{P}_{\neq}^m} f(\boldsymbol{p}_m, \mathcal{P})\Big] = \int_{\mathbb{S}} \mathbb{E}\Big[f(\boldsymbol{p}_m, \mathcal{P} \cup \{\boldsymbol{p}_m\})\Big] \, \lambda^{\otimes m}(\mathrm{d}\boldsymbol{p}_m),$$

where $\mathcal{P}_{\neq}^m$ is the set of all m-tuples of distinct points from $\mathcal{P}$, and $\lambda^{\otimes m}$ is the m-fold product measure of λ.

Finally, the Palm distribution provides a way to study the process from the viewpoint of a typical point or object. Intuitively, this means conditioning on the existence of a point or object, which is often shifted to the origin, and then analyzing how the rest of the process is distributed around it. This perspective is essential in Papers B and C, where local neighborhoods around points play a central role. Note that a point process ξ on $\mathbb{S}$ is locally finite if $\mathbb{P}(\xi(A) < \infty) = 1$ for all bounded sets $A \in \mathcal{S}$.

Definition 2.9 (Palm distribution)**.** *Let $\mathcal{P}$ be a locally finite stationary point process on $\mathbb{R}^d$ with finite positive intensity measure $\lambda \in (0, \infty)$. With $f \colon \mathbb{R}^d \times \mathbf{N}_{\mathsf{loc}} \to [0, \infty)$ being a measurable function, the Palm distribution $\mathbb{P}^0_{\mathcal{P}}$ of $\mathcal{P}$ is the unique probability measure on $\mathbf{N}_{\mathsf{loc}}$ defined by*

$$\mathbb{E}\Big[\sum_{p \in \mathcal{P}} f(p, \mathcal{P} - p)\Big] = \lambda \iint f(p, \mathcal{P})\, \mathbb{P}^0_{\mathcal{P}}(\mathrm{d}\mu)\, \mathrm{d}p,$$

where $\mathcal{P} - p = \sum_{p' \in \mathcal{P}} \delta_{p'-p}$.

From point processes to higher-order networks

By equipping point processes with random connections, one arrives at random connection models, which serve as a bridge to higher-order networks.

In random connection network models vertices are represented by points in a metric space, and edges are formed randomly and independently based on a connection function that determines the probability of an edge existing between any two points.

Definition 2.10 (Random connection model)**.** *A random connection model is a random graph constructed from a point process $\mathcal{P}$ on $\mathbb{R}^d$ by connecting points $p_1, p_2 \in \mathcal{P}$ with an edge independently with probability given by the connection function $\varphi(p_1, p_2)$, where $\varphi \colon \mathbb{R}^d \times \mathbb{R}^d \to [0, 1]$ is a measurable function.*

Random connection models form a fundamental class of spatial random graphs that capture pairwise interactions between nodes.

Higher-order networks are generalizations of traditional networks that allow for the representation of multibody relationships, such as those found in social, biological, and technological systems. Hypergraphs and simplicial complexes are two common mathematical structures used to model higher-order networks.

Definition 2.11 (Hypergraph)**.** *A hypergraph is a pair (V, E), where V is a set of vertices and E is a collection of nonempty subsets of V, called hyperedges. Each hyperedge may contain more than two vertices.*

Random hypergraph models can be constructed by extending random connection models to allow for the formation of hyperedges connecting multiple vertices. For example, as we will see in Paper C, hypergraphs can be modeled as bipartite graphs, where one set of vertices represents the original vertices and the other set represents the hyperedges.

Hypergraphs provide a natural way of representing higher-order interactions, but they do not encode any topological structure beyond the hyperedges themselves. Simplicial complexes constitute a subset of hypergraphs that are combinatorial structures with a topological interpretation, which allows for the application of tools from topology to analyze their properties.

Definition 2.12 (Simplicial complexes)**.** *A simplicial complex on a vertex set V is a family $\mathcal{K}$ of finite subsets of V such that whenever $\sigma \in \mathcal{K}$ and $\tau \subseteq \sigma$, $\tau \in \mathcal{K}$. The elements of $\mathcal{K}$ are called simplices, with 0-simplices corresponding to vertices, 1-simplices to edges, 2-simplices to triangles, and so on.*

A visualization of a simplicial complex is presented in Figure 2. One way to construct a simplicial complex from a graph is through the clique complex, which includes all cliques, fully connected subgraphs of the graph as simplices. Topological data analysis (TDA) provides tools to quantify the shape and connectivity of simplicial complexes. Central among these are Betti numbers, which count topological features of different dimensions: β_0 is the number of connected components, β_1 denotes the number of loops, β_2 the number of voids and so forth.

Definition 2.13 (Betti numbers)**.** *Let $\mathcal{K}$ be a simplicial complex. The k-th Betti number $\beta_k(\mathcal{K})$ is the rank of the k-th homology group $H_k(\mathcal{K})$, and measures the number of k-dimensional holes in the complex.*

For more details on simplicial complexes, homology, and Betti numbers, we refer the reader to [73]. Betti numbers are topological invariants that are robust to perturbations, and thus, they provide a summary of the global structure and connectivity of higher-order networks. In Papers B and C, we study the distribution and scaling behavior of Betti numbers for random simplicial complexes constructed from point processes.

Miscellaneous topics

This section recalls some analytical and probabilistic tools that will be employed throughout the thesis.

Stable distributions and regular variation. Heavy-tailed phenomena play a central role in random graphs and networks, where degrees and weights often exhibit power-law behavior. Two analytical tools to capture such asymptotics are regularly varying functions and stable distributions.

Regular variation provides a mathematical framework for describing heavy tails and scaling properties. It is related to stable distributions through generalized central limit theorems.
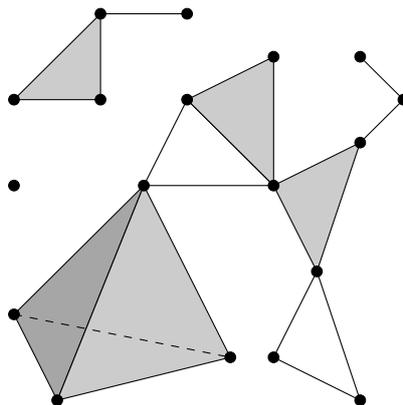
Figure 2: A simplicial complex consisting of vertices (0-simplices), edges (1-simplices), filled triangles (2-simplices), and a filled tetrahedron (3-simplex).

Definition 2.14 (Regular variation). *A measurable function $L\colon (0,\infty) \to (0,\infty)$ is slowly varying at ∞ if for all $c > 0$,*

$$\lim_{x\uparrow\infty} \frac{L(cx)}{L(x)} = 1.$$

A function f is regularly varying with index $\rho \in \mathbb{R}$ if

$$f(x) = x^\rho L(x), \quad x > 0,$$

for some slowly varying function L.

Loosely speaking, a function is regularly varying if it behaves like a power law up to a slowly varying correction.

Next, we define stable distributions, which, as we will see, arise as limits of normalized sums of i.i.d. random variables, possibly with heavy tails.

Definition 2.15 (Stable distribution). *A random variable X is called α-stable, with $\alpha \in (0,2]$, if for all $n \in \mathbb{N}$ there exist $a_n > 0$ and $b_n \in \mathbb{R}$ such that*

$$\sum_{i=1}^{n} X_i \stackrel{d}{=} a_n X + b_n,$$

where $X, X_1, \ldots, X_n$ are i.i.d. random variables.

Stable distributions are characterized by four parameters: the stability parameter $\alpha \in (0,2]$, the skewness parameter $\beta \in [-1,1]$, the scale $\sigma > 0$, and the location $\mu \in \mathbb{R}$. The cumulative distribution functions and probability density functions of stable distributions do not have closed-form expressions in general, except for a few special cases. However, they can be characterized via their characteristic functions. The characteristic function of a stable random variable $X \sim S_\alpha(\beta, \sigma, \mu)$ is given by

$$\mathbb{E}\big[e^{itX}\big] = \exp\big(it\mu - \sigma^\alpha |t|^\alpha \big(1 - i\beta \operatorname{sign}(t)\,\Phi(\alpha, t)\big)\big), \qquad t \in \mathbb{R},$$

where

$$\Phi(\alpha, t) = \begin{cases} \tan(\pi\alpha/2), & \alpha \neq 1, \\ -\frac{2}{\pi}\log(|t|), & \alpha = 1. \end{cases}$$

The stability index α governs the heaviness of the tails since $\mathbb{P}(|X| > x)$ is regularly varying with index $-\alpha$. We also note that Gaussian, Cauchy, and Lévy distributions are special cases of stable distributions:

- $\alpha = 2$ and $\beta = 0$ describes the normal distribution with mean μ and variance $2\sigma^2$,

- if $\alpha = 1$ and $\beta = 0$, then X follows the Cauchy distribution with location μ and scale σ, and finally

- if $\alpha = 1/2$, $\beta = 1$, then X follows the Lévy distribution with density

$$f(x) = \sqrt{\sigma/2\pi}\,(x-\mu)^{-3/2}\exp(-\sigma/(2(x-\mu))), \qquad \text{where } x > \mu.$$

The following generalized central limit theorem states that stable distributions describe the limits of normalized sums of i.i.d. random variables with regularly varying tails.

Theorem 2.16 (Generalized central limit theorem)**.** *Let $X_1, X_2, \ldots$ be i.i.d. random variables. If there exist sequences of constants $a_n > 0$ and $b_n \in \mathbb{R}$ such that the below convergence in distribution holds:*

$$a_n \sum_{i=1}^{n} X_i - b_n \xrightarrow[n\uparrow\infty]{d} X,$$

where X is a non-degenerate random variable, then X is stable distributed.

Skorokhod topology and metric. In Paper D, we study convergence of càdlàg stochastic processes (continuous from the right with left limits) with jumps. In this setting, uniform convergence is often too restrictive. Thus, convergence is considered in the *Skorokhod space* $D([0,1], \mathbb{R})$. The *Skorokhod topology* allows deformations of the time axis, aligning jumps in approximating processes with those of the limit process.

Definition 2.17 (Skorokhod metric)**.** *Let $f, g \in D([0,1], \mathbb{R})$ be two càdlàg functions. The Skorokhod metric $d_{\mathsf{Sk}}(f, g)$ is defined as*

$$d_{\mathsf{Sk}}(f, g) := \inf_{\lambda}\Big(\|\lambda - I\| \vee \|f \circ \lambda^{-1} - g\| \Big),$$

where the infimum is over all homeomorphisms λ from $[0,1]$ to itself, I is the identity map and $\|\cdot\|$ is the supremum norm on $[0,1]$.

Intuitively, the metric allows for small time changes λ to align the jumps of f and g.

3 Research questions and methods

Paper A

In Paper A, which is a result of a collaboration with Christian Hirsch, Benedikt Jahnel, and Sanjoy K. Jhawar, we study the spatial distribution of degree-k nodes in weighted random connection models (WRCMs) with a focus on the influence of the left tail of the weight distribution.

Motivation

Real-world networks, e.g., such as those in the fields of social or biological sciences, often exhibit heavy-tailed degree distributions [3], meaning that although most nodes have a relatively low degree, a few very high-degree nodes exist. In classical random connection models (RCMs), in which edges are formed between a pair of nodes depending on their distance only, such heavy-tailed degree distributions cannot be produced [72, Equation (6.1)]. Thus, their generalized versions, the so-called *weighted random connection models* (WRCMs), are introduced. In WRCMs, edges are formed

between a pair of nodes depending not only on their distance, but also on weights assigned to them. An important early example is the scale-free RCM introduced in the work of Deijfen et al. [28], which generates heavy-tailed degree distributions through suitable choices of vertex weights.

In this paper, we show a Poisson approximation result for the occurrence of degree-k nodes in spatial scale-free random networks in the dense regime. We further examine how the left tail of the weight distribution influences the spatial distribution of these nodes.

Model

The precise model studied in this paper is called *kernel-based spatial random network model*. We build the model from a set of points generated by a homogeneous Poisson point process $\mathcal{P}_s$ on $\mathbb{R}^d$ with intensity $s > 0$, where $\mathbb{R}^d$ denotes the d-dimensional Euclidean space. Next, we assign i.i.d. weights $W_x \in \mathbb{R}_+$ to each of the points $x \in \mathcal{P}_s$ whose cumulative distribution function is denoted by $F(w) := \mathbb{P}(W_x \leqslant w)$. The probability $p_s(x, W_x; y, W_y)$ that a pair of vertices x, y is connected is determined by

$$p_s(x, W_x; y, W_y) = \varphi\left(\frac{|B_{|x-y|}(o)|}{v_s \kappa(W_x, W_y)}\right),$$

where

$$\varphi \colon [0, \infty) \to [0, 1] \qquad \text{is the profile function;}$$
$$B_r(o) \subseteq \mathbb{R}^d \qquad \text{is the Euclidean ball with center } o \text{ and radius } r;$$
$$|B_r(o)| \qquad \text{denotes the volume of the Euclidean ball;}$$
$$\kappa \colon \mathbb{R}_+^2 \to \mathbb{R}_+ \qquad \text{denotes the interpolation kernel;}$$
$$v_s \in \mathbb{R}_+ \qquad \text{is the scaling factor.}$$

The profile function φ translates the ratio of spatial distance (encoded by the volume of the Euclidean ball with radius $|x - y|$) and vertex weights (captured by $\kappa(W_x, W_y)$) into a probability of connection. If φ is a decreasing function, it reflects that if a pair of vertices are closer to each other or have larger weights, they are more likely to connect. We assume that the profile function φ is regularly varying with tail index α at ∞, i.e., $\lim_{r \uparrow \infty} \varphi(tr)/\varphi(r) = t^\alpha$ for all $t > 0$. The interpolation kernel function κ, also introduced in the context of the WRCM in the work of van der Hofstad et al. [104], maps a pair of weights w_1, w_2 to a factor as follows:

$$\kappa(w_1, w_2) = (w_1 \wedge w_2)(w_1 \vee w_2)^a \qquad \text{with } a \geqslant 0.$$

Note that if $a = 0$, then $\kappa(w_1, w_2) = w_1 \wedge w_2$, which is called the *min kernel*. On the other hand, if $a = 1$, then $\kappa(w_1, w_2) = w_1 w_2$, which is known as the *product kernel*. The connection probabilities for an example of a profile function φ and an interpolation kernel κ are shown in Figure 3. We can see that the connection probabilities are influenced not only by the distance of the nodes but also by their weights.
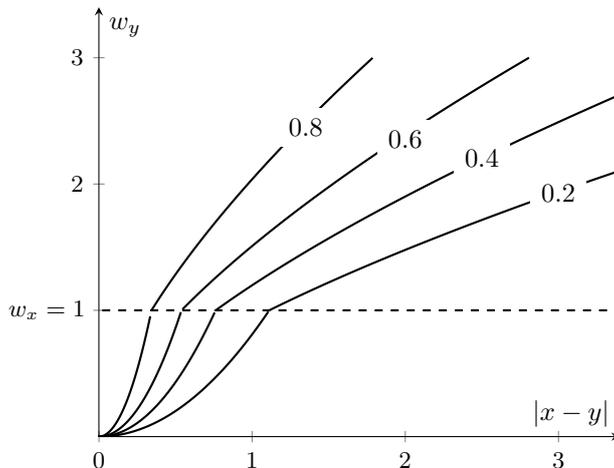
Figure 3: Connection probabilities of a node at location x and weight $w_x = 1$ and a node at location y and weight w_y in a weighted random connection model with parameters $d = 2$, $v_s = \pi$, $\varphi(x) = (1 + x)^{-2}$, and $a = 3$.

Then, the resulting graph $G(\mathcal{P}_s, v_s)$ is therefore random in three ways:

- through the spatial location of the nodes,

- through the weights assigned to the nodes and

- through the random edges connecting the nodes.

Despite these sources of randomness, van der Hofstad et al. [104] showed that many key network properties, such as the scaling of the vertex degrees and the clustering coefficient, are independent of the specific form of the connection function.

We examine the spatial distribution of k-degree nodes in the graph $G(\mathcal{P}_s, v_s)$ in the limit as the intensity s of the Poisson point process $\mathcal{P}_s$ increases. To ensure that the intensity of the k-degree nodes remains bounded, the scaling factor v_s is chosen as a function of the intensity s such that the expected number of degree-k nodes in a bounded region remains constant as $s \to \infty$. In Lemma A.2.1, it turns out that v_s must fulfill the scaling Equation (**SCG**), which is restated below for convenience:

$$k! = s \, \mathbb{E}[A_{v_s}(W)^k \exp(-A_{v_s}(W))] \qquad \text{where} \qquad A_{v_s}(w) = s v_s \, \mathbb{E}[\kappa(W, \cdot)].$$

Main results

Having established the model, we now focus on the spatial distribution of degree-k nodes in the high-density limit as $s \to \infty$, which is given by the point measure

$$\xi_s := \sum_{x \in \mathcal{P}_s \cap H} \mathbb{1}\{\deg(x) = k \text{ in } G(\mathcal{P}_s, v_s)\}\delta_x,$$

where δ_x denotes the Dirac delta, $H \subseteq \mathbb{R}^d$ is a finite-volume Borel set, and $\deg(x)$ denotes the number of edges of a node x.

If $k = 0$, then the point measure ξ_s counts the isolated nodes in $G(\mathcal{P}_s, v_s)$. The typical weight w_s of an isolated node cannot be too small, since these nodes are unlikely to appear. On the other hand, the typical weight w_s cannot be too large, since these nodes are unlikely to be isolated due to their high weight. It turns out that the typical weight w_s of an isolated node is given by the $1/(2s)$-quantile of the weight distribution, i.e., the weight w_s satisfies $F(w_s) = 1/(2s)$.

Before stating the main result, we introduce the notion of the Kantorovich–Rubinstein distance.

Definition 3.1 (Kantorovich–Rubinstein distance)**.** *The Kantorovich–Rubinstein distance d_{KR} between two point measures ξ and ξ' is defined as*

$$d_{\mathsf{KR}}(\xi, \xi') := \sup\{|\mathbb{E}[g(\xi)] - \mathbb{E}[g(\xi')]| \colon g \in \mathrm{LIP}\},$$

where LIP *denotes the set of Lipschitz functions on the space of point measures.*

Then, our main result can be stated as follows:

Theorem A.2.2 (Poisson approximation)**.** *Let $\delta := (\alpha - 1)/2$, and let us assume that for some $K > 0$ and $\eta \in (0, 1)$, the weight distribution F satisfies the following conditions:*

$$
\begin{aligned}
(sv_s)^{-1} w_s^{-\eta} &\in o(1/\log(s)) \\
F(w_s^\eta)\ w_s^{-(K+1)(1-\eta)} &\in o(1/\log(s)) \\
w_s^{-(1-K\delta)(1-\eta)} &\in o(1/\log(s)).
\end{aligned}
$$

Furthermore, let $H \subseteq \mathbb{R}^d$ denote a finite-volume Borel set, and let ζ be a Poisson point process with intensity $\mathbb{1}\{x \in H\}\,\mathrm{d}x$. Then, the point measure ξ_s converges in the Kantorovich–Rubinstein distance d_{KR} to ζ as the intensity s of the point process $\mathcal{P}_s$ increases:

$$\lim_{s \uparrow \infty} d_{\mathsf{KR}}(\xi_s, \zeta) = 0.$$

Note that sv_s is the order of the expected degree of a typical node $\boldsymbol{o}$. With W_o denoting the weight of $\boldsymbol{o}$, this can be seen from the following calculation, which is based on the proof of Lemma A.4.3:

$$\mathbb{E}\big[\deg(\boldsymbol{o}) \,|\, W_o\big] = \mathbb{E}\Big[\sum_{\boldsymbol{x} \in \widetilde{\mathcal{P}}_s \colon \boldsymbol{x} \leftrightarrow \boldsymbol{o}} 1 \,\Big|\, W_o \Big] = s \int_{\mathbb{R}^d} \mathbb{E}\big[p_s(o, W_o; x, W_x) \,|\, W_o\big]\,\mathrm{d}x,$$

where we used Campbell's formula [66, Proposition 2.7] in the second step. Next, we substitute the profile function and switch to spherical coordinates with $v := |B_{|x|}(o)|$:

$$
\begin{aligned}
\mathbb{E}\big[\deg(\boldsymbol{o}) \,|\, W_o\big] &= s \int_0^\infty \mathbb{E}\big[\varphi(v/(v_s\kappa(W_o, W_x))) \,|\, W_o\big]\,\mathrm{d}v \\
&= sv_s \int_0^\infty \mathbb{E}\big[\kappa(W_o, W)\varphi(u) \,|\, W_o\big]\,\mathrm{d}u
\end{aligned}
$$

where we substituted $u := v/(v_s\kappa(W_o, W_x))$, applied Fubini's theorem in the last step, and recognized that the integral is a function of the weights only.

We can see that the left tail, or more precisely, the $1/(2s)$ quantile w_s of the weight distribution plays a crucial role in the three technical assumptions of the theorem. To interpret these assumptions, we can think of η to be close to 1 and K to be small. Then, the first condition roughly tells us that the product of the expected typical degree sv_s and the weight w_s should increase at a rate faster than $\log(s)$ as the intensity s increases. The second at approximately requires that $sw_s^{\varepsilon_1}$ increases with a rate faster than $\log(s)$ for some small $\varepsilon_1 > 0$. Lastly, the third condition states that $w_s^{\varepsilon_2}$ for some small $\varepsilon_2 > 0$ should increase at a rate faster than $\log(s)$. Although the assumptions of the theorem are technical, they can be satisfied by many common weight distributions, such as the polynomial and stretched exponential left tails, as shown in Section A.3.

Finally, we point out that convergence in distribution follows from convergence in Kantorovich–Rubinstein distance, which is the conclusion of Theorem A.2.2.

Methodology

To show Theorem A.2.2, we would like to apply [16, Theorem 4.1], which applies Stein's method to show a convergence result. To state this result in the context of our model, we need to introduce some additional notation.

Let $(\mathbb{X}, \mathcal{X})$ denote a locally compact second countable Hausdorff space. Let $\mathbf{N}_{\mathsf{loc}}$ and $\mathcal{F}$ denote the set of locally finite point sets on $\mathbb{X}$, and the set of closed subsets of $\mathbb{X}$, respectively.

Furthermore, let $\mathcal{S} \colon \mathbb{X} \times \mathbf{N}_{\mathsf{loc}} \to \mathcal{F}$ denote a measurable function that assigns a closed set to each pair $\boldsymbol{x} \in \mathbb{X}$ and $\omega \in \mathbf{N}_{\mathsf{loc}}$. Moreover, we assume that $\mathcal{S}$ is a *stopping set*, which, loosely speaking, means that $\mathcal{S}$ can only depend on points inside the set it assigns [69, Appendix A]. More precisely, $\mathcal{S}$ is a stopping set if for all $\boldsymbol{x} \in \mathbb{X}$ and all closed sets $A \in \mathcal{F}$, the following holds:

$$\{\omega \in \mathbf{N}_{\mathsf{loc}} \colon \mathcal{S}(\boldsymbol{x}, \omega) \subseteq A\} = \{\omega \in \mathbf{N}_{\mathsf{loc}} \colon \mathcal{S}(\boldsymbol{x}, \omega \cap A) \subseteq A\}.$$

Finally, we introduce an indicator function $g \colon \mathbb{X} \times \mathbf{N}_{\mathsf{loc}} \to \{0, 1\}$, which is localized to the stopping set $\mathcal{S}$, i.e., for all $\boldsymbol{x} \in \mathbb{X}$, we have that $g(\boldsymbol{x}, \omega) = g(\boldsymbol{x}, \omega \cap A)$ for all $A \supset \mathcal{S}(\boldsymbol{x}, \omega)$. This means the function values of g are determined solely by the points of ω that are in $\mathcal{S}$.

Theorem 3.2 (Bobrowski, Schulte, Yogeshwaran [16]). *Let ψ and ζ be two Poisson point processes on $\mathbb{X}$ with intensities $\lambda_\psi, \lambda_\zeta < \infty$, respectively. Furthermore, let ξ_s be a Poisson-driven point process defined from the Poisson process ψ as follows:*

$$\xi_s[\psi] := \sum_{\boldsymbol{x} \in \psi} g(\boldsymbol{x}, \psi) \, \delta_{\boldsymbol{x}} \qquad \lambda_\xi = \int \mathbb{E}[g(\boldsymbol{x}, \psi + \delta_{\boldsymbol{x}})] \, \mathrm{d}\lambda_\psi < \infty.$$

For any indicator function g localized to a stopping set $\mathcal{S}$. Then,

$$d_{\mathsf{KR}}(\xi_s, \zeta) \leqslant d_{\mathsf{TV}}(\lambda_\xi, \lambda_\zeta) + E_1 + E_2 + E_3 + E_4,$$

where $d_{\mathsf{TV}}(\lambda_\xi, \lambda_\zeta)$ is the total variation distance of the intensity measures, and $E_1, \ldots, E_4$ are error terms for higher-order deviations as specified in [16, Theorem 4.1].

The form of the intensity measure λ_ξ results from the application of Mecke's formula to the definition of the point process ξ. The error terms $E_1, \ldots, E_4$ quantify deviations when the indicator function g is 1 for two-point configurations that are close to each other, excluding interactions not present in Poisson processes.

To apply this theorem to our model, we would like to use $g((x, W_x), \widetilde{\mathcal{P}}_s) = \mathbb{1}\{\deg(x) = k$ in $G(\mathcal{P}_s, v_s)\}$, where $\deg(x)$ denotes the degree of the point x with mark W_x in the graph $G(\mathcal{P}_s, v_s)$. However, the theorem cannot be directly applied since it requires the indicator function g to be localized to a stopping set $\mathcal{S}$. In our setting, this is not the case: nodes far away from x can influence the degree of x if they have a sufficiently large weight, and in general, nodes can have large weights as well. This problem is visualized in Figure 4.

Thus, our strategy is to follow the two steps below.

(1) First, in Proposition A.4.1, we approximate the indicator function g in two ways.

- **Mark approximation:** we neglect points with marks larger than w_s^η.

- **Reach approximation:** we neglect points that are too far away from x.

In both the mark and the reach approximation, we bound the Kantorovich–Rubinstein distance between the original and the truncated functionals. We need to control two types of errors: the truncations lead to *lost k-degree points* that have edges to truncated points, and some points with degrees larger than k will be k-degree nodes. These truncations allow us to apply the Poisson approximation theorem.
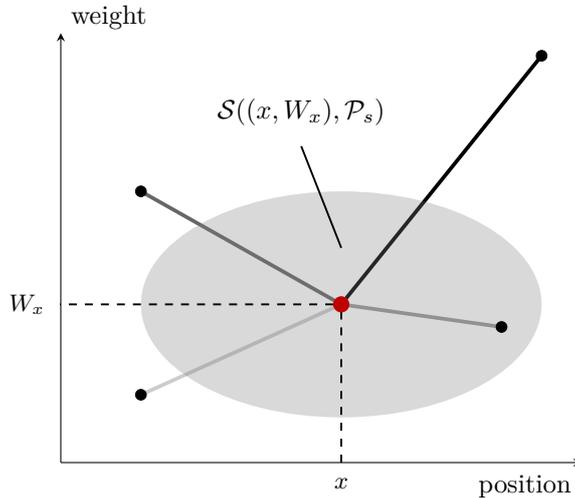
Figure 4: The problem of localization: the degree of the central red point x with mark W_x is influenced by points far away from (x, W_x). Thus, no matter how large the stopping set $\mathcal{S}((x, W_x), \mathcal{P}_s)$ is, we cannot be sure that it contains all points that influence the degree of x.

(2) Then, in Proposition A.4.2, we show that the error terms in the theorem converge to zero as the intensity s increases. The theorem then gives us convergence in the Kantorovich–Rubinstein distance d_{KR}.

Paper B

Paper B, written in collaboration with Christian Hirsch, studies the age-dependent random connection model (ADRCM) viewed as a higher-order network.

Motivation

As mentioned earlier, real-world networks often exhibit heavy-tailed degree distributions. The first widely used model to describe such a system was the Barabási–Albert model introduced by Barabási and Albert [3]. In this model, the network forms gradually by adding new nodes one by one. Each new node connects to existing nodes with a probability proportional to their degree, which means that high-degree nodes are more likely to be connected to new nodes. This mechanism is often referred to as *preferential attachment*. However, the Barabási–Albert model is a non-spatial model that is hard to analyze due to the dependence of the degree of the nodes.

To overcome this difficulty, the age-dependent random connection model (ADRCM) was introduced in [40]. In this model, each node is assigned an arrival time, and its age determines the probability of new, younger nodes connecting to existing older nodes in such a way that the resulting degree distribution is heavy-tailed.

In this paper, we study the ADRCM as a higher-order network model by constructing a simplicial complex on the simple graphs that the ADRCM model generates. To examine how well the clique complex [33] of the ADRCM captures the properties of real-world networks, we compare the higher-order networks with the collaboration network of the arXiv dataset, conducting hypothesis tests for various network characteristics.

Model

The age-dependent random connection model (ADRCM) is defined as follows. Vertices $(x, t) \in [-1/2, 1/2]^d \times \mathbb{R}_+$ arrive to the d-dimensional Euclidean unit cube $[-1/2, 1/2]^d$ at spatial location $x \in [-1/2, 1/2]^d$ and arrival time t according to a homogeneous Poisson point process $\mathcal{P}$. Two vertices (x, u) and (y, v) with $u \leqslant v$ are connected with a probability $p(x, u; y, v)$ defined by the profile function $\varphi \colon [0, \infty) \to [0, 1]$ as follows:

$$p(x, u; y, v) = \varphi\left(\frac{|x - y|}{\beta u^{-\gamma} v^{-(1-\gamma)}} \right),$$

where

$$
\begin{aligned}
&\varphi \colon [0, \infty) \to [0, 1] &&\quad \text{profile function;} \\
&\beta > 0 &&\quad \text{scaling factor;} \\
&\gamma \in (0, 1) &&\quad \text{age parameter.}
\end{aligned}
$$

Remark 3.3. *We remark that in the work of Gracar et al. [40], the ADRCM is defined slightly differently on the d-dimensional torus $\mathbb{T}_1^d = [-1/2, 1/2)^d$ with the torus distance $d_{\text{torus}}(x, y) = [\sum_{i=1}^d (\min_{m \in \{-1,0,1\}^d} |x_i - y_i + m|)^2]^{1/2}$ with $x = (x_1, \ldots, x_d)$ and $y = (y_1, \ldots, y_d)$ instead of the Euclidean distance $|x - y|$. As we will see later, we will consider the limit as the size of the torus grows to infinity, and then the torus distance converges to the Euclidean distance. In the cases of simulation studies of finite-size networks and hypothesis tests on real-world datasets, we will use the torus distance to eliminate boundary effects and to ensure consistency with [40].*

While the parameter β governs the overall edge density, the parameter γ controls the strength of the preferential attachment mechanism and determines the tail index of the degree distribution.

Note that

$$\varphi\left(\frac{d(t^{1/d}x, t^{1/d}y)^d}{\beta(u/t)^{-\gamma}(v/t)^{-(1-\gamma)}}\right) = \varphi\left(\frac{d(x, y)^d}{\beta u^{-\gamma} v^{-(1-\gamma)}}\right),$$

thus, for a finite value of t, the ADRCM can be rescaled using the transformation $h_t \colon [-1/2, 1/2]^d \times (0, t] \to [-t/2, t/2]^d \times (0, 1]$ defined by the map $(x, u) \mapsto (t^{1/d}x, u/t)$, which is visualized in Figure 5. This transformation allows us to examine the ADRCM on the more convenient space $[-t/2, t/2]^d \times (0, 1]$ instead of $[-1/2, 1/2]^d \times \mathbb{R}_+$. From now on, we will study the rescaled ADRCM, and we will not introduce new notations for the rescaled model.

The connection condition can be interpreted similarly to the profile function used in the weighted random connection model (WRCM) from Paper A. First, define the
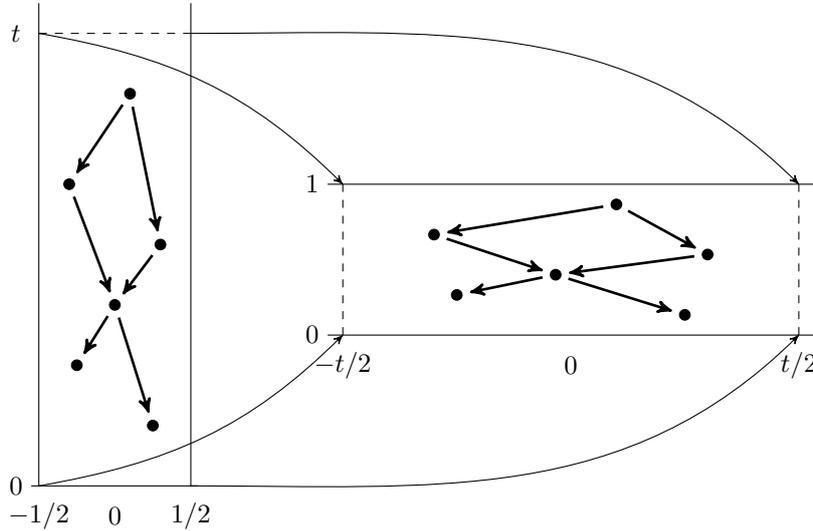
Figure 5: Rescaling of the age-dependent random connection model. The figure was recreated based on [40, Figure 1].

16

kernel function $\kappa_{\mathsf{ADRCM}}(u, v)$ as

$$\kappa_{\mathsf{ADRCM}}(u, v) := (u \wedge v)^{-\gamma}(u \vee v)^{-(1-\gamma)}$$
$$= \left(u^{-(1-\gamma)} \vee v^{-(1-\gamma)}\right)^{-\gamma/(1-\gamma)}\left(u^{-(1-\gamma)} \wedge v^{-(1-\gamma)}\right)$$
$$= \left(\tilde{u} \vee \tilde{v}\right)^{-\gamma/(1-\gamma)}\left(\tilde{u} \wedge \tilde{v}\right),$$

where we introduced the transformed marks $\tilde{u} := u^{-(1-\gamma)}$ and $\tilde{v} := v^{-(1-\gamma)}$ in the last step. The transformed marks $\tilde{u}, \tilde{v}$ are distributed according to a Pareto distribution with tail index $1/(1 - \gamma)$. We note that Gracar et al. [42] introduced a more general class of kernels that includes the kernel κ_{ADRCM} as a special case. Then, the connection probability and the profile function can be interpreted in the framework of the WRCM. Note that the results of Paper A cannot be directly applied to the ADRCM, since the regular variation at ∞ of the profile function φ is not required, and the weight distribution does not fulfill the assumptions of Paper A.

In our paper, we focus on the one-dimensional case $d = 1$ with profile function $\varphi(r) = \mathbb{1}\{r \leqslant 1\}$. This means that the connection between a pair of points $(x, u), (y, v) \in \mathbb{R} \times (0, 1]$ with $u \leqslant v$ is deterministic, and formed if the condition $|x - y| \leqslant \beta u^{-\gamma} v^{-(1-\gamma)}$ holds. This connection condition is visualized in Figure 6 as well. The expected number of edges of a node (x, u) to nodes with smaller arrival times is Poisson distributed with parameter $2\beta/(1 - \gamma)$, which corresponds to the outgoing degree of the node. On the other hand, the expected number of edges to nodes with larger arrival times is Poisson distributed with parameter $\frac{2\beta}{\gamma}(u^{-\gamma} - 1)$, which corresponds to the incoming degree of the node. Since the mark u is uniformly distributed on $(0, 1]$, the expected number of incoming edges of a node has a power-law tail with tail index $1 + 1/\gamma$, which can be seen by the application of Poisson concentration inequalities. These properties make the ADRCM an interesting model to study, as it captures the preferential attachment mechanism while being more tractable than the Barabási–Albert model.

The ADRCM produces a simple graph; therefore, it is not well-suited to study higher-order structures. In this paper, we study the ADRCM as a higher-order network
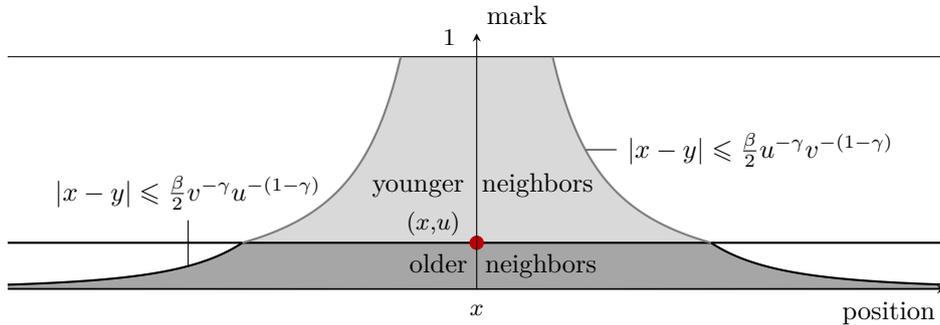
Figure 6: Connection conditions in the ADRCM. In the figure, we have a fixed point (x, u). The gray area shows the domain of points that can be connected to (x, u). Note that the connection condition differs for older and younger neighbors with marks less and larger than u, respectively. The figure was recreated based on Figure B.3 from Paper B.

by considering its clique complex $G := G(\mathcal{P})$, which is a simplicial complex in which each clique of the original graph corresponds to a simplex.

Main results

Let us begin by introducing the Palm distribution of the typical m-simplex $\Delta_m = \{P_0, \ldots, P_m\} \in G$ in the ADRCM for $m \geqslant 0$. Let $\mathbf{N}_{\mathsf{loc}}$ denote the space of locally finite point sets on $\mathbb{R} \times (0, 1]$, let $\mathcal{C}_m$ denote the set of distinct $(m+1)$-tuples of points in $\mathbb{R} \times (0, 1]$, and let $f \colon \mathcal{C}_m \times \mathbf{N}_{\mathsf{loc}} \to [0, \infty)$ be a measurable function that is symmetric in the first $m+1$ arguments. Furthermore, we denote the lowest-mark vertex of a simplex Δ_m by $c(\Delta_m)$. Then, the expectation of the function f of the typical m-simplex Δ_m^* is given by

$$\mathbb{E}[f(\Delta_m^*, \mathcal{P})] = \frac{1}{\lambda_m} \mathbb{E}\Big[\sum_{\Delta \in \mathcal{T}_m(\mathcal{P})} \mathbb{1}\{c(\Delta) \in [0, 1]\} f(\Delta - c(\Delta), \mathcal{P} - c(\Delta)) \Big],$$

where $\lambda_m > 0$ is the simplex density and $\mathcal{T}_m(\mathcal{P})$ is the set of m-simplices in G. Note that the sum is taken over all m-simplices whose lowest-mark vertex is in the interval $[0, 1]$. In our paper, we show that the above expectation exists and the m-simplex intensity is finite.

In our first result, we examine the higher-order degree distribution of the ADRCM, which describes the adjacency structure of simplices in higher dimensions. Let us consider an m-simplex $\Delta_m \subseteq G$. The higher-order m'-degree of the simplex Δ_m is defined as the number of m'-simplices that contain Δ_m:

$$\deg_{m'}(\Delta_m) := |\{\sigma \in G \colon \sigma \supset \Delta_m, |\sigma| = m' + 1\}|.$$

The standard vertex degree corresponds to the case $m = 0$ and $m' = 1$, i.e., $\deg_1(p)$ denotes the number of edges incident to the vertex $p \in G$. The case $m = 1$, $m' = 2$ corresponds to the edge-degree, i.e., the number of triangles incident to an edge in the graph. The edge degree and the triangles formed in the network are of high interest, since they are related to the clustering coefficient studied in—among others—van der Hofstad et al. [103, 104]. Then, the simplex-degree distribution is defined as

$$d_{m,m'}(k) = \mathbb{P}(\deg_{m'}(\Delta_m) \geqslant k),$$

which generalizes the result of Gracar et al. [40, Proposition 4.1], which considers ordinary degree distributions for $m = 0$ and $m' = 1$. Our first result indicates that the higher-order degree distribution of the ADRCM follows a power law.

Theorem B.2.1 (Power law for the typical simplex degree)**.** *Let $\gamma \in (0, 1)$ and $m' > m \geqslant 0$. Then,*

$$\lim_{k \uparrow \infty} \log(d_{m,m'}(k)) / \log(k) = m - (m+1)/\gamma.$$

Note that the left-hand side of the above equation is the power-law exponent of the higher-order degree distribution. Furthermore, note that the right-hand side does not depend on the dimension m', which might be surprising at first.

Next, we study the asymptotic behavior of the Betti numbers of the clique complex $G(\mathcal{P} \cap [0, n])$. In our second main result, we show that the distribution of the appropriately scaled qth Betti number $\beta_{n,q}$ of $G(\mathcal{P} \cap [0, n])$ is asymptotically normal.

Theorem B.2.2 (CLT for the Betti numbers)**.** *Let $q \geqslant 0$ and $0 < \gamma < 1/4$. Then, $n^{-1/2}(\beta_{n,q} - \mathbb{E}[\beta_{n,q}])$ converges in distribution to a normal distribution.*

Our proof requires the constraint $\gamma < 1/4$ since it guarantees a finite fourth moment of the degree distribution. On the other hand, in the paper we also conjectured that Theorem B.2.2 holds for $\gamma < 1/2$, i.e., if the variance of the degree distribution is finite. We note that in the work by Pabst [82], the positivity of the limiting variance was also established; moreover, the convergence in distribution holds even with normalization by the standard deviation. If $\gamma > 1/2$, the model generates long edges, which makes the variance of the degree distribution infinite. Then, the asymptotic normality of the Betti numbers breaks, and we expect that the limiting distribution is stable. The above conjectures are supported by our numerical simulation study, which we present later in this section.

Next, we define the edge count S_n as the number of edges in the clique complex $G(\mathcal{P} \cap [0, n])$:

$$S_n \coloneqq \big|\{(y, v) \rightarrow (x, u) \colon (y, v), (x, u) \in \mathcal{P}, x \in [0, n]\}\big|,$$

where the notation $y \rightarrow x$ means that the edge $(y, v) \rightarrow (x, u)$ is formed in the ADRCM with $u \leqslant v$. For the edge count S_n, we have the following two results.

Theorem B.2.3 (CLT for the edge count)**.** *Let $\gamma < 1/2$. Then, the quantity $\mathrm{Var}(S_n)^{-1/2}(S_n - \mathbb{E}[S_n])$ converges in distribution to a standard normal distribution.*

Theorem B.2.4 (Stable limit law for the edge count)**.** *Let $\gamma \in (1/2, 1)$. Then, $n^{-\gamma}(S_n - \mathbb{E}[S_n])$ converges in distribution to $\mathcal{S}_{\gamma^{-1}}$, where $\mathcal{S}_{\gamma^{-1}}$ is a $1/\gamma$-stable distribution.*

Note that if $\gamma \in (0, 1/2)$, the variance of the degree distribution is finite. In this regime, the limiting edge count distribution is normal. On the other hand, if $\gamma \in (1/2, 1)$, the degree distribution is heavy-tailed, and, in the appropriate sense, the probability of long edges is not negligible. In this regime, the distribution of the edge count S_n converges to a stable distribution as the size n of the observation window grows.

Theorem B.2.1 determines the power-law exponent of the higher-order degree distribution of the ADRCM in terms of the parameter γ, which means that the degree distributions for various dimensions are not independent. However, as we see in the Section B.8, we need a more flexible model to fit it to real-world datasets, in which the tail indices of the higher-order degree distributions do not have such a strong dependence. Thus, we define the *thinned age-dependent random connection model (TADRCM)*. In this modification, we remove edges so that the tail index of the vertex-degree distribution decreases, but the power-law exponent of the edge-degree distribution $d_{1,2}$ describing the distribution of the number of triangles adjacent to an edge is not affected. This allows for the TADRCM model to be fitted to the edge and vertex degrees independently.

While we show that our theoretical results hold for infinitely large networks in the limit, in Section B.7, we conduct a numerical simulation study to verify the theorems for finite settings. Apart from simulating finite networks, we also simulate the Palm distribution of the typical m-simplex Δ_m^* in the ADRCM, eliminating the finite-size effects. We use the software described in Section 4 to simulate the ADRCM.

Simulating several finite networks of various sizes, we find that for large enough networks of size $\sim 10^5$, the fitted power-law exponents of the higher-order degree distributions are close to their theoretical values predicted by Theorem B.2.1.

Next, we use Q-Q plots to compare the edge count distributions for different γ parameters with normal and stable distributions. We find that our simulations are in alignment with Theorems B.2.3 and B.2.4. In particular, the heavy-tailed behavior is prominent in the case when $\gamma > 1/2$.

Finally, we conduct a similar study for the first Betti numbers. Our Q-Q plots support our conjecture that Betti numbers follow a normal distribution as well in the domain $\gamma \in (0, 1/2)$ and a stable distribution if $\gamma \in (1/2, 1)$. This is supposedly because the edge degree distribution has infinite variance if $\gamma > 1/2$.

After the simulation study, we conduct hypothesis tests on the collaboration network of arXiv, including documents published in four different scientific fields: *computer science*, *electrical engineering*, *mathematics*, and *statistics*. To build a simplicial complex from these datasets, we represent authors as vertices, and we establish a higher-order connection for a set of authors whenever there is at least one common publication they published together.

We then conduct hypothesis tests using triangle counts and Betti numbers. The model-generated networks exhibit significantly higher triangle counts and fewer loops compared to the empirical datasets. We believe that this can be partially explained by the specific form of the profile function we use, which leads to vertices connecting to all other vertices in their neighborhood. This leads to a tree-like structure of the ADRCM, which is also supported by our simulation study. Thus, in a future work, it would be worthwhile to study the ADRCM with a more flexible profile function as well. While we conjecture that most parts of the proofs could be adapted to more general profile functions with bounded support, some proofs, e.g., the proof of Equation B.6, would break down if the profile function has unbounded support. This is because, in this case, the common neighborhood of two vertices conditioned on their marks cannot be easily controlled. Furthermore, if the profile function does not converge to 0 fast enough, the weak stabilization part of the Betti number proof may break down.

Methodology

Now, we turn our attention to the proof ideas of the main results of Paper B.

First, we need to show that the Palm distribution of the typical m-simplex Δ_m^* is well-defined and the m-simplex intensity λ_m is finite. To do this, we write λ_m in terms of an integral of the indicator function of the event that the vertices of the typical simplex Δ_m^* form an m-simplex. Then, ordering the vertices of Δ_m^* according to their marks, we apply an iterative approach to calculate the integral.

To prove Theorem B.2.1, we show a lower bound and an upper bound for the higher-order degree distribution $d_{m,m'}(k)$. The key tool to derive these bounds is the

Palm representation of the typical m-simplex Δ_m^*. For the lower bound, we restrict the domain of the points of the typical m-simplex Δ_m^* to a rectangle $B_k \subseteq \mathbb{R} \times (0,1]$ in which it is certain that the $m+1$ points of the simplex are connected. Then, we show that the probability of Δ_m^* having at least k neighboring m'-simplices is bounded away from 0. For the upper bound, we follow two steps.

(1) First, we reduce the problem to the case when $m' = m + 1$.

(2) Then, we show the upper bound for $m' = m + 1$ using Poisson concentration and by bounding the common neighborhood of the $m + 1$ points of the typical simplex Δ_m^*.

The first step is based on the following observation. Consider the oldest vertex $(0, u)$ of the typical m-simplex Δ_m^*, and suppose a younger neighbor of $(0, u)$ is the youngest vertex of some of the neighboring m'-simplices. The number of these neighboring m'-simplices is bounded by the maximum out-degree of the youngest vertex raised to the power $m' - m$. Then, multiplying this number by the number of younger neighbors of $(0, u)$, we get an upper bound for the number of m'-simplices containing the vertex $(0, u)$. Given the mark u, the degree of the vertex $(0, u)$ is Poisson distributed with fast decaying tail probabilities.

To prove Theorem B.2.2, we adapt a general CLT result for stabilizing Poisson functionals [89, Theorem 3.1]. We begin by introducing the add-one cost operator $\delta(\varphi, u) := \beta(\varphi \cup \{(0, u)\}) - \beta(\varphi)$, where β is the Betti number, and $\varphi \in \mathbf{N}_{\mathsf{loc}}$ is a locally finite point set. To apply [89, Theorem 3.1], we verify the following conditions, conceptually similarly to [48, Theorem 5.2].

(1) **Moment condition:** it holds that $\sup_{n \geqslant 1} \mathbb{E}[\delta(\mathcal{P}_n, U)^4] < \infty$.

(2) **Weak stabilization:** it holds that $\delta(\mathcal{P} \cap W_n, U)$ converges almost surely to a finite limit as $n \to \infty$, where $W_n = [-n/2, n/2] \times (0, 1]$.

To verify the moment condition, we show that the add-one cost operator δ is bounded by the number of q- and $(q+1)$-simplices containing the new point. This is the step which introduces the constraint $\gamma < 1/4$ in Theorem B.2.2. The weak stabilization condition requires that the change in the Betti number caused by adding a new point becomes constant as the observation window grows. We analyze the changes in the cycle space and boundary space separately, which define the Betti number. We first show that the number of new cycles or boundaries created by the new point is bounded. Then, we show that the increment of the Betti number is monotonic in the observation window size.

In the proofs of Theorems B.2.3 and B.2.4, we write the edge count as a sum of in-degrees of vertices in a window of size n as follows:

$$S_n = \sum_{i=1}^{n} T_i := \sum_{i=1}^{n} \sum_{P_j \in [i-1,i] \times (0,1]} D_{\mathsf{in}}(P_j),$$

where $D_{\mathsf{in}}(P)$ denotes the in-degree of the point $P \in \mathcal{P}$. For Theorem B.2.3, we apply a CLT for associated random variables [107, Theorem 4.4.3]. Let us first recall the definition of associated random variables.

Definition 3.4 (Associated random variables)**.** *The sequence $\{T_i\}_{i \in \{1,\dots,n\}}$ is associated if and only if for any $f_1, f_2 \colon \mathbb{R}^k \to \mathbb{R}$ coordinatewise non-decreasing functions with $\mathbb{E}[f_{1,2}(T_1,\dots,T_k)^2] < \infty$,*

$$\mathrm{Cov}(f_1(T_1,\dots,T_k), f_2(T_1,\dots,T_k)) \geqslant 0.$$

To apply [107, Theorem 4.4.3], we need to show that the random variables $\{T_i\}$ are associated and that the sum of the covariances $\sum_{k \geqslant 1} \mathrm{Cov}(T_1, T_k) < \infty$ is finite. To show Theorem B.2.4, we apply [107, Theorem 4.5.2], which states the following.

Theorem 3.5 (α-stable convergence)**.** *Let $\{X_i\}_i$ be i.i.d. nonnegative random variables such that $\mathbb{P}(X_i > x) \sim A x^{-\alpha}$ for some $\alpha \in (1,2)$ and $A > 0$. Then, $n^{-1/\alpha}(\sum_{i=1}^n X_i - n \, \mathbb{E}[X_1])$ converges in distribution to an α-stable random variable $\mathcal{S}_\alpha$.*

The main challenge in applying the above theorem is controlling the spatial correlations of the vertex degrees. First, we decompose the edge count by writing $S_n = S_n^{\geqslant} + S_n^{\leqslant}$, where $S_n^{\geqslant}$ and $S_n^{\leqslant}$ denote the sum of the in-degrees of low-mark and high-mark vertices, respectively. After showing that $S_n^{\geqslant}$ converges to 0 in probability, we approximate $S_n^{\leqslant}$ as a sum of i.i.d. random variables with a distribution having power-law tails. Then, [107, Theorem 4.5.2] concludes the proof of Theorem B.2.4.

Paper C

With my coauthors, Christian Hirsch, Moritz Otto, and Morten Brun, in Paper C, we examine a weighted random connection model that describes hypergraphs.

Motivation

While the higher-order networks generated by the age-dependent random connection model (see Paper B) possess many of the characteristics of real-world networks, it does not capture the strength of the interactions of a group of vertices. For instance, in a scientific collaboration network, the age-dependent random connection model only indicates whether a set of authors collaborated. Still, it does not provide information about the number of papers they published.

To address this limitation, we introduce a random connection hypergraph model (RCHM). Our model represents a hypergraph as a bipartite graph, where one vertex set corresponds to nodes of the hypergraph. In contrast, the second vertex set corresponds to the interactions, or hyperedges, connecting the points in the first vertex set. Then, if a network node is connected to an interaction, it indicates that the node is part of that hyperedge.

Model

Similarly to Paper B, we consider the space $\mathbb{S} \coloneqq \mathbb{R} \times (0,1]$, in which $\mathbb{R}$ represents the spatial location and $(0,1]$ the marks. Then, two points $(x, u), (z, w) \in \mathbb{S}$ are connected if

$$|x - z| \leqslant \beta u^{-\gamma} w^{-\gamma'}, \tag{1}$$

where $\gamma, \gamma' \in (0,1)$ and $\beta > 0$ are parameters of the model. Note that the connection condition is similar to the one in Paper B, but now the condition does not distinguish which of the marks u and w is smaller. The neighborhood of a point $(x,u) \in \mathbb{S}$ is defined as

$$B((x,u), \beta) := \{(z,w) \in \mathbb{S} \colon |x - z| \leqslant \beta u^{-\gamma} w^{-\gamma'}\},$$

and for $\Delta \subseteq \mathbb{S}$, the joint neighborhood of the points in Δ is defined as the intersection of the individual neighborhoods $B(\Delta, \beta) := \bigcap_{p \in \Delta} B(p, \beta)$ as the joint neighborhood of the points in Δ.

To define the hypergraph, let $\mathcal{P}, \mathcal{P}'$ be two independent Poisson point processes on $\mathbb{S}$ with intensity measures $\lambda |\cdot|, \lambda' |\cdot|$, respectively, where $\lambda, \lambda' > 0$, and $|\cdot|$ denotes Lebesgue measure on $\mathbb{S}$. In this model, the points in $\mathcal{P}$ represent the vertices of the hypergraph, whereas the points in $\mathcal{P}'$ represent the hyperedges. Then, we denote by $G^{\mathsf{bip}} := G^{\mathsf{bip}}(\mathcal{P}, \mathcal{P}')$ the bipartite graph with vertex set $\mathcal{P} \cup \mathcal{P}'$. A connection between two points $p \in \mathcal{P}$ and $p' \in \mathcal{P}'$ is formed if and only if p and p' fulfill the connection condition (1).

The *random connection hypergraph model (RCHM)* $G^{\mathsf{hyp}} := G^{\mathsf{hyp}}(\mathcal{P}, \mathcal{P}')$ is defined from the bipartite graph G^{bip} using the notion of *Dowker complex* [18]. The set of hyperedges Σ_m consisting of $m + 1$ $\mathcal{P}$-points is defined as the family of those sets of point $\Delta_m \subseteq \mathcal{P}$ such that their common neighborhood in $\mathcal{P}'$ is non-empty:

$$\Sigma_m := \{\Delta_m \subseteq \mathcal{P} \colon \#(\Delta_m) = m + 1, \mathcal{P}'(B(\Delta_m, \beta)) \neq 0\},$$

where $\#(\cdot)$ denotes the cardinality.

A figure illustrating the RCHM is provided in Figure 7.

Note that the hypergraphs generated by the RCHM are simplicial complexes, since by definition, if $\Delta_m \in \Sigma_m$ then $\mathcal{P}'(B(\Delta_{m'}, \beta)) \neq 0$, and thus for $\Delta_{m'} \subseteq \Delta_m$ with $m' \leqslant m$, then $\mathcal{P}'(B(\Delta_{m'}, \beta)) \neq 0$ as well.

The center $c(\Delta_m)$ of an m-simplex $\Delta_m \in \Sigma_m$ is defined as the point in Δ_m with the lowest mark. Note that almost surely, there is a unique point in Δ_m with the lowest mark, since the marks are sampled from a continuous distribution.

Main results

Throughout the presentation of the results, we write $\boldsymbol{p}_m := (p_1, \ldots, p_m) \in \mathbb{S}^m$ for an m-tuple of points. Furthermore, we introduce $\boldsymbol{p}_m(u) := ((0,u), p_1, \ldots, p_m) \in (0,(0,1]) \times \mathbb{S}^m$ for $u \in (0,1]$ and $\overrightarrow{\boldsymbol{p}}_m(u) := \{(0,u), p_1, \ldots, p_m\}$ for the tuple and corresponding set, respectively.

As in Paper B, we begin by showing that the intensity λ_m of m-simplices in the RCHM is finite if $\gamma' < 1/(m + 1)$, which is required to define the Palm distribution of the typical m-simplex Δ_m^*. Then, the distribution of the typical m-simplex is defined in the following proposition.

Proposition C.2.2 (Distribution of the typical m-simplex)**.** *Let $m \geqslant 0$, $\gamma < 1$, $\gamma' < 1/(m + 1)$, and let $f \colon (\mathbb{R} \times (0,1])^{m+1} \times \mathbf{N}_{\mathsf{loc}} \times \mathbf{N}_{\mathsf{loc}} \to \mathbb{R}_+$ be an arbitrary nonnegative measurable functional depending on an m-simplex as well as on the point*
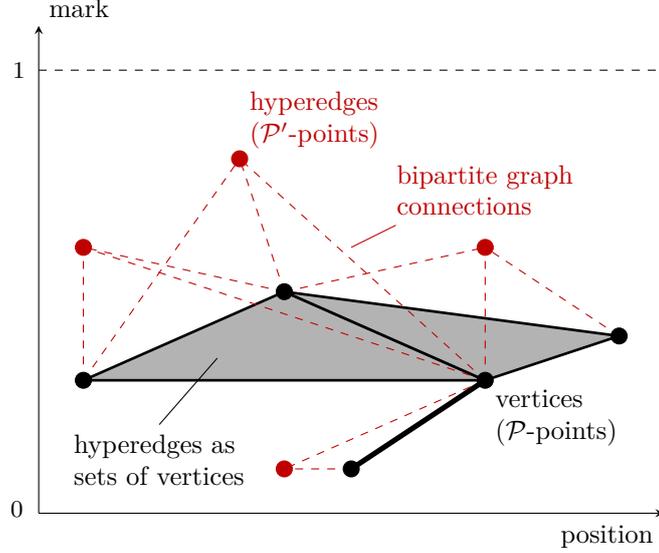
Figure 7: Illustration of the random connection hypergraph model (RCHM). Vertices (black dots) are scattered in space with random marks (vertical axis). Hyperedges (gray shaded areas) are formed between sets of vertices whenever the vertices have a common hyperedge (red dots) they are connected to. The connections can be represented as a bipartite graph (red dashed lines) between vertices and hyperedges.

processes $\mathcal{P}$ and $\mathcal{P}'$. Then,

$$
\mathbb{E}\big[f(\Delta_m^*, \mathcal{P}, \mathcal{P}')\big]
$$
$$
= \frac{\lambda^{m+1}}{\lambda_m(m+1)!} \int_{(0,1]\times\mathbb{S}^m} \mathbb{E}\big[f(\overrightarrow{\boldsymbol{p}}_m(u), \mathcal{P} \cup \overrightarrow{\boldsymbol{p}}_m(u), \mathcal{P}')\, \mathbb{1}\{\overrightarrow{\boldsymbol{p}}_m(u) \in \Sigma_m\}\big]\, \mathrm{d}(u, \boldsymbol{p}_m).
$$

Here, if $\overrightarrow{\boldsymbol{p}}_m(u)$ does not consist of precisely $m+1$ elements, then we let $f(\overrightarrow{\boldsymbol{p}}_m(u), \mathcal{P} \cup \overrightarrow{\boldsymbol{p}}_m(u), \mathcal{P}') := 0$.

After establishing the distribution of the typical m-simplex, we examine the higher-order degree distribution of the RCHM, which we define as follows. The *higher-order degree* of an m-simplex Δ_m is the number $\mathcal{P}'$-points to which all points in Δ_m are connected, i.e., $\deg(\Delta) := \mathcal{P}'(B(\Delta, \beta))$. Our first result is that the higher-order degrees of the RCHM are scale-free, i.e., they have a power-law tail.

Theorem C.2.3 (Scale-freeness of higher-order degrees)**.** *Let $m \geqslant 0$, $\gamma < 1$, $\gamma' < 1/(m+1)$. Then,*

$$
\lim_{k\uparrow\infty} \frac{\log\big(\mathbb{P}\big(\deg(\Delta_m^*) \geqslant k\big)\big)}{\log(k)} = m - \frac{m+1}{\gamma}.
$$

Our next result corresponds to Theorem B.2.2 in Paper B, and it shows that if $\gamma < 1/4$, the Betti numbers of the RCHM are asymptotically normal as the size n of the observation window $\mathbb{S}_n := [0, n] \times (0, 1]$ increases.

Theorem C.2.4 (Asymptotic normality of Betti numbers)**.** *Let $\beta_m^{(n)}$ denote the mth Betti number of $G^{\mathsf{hyp}}(\mathcal{P} \cap \mathbb{S}_n, \mathcal{P}' \cap \mathbb{S}_n)$ with $m \geqslant 0$. If $\gamma < 1/4$ and $\gamma' < 1/(4(m+1))$, then, in distribution,*

$$n^{-1/2}\big(\beta_m^{(n)} - \mathbb{E}\big[\beta_m^{(n)}\big]\big) \xrightarrow[n\uparrow\infty]{d} \mathcal{N}(0,\sigma^2) \qquad \textit{for some } \sigma \geqslant 0,$$

where $\mathcal{N}(0,\sigma^2)$ denotes the normal distribution with mean 0 and variance σ^2.

Note that if $m = 0$, the constraint $\gamma < 1/4$ is almost equivalent to the condition that the degree distribution has a finite fourth moment. As it will be seen from our simulation study, consistently with the results presented in Paper B, the asymptotic normality of the Betti numbers breaks down for $\gamma \geqslant 1/2$. This is expected since in this case, the degree distribution has an infinite variance, and heavy nodes connecting to many other vertices *fill* many of the loops. As for Paper B, the positivity of the limiting variance was also established by Pabst [82], and therefore the convergence in distribution holds also with the normalization by $\mathrm{Var}(\beta_m^{(n)})^{1/2}$.

Next, we state limit laws for the edge count of the RCHM, defined as

$$S_n := \sum_{P_i \in \mathcal{P} \cap \mathbb{S}_n} \deg(P_i),$$

where $\deg(P_i)$ denotes the degree of a point P_i in the bipartite graph G^{bip}.

Theorem C.2.5 (Normal and stable limits of edge counts)**.** *Let $\gamma' < 1/3$. Then, the following distributional limits hold as $n \to \infty$.*

(a) *Let $\gamma \in (0, 1/2)$. Then, $n^{-1/2}(S_n - \mathbb{E}[S_n]) \xrightarrow[n\uparrow\infty]{d} \mathcal{N}(0,\sigma^2)$ for some $\sigma > 0$.*

(b) *Let $\gamma \in (1/2, 1)$. Then, $n^{-\gamma}(S_n - \mathbb{E}[S_n]) \xrightarrow[n\uparrow\infty]{d} \mathcal{S}_{\gamma^{-1}}$, where $\mathcal{S}_{\gamma^{-1}}$ is a γ^{-1}-stable random variable.*

Finally, we define the *m*-simplex count $S_{n,m} := \#\{\Delta_m \in \Sigma_m \colon c(\Delta_m) \in [0,n]\}$ as the number of m-simplices centered in the observation window $\mathbb{S}_n$. Then, we show that the m-simplex count $S_{n,m}$ has a normal limit law for $\gamma < 1/2$ and a stable limit law for $\gamma \in (1/2, 1)$.

Theorem C.2.6 (Normal and stable limits of simplex counts)**.** *Let $\gamma' < 1/(2m+1)$. Then, the following distributional limits hold as $n \to \infty$.*

(a) *Let $\gamma \in (0, 1/2)$. Then, $n^{-1/2}(S_{n,m} - \mathbb{E}[S_{n,m}]) \xrightarrow[n\uparrow\infty]{d} \mathcal{N}(0,\sigma^2)$ for some $\sigma^2 > 0$.*

(b) *Let $\gamma \in (1/2, 1)$. Then, $n^{-\gamma}(S_{n,m} - \mathbb{E}[S_{n,m}]) \xrightarrow[n\uparrow\infty]{d} \mathcal{S}_{\gamma^{-1}}$, where $\mathcal{S}_{\gamma^{-1}}$ is a γ^{-1}-stable random variable.*

In the model considered in Paper B, the corresponding result was not established. The reason is that in Paper C, we could use the formula for the total variance to condition on the point process $\mathcal{P}'$, which is necessary to prove Theorem C.2.6. This

argument could not have been used in Paper B. We note that the proof for the heavy-tailed case has since been provided by Owada and Hirsch [80, Theorem 3.5].

To show that our conjectures and the results proved in the large network limit $n \to \infty$ hold for finite networks, we conducted a simulation study using a Monte Carlo approach. Using the computational framework introduced in Section 4, we generate several higher-order networks and examine their properties.

We find that the degree distribution of the RCHM is scale-free, and the fitted power-law exponents become closer to the theoretical value if the size of the network exceeds $\sim 10^5$ $\mathcal{P}$- and $\mathcal{P}'$-vertices. This value is comparable to the size of many real-world networks, such as the collaboration network of scientific authors.

Next, we examine the distribution of the first Betti numbers with different γ, γ' parameters. Consistent with Theorem C.2.4, the Q-Q plots illustrate that the distribution of the first Betti number is asymptotically normal for $\gamma < 1/4$ and $\gamma' < 1/8$. Moreover, we also find that the first Betti number is asymptotically normal for $\gamma \in [1/4, 1/2)$ and $\gamma' > 1/8$. On the other hand, the Betti number distribution has a fat left tail when $\gamma > 1/2$, in alignment with our conjecture.

Finally, we examine the edge and triangle counts in the network. We found that the edge counts are normally distributed if $\gamma < 1/2$ and $\gamma' < 1/3$, and otherwise, they have a stable distribution. For the triangle counts, we observe a normal distribution for $\gamma < 1/2$ and $\gamma' < 1/5$, and a stable distribution for $\gamma > 1/2$ and $\gamma' < 1/5$. We also conjecture that the triangle counts follow a stable distribution if $\gamma' > 1/5$.

To investigate the applicability of our results to real-world data, we conduct hypothesis tests on the *arXiv* dataset [1], which contains the metadata of scientific papers published on the arXiv platform. In the dataset, we represent the authors as $\mathcal{P}$-vertices and the papers as $\mathcal{P}'$-vertices. Then, we analyze the collaboration network of four scientific fields: *computer science*, *electrical engineering and systems science*, *mathematics*, and *statistics*.

Examining the degree distributions, we found that they are heavy-tailed. Using the fitted power-law exponents, we fit the model parameters γ and γ' using Theorem C.2.3. Then, the network size is fitted so that we compensate for the lack of isolated $\mathcal{P}$- and $\mathcal{P}'$-vertices in the dataset.

After the model parameters are fitted, hypothesis tests for the Betti numbers, edge counts, and triangle counts become available. The datasets are characterized by a much larger Betti number than the simulated networks, and the hypothesis tests for the Betti numbers are rejected. The reason is the same as for Paper B: networks generated by the RCHM are dominated by a couple of very high-degree $\mathcal{P}$-vertices that leads to a tree-like network topology with a few loops. For the edge and triangle counts, the results show that the datasets are more complex than the networks generated by the RCHM.

Methodology

To prove Proposition C.2.2, we examine the common neighborhood of the points in the typical simplex Δ_m^*. Then, employing Markov's inequality, the Mecke formula, and Fubini's theorem we conclude that the m-simplex intensity $\lambda_m < \infty$ is finite if $\gamma' < 1/(m+1)$.

The proof of Theorem C.2.3 follows two steps, namely, we show an upper bound and a lower bound for the degree distributions. For the upper bound, we write the probability $\mathbb{P}(\deg(\Delta_m^*) \geqslant k)$ as an integral, and then we use a Poisson concentration inequality for the number of $\mathcal{P}'$-vertices in the common neighborhood of the points in Δ_m^*. Next, we show an upper bound for the case when $m = 0$, and then we extend this result by bounding the common neighborhood of the points in Δ_m^* by the pairwise intersections of the individual neighborhoods. For the lower bound, we define two rectangles in $\mathbb{S}$ as a function of the degree k such that if a pair of $\mathcal{P}$- and a $\mathcal{P}'$-vertex are in these rectangles, they are surely connected. Lower bounding the integral representation of the probability $\mathbb{P}(\deg(\Delta_m^*) \geqslant k)$ by the integral over the rectangles yields a lower bound for the degree distribution.

The proof of Theorem C.2.4 is similar to the proof of Theorem B.2.2 in Paper B. We use again the CLT for Poisson functionals [89, Theorem 3.1] by examining the add-one cost operator for the mth Betti number in the observation window $\mathbb{S}_n$. In this case, however, the add-one cost operator is more complex than in Paper B, since we need to consider the changes for both the cases of added $\mathcal{P}$- and $\mathcal{P}'$-vertex. More precisely, let us denote by $\beta(\mathcal{P}, \mathcal{P}') := \beta_{n,m}(\mathcal{P}, \mathcal{P}')$ the mth Betti number of the simplicial complex $G_n^{\mathsf{hyp}}(\mathcal{P} \cap \mathbb{S}_n, \mathcal{P}' \cap \mathbb{S}_n)$. Introduce two special points $o := (0, U), o' := (0, W)$ as $\mathcal{P}$- and $\mathcal{P}$-vertices, respectively, we let $G_{n,o}^{\mathsf{hyp}} := G^{\mathsf{hyp}}((\mathcal{P} \cup \{o\}) \cap \mathbb{S}_n, \mathcal{P}' \cap \mathbb{S}_n)$ and $G_{n,o'}^{\mathsf{hyp}}(\mathcal{P} \cap \mathbb{S}_n, (\mathcal{P}' \cup \{o'\}) \cap \mathbb{S}_n)$ be the simplicial complexes in the observation window $\mathbb{S}_n$ with the additional $\mathcal{P}$-vertex o and $\mathcal{P}'$-vertex o', respectively. Then, the add-one cost operators for the Betti number are defined by

$$\delta(G_n^{\mathsf{hyp}}, o) := \beta(G_{n,o}^{\mathsf{hyp}}) - \beta(G_n^{\mathsf{hyp}})$$

$$\delta(G_n^{\mathsf{hyp}}, o') := \beta(G_{n,o'}^{\mathsf{hyp}}) - \beta(G_n^{\mathsf{hyp}}).$$

We then verify the two conditions of [89, Theorem 3.1] for the add-one cost operators $\delta(G_n^{\mathsf{hyp}}, o)$ and $\delta(G_n^{\mathsf{hyp}}, o')$:

- **moment condition:** $\sup_{n \geqslant 1} \mathbb{E}[\delta(G_n^{\mathsf{hyp}}, o)^4] < \infty$ and $\sup_{n \geqslant 1} \mathbb{E}[\delta(G_n^{\mathsf{hyp}}, o')^4] < \infty$

- **weak stabilization:** $\lim_{n \uparrow \infty} \delta(G_n^{\mathsf{hyp}}, o) < \infty$ and $\lim_{n \uparrow \infty} \delta(G_n^{\mathsf{hyp}}, o') < \infty$.

For the moment condition, we bound the add-one cost operator $\delta(G_n^{\mathsf{hyp}}, o')$ by the degree of the added $\mathcal{P}'$-vertex, and then calculate the corresponding expectation. We apply a similar train of thought for $\delta(G_n^{\mathsf{hyp}}, o)$. For the weak stabilization condition, we analyze the changes in the cycle space and boundary space of the simplicial complex G_n^{hyp} caused by adding o and o'. Similarly to Paper B, we show that the number of new cycles or boundaries created by the new point is bounded. Then, we show that the change of the Betti number is monotone increasing as $n \to \infty$, which implies that the limit exists.

To show Theorem C.2.5 (a), we apply the CLT by Whitt [107, Theorem 4.4.3] for stationary sequences of associated random variables $\boldsymbol{T} := T_1, T_2, \ldots$, which requires that $\sum_{k \geqslant 1} \mathrm{Cov}(T_1, T_k) < \infty$. Following the ideas in Paper B, we write the edge count S_n as

$$S_n = \sum_{i=1}^n T_i := \sum_{i=1}^n \sum_{P_j \in [i-1, i] \times (0,1]} \deg(P_j),$$

where $\deg(P_j)$ denotes the degree of the point P_j in the bipartite graph G^{bip}. Then we show that the covariance $\mathrm{Cov}(T_1, T_k)$ is finite for $k \geqslant 1$. To show Theorem C.2.5 (b), we use Theorem 3.5 stated in Section 3. First we decompose S_n into a sum of degrees belonging to the $\mathcal{P}$-vertices with marks larger than $u_n := n^{-2/3}$ and those with marks smaller than u_n:

$$S_n = S_n^{\geqslant} + S_n^{\leqslant} := \sum_{P \in \mathcal{P} \cap \mathbb{S}_{n, \geqslant u_n}} \deg(P) + \sum_{P \in \mathcal{P} \cap \mathbb{S}_{n, \leqslant u_n}} \deg(P),$$

where $\mathbb{S}_{n, \geqslant u} := [0, n] \times [u, 1]$ and $\mathbb{S}_{n, \leqslant u} := [0, n] \times [0, u]$. Using Chebychev's inequality and then bounding the variance, we show that $n^{-\gamma}(S_n^{\geqslant} - \mathbb{E}[S_n^{\geqslant}])$ converges to 0 in probability as $n \to \infty$. Then, we set $\mu(u) := \mathbb{E}[\deg(0, u)]$,

$$S_n^{(1)} := \sum_{(X, U) \in \mathcal{P} \cap \mathbb{S}_{n, \leqslant u_n}} \mu(U), \qquad \text{and} \qquad S_n^{(2)} := \sum_{i \leqslant \lceil \lambda n \rceil} \mu(U_i) \, \mathbb{1}\{U_i \leqslant u_n\},$$

where $\{U_i\}$ are i.i.d. uniformly distributed random variables on $(0, 1]$. Then, we show that $\mathbb{E}[|S_n^{\leqslant} - S_n^{(1)}|] + \mathbb{E}[|S_n^{(1)} - S_n^{(2)}|] \in o(n^{\gamma})$, and finally the application of [107, Theorem 4.5.2] leads to the conclusion that $n^{-\gamma}(S_n^{(2)} - \mathbb{E}[S_n^{(2)}])$ converges in distribution to a stable random variable.

To show Theorem C.2.6, we write the m-simplex count $S_{n,m}$ as

$$S_n := \sum_{P \in \mathcal{P} \cap \mathbb{S}_n} \mathrm{d}_m(P),$$

where

$$\mathrm{d}_m(p) := \frac{1}{m!} \sum_{(P_1, \ldots, P_m) \in (\mathcal{P} \cap \mathbb{S}_{>u})_{\neq}^m} \mathbb{1}\{\mathcal{P}' \cap B(\{p, P_1, \ldots, P_m\}) \neq \varnothing\}$$

is the number of m-simplices containing p. For the proof of Theorem C.2.6 (a), we apply the CLT by Whitt [107, Theorem 4.4.3] once more, extending the result of Theorem C.2.5 (a). Finally, we show Theorem C.2.6 (b) similarly to Theorem C.2.5 (b). We choose $u_n = n^{-b}$, where $b \in (2/3, 1)$, and decompose $S_{n,m}$ as

$$S_{n,m} = S_{n,m}^{\geqslant} + S_{n,m}^{\leqslant} := \sum_{P_i \in \mathcal{P} \cap \mathbb{S}_{n, \geqslant u_n}} \mathrm{d}_m(P_i) + \sum_{P_i \in \mathcal{P} \cap \mathbb{S}_{n, \leqslant u_n}} \mathrm{d}_m(P_i).$$

The first step is showing that the simplex count corresponding to the high-mark vertices is negligible, i.e., $n^{-\gamma}(S_{n,m}^{\geqslant} - \mathbb{E}[S_{n,m}^{\geqslant}])$ converges to 0 in probability. Defining

$$S_{n,m}^{(1)} := \sum_{(X, U) \in \mathcal{P} \cap \mathbb{S}_n} \mu_m(U), \qquad S_{n,m}^{(2)} := \sum_{i \leqslant \lceil \lambda n \rceil} \mu_m(U_i) \, \mathbb{1}\{U_i \leqslant u_n\},$$

with $\mu_m(u) := \mathbb{E}[\mathrm{d}_m(0, u)]$ and $\{U_i\}$ i.i.d. uniform random variables on $(0, 1]$, we prove that $\mathbb{E}[|S_{n,m}^{\leqslant} - S_{n,m}^{(1)}|] + \mathbb{E}[|S_{n,m}^{(1)} - S_{n,m}^{(2)}|] \in o(n^{\gamma})$, and we finish the proof the same way as in Theorem C.2.5 (b).

Paper D

In Paper D, in a joint work with Christian Hirsch and Benedikt Jahnel, we study functional limit theorems in dynamic random connection hypergraphs.

Motivation

Although the models we studied in previous papers describe networks from a static perspective, real-world networks are dynamic and evolve over time. To understand the dynamics of complex random systems, we have to examine the temporal evolution of the system. Thus, establishing functional limit theorems in a random connection model helps to understand the interdependence of the spatial distribution and network dynamics of these systems.

In this paper, we equip the random connection hypergraph model (RCHM) from Paper C with birth-death type dynamics. Then, we prove two functional limit theorems for the edge count of this model. In particular, we derive a functional normal limit theorem and a functional stable limit theorem for the edge count of the bipartite graph.

Model

We begin by defining the *dynamic random connection hypergraph model* (DRCHM) from the random connection hypergraph model introduced in Paper C as follows.

Let us consider two spaces $\mathbb{S} \times \mathbb{T} := (\mathbb{R} \times (0,1]) \times (\mathbb{R} \times \mathbb{R}_+)$ and $\mathbb{S} \times \mathbb{R} := (\mathbb{R} \times (0,1]) \times \mathbb{R}$. Furthermore two independent vertices $p := (x, u, b, \ell) \in \mathbb{S} \times \mathbb{T}$ and $p' := (z, w, r) \in \mathbb{S} \times \mathbb{R}$ are characterized by their coordinates as follows:

- The *positions* $x, z \in \mathbb{R}$ and the *weights* u, w have similar roles to the coordinates in RCHM.

- The *birth time* $b \in \mathbb{R}$ and the *lifetime* $\ell \in \mathbb{R}_+$ of the vertex p govern the temporal dynamics of the vertex p, while vertex p' representing interactions is assigned a single time instant $r \in \mathbb{R}$.

Then, a pair of vertices $p := (x, u, b, \ell) \in \mathbb{S} \times \mathbb{T}$ and $p' := (z, w, r) \in \mathbb{S} \times \mathbb{R}$ are connected if the below two connection conditions hold:

$$|x - z| \leqslant \beta u^{-\gamma} w^{-\gamma'} \qquad \text{and} \qquad b \leqslant r \leqslant b + \ell,$$

where the model parameters $\beta > 0$ and $\gamma, \gamma' \in (0, 1)$ governing the first connection condition have similar roles to the parameters in RCHM. Loosely speaking, the two conditions mean that the vertices p and p' are connected if

- **spatial condition:** their distance is small relative to the product of their weights raised to the power γ and γ', and

- **temporal condition:** the time r of the vertex p' falls into the time interval $[b, b + \ell]$ assigned to the vertex p.
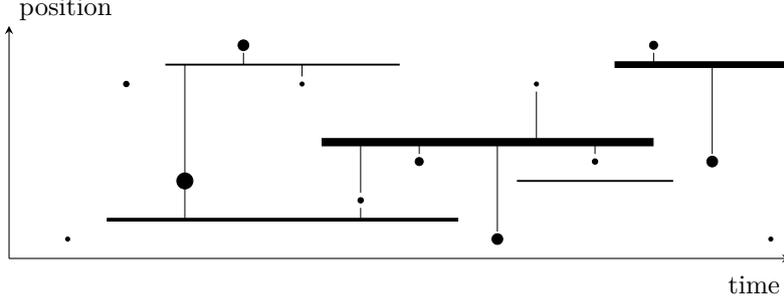
Figure D.2: The horizontal axis represents the time, and the vertical axis represents the position. $\mathcal{P}$-vertices are represented by intervals of different lengths and widths, where the width of the interval corresponds to the weight of the vertex. $\mathcal{P}'$-vertices are represented by points, and the size of the point corresponds to the weight of the vertex. Vertical lines mark if a pair of $\mathcal{P}$- and $\mathcal{P}'$-vertices is connected.

To visualize the model, we include Figure D.2 from Paper D below.

Then, we define two independent Poisson point processes $\mathcal{P}$ and $\mathcal{P}'$ on the spaces $\mathbb{S} \times \mathbb{T}$ and $\mathbb{S} \times \mathbb{R}$, respectively. The coordinates of the points in $\mathcal{P}$ and $\mathcal{P}'$ are denoted by $P \coloneqq (X, U, B, L) \in \mathcal{P}$ and $P' \coloneqq (Z, W, R) \in \mathcal{P}'$. The intensity measure of the stationary Poisson point process $\mathcal{P}$ is $\mu(\mathrm{d}p) = \mu(\mathrm{d}x, \mathrm{d}u, \mathrm{d}b, \mathrm{d}\ell) \coloneqq \mathrm{d}(x, u, b)\, \mathbb{P}_L(\mathrm{d}\ell)$, which is the Lebesgue measure for the position, weight and birth time components, and the distribution $\mathbb{P}_L$ of the lifetime of the $\mathcal{P}$-points is characterized by the exponential measure with parameter 1. Furthermore, the point process $\mathcal{P}'$ is also stationary with Lebesgue intensity measure $\mathrm{d}(z, w, r)$.

Main results

To state our main results, we first define the *neighborhood* $N(p;t)$ of a point $p \in \mathbb{S} \times \mathbb{T}$ as the domain in $\mathbb{S} \times \mathbb{R}$ in which $\mathcal{P}'$-points connect to p up to time t.

$$N(p;t) \coloneqq \{(z, w, r) \in \mathbb{S} \times \mathbb{R} \colon |x - z| \leqslant \beta u^{-\gamma} w^{-\gamma'},\ b \leqslant r \leqslant t \leqslant b + \ell\}.$$

Note that the neighborhood $N(p;t)$ is empty if the point p is not alive at time t, i.e., if $t \notin [b, b+\ell]$. Using the definition of the neighborhood, we define the *degree* $\deg(p;t)$ of point p at time t as the number of $\mathcal{P}'$-points in the neighborhood $N(p;t)$:

$$\deg(p;t) \coloneqq \sum_{P' \in \mathcal{P}'} \mathbb{1}\{P' \in N(p;t)\}.$$

Then, the *edge count* and the *normalized edge count* are defined by the sum of the degrees of the points in the spatial window $[0, n]$:

$$S_n(\,\cdot\,) \coloneqq \sum_{P \in \mathcal{P} \cap (\mathbb{S}_n \times \mathbb{T})} \deg(P; \,\cdot\,) \qquad \text{and} \qquad \overline{S}_n(\,\cdot\,) \coloneqq n^{-1/2}(S_n(\,\cdot\,) - \mathbb{E}[S_n(\,\cdot\,)]),$$

where $\mathbb{S}_n \coloneqq [0, n] \times (0, 1]$ is the *observation window*. The main results of this paper are two functional limit theorems for the edge count $\overline{S}_n(\,\cdot\,)$ when the size n of the observation window grows.

First, we state a univariate normal limit for the edge count $\overline{S}_n(t)$ at a fixed time point t.

Proposition D.2.1 (Univariate normal limit of edge count)**.** *Let $\gamma, \gamma' < 1/2$. Then, for all $t \in \mathbb{R}$, the normalized edge count $\overline{S}_n(t)$ converges weakly to a normal distribution, as $n \to \infty$.*

The limiting covariance function of $\overline{S}_n(t)$ in the thin-tailed case is given by

Proposition D.2.2 (Limiting covariance function of $\overline{S}_n$)**.** *Let $\gamma, \gamma' < 1/2$. Then, for all $t_1 < t_2$, the limiting covariance function of the edge count $\overline{S}_n$ is given by*

$$\lim_{n \uparrow \infty} \mathrm{Cov}\big(\overline{S}_n(t_1), \overline{S}_n(t_2)\big) = (c_1 + c_3 + c_2(2 + t_2 - t_1))\mathrm{e}^{-(t_2 - t_1)},$$

where $c_1 = 2\beta/((1 - \gamma)(1 - \gamma'))$, $c_2 = (2\beta)^2/((1 - 2\gamma)(1 - \gamma')^2)$ and $c_3 = (2\beta)^2/((1 - \gamma)^2(1 - 2\gamma'))$.

The limiting covariance function describes a continuous-time AR(2) process, and it has the form of a Matérn covariance function with appropriate parameters.

Next, we show a multivariate normal limit for the edge counts $\overline{S}_n(t_1), \ldots, \overline{S}_n(t_k)$ at k fixed time points $t_1, \ldots, t_k$.

Proposition D.2.3 (Multivariate normal limit of the edge count)**.** *Let $\gamma < 1/2$ and $\gamma' < 1/3$. Then, for all $k \in \mathbb{Z}_+$ and $t_1, \ldots, t_k \in \mathbb{R}$, the vector of normalized edge counts $(\overline{S}_n(t_1), \ldots, \overline{S}_n(t_k))$ converges weakly to a multivariate normal distribution, as $n \to \infty$.*

Our first functional normal limit theorem for the edge count $\overline{S}_n(\,\cdot\,)$ is stated as follows.

Theorem D.2.4 (Functional normal limit of edge count)**.** *Let $\gamma, \gamma' < 1/4$, and let $X := \{X(t) : t \geqslant 0\}$ denote a Gaussian process with a covariance function specified in Proposition D.2.2. Then,*

$$\overline{S}_n(\,\cdot\,) \xrightarrow[n \uparrow \infty]{d} X(\,\cdot\,)$$

in the Skorokhod space $D([0, 1], \mathbb{R})$.

We also conjecture that Theorem D.2.4 could be proved for the larger domain $\gamma \in (0, 1/2)$ as well.

As in the model from Paper C, the variance of the univariate distribution of the edge count $\overline{S}_n(t)$ diverges as $n \to \infty$ if $\gamma > 1/2$. Thus, if $\gamma > 1/2$, we redefine $\overline{S}_n(\,\cdot\,)$ as follows:

$$\overline{S}_n(\,\cdot\,) := n^{-\gamma}(S_n(\,\cdot\,) - \mathbb{E}[S_n(\,\cdot\,)]).$$

Even though we use the same symbol $\overline{S}_n(\,\cdot\,)$ for two different scalings of the edge count $S_n(\,\cdot\,)$, since they are used in different contexts, it is always clear which scaling we refer to.

Before stating our second functional limit theorem, we need to define further concepts. Let ν be the measure on $\mathbb{J} := [0, \infty)$ defined by $\nu([\varepsilon, \infty)) := ((2\beta)/(1 - \gamma'))^{1/\gamma} \varepsilon^{-1/\gamma}$, and let $\mathcal{P}_\infty$ denote the Poisson point process on $\mathbb{J} \times \mathbb{T}$ with intensity measure $\nu \times \mathrm{Leb} \times \mathbb{P}_L$. In $\mathcal{P}_\infty$, the component $\mathbb{J}$ is related to the limiting scaled size of the spatial neighborhoods of the points in $\mathcal{P}$. We also define the edge counts

$$S_\varepsilon^*(\,\cdot\,) := \sum_{(J,B,L) \in \mathcal{P}_\infty} J(\,\cdot\, - B)\, \mathbb{1}\{J \geqslant \tilde{c}\varepsilon^\gamma\}\, \mathbb{1}\{B \leqslant \cdot \leqslant B + L\}$$

$$\overline{S}_\varepsilon^*(\,\cdot\,) := S_\varepsilon^*(\,\cdot\,) - \mathbb{E}[S_\varepsilon^*(\,\cdot\,)],$$

where $\tilde{c} := 2\beta/(1 - \gamma')$ and $\mathbb{E}[S_\varepsilon^*(\,\cdot\,)] = \tilde{c}^{1/\gamma}\varepsilon^{-(1/\gamma - 1)}/(1 - \gamma)$. Note that $S_\varepsilon^*(t)$ aggregates the contributions from all points in the Poisson process $\mathcal{P}_\infty$ whose spatial neighborhoods are sufficiently large and that are alive at time t. Each such point contributes to the sum by the scaled size J of its spatial neighborhood multiplied by the length of time it is alive at time t. With these definitions at hand, the functional limit theorem for the edge counts when $\gamma > 1/2$ is as follows.

Theorem D.2.6 (Functional stable limit of edge count). *Let $\gamma > 1/2$ and $\gamma' < 1/4$. Then, the limit $\overline{S}(\,\cdot\,) := \lim_{\varepsilon \downarrow 0} \overline{S}_\varepsilon^*(\,\cdot\,)$ exists in the Skorokhod space $D([0,1], \mathbb{R})$, and the centered edge-count process $\overline{S}_n(\,\cdot\,)$ converges weakly to the process $\overline{S}(\,\cdot\,)$ in the Skorokhod space $D([0,1], \mathbb{R})$.*

Note that the limiting process $\overline{S}(\,\cdot\,)$ is not a Lévy process, and it is not even Markov. This is so because the edge count $\overline{S}_n(t)$ and its limit does not contain all the information necessary to predict the process. If a single vertex with many edges dies, all its edges disappear simultaneously. On the other hand, if there are many vertices with a few edges each, the edge count may be identical to the earlier case, but edges will not disappear at once. Similarly, one can argue that the increments of the process $\overline{S}(\,\cdot\,)$ are not independent.

Methodology

In this section, we present the main proof techniques used in the proofs. The content of this section is a summary of Sections D.3–D.11 in Paper D, where the proof outlines are given in more detail.

For some Borel sets $\mathcal{X}, \mathcal{U}, \mathcal{B}, \mathcal{D} \subseteq \mathbb{R}$, we introduce the notations

$$\mathbb{S}_\mathcal{X} := \{(x, u) \in \mathbb{S} : x \in \mathcal{X}\} \quad \mathbb{S}^\mathcal{U} := \{(x, u) \in \mathbb{S} : u \in \mathcal{U}\} \quad \mathbb{S}_\mathcal{X}^\mathcal{U} := \mathbb{S}_\mathcal{X} \cap \mathbb{S}^\mathcal{U}$$
$$\mathbb{T}_\mathcal{B} := \{(b, \ell) \in \mathbb{T} : b \in \mathcal{B}\} \quad \mathbb{T}^\mathcal{D} := \{(b, \ell) \in \mathbb{T} : b + \ell \in \mathcal{D}\} \quad \mathbb{T}_\mathcal{B}^\mathcal{D} := \mathbb{T}_\mathcal{B} \cap \mathbb{T}^\mathcal{D},$$

and employ the shorthand notations for $\mathbb{T}_{\leqslant t_1}^{t_2 \leqslant} = \mathbb{T}_{(-\infty, t_1]}^{(t_2, \infty)}$, $\mathbb{T}_{\leqslant t_1}^{[t_1, t_2]} = \mathbb{T}_{(-\infty, t_1]}^{[t_1, t_2]}$ and $\mathbb{T}_{\leqslant t_2}^{t_2 \leqslant} = \mathbb{T}_{(-\infty, t_2]}^{(t_2, \infty)}$.

The univariate normal limit CLT stated in Proposition D.2.1 is presented using the same idea as in the proof of the CLT for the edge count in RCHM from Papers B and C. Namely, we apply the CLT by Whitt [107, Theorem 4.4.3] for associated random variables to show that the edge count converges to a Gaussian distribution. First, we show that the mean and the variance of the edge count converge to finite values. Then,

we partition the spatial component of the domain $\mathbb{S}_n \times \mathbb{T}$ to intervals of length one and define a sequence of associated random variables $\{T_i\}$ by setting

$$T_i := \sum_{P \in \mathcal{P} \cap (\mathbb{S}_{[i-1,i]} \times \mathbb{T})} \deg(P; t) \qquad S_n = \sum_{i=1}^{n} T_i.$$

Showing that $\sum_{k \geqslant 2} \mathrm{Cov}(T_1, T_k) < \infty$, the application of the CLT for associated random variables concludes the proof.

To show Proposition D.2.2, we decompose the edge counts $S_n(t_1)$ and $S_n(t_2)$ for $t_1 \leqslant t_2$ into three parts

$$S_n^{\mathsf{A}}(t_1, t_2) := \sum_{P \in \mathcal{P} \cap (\mathbb{S}_n \times \mathbb{T}_{\leqslant t_1}^{t_2 \leqslant})} \deg(P; t_1)$$

$$S_n^{\mathsf{B}}(t_1, t_2) := \sum_{P \in \mathcal{P} \cap (\mathbb{S}_n \times \mathbb{T}_{\leqslant t_1}^{[t_1, t_2]})} \deg(P; t_1)$$

$$S_n^{\mathsf{C}}(t_1, t_2) := \sum_{P \in \mathcal{P} \cap (\mathbb{S}_n \times \mathbb{T}_{\leqslant t_2}^{t_2 \leqslant})} \sum_{P' \in \mathcal{P}'} \mathbb{1}\{P' \in N(P; t_2)\} \mathbb{1}\{t_1 \leqslant R\},$$

which are visualized in Figure D.3, also included here from the paper for easier reference. Then, we have the following decomposition:

$$S_n(t_1) = S_n^{\mathsf{A}}(t_1, t_2) + S_n^{\mathsf{B}}(t_1, t_2) \qquad \text{and} \qquad S_n(t_2) = S_n^{\mathsf{A}}(t_1, t_2) + S_n^{\mathsf{C}}(t_1, t_2).$$

Next, writing the covariance function with the help of the above decomposition, we compute the limit of each term separately, and sum the results to obtain the limiting covariance function of $\overline{S}_n(\cdot)$.

To prove Proposition D.2.3, we would like to apply [97, Theorem 1.1], which bounds the d_3 distance of the distribution of Poisson functionals and the normal distribution by the sum of three error terms $E_1(n), E_2(n), E_3(n)$. Then, to show that the finite-dimensional distribution of the edge count converges to a multivariate normal distribution, we need to show that these error terms converge to zero in probability as $n \to \infty$. This, however, can only be shown for $\gamma < 1/3$ for the error term $E_3(n)$. To enlarge the range of γ to $\gamma < 1/2$, we apply a low-mark / high-mark decomposition $S_n(\cdot) = S_n^{\geqslant}(\cdot) + S_n^{\leqslant}(\cdot)$ with

$$S_n^{\geqslant}(\cdot) := \sum_{P \in \mathcal{P} \cap (\mathbb{S}_n^{u_n \leqslant} \times \mathbb{T})} \deg(P; \cdot) \qquad \text{and} \qquad S_n^{\leqslant}(\cdot) := \sum_{P \in \mathcal{P} \cap (\mathbb{S}_n^{\leqslant u_n} \times \mathbb{T})} \deg(P; \cdot),$$

where $u_n := n^{-2/3}$ is a mark that depends on the window size n. We apply a two-step strategy: first, we show that the low-mark edge count is negligible, and then we employ [97, Theorem 1.1] to the high-mark edge count $S_n^{\geqslant}(\cdot)$. To apply [97, Theorem 1.1], we first need to show that the covariance function of the centered and scaled high-mark edge count $\overline{S}_n^{\geqslant}$ converges. Then, we prove that the error terms $E_1(n), E_2(n), E_3(n)$ converge to zero in probability as $n \to \infty$ whenever $\gamma < 1/2$, which involves bounding certain expressions of the add-one and add-two cost operators.

To show that Theorem D.2.4 holds, we need to show convergence of the finite-dimensional distributions of the process and that the process is tight. The tightness criterion is shown by applying [26, Theorem 2]. Since this theorem requires non-decreasing processes, we need to decompose the edge count $S_n(\,\cdot\,)$ into the difference $S_n = S_n^+ - S_n^-$, which we call the *plus-minus decomposition* of the edge count.

To introduce the plus-minus decomposition, we first define the spatial part $p_\mathsf{s} := (x, u)$ and the temporal part $p_\mathsf{t} := (b, \ell)$ of a point $p := (x, u, b, \ell) \in \mathbb{S} \times \mathbb{T}$, and we denote by $p_\mathsf{s}' := (z, w)$ the spatial part of a point $p' := (z, w, r) \in \mathbb{S} \times \mathbb{R}$. Then, we define the spatial and temporal neighborhoods of a point $p \in \mathbb{S} \times \mathbb{T}$ as follows:

$$N_\mathsf{s}(p_\mathsf{s}) := \{(z, w) \in \mathbb{S} \colon |x - z| \leqslant \beta u^{-\gamma} w^{-\gamma'}\}$$
$$N_\mathsf{t}(p_\mathsf{t}, t) := \{r \in \mathbb{R} \colon b \leqslant r \leqslant t \leqslant b + \ell\},$$

and then $N(p; t) = N_\mathsf{s}(p_\mathsf{s}) \times N_\mathsf{t}(p_\mathsf{t}; t)$. The *plus* and *minus* neighborhoods of a point $p \in \mathbb{S} \times \mathbb{T}$ are defined as

$$N^+(p; t) := N_\mathsf{s}(p_\mathsf{s}) \times N_\mathsf{t}^+(p_\mathsf{t}; t) \qquad \text{and} \qquad N^-(p; t) := N_\mathsf{s}(p_\mathsf{s}) \times N_\mathsf{t}^-(p_\mathsf{t}; t),$$

where

$$N_\mathsf{t}^+(p_\mathsf{t}; t) := \begin{cases} \{r \in \mathbb{R} \colon b \leqslant r \leqslant b + \ell\} & \text{if } b + \ell \leqslant t \\ \{r \in \mathbb{R} \colon b \leqslant r \leqslant t\} & \text{if } b + \ell > t \end{cases}$$

$$N_\mathsf{t}^-(p_\mathsf{t}; t) := \begin{cases} \{r \in \mathbb{R} \colon b \leqslant r \leqslant b + \ell\} & \text{if } b + \ell \leqslant t \\ \varnothing & \text{if } b + \ell > t. \end{cases}$$

Note that both neighborhoods $N^+(p; t)$ and $N^-(p; t)$ are monotone increasing in t. Also, observe that with

$$\deg^+(P; t) := \sum_{P' \in \mathcal{P}'} \mathbb{1}\{P' \in N^+(P; t)\} \text{ and}$$
$$\deg^-(P; t) := \sum_{P' \in \mathcal{P}'} \mathbb{1}\{P' \in N^-(P; t)\},$$

we have that $\deg(P; t) = \deg^+(P; t) - \deg^-(P; t)$. The plus-minus decomposition $S_n = S_n^+ - S_n^-$ of the edge count is then defined as

$$S_n^+(t) := \sum_{P \in \mathcal{P} \cap (\mathbb{S}_n \times \mathbb{T}^{0\leqslant})} \deg^+(P; t) \qquad \text{and} \qquad S_n^-(t) := \sum_{P \in \mathcal{P} \cap (\mathbb{S}_n \times \mathbb{T}^{0\leqslant})} \deg^-(P; t),$$

where $\mathbb{T}^{0\leqslant} := \mathbb{T}^{[0,\infty)}$ is the domain for which the death time $b + \ell \geqslant 0$. Note that the sums consider only points $P \in \mathcal{P}$ whose lifetime $[B, B + L]$ intersects the temporal interval $[0, 1]$.

Then, we apply [26, Theorem 2] for the normalized edge counts

$$\overline{S}_n^+ := n^{-1/2}(S_n^+ - \mathbb{E}[S_n^+]) \qquad \text{and} \qquad \overline{S}_n^- := n^{-1/2}(S_n^- - \mathbb{E}[S_n^-])$$

separately. We restate the theorem here.

Theorem D.6.2 (Specialized version of Davydov's theorem)**.** *Let $a_n \to 0$ be a sequence of positive numbers converging to 0, and set $t_k = ka_n$ for $k = 0, 1, \ldots, k_n$ with $k_n = \lfloor 1/a_n \rfloor$ and $t_{k_n+1} = 1$. Then, if $\overline{S}_n^\pm(\,\cdot\,)$ are non-decreasing processes defined on the interval $[0,1]$ such that*

(1) the finite-dimensional distributions of the processes $\overline{S}_n^\pm(\,\cdot\,)$ converge to the finite-dimensional distribution of a limiting process $\overline{S}_\infty^\pm(\,\cdot\,)$,

(2) there exists some constants $\chi_1, \chi_2 > 1$ such that

$$\mathbb{E}\Big[\big|\overline{S}_n^\pm(t) - \overline{S}_n^\pm(s)\big|^{\chi_1}\Big] \in O(|t-s|^{\chi_2})$$

for all n if $|t-s| \geqslant a_n$, and

(3) for the limit of the expected increments, we have

$$\lim_{n\uparrow\infty} \max_{k \leqslant \lfloor 1/a_n \rfloor} \Big|\mathbb{E}\big[\overline{S}_n^\pm(t_{k+1})\big] - \mathbb{E}\big[\overline{S}_n^\pm(t_k)\big]\Big| = 0,$$

then $\overline{S}_\infty^\pm(\,\cdot\,)$ is almost surely continuous and the sequence $\overline{S}_n^\pm(\,\cdot\,)$ converges in distribution to $\overline{S}_\infty^\pm(\,\cdot\,)$.

To show Condition (1) of Theorem D.6.2, we follow the same strategy as in the proof of Proposition D.2.3. Condition (2) is shown after setting $\chi_1 := 4$, $\chi_2 := 1 + \eta$ and $a_n := n^{-1/(1+\eta)}$ for some $\eta > 0$ by bounding the fourth moments of the increments using cumulants. Finally, Condition (3) is shown by bounding the expected increments of the edge count $\overline{S}_n^\pm(t)$.

In the proof of Theorem D.2.6, we need to deal with the infinite-variance regime $\gamma > 1/2$. We make use of the low-mark / high-mark decomposition of the edge count introduced earlier in the context of Proposition D.2.3, and denote the low-mark edge count by $S_n^{(1)} := S_n^{\leqslant}$ to ensure consistency with the notation used in the proof of Theorem D.2.6. In the heavy-tailed case $\gamma > 1/2$, we use the scaling $n^{-\gamma}$ instead of $n^{-1/2}$ to normalize the edge counts:

$$\overline{S}_n^{>}(\,\cdot\,) := n^{-\gamma}\big(S_n^{\geqslant}(\,\cdot\,) - \mathbb{E}[S_n^{\geqslant}(\,\cdot\,)]\big),$$
$$\overline{S}_n^{(1)}(\,\cdot\,) := n^{-\gamma}\big(S_n^{(1)}(\,\cdot\,) - \mathbb{E}[S_n^{(1)}(\,\cdot\,)]\big).$$

We split the proof into two parts. In the first part, we show that the high-mark edge count is negligible, and in the second part, we show that the low-mark edge count converges to a stable process.

Step 1. In Step 1, we show that if $\gamma > 1/2$ and $\gamma' < 1/4$, then $\overline{S}_n^{\geqslant}(\,\cdot\,) \to 0$ in the Skorokhod space $D([0,1], \mathbb{R})$ as $n \to \infty$.

Step 2. Next, in Step 2, the low-mark edge count $S_n^{(1)}$ is approximated by $S_n^{(2)}$ defined by

$$S_n^{(2)}(\,\cdot\,) := \sum_{P \in \mathcal{P} \cap (\mathbb{S}_n \times \mathbb{T})} \mathbb{E}\big[\deg(P; \cdot\,) \mid P\big]\,\mathbb{1}\{U \leqslant u_n\}.$$

Note that the conditional expectation is the size of the neighborhood of the point P, and the indicator function restricts the points to those with small marks. This approximation step is done by showing that the supremum norm of the difference between the two edge counts converges to zero in probability. Note that the spatial correlations of the degrees are eliminated in $\overline{S}_n^{(2)}$. The first part of the proof is concluded here.

For the second part, first recall the definition of the measure ν, the Poisson point process $\mathcal{P}_\infty$, and the edge counts S_ε^* and $\overline{S}$ from Theorem D.2.6. We would like to show that $\overline{S}_n^{(2)}$ converges in distribution to $\overline{S}$ as $n \to \infty$. For all $n, \varepsilon > 0$, we define

$$S_{n,\varepsilon}^{(3)}(\,\cdot\,) := \sum_{P \in \mathcal{P} \cap (\mathbb{S}_n \times \mathbb{T})} \mathbb{E}\big[\deg(P; \cdot\,) \mid P\big]\,\mathbb{1}\{U \leqslant 1/(\varepsilon n)\}.$$

We divide the second part of the proof into three steps, which are illustrated in Figure D.5 taken from the paper. These steps follow [93, Sections 5.5 and 7.2].

Step 3. In Step 3, we show that $\overline{S}_{n,\varepsilon}^{(3)}$ converges to $\overline{S}_n^{(2)}$ with respect to the Skorokhod distance in the space $D([0,1], \mathbb{R})$ as $\varepsilon \to 0$, uniformly for all n. First, we bound the Skorokhod distance d_{Sk} by the supremum metric. Then, we apply again the plus-minus decomposition to the edge count $S_{n,\varepsilon}^{(3)}$ which leads to the sum of a continuous process $S_{n,\varepsilon}^{(3),+}$, which can be written as a sum of integrals and a martingale $S_{n,\varepsilon}^{(3),-}$. Then, the edge count of the heaviest vertices approximates the total edge count.

Step 4. In Step 4, we show that the edge count $\overline{S}_{n,\varepsilon}^{(3)}$ converges in distribution to $\overline{S}_\varepsilon^*$ in $D([0,1], \mathbb{R})$ as $n \to \infty$. We note that $S_{n,\varepsilon}^{(3)}$ and S_ε^* are defined on different probability
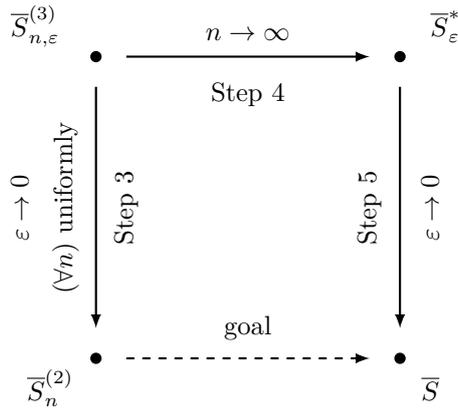
Figure D.5: Main steps of the second part of the proof of Theorem D.2.6. Step 3 shows that $\overline{S}_{n,\varepsilon}^{(3)}$ converges to $\overline{S}_n^{(2)}$ as $\varepsilon \to 0$ uniformly for all n. Step 4 shows convergence of $\overline{S}_{n,\varepsilon}^{(3)}$ to $\overline{S}_\varepsilon^*$ as $n \to \infty$. Finally, Step 5 shows that $\overline{S}_\varepsilon^*$ converges to $\overline{S}$ as $\varepsilon \to 0$.

spaces. First, we show that $n\, \mathbb{P}(n^{-\gamma}|N_{\mathsf{s}}(P_{\mathsf{s}})| \in [\,\cdot\,, \infty))$ converges vaguely to a Lévy measure as $n \to \infty$. The contributions $n^{-\gamma}(|N(P;t)| - \mathbb{E}[|N(P;t)|])$ of single points to the sum $S_{n,\varepsilon}^{(3)}(t)$ are i.i.d. Then,

$$\sum_{P \in \mathcal{P} \cap (\mathbb{S}_n \times \mathbb{T})} \delta_{(n^{-\gamma}|N_{\mathsf{s}}(P_{\mathsf{s}})|, B, L)} \xrightarrow[n\uparrow\infty]{d} \mathrm{PPP}(\nu \otimes \mathrm{Leb} \otimes \mathbb{P}_L),$$

where $\mathrm{PPP}(\nu \otimes \mathrm{Leb} \otimes \mathbb{P}_L)$ is a Poisson point process on $\mathbb{J} \times \mathbb{T}$ with intensity measure $\nu \otimes \mathrm{Leb} \otimes \mathbb{P}_L$. Note that vague convergence requires the state space to be locally compact. On the other hand, since the size of the neighborhood $|N_{\mathsf{s}}(P_{\mathsf{s}})|$ is unbounded, $n^{-\gamma}|N_{\mathsf{s}}(P_{\mathsf{s}})|$ can become arbitrarily large. Thus, our state space is not locally compact unless we compactify it at ∞. This means that instead of working on $[0, \infty)$, we restrict to the domain $(0, \infty]$ so that ∞ becomes a boundary point. Considering $S_{n,\varepsilon}^{(3)}$, the domain of the marks is restricted to $[0, 1/(\varepsilon n)]$, and the domain of the birth and lifetimes are restricted so that the interval $[B, B+L]$ intersects $[0, 1]$. Then, we examine the summation functional

$$\sum_{(J,B,L) \in \mathcal{P}_\infty \cap ([\tilde{c}\varepsilon^\gamma, \infty) \times \mathbb{T})} \delta_{(J,B,L)} \mapsto \sum_{(J,B,L) \in \mathcal{P}_\infty} J(\,\cdot\, - B)\, \mathbb{1}\{J \geqslant \tilde{c}\varepsilon^\gamma\}\, \mathbb{1}\{B \leqslant \,\cdot\, \leqslant B+L\},$$

where $\tilde{c} > 0$ is a constant depending on the model parameters β, γ, γ'. The primary objective of this step is to show that the summation functional is continuous with respect to the Skorokhod metric. Using this partial result, it follows that $n^{-\gamma}S_{n,\varepsilon}^{(3)}(\,\cdot\,) \to S_\varepsilon^*(\,\cdot\,)$ in distribution as $n \to \infty$. Finally, we show that the expectation of the edge count S_ε^* is finite and given by $\mathbb{E}[S_\varepsilon^*] = \tilde{c}\varepsilon^{-(1-\gamma)}/(1-\gamma)$.

Step 5. In Step 5, we show that $\overline{S}_\varepsilon^* \to \overline{S}$ almost surely as $\varepsilon \to 0$ in $D([0,1], \mathbb{R})$. We begin by showing almost sure convergence for fixed time points as $\varepsilon \to 0$. Then, we show that the convergence is almost surely uniform in the supremum norm on $[0, 1]$. First, we prove that the sequence $\overline{S}_{\varepsilon_n}^*$ is Cauchy in probability with respect to the supremum norm, where $\varepsilon_n \to 0$ is a decreasing sequence of positive numbers. Finally, we show that $\lim_{\varepsilon \downarrow 0} \|\overline{S}_\varepsilon^* - \overline{S}\| = 0$ almost surely, and the limit $\overline{S}$ is almost surely in $D([0,1], \mathbb{R})$.

4 Computational framework

Introduction

In this section, we introduce the simulation framework that was developed to complement the theoretical analysis in Papers B and C. The program presented was applied for various tasks.

- First, it was used as a Monte Carlo simulation tool to show convergence rates of theorems proved for the large network limit. This was necessary to validate the application of our theoretical results in real-world scenarios, in which the network size is finite.

- Using this framework, we verified those conjectures for distributions of topological quantities that are not proven in the papers.

- Finally, the program was used to analyze and test real-world datasets, including the estimation of corresponding model parameters, hypothesis testing, and network plotting.

The source code of the simulation framework is made publicly available in the GitHub repository [50] to ensure reproducibility and transparency.

Design, architecture

The simulation framework is designed to handle large-scale networks efficiently, leveraging parallel processing capabilities to ensure rapid computation even for extensive simulations.

Due to the complexity of the models and the need for efficient computation, the software consists of several components, whose dependency structure is illustrated in Figure 8. Please note that the presentation of the module structure is simplified; the actual implementation contains more modules and classes.

The computationally intensive parts of the simulation are implemented in C++ to ensure high performance and efficient parallelization, while the user interface and data handling are done in Python. The communication between the two languages is facilitated by the `pybind11` library, which allows for integration of C++ algorithms into Python scripts.

The C++ code consists of approximately 4200 source lines, and it is organized into two main modules: `CppModel` and `CppNetwork`, the former serving as a factory for the latter. The `CppModel` module is responsible for generating the random higher-order graphs based on various models, and its class hierarchy is illustrated in Figure 9.
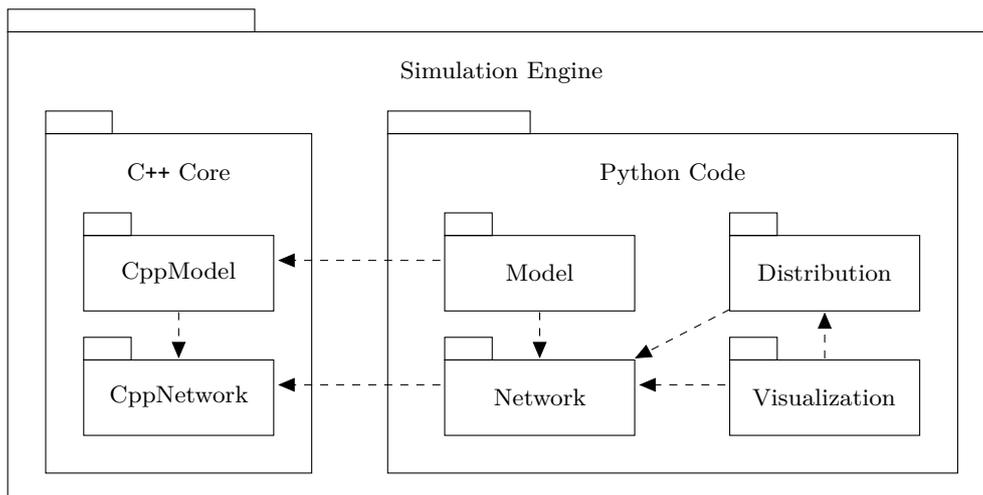
Figure 8: High level overview of the software architecture. Arrows point in the directions of dependencies.
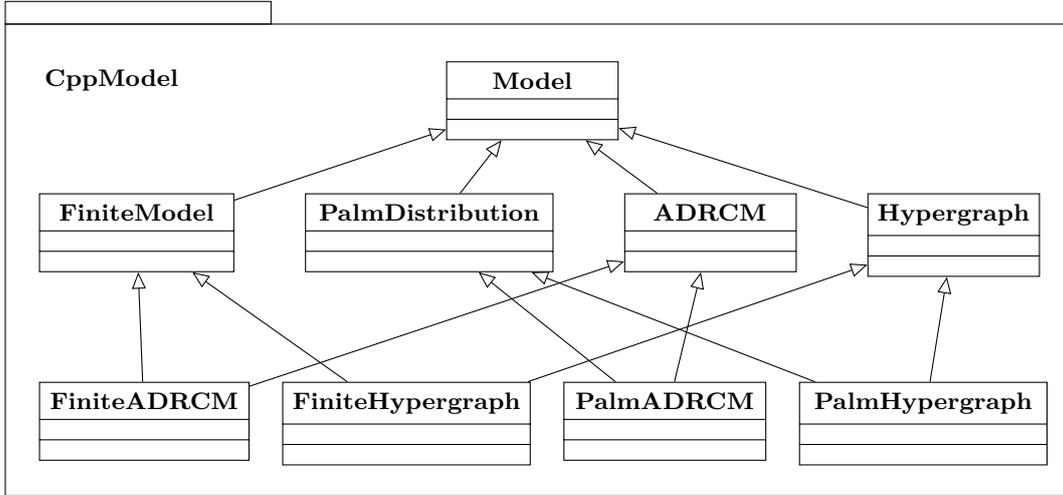
Figure 9: Class diagram of the C++ module. The `CppNetwork` module mirrors the structure of the `CppModel` module: each class in the former has a corresponding class in the latter. The classes in the bottom row inherit from exactly two of the classes in the middle row by employing multiple inheritance.

The specific network models inherit from the interface class `Model` to ensure a consistent API and allow for easy extension with new models. The module is capable of generating both finite networks and Palm distributions free from boundary effects, for both models presented in Papers B (`ADRCM`) and C (`Hypergraph`). The `CppNetwork` efficiently computes topological features, including Betti numbers, degree distributions, and simplex counts, and its class hierarchy mirrors that of the `CppModel` module.

The Python code, consisting of approximately 5000 source lines of code, is responsible for providing the user interface, loading the datasets represented as networks, and visualizing the results. When designing this part of the software, we aimed to delegate most of the computationally intensive tasks to the C++ code, while keeping the Python code as lightweight as possible. The probability distributions of the computed characteristics are estimated using the `scipy.stats` library [105] in Python.

The software was tested through unit tests using the `unittest` framework of Python. We further validated the program by comparing Monte Carlo simulation results against known theoretical distributions for various quantities in increasing network sizes, including higher-order degrees, edge counts, and Betti numbers.

Implementation

The generation of a finite random network has the following steps:

(1) first, random points are generated with positions and marks according to the model parameters;

(2) then, we determine which of the points are connected.

The second step is the most computationally intensive part of the network generation step, since it involves checking the connection condition for each pair of points. This

step is therefore optimized in two ways, which are described below in case of the `Hypergraph` model. First, the marks of the points are transformed in a model-specific manner to enable the efficient computation of the connection kernel. Second, the state space is partitioned into rectangles, which is visualized in Figure C.1 taken from Paper C.
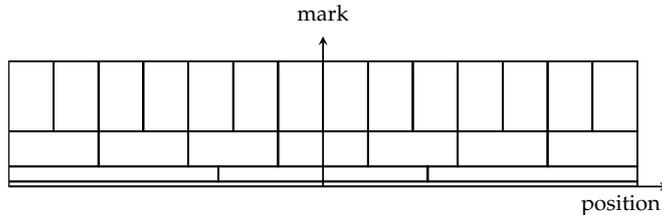
Figure C.1: Partition of the state space into rectangles

The transformed points are then assigned to the rectangles into which they fall. Note that the dimensions of the rectangles are chosen optimally to minimize the number of distance calculations, which is detailed in Paper C. Using the properties of the simulated models, it can be inferred that if all corners of a pair of rectangles satisfy the connection condition, then we can assume that all points within the rectangles are connected, and we can form edges between each pair of points. Conversely, if none of the corners of a pair of rectangles fulfill the connection condition, then we can assume that no points in the rectangles are connected. Then, we only need to check the connection condition between points in pairs of rectangles that do not fall into either of the above two categories. Note that the connections can be generated similarly to the `ADRCM` model.

For the Palm distributions, the algorithm is similar, but not the same:

(1) first, a typical object—point, or simplex—is generated;

(2) next, the neighborhood of the typical object in which other points can influence it is determined;

(3) finally, further points and simplices are generated in the neighborhood of the typical object according to the model parameters.

The generation of these neighborhoods is specific to the simulated model. The above three steps are repeated several times to generate a sufficiently large sample of characteristics for the typical objects.

In the case of the `CliqueComplex` networks generated by the `ADRCM` model, the software employs the `SimplexTree` data structure from the `GUDHI` library [15] to compute all relevant characteristics. Note that, for clique complexes, the `SkeletonBlocker` data structure would be more appropriate; however, it lacks the necessary functionality to compute all the characteristics we need. The `Hypergraph` model, on the other hand, generates hypergraphs whose hyperedges provide an inherent higher-order structure for the generated networks. Thus, to calculate higher-order degrees and simplex counts, the `Hypergraph` network class uses a list of these interactions, called `SimplexList` for computations instead of the heavier `SimplexTree` data structure.

Then, the `SimplexTree` is built only on demand from the list of hyperedges when Betti numbers need to be computed.

Next, we describe how the higher-order degree distributions are computed in the `Hypergraph` model. Since the `SimplexTree` data structure is too memory-intensive and slow for our purposes, we use a custom algorithm to compute the higher-order degrees. The algorithm is described in Algorithm 1, and it is based on the following ideas. We are interested in the distribution of the number of m-simplices neighboring

---

Algorithm 1 Computation of the higher-order degree distribution

Require: Hypergraph H, integers n, m with $0 \leqslant n < m$
Ensure: Distribution of the number of m-simplices adjacent to each n-simplex

1: **procedure** CALC_HIGHER_ORDER_DEGREE_DISTRIBUTION(H, n, m)
2:     **if** $n > 0$ **then**
3:         $\mathcal{P} \leftarrow$ PARTITION(H, n) $\triangleright$ no q-simplices $(q \geqslant n-1)$ in $\bigcup_{\substack{P_i, P_j \in \mathcal{P} \\ i \neq j}} \{P_i \cap P_j\}$
4:     **else**
5:         $\mathcal{P} \leftarrow$ CONNECTED_COMPONENTS(H)
6:     **end if**

7:     **for all** part $P \in \mathcal{P}$ **do**
8:         $S_n, S_m \leftarrow \varnothing$ $\triangleright$ S_n, S_m represented by C++ `std::unordered_set`
9:         **for all** hyperedge $H \in P$ **do**
10:             generate n-, m-faces of H $\triangleright$ use `for_each_combination`
11:             update S_n, S_m with n-, m-faces
12:         **end for**

13:         degree_distribution $\leftarrow \varnothing$ $\triangleright$ represented by C++ `std::unordered_map`
14:         **for all** $\sigma_m \in S_m$ **do**
15:             **for all** $\sigma_n \in S_n$ **do**
16:                 **if** $\sigma_n \subset \sigma_m$ **then** $\triangleright$ use Bloom filter to check membership
17:                     ++ degree_distribution$[\sigma_n]$
18:                 **end if**
19:             **end for**
20:         **end for**
21:     **end for**

22:     **return** degree_distribution
23: **end procedure**

---

n-simplices, where $0 \leqslant n < m$. We begin by partitioning the hypergraph into parts that do not share $n - 1$ or higher-dimensional simplices. If $n = 0$, then we partition the hypergraph into connected components. Note that after partitioning, the different parts of the hypergraph are independent, and we can compute the higher-order degree distribution for each part separately. Next, we generate all n- and m-simplices. To generate simplices of a given dimension, the `SimplexList`

class employs the `for_each_combination` function from the `HinnantCombinations` library [47], capable of efficiently generating combinations of elements. These simplices are collected in the C++ `std::unordered_set` data structure, which utilizes a custom hash function to ensure efficient membership testing and fast lookups. For each possible m-simplex, the algorithm checks whether the simplex at hand is its face. This is done by associating each m-simplex with a 64-bit Bloom filter [14] containing the vertices of the simplex at hand, which allows for membership testing at low computational cost. Then, for each n-simplex, we check which of the m-simplices are its neighbors. The higher-order degree distribution is computed by using the `std::unordered_map` data structure, which stores the simplices as keys, and utilizes the same hash function used for the simplex generation step. All parts of the above algorithm are highly parallelized wherever possible.

Note that the above algorithm only has an advantage over the `SimplexTree` data structure in the case of sparse hypergraphs, where the number of simplices is significantly smaller than the number of vertices. In the case of dense hypergraphs, the `SimplexTree` data structure is more efficient, since it can compute the higher-order degree distribution in a single pass over the simplices.

5   Toy example: the Boolean model

In this section, the main methods of the papers are presented in the context of the Boolean model. Note that the model presented here is neither a special case of the models studied in the papers nor a prerequisite for understanding the results. However, this standalone model serves as a simple example to demonstrate the proof techniques applied in multiple papers included in this thesis, with less technical complexity.

Definition of the model

Let $\mathcal{P}$ denote a stationary Poisson point process on $\mathbb{R}$ with intensity λ, and we will connect points $P_1, P_2 \in \mathcal{P}$ if their distance $|P_1 - P_2|$ is less than or equal to β. We define the neighborhood $N(p) \subseteq \mathbb{R}$ of a point $p \in \mathbb{R}$ as the set of points in the $\mathbb{R}$ that are within distance β from p:

$$N(p) := \{p' \in \mathbb{R} \setminus \{p\} \colon |p - p'| \leqslant \beta\}, \qquad |N(p)| = 2\beta.$$

In this model, the set Σ_m of m-simplices is defined as the family of $m + 1$-tuples of points in the Poisson point process $\mathcal{P}$ in which each pair of points is connected:

$$\Sigma_m := \Sigma_m(\mathcal{P}) := \left\{ \{P_0, P_1, \ldots, P_m\} \subseteq \mathcal{P}_{\neq}^{m+1} \colon \max_{i,j \in \{0,\ldots,m\}} |P_i - P_j| \leqslant \beta \right\}.$$

That is, Σ_m contains m-simplices that are elements of the clique complex of the graph whose vertices are the points in the Poisson point process $\mathcal{P}$ and edges are the pairs of points that are connected. Furthermore, $\Sigma := \Sigma(\mathcal{P}) := \bigcup_m \Sigma_m(\mathcal{P})$ denotes the family of all simplices.

Palm distribution of the typical simplex

We let $\mathbf{N}_{\mathsf{loc}}$ denote the family of all locally finite subsets of $\mathbb{R}$, and let $\mathcal{C}_m$ denote the distinct $(m+1)$-tuples of points in $\mathbb{R}$. Then, we define the center function $c \colon \mathcal{C}_m \to \mathbb{R}$ to be the leftmost point in a set $\{p_0, \dots, p_m\} \in \mathcal{C}_m$ of $m+1$ points: $c(\{p_0, \dots, p_m\}) := \min_{i \in \{0, \dots, m\}} p_i$. Next, we define the Palm distribution of the typical m-simplex Δ_m^*.

Definition 5.1 (Typical m-simplex). *Let $f \colon \mathcal{C}_m \times \mathbf{N}_{\mathsf{loc}} \to [0, \infty)$ be a measurable, translation invariant function that is symmetric in its first $m+1$ arguments. Then, the expectation of f with respect to the Palm distribution of the typical m-simplex Δ_m^* is defined as*

$$\mathbb{E}\big[f(\Delta_m^*, \mathcal{P})\big] = \frac{1}{\lambda_m} \, \mathbb{E}\Big[\sum_{\Delta_m \in \Sigma_m(\mathcal{P})} \mathbb{1}\{c(\Delta_m) \in [0,1]\} f(\Delta_m - c(\Delta_m), \mathcal{P} - c(\Delta_m))\Big],$$

where λ_m is the intensity of the m-simplices.

We can apply Mecke's formula [107, Theorem 4.2.1] to the above expectation. To do so, let $\boldsymbol{o}_m := (o_0, o_1, \dots, o_m) \in \mathcal{C}_m$, and let $g_m \colon \mathcal{C}_m \to \{0,1\}$ be the indicator that a set of $m+1$ points form an m-simplex. Then, we rewrite the expectation of the typical m-simplex as

$$\mathbb{E}\big[f(\Delta_m^*, \mathcal{P})\big] = \frac{1}{\lambda_m} \int_{\mathbb{R}^{m+1}} \mathbb{1}\{c(\boldsymbol{o}_m) \in [0,1]\} \, \mathbb{E}\big[f(\boldsymbol{o}_m, \mathcal{P} \cup \boldsymbol{o}_m)\big] g_m(\boldsymbol{o}_m) \, \mathrm{d}\boldsymbol{o}_m.$$

Proposition 5.2 (Palm distribution of the typical m-simplex). *The Palm distribution of the typical m-simplex Δ_m^* exists.*

Proof. To ensure that the Palm distribution exists, we need to show that the denominator λ_m is finite.

$$\lambda_m = \mathbb{E}\Big[\sum_{\Delta_m \in \Sigma_m(\mathcal{P})} \mathbb{1}\{c(\Delta_m) \in [0,1]\}\Big] = \lambda^{m+1} \int_{\mathbb{R}^{m+1}} \mathbb{1}\{c(\boldsymbol{o}_m) \in [0,1]\} g_m(\boldsymbol{o}_m) \, \mathrm{d}\boldsymbol{o}_m,$$

where we applied Mecke's formula in the second step. As g_m is symmetric in its arguments, we assume without loss of generality that $c(\boldsymbol{o}_m) = o_0$. Next, we apply translation invariance to shift the points by o_0. Then, with $\boldsymbol{o}_m' := (o_1 - o_0, \dots, o_m - o_0)$, Fubini's theorem yields

$$\lambda_m = \lambda^{m+1} \int_{[0,1]} \int_{\mathbb{R}^m} g_m(\{0\} \cup \boldsymbol{o}_m') \, \mathrm{d}\boldsymbol{o}_m' \, \mathrm{d}o_0 = \lambda^{m+1} \int_{[0,\beta]^m} \mathrm{d}\boldsymbol{o}_m' = \lambda^{m+1} \beta^m < \infty,$$

where we used that the points within the neighborhood $[0, \beta]$ of the leftmost point, now shifted to the origin, are connected. $\square$

Higher-order degree distribution

Next, we study the higher-order degree distribution of the Boolean model. For simplicity, we first examine the ordinary degree distribution. The degree $\deg(p) :=$

$\deg(p, \mathcal{P}) := \mathcal{P}(N(p))$ of a point $p \in \mathbb{R}$ is defined as the number of points in $\mathcal{P}$ that are in the neighborhood of p. Due to the properties of the Poisson point process, the degree of a point p is Poisson distributed with parameter $\lambda|N(p)| = 2\lambda\beta$. For $m' > m$, we define the higher-order simplex degree $\deg_{m'} \colon \Sigma \times \mathcal{P} \to \mathbb{N}$ as the number of m'-simplices that are cofaces of a simplex in $\Sigma_{m'}$:

$$\deg_{m'}(\Delta) := |\{\sigma \in \Sigma_{m'} \colon \Delta \subseteq \sigma, |\sigma| = m' + 1\}|,$$

and the higher-order degree distribution $d_{m,m'}(k) := \mathbb{P}(\deg_{m'}(\Delta_m^*) \geqslant k)$ as the probability that the higher-order degree $\deg_{m'}(\Delta_m^*)$ of the typical m-simplex Δ_m^* is greater than or equal to k. Furthermore, for a point $p \in \mathbb{R}$, let $N^{\leqslant}(p) := (p, p + \beta)$ denote the part of the neighborhood of point p which is to the right of the point itself. The neighborhood $N(\{p_0, \ldots, p_m\})$ of a set of points $\{p_0, \ldots, p_m\} \in \mathcal{C}_m$ is defined by the intersection of the neighborhoods $N(\{p_0, \ldots, p_m\}) := \bigcap_{i=0}^{m} N(p_i)$ of the points in the set. Next, we introduce the relation $f \asymp g$ for two functions f, g, denoting that there exist constants $c_1, c_2 > 0$ such that $c_1 g(k) \leqslant f(k) \leqslant c_2 g(k)$ for all sufficiently large k.

Theorem 5.3 (Higher-order degree distribution). *Let $m' > m \geqslant 0$ be integers. Then,*

$$\log(d_{m,m'}(k)) \asymp -k^{1/(m'-m)} \log(k^{1/(m'-m)}),$$

Interestingly, the decay of the higher-order degree distribution is slower for larger values of m'. The reason is that although the ordinary degree distribution $d_{0,1}$ has an exponential decay due to the properties of the Poisson distribution, but the number of m'-simplices is increasing in the number of points in the common neighborhood $N(\Delta_m^*)$.

Proof of Theorem 5.3. Without loss of generality, we assume that the points of the typical m-simplex $\Delta_m^* = \{P_0, \ldots, P_m\}$ are ordered, i.e., $c(\Delta_m^*) = P_0$. Then, $N(\Delta_m^*)$ the common neighborhood $N(\Delta_m^*)$ of the points $P_0, \ldots, P_m$ is determined by P_0, since all points $\mathcal{P} \cap N^{\leqslant}(P_0)$ are connected, and thus

$$N(\Delta_m^*) \subseteq [P_0 - \beta, P_0 + \beta], \qquad |N(\Delta_m^*)| = P_0 + \beta - (P_m - \beta) \in [\beta, 2\beta].$$

The number of points $\mathcal{P}(N(\Delta_m^*))$ of the common neighborhood of the vertices of Δ_m^* is a Poisson random variable with parameter $\lambda|N(\Delta_m)|$. To form an m'-simplex whose m-face is Δ_m^*, we need to choose $m' - m$ vertices from $\mathcal{P} \cap N(\Delta_m^*)$.

Upper bound. First, we bound $\binom{n}{m} \leqslant (en/m)^m$ on the binomial coefficient:

$$d_{m,m'}(k) = \mathbb{P}(\deg_{m'}(\Delta_m^*) \geqslant k) = \mathbb{P}\left(\binom{\mathcal{P}(N(\Delta_m^*))}{m' - m} \geqslant k\right)$$

$$\leqslant \mathbb{P}\left(\left(e \frac{\mathcal{P}(N(\Delta_m^*))}{m' - m}\right)^{m' - m} \geqslant k\right) = \mathbb{P}\left(\mathcal{P}(N(\Delta_m^*)) \geqslant \frac{m' - m}{e} k^{1/(m'-m)}\right).$$

Next, introducing $c(k) := (m' - m)\, k^{1/(m'-m)}/e$ we derive a Chernoff bound. For any $t > 0$,

$$d_{m,m'}(k) \leqslant \mathbb{P}(\mathcal{P}(N(\Delta_m^*)) \geqslant c(k)) = \mathbb{P}\left(\exp(t\mathcal{P}(N(\Delta_m^*))) \geqslant \exp(tc(k))\right)$$

$$\leqslant \exp(-tc(k))\, \mathbb{E}\left[\exp(t\mathcal{P}(N(\Delta_m^*)))\right]$$

where we applied Markov's inequality in the last step. Then, we apply the definition of the Palm distribution of the typical m-simplex:

$$d_{m,m'}(k) \leqslant \frac{\mathrm{e}^{-tc(k)}}{\lambda_m} \int_{\mathbb{R}^{m+1}} \mathbb{1}\{c(\boldsymbol{o}_m) \in [0,1]\} \, \mathbb{E}\Big[\exp(t\mathcal{P}(N(\boldsymbol{o}_m)))\Big] g_m(\boldsymbol{o}_m) \, \mathrm{d}\boldsymbol{o}_m.$$

To calculate the expectation, we use that $\mathcal{P}(N(\boldsymbol{o}_m))$ is Poisson distributed with parameter $\lambda|N(\boldsymbol{o}_m)|$. Thus, the moment generating function of the Poisson distribution yields

$$d_{m,m'}(k) \leqslant \frac{\mathrm{e}^{-tc(k)}}{\lambda_m} \int_{\mathbb{R}^{m+1}} \mathbb{1}\{c(\boldsymbol{o}_m) \in [0,1]\} \exp\Big(\lambda|N(\boldsymbol{o}_m)|(\mathrm{e}^t - 1)\Big) g_m(\boldsymbol{o}_m) \, \mathrm{d}\boldsymbol{o}_m.$$

We assume without loss of generality that $c(\boldsymbol{o}_m) = o_0$ by the symmetry of the integrand, and use translation invariance to shift the points by o_0. Then, with $\boldsymbol{o}'_m := (o_1 - o_0, \ldots, o_m - o_0) \in \mathbb{R}^m$, Fubini's theorem yields

$$
\begin{aligned}
d_{m,m'}(k) &\leqslant \frac{\mathrm{e}^{-tc(k)}}{(m+1)\lambda_m} \int_0^1 \int_{\mathbb{R}^m} \exp\Big(\lambda|N(\{0\} \cup \boldsymbol{o}'_m)|(\mathrm{e}^t - 1)\Big) g_m(\{0\} \cup \boldsymbol{o}'_m) \, \mathrm{d}\boldsymbol{o}'_m \, \mathrm{d}o_0 \\
&\leqslant \frac{\exp(2\beta\lambda(\mathrm{e}^t - 1) - tc(k))}{(m+1)\lambda_m} \int_0^1 \int_{[0,\beta]^m} \mathrm{d}\boldsymbol{o}'_m \, \mathrm{d}o_0 \\
&= \frac{\exp(2\beta\lambda(\mathrm{e}^t - 1) - tc(k))}{(m+1)\lambda^{m+1}},
\end{aligned}
$$

where we used that $|N(\{0\} \cup \boldsymbol{o}'_m)| \leqslant 2\beta$ in the second step. We optimize over t to minimize the right-hand side. Setting $t = \log(c(k)/(2\beta\lambda))$, which is positive for a large enough $c(k)$, we have

$$d_{m,m'}(k) \leqslant \frac{\mathrm{e}^{-2\beta\lambda}}{(m+1)\lambda^{m+1}} \exp\Big(-c(k)\Big(\log\Big(\frac{c(k)}{2\beta\lambda}\Big) - 1\Big)\Big).$$

Then, taking the logarithm, we obtain

$$
\begin{aligned}
\log(d_{m,m'}(k)) &\leqslant -2\beta\lambda - \log((m+1)\lambda^{m+1}) - c(k)\Big(\log\Big(\frac{c(k)}{2\beta\lambda}\Big) - 1\Big) \\
&\asymp -c(k)\log(c(k)) \asymp -k^{1/(m'-m)} \log(k^{1/(m'-m)}).
\end{aligned}
$$

Lower bound. We are following a similar strategy for the lower bound. For the binomial coefficient, $\binom{n}{m} \geqslant (n/m)^m$, and then

$$
\begin{aligned}
d_{m,m'}(k) = \mathbb{P}(\deg_{m'}(\Delta_m^*) \geqslant k) &= \mathbb{P}\Big(\binom{\mathcal{P}(N(\Delta_m^*))}{m'-m} \geqslant k\Big) \\
&\geqslant \mathbb{P}\Big(\Big(\frac{\mathcal{P}(N(\Delta_m^*))}{m'-m}\Big)^{m'-m} \geqslant k\Big) \geqslant \mathbb{P}(\mathcal{P}(N(\Delta_m^*)) \geqslant k'),
\end{aligned}
$$

where $k' := (m'-m) \, k^{1/(m'-m)}$. Writing the probability as the expectation of the indicator, we apply the Palm distribution of the typical m-simplex to obtain

$$d_{m,m'}(k) \geqslant \frac{1}{\lambda_m} \int_{\mathbb{R}^{m+1}} \mathbb{1}\{c(\boldsymbol{o}_m) \in [0,1]\} \, \mathbb{P}(\mathcal{P}(N(\boldsymbol{o}_m)) \geqslant k') g_m(\boldsymbol{o}_m) \, \mathrm{d}\boldsymbol{o}_m.$$

We proceed in the same manner as for the upper bound. Without loss of generality, we assume that $c(\boldsymbol{o}_m) = o_0$ by the symmetry of the integrand, and use translation invariance to shift the points by o_0. Then, introducing $\boldsymbol{o}'_m := (o_1 - o_0, \ldots, o_m - o_0) \in \mathbb{R}^m$ again, Fubini's theorem yields

$$d_{m,m'}(k) \geqslant \frac{1}{(m+1)\lambda_m} \int_0^1 \int_{\mathbb{R}^m} \mathbb{P}\big(\mathcal{P}(N(\{0\} \cup \boldsymbol{o}'_m)) \geqslant k'\big) g_m(\{0\} \cup \boldsymbol{o}'_m) \, \mathrm{d}\boldsymbol{o}'_m \, \mathrm{d}o_0.$$

Next, we restrict the integration domain with respect to $\boldsymbol{o}'_m$ to the set $[0, \beta]^m$. Then, on the one hand, $g_m(\{0\} \cup \boldsymbol{o}'_m) = 1$, and on the other hand, the neighborhood $N(\{0\} \cup \boldsymbol{o}'_m)$ contains the interval $[0, \beta]$, and thus $|N(\{0\} \cup \boldsymbol{o}'_m)| \geqslant \beta$. Therefore,

$$d_{m,m'}(k) \geqslant \frac{\mathbb{P}(X_{\mathsf{low}} \geqslant k')}{(m+1)\lambda_m} \int_0^1 \int_{[0,\beta]^m} \mathrm{d}\boldsymbol{o}'_m \, \mathrm{d}o_0 = \frac{\mathbb{P}(X_{\mathsf{low}} \geqslant k')}{(m+1)\lambda^{m+1}},$$

where X_{low} is a Poisson random variable with parameter $\beta\lambda$, and we used that $\lambda_m = \lambda^{m+1}\beta^m$ in the last step. We lower bound the probability that X_{low} is greater than or equal to k' by the probability that it is equal to $\lfloor k' \rfloor$:

$$d_{m,m'}(k) \geqslant \frac{\mathbb{P}(X_{\mathsf{low}} = \lfloor k' \rfloor)}{(m+1)\lambda^{m+1}} = \frac{(\beta\lambda)^{\lfloor k' \rfloor} \mathrm{e}^{-\beta\lambda}}{(m+1)\lambda^{m+1}\lfloor k' \rfloor!}.$$

Using Stirling's approximation for the factorial and taking the logarithm yields

$$\log\big(d_{m,m'}(k)\big) \geqslant -\lfloor k' \rfloor \Big(\log\Big(\frac{\lfloor k' \rfloor}{\beta\lambda}\Big) - 1\Big) + \log\Big(\frac{\mathrm{e}^{-\beta\lambda}}{(m+1)\lambda^{m+1}}\Big) \asymp -k' \log(k').$$

Then, for large enough k, the lower bound follows from $k' \asymp k^{1/(m'-m)}$. $\qquad\square$

CLT for the number of components

The following theorem characterizes the distribution of the number of components β_0 in the Boolean model.

Theorem 5.4. *Let $W_n \subseteq \mathbb{R}$ denote the window $[-n/2, n/2]$ of size n. The number of components $\beta_{n,0} := \beta_0(\mathcal{P} \cap W_n)$ in the Boolean model converges to a normal distribution:*

$$n^{-1/2}\big(\beta_{n,0} - \mathbb{E}[\beta_{n,0}]\big) \xrightarrow[n\uparrow\infty]{d} \mathcal{N}(0, \sigma^2) \qquad \text{with some } \sigma^2 \geqslant 0.$$

Proof. First, we introduce the add-one cost operator $\delta(\mathcal{P}, o) := \beta_0(\mathcal{P} \cup \{o\}) - \beta_0(\mathcal{P})$ to be the change in the number of components when we add a new point o to the Poisson point process $\mathcal{P}$. Note that the addition of the point o can result in at most 1 new component if it is not connected to any other points, or it can merge at most $\mathcal{P}(N(o))$ components to a single component. Thus, $|\delta(\mathcal{P}, o)| \leqslant \mathcal{P}(N(o)) + 1 = \deg(o) + 1$. To show that the CLT holds, we follow the steps of the proof of Hiraoka et al. [48, Theorem 5.2], and we apply the CLT by Penrose and Yukich [89, Theorem 3.1]. To do so, we need to verify the following conditions.

- **Moment bound**: the supremum of the fourth moment of the add-one cost operator $\delta(\mathcal{P}, o)$ is finite: $\sup_{n\geqslant 1} \mathbb{E}[\delta(\mathcal{P} \cap W_n, o)^4] < \infty$.

- **Weak stabilization**: the add-one cost operator $\delta(\mathcal{P}, o)$ converges to a finite limit as $n \to \infty$: $\lim_{n\uparrow\infty} \delta(\mathcal{P} \cap W_n, o) < \infty$.

Moment bound. For the moment bound, using that $|\delta(\mathcal{P}, o)| \leqslant \deg(o) + 1$, we have

$$\mathbb{E}[\delta(\mathcal{P} \cap W_n, o)^4] = \int_0^\infty \mathbb{P}(\delta(\mathcal{P} \cap W_n, o) \geqslant s^{1/4}) \, \mathrm{d}s \leqslant \int_0^\infty \mathbb{P}(\deg(o) + 1 \geqslant s^{1/4}) \, \mathrm{d}s$$

$$\leqslant 4 \int_{-1}^\infty \mathbb{P}(\deg(o) \geqslant t)(t+1)^3 \, \mathrm{d}t,$$

where in the third step we used the substitution $t := s^{1/4} - 1$. As $\deg(o)$ is Poisson distributed with parameter $2\beta\lambda$, we have by Bennett's inequality [8] that if $t \geqslant 2\beta\lambda \vee e^2$,

$$\mathbb{P}(\deg(o) \geqslant t) \leqslant \exp\left(-2\beta\lambda t(\log(t) - 1 + 1/t)\right) \leqslant e^{-2\beta\lambda t},$$

since $\log(t) - 1 + 1/t \geqslant 1$ whenever $t \geqslant e^2$. Then, bounding the probability by 1 for $t < 2\beta\lambda \vee e^2$,

$$\mathbb{E}[\delta(\mathcal{P} \cap W_n, o)^4] \leqslant 4 \int_{-1}^{2\beta\lambda \vee e^2} (t+1)^3 \, \mathrm{d}t + 4 \int_{2\beta\lambda \vee e^2}^\infty (t+1)^3 e^{-2\beta\lambda t} \, \mathrm{d}t < \infty,$$

where the first integral is finite since it is an integral of a polynomial over a finite domain, and the second integral is finite since an exponential function dominates it.

Weak stabilization. For the weak stabilization, we have

$$\lim_{n\uparrow\infty} \delta(\mathcal{P} \cap W_n, o) = \delta(\mathcal{P}, o) < \deg(o) + 1 < \infty$$

almost surely, since the degree of a point is Poisson distributed. $\qquad\square$

CLT for the number of edges

In the following, we will show that a CLT also holds for the number of edges in the Boolean model. We define the edge count S_n as the number of edges whose center (leftmost point) is in $[0, n]$:

$$S_n = \sum_{\Delta \in \Sigma_1} \mathbb{1}\{c(\Delta) \in [0, n]\}.$$

Theorem 5.5 (CLT for the edge counts). *The centered and scaled edge count converges to a normal distribution:*

$$n^{-1/2}\big(S_n - \mathbb{E}[S_n]\big) \xrightarrow[n\uparrow\infty]{d} \mathcal{N}(0, \sigma^2) \qquad \text{with some } \sigma^2 \geqslant 0.$$

Proof. To show this result, Penrose and Yukich [89, Theorem 3.1] could be used for the number of components as in the proof of Theorem 5.4, but this time, we use a different approach, on which proofs in more general settings are based in the following chapters. Setting $\Delta := \{P_0, P_1\}$, we assume without loss of generality that $c(\Delta) = P_0$ is the leftmost point. Thus,

$$S_n = \sum_{\Delta \in \Sigma_1} \mathbb{1}\{P_0 \in [0, n]\} \mathbb{1}\{P_1 \in N^{\leqslant}(P_0)\} = \sum_{P \in \mathcal{P} \cap [0,n]} \deg^{\leqslant}(P),$$

where

$$\deg^{\leqslant}(P) := \deg^{\leqslant}(P, \mathcal{P}) := \sum_{P_j \in \mathcal{P}} \mathbb{1}\{P_j \in N^{\leqslant}(P)\}.$$

We divide the interval $[0, n]$ into n intervals of length 1. Then, we write the edge count S_n as the sum of the edge counts in each interval $[i-1, i]$:

$$S_n = \sum_{i=1}^{n} T_i, \qquad T_i := \sum_{P \in \mathcal{P} \cap [i-1, i]} \deg^{\leqslant}(P).$$

To show that the CLT holds, we would like to apply the CLT by Whitt [107, Theorem 4.4.3], which states the following. If $\{T_i\}_{i \in \{1,\dots,n\}}$ is an associated stationary sequence of random variables with finite variance $\mathrm{Var}(T_i) < \infty$, and if $\sum_{i=1}^{\infty} \mathrm{Cov}(T_1, T_{1+i}) < \infty$, then the centered and scaled sum converges in distribution to a normal random variable:

$$n^{-1/2}(S_n - \mathbb{E}[S_n]) \xrightarrow[n \uparrow \infty]{d} \mathcal{N}(0, \sigma^2) \qquad \text{for some } \sigma^2 \geqslant 0.$$

The sequence $\{T_i\}_{i \in \{1,\dots,n\}}$ is stationary by the stationarity assumption of the Poisson process, and thus $\mathbb{E}[S_n] = n\,\mathbb{E}[T_1]$.

Let us recall the definition of associated random variables from Definition 3.4. If we add a new point to the Poisson point process, then the degrees of the points in the Poisson point process cannot decrease. In other words, the degrees are an increasing function of the Poisson point process. Thus, by the Harris-FKG theorem [66, Theorem 20.4], the random variables $\{T_i\}_{i \in \{1,\dots,n\}}$ are associated.

Next, we show that the variance $\mathrm{Var}(T_i)$ is finite. Let $\mathcal{P}_i := \mathcal{P} \cap [i-1, i]$. Then, writing T_i as the sum of degrees, we have

$$\mathrm{Var}(T_i) = \mathbb{E}\Big[\sum_{P \in \mathcal{P}_i} \deg^{\leqslant}(P)^2\Big] + \mathbb{E}\Big[\sum_{(P_1, P_2) \in (\mathcal{P}_i)^2_{\neq}} \mathrm{Cov}(\deg^{\leqslant}(P_1), \deg^{\leqslant}(P_2))\Big]$$

Next, we apply Mecke's formula to the above terms. For the first term,

$$\mathbb{E}\Big[\sum_{P \in \mathcal{P}_i} \deg^{\leqslant}(P)^2\Big] = \lambda \int_{i-1}^{i} \mathbb{E}[\deg^{\leqslant}(p)^2]\,\mathrm{d}p.$$

For the second term, we need to use the multivariate Mecke formula, and we add two points $p_1, p_2 \in \mathbb{R}$ to the Poisson point process. As these two points can connect, we need to decompose the degree $\deg^{\leqslant}(p_1)$ as below:

$$\deg^{\leqslant}(p_1; \mathcal{P}_i \cup \{p_1, p_2\}) = \deg^{\leqslant}(p_1; \mathcal{P}_i \cup \{p_1\}) + \mathbb{1}\{p_2 \in N^{\leqslant}(p_1)\},$$

and thus the product is

$$
\begin{aligned}
\deg^{\leqslant}&(p_1; \mathcal{P}_i \cup \{p_1, p_2\}) \deg^{\leqslant}(p_2; \mathcal{P}_i \cup \{p_1, p_2\}) \\
&= \deg^{\leqslant}(p_1; \mathcal{P}_i \cup \{p_1\}) \deg^{\leqslant}(p_2; \mathcal{P}_i \cup \{p_2\}) + \mathbb{1}\{p_1 \in N^{\leqslant}(p_2)\}\,\mathbb{1}\{p_2 \in N^{\leqslant}(p_1)\} \\
&\quad + \mathbb{1}\{p_2 \in N^{\leqslant}(p_1)\} \deg^{\leqslant}(p_1; \mathcal{P}_i \cup \{p_1\}) + \mathbb{1}\{p_1 \in N^{\leqslant}(p_2)\} \deg^{\leqslant}(p_2; \mathcal{P}_i \cup \{p_2\}) \\
&= \deg^{\leqslant}(p_1; \mathcal{P}_i \cup \{p_1\}) \deg^{\leqslant}(p_2; \mathcal{P}_i \cup \{p_2\}) + \mathbb{1}\{p_1 = p_2\} \\
&\quad + 2\,\mathbb{1}\{p_2 \in N^{\leqslant}(p_1)\} \deg^{\leqslant}(p_1; \mathcal{P}_i \cup \{p_1\}),
\end{aligned}
$$

where the last equality follows from the symmetry of the last two terms of the expression with respect to the points p_1 and p_2. The indicator $\mathbb{1}\{p_1 = p_2\}$ is always zero since we consider only distinct pairs $(P_1, P_2) \in (\mathcal{P}_i)_{\neq}^2$. Then, the application of the Mecke formula on the second term gives

$$\mathbb{E}\Big[\sum_{(P_1, P_2) \in (\mathcal{P}_i)_{\neq}^2} \mathrm{Cov}(\deg^{\leqslant}(P_1), \deg^{\leqslant}(P_2)) \Big]$$

$$= \lambda^2 \int_{i-1}^i \int_{i-1}^i \mathrm{Cov}\big(\deg^{\leqslant}(p_1), \deg^{\leqslant}(p_2)\big) \, \mathrm{d}p_1 \, \mathrm{d}p_2$$

$$+ 2\lambda^2 \int_{i-1}^i \mathbb{E}[\deg^{\leqslant}(p_1)] \int_{i-1}^i \mathbb{1}\{p_2 \in N^{\leqslant}(p_1)\} \, \mathrm{d}p_2 \, \mathrm{d}p_1,$$

and thus

$$\mathrm{Var}(T_i) = \lambda \int_{i-1}^i \mathbb{E}[\deg^{\leqslant}(p)^2] \, \mathrm{d}p + \lambda^2 \int_{i-1}^i \int_{i-1}^i \mathrm{Cov}\big(\deg^{\leqslant}(p_1), \deg^{\leqslant}(p_2)\big) \, \mathrm{d}p_1 \, \mathrm{d}p_2$$

$$+ 2\lambda^2 \int_{i-1}^i \mathbb{E}[\deg^{\leqslant}(p_1)] \int_{i-1}^i \mathbb{1}\{p_2 \in N^{\leqslant}(p_1)\} \, \mathrm{d}p_2 \, \mathrm{d}p_1.$$

As $\deg^{\leqslant}(p)$ is Poisson distributed with parameter $\beta\lambda$, the first integrand is the second moment of a Poisson random variable, and thus the first integral is

$$\lambda \int_{i-1}^i \mathbb{E}[\deg^{\leqslant}(p)^2] \, \mathrm{d}p = \beta\lambda^2(\beta\lambda + 1).$$

For the second integrand, we have

$$\mathrm{Cov}\big(\deg^{\leqslant}(p_1), \deg^{\leqslant}(p_2)\big) = \mathbb{E}\Big[\sum_{P_1 \in \mathcal{P}} \sum_{P_2 \in \mathcal{P}} \mathbb{1}\{P_1 \in N^{\leqslant}(p_1)\} \, \mathbb{1}\{P_2 \in N^{\leqslant}(p_2)\} \Big]$$

$$- \mathbb{E}\Big[\sum_{P \in \mathcal{P}} \mathbb{1}\{P \in N^{\leqslant}(p_1)\} \Big] \mathbb{E}\Big[\sum_{P \in \mathcal{P}} \mathbb{1}\{P \in N^{\leqslant}(p_2)\} \Big].$$

We decompose the first term based on two cases: when $P_1 = P_2$ and $P_1 \neq P_2$. For the case $P_1 \neq P_2$, by the independence of the Poisson process, the expectation of the product is the product of the expectations, which makes this summand cancel with the second term, thus

$$\mathrm{Cov}\big(\deg^{\leqslant}(p_1), \deg^{\leqslant}(p_2)\big) = \mathbb{E}\Big[\sum_{P \in \mathcal{P}} \mathbb{1}\{P \in N^{\leqslant}(p_1) \cap N^{\leqslant}(p_2)\} \Big].$$

Applying the Mecke formula yields

$$\mathrm{Cov}\big(\deg^{\leqslant}(p_1), \deg^{\leqslant}(p_2)\big) = \lambda \int_{\mathbb{R}} \mathbb{1}\{p \in N^{\leqslant}(\{p_1, p_2\})\} \, \mathrm{d}p = \lambda \big| N^{\leqslant}(\{p_1, p_2\}) \big|.$$

Note that the covariance is nonzero only if $|p_1 - p_2| \leqslant \beta$, thus we bound the covariance as

$$\mathrm{Cov}\big(\deg^{\leqslant}(p_1), \deg^{\leqslant}(p_2)\big) = \lambda\beta \, \mathbb{1}\{|p_1 - p_2| \leqslant \beta\}.$$

Then, the integral of the covariance is

$$\lambda^3 \int_{i-1}^{i} \int_{i-1}^{i} \mathrm{Cov}\big(\deg^{\leqslant}(p_1), \deg^{\leqslant}(p_2)\big) \,\mathrm{d}p_1 \,\mathrm{d}p_2 \leqslant \lambda^3 \int_{i-1}^{i} \int_{p_1-\beta}^{p_1+\beta} \beta \,\mathrm{d}p_2 \,\mathrm{d}p_1 = 2\beta^2 \lambda^3,$$

which is finite. We write the third term as follows:

$$2\lambda^2 \int_{i-1}^{i} \mathbb{E}\big[\deg^{\leqslant}(p_1)\big] \int_{i-1}^{i} \mathbb{1}\{p_2 \in N^{\leqslant}(p_1)\} \,\mathrm{d}p_2 \,\mathrm{d}p_1 \leqslant 2\lambda^2 \int_{i-1}^{i} |N^{\leqslant}(p_1)| \,\mathrm{d}p_1 = 2\beta\lambda^2.$$

Thus,

$$\mathrm{Var}(T_i) \in O(1).$$

To apply the CLT for associated random variable, we show that the covariance $\mathrm{Cov}(T_1, T_{1+i})$ is summable.

$$\sum_{i=1}^{\infty} \mathrm{Cov}(T_1, T_{1+i}) = \sum_{i=1}^{\lceil 1+\beta \rceil} \mathrm{Cov}(T_1, T_{1+i}) < \infty,$$

where we used again that the common neighborhood $N^{\leqslant}(\{p_1, p_2\})$ of two points p_1, p_2 is empty if $|p_1 - p_2| > \beta$, and the sum is finite by similar arguments as above. $\qquad\square$

Poisson approximation for isolated points

Finally, we show a Poisson approximation result for the isolated points. So far, we examined the distribution of the number of m-simplices in a growing window $[0, n]$ with constant intensity measure λ. Now, we consider the distribution of isolated points in the unit interval $[0, 1]$, with the Poisson process $\mathcal{P}_n$ having an increasing intensity $\lambda_n := \lambda n$. As we will see later, to keep the intensity of isolated points finite, we need to scale the parameter $\beta_n := (2\lambda n)^{-1} \log(\lambda n/\beta)$. In this model, the following theorem holds.

Theorem 5.6 (Poisson approximation for isolated points)**.** *The distribution of isolated points converges to a homogeneous Poisson point process with intensity $\lambda_{\mathsf{isolated}} = \beta$ as $n \to \infty$.*

Proof. This theorem can be proved using simpler methods than the one we will use here, as cited in [86, Theorem 8.12]. However, to demonstrate the techniques that we will use in Paper A, we apply a more complex approach here.

Our proof relies on the Poisson approximation theorem [16, Theorem 4.1], which we introduce in our context. Let us define the measurable function $\mathcal{S} \colon \mathcal{P} \to \mathcal{F}$ by

$$\mathcal{S}(p) := [p - \beta_n, p + \beta_n],$$

where $\mathcal{F}$ is the set of all closed subsets of $\mathbb{R}$. Furthermore, let $g \colon \mathcal{P} \times \mathbf{N}_{\mathsf{loc}} \to \{0, 1\}$ be the measurable function indicating that a point p is isolated:

$$g(p, \mathcal{P}) := \mathbb{1}\{\deg(p) = 0\}.$$

Note that g is localized to $\mathcal{S}$, since its value depends only on points inside $\mathcal{S}$. Next, we define the point process ξ marking the isolated points of $\mathcal{P}$ as follows:

$$\xi[\mathcal{P}] := \sum_{p \in \mathcal{P}} g(p, \mathcal{P}) \delta_p.$$

Applying the multivariate Mecke formula to the above point process ξ, we have that its intensity $\lambda_{\mathsf{isolated}}$ is given by

$$\lambda_{\mathsf{isolated}}(A) = \lambda_n \int_A \mathbb{E}[g(p, \mathcal{P})] \, \mathrm{d}p = \lambda_n \int_A \mathbb{P}(\deg(p) = 0) \, \mathrm{d}p = \lambda_n |A| \, \mathbb{P}(\deg(p) = 0),$$

where $A \subseteq [0, 1]$ is an arbitrary Borel set, we substituted the definition of g in the second step, and calculated the integral using translation invariance and the stationarity of the Poisson point process. Using the Poisson distribution property of the Poisson process, we have $\mathbb{P}(\deg(p) = 0) = \mathrm{e}^{-2\beta_n \lambda_n}$, and thus

$$\lambda_{\mathsf{isolated}}(A) = \lambda_n |A| \mathrm{e}^{-2\beta_n \lambda_n} = \beta |A| < \infty,$$

where in the second step we used that $\beta_n = (2\lambda n)^{-1} \log(\lambda n / \beta)$.

Let η be a Poisson point process with intensity measure $\lambda_{\mathsf{isolated}}$, and let $S_p := \mathcal{S}(p) = [p - \beta_n, p + \beta_n]$ be a measurable map from $\mathcal{P}$ to $\mathcal{F}$, thus $\mathcal{S}(p) \subseteq S_p$. Then, by Bobrowski et al. [16, Theorem 4.1],

$$\mathrm{d}_{\mathsf{KR}}(\xi, \eta) \leqslant E_1 + E_2 + E_3,$$

where d_{KR} is the Kantorovich–Rubinstein distance, and

$$E_1 = 2\lambda_n \int_{[0,1]} g(p, \mathcal{P} \cup \{p\}) \, \mathbb{1}\{\mathcal{S}(p) \not\subset S_p\} \, \mathrm{d}p$$

$$E_2 = 2\lambda_n^2 \iint_{[0,1]^2} \mathbb{1}\{S_{p_1} \cap S_{p_2} \neq \varnothing\} \, \mathbb{E}\Big[g(p_1, \mathcal{P} \cup \{p_1\})\Big] \mathbb{E}\Big[g(p_2, \mathcal{P} \cup \{p_2\})\Big] \, \mathrm{d}(p_1, p_2)$$

$$E_3 = 2\lambda_n^2 \iint_{[0,1]^2} \mathbb{1}\{S_{p_1} \cap S_{p_2} \neq \varnothing\} \, \mathbb{E}\Big[g(p_1, \mathcal{P} \cup \{p_1, p_2\}) g(p_2, \mathcal{P} \cup \{p_1, p_2\})\Big] \, \mathrm{d}(p_1, p_2).$$

Note that convergence in the Kantorovich–Rubinstein distance implies convergence in distribution.

For the first term, $E_1 = 0$, since the indicator in the integrand is always 0.

In the error term E_2,

$$\mathbb{E}\Big[g(p_1, \mathcal{P} \cup \{p_1\})\Big] = \mathbb{E}[g(p_1, \mathcal{P})] = \mathbb{P}(\deg(p_1) = 0) = \mathrm{e}^{-2\beta_n \lambda_n},$$

and similarly for p_2. Then, recognizing that $\mathbb{1}\{S_{p_1} \cap S_{p_2} \neq \varnothing\} = \mathbb{1}\{|p_1 - p_2| \leqslant 2\beta_n\}$, we can bound the error term as follows:

$$E_2 = 2\lambda_n^2 \mathrm{e}^{-4\beta_n \lambda_n} \iint_{[0,1]^2} \mathbb{1}\{|p_1 - p_2| \leqslant 2\beta_n\} \, \mathrm{d}(p_1, p_2) \leqslant 8\beta_n \lambda_n^2 \mathrm{e}^{-4\beta_n \lambda_n}.$$

Taking the limit $n \to \infty$, we have

$$\lim_{n \uparrow \infty} E_2 = \lim_{n \uparrow \infty} 8\beta_n \big(\lambda_n \mathrm{e}^{-2\beta_n \lambda_n}\big)^2 = 8 \lim_{n \uparrow \infty} \beta_n \beta^2 = 0.$$

51

It remains to show that $E_3 \to 0$ as $n \to \infty$. Since

$$\mathbb{E}\Big[g(p_1, \mathcal{P} \cup \{p_1, p_2\})g(p_2, \mathcal{P} \cup \{p_1, p_2\})\Big] = \mathbb{E}\Big[g(p_1, \mathcal{P} \cup \{p_2\})g(p_2, \mathcal{P} \cup \{p_1\})\Big],$$

the expectation is 0 whenever $|p_1 - p_2| \leqslant \beta_n$. On the other hand, the indicator $\mathbb{1}\{S_{p_1} \cap S_{p_2} \neq \varnothing\}$ requires that $|p_1 - p_2| \leqslant 2\beta_n$. Thus,

$$E_3 = 2\lambda_n^2 \iint_{[0,1]^2} \mathbb{1}\{|p_1 - p_2| \in [\beta_n, 2\beta_n]\}\, \mathbb{P}(\deg(p_1) = 0, \deg(p_2) = 0)\, \mathrm{d}(p_1, p_2),$$

where we substituted the definition of g in the expectation. The event in the probability happens whenever there are no points in the union of the two neighborhoods $N(p_1) \cup N(p_2)$, and thus

$$\mathbb{P}(\deg(p_1) = 0, \deg(p_2) = 0) = \mathbb{P}(\mathcal{P}(N(p_1) \cup N(p_2)) = 0) = \mathrm{e}^{-\lambda_n |N(p_1) \cup N(p_2)|}.$$

Note that $|N(p_1) \cup N(p_2)| = 2\beta_n + |p_1 - p_2|$ whenever $|p_1 - p_2| \leqslant 2\beta_n$, and thus

$$E_3 = 2\lambda_n^2 \mathrm{e}^{-2\beta_n \lambda_n} \iint_{[0,1]^2} \mathbb{1}\{|p_1 - p_2| \in [\beta_n, 2\beta_n]\}\mathrm{e}^{-\lambda_n |p_1 - p_2|}\, \mathrm{d}(p_1, p_2).$$

We bound the first integral using translation invariance. We set $p_1 = 0$ and integrate with respect to p_1. Then, using that $\lambda_n \mathrm{e}^{-2\beta_n \lambda_n} = \beta$, we have

$$E_3 \leqslant 2\beta\lambda_n \int_{[0,1]} \mathbb{1}\{|p_2| \in [\beta_n, 2\beta_n]\}\mathrm{e}^{-\lambda_n |p_2|}\, \mathrm{d}p_2$$

$$\leqslant 4\beta\lambda_n \int_{\beta_n}^{\infty} \mathrm{e}^{-\lambda_n p_2}\, \mathrm{d}p_2 = 4\beta\mathrm{e}^{-\beta_n \lambda_n},$$

where we bounded the indicator by $\mathbb{1}\{|p_2| \in [\beta_n, 2\beta_n]\} \leqslant \mathbb{1}\{|p_2| \geqslant \beta_n\}$, and we used the symmetry of $|\cdot|$ in the second step. Finally, we take the limit $n \to \infty$:

$$\lim_{n \uparrow \infty} E_3 = 4\beta \lim_{n \uparrow \infty} \mathrm{e}^{-\beta_n \lambda_n} = 0$$

since $\lim_{n \uparrow \infty} \beta_n \lambda_n = \infty$. $\qquad\qquad\qquad\qquad\qquad\qquad\qquad\qquad\qquad\quad \square$

Paper A

Poisson approximation of fixed-degree nodes in weighted random connection models

Christian Hirsch, Benedikt Jahnel, Sanjoy K. Jhawar, and Péter Juhász

Abstract: We present a process-level Poisson approximation result for the degree-k vertices in a high-density weighted random connection model with a preferential-attachment kernel in a finite-volume Borel set. Our main focus lies on the impact of the left tails of the weight distribution, for which we establish general criteria based on their small-weight quantiles. To illustrate that our conditions are broadly applicable, we verify them for weight distributions with polynomial and stretched exponential left tails. The proofs rest on truncation arguments and a recently established quantitative Poisson approximation result for functionals of Poisson point processes.

A.1 Introduction

Spatial random networks are found in a wide variety of applications ranging from social networks to material science to telecommunication systems [43, 59]. In particular, in the context of such networks, it is essential to estimate the probability that we observe extreme realizations of the key network characteristics, and to understand the reasons leading to such extreme behavior. This need motivates the extension of the classical findings from extreme-value theory to the context of spatial random networks.

To make our results accessible to a larger audience, we first explain the classical non-spatial models for preferential attachment, which go back to Barabási and Albert [3]. Here, nodes arrive over time and connect to already existing nodes. The important feature of the model is that it is more likely to connect to nodes that already have many connections.

However, the classical *preferential attachment model* is not a spatial network. On the other hand, one of the most fundamental spatial network models is the *random connection model* (RCM) from [85]. It is defined on a vertex set in Euclidean space where edges are put independently with some distance-dependent probability. We also refer to Franceschetti et al. [38], Last et al. [68] for further properties. However, the RCM does not have a heavy-tailed degree distribution. This motivated the introduction of the *weighted RCM* (WRCM) [see 40, 42, 41, 64]. Here, the connection probability not only depends on the distance but also on the weights.

A seminal paper in this context is [88], which studies the asymptotic behavior of the number of degree-k nodes in the inhomogeneous RCM. More precisely, the main result of [88] states that the number of degree-k nodes converges to a Poisson distribution under a suitable scaling of the connectivity threshold in the connection function.

While the extensions of Stein's method developed in [88] are interesting from a mathematical point of view, it is not always easily applicable in practice. The reason is that the RCM can only produce light-tailed degree distributions [72, Equation (6.1)], whereas many real-world networks exhibit heavy tails [3, 75]. To overcome this limitation, Iyer and Jhawar [55] extended the results to the scale-free RCM introduced in [29, 28]. These networks generate heavy-tailed degree distributions by assigning suitable weights to the vertices, which significantly influence their ability to connect to other vertices.

While the scale-free RCM involves many parameters, an important finding in [55] is that most of them influence the connectivity threshold only through multiplication by a constant. This points to a limitation of the scale-free RCM since, depending on the application, we expect a wide variety of extreme-value scalings.

In this paper, we resolve this potential misconception by showing that scale-free RCMs can indeed give rise to a wide range of extreme-value scalings. We stress that these findings do not contradict the results in [55], since, in contrast to that work, where the weights are bounded away from zero, we allow variations of the left tail of the weight distribution, i.e., the behavior of the distribution near zero. While the majority of the existing literature focuses exclusively on studying the effects of the right tail due to its importance for the degree distribution, one of the core findings of our work

is showing that the left tail of the weight distribution is crucial for understanding the extreme-value behavior of degree-k nodes.

While this may be surprising at first sight, it is not entirely unexpected. Indeed, our analysis shows that the most likely reason for observing a constant order of isolated nodes is that these nodes have an extremely small weight, making it easier for them to be isolated. On the other hand, it is the left tail that determines how difficult it is for a node to have an extremely small weight. Hence, by allowing modification to the left tail of the distribution of the weights, we can observe a variety of different extreme-value behaviors.

Let us illustrate these findings through simulations set up with a constant order of isolated nodes. In the left panel of Figure A.1, we consider a typical realization of an *isolated node* (red) in a weighted RCM of intensity 1000, whose weight distribution has a power-law left tail of tail index 2. The horizontal axis corresponds to the positions of the nodes, whereas the vertical axis shows their weights. Edges are not shown. Loosely speaking, most of the network resembles a typical realization of a Poisson point process. However, the weight of the red node at the origin is atypically small, making it easy to avoid connections. Our main result makes this intuition precise by providing a quantitative prediction for how small the weight of the origin must be to see a constant order of isolated nodes. In the right panel of Figure A.1, we show a log-log plot of the weight of a typical isolated node against the point-process intensity. The plot is approximately linear with a slope of -0.4682, which is close to our theoretical prediction of $-1/2$.

The main contribution of our paper can be summarized as follows.

(1) While the results in [88, 55] tentatively indicate that the rare-event behavior of the degree-k nodes is not strongly affected by the parameters, we show that, in fact, a wide variety of extreme-value scalings can be obtained. This is achieved by modifying the left tail of the weight distribution. As specific examples, we consider the case where the left tail is of power-law or of Fréchet type.
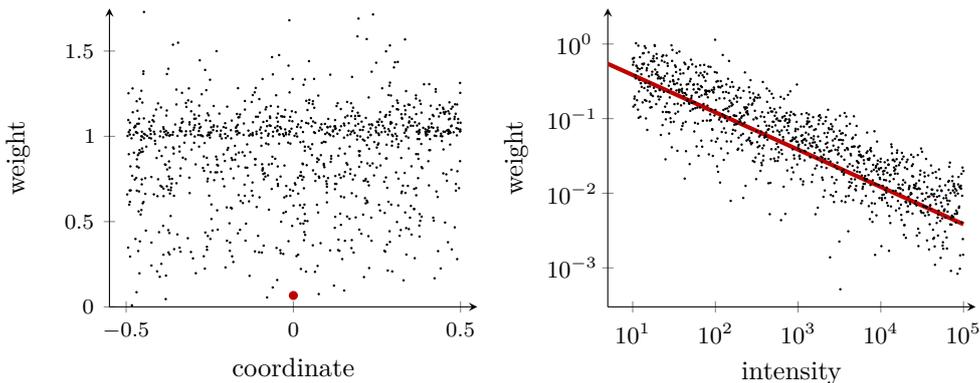
Figure A.1: Realization of an isolated node (red) in a weighted RCM with intensity 1000 and weight distribution with power-law left tails of tail index 2 (left). Log-log plot of the weight of a typical isolated point against varying point-process intensities (right).

(2) Our results go beyond the scale-free RCM and consider the *weighted RCM (WRCM)* introduced by Gracar et al. [40, 42, 41], Komjáthy and Lodewijks [64]. WRCMs specify a kernel function and, therefore, allow one to consider models of spatial preferential attachment.

(3) In contrast to [88, 55], we not only look at the number of degree-k nodes, but also at their spatial distribution. In other words, we prove convergence of the degree-k nodes to a Poisson point process. This is accomplished through the application of a recently developed functional Poisson-approximation result from Bobrowski et al. [16].

Our results focus on models where weights are assigned to vertices, which distinguishes our work from the WRCMs explored in [64]. On the other hand, a connection arises through the influence of the left tail of the weight distribution. Although the criteria for explosion in [64, Equation (1.1)] is satisfied in both of our examples discussed in Section A.3, it is not directly connected to the Assumptions A.1–A.3 introduced later in our paper.

The rest of the manuscript is organized as follows. In Section A.2, we recall the definition of the WRCM and state Theorem A.2.2 as our main result on the Poisson approximation of the degree-k nodes. Loosely speaking, the precise rare-event behavior is encoded in a characterizing equation that prominently involves the weight distribution. Next, in Section A.3, we illustrate that the conditions on the weight distribution are meaningful as they cover a wide range of natural models. Finally, in Section A.4, we present the proofs of the above results.

A.2 The inhomogeneous random connection model and main results

We now recall the precise definition of the kernel-based spatial random networks, which are the object of our study, as presented by Gracar et al. [41, 40]. We consider, henceforth, a random graph with vertex set given by a homogeneous Poisson point process $\mathcal{P}_s$ on $\mathbb{R}^d$ with intensity $s > 0$ and $d \geqslant 1$. Independently to each $x \in \mathcal{P}_s$, we associate a random weight W_x drawn from a distribution with cumulative distribution function $F \colon \mathbb{R}_+ \to [0,1]$, $F(w) \coloneqq F_W(w) = \mathbb{P}(W \leqslant w)$ on $(0, \infty)$. Edges between pairs of points are drawn independently, and the probability that there is an edge between any two vertices $x, y \in \mathcal{P}_s$ is a function of their distance and their weights W_x and W_y, i.e.,

$$p_s(x, W_x; y, W_y) \coloneqq \varphi\big(|B_{|x-y|}(o)|/(v_s \kappa(W_x, W_y))\big), \tag{A.1}$$

where v_s is the scaling factor depending on the intensity, $|B_{|x-y|}(o)|$ is the volume of the centered Euclidean ball with radius $|x - y|$, and κ and φ are the *kernel* and the *profile function* of the model that are specified as follows. Note that the scaling factor v_s has a specific value, which is discussed in (**SCG**) below. As kernel, we consider the interpolation kernel, i.e.,

$$\kappa(w_1, w_2) = (w_1 \wedge w_2)(w_1 \vee w_2)^a$$

for some $a \geqslant 0$, which is a special case of the kernel considered in [70, Equation (2.2)] with parameters $\alpha = 1$ and $\gamma = a$. Note that the interpolation kernel was also introduced in the context of the WRCM in [104] under a different parametrization. In particular, it interpolates between the cases $a = 0$ and $a = 1$, which are considered under the names *min kernel* and *product kernel* earlier in the literature.

The profile function is a non-negative function $\varphi \colon [0, \infty) \to [0, 1]$ satisfying the normalization condition $\int_0^\infty \varphi(r) \, \mathrm{d}r = 1$, and regularly varying [13] at infinity with tail index $\alpha > 1$, that is,

$$\lim_{r \uparrow \infty} \varphi(tr)/\varphi(r) = t^{-\alpha} \qquad \text{for all } t > 0.$$

We assume that $1 - F$ is also regularly varying at infinity with tail index $\beta > a\alpha$, in particular, $\mu_{a\alpha} < \infty$ with $\mu_r := \mathbb{E}[W^r]$. The resulting random graph is denoted by $G(\mathcal{P}_s, v_s)$. We highlight that the parameter sv_s has a natural interpretation in terms of the network model. Indeed, as we will see in Application A.4.4 in Section A.4, sv_s is the order of the expected number of neighbors of a typical network node.

We are interested in the spatial distribution of nodes with a given degree, i.e.,

$$\xi_{s,k} := \sum_{x \in \mathcal{P}_s \cap H} \mathbb{1}\{\deg(x) = k \text{ in } G(\mathcal{P}_s, v_s)\} \delta_x, \tag{A.2}$$

where $H \subseteq \mathbb{R}^d$ a Borel set with finite volume $|H|$. Note that $\deg(x)$ is the number of all points connected to x, including those that lie outside H. In order to specify the scaling v_s, we first consider $D_{s,k} := \xi_{s,k}(H)$, the number of degree-k vertices in $G(\mathcal{P}_s, v_s)$ that are contained in H. We identify the correct scaling $v_{s,k}$ such that $\mathbb{E}[D_{s,k}]$ is constant. For this, let us introduce the decomposition

$$h(w) := w\mu_+(w) + w^a \mu_-(w) := w \, \mathbb{E}\big[\mathbb{1}\{W \geqslant w\}W^a\big] + w^a \, \mathbb{E}\big[\mathbb{1}\{W < w\}W\big], \tag{A.3}$$

of $h(w) = \mathbb{E}[\kappa(w, \cdot)]$ and consider the scaling v_s defined as the largest solution of the equation

$$k! = s \, \mathbb{E}[(sv_{s,k}h(W))^k \exp(-sv_{s,k}h(W))], \tag{SCG}$$

for $k \geqslant 0$. We note that such a solution must exist at least for all sufficiently large s. Indeed, take for example $v_{s,k} = c/s$, then (**SCG**) can be rewritten as $s = k!/\mathbb{E}[(ch(W))^k \exp(-ch(W))]$, where the right-hand side tends to infinity for $c \to \infty$. We emphasize that the scaling $v_{s,k}$ depends on the chosen value of k. From now on, we fix the degree $k \geqslant 0$, and write v_s instead of $v_{s,k}$ going forward. We use the same convention for D_s, $D_{s,k}$, and ξ_s, $\xi_{s,k}$ as well. The following result establishes the correct scaling, with its proof presented in Section A.4.

Lemma A.2.1 (Expected typical degree). *Let us fix $k \geqslant 0$ and consider the random graph $G(\mathcal{P}_s, v_s)$ with the connection function p_s of the form (A.1) and scaling parameter v_s as defined by (**SCG**). Then,*

$$\mathbb{E}[D_s] = |H|. \tag{A.4}$$

While the definition of v_s is indirect, in Section A.3, we illustrate that the order of v_s can be computed for given natural choices of the weight distribution as a function

of the intensity s. The value of the parameter v_s has important implications for the network topology, as it reveals the order of the expected number of neighbors of a typical node, sv_s. More precisely, we will see that, for polynomial tails, sv_s is of polynomial order, while for stretched exponential tails, it is of polylogarithmic order. This reflects the intuition that for polynomial tails, it is more likely that low-weight nodes appear, which means that even for relatively large values of sv_s, it is reasonably likely that a low-weight node is isolated. For stretched exponential tails, it is less likely to create low-weight nodes, which means that even for smaller values of sv_s, it is unlikely that a low-weight node is isolated. These observations are to be contrasted with the finding from Iyer and Jhawar [55] that for a lower-bounded weight distribution, sv_s is of a much smaller, namely, logarithmic order.

Having established the convergence of the expected degree counts in Lemma A.2.1, in Theorem A.2.2 below, we prove the convergence of the degree distribution itself in the sense of a Poisson point process approximation result. Note that this result is only valid under certain assumptions on the distributions of the weights W, which we now collect. These assumptions are rather technical but are a key component of the approximation arguments in our proof. In Section A.3, we illustrate how to verify these assumptions and present examples for weight distributions exhibiting a variety of left tails.

A central role in our proof is played by the $1/(2s)$-quantile of the weight distribution, which we denote by w_s. That is, $F(w_s) = 1/(2s)$. The importance of this quantity stems from the intuition that it is a first indication for the typical weight of an isolated node in H. Indeed, nodes of weights much smaller than w_s are unlikely to appear in H, whereas nodes of weights much larger than w_s are unlikely to be isolated. We stress that the precise interpretation of *much smaller* and *much larger* may depend on the tail distribution. This is one of the main reasons why the following assumptions are rather technical. Let $\delta := (\alpha - 1)/2$. Our assumptions require that, for some $K > 0$ and $\eta \in (0, 1)$,

A.1 $\lim_{s \uparrow \infty} sv_s w_s^\eta / \log(s) = \infty$,

A.2 $\lim_{s \uparrow \infty} \log(s) w_s^{-(K+1)(1-\eta)} F(w_s^\eta) = 0$, and

A.3 $\lim_{s \uparrow \infty} \log(s) w_s^{(K\delta - 1)(1-\eta)} = 0$.

To present our main result, let ζ denote a Poisson point process with intensity $\mathrm{Leb}(\mathrm{d}x) := \mathbb{1}\{x \in H\}\,\mathrm{d}x$ and let

$$d_{\mathsf{KR}}(\xi, \xi') := \sup\{|\mathbb{E}[g(\xi)] - \mathbb{E}[g(\xi')]| \colon g \in \mathrm{LIP}\}$$

denote the Kantorovich–Rubinstein distance between the distributions of the two processes ξ and ξ'. Here LIP is the class of measurable 1-Lipschitz functions with respect to the total variation distance on the space of finite point configurations in H.

Theorem A.2.2 (Poisson approximation)**.** *Let us fix $k \geqslant 0$, and consider the random graph $G(\mathcal{P}_s, v_s)$ with the connection function p_s of the form* (A.1) *and the scaling parameter v_s as defined by* (**SCG**)*. Then, under Assumptions A.1–A.3,*

$$\lim_{s \uparrow \infty} d_{\mathsf{KR}}(\xi_s, \zeta) = 0$$

for any Borel set $H \subset \mathbb{R}^d$ of finite volume.

Note that convergence in Kantorovich–Rubinstein distance implies convergence in distribution in the sense of random measures supported on a finite volume H. In fact, by [61, Theorem 4.11], this implies that the random measure ξ_s defined on the entire $\mathbb{R}^d$ converges vaguely in distribution to a homogeneous Poisson point process. However, we stress that for these infinite-volume objects, we do not obtain the convergence in Kantorovich–Rubinstein distance.

We note also that Theorem A.2.2 is the analog of [55, Theorem 3.2] for the case where the weight distribution has positive mass arbitrarily close to 0. More precisely, we note that in [55], the connection probability is given by

$$1 - \exp\Big(-\frac{\eta r_s^\alpha W_x W_y}{|x - y|^\alpha}\Big)$$

for some parameters η, r_s, α. Hence, this can be written as $\varphi(|B_{|x-y|}(o)|/(v_s \kappa(W'_x, W'_y)))$, where $v_s := r_s^d$, $W'_x := W_x^{d/\alpha}$, the parameter $a = 1$ in the kernel κ and

$$\varphi(r) := 1 - \exp\Big(-\eta|B_1(o)|^{\alpha/d} r^{-\alpha/d}\Big).$$

Since in [55], there exists $\varepsilon > 0$ such that $w_s > \varepsilon$ for all intensity s, the Assumptions A.2 and A.3 are violated. This means that the results for the model discussed by Iyer and Jhawar [55] are not implied by Theorem A.2.2.

We also note that in [88], a straightforward extension of the arguments for the degree-k vertices also yields the Poisson approximation for size-k components. However, in our setting, the introduction of weights makes the analysis of size-k components substantially more involved. Indeed, such an analysis would rely on a highly delicate configurational analysis of the weights in such components. These weights need to be small enough to ensure that there are no connections to outside nodes, while simultaneously being large enough to ensure connectivity between the nodes within the component. While such an analysis is not entirely out of range, it would require additional constraints on the weight distribution as well as a substantially more refined analysis. Hence, to provide a focused presentation of the main ideas, we refrain from conducting such an analysis here.

Moreover, as mentioned in the introduction, the main tool of the proof is a recently developed functional Poisson-approximation result from Bobrowski et al. [16, Theorem 4.1]. Here, we note that Bobrowski et al. [16] also gives a functional Poisson-approximation result for the nearest-neighbor radii. However, this result heavily relies on the specific form of the isolation probability for the standard random geometric graph on a Poisson point process. In particular, such a result does not extend easily to the present setting, where the isolation probability depends in a complicated way on both the weights and the profile function.

Finally, we note that, while Bobrowski et al. [16, Theorem 4.1] provides a rate of convergence, we refrain from stating such rates here. This is because the complexity of our model forces us to make approximations at several instances that are presumably suboptimal. Hence, while it would be possible to extract specific convergence rates from our proof, they would be far from optimal as well. Since a streamlined proof without tracking the rates is substantially more accessible, we decided to present the proof in this form.

A.3 Examples

The goal of this section is to provide examples for the weight distributions and show that they fulfill the Assumptions A.1–A.3 listed in Section A.2. In Sections A.3 and A.3, we discuss examples for weight distributions with polynomial and stretched exponential left tails, respectively.

Let us start by stating some a priori estimates of our parameters; recall the definitions in (A.3).

Lemma A.3.1. *It holds that*

(1) $\mu_-(w) \leqslant wF(w)$,

(2) $w^a(1 - F(w)) \leqslant \mu_+(w) \leqslant \mu_a$,

(3) $\lim_{w\downarrow 0} \mu_+(w) = \mu_a$,

(4) $\lim_{w\downarrow 0} h(w)/w = \mu_a$, *and*

(5) $sv_s w_s \in O(\log(s))$.

Proof. The first three statements are immediate. For the fourth statement, as $w \to 0$, we can bound the fraction of the two terms of $h(w)$ as

$$\lim_{w\downarrow 0} \frac{w^a \mu_-(w)}{w\mu_+(w)} \leqslant \lim_{w\downarrow 0} w^a \frac{F(w)}{\mu_a} = 0.$$

For the fifth statement we use the indicators for the events $W \leqslant w_s$ and $W > w_s$ to bound

$$1 = s\,\mathbb{E}\Big[\frac{1}{k!}(sv_s h(W))^k \exp(-sv_s h(W))\Big]$$

$$\leqslant s\,\mathbb{P}(W \leqslant w_s) + s\,\mathbb{E}\Big[\frac{1}{k!}(sv_s h(W))^k \exp(-sv_s h(W))\,\mathbb{1}\{W > w_s\}\Big].$$

As w_s is the $1/(2s)$-quantile, the first term is $1/2$, and as $\sup\{x^k \exp(-x/2)\colon x \geqslant 0\} < \infty$, we can upper bound the second term as

$$1/2 \leqslant cs\,\mathbb{E}\big[\exp(-sv_s h(W)/2)\,\mathbb{1}\{W > w_s\}\big]$$

$$\leqslant c's\,\mathbb{E}\big[\exp(-sv_s h(W)/2)\,\mathbb{1}\{w_s < W < c''\}\big]$$

for some constants $c, c', c'' > 0$ with $\mu(c'') > 0$. In the last step, we used that $h(W)$ is a monotone increasing function. Finally, using the definition of $h(W)$, we have that $1/2 \leqslant c's \exp(-sv_s w_s \mu_+(c'')/2)$ and therefore $sv_s w_s \mu_+(c'') \leqslant 2\log(2c's)$, as asserted. $\qquad\square$

The starting point of the computations in this section is (**SCG**). We use that $\lim_{s\uparrow\infty} sv_s = \infty$. This is so because the expectation in (**SCG**) must be zero in the limit so that the left-hand side of (**SCG**) is constant.

Polynomial left tails

First, we consider the setting with polynomial left tails. That is, we assume that there exist parameters $p, \rho, b > 0$ such that

$$F(w) = pw^\rho \qquad \text{for all } w \leqslant b.$$

Note that, for sufficiently large values of s, the $1/(2s)$-quantile w_s of the weight distribution is given by

$$\mathbb{P}(W \leqslant w_s) = 1/(2s) \quad \Longleftrightarrow \quad pw_s^\rho = 1/(2s) \quad \Longleftrightarrow \quad w_s = (2ps)^{-1/\rho}.$$

Let us first establish the scaling v_s.

Lemma A.3.2 (Scaling for polynomial left tails)**.** *Let $k \geqslant 0$ and let v_s be as defined in (**SCG**). Then*

$$\lim_{s\uparrow\infty} s^{\rho-1} v_s^\rho = \frac{p\rho}{k!\mu_a^\rho}\Gamma(k+\rho).$$

Proof. Let $0 < \varepsilon < b$. Then, using (**SCG**), we have that

$$\begin{aligned}
\lim_{s\uparrow\infty} s^{\rho-1} v_s^\rho &= \lim_{s\uparrow\infty} \frac{(sv_s)^\rho}{k!} \mathbb{E}\big[(sv_s h(W))^k \exp(-sv_s h(W))\big] \\
&= \lim_{s\uparrow\infty} \frac{(sv_s)^\rho}{k!} \big(\mathbb{E}\big[(sv_s h(W))^k \exp(-sv_s h(W)) \mathbb{1}\{W \leqslant \varepsilon\}\big] \\
&\qquad + \mathbb{E}\big[(sv_s h(W))^k \exp(-sv_s h(W)) \mathbb{1}\{W > \varepsilon\}\big]\big),
\end{aligned}$$

where the second term decays exponentially fast in sv_s since $h(W) > 0$ whenever $W > \varepsilon$. Thus, we keep only the case when $W \leqslant \varepsilon$, which leads to

$$\lim_{s\uparrow\infty} s^{\rho-1} v_s^\rho = \lim_{s\uparrow\infty} \frac{(sv_s)^\rho}{k!} \mathbb{E}\big[(sv_s h(W))^k \exp(-sv_s h(W)) \mathbb{1}\{W \leqslant \varepsilon\}\big].$$

Note that, for $w \leqslant b$, the weight distribution has the density $p\rho w^{\rho-1}$. Since $\varepsilon \to 0$, we can use that $\lim_{w\downarrow 0} h(w)/w = \mu_a$. We use Lemma A.3.1 to see that

$$\lim_{s\uparrow\infty} s^{\rho-1} v_s^\rho = \lim_{\varepsilon\downarrow 0}\lim_{s\uparrow\infty} \frac{(sv_s)^{\rho+k}p\rho\mu_a^k}{k!} \int_0^\varepsilon (1+o_\varepsilon(1))w^{k+\rho-1}\exp(-sv_s\mu_a w(1+o_\varepsilon(1)))\,\mathrm{d}w.$$

Finally, substituting $u := sv_s\mu_a w$ we have that

$$\begin{aligned}
\lim_{s\uparrow\infty} s^{\rho-1} v_s^\rho &= \lim_{\varepsilon\downarrow 0}\lim_{s\uparrow\infty} \frac{p\rho}{k!\mu_a^\rho} \int_0^{sv_s\varepsilon\mu_a} (1+o_\varepsilon(1))u^{k+\rho-1}\exp(-u(1+o_\varepsilon(1)))\,\mathrm{d}u \\
&= \frac{p\rho}{k!\mu_a^\rho}\Gamma(k+\rho),
\end{aligned}$$

as asserted. $\qquad\square$

After having shown Lemma A.3.2, we verify Assumptions A.1–A.3. First, we deal with Assumption A.1. As $w_s = (2ps)^{-1/\rho}$, we have that for $\eta \in (0,1)$,

$$\liminf_{s\uparrow\infty} \frac{sv_s(2ps)^{-\eta/\rho}}{\log(s)} = \liminf_{s\uparrow\infty} \frac{(2ps)^{-\eta/\rho}}{\log(s)} \Big(\frac{sp\rho}{k!\mu_a^\rho}\Gamma(k+\rho)\Big)^{1/\rho}$$

$$= \liminf_{s\uparrow\infty} \Big(\frac{p^{1-\eta}\rho\Gamma(k+\rho)}{2^\eta k!\mu_a^\rho}\Big)^{1/\rho} \frac{s^{(1-\eta)/\rho}}{\log(s)} = \infty,$$

where in the first step we used Lemma A.3.2.

Now, we choose $K := 2/\delta$ and subsequently η sufficiently close to 1 such that $(K+1)(1-\eta)/\rho < \eta$, or, equivalently,

$$\frac{(1+K)/\rho}{1+(1+K)/\rho} < \eta < 1.$$

We now turn our attention to Assumption A.2. Note that $F(w_s^\eta) = pw_s^{\eta\rho} = p/(2ps)^\eta$. Therefore,

$$\limsup_{s\uparrow\infty} \log(s)w_s^{-(K+1)(1-\eta)}F(w_s^\eta) = \limsup_{s\uparrow\infty} \log(s)(2ps)^{(K+1)(1-\eta)/\rho}\frac{p}{(2ps)^\eta}$$

$$= p\limsup_{s\uparrow\infty} \log(s)(2ps)^{(K+1)(1-\eta)/\rho-\eta} = 0,$$

where we used that the exponent is negative for the chosen η. Thus, Assumption A.2 is satisfied.

Finally, for Assumption A.3 we have that

$$\limsup_{s\uparrow\infty} \log(s)w_s^{(K\delta-1)(1-\eta)} = \limsup_{s\uparrow\infty} \log(s)(2sp)^{-(K\delta-1)(1-\eta)/\rho} = 0,$$

as the exponent is negative by the choice of K.

Stretched exponential left tails

Now, we consider stretched-exponential left tails. That is, we assume that there exist parameters $p, \rho, b > 0$ such that

$$F(w) = p\exp(-w^{-\rho}) \qquad \text{for all } w \leqslant b.$$

Note that, for large values of s, the $1/(2s)$-quantile w_s of the weight distribution is given by

$$\mathbb{P}(W \leqslant w_s) = 1/(2s) \iff p\exp(-w_s^{-\rho}) = 1/(2s) \iff w_s = \log(2ps)^{-1/\rho}.$$

Next, we identify the v_s-scaling.

Lemma A.3.3 (Scaling for stretched exponential left tails)**.** *Let v_s be as defined in* (**SCG**)*. Then, for $k \geqslant 0$,*

$$0 < \liminf_{s\uparrow\infty} \frac{sv_s}{\log(s)^{1+1/\rho}} \leqslant \limsup_{s\uparrow\infty} \frac{sv_s}{\log(s)^{1+1/\rho}} < \infty.$$

Since the proof of Lemma A.3.3 is rather technical, we first explain how to verify Assumptions A.1–A.3. For this, let $\eta = 1/2$ and fix $K > (2\rho + 1)/\delta$. First, we examine Assumption A.1. As $w_s = \log(2ps)^{-1/\rho}$, using Lemma A.3.3, for some $M > 0$,

$$\liminf_{s\uparrow\infty} \frac{sv_s w_s^\eta}{\log(s)} = \liminf_{s\uparrow\infty} \frac{sv_s \log(2ps)^{-\eta/\rho}}{\log(s)} \geqslant \lim_{s\uparrow\infty} \frac{1}{M} \log(s)^{-\eta/\rho-1} \log(s)^{1+1/\rho} = \infty,$$

where we applied that $\lim_{s\uparrow\infty} \log(s)/\log(2ps) = 1$. Let us consider Assumption A.2. As

$$F(w_s^\eta) = p\exp(-w_s^{-\rho\eta}) = p\exp(-\log(2ps)^{1/2}),$$

we have that

$$\limsup_{s\uparrow\infty} \log(s)w_s^{-(K+1)(1-\eta)} F(w_s^\eta) = \lim_{s\uparrow\infty} \log(s) \log(2ps)^{(K+1)/(2\rho)} p\exp(-\log(2ps)^{1/2})$$

$$= p\lim_{s\uparrow\infty} \log(s)^{1+(K+1)/(2\rho)} \exp(-\log(s)^{1/2}).$$

Noting that $\log(\log(s)^{1+(K+1)/2\rho}) \in o(\log(s)^{1/2})$, independently of the value of K, we conclude that

$$\limsup_{s\uparrow\infty} \log(s)w_s^{-(K+1)(1-\eta)} F(w_s^\eta) = p\limsup_{s\uparrow\infty} \exp(-\log(s)^{1/2}) = 0.$$

Thus, the Assumption A.2 holds. Similarly, we can see that Assumption A.3 is satisfied since for our choice of K,

$$\limsup_{s\uparrow\infty} \log(s)w_s^{(K\delta-1)(1-\eta)} = \lim_{s\uparrow\infty} \log(s) \log(2ps)^{-(K\delta-1)/(2\rho)} = 0.$$

Now, we prove Lemma A.3.3. In the proof, we use the Landau notation $f \asymp g$ for $f \in O(g)$ and $g \in O(f)$.

Proof of Lemma A.3.3. To prove the statement for general $k \geqslant 0$, we show lower and upper bounds for $\sigma_s := sv_s$, defined via (**SCG**). Let us introduce the following notations:

$$\sigma_s^- := M^{-1} \log(s)^{1+1/\rho} \qquad \text{and} \qquad \sigma_s^+ := M \log(s)^{1+1/\rho},$$

for a suitable $M > 0$ chosen below.

Our goal is to show that for some $M > 0$ and all sufficiently large s, the largest solution σ_s of (**SCG**) lies in $\sigma_s^- < \sigma_s < \sigma_s^+$. For a fixed intensity s, Figure A.2 shows the right-hand side

$$L(s, \sigma) := s\,\mathbb{E}[(\sigma h(W))^k \exp(-\sigma h(W))]$$

of (**SCG**) as a function of σ compared to its left-hand side $k!$.
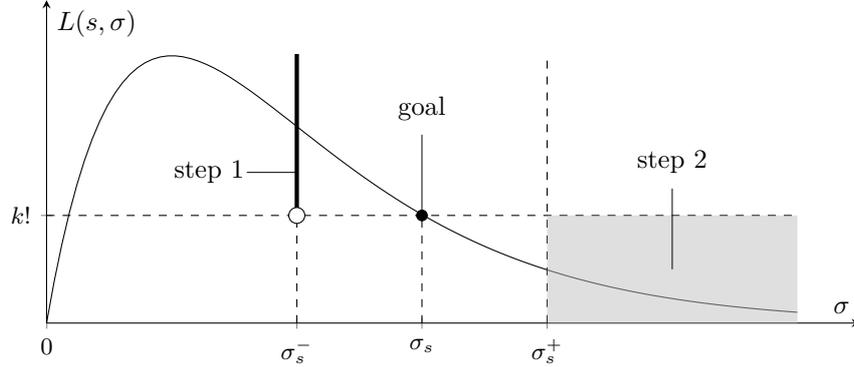
Figure A.2: The right-hand side $L(s, \sigma)$ of (**SCG**) as a function of σ in three intervals. In the first step of the proof, we show that $L(s, \sigma_s^-) > k!$ for large s. The second step proves that if s is large and $\sigma \geqslant \sigma_s^+$, then $L(s, \sigma) < k!$. Finally, we use the intermediate-value theorem to show that the largest solution of (**SCG**) must lie in the third interval.

To prove Lemma A.3.3, we use two steps.

(1) First, we show that $\lim_{s\uparrow\infty} L(s, \sigma_s^-) = \infty$.

(2) Next, we will see that $\lim_{s\uparrow\infty} \sup_{\sigma \geqslant \sigma_s^+} L(s, \sigma) = 0$.

These two steps conclude the proof. Indeed, we note that $\lim_{s\uparrow\infty} L(s, \sigma_s^-) > k!$ (Step (1)), while also $\lim_{s\uparrow\infty} \sup_{\sigma \geqslant \sigma_s^+} L(s, \sigma) < k!$ (Step (2)). As $L(s, \sigma)$ is a continuous function of σ, the intermediate-value theorem leads to the conclusion that for large s, there is at least one solution of (**SCG**) if $\sigma_s^- < \sigma < \sigma_s^+$. It also follows from Step (2) that we cannot have a solution if $\sigma \geqslant \sigma_+$. Thus, the largest solution σ_s must exist and lie in $\sigma_s^- < \sigma_s < \sigma_s^+$, thus proving the lemma.

Step (1). Let us first assume that $\sigma = \sigma_s^-$. Then, for every $K > 0$,

$$L(s, \sigma_s^-) = s\, \mathbb{E}\big[(\sigma_s^- h(W))^k \mathrm{e}^{-\sigma_s^- h(W)}\big] \geqslant s\, \mathbb{E}\big[\mathbb{1}\{\sigma_s^- h(W) \geqslant 1, W \leqslant Kw_s\}\mathrm{e}^{-\sigma_s^- h(W)}\big].$$

We choose K and M large enough such that $K^{-\rho} + 2M^{-1}K\mu_a < 1$. Since $w_s \to 0$ as $s \to \infty$, independently of the chosen K in the indicator function, we use again that $\lim_{w\downarrow 0} h(w)/w = \mu_a$ from of Lemma A.3.1 (3) to see that

$$\lim_{s\uparrow\infty} L(s, \sigma_s^-) \geqslant \lim_{s\uparrow\infty} s\, \mathbb{E}\big[\exp\big(-2\sigma_s^- W\mu_a\big) \mathbb{1}\{2/(\sigma_s^- \mu_a) \leqslant W \leqslant Kw_s\}\big]$$
$$\geqslant \lim_{s\uparrow\infty} s\exp\big(-2\sigma_s^- Kw_s\mu_a\big) \mathbb{P}\big(2/(\sigma_s^- \mu_a) \leqslant W \leqslant Kw_s\big).$$

We can simplify the above exponential by using the specific form of σ_s^- and w_s, which leads to

$$\exp\big(-2\sigma_s^- Kw_s\mu_a\big) = \exp\big(-2K\mu_a \log(s)^{1+1/\rho} \log(2ps)^{-1/\rho}/M\big) \asymp s^{-2M^{-1}K\mu_a},$$

where we also used that $\lim_{s\uparrow\infty}\log(s)/\log(2ps) = 1$. We can determine the probability for large s as

$$\mathbb{P}\big((\sigma_s^- \mu_a)^{-1} \leqslant W \leqslant Kw_s\big) \geqslant \mathbb{P}(W \leqslant Kw_s) - \mathbb{P}(W \leqslant Kw_s/2)$$
$$\asymp p(2ps)^{-K^{-\rho}} - p(2ps)^{-(K/2)^{-\rho}} \asymp s^{-K^{-\rho}}.$$

Thus, using these results, we deduce that

$$\lim_{s\uparrow\infty} L(s,\sigma_s^-) \geqslant \lim_{s\uparrow\infty} s^{1-K^{-\rho}-2M^{-1}K\mu_a} = \infty,$$

since our choice of K ensures $K^{-\rho} + 2M^{-1}K\mu_a < 1$.

Step (2).   Here, we have that

$$\limsup_{s\uparrow\infty}\ \sup_{\sigma\geqslant\sigma_s^+}\ L(s,\sigma) = \limsup_{s\uparrow\infty}\ \sup_{\sigma\geqslant\sigma_s^+}\ s\,\mathbb{E}\big[(\sigma h(W))^k \exp(-\sigma h(W))\big]$$
$$\leqslant \limsup_{s\uparrow\infty}\ \sup_{\sigma\geqslant\sigma_s^+}\ s\,\mathbb{E}\big[C\exp(-\sigma h(W)/2)\big]$$
$$\leqslant C\limsup_{s\uparrow\infty} s\,\mathbb{E}\big[\exp(-\sigma_s^+ h(W)/2)\big],$$

where $C := (2k)^k \exp(-k)$. For the right tail of the weight distribution when $W > b$, we estimate

$$\mathbb{E}\big[\exp(-\sigma_s^+ h(W)/2)\,\mathbb{1}\{W > b\}\big] \leqslant \exp(-\sigma_s^+ h(b)/2) = s^{-M\log(s)^{1/\rho}h(b)/2} \in o(s^{-2}),$$

where we used the monotonicity of $h(W)$ in the first step. Fixing $K > 0$ with $K^{-\rho} \geqslant 2$, we calculate the upper bound for the case when $W < Kw_s$ via

$$\mathbb{E}\big[\exp(-\sigma_s^+ h(W)/2)\,\mathbb{1}\{W < Kw_s\}\big] \leqslant \mathbb{P}(W < Kw_s),$$

where the choice of K, as we will see below, implies that the second term is negligible compared to the case when $W \in [Kw_s, b]$. Finally, for $W \in [Kw_s, b]$, we have $h(w) \geqslant w\mu_+(b)$, and therefore, since $w_s = \log(2ps)^{-1/\rho}$, choosing $M > 4/(K\mu_+(b))$ gives that

$$\mathbb{E}\big[\exp(-\sigma_s^+ h(W)/2)\,\mathbb{1}\{Kw_s \leqslant W \leqslant b\}\big] \leqslant \exp(-\sigma_s^+ Kw_s\mu_+(b)/2) \in o(s^{-2}).$$

We obtain that $\lim_{s\uparrow\infty} s\,\mathbb{E}[\exp(-\sigma_s^+ h(W)/2)] = 0$, as asserted. $\qquad\square$

A.4   Proofs

To apply the result Bobrowski et al. [16, Theorem 4.1], it is convenient to express the examined scale-free network via i.i.d. marked Poisson point processes. More precisely, we define

$$\xi[\omega; v] := \sum_{\boldsymbol{x}\in\omega} g_k(\boldsymbol{x},\omega;v)\delta_x \tag{A.5}$$

for locally finite ω in the suitable space $\Omega = \mathbb{R}^d \times [0,\infty) \times [0,1]^{\mathbb{Z}_{\geqslant 0}}$. Here $g_k(\boldsymbol{x},\omega;v)$ denotes the indicator that the node x is in H and has degree k in the graph $G(\omega;v)$.

We consider $\xi_s = \xi[\widetilde{\mathcal{P}}_s; v_s]$ where $\widetilde{\mathcal{P}}_s$ is a Poisson point process on Ω with intensity measure $\mathbb{K}_s(\mathrm{d}\boldsymbol{x}) = s\,\mathrm{d}x \otimes \mathbb{P}^W \otimes \mathrm{Leb}_{[0,1]}^{\otimes \mathbb{Z}_{\geqslant 0}}$. Based on the marks, we draw an edge between any two points $\boldsymbol{x} = (x, W_x, T_x)$ and $\boldsymbol{y} = (y, W_y, T_y)$ with $W_x < W_y$ if $T_y^{(i)} < p_s(x, W_x, y, W_y)$, where $i \geqslant 0$ is chosen such that x is the ith closest point to y within $\widetilde{\mathcal{P}}_s$. In words, similarly to [88], we encode the randomness associated with the existence of an edge (conditioned on the positions x, y and weights W_x, W_y of the endpoints) into an additional i.i.d. marking of the points, where the vertex with the larger mark makes the decision. The measure $\mathrm{Leb}_{[0,1]}^{\otimes \mathbb{Z}_{\geqslant 0}}$ then guarantees that any edge in the complete graph has an independent choice, using the fact that with probability one no two points have the same distance.

Now, we can break down the proof of our main theorem into two key steps: an approximation step and then the Poisson-convergence proof for the approximating process. As mentioned above, to employ [16, Theorem 4.1], we need to control certain bounding terms. However, due to the long-range correlations in the spatial random network, it is difficult to directly apply this result. Moreover, they are also not easily expressible in the usual framework of stopping sets from Bobrowski et al. [16]. Therefore, we work with suitable truncations in the weight space and the spatial domain. Thus, we consider the truncated point count

$$\hat{g}_k^c(\boldsymbol{x}, \omega; v) := g_k(\boldsymbol{x}, \omega \cap \Omega_{\geqslant W_x}; v)\,\mathbb{1}\{W_x < c\},$$

where $\Omega_{\geqslant W_x} = \mathbb{R}^d \times [W_x, \infty) \times [0,1]^{\mathbb{Z}_{\geqslant 0}}$. To spatially localize the edge count, let us introduce

$$\bar{g}_k^{V,c}(\boldsymbol{x}, \omega; v) = \hat{g}_k^c(\boldsymbol{x}, \omega \cap \Omega^V(x); v),$$

where $\Omega^V(x) = B_{(V/\nu_d)^{1/d}}(x) \times [0, \infty) \times [0,1]^{\mathbb{Z}}$. Here $\nu_d = |B_1(o)|$ and hence, the ball $B_{(V/\nu_d)^{1/d}}(x)$ with radius V/ν_d centered at x has volume V. We write $\Omega_{\geqslant a}^V(x) = \Omega^V(x) \cap \Omega_{\geqslant a}$ and consider the random variable

$$\bar{\xi}_s^{V_o, w} := \bar{\xi}_s^{V_o, w}[\widetilde{\mathcal{P}}_s; v_s] := \sum_{\boldsymbol{x} \in \widetilde{\mathcal{P}}_s} \bar{g}_k^{v_s W_x V_o, w}(\boldsymbol{x}, \widetilde{\mathcal{P}}_s; v_s)\delta_x,$$

where, we fix the cut-off $V_o(s) = w_s^{K(\eta-1)}$ for $\eta \in (0,1)$ and $K > 0$ satisfying the Assumptions A.1–A.3. The proof of Theorem A.2.2 is a direct consequence of the following two statements.

Proposition A.4.1 (Truncations are negligible)**.** *Under Assumptions A.1–A.3, we have that*

$$\lim_{s \uparrow \infty} d_{\mathsf{KR}}(\xi_s, \bar{\xi}_s^{V_o(s), w_s^\eta}) = 0.$$

Proposition A.4.2 (Poisson approximation)**.** *Under Assumptions A.1–A.3, we have that*

$$\lim_{s \uparrow \infty} d_{\mathsf{KR}}(\bar{\xi}_s^{V_o(s), w_s^\eta}, \zeta) = 0.$$

Before presenting the proofs of Propositions A.4.1 and A.4.2 in Sections A.4 and A.4, respectively, let us collect some supporting results that will be used multiple times later.

Supporting results

A key property of the considered model is that the expected typical degree conditioned on the typical weight W_o can be expressed in closed form. This is the content of the following auxiliary result from Deprez and Wüthrich [29, Lemma 4.1]. To make our presentation self-contained, we reproduce the short proof here. Let us introduce the notation $\boldsymbol{o} := (o, W_o, T_o)$ for the marked typical vertex. Furthermore, let $f \colon [0, \infty)^3 \to [0, \infty)$ be a measurable function. We define an f-weighted degree of a marked vertex $\boldsymbol{x}$ as

$$\deg_f(\boldsymbol{x}) := \sum_{\boldsymbol{y} \in \widetilde{\mathcal{P}}_s \,:\, \boldsymbol{y} \leftrightarrow \boldsymbol{x}} f(|B_{|x-y|}(o)|, W_x, W_y).$$

In particular, by choosing f as a suitable indicator, we can filter only those neighbors of x satisfying a desired property. To ease notation, we set

$$f^*(w_o, w) := \int_0^\infty f(uv_s\kappa(w_o, w), w_o, w)\varphi(u)\, \mathrm{d}u, \quad w_o, w > 0.$$

Lemma A.4.3 (Expected typical degree). *It holds that*

$$\mathbb{E}[\deg_f(\boldsymbol{o}) \mid W_o] = sv_s W_o\, \mathbb{E}\big[\mathbb{1}\{W \geqslant W_o\}W^a f^*(W_o, W) \mid W_o\big]$$
$$+ sv_s W_o^a\, \mathbb{E}\big[\mathbb{1}\{W \leqslant W_o\}W f^*(W_o, W) \mid W_o\big].$$

Before proving Lemma A.4.3, we discuss how to simplify it for specific choices of f. Recall that

$$h(W_o) = W_o\mu_+(W_o) + W_o^a\mu_-(W_o)$$
$$= W_o\, \mathbb{E}\big[\mathbb{1}\{W \geqslant W_o\}W^a \mid W_o\big] + W_o^a\, \mathbb{E}\big[\mathbb{1}\{W < W_o\}W \mid W_o\big].$$

Application A.4.4 (Degree of a typical vertex). *For $f \equiv 1$, we have that $f^*(w_o, w) = 1$ and hence,*

$$\mathbb{E}[\deg_f(\boldsymbol{o}) \mid W_o] = sv_s W_o\, \mathbb{E}\big[\mathbb{1}\{W \geqslant W_o\}W^a \mid W_o\big] + sv_s W_o^a\, \mathbb{E}\big[\mathbb{1}\{W \leqslant W_o\}W \mid W_o\big]$$
$$= sv_s\, \mathbb{E}[\kappa(W_o, W) \mid W_o] = sv_s W_o\mu_+(W_o) + sv_s W_o^a\mu_-(W_o).$$

Application A.4.5 (Outdegree of a typical vertex). *Since $f^*(w_o, w) = \mathbb{1}\{w \geqslant w_o\}$ for $f(u, w_o, w) = \mathbb{1}\{w \geqslant w_o\}$, we have that*

$$\mathbb{E}[\deg_f(\boldsymbol{o}) \mid W_o] = sv_s h(W_o) = sv_s W_o\mu_+(W_o).$$

Application A.4.6 (Finite-range truncation). *For $f(u, w_o, w) = \mathbb{1}\{u \geqslant V_o v_s w_o, w \geqslant w_o\}$, we have that $f^*(w_o, w) = \mathbb{1}\{w \geqslant w_o\} \int_{V_o/W^a}^\infty \varphi(u)\, \mathrm{d}u$, and hence,*

$$\mathbb{E}[\deg_f(\boldsymbol{o}) \mid W_o] = sv_s W_o\, \mathbb{E}\Big[\mathbb{1}\{W \geqslant W_o\}W^a \int_{V_o/W^a}^\infty \varphi(u)\, \mathrm{d}u \,\Big|\, W_o\Big]$$
$$\leqslant sv_s W_o\, \mathbb{E}\Big[W^a \int_{V_o/W^a}^\infty \varphi(u)\, \mathrm{d}u\Big].$$

We further bound the expression in Application A.4.6 using the fact that φ and $1 - F$ are assumed to be regularly varying with suitable indices.

Lemma A.4.7. *As $s \to \infty$, we have that*

$$\mathbb{E}\Big[W^a \int_{V_o/W^a}^\infty \varphi(u)\,\mathrm{d}u\Big] \in O(V_o^{(1-\alpha)/2}).$$

Proof. We first consider the simple case where $a = 0$. Then, Karamata's theorem [94, Theorem 0.6] implies that for large V_o we have that $\mathbb{E}[\deg_f(\boldsymbol{o})\,|\,W_o] \leqslant c_1 s v_s W_o V_o \varphi(V_o)$, for some constant $c_1 > 0$. Again, by the regular variation of φ, for all sufficiently large V_o, we have that $\varphi(V_o) \leqslant c_2 V_o^{-\alpha+(\alpha-1)/2}$.

For $a > 0$, we distinguish between the cases, where $V_o \leqslant MW^a$ and where $V_o > MW^a$, for some large $M > 0$. This allows us to bound the integral with respect to the function φ, and we obtain that

$$\mathbb{E}\Big[W^a \int_{V_o/W^a}^\infty \varphi(u)\,\mathrm{d}u\Big] \leqslant \mu_+((V_o/M)^{1/a}) + c_3 V_o\, \mathbb{E}\big[\mathbb{1}\{(V_o/M)^{1/a} \geqslant W\}\varphi(V_o/W^a)\big],$$

for some constant $c_3 > 0$. Let $\varepsilon \coloneqq (\alpha - 1)/2$. Then, the regular variation of φ implies that for a suitable $c_4 > 0$ we have

$$\int_0^{(V_o/M)^{1/a}} \varphi(V_o/w^a) F(\mathrm{d}w) \leqslant c_4 V_o^{-\alpha+\varepsilon} \int_0^{(V_o/M)^{1/a}} w^{a(\alpha-\varepsilon)} F(\mathrm{d}w)$$
$$\leqslant c_4 \mu_{a(\alpha-\varepsilon)} V_o^{-\alpha+(\alpha-1)/2},$$

where we also used that regularly varying functions can be bounded by polynomials with a slightly weaker exponent [see 94, Proposition 0.8]. On the other hand, we can express the first term using the ath moment of $W\,\mathbb{1}\{W \geqslant (V_0/M)^{1/a}\}$ as

$$\mu_+((V_o/M)^{1/a}) = \int_{(V_o/M)^{1/a}}^\infty w^a F(\mathrm{d}w)$$
$$= a \int_0^\infty r^{a-1}\, \mathbb{P}(W \geqslant \max\{r, (V_0/M)^{1/a}\})\,\mathrm{d}r.$$

Handling the cases $r \leqslant (V_0/M)^{1/a}$ and $r > (V_0/M)^{1/a}$ separately,

$$\mu_+((V_o/M)^{1/a}) = \frac{V_o}{M}\Big(1 - F((V_o/M)^{1/a})\Big) + a \int_{(V_o/M)^{1/a}}^\infty r^{a-1}(1 - F(r))\,\mathrm{d}r.$$

Since $1 - F$ is a regularly varying function with tail index β, we can bound $1 - F(r)$ by $c_5 r^{-\beta+a(\alpha-1)/2}$ for all suitably large r, where $c_5, c_6 > 0$ are constants:

$$\mu_+((V_o/M)^{1/a}) \leqslant c_5\Big(\frac{V_o}{M}\Big)^{1-\beta/a+(\alpha-1)/2} + c_5 a \int_{(V_o/M)^{1/a}}^\infty r^{a-1-\beta+a(\alpha-1)/2}\,\mathrm{d}r$$
$$= c_6 V_o^{1-(\beta-a(\alpha-1)/2)/a},$$

where we used again [94, Theorem 0.6 and Proposition 0.8]. Now, since $\beta > a\alpha$ we see that $1 - (\beta - a(\alpha - 1)/2)/a < (1 - \alpha)/2$, which finishes the proof. $\qquad\square$

After having discussed these specific applications, we now turn to the proof of Lemma A.4.3.

Proof of Lemma A.4.3. First, by Campbell's formula [66, Proposition 2.7],

$$\mathbb{E}[\deg_f(\boldsymbol{o}) \mid W_o] = s \int_{\mathbb{R}^d} \mathbb{E}\big[f(|B_{|x|}(o)|, W_o, W_x)p_s(o, W_o; x, W_x) \mid W_o\big]\, \mathrm{d}x.$$

Now, switching to spherical coordinates, substituting $u := v/(v_s \kappa(W_o, W))$, and applying Fubini's theorem yields

$$\begin{aligned}
\mathbb{E}[\deg_f(\boldsymbol{o}) \mid W_o] &= s \int_0^\infty \mathbb{E}\big[f(v, W_o, W)\varphi(v/(v_s\kappa(W_o, W))) \mid W_o\big]\, \mathrm{d}v \\
&= sv_s \int_0^\infty \mathbb{E}\big[\kappa(W_o, W)f(uv_s\kappa(W_o, W), W_o, W)\varphi(u) \mid W_o\big]\, \mathrm{d}u \\
&= sv_s W_o\, \mathbb{E}\Big[\mathbb{1}\{W \geqslant W_o\}W^a \int_0^\infty f(uv_s W_o W^a, W_o, W)\varphi(u)\, \mathrm{d}u \,\Big|\, W_o\Big] \\
&\quad + sv_s W_o^a\, \mathbb{E}\Big[\mathbb{1}\{W \leqslant W_o\}W \int_0^\infty f(uv_s W_o^a W, W_o, W)\varphi(u)\, \mathrm{d}u \,\Big|\, W_o\Big],
\end{aligned}$$

as asserted. $\qquad\square$

As an immediate application of the above discussion, we can prove Lemma A.2.1.

Proof of Lemma A.2.1. By the Mecke formula and reparametrization, we have

$$\begin{aligned}
\mathbb{E}[D_s] &= \mathbb{E}\Big[\sum_{\boldsymbol{x} \in \widetilde{\mathcal{P}}_s \cap H} \mathbb{1}\{\deg(\boldsymbol{x}) = k \text{ in } G(\widetilde{\mathcal{P}}_s, v_s)\}\Big] \\
&= s\, \mathbb{P}\big(\deg(\boldsymbol{o}) = k \text{ in } G(\widetilde{\mathcal{P}}_s, v_s)\big)|H| \\
&= s\, \mathbb{E}\Big[\frac{1}{k!}(sv_s h(W_o))^k \exp(-sv_s h(W_o))\Big]|H| = |H|,
\end{aligned}$$

where we also used that, given a fixed value of W_o, $\deg(\boldsymbol{o})$ is a Poisson random variable with parameter

$$\mathbb{E}[\deg(\boldsymbol{o}) \mid W_o] = s \int_{\mathbb{R}^d} \mathbb{E}[p_s(o, W_o; x, W_x) \mid W_o]\, \mathrm{d}x = sv_s h(W_o).$$

This finishes the proof. $\qquad\square$

Proof of Proposition A.4.1

Proof of Proposition A.4.1 Part 1: Mark approximation. We perform the proof in three steps.

Step 1. Before performing the main mark approximation, we neglect the largest marks. For this, let

$$\xi_s^c = \sum_{\boldsymbol{x} \in \widetilde{\mathcal{P}}_s} g_k^c(\boldsymbol{x}, \widetilde{\mathcal{P}}_s; v_s)\delta_x,$$

where $g_k^c(\boldsymbol{x}, \widetilde{\mathcal{P}}_s; v_s) := g_k(\boldsymbol{x}, \widetilde{\mathcal{P}}_s; v_s)\mathbb{1}\{W_x < c\}$ and c is such that $\mu_-(c) > 0$. Then, using that ξ_s and ξ_s^c are defined on the same probability space, Markov's inequality and the Mecke theorem,

$$d_{\mathsf{KR}}(\xi_s, \xi_s^c) \leqslant \mathbb{E}[d_{\mathsf{TV}}(\xi_s, \xi_s^c)] = \mathbb{E}[(\xi_s - \xi_s^c)(H)] \leqslant s\, \mathbb{E}[\psi^c(s)],$$

where $\psi^c(s) := \mathbb{1}\{W_o \geqslant c, \deg(o) = k \text{ in } G(\widetilde{\mathcal{P}}_s, v_s)\}$. Then, $s\,\mathbb{E}[\psi^c(s)] = \mathbb{E}[f_s^c(W_o)\,\mathbb{1}\{W_o \geqslant c\}]$, with

$$f_s^c(W_o) := \frac{s}{k!}\big(sv_s h(W_o)\big)^k \exp(-sv_s h(W_o)) \leqslant C_k s \exp(-sv_s h(W_o)/2),$$

where we used that $\sup\{x^k \exp(-x/2)\colon x \geqslant 0\} < \infty$. Now we can further bound,

$$s\exp(-sv_s h(W_o)/2)\,\mathbb{1}\{W_o \geqslant c\} \leqslant s\exp(-sv_s c^a \mu_-(c)/2) = s\exp\big(-sv_s w_s^\eta c_s/2\big),$$

with $c_s = c^a \mu_-(c)/w_s^\eta$. Note that $\lim_{s\uparrow\infty} c_s \geqslant 2$ since $w_s \to 0$ and, invoking Assumption A.1, $sv_s w_s^\eta \geqslant 2\log(s)$ for all sufficiently large s. Hence,

$$\lim_{s\uparrow\infty} s\exp(-sv_s c^a \mu_-(c)/2) \leqslant \lim_{s\uparrow\infty} s\exp(-2\log(s)) = 0.$$

Step 2. Following the same initial arguments as in Step 1, we now remove marks $W_o \geqslant w_s^\eta$. More precisely, we then have that $d_{\mathsf{KR}}(\xi_s^c, \xi_s^{w_s^\eta}) \leqslant \mathbb{E}[f_s(W_o)\,\mathbb{1}\{w_s^\eta \leqslant W_o < c\}]$, where

$$f_s(W_o) := \frac{s}{k!}\big(sv_s h(W_o)\big)^k \exp(-sv_s h(W_o)) \leqslant C_k s\exp(-sv_s h(W_o)/2).$$

Now, we bound slightly differently. For large values of s,

$$s\exp(-sv_s h(W_o)/2)\,\mathbb{1}\{w_s^\eta \leqslant W_o < c\} \leqslant s\exp(-sv_s w_s^\eta \mu_+(c)).$$

Again, using Assumption A.1, the right-hand side tends to zero as $s \to \infty$.

Step 3. We now come to the main mark-approximation step. We may bound, as above,

$$d_{\mathsf{KR}}(\xi_s^{w_s^\eta}, \hat{\xi}_s^{w_s^\eta}) \leqslant s\,\mathbb{E}\big[\psi(s)\big],$$

where $\hat{\xi}_s^{w_s^\eta} = \sum_{x\in\widetilde{\mathcal{P}}_s} \hat{g}_k^{w_s^\eta}(x, \widetilde{\mathcal{P}}_s; v_s)\delta_x$ and $\psi(s) = \psi_1(s)\,\mathbb{1}\{W_o < w_s^\eta\} + \psi_2(s)\,\mathbb{1}\{W_o < w_s^\eta\}$ with

$$\psi_1(s) := \mathbb{1}\{\deg(o) = k \text{ in } G(\widetilde{\mathcal{P}}_s^{\geqslant W_o}, v_s)\}\,\mathbb{1}\{\deg(o) > 0 \text{ in } G(\widetilde{\mathcal{P}}_s^{<W_o}, v_s)\}$$

$$\psi_2(s) := \mathbb{1}\{\deg(o) = k \text{ in } G(\widetilde{\mathcal{P}}_s, v_s)\}\,\mathbb{1}\{\deg(o) > 0 \text{ in } G(\widetilde{\mathcal{P}}_s^{<W_o}, v_s)\}.$$

Here, $\widetilde{\mathcal{P}}_s^{\geqslant W_o}$ denotes the Poisson point process $\widetilde{\mathcal{P}}_s$ restricted to points with marks $\geqslant W_o$. In words, $\psi(s)$ bounds the indicators of the two events that $\hat{\xi}_s^{w_s^\eta}$ contains a point not contained in $\xi_s^{w_s^\eta}$ and vice versa.

Using the fact that $\widetilde{\mathcal{P}}_s$ is an independent superposition of $\widetilde{\mathcal{P}}_s^{\geqslant W_o}$ and $\widetilde{\mathcal{P}}_s^{<W_o}$, we can use the Mecke formula to write $s\,\mathbb{E}[\psi_1(s)\,\mathbb{1}\{W_o < w_s^\eta\}] = \mathbb{E}[f_s^1(W_o)\,\mathbb{1}\{W_o < w_s^\eta\}]$, with

$$f_s^1(W_o) := \frac{s}{k!}\big(sv_s W_o \mu_+(W_o)\big)^k \exp(-sv_s W_o \mu_+(W_o))\big(1 - \exp(-sv_s W_o^a \mu_-(W_o))\big).$$

Now, under the event $\{W_o < w_s^\eta\}$, we have that $sv_s W_o^a \mu_-(W_o) \leqslant sv_s w_s^{(a+1)\eta} F(w_s^\eta)$, where we used Lemma A.3.1 (1) to upper bound $\mu_-(W_o)$. Next, we invoke Part 5

of Lemma A.3.1 to argue that $s v_s w_s^{(a+1)\eta} F(w_s^\eta) < w_s^{(a+1)\eta-1} \log(s) F(w_s^\eta)$. But, since $w_s^{(a+1)\eta-1} \leqslant w_s^{-(1-\eta)}$, we have that $w_s^{(a+1)\eta-1} \log(s) F(w_s^\eta) < w_s^{-(1-\eta)} \log(s) F(w_s^\eta)$. Now, we employ Assumption A.2 with an arbitrary value of $K > 0$ to conclude that

$$s v_s W_o^a \mu_-(W_o) \in o(1) \qquad \text{if } \{W_o < w_s^\eta\}. \tag{A.6}$$

Hence,

$$\mathbb{E}[f_s^1(W_o) \mid W_o] \leqslant \exp(s v_s w_s^{(a+1)\eta} F(w_s^\eta))(1 - \exp(-s v_s w_s^{(a+1)\eta} F(w_s^\eta))) \to 0.$$

For the second term ψ_2, we write $s \mathbb{E}[\psi_2(s) \mathbb{1}\{W_o < w_s^\eta\}] = \mathbb{E}[f_s^2(W_o) \mathbb{1}\{W_o < w_s^\eta\}]$, with

$$f_s^2(W_o) := s \sum_{\ell=1}^k \frac{1}{\ell!} (s v_s W_o^a \mu_-(W_o))^\ell \exp(-s v_s W_o^a \mu_-(W_o))$$

$$\times \frac{1}{(k-\ell)!} (s v_s W_o \mu_+(W_o))^{k-\ell} \exp(-s v_s W_o \mu_+(W_o))$$

$$= \frac{s}{k!} (s v_s h(W_o))^k \exp(-s v_s h(W_o)) \sum_{\ell=1}^k \binom{k}{\ell} \Big(\frac{W_o^a \mu_-(W_o)}{h(W_o)}\Big)^\ell \Big(\frac{W_o \mu_+(W_o)}{h(W_o)}\Big)^{k-\ell}.$$

Again, invoking (**SCG**), it suffices to show that

$$\sum_{\ell=1}^k \binom{k}{\ell} \Big(\frac{W_o^a \mu_-(W_o)}{h(W_o)}\Big)^\ell \Big(\frac{W_o \mu_+(W_o)}{h(W_o)}\Big)^{k-\ell} = 1 - \Big(\frac{W_o \mu_+(W_o)}{h(W_o)}\Big)^k$$

tends to zero, which is true by Lemma A.3.1 (4). □

Proof of Proposition A.4.1 Part 2: Reach approximation. We again invoke the Markov inequality and the Mecke formula to estimate,

$$d_{\mathsf{KR}}(\hat{\xi}_s^{w_s^\eta}, \bar{\xi}_s^{V_o(s), w_s^\eta}) \leqslant s \mathbb{E}[\psi'(s)],$$

where $\psi' = \psi_1' \mathbb{1}\{W_o < w_s^\eta\} + \psi_2' \mathbb{1}\{W_o < w_s^\eta\}$ with $E_s := B_{(v_s W_o V_o(s)/\nu_d)^{1/d}}(o)$ and

$$\psi_1'(s) := \mathbb{1}\Big\{\deg(o) = k \text{ in } G(\widetilde{\mathcal{P}}_s^{\geqslant W_o} \cap E_s, v_s)\Big\} \mathbb{1}\Big\{\deg(o) > 0 \text{ in } G(\widetilde{\mathcal{P}}_s^{\geqslant W_o} \cap E_s^c, v_s)\Big\}$$

$$\psi_2'(s) := \mathbb{1}\Big\{\deg(o) = k \text{ in } G(\widetilde{\mathcal{P}}_s^{\geqslant W_o}, v_s)\Big\} \mathbb{1}\Big\{\deg(o) > 0 \text{ in } G(\widetilde{\mathcal{P}}_s^{\geqslant W_o} \cap E_s^c, v_s)\Big\}.$$

Recall that we set $V_o(s) = w_s^{K(\eta-1)}$ for $\eta \in (0,1)$ and $K > 0$ and hence $\lim_{s \uparrow \infty} V_o(s) = \infty$. Note that, conditioned on W_o, the Poisson point processes $\widetilde{\mathcal{P}}_s^{\geqslant W_o} \cap E_s$ and $\widetilde{\mathcal{P}}_s^{\geqslant W_o} \cap E_s^c$ are independent and thus, $s \mathbb{E}[\psi_1'(s)] = \mathbb{E}[f_s'^1(W_o) \mathbb{1}\{W_o < w_s^\eta\}]$ with

$$f_s'^1(W_o) := \frac{s}{k!} (s v_s W_o \bar{\mu}_+(W_o, V_o(s)))^k \exp(-s v_s W_o \bar{\mu}_+(W_o, V_o(s)))$$
$$\times (1 - \exp(-s v_s W_o \bar{\mu}_-(W_o, V_o(s))))$$

where we used the notation

$$\bar{\mu}_+(W_o, V_o) := \mathbb{E}\Big[\mathbb{1}\{W \geqslant W_o\} W^a \int \mathbb{1}\{u \leqslant V_o/W^a\} \varphi(u) \, du \,\Big|\, W_o\Big] \quad \text{and}$$

$$\bar{\mu}_-(W_o, V_o) := \mathbb{E}\Big[\mathbb{1}\{W \geqslant W_o\} W^a \int \mathbb{1}\{u \geqslant V_o/W^a\} \varphi(u) \, du \,\Big|\, W_o\Big].$$

As before, we use the first part of f'^1_s to compensate for the coefficient s and the second part to achieve the convergence to zero. Using Lemma A.4.7, we upper bound $\bar{\mu}_-(W_o, V_o)$ as follows:

$$\bar{\mu}_-(W_o, V_o) \leqslant \mathbb{E}\Big[W^a \int_{V_o/W^a}^{\infty} \varphi(u)\,\mathrm{d}u\Big] \leqslant cV_0^{-\delta}$$

for some constant $c > 0$, where $\delta = (\alpha - 1)/2$. Noting that $W_o\bar{\mu}_+(W_o, V_o(s)) \leqslant h(W_o)$ we have

$$f'^1_s(W_o) \leqslant \frac{s}{k!}\big(sv_s h(W_o)\big)^k \exp(-sv_s h(W_o)) \exp\Big(sv_s w_s^{\eta}\big(cw_s^{K(1-\eta)\delta} + w_s^{a\eta}F(w_s^{\eta})\big)\Big)$$
$$\times \Big(1 - \exp\big(-csv_s w_s^{\eta + K(1-\eta)\delta}\big)\Big),$$

where we used that, employing Lemmas A.3.1 and A.4.7,

$$h(W_o) - W_o\bar{\mu}_+(W_o, V_o) = W_o\bar{\mu}_-(W_o, V_o) + W_o^a\mu_-(W_o) \leqslant cW_oV_o^{-\delta} + W_o^{a+1}F(W_o).$$

Arguing as in the third step of the mark-approximation proof above, by (A.6), we have that $\exp(sv_s w_s^{(a+1)\eta})F(w_s^{\eta}) \to 1$, and hence, using (**SCG**),

$$\mathbb{E}[f'^1_s(W_o) \mid W_o] \leqslant C\exp\big(csv_s w_s^{\eta + K(1-\eta)\delta}\big)\Big(1 - \exp\big(-csv_s w_s^{\eta + K(1-\eta)\delta}\big)\Big).$$

To see that $sv_s w_s^{\eta + K(1-\eta)\delta} \in o(1)$, we invoke again Lemma A.3.1 (3) and Assumption A.3 to see that for some $c' > 0$,

$$sv_s w_s^{\eta + K(1-\eta)\delta} \leqslant c'\log(s)w_s^{\eta + K(1-\eta)\delta - 1} \to 0.$$

For ψ'_2, we can argue similarly to the second error term in Step 3 of the proof of the mark approximation. More precisely, we have $s\,\mathbb{E}[\psi'_2(s)\mathbb{1}\{W_o < w_s^{\eta}\}] = \mathbb{E}[f'^2_s(W_o)\mathbb{1}\{W_o < w_s^{\eta}\}]$ with $f'^2_s(W_o)$ defined as

$$s\sum_{\ell=1}^{k}\frac{1}{\ell!}\big(sv_s W_o\bar{\mu}_-(W_o, V_o(s))\big)^{\ell}\exp(-sv_s W_o\bar{\mu}_-(W_o, V_o(s)))$$
$$\times \frac{1}{(k-\ell)!}\big(sv_s W_o\bar{\mu}_+(W_o, V_o(s))\big)^{k-\ell}(1 - \exp(-sv_s W_o\bar{\mu}_+(W_o, V_o(s))))$$
$$= \frac{s}{k!}\big(sv_s W_o\mu_+(W_o)\big)^k e^{-sv_s W_o\mu_+(W_o)}\sum_{\ell=1}^{k}\binom{k}{\ell}\Big(\frac{\bar{\mu}_-(W_o, V_o(s))}{\mu_+(W_o)}\Big)^{\ell}\Big(\frac{\bar{\mu}_+(W_o, V_o(s))}{\mu_+(W_o)}\Big)^{k-\ell}$$
$$\leqslant \frac{Cs}{k!}\big(sv_s h(W_o)\big)^k e^{-sv_s h(W_o)}e^{sv_s w_o^{(a+1)\eta}F(w_s^{\eta})}\Big[1 - \Big(\frac{\bar{\mu}_+(W_o, V_o(s))}{\mu_+(W_o)}\Big)^k\Big].$$

Again, using (**SCG**) and (A.6), it suffices to show that, under the event $W_o < w_s^{\eta}$,

$$\frac{\bar{\mu}_-(W_o, V_o(s))}{\bar{\mu}_+(W_o, V_o(s))} \leqslant \frac{\mathbb{E}\Big[W^a \int_{V_o(s)/W^a}^{\infty}\varphi(u)\,\mathrm{d}u\Big]}{\mathbb{E}\Big[W^a \mathbb{1}\{W \geqslant w_s^{\eta}\}\int_0^{V_o(s)/W^a}\varphi(u)\,\mathrm{d}u\Big]} \in o(1).$$

This is true since, first for the numerator, for all u, we have $\mathbb{E}[W^a \mathbb{1}\{W^a \geqslant V_o(s)/u\}] \leqslant \mu_a$ and also $\lim_{s\uparrow\infty} \mathbb{E}[W^a \mathbb{1}\{W^a \geqslant V_o(s)/u\}] = 0$ and thus, using dominated convergence,

$$\lim_{s\uparrow\infty} \mathbb{E}\Big[W^a \int_{V_o(s)/W^a}^\infty \varphi(u)\,\mathrm{d}u\Big] = \int_0^\infty \varphi(u)\, \mathbb{E}\Big[W^a \mathbb{1}\{W^a \geqslant V_o(s)/u\}\Big]\,\mathrm{d}u = 0.$$

On the other hand, for the denominator, for all u, we have $\mathbb{E}[W^a \mathbb{1}\{W \geqslant w_s^\eta\} \mathbb{1}\{W^a \leqslant V_o(s)/u\}] \leqslant \mu_a$ and $\lim_{s\uparrow\infty} \mathbb{E}[W^a \mathbb{1}\{W \geqslant w_s^\eta\} \mathbb{1}\{W^a \leqslant V_o(s)/u\}] = \mu_a$ and thus, again by dominated convergence,

$$\lim_{s\uparrow\infty} \mathbb{E}\Big[W^a \int_{V_o(s)/W^a}^\infty \varphi(u)\,\mathrm{d}u\Big] = \int_0^\infty \varphi(u)\, \mathbb{E}\Big[W^a \mathbb{1}\{W^a \geqslant V_o(s)/u\}\Big]\,\mathrm{d}u = \mu_a.$$

This finishes the proof. $\qquad\square$

Proof of Proposition A.4.2

To prove Proposition A.4.2, we employ [16, Theorem 4.1]. To express the considered functional in the framework of [16, Theorem 4.1], we first introduce additional notation. To each point $\boldsymbol{x}$ we associate a deterministic compact set $S^V(\boldsymbol{x})$ from which the score function of interest can be computed with high probability. In addition to $S^V(\boldsymbol{x})$, [16, Theorem 4.1] also allows for the use of a more refined localization set $\mathcal{S}(\boldsymbol{x}, \omega)$, which may be random in general. In the current setting, we do not require this additional flexibility, as we have already implemented a truncation step the beginning of Section A.4. Therefore, we set $\mathcal{S}(\boldsymbol{x}, \omega) \coloneqq S^V(\boldsymbol{x}) \coloneqq B_{(v_s W_x V/\nu_d)^{1/d}}(x)$, to be the ball of volume $v_s W_x V$ around x.

Then, [16, Theorem 4.1] bounds the KR-distance between the process of interest and a Poisson point process by a sum of four quantities. The first of them is the total variation between the corresponding intensity measures. The remaining three quantities, denoted by E_1, E_2, E_3, concern higher-order deviations. Note that, since we choose $\mathcal{S}(\boldsymbol{x}, \omega) = S^V(\boldsymbol{x})$, the E_1 term is identically 0. Hence, we formally state three remaining separate auxiliary results, Lemmas A.4.8–A.4.11 below. The proofs follow afterward.

We begin with the intensity measures. By the homogeneity of the approximations, the intensity measure $L_s(\mathrm{d}x)$ of $\bar{\xi}_s^{V_o(s), w_s^\eta}$ has the constant Lebesgue density $\int_\Omega \mathbb{E}[\bar{g}_k^{V_o(s), w_s^\eta}(\boldsymbol{x}, \widetilde{\mathcal{P}}_s)]\mathbb{K}_s(\mathrm{d}\boldsymbol{x})$, where $\bar{g}_k^{V_o(s), w_s^\eta} \equiv \bar{g}_k^{v_s W_x V_o(s), w_s^\eta}$ for brevity.

Lemma A.4.8 (Convergence of intensity measures)**.** *Under Assumptions A.1–A.3, we have that*

$$\lim_{s\uparrow\infty} d_{\mathsf{TV}}(L_s, \mathrm{Leb}) = 0. \tag{A.7}$$

Proof. First, note that

$$\begin{aligned}
d_{\mathsf{TV}}(L_s, \mathrm{Leb}) &\leqslant \Big|\int_\Omega \mathbb{E}[\bar{g}_k^{V_o(s), w_s^\eta}(\boldsymbol{x}, \widetilde{\mathcal{P}}_s)]\beta K_s(\mathrm{d}\boldsymbol{x}) - 1\Big| \\
&\leqslant \int_\Omega \mathbb{E}\big[|\bar{g}_k^{V_o(s), w_s^\eta}(\boldsymbol{x}, \widetilde{\mathcal{P}}_s) - g_k(\boldsymbol{x}, \widetilde{\mathcal{P}}_s)|\big]\beta K_s(\mathrm{d}\boldsymbol{x}) \\
&\leqslant s\, \mathbb{E}\big[|\bar{g}_k^{V_o(s), w_s^\eta}(\boldsymbol{o}, \widetilde{\mathcal{P}}_s) - g_k(\boldsymbol{o}, \widetilde{\mathcal{P}}_s)|\,|\,W_o\big],
\end{aligned}$$

where we used Lemma A.2.1 and the Mecke formula. Step-by-step reintroducing the mark- and reach approximations, we see that

$$s\mathbb{E}^o\big[|\bar{g}_k^{V_o(s),w_s^\eta}(\boldsymbol{o},\widetilde{\mathcal{P}}_s) - g_k(\boldsymbol{o},\widetilde{\mathcal{P}}_s)|\big] \leqslant s\mathbb{E}^o[\psi^c(s) + \psi(s) + \psi'(s)],$$

where the right-hand side tends to zero as s tends to infinity using the same arguments as in the proof of Proposition A.4.1. $\qquad\square$

As described above, the following statement is immediate.

Lemma A.4.9 (Convergence of E_1). *We have that*

$$\lim_{s\uparrow\infty}\int_\Omega \mathbb{E}\Big[\mathbb{1}\{\mathcal{S}(\boldsymbol{x},\widetilde{\mathcal{P}}_s) \not\subseteq S^{V_o(s)}(\boldsymbol{x})\}\bar{g}_k^{V_o(s),w_s^\eta}(\boldsymbol{x},\widetilde{\mathcal{P}}_s)\Big]\mathbb{K}_s(\mathrm{d}\boldsymbol{x}) = 0. \qquad (A.8)$$

Here are the remaining requirements.

Lemma A.4.10 (Convergence of E_2). *If Assumption A.2 holds, then we have that*

$$\lim_{s\uparrow\infty}\int_{\Omega^2} \mathbb{1}\{S^{V_o(s)}(\boldsymbol{x}) \cap S^{V_o(s)}(\boldsymbol{z}) \neq \varnothing\} \tag{A.9}$$
$$\times \mathbb{E}\big[\bar{g}_k^{V_o(s),w_s^\eta}(\boldsymbol{x},\widetilde{\mathcal{P}}_s)\big]\,\mathbb{E}\big[\bar{g}_k^{V_o(s),w_s^\eta}(\boldsymbol{z},\widetilde{\mathcal{P}}_s)\big]\mathbb{K}_s(\mathrm{d}\boldsymbol{z})\mathbb{K}_s(\mathrm{d}\boldsymbol{x}) = 0.$$

Proof. By symmetry, we can insert $2\,\mathbb{1}\{W_z \geqslant W_x\}$. Then, under this event,

$$\mathbb{1}\{S^{V_o(s)}(\boldsymbol{x}) \cap S^{V_o(s)}(\boldsymbol{z}) \neq \varnothing\} \leqslant \mathbb{1}\{x \in B_{2(v_s V_o(s)W_z/\nu_d)^{1/d}}(z)\},$$

and hence, also using that $W_z \leqslant w_s^\eta$ and translation invariance, the integral on the left-hand side of (A.9) is bounded from above by

$$2^d v_s w_s^\eta V_o(s)\,\mathbb{E}[s\bar{g}_k^{V_o(s),w_s^\eta}(\boldsymbol{o},\widetilde{\mathcal{P}}_s)]^2,$$

where $\lim_{s\uparrow\infty}\mathbb{E}[s\bar{g}_k^{V_o(s),w_s^\eta}(\boldsymbol{o},\widetilde{\mathcal{P}}_s)] = 1$ by Lemma A.4.8. Hence, using $1 \leqslant 2sF(w_s^\eta)$ and Lemma A.3.1 (5) we have for some $c > 0$,

$$v_s w_s^{\eta - K(1-\eta)} \leqslant c\log(s)w_s^{-(K+1)(1-\eta)}F(w_s^\eta),$$

which by Assumption A.2 tends to zero as $s \to \infty$. $\qquad\square$

Lemma A.4.11 (Convergence of E_3). *Under Assumption A.2, we have that*

$$\lim_{s\uparrow\infty}\int_{\Omega^2} \mathbb{1}\{S^{V_o(s)}(\boldsymbol{x}) \cap S^{V_o(s)}(\boldsymbol{z}) \neq \varnothing\} \tag{A.10}$$
$$\times \mathbb{E}\big[\bar{g}_k^{V_o(s),w_s^\eta}(\boldsymbol{x},\widetilde{\mathcal{P}}_s \cup \{\boldsymbol{z}\})\bar{g}_k^{V_o(s),w_s^\eta}(\boldsymbol{z},\widetilde{\mathcal{P}}_s \cup \{\boldsymbol{x}\})\big]\mathbb{K}_s(\mathrm{d}\boldsymbol{z})\mathbb{K}_s(\mathrm{d}\boldsymbol{x}) = 0.$$

Proof. Again, by symmetry, we may insert the indicator of the event $\mathbb{1}\{W_z \leqslant W_x\}$, to obtain $\mathbb{1}\{S^{V_o(s)}(\boldsymbol{x}) \cap S^{V_o(s)}(\boldsymbol{z}) \neq \varnothing\} \leqslant \mathbb{1}\{x \in B_{2(v_s V_o(s)W_x/\nu_d)^{1/d}}(z)\}$. The important observation is that $\bar{g}_k^{V_o(s),w_s^\eta}(\boldsymbol{x},\widetilde{\mathcal{P}}_s \cup \{\boldsymbol{z}\})$ only takes into account nodes with weight

exceeding W_x and therefore the point $\boldsymbol{z}$ can be neglected. As $W_z \leqslant w_s^\eta$, the integral in the left-hand side of (A.10) is bounded above by

$$2F(w_s^\eta) \int_{\Omega^2} \mathbb{1}\{S^{V_o(s)}(\boldsymbol{x}) \cap S^{V_o(s)}(\boldsymbol{z}) \neq \varnothing\} \, \mathbb{E}[\bar{g}_k^{V_o(s),w_s^\eta}(\boldsymbol{x},\widetilde{\mathcal{P}}_s)] \mathbb{K}_s(\mathrm{d}\boldsymbol{z}) \mathbb{K}_s(\mathrm{d}\boldsymbol{x})$$

$$\leqslant 2F(w_s^\eta) \int_{\Omega^2} \mathbb{1}\{x \in B_{2(v_s V_o(s) w_s^\eta)^{1/d}}(z)\} \, \mathbb{E}[\bar{g}_k^{V_o(s),w_s^\eta}(\boldsymbol{x},\widetilde{\mathcal{P}}_s)] \mathbb{K}_s(\mathrm{d}\boldsymbol{z}) \beta K_s(\mathrm{d}\boldsymbol{x})$$

$$\leqslant 4s v_s w_s^\eta V_o(s) F(w_s^\eta) \, \mathbb{E}[s \bar{g}_k^{V_o(s),w_s^\eta}(\boldsymbol{o},\widetilde{\mathcal{P}}_s)],$$

where $\lim_{s\uparrow\infty} \mathbb{E}[s\bar{g}_k^{V_o(s),w_s^\eta}(\boldsymbol{o},\widetilde{\mathcal{P}}_s)] = 1$ by Lemma A.4.8. For this, invoking again Lemma A.3.1 (5), we have for some $c > 0$

$$s v_s w_s^{\eta - K(1-\eta)} F(w_s^\eta) \leqslant c \log(s) w_s^{-(K+1)(1-\eta)} F(w_s^\eta),$$

which by Assumption A.2 tends to 0 as $s \to \infty$. $\qquad\square$

Paper B

On the topology of higher-order age-dependent random connection models

Christian Hirsch and Péter Juhász

Abstract: In this paper, we investigate the potential of the age-dependent random connection model (ADRCM) to represent higher-order networks. A key contribution of our work is the derivation of probabilistic limit results in large domains. More precisely, we first prove that the higher-order degree distributions have a power-law tail. Second, we establish central limit theorems for the edge counts and Betti numbers of the ADRCM in the regime where the degree distribution is light-tailed. Moreover, in the heavy-tailed regime, we prove that asymptotically, the recentered and suitably rescaled edge counts converge to a stable distribution. We also propose a modification of the ADRCM in the form of a thinning procedure that enables independent adjustment of the power-law exponents for vertex and edge degrees. To apply the derived theorems to finite networks, we conduct a simulation study illustrating that the power-law degree distribution exponents approach their theoretical limits for large networks. It also indicates that in the heavy-tailed regime, the limit distribution of the recentered and suitably rescaled Betti numbers is stable. We demonstrate the practical application of the theoretical results to real-world datasets by analyzing scientific collaboration networks based on data from arXiv.

B.1 Introduction

In recent decades, the field of complex networks has emerged as a powerful framework for analyzing systems whose properties cannot be understood by studying their parts in isolation. The human brain, collaboration among researchers, the interaction of chemical elements, technological infrastructures, or the evolution of species are some examples of complex systems in which studying the relationships between the parts is inevitable [6, 53]. For instance, a collaboration network of scientists based on data from arXiv is illustrated in Figure B.1, where vertices represent authors of publications and a simplex represents each document.

In addition to a descriptive approach, it is often desirable to develop a stochastic model for generating synthetic networks. The key advantage of creating such a stochastic model representation is that it enables a more refined analysis and a tool to understand properties of a complex system more deeply. Through this approach, it becomes feasible to reveal effects that remain hidden in an actual dataset, particularly if its size is not large enough. For an excellent discussion on complex network models as null models, we also refer the reader to van der Hofstad et al. [103].

The traditional approach to modeling complex systems relies on binary networks, where vertices represent the parts of the system, and the connections between them define their relationships. At the turn of the century, the field of complex networks experienced a rapid growth due to the insight that networks occurring in a wide variety of disciplines share a common set of key characteristics.

In their seminal work, Barabási and Albert [3] discovered that many key empirical features of complex networks are explained by a surprisingly simple *preferential attachment model*. Loosely speaking, it provides mathematical precision to the idea that many real networks emerge through a *rich-get-richer* mechanism. In addition to the broad impact of network science in various application domains, complex networks have also become the subject of intense research activity in mathematics, where rigorous mathematical proofs have been provided for many of the effects previously empirically identified in network science [102]. In particular, the analysis of large
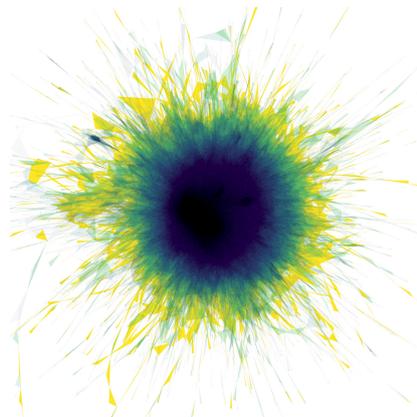
Figure B.1: The largest component of a higher-order network of scientists

preferential attachment models has become a highly fruitful research topic leading to results such as the limiting distributions of various network characteristics [30, 31].

One of the shortcomings of the standard preferential attachment models is that they lead to tree-like structures, thus failing to reproduce the clustering property observed in real-world networks. To address this issue, among others, spatial variants of the preferential attachment models have been proposed [57, 58]. Here, the network nodes are embedded in Euclidean space, allowing the preferential-attachment rule to take spatial positions into account. While the embedding produces the desired clustering effects, it complicates the mathematical analysis. Subsequently, it was realized by Gracar et al. [40] that a simplified construction rule could also realize the decisive scale-free and clustering properties of the spatial preferential attachment mechanism. In the *age-dependent random connection model (ADRCM)*, the connection probability to an existing vertex now depends on the age rather than the in-degree of that vertex. In particular, knowing the age of a vertex does not require any information on the network structure in the neighborhood of that vertex. This provides a significantly greater degree of spatial independence, which substantially simplifies many mathematical derivations. Later, Komjáthy and Lodewijks [64], Gracar et al. [42] described a more general framework for incorporating weights into the connection mechanism.

As traditional network analysis was designed to study pairwise relationships between entities, simple network models are not capable of modeling higher-order interactions involving more than two entities. The study of higher-order network models has recently gained special attention due to its ability to capture these multibody relationships that a simple network model cannot handle. Among others, the need for higher-order relationships arises in scientific collaboration networks. Beyond collaboration networks, the study of group relationships can already explain several phenomena, such as the synchronization of neurons or the working mechanism of supply chain routes [108].

We model higher-order networks using simplicial complexes, which generalizes a graph to represent group interactions among more than two entities. In this framework, relationships are represented by simplices of various dimensions. For example, a 0-simplex is a vertex, a 1-simplex is an edge, a 2-simplex is a triangle representing a three-way relationship, and in general, a k-simplex corresponds to a set of $k + 1$ interconnected vertices. The key benefit of modeling higher-order networks with simplicial complexes is that we can describe the networks using tools from topological data analysis (TDA), which provide further insights compared to those of traditional graph-theoretic analysis. This form of analysis was carried out in several studies [2, 20, 83, 90].

While these studies investigate different datasets and rely on different TDA tools to analyze them, none of these works proposes a mathematical model to represent such higher-order networks. Previously, Fountoulakis et al. [37] considered a stochastic model for higher-order complex networks. However, as this model relies on a form of preferential attachment mechanism, even deriving the asymptotic degree distribution is highly involved. In contrast, since the ADRCM relies on a far simpler connection mechanism, we can derive results in the present paper that are substantially more refined than those based on the degree distribution.

The main contributions of the present work are as follows:

(1) We begin by rigorously proving that the higher-order degree distributions follow a power law.

(2) As a basis for hypothesis tests, we provide central limit theorems (CLTs) and stable limit theorems for the edge count and Betti numbers.

(3) Recognizing the limitations of the ADRCM, we propose a model extension of the ADRCM capable of matching both any given admissible vertex- and edge-degree exponents.

(4) Since these results are proved in the limit for large networks, we support the validity of these results for finite-size networks through conducting a simulation study.

(5) Showing the convergence of the related quantities for finite-size networks, we proceed by developing statistical tests for finite networks based on the number of triangles and the Betti numbers for different parameter regimes.

(6) Finally, we illustrate the use of these hypothesis tests for analyzing real-world collaboration networks.

We now expand on the above points in more detail, referring to Section B.2 for further information.

As discussed earlier, the ADRCM stands out as an appealing model due to its ability to replicate key features—power-law distributed vertex degrees and a high clustering coefficient—observed in real-world complex networks, while also being mathematically tractable. In light of this, our approach utilizes the ADRCM as a foundation and endows it with a higher-order structure by forming the *clique complex*. That is, the simplices in this complex are the cliques of the underlying graph. A set of $k+1$ vertices forms a k-simplex if and only if it is a k-clique, i.e., if and only if there is an edge between every pair of the $k+1$ vertices.

While for binary networks, the degree distribution is arguably the most fundamental characteristic, for higher-order networks, it is essential to understand also higher-order adjacencies. Hence, to extend the concept of degree distributions to higher-order networks, we draw upon the idea of *generalized degrees* introduced by Bianconi and Rahmede [11]. For $m' \geqslant m$, one considers the distribution of the number of m'-simplices containing a typical m-simplex as a face. For instance, the standard vertex degree corresponds to the scenario where $(m, m') = (0, 1)$. One of the fundamental findings by Gracar et al. [40] is that in the ADRCM, the vertex-degree distribution satisfies a power law. As another example, for $(m, m') = (1, 2)$ the *edge degree* counts the number of triangles adjacent to a given edge. In Theorem B.2.1, we show that the generalized degrees also adhere to a power-law distribution. Furthermore, we relate the exponents of the higher-order degree distribution to the exponent governing the vertex-degree distribution. We pay special attention to the edge-degree distribution, since the formation of triangles in complex spatial networks is also of high interest for determining the clustering coefficient, as explored by van der Hofstad et al. [103, 104].

In our second main result, we find that the distribution of the recentered and rescaled edge count in the ADRCM converges to a normal distribution for light-tailed degree distribution and to a stable distribution for heavy-tailed degree distributions (Theorems B.2.3 and B.2.4). Based on our simulation study, we conjecture that these asymptotic results can be extended to higher-dimensional simplices.

Next, turning our focus to the features relevant in TDA, we continue with the analysis of the distribution of the *Betti numbers* of the clique complexes generated by the ADRCM. Betti numbers are topological invariants that quantify the number of *holes* in different dimensions within a simplicial complex, which describe the higher-order connectivity of a network:

- the 0th Betti number β_0 counts the number of connected components;

- the 1st Betti number β_1 is the number of independent loops in the network;

- the 2nd Betti number β_2 captures the number of voids enclosed by triangular faces.

Higher Betti numbers continue this pattern, corresponding to higher-dimensional *holes*. Siu et al. [98] derived asymptotic expressions for the growth rate of the expected Betti numbers in non-spatial preferential attachment models. In contrast, the focus of our study is on the fluctuations around the expectation, enabling the application of hypothesis tests. In Theorem B.2.2, we prove a CLT for the Betti numbers if the degree distribution is sufficiently light-tailed. We also conjecture that for other values of the model parameters, the distribution of Betti numbers follows a stable distribution. Again, this hypothesis gains credibility through the results of our simulation study, supporting the above conjecture.

By analyzing the empirical distributions within the arXiv dataset, we find that the relationship between the exponents governing vertex and edge degrees, as stated in Theorem B.2.1, is too rigid to be applicable in real-world scenarios. To address this limitation, we present a model extension that provides greater flexibility to the original ADRCM by introducing a new parameter. The primary challenge in establishing this result is to ensure that we can independently adjust the edge-degree exponent while maintaining the vertex-degree exponent. More precisely, we proceed as follows: First, we adjust the original parameters of the ADRCM to increase both the vertex- and edge-degree exponents, so that the edge-degree exponent reaches the desired value. Then, we apply a dependent thinning operation involving the random removal of a fraction of certain edges that do not affect the edge-degree exponent, but which decrease the vertex-degree exponent. These steps lead to the desired greater flexibility between vertex and edge degrees formalized in Theorem B.2.5.

Our theoretical results presented above hold in the limit for extensive networks. For applications to real data, we accompany our theoretical results with a simulation study.

- First, we explore the finite-size effects on higher-order degree distributions by examining the rate of convergence of the degree distribution exponents to their theoretical limits. We observe that the fluctuations of the exponents around

their theoretical values decrease as the network size increases. The simulations also reveal that apart from their fluctuations, the exponents have a bias due to the finite size. An interesting aspect of the simulation study is that, through Palm theory, we can simulate typical simplices in infinite networks that are free from finite-size effects.

- Simulating three sets of networks with different model parameters, we validate our theoretical results regarding the edge-count distributions. Furthermore, we also estimate the parameters of the distributions that are not explicitly derived in the theorems. Finally, we discover the finite-size effects that are the most prominent in certain boundary cases.

- As for the exploration of the edge-count distribution, we conduct a similar analysis for the Betti numbers. This analysis supports our conjectures concerning the stable distribution of Betti numbers.

Next, we demonstrate the application of the theorems to four real-world collaboration networks of scientists based on arXiv data. After a general exploratory analysis, we analyze the vertex- and edge-degree distribution exponents.

Based on the fitted vertex-degree exponents of the datasets, we fix the model parameters to use the ADRCM for further analysis of collaboration networks. These fitted parameters guarantee that the vertex-degree exponent and the edge count are modeled correctly. Thus, instead of the edge count, we conduct hypothesis tests based on the triangle count, where the null hypothesis is that the ADRCM well describes the dataset. Similar tests are also conducted for the Betti numbers.

The results of the hypothesis tests reveal that the topological structure of scientific collaboration networks is highly complex. In particular, an elementary two-parameter model, such as the ADRCM, is not enough to capture all aspects of higher-order networks.

The rest of the manuscript is organized as follows. Section B.2 presents our main theoretical results regarding higher-order networks generated by extending the ADRCM model to a clique complex. Sections B.3, B.4, B.5, B.6 contain the proofs of the theorems stated in Section B.2. Section B.7 details the simulation study to demonstrate the validity of the asymptotic results discussed in Section B.2 for finite networks. Section B.8 illustrates the application of the ADRCM model to higher-order networks of scientific collaborations. Lastly, Section B.9 provides a summary and outlines ideas for future research directions.

B.2 Model and main results

The higher-order network model discussed in this paper is an extension of the ADRCM, which we recall here for the reader's convenience. In this network model, vertices arrive according to a Poisson process and are placed uniformly at random in the Euclidean space. Two vertices are connected with a probability given by the profile function, which is a function of the distance and the ages of the vertices.

As justified below, we restrict our attention to the special case of latent Euclidean dimension $d = 1$ and profile function $\varphi(r) := \mathbb{1}\{r \in [0, 1]\}$. Let $\mathcal{P} := \{P_i\} := \{(X_i, U_i)\}_{i \geqslant 1}$ be a unit-intensity Poisson point process on $\mathbb{R} \times (0, 1]$, let $\beta > 0$ and $\gamma \in (0, 1)$. Then, for $(x, u), (y, v) \in \mathbb{R} \times (0, 1]$ with $u \leqslant v$, there is an edge from (y, v) to (x, u), in symbols $(y, v) \to (x, u)$, if and only if

$$|x - y| \leqslant \tfrac{\beta}{2} u^{-\gamma} v^{-(1-\gamma)},$$

where $\beta > 0$ is a parameter governing the edge density. We henceforth denote this network by $G := G(\mathcal{P})$.

We stress that the framework developed by Gracar et al. [40] allows treating arbitrary dimensions and far more general connection functions. However, the results by Gracar et al. [40], van der Hofstad et al. [104] indicate that many of the key network properties, such as the scaling of the vertex degrees or the clustering coefficient, depend neither on the dimension nor the connection function. We expect that a similar observation holds for higher-order characteristics; therefore, we decided to work with the simplest form of the ADRCM, which significantly reduces the level of technicality in the presentation of the proofs.

While G determines the binary vertex interactions, in many applications, higher-order interactions play a crucial role. The key idea for taking this observation into account is to extend G to a simplicial complex. The most popular approach for achieving this goal relies on the *clique complex* [33]. Here, a set of $k + 1$ vertices forms a k-simplex if and only if it is a k-clique, i.e., if and only if there is an edge between every pair of the $k + 1$ vertices. To ease readability, we will henceforth also write $G = G(\mathcal{P})$ not only for the binary ADRCM network but also for the clique complex generated by it.

While Gracar et al. [40] analyzes several key characteristics of the ADRCM considered as a binary network, we focus on its simplicial structure. Specifically, we deal with the higher-order degrees and the Betti numbers, which we introduce in Sections B.2 and B.2, respectively.

Higher-order degree distribution

Arguably, the most fundamental characteristic of complex networks is the degree distribution. While the standard degree distribution provides an important summary of a complex network, it ignores higher-order structures. Therefore, Courtney and Bianconi [24] argues to consider generalized degrees that can convey information on the adjacency structure of simplices of varying dimensions.

To define the typical vertex degree, the idea is to add to $\mathcal{P}$ a distinguished typical vertex of the form $o = (0, U)$ where U is uniform in $(0, 1]$ and independent of $\mathcal{P}$ [40]. We let $G_* = G(\mathcal{P} \cup \{o\})$ denote the ADRCM constructed on the extended vertex set. Then, the typical vertex degree is that of o in G_*. We define the tail of the vertex-degree distribution $d_{0,1}(k)$ to be

$$d_{0,1}(k) = \mathbb{P}(\deg_1(o) \geqslant k),$$

i.e., the probability that the typical vertex degree exceeds $k \geqslant 0$. In this context, Gracar et al. [40] proved that the ADRCM is scale-free in the sense that the degree

distribution satisfies a power law:

$$\lim_{k\uparrow\infty} \log(d_{0,1}(k))/\log(k) = -1/\gamma.$$

While higher-order vertex degrees provide a more refined picture than the standard vertex degrees, it is also important to go beyond vertices by considering higher-dimensional simplices as well.

To study generalized degrees, we define the higher-order degree of an m-simplex $\Delta \subseteq G$ as

$$\deg_{m'}(\Delta) := |\{\sigma \in G \colon \sigma \supset \Delta, |\sigma| = m' + 1\}|,$$

represented as the number of m'-simplices containing Δ. For instance, $(m, m') = (0, 1)$ recovers the standard vertex degree and the higher-order vertex degree $\deg_{m'}(v)$ of the vertex v denotes the number of m'-simplices that are incident to v.

To study the generalized degree distributions, we consider typical simplices via the concept of the Palm distribution. Palm theory provides a rigorous framework for analyzing typical objects in point processes. In our context, this allows us to define and study a typical representative of the simplices in the network. Here, we describe the specific setting needed in the present paper, and refer the reader to Last and Penrose [66] for a more general introduction to Palm theory. For $m \geqslant 0$, we can consider the m-simplices $\Delta_m = \{P_0, \dots, P_m\}$ in G as a marked point process by centering Δ_m at its oldest vertex $c(\Delta_m)$. Let $\mathcal{T}_m(\mathcal{P})$ denote the family of m-simplices in the clique complex on G. Then, the expectation of a function f of the typical m-simplex Δ_m^* is given by

$$\mathbb{E}[f(\Delta_m^*, \mathcal{P})] = \frac{1}{\lambda_m} \mathbb{E}\Big[\sum_{\Delta \in \mathcal{T}_m(\mathcal{P})} \mathbb{1}\{c(\Delta) \in [0,1]\} f\big(\Delta - c(\Delta), \mathcal{P} - c(\Delta)\big)\Big], \qquad \text{(B.1)}$$

where $\lambda_m > 0$ is the simplex density and where $f \colon \mathcal{C}_m \times \mathbf{N}_{\mathsf{loc}} \to [0, \infty)$ is any measurable function from the space $\mathcal{C}_m$ of distinct $(m+1)$-tuples of points in $\mathbb{R} \times (0,1]$ and the space of locally finite point processes to $[0, \infty)$, and which is symmetric in the first $m + 1$ arguments.

In the present paper, we extend the result of Gracar et al. [40, Proposition 4.1] by considering the generalized simplex-degree distribution

$$d_{m,m'}(k) = \mathbb{P}\big(\deg_{m'}(\Delta_m) \geqslant k\big),$$

represented as the distribution of the number of m'-simplices incident to Δ_m^*.

Theorem B.2.1 (Power law for the typical simplex degree)**.** *Let $\gamma \in (0,1)$ and $m' > m \geqslant 0$. Then,*

$$\lim_{k\uparrow\infty} \log(d_{m,m'}(k))/\log(k) = m - (m+1)/\gamma.$$

Central and stable limit theorems

As outlined in Section B.1, to decide whether a given model is a good fit for a dataset, it is important to be able to carry out statistical hypothesis tests. In this work, we discuss possible hypothesis tests that become asymptotically exact for growing networks. While higher-order degree distributions are an important tool for describing higher-order networks, they only provide a highly restricted view of the topological structure. The idea behind TDA is to rely on invariants from algebraic topology for extracting more refined shape-related information. In this context, one of the most celebrated characteristics is the Betti numbers, which can be interpreted as the number of topological holes in a dataset. For a more detailed explanation of Betti numbers, we refer the reader to Hiraoka et al. [48]. One attractive way to develop a hypothesis test is to show that the considered test statistic becomes asymptotically normal. This is the content of the following theorem. Here, we write $\beta_{n,q}$ for the qth Betti number of the clique complex $G(\mathcal{P} \cap [0, n])$.

Theorem B.2.2 (CLT for the Betti numbers)**.** *Let $q \geqslant 0$ and $0 < \gamma < 1/4$. Then, $n^{-1/2}(\beta_{n,q} - \mathbb{E}[\beta_{n,q}])$ converges in distribution to a normal distribution.*

A disadvantage of Theorem B.2.2 is that our proof imposes a substantial constraint on the parameter γ. In particular, Theorem B.2.2 considers a regime where the variance of the degree distribution is finite, while for many real-world datasets it is infinite. Note that for large values γ, the ADRCM gives rise to extremely long edges, which makes it difficult to control spatial correlations over long distances, which is the main challenge in the proof. While we expect that by a more careful argumentation in the proof of Theorem B.2.2, the range of γ could be extended, we conjecture that the asymptotic normality breaks down for values of $\gamma > 1/2$. To provide evidence for this conjecture, we now illustrate that a similar effect occurs for a more elementary test statistic, namely, the edge count

$$S_n := |\{(y, v) \to (x, u) \colon (y, v), (x, u) \in \mathcal{P}, x \in [0, n]\}|.$$

The key observation is that depending on whether γ is smaller or larger than $1/2$, the variance of S_n at a typical vertex is either finite or infinite. Hence, we should only expect a CLT in the finite variance regime. We show that this is indeed the case.

Theorem B.2.3 (CLT for the edge count)**.** *Let $\gamma < 1/2$. Then, the quantity $\mathrm{Var}(S_n)^{-1/2}(S_n - \mathbb{E}[S_n])$ converges in distribution to a standard normal distribution.*

For $\gamma > 1/2$ since the degree distribution is heavy-tailed, the right tails in the edge count are more pronounced than those of a normal distribution. For many combinatorially defined network models, such as the configuration model, the degrees are taken to be i.i.d. from a given distribution. Hence, here the limiting vertex-degree distribution follows from the classical stable central limit theorem [107, Theorem 4.5.2]. We also refer the reader to van der Hofstad et al. [103] for a discussion in this direction. However, we are not aware of any existing corresponding results for spatial networks, which often feature strong spatial correlations between the individual vertex degrees. Hence, the main challenge in proving Theorem B.2.4 is to understand and overcome

these correlations to extend the results from the combinatorial networks to spatial network models.

Theorem B.2.4 (Stable limit law for the edge count)**.** *Let $\gamma \in (1/2, 1)$. Then, $n^{-\gamma}(S_n - \mathbb{E}[S_n])$ converges in distribution to $\mathcal{S}_{\gamma^{-1}}$, where $\mathcal{S}$ is a $1/\gamma$-stable distribution.*

Model extensions

Theorem B.2.1 expresses the power-law exponent of the vertex-degree distribution and the edge-degree distribution in terms of γ. However, as we will illustrate in Section B.8, when analyzing datasets of scientific collaborations, the relation between the vertex and edge exponents suggested in Theorem B.2.1 may often be violated in real datasets. More precisely, for a given vertex-degree exponent, we found the edge degrees in the data to be substantially more heavy-tailed than suggested in Theorem B.2.1. In other words, real datasets exhibit a larger proportion of edges incident to many triangles than what can be realized by the ADRCM. Alternatively, we could choose γ to match the power-law exponent of the edge degrees in the data. In this case, however, the vertex degrees of the fitted model would exhibit too heavy tails.

To address this shortcoming, we propose a model extension *thinned age-dependent random connection model (TADRCM)*, where we remove some edges so that the power-law exponent of the edge degrees is not affected. The key observation is that for edges with high edge degrees, typically, both endpoints are very old. However, only a tiny proportion of vertices connect to more than one very old vertex. More precisely, we say that an edge $(z, w) \to (x, u)$ is *protected* if $w \leqslant 2u$ or if there exists a vertex (y, v) with $v \leqslant 2u \leqslant 4v$ with $(z, w) \to (y, v)$. An edge is *exposed* if it is not protected. Then, we define the TADRCM G^{th}, η of G by removing independently exposed edges. The key idea is to use a retention probability of u^η, where $\eta > 0$ is a new model parameter. Our next main result is the following analog of Theorem B.2.1 for the thinned model, where $d_{m,m'}^{\mathsf{th},\eta}$ is defined as $d_{m,m'}$, except that we use the TADRCM instead of the ADRCM.

Theorem B.2.5 (Power law for the thinned typical vertex and edge degree)**.** *Let $\gamma \in (1/2, 1)$ and $\eta > 0$ be such that $2/\gamma - 1 > 1/(\gamma - \eta)$. Then,*

(a) $\lim_{k \uparrow \infty} \log(d_{0,m'}^{\mathsf{th},\eta}(k))/\log(k) = -1/(\gamma - \eta)$, and

(b) $\lim_{k \uparrow \infty} \log(d_{1,m'}^{\mathsf{th},\eta}(k))/\log(k) = 1 - 2/\gamma$.

We stress that alternative approaches also exist to enhance the flexibility of the ADRCM. For instance, van der Hofstad et al. [104] introduced a different extension, focusing on clustering properties. However, in the scope of our work, we found the thinning-based model more convenient for two reasons. First, as shown in Theorem B.2.5, the parameters γ and η are transparently related to the vertex and edge degrees, which substantially simplifies fitting the model to datasets. In contrast, van der Hofstad et al. [104] discussed a model where the connection between the model parameters and degree exponents is less obvious, and it is not immediate which combinations of higher-order degrees can be realized in the model. Second, when carrying out the proofs, it is convenient that in the ADRCM, the out-degree is Poisson-distributed

independently of the vertex age. Although we expect that our proofs could be adapted to the extension from van der Hofstad et al. [104], some steps would require additional work.

B.3 Proof of Theorem B.2.1—power-law exponents for higher-order simplex degrees

In this section, we establish Theorem B.2.1, i.e., we compute the power-law exponents for the higher-order simplex degrees in the ADRCM. To achieve this goal, we consider the lower and upper bounds separately in Sections B.3 and B.3, respectively.

To prepare the proof, we start with an integral representation for the distribution of the typical m-simplex Δ_m^*. While (B.1) provides a conceptually clean definition of the expectation of a function of a typical m-simplex, it is not ideal for carrying out actual computations. For this reason, we derive an alternative representation in Proposition B.3.1 below.

In this representation, we write $o := o_0 := (0, u)$ with $u \in (0, 1]$ for the typical vertex at the origin and

$$\boldsymbol{o}_m := (o_1, \ldots, o_m) := ((y_1, v_1), \ldots, (y_m, v_m)) \in \mathbb{S}^m := (\mathbb{R} \times (0, 1])^m$$

for the remaining vertices. Then, we let $g_m(u, \boldsymbol{o}_m)$ denote the indicator of the event that $(o_0, \boldsymbol{o}_m)$ forms an m-simplex in the ADRCM with $u \leqslant v_1 \leqslant \cdots \leqslant v_m$. Henceforth, we let $I_r(x) := [x - r/2, x + r/2]$ denote the interval of side length $r > 0$ centered at $x \in \mathbb{R}$. We let $\mathbf{N}_{\mathsf{loc}}$ denote the family of all locally finite subsets of $\mathbb{S}$.

Proposition B.3.1 (Distribution of the typical m-simplex)**.** *Let $m \geqslant 1$. Then,*

$$\mathbb{E}[f(\Delta_m^*, \mathcal{P})] = \frac{\int_0^1 \int_{\mathbb{S}^m} \mathbb{E}[f(\{o, \boldsymbol{o}_m\}, \mathcal{P} \cup \{o, \boldsymbol{o}_m\})] g_m(u, \boldsymbol{o}_m) \, \mathrm{d}\boldsymbol{o}_m \, \mathrm{d}u}{\int_0^1 \int_{\mathbb{S}^m} g_m(u, \boldsymbol{o}_m) \, \mathrm{d}\boldsymbol{o}_m \, \mathrm{d}u}$$

for any measurable $f \colon \mathcal{C}_m \times \mathbf{N}_{\mathsf{loc}} \to [0, \infty)$, which is translation-covariant in the sense that $f((x + y, u), \varphi + y) = f((x, u), \varphi)$ for every $(x, u) \in \mathbb{S}, y \in \mathbb{R}$ and $\varphi \in \mathbf{N}_{\mathsf{loc}}$.

To ensure that the Palm version is well-defined, we need to show that the denominator is finite. We formulate this property as a separate auxiliary result. First, define the function

$$\mu_m(u) := \int_{\mathbb{S}^m} g_m(u, \boldsymbol{o}_m) \, \mathrm{d}\boldsymbol{o}_m.$$

For instance, $\mu_0 \equiv 1$ and also for $m = 1$, the expression simplifies. To that end, we write

$$M(p) := \{p' \in \mathbb{S} \colon p' \to p\}$$

for the set of all space-time points connecting to $p \in \mathbb{S}$. Then,

$$\mu(u) := \mu_1(u) = |M(o)| = \int_u^1 \left| I_{\beta u^{-\gamma} v^{-(1-\gamma)}}(0) \right| \mathrm{d}v = \frac{\beta}{\gamma}(u^{-\gamma} - 1) \qquad \text{(B.2)}$$

is the expected in-degree of the typical vertex. That is, $\mu_1(u) = \mathbb{E}[D_{\mathsf{in}}(u)]$, where

$$D_{\mathsf{in}}(u) := |\mathcal{P} \cap M(o)|$$

is the in-degree of the typical vertex o.

For general $m \geqslant 1$, we can derive the small-u asymptotics.

Lemma B.3.2 (Asymptotics for $\mu_m(u)$)**.** *Let* $m \geqslant 1$, $\gamma \in (0,1)$ *and* $\eta > 0$. *Then,* $\mu_m(u) \in O(u^{-\gamma-\eta})$.

Proof. First,

$$\int_{\mathbb{S}} g_m(u, \boldsymbol{o}_m) \, \mathrm{d}o_m \leqslant g_{m-1}(u, \boldsymbol{o}_{m-1}) \int_0^1 \big| I_{\beta v_{m-1}^{-\gamma} v_m^{-(1-\gamma)}}(y_{m-1}) \big| \, \mathrm{d}v_m$$
$$= \tfrac{\beta}{\gamma} g_{m-1}(u, \boldsymbol{o}_{m-1}) v_{m-1}^{-\gamma}.$$

Next,

$$\int_{\mathbb{S}} g_{m-1}(u, \boldsymbol{o}_{m-1}) v_{m-1}^{-\gamma-\eta} \, \mathrm{d}o_{m-1} \leqslant g_{m-2}(u, \boldsymbol{o}_{m-2}) \int_{v_{m-2}}^1 \beta v_{m-2}^{-\gamma} v_{m-1}^{-1-\eta} \, \mathrm{d}v_{m-1}$$
$$\leqslant \tfrac{\beta}{\eta} g_{m-2}(u, \boldsymbol{o}_{m-2}) v_{m-2}^{-\gamma-\eta}.$$

Hence, iterating this bound yields that $\mu_m(u) \leqslant \beta^m u^{-\gamma-\eta}/(\gamma\eta^{m-1})$, as asserted. $\qquad\square$

Proof of Proposition B.3.1. Let $g'_m(P_0, \ldots, P_m)$ be the indicator of the event that $\{P_0, \ldots, P_m\}$ forms an m-simplex in the ADRCM with $U_0 \leqslant \cdots \leqslant U_m$. Let $A \subseteq \mathbb{R}$ be a Borel set with $|A| = 1$. Then

$$\lambda_m \, \mathbb{E}[f(\Delta_m^*, \mathcal{P})] = \mathbb{E}\Big[\sum_{\substack{P_0, \ldots, P_m \in \mathcal{P}_{\neq}^{m+1} \\ U_0 \leqslant \cdots \leqslant U_m}} \mathbb{1}\{X_0 \in A\} f(\{P_0, \ldots, P_m\}, \mathcal{P}) g'_m(P_0, \ldots, P_m) \Big].$$

Then, writing $\boldsymbol{p} = (p_1, \ldots, p_m)$, by the Mecke formula [66, Theorem 4.4],

$$\lambda_m \, \mathbb{E}[f(\Delta_m^*, \mathcal{P})] = \int_{A \times (0,1]} \int_{\mathbb{S}^m} \mathbb{E}[f(\{p_0, \boldsymbol{p}\}, \mathcal{P})] g'_m(\{p_0, \boldsymbol{p}\}) \, \mathrm{d}\boldsymbol{p} \, \mathrm{d}p_0.$$

As $|A| = 1$, a substitution $\mathbf{p}_m = \mathbf{o}_m + p_0$ and an application of Fubini's theorem give that

$$\lambda_m \, \mathbb{E}[f(\Delta_m^*, \mathcal{P})] = \int_0^1 \int_{\mathbb{S}^m} \mathbb{E}[f(\{o, \boldsymbol{o}_m\}, \mathcal{P})] g_m(u, \boldsymbol{o}_m) \, \mathrm{d}\boldsymbol{o}_m \, \mathrm{d}u.$$

Hence, evaluating this equality for $f = 1$ concludes the proof. $\qquad\square$

Proof of the lower bound

Next, we prove the lower bound by relying on the Palm representation derived in Proposition B.3.1. More precisely, we produce specific configurations of $u, \boldsymbol{o}_m$ that occur with sufficiently high probability and such that $\mathbb{P}(\deg_{m'}(u, \boldsymbol{o}_m) \geqslant k)$ is bounded away from 0.

Proof of Theorem B.2.1, lower bound. To ease notation, we put $\beta' := \beta/2$. First, let $p := \mathbb{P}(\mathcal{P}([0, \beta'] \times [3/4, 1]) \geqslant m')$ denote the probability that a $(\beta' \times 1/4)$-box contains at least m' Poisson points. Furthermore, let $M := \lceil 2/p \rceil$. Then, consider the set $B_k \subseteq (0, 1]^{m+1} \times \mathbb{R}^m$ given by

$$B_k := [0, \beta'k]^m \times B_k' \qquad \text{with} \qquad B_k' := \prod_{j=0}^{m} \Big[\Big(\frac{j}{Mmk}\Big)^{1/\gamma}, \Big(\frac{j+1}{Mmk}\Big)^{1/\gamma}\Big].$$

Since $|B_k| \in \Omega(k^{-(m+1)/\gamma + m})$, we only need to verify the following two items for every $(u, \boldsymbol{o}_m) \in B_k$.

(a) The $(o, \boldsymbol{o}_m)$ points form an m-simplex in the clique complex of the ADRCM.

(b) It holds that $\mathbb{P}(\deg_{m'}(u, \boldsymbol{o}_m) \geqslant k) \geqslant 1/2$.

For Part (a), note that every $(u, \boldsymbol{o}_m) \in B_k$ indeed defines an m-simplex since

$$\max_{i \leqslant m}|y_i| \leqslant \beta'k \leqslant \beta'((Mk)^{-1/\gamma})^{-\gamma} \quad \text{and} \quad \max_{i,j \leqslant m}|y_i - y_j| \leqslant \beta'k \leqslant \beta'((Mk)^{-1/\gamma})^{-\gamma}.$$

For Part (b), we note that the events $E_{i,k} := \{\mathcal{P}([i\beta', (i+1)\ \beta'] \times [3/4, 1]) \geqslant m'\}$ are independent for $i \leqslant kM$. Moreover, let $N_k := \sum_{i \leqslant kM} \mathbb{1}\{E_{i,k}\}$ be the number of events that occur. Then, N_k is a binomial random variable with kM trials and success probability p. Since $kMp \geqslant 2k$, the binomial concentration result implies that $\mathbb{P}(N_k \geqslant k) \geqslant 1/2$ holds for sufficiently large k.

Hence, it suffices to show that almost surely, $N_k \leqslant \deg_{m'}(u, \boldsymbol{o}_m)$. To achieve this goal, we first note that for fixed $i \leqslant kM$ any two points in $[i\,\beta', (i+1)\beta'] \times (0, 1]$ are connected by an edge. Moreover, we claim that any $(Z, W) \in [0, \beta'kM] \times [3/4, 1]$ connects to o and to every o_i, $i \leqslant m$. Now,

$$|Z - 0| \leqslant \beta'kM = \beta'((kM)^{-1/\gamma})^{-\gamma} \quad \text{and} \quad \max_{i \leqslant m}|Z - y_i| \leqslant \beta'kM = \beta'((kM)^{-1/\gamma})^{-\gamma}.$$

This concludes the proof since the Poisson concentration inequality [88, Lemma 1.2] implies that $\mathbb{P}(\mathcal{P}(B_k) \geqslant k) \to 1$ as $k \to \infty$. $\qquad\square$

Proof of the upper bound

In this subsection, we prove the upper bound for the simplex degree in Theorem B.2.1. First, to provide the reader with a gentle introduction, we present the case of the in-degree, which was considered previously by Gracar et al. [40, Proposition 4.1]. In fact, [41, Lemma 4] is slightly more refined than Theorem B.2.1 in the sense that it provides not only the asymptotics for the tail probabilities but for the entire probability mass function. Nevertheless, we include the short argument here because it makes the presentation self-contained and provides an intuition for the more complicated higher-order case.

The key observation is that conditioned on the arrival time u of the typical vertex $o = (0, u)$, the in-degree is Poisson distributed. Indeed, by the restriction theorem, the in-neighbors form a Poisson point process for fixed u [66, Theorem 5.2].

Proof of the upper bound for the in-degree. First, note that if $\mu(u) \leqslant k/2$—where $\mu(u)$ is the expected in-degree of the typical vertex introduced in (B.2)—, then by the Poisson concentration inequality, the probability $\mathbb{P}(D_{\mathsf{in}}(u) \geqslant k)$ vanishes exponentially fast in k. Hence, we may assume that $u \leqslant \mu^{-1}(k/2)$. Noting that (B.2) gives that $\mu^{-1}(k/2) \in O(k^{-1/\gamma})$ concludes the proof. $\qquad\square$

To tackle the general case, we proceed in two steps. First, we reduce to the case where $m' = m + 1$, and then deal with this case. For the reduction step, the key idea is that the out-degree of a given vertex is Poisson distributed with a finite parameter [40]. Hence, the number of simplices containing a given point as its youngest vertex has rapidly decaying tail probabilities. In particular, only a few simplices contain a given vertex as its youngest vertex, as this number is bounded from above by the out-degree of the vertex at hand.

We would like to show that for the higher-order degree of the typical simplex Δ_m^*,

$$\limsup_{k\uparrow\infty} \frac{1}{\log(k)} \log\big(\mathbb{P}(\deg_{m'}(\Delta_m^*) \geqslant k)\big) \leqslant m - \frac{m+1}{\gamma}. \tag{B.3}$$

Hence, using Proposition B.3.1, we see that (B.3) is equivalent to

$$\limsup_{k\uparrow\infty} \frac{1}{\log(k)} \log\Big(\int_0^1 \varphi_{k,m,m'}(u)\,\mathrm{d}u\Big) \leqslant m - \frac{m+1}{\gamma}, \tag{B.4}$$

where

$$\varphi_{k,m,m'}(u) := \int_{\mathbb{S}^m} \mathbb{P}(\deg_{m'}(u, \boldsymbol{o}_m) \geqslant k) g_m(u, \boldsymbol{o}_m)\,\mathrm{d}\boldsymbol{o}_m.$$

Proof of reduction to $m' = m+1$. Let $M(\boldsymbol{o}_m) := \bigcap_{j \leqslant m} M(o_j)$ denote the common in-neighbors of $o_1, \ldots, o_m$. Then, the goal of this step is to reduce the problem to deriving the asserted power-law bound for the expression $\mathbb{P}(\mathcal{P}(M(\boldsymbol{o}_m)) \geqslant k)$. First, Lemma B.3.2 gives that $\varphi_{k,m,m'}(u) \in O(u^{-\gamma})$. Hence, we may assume that $u \geqslant k^{-2K}$, where K is chosen such that $(1 - \gamma)K = (m+1)/\gamma - m$.

Now, we note that any m'-simplex containing the typical m-simplex consists of the $m + 1$ vertices of the typical simplex and $m' - m$ additional Poisson points. In particular, the number of $(m' - m)$-simplices containing the typical vertex o as its youngest vertex is at most $D_{\mathsf{out}}(o)^{m'-m}$. Moreover,

$$\mathbb{P}\big(D_{\mathsf{out}}(o)^{m'-m} \geqslant k\big) = \mathbb{P}\big(D_{\mathsf{out}}(o) \geqslant k^{1/(m'-m)}\big), \tag{B.5}$$

which decays stretched exponentially by [40, Proposition 4.1] and Poisson concentration [88, Lemma 1.2].

Hence, it suffices to consider the number $N_{m,m'}$ of m' simplices incident to the typical m-simplex with the property that the youngest vertex is one of the $m' - m$ Poisson points $P_i \in \mathcal{P}$. Again, the number of $(m' - m)$-simplices having P_i as its youngest vertex is bounded above by $D_{\mathsf{out}}(P_i)^{m'-m}$. Hence, we have for any $\varepsilon > 0$ that

$$\mathbb{P}(N_{m,m'} \geqslant k) \leqslant \mathbb{P}\Big(\sum_{P_i \in M(\boldsymbol{o}_m)} D_{\mathsf{out}}(P_i)^{m'-m} \geqslant k \Big)$$

$$\leqslant \mathbb{P}\big(\mathcal{P}(M(\boldsymbol{o}_m)) \geqslant k^{1-\varepsilon}\big) + \mathbb{P}\big(\max_{P_i \in M(o)} D_{\mathsf{out}}(P_i)^{m'-m} \geqslant k^\varepsilon \big).$$

In particular, by the Mecke formula,

$$\mathbb{P}\big(\max_{P_i \in M(o)} D_{\mathsf{out}}(P_i)^{m'-m} \geqslant k^\varepsilon\big)$$

$$\leqslant \int_{\mathbb{R}} \int_u^1 \mathbb{P}(D_{\mathsf{out}}(x)^{m'-m} \geqslant k^\varepsilon)\, \mathbb{1}\{(x,v) \in M(o)\}\, \mathrm{d}x\, \mathrm{d}v$$

$$= \mathbb{P}(D_{\mathsf{out}}(o) \geqslant k^{\varepsilon/(m'-m)})\mu(u).$$

Now, the Poisson concentration inequality shows that the probability on the right-hand side decays to 0 exponentially fast in k, whereas the assumption $u \geqslant k^{-2K}$ gives a polynomial upper bound on $\mu(u)$. In particular, this step reduces the proof to bounding the expression $\mathbb{P}(\mathcal{P}(M(\boldsymbol{o}_m)) \geqslant k^{1-\varepsilon})$. $\qquad\square$

It remains to consider $m' = m + 1$. During the proof, it is important to control the conditional mean

$$\mu(p,q) := |M(p,q)| := |M(p) \cap M(q)|, \tag{B.6}$$

i.e., the area of the set of space-time points connecting to both $p = (x,u)$ and $q = (y,v)$, where we henceforth assume that $v \geqslant u$.

Lemma B.3.3 (Bound on $\mu(p,p')$)**.** *Put* $s(r,u) := (\beta u^{-\gamma}/|r|)^{1/(1-\gamma)}$ *and* $s_\wedge(r,u) := s(r,u) \wedge 1$. *Then,*

$$\mu(p,q) \leqslant \tfrac{\beta}{\gamma} v^{-\gamma} s_\wedge(x-y,u)^\gamma\, \mathbb{1}\{u|x-y| \leqslant \beta\}.$$

Proof. The key observation is that $|x-y| \leqslant |z-x| + |z-y| \leqslant \beta u^{-\gamma} w^{-(1-\gamma)}$ for every $(z,w) \in M(p,q)$. Hence, $u \leqslant w \leqslant s_\wedge(x-y,u)$. In particular,

$$\mu(p,q) \leqslant \mathbb{1}\{u \leqslant s_\wedge(x-y,u)\} \int_v^{s_\wedge(x-y,u)} \big|I_{\beta v^{-\gamma} w^{-(1-\gamma)}}\big|\, \mathrm{d}w.$$

Hence, a computation of the integral concludes the proof. $\qquad\square$

Next, we need to bound suitable integrals on $s(r,u)$.

Lemma B.3.4 (Integrals of $s(r,u)$)**.** *Let* $\gamma < 1$ *and* $0 < \eta < 1 - \gamma < \rho$. *Then,*

(a) $\displaystyle\int_0^\infty s_\wedge(r,u)^\rho\, \mathrm{d}r \in O(u^{-\gamma}).$

(b) $\displaystyle\int_0^{\beta/u} s_\wedge(r,u)^{1-\gamma-\eta}\, \mathrm{d}r \in O(u^{-\gamma-\eta}).$

(c) $\displaystyle\int_0^{\beta/r} s_\wedge(r,u)^\gamma\, \mathrm{d}u \in O(r^{-1-\gamma})$ *if* $\gamma < 1/2.$

Proof. **Part (a).** We distinguish two cases. First, note that $|I_{\beta u^{-\gamma}}| \in O(u^{-\gamma})$. Hence, we may assume that $y \in \mathbb{R} \setminus I_{\beta u^{-\gamma}}$ so that $s_\wedge(r,u) = s(r,u)$. Then, as asserted,

$$\int_{\mathbb{R} \setminus I_{\beta u^{-\gamma}}} s(r,u)^\rho\, \mathrm{d}r \leqslant 2 \int_{\beta u^\gamma}^\infty \Big(\frac{u^\gamma r}{\beta}\Big)^{-\rho/(1-\gamma)}\, \mathrm{d}r \in O(u^{-\gamma}).$$

Part (b). We compute that

$$\int_0^{\beta/u} s(r,u)^{1-\gamma-\eta}\,\mathrm{d}r \leqslant 2\int_0^{\beta u^{-1}} \left(\frac{u^\gamma r}{\beta}\right)^{-(1-\gamma-\eta)/(1-\gamma)}\,\mathrm{d}r \leqslant \frac{2(1-\gamma)}{\eta}u^{-\gamma-\eta}.$$

Part (c). We compute that

$$\int_0^{\beta/r} s(r,u)^\gamma\,\mathrm{d}u = \left(\frac{r}{\beta}\right)^{-\gamma/(1-\gamma)}\int_0^{\beta/r} u^{-\gamma^2/(1-\gamma)}\,\mathrm{d}u.$$

The latter integral is of the order $O(r^\zeta)$ where $\zeta = -\gamma/(1-\gamma)+\gamma^2/(1-\gamma)-1 = -1-\gamma$, as asserted. $\qquad\square$

Finally, we complete the proof of the upper bound in the case $m' = m+1$.

Proof of the upper bound; $m' = m+1$. We need to bound the tail probabilities of the Poisson random variable $D'_m(u,\boldsymbol{o}_m) := \mathcal{P}(M(o,\boldsymbol{o}_m))$, which has parameter $\mu'_m(u,\boldsymbol{o}_m)$ $:= \mathbb{E}[D'_m(u,\boldsymbol{o}_m)]$. Note that

$$\mathbb{P}(D'_m(u,\boldsymbol{o}_m) \geqslant k)$$
$$\leqslant \mathbb{P}\Big(D'_m(u,\boldsymbol{o}_m) \geqslant k, \mu'_m(u,\boldsymbol{o}_m) \leqslant k/2\Big) + \mathbb{1}\{\mu'_m(u,\boldsymbol{o}_m) \geqslant k/2\},$$

where the first probability on the right vanishes exponentially by Poisson concentration. Moreover, $\mu'_m(u,\boldsymbol{o}_m) \leqslant \min_{n\leqslant m} \mu(o_{n-1},o_n)$, where we set $\mu(o_{-1},o_0) := \mu(u)$. Hence, it remains to bound

$$\int_0^1 \int_{\mathbb{S}^m} \prod_{n\leqslant m} \mathbb{1}\{\mu(o_{n-1},o_n) \geqslant k\}\,\mathrm{d}\boldsymbol{o}_m\,\mathrm{d}u.$$

We start with the innermost integral. Here, by Lemma B.3.3, we deduce that if $\mu(o_{m-1},o_m) \geqslant k$, then

$$v_m \leqslant (\beta/\gamma)^{1/\gamma}k^{-1/\gamma}s_\wedge(y_{m-1}-y_m, v_{m-1}).$$

Therefore,

$$\int_{\mathbb{S}} \mathbb{1}\{\mu(o_{m-1},o_m) \geqslant k\}\,\mathrm{d}o_m$$
$$\leqslant (\beta/\gamma)^{1/\gamma}k^{-1/\gamma}\int_{\mathbb{R}} s_\wedge(y_{m-1}-y_m, v_{m-1})\,\mathrm{d}y_m. \tag{B.7}$$

Hence, applying Lemma B.3.4 (a) shows that for some $c > 0$,

$$\int_0^1 \int_{\mathbb{S}^m} \prod_{n\leqslant m} \mathbb{1}\{\mu(o_{n-1},o_n) \geqslant k\}\,\mathrm{d}\boldsymbol{o}_m\,\mathrm{d}u$$
$$\leqslant ck^{-1/\gamma}\int_0^1 \int_{\mathbb{S}^{m-1}} \prod_{n\leqslant m-1} \mathbb{1}\{\mu(o_{n-1},o_n) \geqslant k\}v_{m-1}^{-\gamma}\,\mathrm{d}\boldsymbol{o}_{m-1}\,\mathrm{d}u.$$

We now continue to compute the integral over o_{m-1}, which is the next innermost integral. More generally, we claim that for every $n \geqslant 1$ and sufficiently small $\eta > 0$, we have that

$$\int_{\mathbb{S}} \mathbb{1}\{\mu(o_{n-1},o_n) \geqslant k\}v_n^{-\gamma-\eta}\,\mathrm{d}o_n \in O\big(k^{-(1-\gamma-\eta)/\gamma}v_{n-1}^{-\gamma-\eta}\big).$$

93

First, similarly to (B.7), for some $c > 0$,

$$\int_{\mathbb{S}} \mathbb{1}\{\mu(o_{n-1}, o_n) \geqslant k\} v_n^{-\gamma-\eta} \, \mathrm{d}o_n$$

$$\leqslant ck^{-(1-\gamma-\eta)/\gamma} \int_{-I_{\beta v_{n-1}^{-1}}} s_\wedge(y_{n-1} - y_n, v_{n-1})^{1-\gamma-\eta} \, \mathrm{d}y_n.$$

Therefore, by Lemma B.3.4 (b),

$$\int_{\mathbb{S}} \mathbb{1}\{\mu(o_{n-1}, o_n) \geqslant k\} v_n^{-\gamma-\eta} \, \mathrm{d}o_n \in O\big(k^{-(1-\gamma-\eta)/\gamma} v_{n-1}^{-\gamma-\eta}\big)$$

as asserted. □

B.4   Proof of Theorem B.2.2—CLT for Betti numbers

In this section, we prove Theorem B.2.2. The idea is to proceed similarly to [48, Theorem 5.2] and apply the general Poisson CLT by Penrose and Yukich [89, Theorem 3.1]. While the general strategy is similar to that chosen by Hiraoka et al. [48, Theorem 5.2], the long-range dependencies in the ADRCM require more refined argumentation. Therefore, we provide additional details here. For a locally finite set $\varphi \subseteq \mathbb{R} \times (0, 1]$ we let $\beta(\varphi) = \beta_q(\varphi)$ denote the qth Betti number computed for the ADRCM on φ. To state the conditions of [89, Theorem 3.1] precisely, we introduce the add-one cost operator

$$\delta(\varphi, u) := \beta(\varphi \cup \{(0, u)\}) - \beta(\varphi).$$

Now, to apply [89, Theorem 3.1], we need to verify the following two conditions.

- It holds that $\sup_{n \geqslant 1} \mathbb{E}[\delta(\mathcal{P}_n, U)^4] < \infty$ (**moment condition**).

- It holds that $\delta(\mathcal{P} \cap W_n, U)$ converges almost surely to a finite limit as $n \to \infty$ (**weak stabilization**), where $W_n = [-n/2, n/2] \times (0, 1]$.

We now verify the weak stabilization and the moment condition separately. In both cases, we follow the general strategy outlined by Hiraoka et al. [48, Theorem 5.2]. To make the presentation self-contained, we provide the most important steps of the proof. First, we consider the moment condition.

Proof of Theorem B.2.2, moment condition. As in the proof by Hiraoka et al. [48, Theorem 5.2], we note that $\delta(\varphi, U)$ is bounded above by the number of q- and $(q+1)$-simplices containing o. Thus,

$$\mathbb{E}[\delta(\varphi, U)^4] = \int_0^\infty \mathbb{P}(\delta(\varphi, U) \geqslant s^{1/4}) \, \mathrm{d}s \leqslant \int_0^\infty \mathbb{P}(\deg_q(o) + \deg_{q+1}(o) \geqslant s^{1/4}) \, \mathrm{d}s$$

$$\leqslant \int_0^\infty d_{0,q}(s^{1/4}/2) + d_{0,q+1}(s^{1/4}/2) \, \mathrm{d}s,$$

where the last inequality holds as if $\deg_q(o) + \deg_{q+1}(o) \geqslant s^{1/4}$, then at least one of $\deg_q(o)$ or $\deg_{q+1}(o)$ is larger than $s^{1/4}/2$. Now, by Theorem B.2.1, both $d_{0,q}$ and $d_{0,q+1}$ have tail index $1/\gamma > 4$, thereby showing the finiteness of the above integral. □

Second, we consider the weak stabilization.

Proof of Theorem B.2.2, weak stabilization. For $n \geqslant 1$, we write

$$\beta_n := \dim(Z_n) - \dim(B_n) := \dim(Z(\mathcal{P}_n)) - \dim(B(\mathcal{P}_n))$$

for the Betti number of the ADRCM constructed on $\mathcal{P}_n$, noting that this characteristic is the dimension difference of the corresponding cycle space Z_n and boundary space B_n, respectively. Similarly, we set

$$\beta'_n := \dim(Z'_n) - \dim(B'_n) := \dim(Z(\mathcal{P}_n \cup \{o\})) - \dim(B(\mathcal{P}_n \cup \{o\})),$$

where we have now added the typical vertex, $o = (0, U)$. Hence, it suffices to show the weak stabilization with respect to $\dim(Z_n)$ and $\dim(B_n)$ separately. We now discuss the case of $\dim(Z_n)$, noting that the arguments for $\dim(B_n)$ are very similar. To check weak stabilization, we show that the sequence $\dim(Z'_n) - \dim(Z_n)$ is increasing and bounded.

First, to show that $\dim(Z'_n) - \dim(Z_n)$ is bounded, we note that $\dim(Z'_n) - \dim(Z_n) \leqslant \deg_{q,n}(o)$, where, $\deg_{q,n}(o)$ denotes the number of q-simplices in W_n containing the typical vertex o. This is because the q-simplices constructed from $\mathcal{P}_n \cup \{o\}$ can be decomposed into the set of q-simplices containing the typical vertex o and into the family of all simplices formed in $\mathcal{P}_n$. We refer to the arguments by Hiraoka et al. [48, Lemma 2.9] for the rigorous result. Now, almost surely, there exists $n_0 \geqslant 1$ such that for $n \geqslant n_0$, the neighbors of o do not change any further. In particular, $\dim(Z'_n) - \dim(Z_n) \leqslant |K_n^0|$.

Second, we show that $\dim(Z'_n) - \dim(Z_n)$ is non-decreasing. To that end, we take $n_2 \geqslant n_1$ and consider the canonical map

$$Z'_{n_1,q} \to Z'_{n_2,q}/Z_{n_2,q},$$

where the index q refers to the dimension of the cycle space. Then, any cycle contained in the kernel of this map consists of simplices formed by vertices in $\mathcal{P}_n$. In other words, the kernel equals $Z_{n_1,q}$, which shows that the induced map

$$Z'_{n_1,q}/Z_{n_1,q} \to Z'_{n_2,q}/Z_{n_2,q}$$

is injective. In particular, $\dim(Z'_{n_1}) - \dim(Z_{n_1}) \leqslant \dim(Z'_{n_2}) - \dim(Z_{n_2})$, as asserted. $\quad\square$

B.5 Proof of Theorems B.2.3 and B.2.4—asymptotics of edge counts

In this section, we prove Theorems B.2.3 and B.2.4. In both results, the idea is to write

$$S_n = \sum_{i \leqslant n} T_i := \sum_{i \leqslant n} \sum_{P_j \in \mathcal{P} \cap ([i-1,i] \times (0,1])} D_{\mathsf{in}}(P_j),$$

i.e., to express the edge count S_n as the sum of the in-degrees of all vertices within $[i-1, i] \times (0, 1]$. For the proofs of Theorems B.2.3 and B.2.4, it will be important to

compute variances of suitable sums of in-degrees. For ease of reference, we therefore state such bounds as a general auxiliary result. To make this precise, we henceforth let

$$S(B) := \sum_{P_j \in B} D_{\mathsf{in}}(P_j)$$

denote the in-degree sum for all vertices contained in the space-time region $B \subseteq \mathbb{S}$.

Lemma B.5.1 (Variance of accumulated in-degrees)**.** *Let $\gamma \neq 1/2$, $A \subseteq \mathbb{R}$ and $u_- > 0$. Then, there exists a constant $c_{\mathsf{VI}} > 0$ such that*

$$\mathrm{Var}(S(A \times [u_-, 1]))$$

$$\leqslant c_{\mathsf{VI}} \Big(|A|(1 + u_-^{1-2\gamma}) + \int_{A^2} \int_{u_-}^{1 \wedge (\beta/|x-y|)} s_\wedge(x-y,u)^\gamma \, \mathrm{d}u \, \mathrm{d}(x,y) \Big).$$

Proof. First, we note that

$$D_{\mathsf{in}}\big((x,u), \mathcal{P} \cup \{(x,u), (y,v)\}\big) = D_{\mathsf{in}}\big((x,u), \mathcal{P} \cup \{(x,u)\}\big) + \mathbb{1}\{(y,v) \in M(x,u)\}.$$

Hence, by the Mecke formula [66, Theorem 4.4] with $B := A \times [u, 1]$,

$$\mathrm{Var}(S(B)) = \int_B \mathbb{E}[D_{\mathsf{in}}(x,u)^2] \, \mathrm{d}(x,u) + \iint_{B^2} \mathrm{Cov}\big(D_{\mathsf{in}}(x,u), D_{\mathsf{in}}(y,v)\big) \, \mathrm{d}(x,u) \, \mathrm{d}(y,v)$$

$$+ 2 \int_B \mathbb{E}[D_{\mathsf{in}}(x,u)] \big|\{(y,v) \in B \colon (x,u) \in M(y,v)\}\big| \, \mathrm{d}(x,u),$$

where $D_{\mathsf{in}}(x,u)$ denotes the in-degree of the vertex (x,u) on the ADRCM constructed on $\mathcal{P} \cup \{(x,u)\}$. Now, note that $|\{(y,v) \in B \colon (x,u) \in M(y,v)\}| \in O(1)$ and that $\mathbb{E}[D_{\mathsf{in}}(x,u)] \leqslant \mathbb{E}[D_{\mathsf{in}}(x,u)^2]$. Hence, it suffices to bound the sum

$$\int_B \mathbb{E}[D_{\mathsf{in}}(x,u)^2] \, \mathrm{d}(x,u) + \iint_{B^2} \mathrm{Cov}\big(D_{\mathsf{in}}(x,u), D_{\mathsf{in}}(y,v)\big) \, \mathrm{d}(x,u) \, \mathrm{d}(y,v),$$

and we deal with the two summands separately.

We start by bounding $\mathbb{E}[D_{\mathsf{in}}(x,u)^2]$. Since $D_{\mathsf{in}}(x,u)$ is a Poisson random variable with mean $\mu(u) \in O(u^{-\gamma})$, the Poisson concentration inequality shows that $\mathbb{E}[D_{\mathsf{in}}(x,u)^2] \in O(u^{-2\gamma})$. Now, we note that $\int_{u_-}^1 u^{-2\gamma} \, \mathrm{d}u = (1 - 2\gamma)^{-1}(1 - u_-^{1-2\gamma})$, which is of order $O(u^{1-2\gamma})$ for $\gamma > 1/2$ and of order $O(1)$ for $\gamma < 1/2$.

To bound the covariance $\mathrm{Cov}(D_{\mathsf{in}}(x,u), D_{\mathsf{in}}(y,v))$, recall from (B.6) that a point (z,w) connects to both (x,u) and (y,v) if and only if $(z,w) \in M((x,u),(y,v))$:

$$\mathrm{Cov}\big(D_{\mathsf{in}}(x,u), D_{\mathsf{in}}(y,v)\big) = \mathbb{E}\Big[\sum_{(z,w) \in \mathcal{P}} \mathbb{1}\{(z,w) \in M((x,u),(y,v))\} \Big]$$

$$+ \sum_{(z,w),(z',w') \in \mathcal{P}^2_{\neq}} \mathbb{1}\{(z,w) \in M(x,u)\} \, \mathbb{1}\{(z',w') \in M(y,v)\}$$

$$- \mathbb{E}\Big[\sum_{(z,w) \in \mathcal{P}} \mathbb{1}\{(z,w) \in M(x,u)\} \Big] \mathbb{E}\Big[\sum_{(z,w) \in \mathcal{P}} \mathbb{1}\{(z,w) \in M(y,v)\} \Big],$$

where the last two terms cancel by the independence property of the Poisson process. Then, applying the Mecke formula [66, Theorem 4.4] gives

$$\mathrm{Cov}\big(D_{\mathsf{in}}(x, u), D_{\mathsf{in}}(y, v)\big) = \int_{(z,w)} \mathbb{1}\{(z, w) \in M((x, u), (y, v))\} \, \mathrm{d}(z, w)$$
$$= \mu((x, u), (y, v)).$$

In particular, Lemma B.3.3 concludes the proof:

$$\iint_{B^2} \mu((x, u), (y, v)) \, \mathrm{d}(x, u) \, \mathrm{d}(y, v)$$
$$\leqslant c_{\mathsf{VI}} \iint_{A^2} \int_{u_-}^{1 \wedge (\beta|x-y|)} s_\wedge(x - y, u)^\gamma \, \mathrm{d}u \, \mathrm{d}(x, y).$$

$\square$

First, we prove the CLT for the simplex count in the regime $\gamma < 1/2$, where we will rely on a general CLT for associated random variables [107, Theorem 4.4.3]. Here, we recall that the real-valued random variables $T_1, \ldots, T_k$ are *associated* if

$$\mathrm{Cov}\big(f_1(T_1, \ldots, T_k), f_2(T_1, \ldots, T_k)\big) \geqslant 0$$

holds for any coordinate-wise increasing functions $f_1, f_2 \colon \mathbb{R}^k \to [0, \infty)$.

Proof of Theorem B.2.3. Since the in-degrees are an increasing function in the underlying Poisson point process, we conclude from the Harris-FKG theorem [66, Theorem 20.4] that the random variables $\{T_i\}$ are associated. Hence, to apply [107, Theorem 4.4.3], it remains to prove that $\mathrm{Var}(T_1) < \infty$ and $\sum_{k \geqslant 2} \mathrm{Cov}(T_1, T_k) < \infty$. The finiteness of $\mathrm{Var}(T_1)$ follows from Lemma B.5.1, so it remains to consider the covariance sum.

We prove that $\mathrm{Cov}(T_1, T_k) \in O(k^{-1-\gamma})$, recalling that $\gamma < 1/2$. Proceeding similarly to Lemma B.5.1, and setting $a := |x - y|$, we need to show that $\int_0^{\beta/a} s_\wedge(a, u)^\gamma \, \mathrm{d}u \in O(k^{-1-\gamma})$. Hence, applying Lemma B.3.4 (c) concludes the proof. $\square$

Next, we prove Theorem B.2.4, i.e., the stable limit theorem for the edge count. Before proving Theorem B.2.4, we stress that while there are several general limit results in the literature for deriving the distributional convergence to α-stable limits [5, 27, 46], these do not apply in our setting. More precisely, it is difficult to verify [5, Condition 3.3] since the ADRCM is mixing but not ϕ-mixing. Second, Decreusefond et al. [27, Theorem 7.8] gives a general convergence result of Poisson functionals to α-stable random variables with $\alpha \in (0, 1)$. However, this corresponds to the case where $\gamma > 1$, which is not possible due to the model constraints. While Decreusefond et al. [27, Remark 7.9] states that in principle, the method should generalize to $\alpha \in (1, 2)$, the ensuing computations may lead to difficulties that are challenging to tackle. Third, Heinrich and Wolf [46] derived a general limit result for U-statistics based on i.i.d. input. However, in our setting, we work in a growing domain, so the distributions change after every step.

Before starting the proof of Theorem B.2.4, it will be convenient to review the classical stable limit theorem for i.i.d. sequences from [107, Theorem 4.5.2]. To ease

presentation, we restrict to the present setting of nonnegative random variables. More precisely, let $\{X_i\}_i$ be i.i.d. nonnegative random variables such that $\mathbb{P}(X_i > x) \sim Ax^{-\alpha}$ for some $\alpha \in (1, 2)$ and $A > 0$. Then, $n^{-1/\alpha}(\sum_{i \leqslant n} X_i - n\,\mathbb{E}[X_1])$ converges in distribution to an α-stable random variable $\mathcal{S}_\alpha$.

A key step in proving Theorem B.2.4 is a truncation argument, which we first discuss in the i.i.d. case.

Lemma B.5.2 (Truncation in the i.i.d. case)**.** *Let $\{X_i\}_i$ be i.i.d. random variables with $\mathbb{P}(X_i > x) \sim Ax^{-\alpha}$ for some $\alpha \in (1, 2)$ and $A > 0$. Then, for every $a < 1/\alpha$,*

$$n^{-1/\alpha}\Big(\sum_{i \leqslant n} X_i \,\mathbb{1}\{X_i \leqslant n^a\}\Big) - n\,\mathbb{E}[X_1\,\mathbb{1}\{X_1 \leqslant n^a\}] \xrightarrow{L^2} 0.$$

Proof. Since the random variables X_i are i.i.d., the claim follows by showing that $\mathrm{Var}(X_i\,\mathbb{1}\{X_i \leqslant n^a\}) \in o(n^{2/\alpha-1})$. Now,

$$\mathbb{E}[X_i^2\,\mathbb{1}\{X_i^2 \leqslant n^{2a}\}] = \int_0^{n^{2a}} \mathbb{P}(X_1^2 \in [r, n^{2a}])\,\mathrm{d}r.$$

Since $\mathbb{P}(X_1^2 \geqslant r) \asymp Ar^{-\alpha/2}$ we note that $\int_1^{n^{2a}} \mathbb{P}(X_1^2 > r)\,\mathrm{d}r \in O(n^{2a(1-\alpha/2)})$. Hence, observing that $2a(1 - \alpha/2) < 2/\alpha - 1$ concludes the proof. $\square$

Now, we return to the case of the edge count in the ADRCM. The idea of proof is to decompose S_n as $S_n^{\geqslant} + S_n^{\leqslant}$, where $S_n^{\geqslant}$ and $S_n^{\leqslant}$ contain the contributions of the young and the old vertices, respectively. More precisely, for $u_n := n^{-0.9}$ put

$$S_n^{\geqslant} := \sum_{P_i \in [0,n] \times [u_n, 1]} D_{\mathsf{in}}(P_i), \qquad \text{and} \qquad S_n^{\leqslant} := \sum_{P_i \in [0,n] \times [0, u_n]} D_{\mathsf{in}}(P_i).$$

First, we control the deviations of $S_n^{\geqslant}$ via the Chebyshev inequality.

Proposition B.5.3 ($S_n^{\geqslant}$ is negligible)**.** *It holds that $n^{-\gamma}(S_n^{\geqslant} - \mathbb{E}[S_n^{\geqslant}])$ converges to 0 in probability.*

Proof. To prove the claim, we apply Lemma B.5.1 with $A = [0, n]$ and $u_- = u_n$. In particular, the first summand in Lemma B.5.1 is then of order $O(nu_n^{1-2\gamma})$. Now, since $-0.9(1 - 2\gamma) + 1 < 2\gamma$, we get $nu_n^{1-2\gamma} \in o(n^{2\gamma})$. Hence, it suffices to bound the second summand in Lemma B.5.1. Here, we can apply Lemma B.3.4 (a) which shows that $\int_{\mathbb{S}} s_\wedge(a, u)^\gamma\,\mathrm{d}(a, u) \in O(1)$, thereby concluding the proof. $\square$

Second, we approximate $S_n^{\leqslant}$ by a sum of i.i.d. Pareto random variables so that we can apply the stable CLT by Whitt [107, Theorem 4.5.2].

Proposition B.5.4 ($S_n^{\leqslant}$ converges to a stable distribution)**.** *It holds that $n^{-\gamma}(S_n^{\leqslant} - \mathbb{E}[S_n^{\leqslant}])$ converges in distribution to a stable random variable.*

To maintain a clear structure, we conclude the proof of Theorem B.2.4 before establishing Proposition B.5.4.

Proof of Theorem B.2.4. By Proposition B.5.3, $n^{-\gamma}(S_n^{\geqslant} - \mathbb{E}[S_n^{\geqslant}])$ tends to 0 in probability, and $n^{-\gamma}(S_n^{\leqslant} - \mathbb{E}[S_n^{\leqslant}])$ tends in distribution to a stable random variable. Hence, also

$$n^{-\gamma}(S_n - \mathbb{E}[S_n]) = n^{-\gamma}(S_n^{\geqslant} - \mathbb{E}[S_n^{\geqslant}]) + n^{-\gamma}(S_n^{\leqslant} - \mathbb{E}[S_n^{\leqslant}])$$

tends in distribution to a stable random variable. $\square$

It remains to prove Proposition B.5.4. That is, the renormalized sum of the large in-degrees converges to a stable distribution. To make this precise, we introduce two further approximations, namely $S_n^{(1)}$ and $S_n^{(2)}$, that we define now. In these approximations, we replace the in-degree by its expectation, and replace the Poisson number of points in $[0, n]$ by a fixed number, respectively. More precisely, we set

$$S_n^{(1)} := \sum_{\substack{X_i \in [0,n] \\ U_i \leqslant u_n}} \mu(U_i) \qquad \text{and} \qquad S_n^{(2)} := \sum_{\substack{i \leqslant n \\ U_i \leqslant u_n}} \mu(U_i).$$

The key step in the proof of Proposition B.5.4 is to show that each of these expressions is close in L^1-norm.

Lemma B.5.5 ($S_n^{\leqslant}, S_n^{(1)}$ and $S_n^{(2)}$)**.** *It holds that* $\mathbb{E}[|S_n^{\leqslant} - S_n^{(1)}|] + \mathbb{E}[|S_n^{(1)} - S_n^{(2)}|] \in o(n^{\gamma})$.

Before proving Lemma B.5.5, we explain how to conclude the proof of Proposition B.5.4.

Proof of Proposition B.5.4. By Lemma B.5.5, it suffices to show that $n^{-\gamma}(S_n^{(2)} - \mathbb{E}[S_n^{(2)}])$ converges in distribution to a stable random variable. We note that, by construction, the summands $\mu(U_i)$, $i \leqslant n$, are i.i.d. Moreover, by Lemma B.3.3, $\mu(u) \sim (\beta/\gamma)u^{-\gamma}$. Hence, an application of Lemma B.5.2 concludes the proof. $\square$

It remains to prove Lemma B.5.5.

Proof of Lemma B.5.5. We prove the two parts separately.

Part $\mathbb{E}[|S_n^{\leqslant} - S_n^{(1)}|]$**.** By the Mecke formula, it suffices to show that

$$n \int_{[0,u_n]} \mathbb{E}\big[|D_{\mathsf{in}}(o) - \mu(u)|\big] \, \mathrm{d}u \in o(n^{\gamma}).$$

To achieve this goal, we use the fact that the centered moment of a Poisson random variable with parameter λ is given by $2\lambda^{\lfloor \lambda \rfloor + 1}e^{-\lambda}/\lfloor \lambda \rfloor!$. Specializing to $\lambda = \mu(u)$ and applying the Stirling formula shows that $\mathbb{E}[|D_{\mathsf{in}}(o) - \mu(u)|] \in O(u^{-0.6\gamma})$. Therefore,

$$n \int_{[0,u_n]} \mathbb{E}[|D_{\mathsf{in}}(o) - \mu(u)|] \, \mathrm{d}u \in O(nu_n^{1-0.6\gamma}).$$

Now, since $1 - 0.9(1 - 0.6\gamma) < \gamma$, we deduce that $nu_n^{1-0.6\gamma} \in o(n^{\gamma})$, thereby concluding the proof.

Part $\mathbb{E}[|S_n^{(1)} - S_n^{(2)}|]$**.**   Let N be a Poisson random variable with parameter n. Then,

$$\mathbb{E}[|S_n^{(1)} - S_n^{(2)}|] \leqslant \mathbb{E}[|N - n|] \int_0^{u_n} \mu(u)\, \mathrm{d}u.$$

First, the CLT for i.i.d. random variables gives that $\mathbb{E}[|N-n|] \in O(n^{1/2})$. Furthermore,

$$\int_0^{u_n} \mu(u)\, \mathrm{d}u \in O(u_n^{1-\gamma}).$$

Therefore, $\mathbb{E}[|S_n^{(1)} - S_n^{(2)}|] \in O(n^{1/2} u_n^{1-\gamma})$. Hence, noting that $1/2 - 0.9(1-\gamma) < \gamma$ concludes the proof. $\qquad\square$

B.6   Proof of Theorem B.2.5

We deal with Parts (a) and (b) of Theorem B.2.5 separately.

Proof of Part (a)

We start with Part (a). In the assertion, we need to establish upper and lower bounds for the probability that the typical degree in the thinned graph G^{th}, η is large. First, we discuss the lower bound, as the proof allows us to ignore the distinction between exposed and protected edges.

Proof of Theorem B.2.5 (a), lower bound. Let G' be obtained by independent edge thinning, where all edges of the ADRCM G are eligible to be removed. Moreover, the retention probability of an edge $(Y, V) \to o = (0, U)$ is set as U^η. Then, $G' \subseteq G^{\mathsf{th}}, \eta$ so that $\mathbb{P}(\deg_{G^{\mathsf{th}},\eta,\mathsf{in}}(o) \geqslant k) \geqslant \mathbb{P}(\deg_{G',\mathsf{in}}(o) \geqslant k)$.

Now, the thinning theorem for Poisson point processes implies that, conditioned on U, the retained in-neighbors form a Poisson point process. Hence, conditioned on U, the in-degree is a Poisson random variable with a mean $U^\eta \mu(U)$. Moreover,

$$\mathbb{P}(\deg_{G',\mathsf{in}}(o) \geqslant k) \geqslant \mathbb{P}(U^\eta \mu(U) \geqslant 2k) - \mathbb{P}(\deg_{G',\mathsf{in}}(o) \leqslant k, U^\eta \mu(U) \geqslant 2k).$$

By Poisson concentration, the second probability on the right decays exponentially in k, whereas (B.2) yields the asserted $\mathbb{P}(U^\eta \mu(U) \geqslant 2k) \in O(k^{-1/(\gamma-\eta)})$. $\qquad\square$

Next, we prove the upper bound for the tail probabilities of the vertex degrees. That is, an upper bound for the probability that the typical degree is considerable. Since in the model G^{th}, η only the exposed edges are thinned out, this is more difficult than the lower bound. Loosely speaking, we need to ensure that the number of protected edges is negligible so that it does not matter whether they are considered in the thinning. To achieve this goal, in Lemma B.6.1, we bound the power-law exponent of the number of protected edges leading to the typical node o.

Lemma B.6.1 (Power-law for the vertex degree of protected edges)**.** *It holds that*

$$\lim_{k \uparrow \infty} \log(d_k^{\mathsf{pr},\eta}) / \log(k) = 1 - 2/\gamma.$$

Before proving Lemma B.6.1, we conclude the proof of the upper bound in Theorem B.2.5 (a).

Proof of Theorem B.2.5 (a), upper bound. As in the proof of the lower bound, we let G' be the graph obtained by independent edge thinning, where we allow all edges to be thinned. Moreover, we let I_{pr} denote the number of protected edges incident to Δ_m. Then,

$$\mathbb{P}\big(\deg_{G^{\mathsf{th},\eta}}(o) \geqslant k\big) \leqslant \mathbb{P}\big(\deg_{G'}(o) \geqslant k/2\big) + \mathbb{P}\big(I_{\mathsf{pr}} \geqslant k/2\big).$$

By Lemma B.6.1, the second probability on the right-hand side is of order at most $k^{1-2/\gamma+o(1)}$. Hence, to conclude the proof, we need to show that the first probability is of order at most $k^{-1/(\gamma-\eta)+o(1)}$. To that end, we proceed as in the proof of the lower bound. More precisely,

$$\mathbb{P}\big(\deg_{G'}(o) \geqslant k\big) \leqslant \mathbb{P}\big(\deg_{G'}(o) \geqslant k, U^\eta \mu(U) \leqslant k/2\big) + \mathbb{P}\big(U^\eta \mu(U) \geqslant k/2\big).$$

Again, by Poisson concentration, the first probability on the right-hand side decays exponentially in k, whereas the second one is of order $k^{-1/(\eta-\gamma)+o(1)}$, as asserted. $\square$

Now, we prove Lemma B.6.1. The idea is to carefully distinguish between different cases of how an edge can be protected, and then to bound each of the resulting probabilities separately.

Proof of Lemma B.6.1. Our goal is to bound the probability that the number of protected edges leading to o is at least $k \geqslant 1$. By definition, it suffices to bound $\mathbb{P}(\mathcal{P}^{(1)} \geqslant k)$, and $\mathbb{P}(\mathcal{P}^{(2)} \geqslant k)$, where

$$\mathcal{P}^{(1)} := \{(Z,W) \in M(o) : U \leqslant W \leqslant 2U\},$$
$$\mathcal{P}^{(2)} := \{(Z,W) \in M(o) : (Z,W) \to (Y,V) \text{ for some } (Y,V) \in \mathcal{P} \text{ with } V \leqslant 2U \leqslant 4V\}.$$

We now deal with the two cases separately and heavily rely on the result from [40, Proposition 4.1], that conditioned on $U = u$, the in-degree of o is Poisson-distributed with mean in $\mu(u)$.

$\mathbb{P}(|\boldsymbol{\mathcal{P}^{(1)}}| \geqslant \boldsymbol{k})$. We note that conditioned on $U = u$, the quantity $|\mathcal{P}^{(1)}|$ is a Poisson random variable with mean $\int_u^{2u} |I_{\beta u^{-\gamma} v^{-(1-\gamma)}}| \, dv = \beta(2^\gamma - 1)/\gamma$. Hence, $\mathbb{P}(|\mathcal{P}^{(1)}| \geqslant k)$ decays exponentially fast in k.

$\mathbb{P}(|\boldsymbol{\mathcal{P}^{(2)}}| \geqslant \boldsymbol{k})$. Note that if $(Z,W) \to (0,U)$ and $(Z,W) \to (Y,V)$, then

$$|Y| \leqslant \beta|Z|/2 + \beta|Z-Y|/2 \leqslant \beta U^{-\gamma} W^{-(1-\gamma)}.$$

For any $\varepsilon > 0$, the probabilities $\mathbb{P}(\mathcal{P}([-\beta U^{-1}, \beta U^{-1}] \times [U, 2U]) \geqslant k^\varepsilon)$ decay at stretched exponential speed. Indeed, conditioned on $U = u$, the random variable $\mathcal{P}([-\beta u^{-1}, \beta u^{-1}] \times [u, 2u])$ is Poisson distributed with mean 2β so that the asserted decay is a consequence of the Poisson concentration inequality.

Therefore, recalling (B.6), it suffices to bound

$$\int_0^1 \int_{u/2}^1 \int_{-\infty}^\infty \mathbb{P}\big(\mathcal{P}\big(M\big((0,u),(y,v)\big)\big) \geqslant k^{1-\varepsilon}\big) \, \mathrm{d}y \, \mathrm{d}v \, \mathrm{d}u.$$

Again, applying the Poisson concentration inequality reduces this task to bounding

$$\int_0^1 \int_{u/2}^1 \int_{-\infty}^\infty \mathbb{1}\{\mu\big((0,u),(y,v)\big) \geqslant k^{1-\varepsilon}\} \, \mathrm{d}y \, \mathrm{d}v \, \mathrm{d}u. \tag{B.8}$$

Since $\mu\big((0,u),(y,v)\big) \leqslant \mu(u)$, we conclude that if $\mu\big((0,u),(y,v)\big) \geqslant k^{1-\varepsilon}$, then $u \leqslant ck^{-(1-\varepsilon)/\gamma}$ for some $c > 0$. Moreover, we deduce from Lemma B.3.3 that $\mu\big((0,u),(y,v)\big) \leqslant (\beta/\gamma)v^{-\gamma}s_\wedge(y,u)^\gamma$. Therefore, (B.8) is bounded above by

$$(\beta/\gamma)^{1/\gamma}k^{-(1-\varepsilon)/\gamma} \int_0^{ck^{-(1-\varepsilon)/\gamma}} \int_{-\infty}^\infty s_\wedge(y,u) \, \mathrm{d}y \, \mathrm{d}u.$$

Hence, an application of Lemma B.3.4 (a) concludes the proof. □

Proof of Part (b)

Next, we prove Part (b) of Theorem B.2.5. That is, the thinning operation does not affect the power-law exponent of the edge degrees. Loosely speaking, the idea is that even after removing all exposed edges, the protected edges are sufficient to sustain a positive proportion of all the triangles, resulting in a high edge degree in the ADRCM.

As in the proof of (a), we show upper and lower bounds for the tail probabilities separately. We start with the proof of the upper bound. Intuitively, it is not surprising that removing edges reduces the edge degrees. Nevertheless, to make the presentation self-contained, we give a rigorous proof.

Proof of Part (b) of Theorem B.2.5, upper bound. The key idea is to use the Palm representation of the typical edge degree. More precisely,

$$\begin{aligned} d_{1,k} &= \mathbb{P}(\deg_2(\Delta_1) \geqslant k) \\ &= \frac{1}{\lambda_2} \mathbb{E}\Big[\sum_{\substack{(X,U),(Y,V)\in\mathcal{P} \\ (Y,V)\to(X,U)}} \mathbb{1}\{X \in [0,1]\} \, \mathbb{1}\{\deg_2\big((X,U),(Y,V)\big) \geqslant k\}\Big], \end{aligned}$$

where $\lambda_2 > 0$ denotes the edge intensity of G. Similarly, by writing $\to^\eta$ to indicate a directed edge in the graph G^{th}, η, we get that

$$d_{1,k}^{\mathsf{th},\eta} = \frac{1}{\lambda_2^{(\eta)}} \mathbb{E}\Big[\sum_{\substack{(X,U),(Y,V)\in\mathcal{P} \\ (Y,V)\to^\eta(X,U)}} \mathbb{1}\{X \in [0,1]\} \, \mathbb{1}\{\deg_G\big((X,U),(Y,V)\big) \geqslant k\}\Big],$$

where $\lambda_2^{(\eta)}$ is the edge intensity of the thinned graph. Now, noting that G^{th}, η is a subgraph of G implies that $d_{1,k}^{\mathsf{th},\eta}\lambda_2^{(\eta)} \leqslant d_{1,k}\lambda_2$. In particular, $\limsup_{k\uparrow\infty} \log(d_{1,k}^{\mathsf{th},\eta})/\log(k) \leqslant 1 - 2/\gamma$, as asserted. □

The lower bound is more delicate since we need to show that triangles formed by the protected edges are sufficient to sustain the original edge degree even after the thinning. By monotonicity, it suffices to establish the asserted lower bound for the graph $G'' := G^{(\infty)}$, i.e., the graph where only the protected edges are retained.

Proof of Part (b) of Theorem B.2.5, lower bound. As a preliminary observation, we note that a directed edge of the form $(Y, V) \to (X, U)$ with $V \leqslant 2U$ is never exposed. Hence, as in the non-thinned case in Theorem B.2.1, we need to derive a lower bound for the expression

$$\int_0^1 \int_u^{2u} \int_{-\infty}^{\infty} T(u, v, y) \, \mathrm{d}y \, \mathrm{d}v \, \mathrm{d}u,$$

where $T(u, v, y) := \mathbb{P}(\deg_2((y, v), (o, u)) \geqslant k)$. To achieve this goal, we derive a lower bound for $T(u, v, y)$ when (u, v, y) is in the domain

$$B_k := [(\beta/(64k))^{1/\gamma}, (\beta/(32k))^{1/\gamma}] \times [(\beta/(32k))^{1/\gamma}, (\beta/(16k))^{1/\gamma}] \times [0, 8k].$$

First, note that $(y, v) \to (0, u)$ for every $(u, v, y) \in B_k$ as $(\beta/2)u^{-\gamma}v^{-(1-\gamma)} \geqslant 16k \geqslant y$. Since $|B_k| \in O(k^{1-2/\gamma})$, it therefore suffices to show that $T(u, v, y)$ is uniformly bounded away from 0 for $(u, v, y) \in B_k$.

To achieve this goal, we first note that any point $(z, w) \in C_k := [0, 8k] \times [3/4, 1]$ connects to both (o, u) and (y, v). Indeed,

$$|z - 0| \leqslant 8k \leqslant (\beta/2)((\beta/(32k))^{1/\gamma})^{-\gamma} \quad \text{and} \quad |z - y| \leqslant 8k \leqslant (\beta/2)((\beta/(16k))^{1/\gamma})^{-\gamma}.$$

Noting that $v \leqslant 2u$ implies that both edges are protected and therefore also exist in G^{th}, η. Now, we conclude since the Poisson concentration inequality implies that $\mathbb{P}(\mathcal{P}(C_k) \geqslant k) \to 1$ as $k \to \infty$. $\qquad\square$

B.7   Simulation study

This section serves as a bridge between the theory and its applications to real-world data. Specifically, we study how well the methods and limit theorems derived for the ADRCM apply to finite networks. Our Monte Carlo approach involves simulating multiple networks with identical model parameters. Subsequently, we calculate various network properties and subject them to statistical analysis, often entailing parameter estimation for theoretical probability distributions. Relying on Palm calculus, we also explore the simulation of typical simplices in infinite networks to examine fluctuations of different quantities around the limit, devoid of finite-size effects.

To ensure efficiency, performance-critical parts of our simulation software—such as network generation and the computation of quantities of large networks—are implemented in C++. For topological data analysis, we use the GUDHI C++ library [15], which provides robust tools for the calculation of Betti numbers. These C++ algorithms are exposed to Python using pybind11 [60]. Data processing and statistical analysis are performed in Python using packages such as NumPy [45], SciPy [105], and NetworkX [44]. Finally, all visualizations in the paper were created using the LaTeX package TikZ and the Python package Matplotlib [54].

Simulation methods

Simulating finite networks.   To simulate a finite network, we follow a step-by-step process as outlined below.

(1) We begin by fixing the network size, setting the volume V of the sampling window equal to the expected number of vertices in the network. The vertex number N is drawn from a Poisson distribution with parameter V. This step determines the actual vertex number in the network.

(2) Next, we generate the birth times of the N vertices. Conditioned on the vertex number, the birth times are uniformly distributed. Thus, the birth times are generated by drawing N i.i.d. uniformly distributed random variables from the interval $(0, 1]$. For each vertex, its position is also generated independently and uniformly across the entire sampling window. This process corresponds to sampling the spatial Poisson point process conditioned on the point count.

(3) Connections between vertices are created based on the following condition. For every pair of vertices (x, u) and (y, v), where $u \leqslant v$, a connection is formed if the distance between the vertices satisfies $|x - y| \leqslant \frac{1}{2}\beta u^{-\gamma} v^{-(1-\gamma)}$. This criterion governs the establishment of connections in the network.

(4) Finally, the generated binary network is expanded to a clique complex. This simplicial complex enables topological analysis and the examination of higher-order network properties.

Figure B.2 shows the largest component of a generated network of size $1\,000\,000$ with $\gamma = 0.7$.

Simulating Palm distributions.   To avoid the influence of finite-size effects and simulate typical simplices in infinite networks, we use Palm calculus. The main idea is to focus only on the immediate neighborhood of a typical vertex placed at the origin, thereby eliminating the presence of finite-size effects for the central vertex. In this neighborhood, other vertices can form connections with the central vertex and with
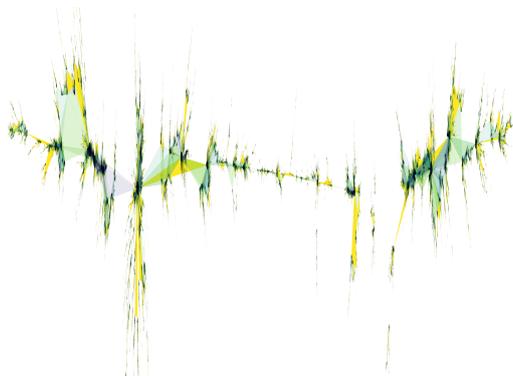
Figure B.2: The largest component of a network sample generated by the ADRCM

each other as well. Any vertex that cannot form a connection with the vertex at the origin is not considered. The simulation of a single network is visualized in Figure B.3.

(1) **Typical vertex**. We begin by randomly placing a vertex $(0, u)$ at the origin of the sampling window with a uniformly distributed birth time u.

(2) **Simulation of older vertices**. We create older vertices to which the vertex $(0, u)$ connects by simulating a homogeneous Poisson point process in the red shaded area. The number of older vertices in the red area born up to time $v_0 \leqslant u$ is Poisson distributed with parameter

$$\int_0^{v_0} |I_{\beta v^{-\gamma} u^{-(1-\gamma)}}| \, \mathrm{d}v = \frac{\beta}{1 - \gamma} u^{-(1-\gamma)} v_0^{1-\gamma}.$$

To generate the birth times $\{v_i\}$ of the points, we simulate a homogeneous Poisson point process $\{w_i\}$ in the domain $[0, u^{1-\gamma}]$ with intensity $\beta u^{-(1-\gamma)}/(1 - \gamma)$. The cardinality of $\{w_i\}$ will have the same distribution as the point count in the red area. We then transform $\{w_i\}$ to obtain the set of birth times: $\{v_i\} = \{w_i^{1/(1-\gamma)}\}$. The transformation ensures that the birth times $\{v_i\}$ have the required density. The positions y_i of the vertices are chosen uniformly in the respective domain $[-\frac{1}{2}\beta v_i^{-\gamma} u^{-(1-\gamma)}, \frac{1}{2}\beta v_i^{-\gamma} u^{-(1-\gamma)}]$.

(3) **Simulation of younger vertices**. Simulation of the younger neighbors of the typical vertex is similar. The number of younger vertices in the green area born up to time $v_0 \geqslant u$ is again Poisson distributed with parameter

$$\int_u^{v_0} |I_{\beta v^{-\gamma} u^{-(1-\gamma)}}| \, \mathrm{d}v = \frac{\beta}{\gamma} \big(u^{-\gamma} v_0^\gamma - 1\big).$$

To generate the birth times $\{v_i\}$ using a homogeneous Poisson point process $\{w_i\}$ in the domain $[u^\gamma, 1]$ with intensity $\beta u^{-\gamma}/\gamma$, which means that the number of elements in $\{w_i\}$ will have the same distribution as the number of younger vertices connecting to the typical vertex. Then, we transform $\{w_i\}$ as before
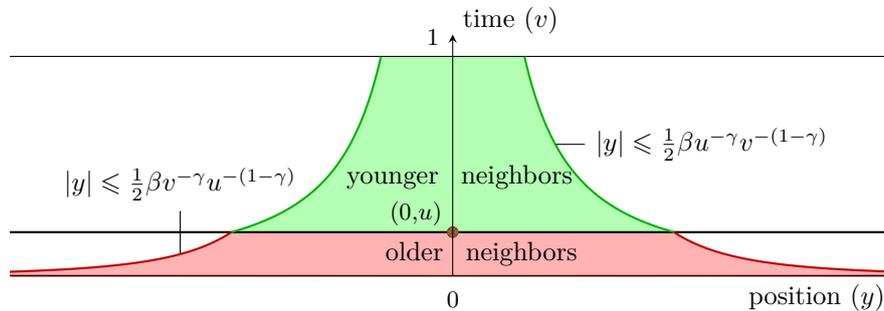
Figure B.3: Simulation of the Palm distribution. A typical vertex is placed at the origin with fixed birth time u. The typical vertex connects to older vertices in the red shaded area, whereas younger vertices connect to the typical vertex in the green shaded area of the graph.

to get the birth times $\{v_i\} = \{w_i^{1/\gamma}\}$. The positions y_i are chosen uniformly in $[-\frac{1}{2}\beta u^{-\gamma}v_i^{-(1-\gamma)}, \frac{1}{2}\beta u^{-\gamma}v_i^{-(1-\gamma)}]$.

(4) **Clique complex**. As before, the generated simple graph is expanded to a clique complex. Note that those simplices in the clique complex are not subject to finite-size effects, which include the central vertex $(0, u)$ at the origin.

Higher-order degree distributions of the ADRCM

First, we demonstrate that the higher-order degree distributions converge to their theoretical limit as the network size increases.

To estimate the parameters of power-law distributions, we face two problems. First, the domain in which the power-law distribution holds is not identical to the entire domain of the data. As discussed in Section B.2, the degree of a typical vertex is a Poisson random variable whose parameter is itself a heavy-tailed random variable. Thus, the power-law distribution will only be visible for empirical values that are larger than a minimal value x_{min}, from where the influence of the Poisson distribution is negligible. On the other hand, x_{min} cannot be too large since in this case the estimation of the power-law exponent becomes too inaccurate due to the low number of values above x_{min}. Considering these two effects, we conducted a pilot study and found $x_{\mathsf{min}} = 30$ to be a suitable compromise. We estimated the exponent a of the power-law distributions via maximum likelihood [23]. In our setting, this means that

$$\hat{a} = 1 + n\Big[\sum_{i \leqslant n} \log\Big(\frac{x_i}{x_{\mathsf{min}} - 1/2}\Big)\Big]^{-1},$$

where the index i goes over the data points $x_i \geqslant x_{\mathsf{min}}$. We fixed the network size to $100\,000$ and set $\beta = 1$. For several choices of the parameter γ, we estimated the power-law exponent $\hat{a}$ for each candidate x_{min} using the maximum likelihood method. We found that the inferred γ values computed from the exponents $\hat{a}$ were close to theoretical values when $x_{\mathsf{min}} \geqslant 30$. The vertex, edge, and triangle degree distributions of a generated network sample with a network size of $100\,000$ and $\gamma = 0.7$ can be seen in Figure B.4, which illustrates the challenges in estimating power-law exponents for degree distributions. In the small-degree range, the power-law tail of the distribution is hidden due to the Poisson distribution. However, as the degrees exceed ~ 30, the power-law tail is apparent.

In Theorem B.2.1, we demonstrated that both the ordinary and the higher-order degree distributions follow a power-law tail. However, this result is rigorously established only for infinitely large networks. To apply this theorem to real datasets of finite size, it is essential to investigate the extent to which these findings hold for finite networks.

To address this, we conducted Monte Carlo simulations for finite network sizes. For each network size, we generated 100 networks with a parameter $\gamma = 0.7$. The power-law distribution was then fitted to their degree distributions using the described method. This process yielded 100 exponents for the vertex, edge, and triangle degree distributions. Given that the parameters of the underlying ADRCM remained constant, this set of exponents provided a basis for statistical analysis. By repeating
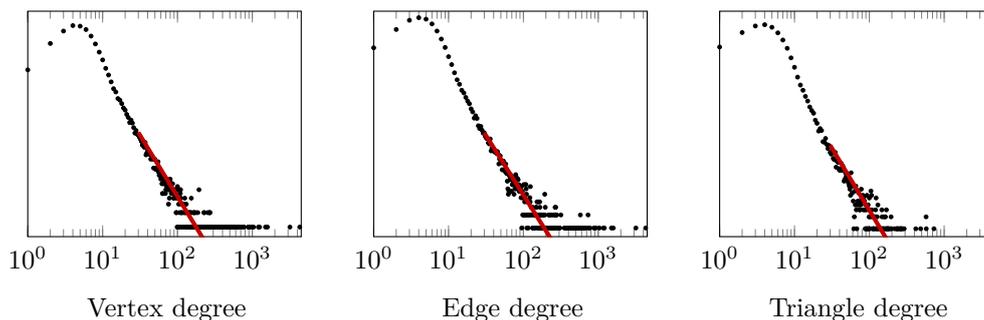
Figure B.4: Degree distributions of the ADRCM

this procedure for networks of varying size, we assessed the convergence of degree distribution exponents to the theoretical limit established in Theorem B.2.1.

Additionally, we examined the simulation of Palm distributions using the same approach. For this case, 100 000 infinite networks were simulated to fit the degree distribution exponents, equivalent to sampling 100 000 typical vertices. The edges and triangles considered in the simulation of the Palm distribution were those involving a special vertex placed at the origin.

The results of the simulations are depicted in Figure B.5, presenting three sets of boxplots summarizing the distribution of the fitted exponents. The three figures visually illustrate the convergence of fitted exponents towards the theoretical limit, indicated by a red horizontal line. From the observed results, the following conclusions can be drawn.
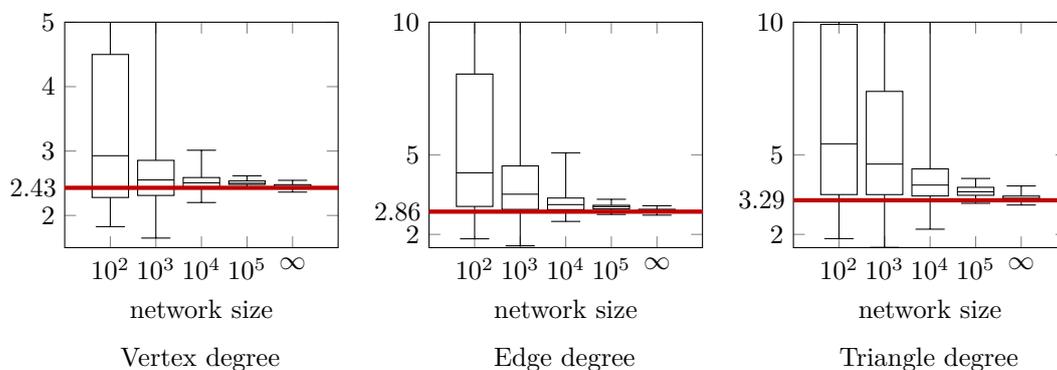
Figure B.5: Degree distribution exponents

- As the network size increases, the fluctuation of fitted exponents decreases. Smaller networks (with fewer than 1000 vertices) exhibit significant fluctuations, while larger networks (with over 10 000 vertices) tend to approach the theoretical limit more closely. Infinite networks display the least fluctuations.

- For a given network size, higher dimensions lead to larger fluctuations in the fitted exponents. This suggests that considering higher dimensions introduces more variability in estimating the exponents of degree distributions.

107

- Fitted exponents for finite networks tend to be higher than the theoretical values, indicating a bias in the estimation process. This bias is attributed to the constraint on the maximum degree in each dimension due to the finite size, resulting in the truncation of the degree distribution tails. For small degrees, such truncation is absent. These effects lead to higher degree distribution exponents. The negligible bias observed in the distribution of exponents for *infinite* networks supports this explanation.

Edge count of the ADRCM

In Theorem B.2.3, we demonstrated that the edge count in large networks follows a normal distribution if $\gamma < 0.5$. Conversely, Theorem B.2.4 established that the edge count distribution can be described by a stable distribution if $\gamma > 0.5$. To validate these claims in finite networks, we analyzed the edge count distribution in networks containing $100\,000$ vertices.

For each of the three selected values of the parameter γ (0.25, 0.50, and 0.60), we simulated 1000 networks with $\beta = 1$. Then, we examined the distributions of the edge counts for each of the three cases by fitting both a normal and a stable distribution to the empirical values.

To fit a normal distribution, we estimated the expectation as the sample mean and the variance as the sample variance. When fitting the stable distribution, we utilized the insights from Theorem B.2.4 to set the α and β parameters directly: $\alpha = 1/\gamma$ (if $\gamma < 0.5$, otherwise $\alpha = 2$) and $\beta = 1$. The *location* and *scale* parameters needed to be estimated from the empirical distribution. For this purpose, we employed maximum likelihood estimation [77].

Figure B.6 visually represents the results of our analysis, showing the distributions of the edge counts for each of the three cases: $\gamma = 0.25$, $\gamma = 0.50$, and $\gamma = 0.60$. The subfigures in Figure B.6 provide a comprehensive view of the empirical and fitted distributions of the edge counts, along with Q-Q (Quantile-Quantile) plots for comparing the empirical and fitted distributions. The top row displays the empirical and fitted distributions, while the second and third rows present the Q-Q plots for the fitted normal distributions and the fitted stable distributions.

When $\gamma = 0.25$, the distribution of edge counts appears symmetric, and the fitted normal distribution closely aligns with the empirical data. However, for $\gamma = 0.6$, a fat right tail is clearly visible in the empirical distribution. This heavy-tailed behavior is not adequately captured by the fitted normal distribution, as evidenced by the deviation from the diagonal line in the Q-Q plot for the normal distribution. In contrast, the stable distribution provides a better fit, aligning well with the data points in the Q-Q plot. Interestingly, for $\gamma = 0.5$, the normal distribution does not describe the data as effectively as it does for $\gamma = 0.25$. We offer two potential reasons for this observation.

- **The finite size of the network:** In this case, a few high-degree vertices may contribute significantly to the total edge count. However, for a sufficiently large network, these contributions would be spread among many such vertices, leading to a more normal-like distribution.
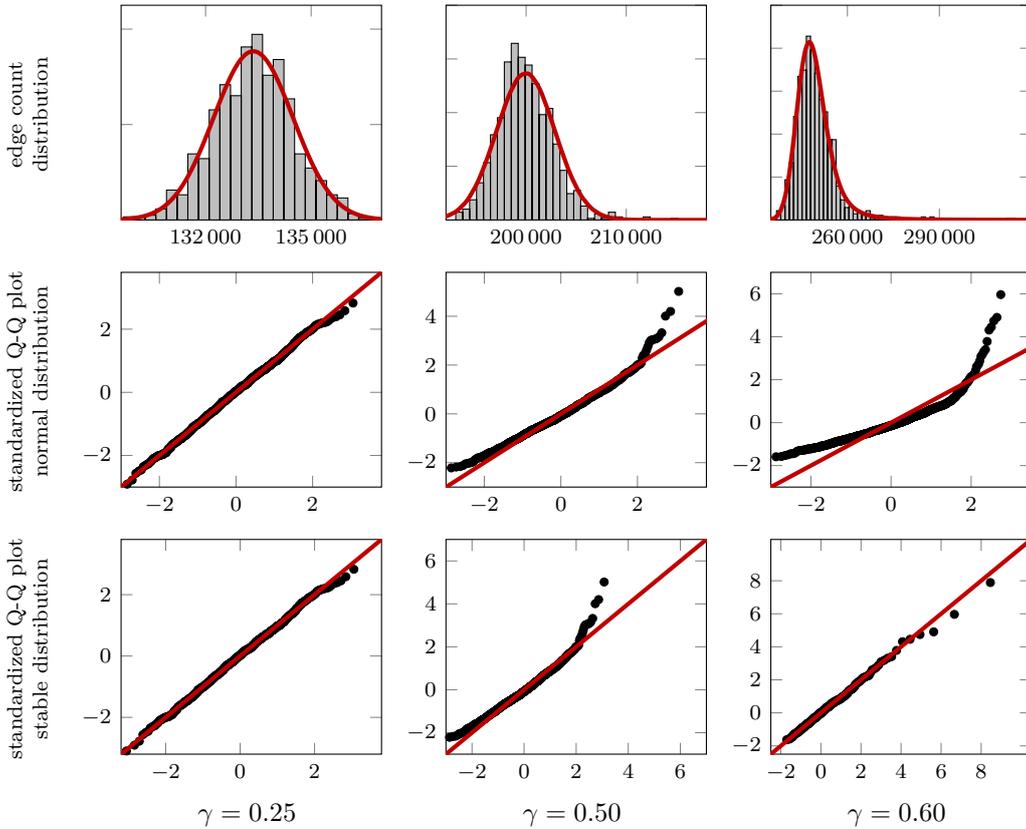
Figure B.6: Distribution of the edge count for different γ parameters

- **The boundary case of $\gamma = 0.5$:** At this value, the degree distributions have an infinite variance, which can affect the distribution characteristics and may not be accurately captured by a normal distribution.

Supporting the validity of Theorem B.2.4, the above observations suggest that the normal distribution appears to be a reasonably good fit when $\gamma < 0.5$, but the stable distribution explains the data more accurately if $\gamma > 0.5$.

Betti numbers of the ADRCM

To establish the validity of Theorem B.2.2 for finite networks, we conducted simulations on finite networks containing 100 000 vertices. In this case, due to the computational costs of computing Betti numbers, we performed 100 simulations for each of the three different values of the parameter γ: 0.25, 0.50, and 0.67.

For values of $\gamma = 0.25$, aligning with the findings of Theorem B.2.2, we approximated the empirical values of the first Betti numbers with a normal distribution. For values of $\gamma = 0.6$, we observed the distribution of the Betti numbers and conjectured that they follow a stable distribution with stability parameter $\alpha = 1/\gamma$. We posit this

based on the expectation that the infinite variance of the simplex count leads to a corresponding infinite variance of the Betti numbers.

In all cases, the parameter β of the stable distribution remained constant at -1. As in Section B.7, we estimated the remaining parameters of the fitted distributions via maximum likelihood. The results are visualized in Figure B.7.

From the Q-Q plots, it is evident that the fitted normal distribution provides a satisfactory approximation to the distribution of the Betti numbers for the simulations with $\gamma = 0.25$ and $\gamma = 0.50$. The points on the Q-Q plots are closely aligned with the diagonal line, indicating a good fit.

However, for $\gamma = 0.67$, the distribution displays a heavy left tail, which is clearly visible both from the histogram and the Q-Q plot against the normal distribution: the points on the Q-Q plot significantly deviate from the diagonal line in the lower quantiles. The shallow slope of the points in the central section suggests that the standard deviation is not accurately captured by the normal distribution, which is also an artifact of the heavy left tail. In contrast, the stable distribution fits the histogram more accurately, as visualized in the Q-Q plot shown in the bottom right part of Figure B.7. We can also see that the left tail is not entirely accurate in the stable distribution case. This is explained by two effects:

- the simulation number is low, thus there are not enough values in the left tail to precisely estimate the distribution;

- the minimum value in the distribution is 0, suggesting the presence of finite-size effects.

All in all, the points on the Q-Q plot against the stable distribution follow more closely the diagonal line both in the central region and in the left tail of the distribution, reinforcing our earlier conjecture about the stable distribution of Betti numbers for $\gamma > 0.5$.

B.8   Analysis of collaboration networks

In this section, we analyze four datasets collected from arXiv to showcase the applications of our results and to motivate our model extensions further. As higher-order relationships naturally emerge in the context of scientific collaborations, we chose to analyze a publicly available dataset of scientific papers. The authors of the papers are represented as vertices in a simplicial complex, and each paper corresponds to a higher-order interaction of the authors.

Patania et al. [83] also investigates higher-order collaboration networks on the arXiv data and extends the concept of triadic closure to higher dimensions. However, their analysis was purely empirical in nature and did not consider the question of using a stochastic higher-order network model. In contrast, we compare the arXiv dataset with the ADRCM, and also perform hypothesis tests. We also note that although we consider a different time frame, the Betti numbers we found are mainly consistent with the results published by Patania et al. [83].
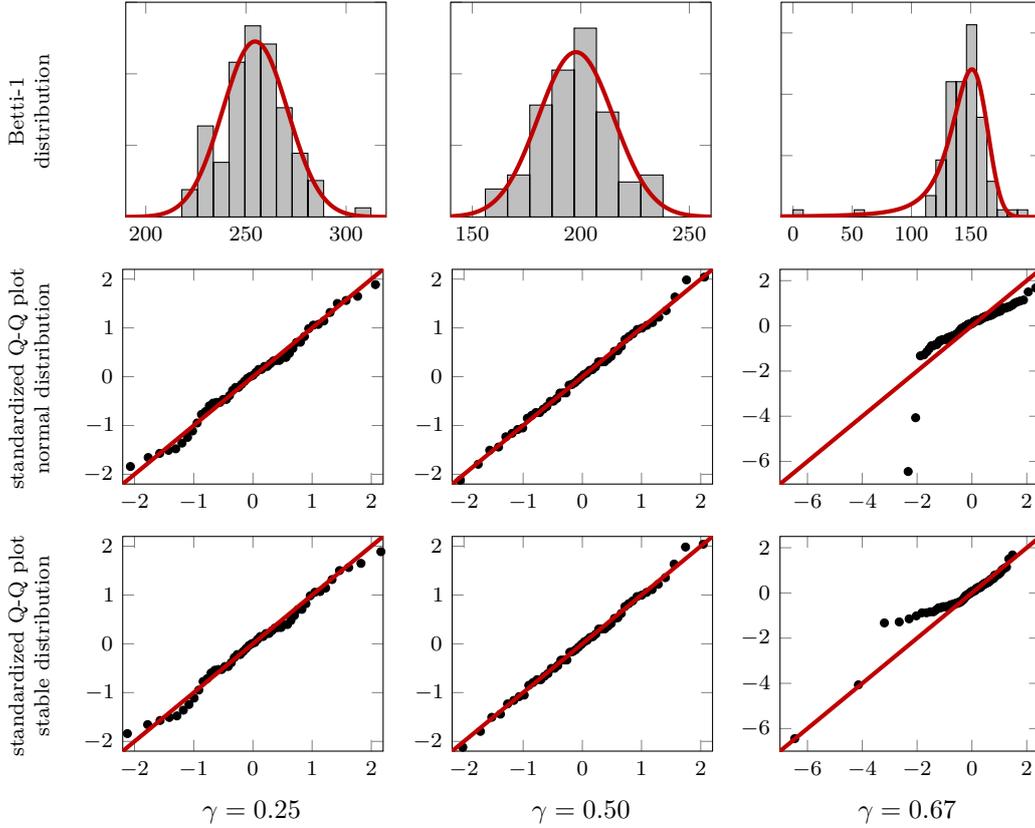
Figure B.7: Distribution of Betti-1 with different γ parameters

Datasets

We analyze all available documents uploaded to arXiv from various scientific fields. For each document, we extracted the author names, the publication time, and its primary category. The datasets were constructed using the primary categories of the documents specified by the authors.

- **Computer Science (`cs`):** The computer science dataset is the largest we analyze, with more than 400 000 authors.

- **Engineering (`eess`):** The second dataset we analyze consists of documents from the scientific field of electrical engineering, which was built from approximately 80 000 authors.

- **Mathematics (`math`):** The mathematics dataset encompasses around 200 000 authors.

- **Statistics (`stat`):** The smallest dataset we analyze contains documents from the field of statistics, including around 45 000 authors.

The largest components of the datasets are visualized in Figure B.8, and their most important characteristics are summarized in Table B.1.

<div align="center">cs   eess   math   stat</div>
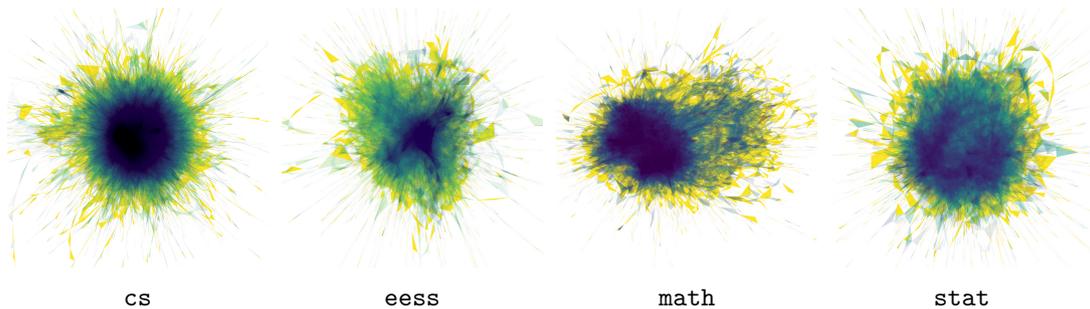
Figure B.8: The largest components of the simplicial complexes built from the datasets

As arXiv does not uniquely identify authors, we chose to use their full names as identifiers. Although, in the case of a common full name, this method will result in treating distinct authors as if they were the same, the effect of these identifier collisions is significantly reduced when considering scientific fields separately.

After identifying the authors as vertices, each document is considered as a higher-order interaction of the authors. This means that every document with $n+1$ authors is represented by an n-simplex. Furthermore, as our goal is to build a simplicial complex, every lower-dimensional face of this n-simplex is also added to the simplicial complex to ensure that it is closed under taking subsets.

A document with $n + 1$ authors has $\binom{n+1}{m+1}$ m-faces, so in total $\sum_{m=0}^{n}\binom{n+1}{m+1} = 2^{n+1} - 1$ number of simplices needs to be considered. This poses a twofold practical implementation challenge.

(1) Due to computational reasons, we must limit the maximum dimension of the simplicial complex.

(2) The more authors a document has, the higher its influence is on the simplicial complex, as the number of simplices grows exponentially with the number of authors. Carstens and Horadam [20] has also found the same problem when analyzing collaboration networks. They tackled this problem by weighting the simplices: they assigned greater weights to smaller simplices and to those in which the represented collaboration occurred frequently. Although introducing weighted simplices is possible, it is beyond the scope of our present work.

Taking into account the above aspects, we consider interactions with a dimension of at most 20 (which, including all the faces, means more than 2 million simplices in total for a document with 21 authors). To further reduce computational complexity, we analyzed the 2-skeleton of the collaboration network, with the triangles being the highest-dimensional simplices.

Using this procedure, we built four separate datasets, each representing publications of a specific scientific field published up to 4 August 2023. As we will see, the nature of collaborations significantly differs in the four cases; thus, by considering the four scientific fields separately, we can examine how the ADRCM model behaves for four distinct scientific communities.

Table B.1: Main properties of the datasets

dataset	authors	documents	components	size of largest component
cs	433244	452881	22576	370494
eess	77686	69594	5533	54147
math	198601	466428	26197	152441
stat	44380	36689	4049	32373

It is also interesting to analyze the distribution of the dimension of the higher-order interactions, or, equivalently, of the per-document author count. Figure B.9 visualizes the distribution of the per-document author count for each dataset, revealing the typical size of the collaborations scientists participate in within each of the examined scientific fields. The distributions related to the cs and eess datasets have the fattest tails, i.e., a relatively higher number of documents have more authors. On the other hand, the opposite is true for the math and stat datasets, where most papers tend to have a lower number of authors. The dataset diversity across different fields opens the opportunity to examine the comprehensive application of the theorems stated in Section B.2.

To fit the ADRCM to the datasets, we need to set two model parameters. First, we can use Theorem B.2.1 to estimate the parameter γ that describes the datasets based on their vertex- or higher-order degree distributions. The vertex- and edge-degree distributions are visualized in Figure B.10.

All plots exhibit a drop in the empirical distributions at value 20. This is explained by the exclusion of documents with more than 21 authors. For combinatorial reasons, this discontinuity is more pronounced in the case of the edge-degree distributions. For heavier-tailed distributions, a larger number of documents have more than 21 authors, leading to a greater drop for the cs and eess datasets. As explained at the beginning of Section B.8, including these documents would lead to the problem of the high influence of a few high-dimensional interactions, as described earlier.
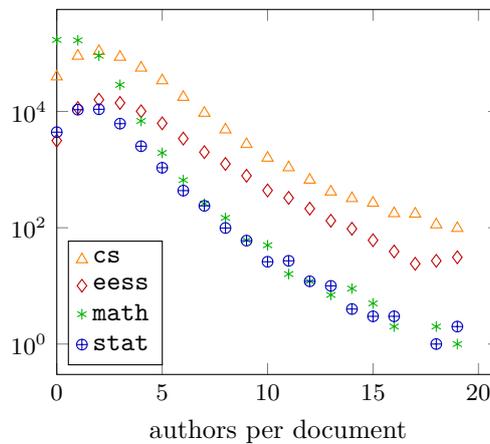
Figure B.9: Distribution of authors per documents
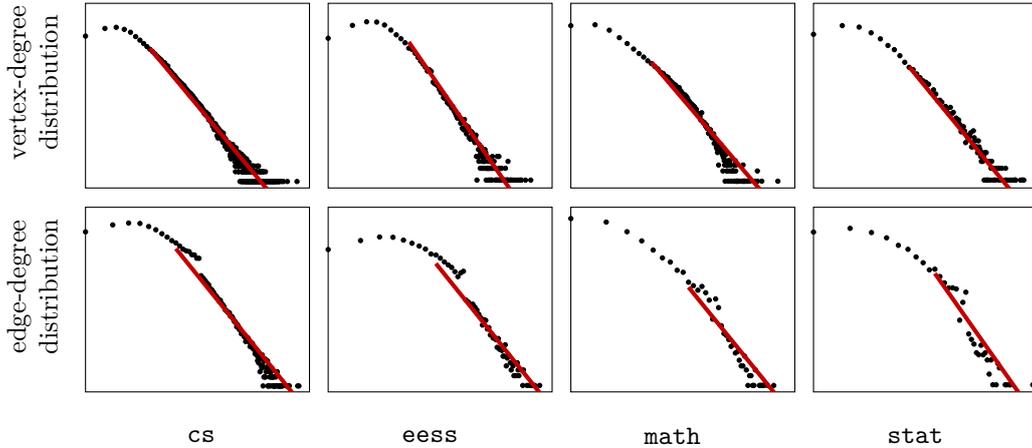
Figure B.10: Vertex-degree distributions (top) and edge-degree distributions (bottom) of the datasets

Higher-order degree distributions

Just as in the case of the simulations, fitting the parameters of the power-law distribution poses computational challenges once again. When determining the minimum value x_{min} from which the power law is visible, the goal is to find a balance between two conflicting interests.

- On the one hand, choosing a low minimum degree value would ensure enough data points in the degree distributions so that the estimates of the exponent are less noisy.

- On the other hand, choosing a high minimum degree value would remove the noise from light-tailed components of the degree.

Considering both effects, we found that setting the minimum value $x_{\mathsf{min}} = 10$ is a good compromise for fitting the power-law distributions. We note that this choice is more conservative than the one used in Section B.7, where we set $x_{\mathsf{min}} = 30$. This is because we found the datasets to be noisier than the simulated networks. Specifically, the imperfections in the data at high degrees can significantly impact the estimation of the power-law exponent, motivating a more conservative choice of x_{min}. In contrast to the controlled setting of the simulation study in Section B.7, when working with real data, the deviations from the power law can be far more erratic. In particular, the effects of noise in the tail—where data points are sparse—are more pronounced. Therefore, we gave greater weight to the second consideration and chose to use a smaller minimum value of $x_{\mathsf{min}} = 10$ to enlarge the number of data points used for the fitting. After fitting the power-law distributions, we can use Theorem B.2.1 to infer the γ model parameter based on the fitted power-law exponents.

The fitted exponents and the γ model parameters inferred from these exponents are summarized in Table B.2.

Table B.2: Fitted exponents of the degree
distributions and the inferred γ model parameters

dataset	vertex degree		edge degree	
	exponent	inferred γ	exponent	inferred γ
`cs`	-2.39	0.72	-3.76	0.53
`eess`	-2.98	0.50	-4.14	0.48
`math`	-2.79	0.56	-4.47	0.45
`stat`	-2.96	0.51	-4.86	0.41

Table B.3: Mean vertex degree and $\hat{\beta}$

dataset	mean vertex degree	$\hat{\beta}$
`cs`	9.57	2.69
`eess`	7.13	3.54
`math`	4.58	2.02
`stat`	5.14	2.52

In general, the edge-degree distributions have a thinner tail compared to that of the related vertex-degree distributions. We can see that the parameter γ differs substantially when inferred from the vertex- and edge-degree distributions, respectively. This observation suggests that the ADRCM with the connection kernel we apply is not flexible enough to capture both binary and higher-order features simultaneously. We henceforth infer γ from the vertex-degree distributions due to the following reasons. First, they are less affected by the high-dimensional interactions: a document with n authors contributes with n values in case of the vertex degrees, while it is represented by $\binom{n}{2}$ values in the edge-degree distribution. Additionally, the computation of the vertex-degree distribution only requires the consideration of pairwise relationships, which the original ADRCM was designed to describe.

As discussed by Gracar et al. [40], the parameter β governs the asymptotic edge density (the expected number of edges containing a vertex) of the generated networks through the formula $\mathbb{E}[d_{0,1}] = \beta/(1 - \gamma)$. Thus, using the above formula, we estimate the parameter β from the mean vertex degree of the datasets. The mean vertex degree and the estimated parameter $\hat{\beta}$ are shown in Table B.3.

After fitting the model parameters, we can generate synthetic networks. We simulated a representative network for each dataset, whose largest components are visualized in Figure B.11. When comparing the plots of the actual datasets with those of the ADRCM, we observe that although the ADRCM is capable of generating triangles and tetrahedra, it tends to produce globally tree-like structures.

Triangle counts

Next, we examine if the simplex counts in the ADRCM match those in the datasets. The simplex counts of the datasets are presented in Table B.4. The number of vertices is matched by the model on expectation, as we choose the size of the sampling window

| cs | eess | math | stat |
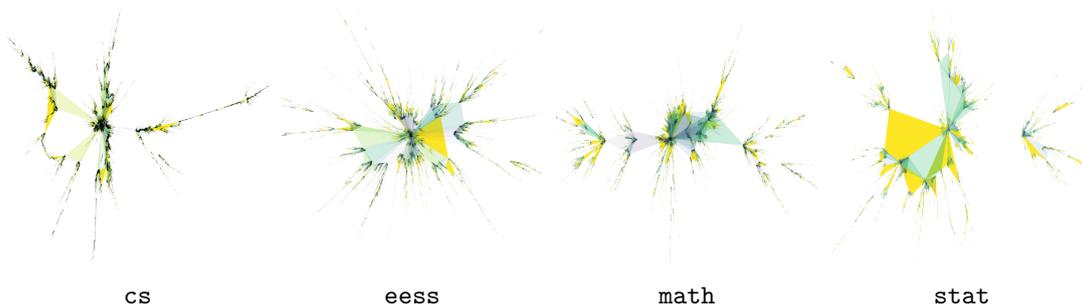
Figure B.11: The largest components of simulated ADRCMs with fitted parameters

Table B.4: Number of simplices of different dimensions in the datasets

dataset	vertices	edges	triangles
cs	433244	2073235	4055220
eess	77686	276947	562382
math	198601	455130	321406
stat	44380	114003	135800

Table B.5: Estimated parameters of the stable distributions for triangle counts

dataset	$\hat{\alpha}$	$\hat{\beta}$	location	scale
cs	1.39	1.0	18785263	504582
eess	1.98	1.0	1911396	38527
math	1.79	1.0	2027542	28774
stat	1.96	1.0	566665	15352

accordingly. It is also irrelevant to examine the edge count, being asymptotically fixed through the parameter β. Consequently, the first nontrivial dimension to consider is the triangle count.

As shown in Theorem B.2.3, the number of edges follows a stable distribution if the model parameter γ is larger than 0.5, which is the case for our datasets. We conjecture that the distributions of higher-dimensional simplex counts also follow a stable distribution for $\gamma > 0.5$.

To study the distribution of the triangle counts, we simulated 100 networks with estimated parameters $\hat{\beta}$ and $\hat{\gamma}$, which were determined according to the datasets. For fitting stable distributions to the triangle counts, we use the method detailed in Section B.7. While the parameters α and β of the stable distribution are predicted based on our mathematical conjecture, the location and scale parameters are estimated using the maximum likelihood method. The fitted parameters are presented in Table B.5.

In Section B.7, we empirically verified for 1-simplices the limit for the simplex-count distribution. This was done by comparing histograms and Q-Q plots of simulated

quantities on bounded windows with the theoretical limit. Now, we conduct a hypothesis test based on the triangle counts. Our null model is the ADRCM model with the connection kernel from Section B.2. The dataset values are marked by vertical green dashed lines in Figure B.12. We conclude that in all cases, the ADRCM contains substantially more triangles compared to the dataset. In particular, the null hypothesis is rejected at the 5% level.

Betti numbers

The presence of loops is an important feature of collaboration networks, as it quantifies their interconnectedness. In Section B.7, we provided numerical evidence for the conjecture that the Betti numbers follow a stable distribution if $\gamma > 0.5$. On this basis, we can conduct a similar hypothesis test as above on the first Betti numbers, using the ADRCM as the null model. The Betti numbers of the datasets we aim to test are presented in Table B.6.

We again simulated 100 networks using the ADRCM with the fitted model parameters. As in Section B.8, the parameters α and β of the stable distributions are predicted by our conjecture, while the location and scale parameters are fitted via the maximum likelihood. After fitting the stable distributions, we visualize the hypothesis testing in Figure B.13. The parameters of the considered stable distributions are given in Table B.7. In particular, the real datasets contain a significantly greater number of loops than the networks generated by the ADRCM; thus, the null hypothesis is rejected.
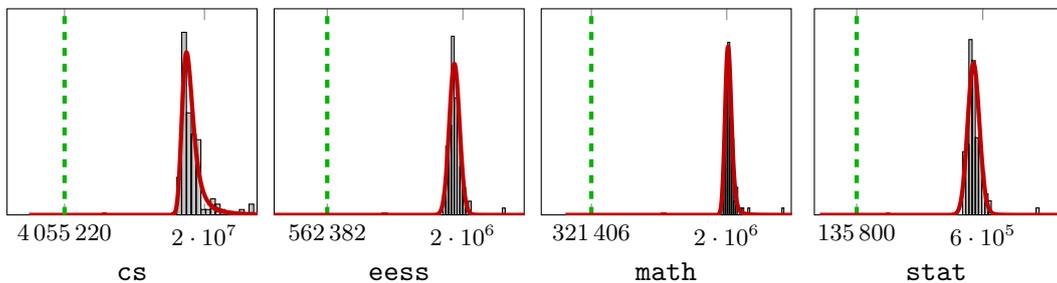
Figure B.12: Stable distribution and hypothesis testing of the triangle counts for the datasets. The model parameters were determined based on the parameters of the datasets. Each of the p-values is smaller than 0.0001.

Table B.6:
Betti numbers of the datasets

dataset	Betti-0	Betti-1
cs	22576	168770
eess	5533	7419
math	26197	78009
stat	4049	7275

Table B.7: Parameter estimates of the stable distributions for Betti-1

dataset	$\hat{\alpha}$	$\hat{\beta}$	location	scale
cs	1.39	-1.0	37	12.83
eess	1.98	-1.0	105	9.66
math	1.79	-1.0	490	19.16
stat	1.96	-1.0	126	8.99
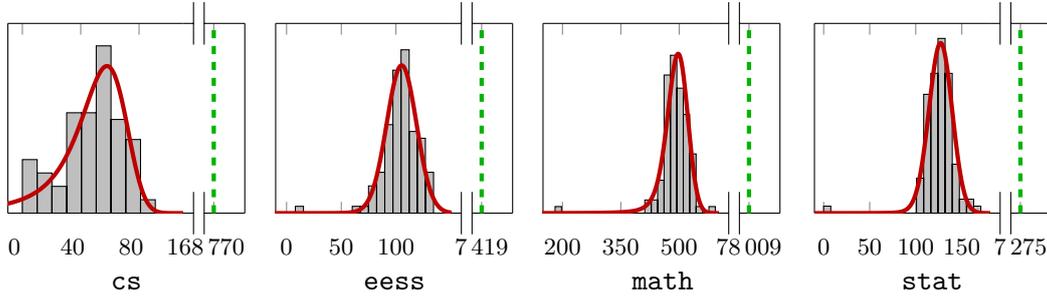
Figure B.13: Hypothesis testing of Betti-1 for the datasets. Each of the *p*-values is smaller than 0.0001.

As explained by Patania et al. [83], the loops in the network can be interpreted as bridges between communities. Hence, they are important features of scientific collaboration networks. Our analysis indicates that this community structure exhibits a rich spatial correlation pattern, which a simple two-parameter model, such as the ADRCM cannot fully capture.

The reason for this phenomenon is at least partly due to the chosen connection kernel. The vertices connect to many vertices within their neighborhood with probability 1, thereby making it difficult to form loops. This suggests that the ADRCM generates networks that appear tree-like on a global level with relatively few large loops.

To illustrate this idea, we conducted a pilot study examining the influence of the connection kernel on the first Betti numbers. More precisely, we can employ the more general connection kernel where two vertices $(x, u), (y, v) \in \mathcal{P}$ with $u \leqslant v$ connect with probability $1/(2a)$ $(a \geqslant 1/2)$, whenever $|x - y| \leqslant a\beta u^{-\gamma} v^{-(1-\gamma)}$ [40]. Note that for $a = 0.5$, the connection kernel coincides with the one introduced in Section B.2. Increasing the newly introduced model parameter a increases the distance of the vertices in which connections can be established. On the other hand, to maintain the expected number of connections of the vertices, it simultaneously reduces the connection probability.

For $\beta = 1$ and $\gamma = 0.6$, we simulated six sets of 100 networks each, with a network size of $100\,000$. We then gradually increased the value of the parameter a from its default value of 0.5 and kept track of the corresponding increase in the first Betti numbers. The results are shown in Table B.8, and we conclude that even a slight increase of a results in a drastic growth of the first Betti numbers.

Table B.8: Influence of the profile function on Betti-1

parameter a	0.5	0.6	0.7	0.8	0.9	1.0
mean of Betti-1	170	4873	10976	17786	24914	31961

B.9 Conclusion and outlook

To analyze higher-order network structures, we investigated the ADRCM as a clique complex.

First, we examined how the neighborhood of simplices of different dimensions is organized, and proved that the higher-order degree distributions have a power-law tail in the limit for large networks. Next, we proved that in the limit for large networks, the recentered and suitably rescaled edge count follows a normal distribution if the model parameter γ is less than 0.5, and a stable distribution for $\gamma > 0.5$. Turning our attention to the topological features, we proved a CLT for the Betti numbers if $\gamma < 0.25$. Recognizing the limitations of the ADRCM model, we devised a *thinning* procedure where certain types of edges are removed independently with a given thinning probability. This allowed us to adjust the edge-degree exponents while keeping the power-law exponent of the vertex-degree distribution intact.

To show that the above theoretical results can be applied in real-world datasets, we examined the extent to which the theorems are valid for finite networks by simulating several networks using identical model parameters. We found that the convergence of specific quantities to their limiting behavior is already clearly visible in networks of reasonable size. Furthermore, we also provided numerical evidence supporting our conjectures regarding the stable distribution of the Betti numbers when $\gamma > 0.5$.

Finally, after showing that the theoretical results are applicable to networks of finite size, we analyzed real-world scientific collaboration networks from arXiv. Following an exploratory analysis of these higher-order collaboration networks, we fitted the model parameters to the data. Developing hypothesis tests, we showed that—although several properties are well described by the higher-order ADRCM—topologically important quantities, such as Betti numbers or the higher-dimensional simplex counts, are not well explained. Looking ahead, we present several directions for future research.

One promising avenue is to introduce Dowker complexes or weighted simplices in the network representation as proposed by Baccini et al. [2]. Similarly to binary networks, incorporating weighted connections can describe a richer set of phenomena with simplicial complex models. Furthermore, by carefully tuning these weights, we can control and bound the influence of large simplices, thereby avoiding the large effects that high-dimensional interactions introduce due to the combinatorial explosion.

Incorporating time-dependent information into the analysis of higher-order networks would enrich our understanding of their evolution and temporal behavior. Exploring the dynamic aspect in the arXiv datasets opens up possibilities for detecting changes in the topology of scientific fields over time.

To gain a comprehensive understanding of network structures, we can investigate different embedding spaces to examine how the embedding space influences the topological and geometric features of the generated networks. Related to alternative embedding spaces, investigating alternative connection kernels could also lead to novel network models that better describe the topological properties of higher-order networks that traditional network representations may miss.

Acknowledgement

Paper C

Random Connection Hypergraphs

Morten Brun, Christian Hirsch, Péter Juhász, and Moritz Otto

Abstract: In this paper, we introduce a novel model for random hypergraphs based on weighted random connection models. In accordance with the standard theory for hypergraphs, this model is constructed from a bipartite graph. In our stochastic model, both vertex sets of this bipartite graph form marked Poisson point processes, and the connection radius is inversely proportional to a product of suitable powers of the marks. Hence, our model is a common generalization of weighted random connection models and AB random geometric graphs. For this hypergraph model, we investigate the limit theory of various graph-theoretic and topological characteristics, including higher-order degree distributions, Betti numbers of the associated Dowker complex, and simplex counts. In particular, for the latter quantity, we identify regimes of convergence to normal and to stable distribution depending on the heavy-tailedness of the weight distribution. We conclude our investigation with a simulation study and an application to the collaboration network extracted from the arXiv dataset.

C.1 Introduction

Since the seminal work of Barabási and Albert [3], the study of complex networks has become a very active field of research. The primary reason for this is that many real-world systems can be represented as networks, where nodes represent the elements of the system and links represent the interactions between them. Examples of such systems include the Internet, social networks, and biological networks, among others. The study of complex networks has led to the development of new tools and methods for analyzing and modeling the structure and dynamics of these systems.

The popularity of complex network models can be attributed to their ability to capture the main features of real-world networks such as the presence of a scale-free degree distribution and the small-world property, which means that the average distance between any two nodes in the network is relatively short. Despite these promising results, the most basic complex network models struggle to capture clustering structures that are essential in various application domains. An elegant approach to implementing these clustering effects involves embedding the network nodes in a suitable ambient space, where nearby nodes have a greater tendency to be connected. This geometric embedding, therefore, encourages the formation of clusters of nodes in a spatial vicinity. While there are various ways to endow complex networks with a spatial structure, one of the most elegant and mathematically tractable approaches is the age-dependent random connection model (ADRCM) by Gracar et al. [40, 41]. These models enable the combination of a geometric embedding with possibly heavy-tailed vertex weights, which can create a hierarchy of hubs often observed in real data. This idea also lies at the core of kernel-based networks as considered by Gracar et al. [42], Komjáthy and Lodewijks [64].

Besides the spatial structure, another important advantage of the ADRCM is that it can be used to model higher-order interactions in complex networks. For instance, in the context of collaboration networks, scientific papers often involve more than one or two authors, thereby illustrating the need to go beyond binary networks. One of the challenges in investigating higher-order networks is that their topology can become highly complex, which is why tools from the field of algebraic topology are now being applied in the context of network analysis. For instance, Siu et al. [98] considered a higher-order model for preferential attachment and computed the asymptotic growth rate of the expected Betti numbers. Moreover, in an earlier work, we studied the potential of the ADRCM as a model for arXiv collaboration data from different fields (Paper B).

While the ADRCM is an exciting model for scale-free networks with a spatial structure, it is too coarse to capture some key features in collaboration networks. Indeed, from the ADRCM, we can tell whether two scientists have collaborated, but there is no way to determine how many papers they have written together. To address this shortcoming, we propose a spatial hypergraph structure, which we call the *random connection hypergraph model (RCHM)*. This hypergraph, which we think of as a collection of subsets of vertices, will be defined through its incidence graph, i.e., the bipartite graph whose two vertex sets are given by the set of hypergraph vertices and relations, respectively [9]. In our setting, this bipartite graph has vertex sets

corresponding to the authors and documents, respectively, with an edge indicating that an author has collaborated on a document.

On the model side, the RCHM removes one of the key drawbacks of the ADRCM, namely that the latter does not allow for capturing the number of documents that a collection of authors has collaborated on. Despite this improvement, we show that the RCHM remains mathematically tractable. Indeed, we can recover many of the central higher-order characteristics considered in Paper B such as higher-order degree distributions, simplex counts, and Betti numbers. However, the bipartite structure often induces additional complexities that require substantially more involved mathematical machinery compared to the ADRCM. Surprisingly, in the case of simplex counts, the bipartite structure allows us to go further than the ADRCM.

Hence, the main contributions of this manuscript are the following:

- We introduce the RCHM, a higher-order model for bipartite networks. Note that in the setting of traditional spatial networks, the *AB random geometric graphs* are an intensively studied model [32, 56, 87, 99]. However, while bipartite AB random geometric bipartite graphs have previously received substantial attention in telecommunication networks, they are not suited for collaboration networks, as they are not scale-free. To the best of our knowledge, the RCHM is the first spatial model applicable to scale-free bipartite networks.

- While the bipartite structure of the RCHM induces additional complexities, we show that the RCHM is mathematically tractable. In fact, surprisingly, in the case of simplex counts, the bipartite structure allows us to go further than the ADRCM. We note that the triangle count is of high interest in the context of complex networks since it is intimately related to the clustering coefficients. For both geometric and combinatorial network models, the clustering coefficient has recently been the subject of intense research [103, 104].

- We illustrate the usefulness of our asymptotic results in finite sample sizes through an extensive simulation study. Finally, we also compare the model to real-world data from the arXiv network.

The rest of the manuscript is organized as follows. In Section C.2, we introduce the RCHM and discuss its main properties. We also present the main results of the manuscript. Sections C.3–C.8 are devoted to the proofs of the main results. Next, in Section C.8 we illustrate the applicability of our asymptotic results in finite sample sizes through an extensive simulation study. Finally, in Section C.9, we compare the model to real-world data from the arXiv network.

C.2   Model and main results

We work on the space $\mathbb{S} := \mathbb{R} \times (0,1]$ and interpret $\mathbb{R}$ as the *location* and $(0,1]$ as the *mark space*. Given parameters $0 < \gamma, \gamma' < 1$, $\beta > 0$, we introduce our notion of connectivity of elements in $\mathbb{S}$. For $p := (x,u) \in \mathbb{S}$ and $p' := (z,w) \in \mathbb{S}$ we let

$$F(p,p') = F(p,p';\gamma,\gamma') := |x-z|u^\gamma w^{\gamma'} \tag{C.1}$$

and say that $p \in \mathbb{S}$ and $p' \in \mathbb{S}$ are *connected* if

$$F(p, p'; \gamma, \gamma') \leqslant \beta. \tag{C.2}$$

We define the *neighborhood* of a point $p \in \mathbb{S}$ by

$$B(p, \beta) = B_F(p, \beta) \coloneqq \{p' \in \mathbb{S} \colon F(p, p'; \gamma, \gamma') \leqslant \beta\}. \tag{C.3}$$

Loosely speaking, we can think of B as a non-metric ball centered at a point $p \in \mathbb{S}$ with radius β. For $\Delta \subseteq \mathbb{S}$, we also put $B_F(\Delta, \beta) \coloneqq \bigcap_{p \in \Delta} B_F(p, \beta)$ as the joint neighborhood of the points in Δ.

Next, we define a random bipartite graph. Let $\mathcal{P}, \mathcal{P}'$ be independent Poisson processes on $\mathbb{S}$ with intensity measures $\lambda |\cdot|, \lambda' |\cdot|$, respectively, where $\lambda, \lambda' > 0$ are fixed parameters and $|\cdot|$ denotes Lebesgue measure on $\mathbb{S}$. Let $G^{\mathsf{bip}} \coloneqq G^{\mathsf{bip}}(\mathcal{P}, \mathcal{P}') \coloneqq G^{\mathsf{bip}}(\mathcal{P}, \mathcal{P}'; \gamma, \gamma', \beta)$ be the bipartite graph with vertex set $\mathcal{P} \cup \mathcal{P}'$, where there is an edge between two points $p \in \mathcal{P}$ and $p' \in \mathcal{P}'$ if and only if p and p' are connected. Note that given $\mathcal{P}$ and $\mathcal{P}'$, the number of edges in G^{bip} is increasing in the parameters γ, γ' and β and that $\mathcal{P}' \cap B_F(p, \beta)$ is the subset of points in $\mathcal{P}'$ connected to p in G^{bip}.

In the collaboration network example discussed in Section C.9 below, the Poisson processes $\mathcal{P}$ and $\mathcal{P}'$ can be thought of as sets of authors and documents, respectively. An edge (p, p') can be interpreted as the relation that author $p \in \mathcal{P}$ has collaborated on manuscript $p' \in \mathcal{P}'$. Considering the product on the right-hand side of (C.1) illustrates that G^{bip} is a natural bipartite extension of the age-dependent random connection models from Gracar et al. [40, 41]. As will be made precise below, $\gamma, \gamma' < 1$ determine the power-law exponent of the degree distribution for vertices in $\mathcal{P}, \mathcal{P}'$, respectively. Once γ, γ' are fixed, the parameter $\beta > 0$ can be used to tune the overall number of expected edges in the bipartite graph G^{bip}.

Note that it follows from identity (C.1) that the roles of $\mathcal{P}$ and $\mathcal{P}'$ are symmetric when switching the parameters γ and γ'. Hence, when in the following we describe more elaborate graph-theoretic and topological quantities of G^{bip} that are defined with reference to $\mathcal{P}$, the symmetry between $\mathcal{P}$ and $\mathcal{P}'$ implies that our results also hold for the corresponding quantities defined in terms of $\mathcal{P}'$, when switching the assumptions on γ and γ'.

We now introduce the *random connection hypergraph model (RCHM)* $G^{\mathsf{hyp}} \coloneqq G^{\mathsf{hyp}}(\mathcal{P}, \mathcal{P}')$ through the construction known as *Dowker complex* [18]. We stress here that G^{hyp} is a specific type of hypergraph, namely, a simplicial complex. In the following, we rely on this structure as a simplicial complex to investigate Betti numbers. More precisely, the set of hyperedges Σ_m of G^{hyp} of cardinality $m + 1$ is given by

$$\Sigma_m \coloneqq \{\Delta_m \subseteq \mathcal{P} \colon \#(\Delta_m) = m + 1, \mathcal{P}' \cap B_F(\Delta_m, \beta) \neq \varnothing\}, \tag{C.4}$$

where $\#(\cdot)$ denotes the cardinality of a set.

Following the terminology in topological data analysis, we also refer to the elements of Σ_m as *m-simplices*. If there is a unique vertex of an m-simplex Δ_m with the lowest mark, then we define $c(\Delta_m) \in \mathbb{R}$ as the location coordinate of this vertex. Otherwise, let $c(\Delta_m)$ be the location of the left-most vertex among all vertices with minimal mark. Although not explicitly stated, the set of m-simplices Σ_m depends on the point

process $\mathcal{P}'$. In our interpretation, $m+1$ authors form an m-simplex if and only if they have coauthored at least one common paper.

In classical binary networks, the degree distribution of a typical vertex is of central importance. Due to the translation-invariance of the edge rule (C.2), such a vertex can be chosen to be of the form $o = (0, U)$ with U uniform in $(0,1]$. For higher-order networks, it is essential to go beyond single vertices and describe properties of typical m-simplices. However, rigorously defining the notion of a typical simplex is a far more involved process. To address this problem, we will rely on the established theory of Palm calculus as explained in [66, Chapter 9]. As a first step, we need to establish that the m-simplex intensity is finite. Given a subset A of $\mathbb{R}$, we denote the subset of m-simplices centered in A by

$$\Sigma_m^A := \{\Delta_m \in \Sigma_m \colon c(\Delta_m) \in A\}.$$

Proposition C.2.1 (Finiteness of the m-simplex-intensity)**.** *Let $\mathcal{P}$ and $\mathcal{P}'$ be independent Poisson point processes on $\mathbb{S}$, let $A \subseteq \mathbb{R}$ be a Borel set with Lebesgue measure one. Given $m \geqslant 0$, $\gamma < 1$, $\gamma' < 1/(m+1)$ and $\beta > 0$, the m-simplex intensity $\lambda_m := \mathbb{E}[\#\Sigma_m^A]$ is a non-zero finite value not depending on the choice of A.*

Now, we define the distribution of the typical m-simplex Δ_m^*. To do so, we first introduce the following notations. More precisely, f denotes an arbitrary nonnegative measurable functional that may depend on a considered m-simplex as well as on the point processes $\mathcal{P}$ and $\mathcal{P}'$. Then, we define the distribution of the typical m-simplex as

$$\mathbb{E}[f(\Delta_m^*, \mathcal{P}, \mathcal{P}')] = \frac{1}{\lambda_m} \mathbb{E}\Big[\sum_{\Delta_m \in \Sigma_m^A} f(\Delta_m - c(\Delta_m), \mathcal{P} - c(\Delta_m), \mathcal{P}' - c(\Delta_m)) \Big] \quad \text{(C.5)}$$

where $A \subseteq \mathbb{R}$ is an arbitrary Borel set with $|A| = 1$ and for a set $R \subseteq \mathbb{S}$ and $x \in \mathbb{R}$, we write $R - x := \{(y - x, u) \colon (y, u) \in R\}$. Note that for translation-invariant f, we can replace $f(\Delta_m - c(\Delta_m), \mathcal{P} - c(\Delta_m), \mathcal{P}' - c(\Delta_m))$ by $f(\Delta_m, \mathcal{P}, \mathcal{P}')$. Note also that if f is bounded, Proposition C.2.1 shows that the expectation (C.5) is well-defined.

Now we can derive an integral representation of the Palm distribution. We write $\boldsymbol{p}_m := (p_1, \ldots, p_m)$ for an m-tuple of points, and for $u \in (0,1]$, we introduce the notations $\boldsymbol{p}_m(u) := ((0, u), p_1, \ldots, p_m)$ and $\overrightarrow{\boldsymbol{p}}_m(u) := \{(0, u), p_1, \ldots, p_m\}$ for the tuple and corresponding set, respectively.

Proposition C.2.2 (Distribution of the typical m-simplex)**.** *Let $m \geqslant 0$, $\gamma < 1$, $\gamma' < 1/(m+1)$, and let $f \colon (\mathbb{R} \times (0,1])^{m+1} \times \mathbf{N}_{\mathsf{loc}} \times \mathbf{N}_{\mathsf{loc}} \to \mathbb{R}_+$ be an arbitrary nonnegative measurable functional depending on an m-simplex as well as on the point processes $\mathcal{P}$ and $\mathcal{P}'$. Then,*

$$\mathbb{E}[f(\Delta_m^*, \mathcal{P}, \mathcal{P}')]$$
$$= \frac{\lambda^{m+1}}{\lambda_m(m+1)!} \int_{(0,1] \times \mathbb{S}^m} \mathbb{E}[f(\overrightarrow{\boldsymbol{p}}_m(u), \mathcal{P} \cup \overrightarrow{\boldsymbol{p}}_m(u), \mathcal{P}') \mathbb{1}\{\overrightarrow{\boldsymbol{p}}_m(u) \in \Sigma_m\}] \, \mathrm{d}(u, \boldsymbol{p}_m).$$

Here, if $\overrightarrow{\boldsymbol{p}}_m(u)$ does not consist of precisely $m+1$ elements, then we let $f(\overrightarrow{\boldsymbol{p}}_m(u), \mathcal{P} \cup \overrightarrow{\boldsymbol{p}}_m(u), \mathcal{P}') := 0$.

As a first application of the Palm distribution, we show that the higher-order degree distributions are scale-free. In classical binary networks, the degree of a vertex equals the number of edges it is incident to. For instance, in the bipartite graph G^{bip}, the degree of an author-vertex equals the number of papers this author has written. Hence, similarly, for an $(m + 1)$-element subset of authors, we define its higher-order degree as the number of papers this subset has collaborated on. With $\mathrm{Fin}(\mathcal{P})$ denoting the family of finite subsets of $\mathcal{P}$, we define the bipartite graph with vertex sets $\mathrm{Fin}(\mathcal{P})$ and $\mathcal{P}'$, and there is an edge between a simplex $\Delta \in \mathrm{Fin}(\mathcal{P})$ and $p' \in \mathcal{P}'$ if and only if $\max_{p \in \Delta} F(p, p'; \gamma, \gamma') \leqslant \beta$. The degree $\deg(\Delta)$ of a simplex Δ is then the number of points in $\mathcal{P}'$ to which all points in Δ are connected to:

$$\deg(\Delta) := \mathcal{P}'(B_F(\Delta, \beta)) := \#(\mathcal{P}' \cap B_F(\Delta, \beta)).$$

Note that $\deg(\Delta)$ depends in fact on G^{bip} and not only on G^{hyp}. In the context of the Dowker complex, $\deg(\Delta)$ can also be interpreted as the number of witnesses for the m-simplex Δ. We now show that the typical higher-order degrees are scale-free, characterized by a power-law distribution. In particular, for $m = 0$, we recover the classical degree distribution of the authors.

Theorem C.2.3 (Scale-freeness of higher-order degrees)**.** *Let $m \geqslant 0$, $\gamma < 1$, $\gamma' < 1/(m + 1)$. Then,*

$$\lim_{k \uparrow \infty} \frac{\log\big(\mathbb{P}(\deg(\Delta_m^*) \geqslant k)\big)}{\log(k)} = m - \frac{m + 1}{\gamma}.$$

We note that given a subset σ of $\mathcal{P}$ and a subset τ of $\mathcal{P}'$, one can say that (σ, τ) forms a biclique in the bipartite graph G^{bip} if every $\mathcal{P}$-vertex in σ is connected to every $\mathcal{P}'$-vertex in τ and vice versa. Then, the degree of σ is the number of bicliques of the form (σ, τ) where τ is a set of cardinality exactly one.

From a topological perspective, we note that Theorem C.2.3 is loosely related to the multicover bifiltration. Here, considering a union of balls, a point is k-covered if it is contained in at least k of the balls. Similarly, in Theorem C.2.3 we have $\deg(\Delta_m^*) \geqslant k$ if there are at least k points in the set $B_F(\Delta_m, \beta)$.

One of the key advantages of a stochastic network model is that, when working with data, we can statistically test whether the model is a good fit for the considered data. To carry out this approach rigorously, we aim to use test statistics that reflect the key topological properties of the Dowker complex associated with G^{hyp}.

This opens the door towards considering invariants from topological data analysis, such as the Betti numbers. Thus, we start by establishing the asymptotic normality of the Betti numbers in the regime $\gamma < 1/4$ in the window $\mathbb{S}_n := [0, n] \times (0, 1]$. To make this precise, fix $m \geqslant 0$ and let $\beta_m^{(n)}$ denote the mth Betti number of $G^{\mathsf{hyp}}(\mathcal{P} \cap \mathbb{S}_n, \mathcal{P}' \cap \mathbb{S}_n)$. Moreover, let $\mathcal{N}(0, \sigma^2)$ denote the normal distribution with mean 0 and variance σ^2.

Theorem C.2.4 (Asymptotic normality of Betti numbers)**.** *Let $m \geqslant 0$. Let $\gamma < 1/4$ and $\gamma' < 1/(4(m + 1))$. Then, in distribution,*

$$n^{-1/2}\big(\beta_m^{(n)} - \mathbb{E}[\beta_m^{(n)}]\big) \xrightarrow[n \uparrow \infty]{d} \mathcal{N}(0, \sigma^2) \qquad \text{for some } \sigma^2 \geqslant 0.$$

Note that instead of letting $n \to \infty$, one could alternatively let λ, λ', and β tend to infinity.

Note also that by the Dowker duality theorem [18], $\beta_m^{(n)}$ coincides with the Betti number that is obtained from the dual Dowker complex, where the roles of $\mathcal{P}$ and $\mathcal{P}'$ are reversed.

While the asymptotic normality of test statistics is highly convenient in applied statistics, we stress that Theorem C.2.4 requires that $\gamma < 1/4$. Taking into account Theorem C.2.3 for $m = 0$, we see that this means that the typical degree distribution has a finite fourth moment. However, when considering complex networks, we often encounter the situation where even the variance is infinite. Hence, it is no longer reasonable to expect a normal distribution in the limit, since the latter exhibits light tails. In analogy to the classical setting of sums of independent heavy-tailed random variables, we expect that the suitably recentered and rescaled distribution converges to a stable distribution.

However, since the Betti numbers are a highly refined topological quantity, giving a rigorous proof of the stable limit convergence in the delicate heavy-tailed setting is difficult. We also note that while there is an ample variety of asymptotically normal test statistics for spatial network models [48, 89], the stable setting has been considered so far only in selected isolated cases [27].

While establishing a stable limit for the Betti numbers seems to be out of reach for the moment, similarly to Paper B, we can prove a stable limit for a much simpler test statistic, namely the edge count

$$S_n := \sum_{P_i \in \mathcal{P} \cap \mathbb{S}_n} \deg(P_i),$$

where we recall that $\deg(P_i)$ denotes the degree of a point P_i in the bipartite graph G^{bip}.

Theorem C.2.5 (Normal and stable limits of edge counts)**.** *Let $\gamma' < 1/3$. Then, the following distributional limits hold as $n \to \infty$.*

(a) *Let $\gamma \in (0, 1/2)$. Then, $n^{-1/2}(S_n - \mathbb{E}[S_n]) \xrightarrow[n\uparrow\infty]{d} \mathcal{N}(0, \sigma^2)$ for some $\sigma^2 > 0$.*

(b) *Let $\gamma \in (1/2, 1)$. Then, $n^{-\gamma}(S_n - \mathbb{E}[S_n]) \xrightarrow[n\uparrow\infty]{d} \mathcal{S}_{\gamma^{-1}}$, where $\mathcal{S}_{\gamma^{-1}}$ is a γ^{-1}-stable random variable.*

While Theorem C.2.5 establishes rigorously the desired normal and stable limits in the asserted regimes, it is difficult to apply to hypothesis tests in an actual data analysis. This is because the parameter β is typically tuned such that the expected number of edges in the bipartite model matches the quantity observed in the data.

Hence, to have practically useful test statistics, we now define

$$S_{n,m} := \#\{\Delta_m \in \Sigma_m \colon c(\Delta_m) \in [0, n]\}$$

as the number of m-simplices centered in $[0, n]$.

The fact that we can extend the proof of Theorem C.2.5 to the case of m-simplex count is remarkable. Indeed, in the simpler model considered in Paper B, this functional seemed out of reach. The explanation is that for the task of proving central and stable

limit theorems, our bipartite model is surprisingly more accessible than the one from Paper B. The reason is that in the present model, the crucial covariance between simplex counts in disjoint regions becomes accessible since we can condition on the set $\mathcal{P}'$ and then apply the formula for total covariance. These essential variance and covariance computations are summarized in the following auxiliary result.

Theorem C.2.6 (Normal and stable limits of simplex counts)**.** *Let $\gamma' < 1/(2m+1)$. Then, the following distributional limits hold as $n \to \infty$.*

(a) *Let $\gamma \in (0, 1/2)$. Then, $n^{-1/2}(S_{n,m} - \mathbb{E}[S_{n,m}]) \xrightarrow[n\uparrow\infty]{d} \mathcal{N}(0, \sigma^2)$ for some $\sigma^2 > 0$.*

(b) *Let $\gamma \in (1/2, 1)$. Then, $n^{-\gamma}(S_{n,m} - \mathbb{E}[S_{n,m}]) \xrightarrow[n\uparrow\infty]{d} \mathcal{S}_{\gamma^{-1}}$, where $\mathcal{S}_{\gamma^{-1}}$ is a γ^{-1}-stable random variable.*

To relate our model to existing concepts in the literature, we note that a standard construction exists to retrieve a hypergraph from a bipartite graph. This could also be done in our setting with the bipartite graph G^{bip}. After taking closures under subsets, we recover the hypergraph G^{hyp} introduced above.

In the remainder of the paper, the parameter β is held fixed. Hence, to ease notation, in the rest of the paper, we write $B_F(\overrightarrow{\boldsymbol{p}}_m)$ instead of $B_F(\overrightarrow{\boldsymbol{p}}_m, \beta)$.

C.3 Proof of Propositions C.2.1 and C.2.2

Proof of Proposition C.2.1. As before, let $A \subseteq \mathbb{R}$ be an arbitrary Borel set with $|A| = 1$. Furthermore, let $g_m(p_0, \dots, p_m, \mathcal{P}')$ denote the indicator of the event that an m-tuple of points forms an m-simplex and that the marks of $p_0, \dots, p_m$ are ordered ascending. The m-simplex intensity λ_m is then given by

$$
\begin{aligned}
\lambda_m &= \mathbb{E}\Big[\sum_{\Delta_m \in \Sigma_m} \mathbb{1}\{c(\Delta_m) \in A\} \Big] \\
&= \lambda^{m+1} \int_{(A \times (0,1]) \times \mathbb{S}^m} \mathbb{E}\big[g_m((p_0, p_1, \dots, p_m), \mathcal{P}') \big] \, \mathrm{d}(p_0, \boldsymbol{p}_m) \\
&= \lambda^{m+1} \int_{(0,1] \times \mathbb{S}^m} \mathbb{E}\big[g_m(\boldsymbol{p}_m(u), \mathcal{P}') \big] \, \mathrm{d}(u, \boldsymbol{p}_m),
\end{aligned}
$$

where we used the Mecke formula [66, Theorem 4.4] in the first step, and integrated with respect to the location of p_0 in the second step. Note that the number of points in the common neighborhood $B(\overrightarrow{\boldsymbol{p}}_m(u))$ of the vertices is Poisson-distributed. Hence, by the Markov inequality, the probability that this set is nonempty is given by:

$$
\begin{aligned}
\lambda_m &= \frac{\lambda^{m+1}}{(m+1)!} \int_0^1 \int_{\mathbb{S}^m} \mathbb{P}(\mathcal{P}'(B(\overrightarrow{\boldsymbol{p}}_m(u))) \geqslant 1) \, \mathrm{d}\boldsymbol{p}_m \, \mathrm{d}u \\
&\leqslant \frac{\lambda^{m+1} \lambda'}{(m+1)!} \int_0^1 \int_{\mathbb{S}^m} |B(\overrightarrow{\boldsymbol{p}}_m(u))| \, \mathrm{d}\boldsymbol{p}_m \, \mathrm{d}u.
\end{aligned}
$$

The inner integral is given by

$$\int_{\mathbb{S}^m} |B(\overrightarrow{\boldsymbol{p}}_m(u))| \, \mathrm{d}\boldsymbol{p}_m$$
$$= \int_{\mathbb{S}} \mathbb{1}\{|z| \leqslant \beta u^{-\gamma} w^{-\gamma'}\} \int_{\mathbb{S}^m} \mathbb{1}\{|z - y_i| \leqslant \beta v_i^{-\gamma} w^{-\gamma'} : 1 \leqslant i \leqslant m\} \, \mathrm{d}\boldsymbol{p}_m \, \mathrm{d}p'.$$

Next, we integrate with respect to the location coordinates $\boldsymbol{y} := (y_1, \ldots, y_m)$, the marks $\boldsymbol{v} := (v_1, \ldots, v_m)$ as well as z, w, u. This gives for the above

$$\int_{\mathbb{S}} \mathbb{1}\{|z| \leqslant \beta u^{-\gamma} w^{-\gamma'}\} \int_{(0,1]^m} \prod_{i=1}^m (2\beta v_i^{-\gamma} w^{-\gamma'}) \, \mathrm{d}\boldsymbol{v} \, \mathrm{d}p'$$
$$= \Big(\frac{2\beta}{1-\gamma}\Big)^m \int_{\mathbb{S}} \mathbb{1}\{|z| \leqslant \beta u^{-\gamma} w^{-\gamma'}\} w^{-m\gamma'} \, \mathrm{d}p'$$
$$= \frac{(2\beta)^{m+1}}{(1-\gamma)^m} u^{-\gamma} \int_0^1 w^{-(m+1)\gamma'} \, \mathrm{d}w = \frac{(2\beta)^{m+1}}{(1-\gamma)^m} \frac{u^{-\gamma}}{1 - (m+1)\gamma'},$$

where we have used that $\gamma < 1$ and $\gamma' < 1/(m+1)$. Using again that $\gamma < 1$, we conclude that $\lambda_m < \infty$. $\qquad\square$

Proof of Proposition C.2.2. Let $A \subseteq \mathbb{R}$ be an arbitrary Borel set with $|A| = 1$. Let the lowest-mark $\mathcal{P}$-vertex $c(\Delta_m)$ of a set of $m + 1$ points Δ_m be denoted by $p_0 := (x, u)$. The expectation of a nonnegative functional f is given by (C.5). By another application of the Mecke formula, and by integrating over x, we obtain

$$\mathbb{E}\big[f(\Delta_m^*, \mathcal{P}, \mathcal{P}')\big]$$
$$= \frac{\lambda^{m+1}}{\lambda_m} \int_{(0,1] \times \mathbb{S}^m} \mathbb{E}\Big[f(\overrightarrow{\boldsymbol{p}}_m(u), \mathcal{P} \cup \overrightarrow{\boldsymbol{p}}_m(u), \mathcal{P}') g_m(\boldsymbol{p}_m(u), \mathcal{P}')\Big] \, \mathrm{d}(u, \boldsymbol{p}_m),$$

as asserted. $\qquad\square$

C.4 Proof of Theorem C.2.3

Since the proofs of the upper and lower bounds are very different, we deal with them in Sections C.4 and C.4, separately. We start with two lemmas that are used in both the proof of the upper and lower bounds.

Lemma C.4.1 (Pairwise intersections). *Let $0 \leqslant u \leqslant v \leqslant 1$, and set $o := (0, u) \in \mathbb{S}$ and $p := (y, v) \in \mathbb{S}$. Then, the measure of the intersection of their neighborhood $|B(\{o, p\})|$ can be upper bounded as follows:*

$$|B(\{o, p\})| \leqslant \frac{2\beta}{1-\gamma'} v^{-\gamma} s_\wedge(u, y)^{1-\gamma'} \qquad where \qquad s_\wedge(u, y) := (2\beta u^{-\gamma} |y|^{-1})^{1/\gamma'} \wedge 1.$$

Proof. For a point $(z, w) \in \mathbb{S}$ to be connected to both $(0, u)$ and (y, v), it must hold that $|z| \leqslant \beta u^{-\gamma} w^{-\gamma'}$ and that $|y - z| \leqslant \beta v^{-\gamma} w^{-\gamma'}$. As $u \leqslant v$, we find from the triangle

inequality that $|y| \leqslant 2\beta u^{-\gamma} w^{-\gamma'}$ and hence $w \leqslant (2\beta u^{-\gamma}|y|^{-1})^{1/\gamma'}$. On the other hand, $w \leqslant 1$, so $w \leqslant s_\wedge(u,v)$ and using only the second condition above for z,

$$
\begin{aligned}
|B(\{o,p\})| &\leqslant \int_0^{s_\wedge(u,y)} \int_{-\beta v^{-\gamma} w^{-\gamma'}}^{\beta v^{-\gamma} w^{-\gamma'}} \mathrm{d}z \, \mathrm{d}w \\
&= \int_0^{s_\wedge(u,y)} 2\beta v^{-\gamma} w^{-\gamma'} \, \mathrm{d}w = \frac{2\beta}{1-\gamma'} v^{-\gamma} s_\wedge(u,y)^{1-\gamma'},
\end{aligned}
$$

as asserted. $\qquad\square$

Lemma C.4.2 (Upper bound of $\int F(s_\wedge(u,y)) \, \mathrm{d}y$). *Let $\rho > \gamma'$ and $F\colon (0,\infty) \to [0,1]$ be an integrable function. Assume that $c := \sup_{x>0} x^{-\rho} F(x) < \infty$. Then, for all $a \geqslant 0$,*

$$
\int_{-\infty}^{\infty} F(s_\wedge(u,y)) \, \mathrm{d}y \leqslant 2a + \frac{2c\gamma'}{\rho - \gamma'} (2\beta)^{\rho/\gamma'} a^{1-\rho/\gamma'} u^{-\rho\gamma/\gamma'}.
$$

Proof. We use the upper bound of F and the symmetry of $|y|$ to write

$$
\begin{aligned}
\int_{-\infty}^{\infty} F(s_\wedge(u,y)) \, \mathrm{d}y &\leqslant 2 \int_0^a 1 \, \mathrm{d}y + 2c \int_a^\infty s_\wedge(u,y)^\rho \, \mathrm{d}y \\
&\leqslant 2a + 2c(2\beta u^{-\gamma})^{\rho/\gamma'} \int_a^\infty y^{-\rho/\gamma'} \, \mathrm{d}y \leqslant 2a + \frac{2c\gamma'}{\rho - \gamma'} (2\beta)^{\rho/\gamma'} a^{1-\rho/\gamma'} u^{-\rho\gamma/\gamma'},
\end{aligned}
$$

where we have used that $\rho > \gamma'$. $\qquad\square$

Proof of the upper bound

The key idea for the proof of the upper bound is to note that if all points of Δ_m have a common neighbor in $\mathcal{P}'$, then also all pairs of $\mathcal{P}$-vertices in Δ_m have a common neighbor. This observation will be used to subsequently bound the integrals in the Palm probabilities.

Proof of the upper bound. By Proposition C.2.2 we obtain that

$$
\mathbb{P}(\deg(\Delta_m^*) \geqslant k) = \frac{\lambda^{m+1}}{\lambda_m(m+1)!} \int_{(0,1]} \int_{\mathbb{S}^m} \mathbb{P}(\mathcal{P}'(B(\overrightarrow{\boldsymbol{p}}_m(u))) \geqslant k) \, \mathrm{d}\boldsymbol{p}_m \, \mathrm{d}u.
$$

Let $b := \lambda' |B(\overrightarrow{\boldsymbol{p}}_m(u))|$ and note that $X := \mathcal{P}'(B(\overrightarrow{\boldsymbol{p}}_m(u)))$ is Poisson-distributed with parameter b. Next, we bound the probability by distinguishing whether $b \geqslant k/2$:

$$
\mathbb{P}(X \geqslant k) \leqslant \mathbb{1}\{b \geqslant k/2\} + \mathbb{P}(X \geqslant k) \mathbb{1}\{b < k/2\}.
$$

Our goal is to show that the second term is negligible compared to the first for large values of k. First,

$$
\mathbb{P}(X \geqslant k) = \mathbb{P}(X \geqslant 1) \frac{\mathbb{P}(X \geqslant k)}{\mathbb{P}(X \geqslant 1)}.
$$

Let $b_\vee := 2 \vee e^2 b$. The numerator is upper bounded by $(b/k)^{k/2}$ whenever $k \geqslant b_\vee$ using [86, Lemma 1.2]. If $b < 1/2$, the denominator can be bounded from below by

$1 - \exp(-b) \geqslant b/2$. Otherwise, the denominator can be bounded from below by a finite constant $1/c_2$. Thus, for $k \geqslant b_\vee$, we have

$$\frac{\mathbb{P}(X \geqslant k)}{\mathbb{P}(X \geqslant 1)} \leqslant c_1 \Big(\frac{b}{k}\Big)^{k/2} \Big(\frac{2}{b} \mathbb{1}\Big\{b < \frac{1}{2}\Big\} + c_2 \mathbb{1}\Big\{b \geqslant \frac{1}{2}\Big\}\Big) \leqslant c_3 \Big(\frac{b}{k}\Big)^{k/2-1}$$

for some $c_1, c_2, c_3 > 0$. Considering the indicator $\mathbb{1}\{b < k/2\}$ in the integrand, we can conclude that

$$\int_{(0,1] \times \mathbb{S}^m} \mathbb{P}(X \geqslant k) \, \mathbb{1}\{b < k/2\} \, \mathrm{d}(u, \boldsymbol{p}_m)$$
$$\leqslant c_3 2^{1-k/2} \int_{(0,1] \times \mathbb{S}^m} \mathbb{P}(X \geqslant 1) \, \mathrm{d}(u, \boldsymbol{p}_m) = c_4 2^{-k/2},$$

where $c_4 > 0$ and in the last step we used that the integral above is finite due to Proposition C.2.1. As shown below, the $\mathbb{1}\{b \geqslant k/2\}$ term decays as a power law with increasing k. Thus,

$$\limsup_{k \uparrow \infty} \frac{\log\big(\mathbb{P}(\deg(\Delta_m^*) \geqslant k)\big)}{\log(k)} \leqslant \limsup_{k \uparrow \infty} \frac{\log\big(\int_{(0,1] \times \mathbb{S}^m} \mathbb{1}\{b \geqslant k/2\} \, \mathrm{d}(u, \boldsymbol{p}_m)\big)}{\log(k)}.$$

In particular, for $m = 0$,

$$\int_{(0,1]} \mathbb{1}\{b \geqslant k/2\} \, \mathrm{d}u = \int_{(0,1]} \mathbb{1}\Big\{\lambda' \int_{\mathbb{R} \times (0,1]} \mathbb{1}\{|z| \leqslant \beta u^{-\gamma} w^{-\gamma'}\} \, \mathrm{d}(z, w) \geqslant k/2\Big\} \, \mathrm{d}u$$
$$= \int_{(0,1]} \mathbb{1}\Big\{\frac{2\beta\lambda'}{1 - \gamma'} u^{-\gamma} \geqslant \frac{k}{2}\Big\} \, \mathrm{d}u \in O(k^{-1/\gamma}).$$

This concludes the proof for $m = 0$.

From now on, we assume $m \geqslant 1$. Our goal is to upper bound the expression

$$\limsup_{k \uparrow \infty} \frac{\log\big(\mathbb{P}(\deg(\Delta_m^*) \geqslant k)\big)}{\log(k)} \leqslant \limsup_{k \uparrow \infty} \Big(\frac{1}{\log(k)} \log\Big(\int_{(0,1] \times \mathbb{S}^m} \mathbb{1}\Big\{b \geqslant \frac{k}{2}\Big\} \, \mathrm{d}(u, \boldsymbol{p})\Big)\Big).$$

We assume that the points p_i are ordered in increasing order of their marks, i.e., $u \leqslant v_1 \leqslant \cdots \leqslant v_m$. Note that

$$b \leqslant \lambda' |B(\overrightarrow{\boldsymbol{p}}_1(u))| \wedge \min_{i=1,\ldots,m-1} \lambda' |B(\{p_i, p_{i+1}\})|.$$

Due to translation invariance and Lemma C.4.1 we find that for some constant $c > 0$,

$$\lambda' |B(\{p_i, p_{i+1}\})| = \lambda' |B(\{(0, v_i), (y_{i+1} - y_i, v_{i+1})\})| \leqslant c v_{i+1}^{-\gamma} s_\wedge(v_i, y_{i+1} - y_i)^{1-\gamma'}.$$

Using this upper bound,

$$\int_{(0,1] \times \mathbb{S}^m} \mathbb{1}\{b \geqslant k/2\} \, \mathrm{d}(u, \boldsymbol{p}_m)$$
$$\leqslant \int_{(0,1] \times \mathbb{S}^m} \prod_{i=0}^{m-1} \mathbb{1}\Big\{c v_{i+1}^{-\gamma} s_\wedge(v_i, y_{i+1} - y_i)^{1-\gamma'} \geqslant k\Big\} \, \mathrm{d}(u, \boldsymbol{p}_m),$$

132

where we have set $v_0 := u$ and $y_0 := 0$. In the indicators, we can express the upper limit of the marks v_i,

$$\int_0^{ck^{-1/\gamma}} \int_{\mathbb{S}^m} \prod_{i=0}^{m-1} \mathbb{1}\left\{v_{i+1} \leqslant cs_\wedge(v_i, y_{i+1} - y_i)^{(1-\gamma')/\gamma}k^{-1/\gamma}\right\} \mathrm{d}\boldsymbol{p}_m \,\mathrm{d}u,$$

where we set the upper limit of the integral with respect to u to $ck^{-1/\gamma}$ as $u \leqslant v_1 \leqslant ck^{-1/\gamma}$. We now substitute $y'_{i+1} := y_{i+1} - y_i$ for $i = 0, \ldots, m-1$. Furthermore, let $p'_i := (y'_i, v_i)$ denote the ith point with the new coordinates. Then, we have

$$\int_0^{ck^{-1/\gamma}} \int_{\mathbb{S}^m} \prod_{i=0}^{m-1} \mathbb{1}\left\{v_{i+1} \leqslant cs_\wedge(v_i, y'_{i+1})^{(1-\gamma')/\gamma}k^{-1/\gamma}\right\} \mathrm{d}\boldsymbol{p}'_m \,\mathrm{d}u.$$

Note that the point $p'_m = (y'_m, v_m)$ only appears in one of the indicators in the product. We integrate this indicator with respect to p'_m. Then, for large k,

$$\int_{\mathbb{R}\times(0,1]} \mathbb{1}\left\{v_m \leqslant cs_\wedge(v_{m-1}, y'_m)^{(1-\gamma')/\gamma}k^{-1/\gamma}\right\} \mathrm{d}p'_m$$
$$= \int_{\mathbb{R}} ck^{-1/\gamma}s_\wedge(v_{m-1}, y'_m)^{(1-\gamma')/\gamma} \,\mathrm{d}y'_m \in O(k^{-1/\gamma}v_{m-1}^{-\gamma}),$$

where in the first step we noted that the indicator represents an upper bound of v_m and integrated it out, and in the second step we used Lemma C.4.2 with $\rho = (1-\gamma')/\gamma$ and $a = u^{-\gamma}$. Note that the finiteness of the integral requires that $\gamma < (1-\gamma')/\gamma'$. We can follow the same steps for integrating out with respect to p'_{m-1}. The only difference is that now a $v_{m-1}^{-\gamma}$ appears in the integration, resulting in a $k^{(1-\gamma)/\gamma}$ factor. Then,

$$\int_{(0,1]\times\mathbb{S}^m} \mathbb{1}\{b \geqslant k/2\} \,\mathrm{d}(u, \boldsymbol{p}_m)$$
$$\leqslant ck^{-(1+(m-2)(1-\gamma))/\gamma} \int_0^{ck^{-1/\gamma}} \int_{\mathbb{R}\times(0,1]} \mathbb{1}\left\{cv_1^{-\gamma}s_\wedge(u, y'_1)^{1-\gamma'} \geqslant k\right\} v_1^{-\gamma} \,\mathrm{d}p'_1 \,\mathrm{d}u$$
$$\leqslant ck^{-(1+(m-1)(1-\gamma))/\gamma} \int_0^{ck^{-1/\gamma}} u^{-\gamma} \,\mathrm{d}u \in O(k^{m-(m+1)/\gamma}).$$

This leads to

$$\lim_{k\uparrow\infty} \left(\frac{1}{\log(k)} \log\left(\int_{(0,1]\times\mathbb{S}^m} \mathbb{1}\{b \geqslant k/2\} \,\mathrm{d}(u, \boldsymbol{p}_m)\right)\right) = m - \frac{m+1}{\gamma},$$

as asserted. $\qquad\square$

Proof of the lower bound

The idea for proving the lower bound is to construct specific configurations that lead to higher-order degrees exceeding k. We then show that these configurations occur with a sufficiently high probability.

Proof of the lower bound. Let $R_k := [0, k] \times [0, (\beta/k)^{1/\gamma}] \subseteq \mathbb{S}$ and note that for $p := (y, v) \in R_k$ and $p' := (z, w) \in [0, k] \times (0, 1]$, p and p' are connected. Indeed, $|y - z| \leqslant k \leqslant \beta u^{-\gamma} w^{-\gamma'}$. This gives for $\nu(k) := \lambda' k - \log(2)$ by Proposition C.2.2

$$\mathbb{P}(\deg(\Delta_m^*) \geqslant \nu(k)) \geqslant \frac{\lambda^{m+1}}{\lambda_m(m+1)!} \int_{R_k^m} \int_{[0,(\beta/k)^{1/\gamma}]} \mathbb{P}(\deg(\overrightarrow{\boldsymbol{p}}_m(u)) \geqslant \nu(k)) \, \mathrm{d}u \, \mathrm{d}\boldsymbol{p}_m$$

$$\geqslant \frac{\lambda^{m+1}(\beta/k)^{1/\gamma}}{\lambda_m(m+1)!} \int_{R_k^m} \mathbb{P}\Big(\mathcal{P}'([0,k] \times (0,1]) \geqslant \nu(k)\Big) \, \mathrm{d}\boldsymbol{p}_m.$$

As $\mathcal{P}'([0, k] \times (0, 1]) \sim \mathrm{Poi}(\lambda' k)$, its median can be lower bounded by $\nu(k)$ [21, Theorem 2]. Thus, lower bounding the integrand, we obtain

$$\mathbb{P}(\deg(\Delta_m^*) \geqslant \nu(k)) \geqslant \frac{\lambda^{m+1}(\beta/k)^{1/\gamma}}{2\lambda_m(m+1)!} |R_k|^m = \frac{\lambda^{m+1}\beta^{(m+1)/\gamma}}{2\lambda_m(m+1)!} k^{m-(m+1)/\gamma}.$$

Hence,

$$\liminf_{k \uparrow \infty} \frac{\log\big(\mathbb{P}(\deg(\Delta_m^*) \geqslant k)\big)}{\log(k)} = \liminf_{k \uparrow \infty} \frac{\log\big(\mathbb{P}(\deg(\Delta_m^*) \geqslant \nu(k))\big)}{\log(k)} \geqslant m - \frac{m+1}{\gamma}$$

as asserted. □

C.5 Proof of Theorem C.2.4

The proof of the CLT for the Betti numbers relies on the general Poisson CLT by Penrose and Yukich [89, Theorem 3.1]. This result requires verification of two conditions: a stabilization condition and a moment condition.

The stabilization condition follows from an adaptation of the arguments provided in Paper B and [48]. However, the moment condition is more involved than in Paper B or in [48]. This is because, in contrast to Paper B and [48], the existence of an m-simplex can no longer be determined just from the knowledge of the positions of the $m + 1$ $\mathcal{P}$-vertices. Indeed, the existence fundamentally involves the second Poisson process $\mathcal{P}'$.

Let $\beta(\mathcal{P}, \mathcal{P}') := \beta_{n,m}(\mathcal{P}, \mathcal{P}')$ be the mth Betti number of $G_n^{\mathsf{hyp}}(\mathcal{P} \cap \mathbb{S}_n, \mathcal{P}' \cap \mathbb{S}_n)$. We introduce the two special points $o := (0, U)$, $o' := (0, W)$. Furthermore, let $G_{n,o}^{\mathsf{hyp}} := G^{\mathsf{hyp}}((\mathcal{P} \cup \{o\}) \cap \mathbb{S}_n, \mathcal{P}' \cap \mathbb{S}_n)$ denote the hypergraph in the window $\mathbb{S}_n$ with the additional $\mathcal{P}$-vertex o, and similarly, let $G_{n,o'}^{\mathsf{hyp}}(\mathcal{P} \cap \mathbb{S}_n, (\mathcal{P}' \cup \{o'\}) \cap \mathbb{S}_n)$ denote the hypergraph in the window $\mathbb{S}_n$ with the additional $\mathcal{P}'$-vertex o'. Using these notations, the add-one cost operators

$$\delta(G_n^{\mathsf{hyp}}, o) := \beta(G_{n,o}^{\mathsf{hyp}}) - \beta(G_n^{\mathsf{hyp}})$$

$$\delta(G_n^{\mathsf{hyp}}, o') := \beta(G_{n,o'}^{\mathsf{hyp}}) - \beta(G_n^{\mathsf{hyp}}).$$

To apply [89, Theorem 3.1], we need to verify the following conditions:

- **moment condition:** $\sup_{n \geqslant 1} \mathbb{E}[\delta(G_n^{\mathsf{hyp}}, o)^4] < \infty$ and $\sup_{n \geqslant 1} \mathbb{E}[\delta(G_n^{\mathsf{hyp}}, o')^4] < \infty$

- **weak stabilization:** $\lim_{n \uparrow \infty} \delta(G_n^{\mathsf{hyp}}, o) < \infty$ and $\lim_{n \uparrow \infty} \delta(G_n^{\mathsf{hyp}}, o') < \infty$

Proof of the moment condition. By Hiraoka et al. [48, Lemma 2.9] and Edelsbrunner and Harer [35, Chapter VII], $\delta(G_n^{\mathsf{hyp}}, o)$ and $\delta(G_n^{\mathsf{hyp}}, o')$ are bounded above by the number of m- and $(m+1)$-simplices containing the additional $\mathcal{P}$-vertex $o = (0, U) \in \mathcal{P}$ or $o' = (0, W) \in \mathcal{P}'$.

We first consider the case of $\delta(G_n^{\mathsf{hyp}}, o')$. The number of new $m-1$-simplices is given as the number of m-tuples of points in the neighborhood $B(o')$ of the new point $(0, W) \in \mathcal{P}'$:

$$\mathbb{E}[\delta(G_n^{\mathsf{hyp}}, o')^4] \leqslant \mathbb{E}\left[\binom{\mathcal{P}(B(o'))}{m}^4\right] \leqslant \mathbb{E}[\mathcal{P}(B(o'))^{4m}].$$

The number of points in the neighborhood $\mathcal{P}(B(o'))$ is Poisson distributed with mean $\lambda |B(o')| = (2\beta\lambda)/(1-\gamma)w^{-\gamma'}$, as shown in Proposition C.2.1. Since the rth factorial moment of a Poisson random variable with parameter $\mu > 0$ equals μ^r, the rth moment itself is bounded above by $c_{\mathsf{M},r}\mu^r$ for some constant $c_{\mathsf{M},r} > 0$. Noting that $\gamma' < 1/(4m)$, we conclude that

$$\mathbb{E}[\mathcal{P}(B(o'))^{4m}] \leqslant c_{\mathsf{M},4m} \mathbb{E}\left[\left(\frac{2\beta}{1-\gamma}W^{-\gamma'}\right)^{4m}\right] \leqslant c \int_0^1 w^{-4m\gamma'}\, \mathrm{d}w < \infty$$

for some $c > 0$.

Next, we show that $\mathbb{E}[\delta(G_n^{\mathsf{hyp}}, o)^4] < \infty$. The number of new m-simplices are formed by the sets of m points $\overrightarrow{\boldsymbol{P}}_m := \{P_1, \ldots, P_m\} \in \mathcal{P}_{\neq}^m$ for which a common neighbor $P' \in \mathcal{P}'$ exists with the new $\mathcal{P}$-vertex o. As this number upper bounds $\delta(G_n^{\mathsf{hyp}}, o)$, we have

$$\mathbb{E}[\delta(G_n^{\mathsf{hyp}}, o)^4] \leqslant \mathbb{E}\left[\left(\sum_{\boldsymbol{P}_m \in \mathcal{P}_{\neq}^m} \mathbb{1}\left\{\mathcal{P}'(B(\{o\} \cup \overrightarrow{\boldsymbol{P}}_m)) \geqslant 1\right\}\right)^4\right]$$

$$\leqslant \mathbb{E}\left[\left(\sum_{P' \in \mathcal{P}'} \binom{\mathcal{P}(B(P'))}{m} \mathbb{1}\{P' \in B(o)\}\right)^4\right],$$

where $\overrightarrow{\boldsymbol{P}'}_m := \{P_1', \ldots, P_m'\}$, and in the second step each term of the sum represents the number of m-tuples of $\mathcal{P}$-vertices in the neighborhood of a point $P' \in \mathcal{P}'$, and the indicator ensures that this point is in turn connected to the new $\mathcal{P}$-vertex o. We bound the binomial coefficient by $\mathcal{P}(B(P'))^m$, and expand the fourth power of the

sum by using the multinomial theorem to obtain

$$\mathbb{E}[\delta(G_n^{\mathsf{hyp}}, o)^4]$$
$$\leqslant c_1 \, \mathbb{E}\Big[\textstyle\sum_{\boldsymbol{P}'_4 \in \mathcal{P}'^4_{\neq}} \prod_{i \leqslant 4} \mathcal{P}(B(P'_i))^m \, \mathbb{1}\{\overrightarrow{\boldsymbol{P}'}_4 \subseteq B(o)\}\Big] \qquad - \quad \text{term I}$$
$$+ c_2 \, \mathbb{E}\Big[\textstyle\sum_{\boldsymbol{P}'_3 \in \mathcal{P}'^3_{\neq}} \mathcal{P}(B(P'_1))^{2m} \prod_{i=2}^{3} \mathcal{P}(B(P'_i))^m \, \mathbb{1}\{\overrightarrow{\boldsymbol{P}'}_3 \subseteq B(o)\}\Big] \quad - \quad \text{term II}$$
$$+ c_3 \, \mathbb{E}\Big[\textstyle\sum_{\boldsymbol{P}'_2 \in \mathcal{P}'^2_{\neq}} \mathcal{P}(B(P'_1))^{2m} \mathcal{P}(B(P'_2))^{2m} \, \mathbb{1}\{\overrightarrow{\boldsymbol{P}'}_2 \subseteq B(o)\}\Big] \qquad - \quad \text{term III}$$
$$+ c_4 \, \mathbb{E}\Big[\textstyle\sum_{\boldsymbol{P}'_2 \in \mathcal{P}'^2_{\neq}} \mathcal{P}(B(P'_1))^{3m} \mathcal{P}(B(P'_2))^m \, \mathbb{1}\{\overrightarrow{\boldsymbol{P}'}_2 \subseteq B(o)\}\Big] \qquad - \quad \text{term IV}$$
$$+ c_5 \, \mathbb{E}\Big[\textstyle\sum_{P' \in \mathcal{P}'} \mathcal{P}(B(P'))^{4m} \, \mathbb{1}\{P' \in B(o)\}\Big] \qquad\qquad - \quad \text{term V}$$

for some $c_1, \ldots, c_5 > 0$. To show the moment bound, it is enough to show that each of the above terms is finite. We begin with using the multivariate Mecke formula for term I:

$$I := c_1 \, \mathbb{E}\Big[\sum_{\boldsymbol{P}'_4 \in \mathcal{P}'^4_{\neq}} \prod_{i \leqslant 4} \mathcal{P}(B(P'_i))^m \, \mathbb{1}\{\overrightarrow{\boldsymbol{P}'}_4 \subseteq B(o)\}\Big]$$
$$= c_1 \iint_{(0,1] \times \mathbb{S}^4} \mathbb{E}\Big[\prod_{i \leqslant 4} \mathcal{P}(B(p'_i))^m \, \mathbb{1}\{p'_i \in B(o)\}\Big] \, \mathrm{d}(u, \boldsymbol{p}'_4).$$

Introducing the notation $p'_i := (z_i, w_i)$ for the coordinates of the points p'_i, the indicator represents an upper bound for the coordinates $|z_i| \leqslant \beta u^{-\gamma} w_i^{-\gamma'}$. Next, we use Hölder's inequality to upper bound the expectation of the product:

$$I \leqslant 2^4 c_1 \iint_{(0,1] \times (0,1]^4} \prod_{i \leqslant 4} \Big(\int_0^{\beta u^{-\gamma} w_i^{-\gamma'}} \mathbb{E}\Big[\mathcal{P}\Big(B((z_i, w_i))\Big)^{4m}\Big]^{1/4} \, \mathrm{d}z_i \Big) \, \mathrm{d}(u, \boldsymbol{w}).$$

Hence,

$$I \leqslant 2^4 c_1 \iint_{(0,1] \times (0,1]^4} \prod_{i \leqslant 4} \Big(\int_0^{\beta u^{-\gamma} w_i^{-\gamma'}} c_{\mathsf{M},4m} \Big(\frac{2\beta}{1-\gamma} w_i^{-\gamma'} \Big)^m \, \mathrm{d}z_i \Big) \, \mathrm{d}(u, \boldsymbol{w}).$$

Note that the upper bound does not depend on the variable z_i, as it is translation invariant. Also, we can upper bound the exponential term by a sufficiently large constant C to get

$$I \leqslant \Big(\frac{C(2\beta)^{(m+1)}}{(1-\gamma)^m} \Big)^4 c_1 \int_0^1 u^{-4\gamma} \, \mathrm{d}u \int_{(0,1]^4} \prod_{i=1}^{4} w_i^{-(m+1)\gamma'} \, \mathrm{d}\boldsymbol{w}.$$

The integral over the w_i is finite whenever $\gamma' < 1/(m+1)$, and the integral over u is finite if $\gamma < 1/4$. The other terms can be bounded similarly, and we obtain a finite bound for $\mathbb{E}[\delta(G_n^{\mathsf{hyp}}, o)^4]$. The conditions for the finiteness of the integrals are given as follows:

- term I: $\gamma < 1/4$ and $\gamma' < 1/(m+1)$,

- term II: $\gamma < 1/3$ and $\gamma' < 1/(2m+1)$,

- term III: $\gamma < 1/2$ and $\gamma' < 1/(2m+1)$,

- term IV: $\gamma < 1/2$ and $\gamma' < 1/(3m+1)$,

- term V: $\gamma < 1$ and $\gamma' < 1/(4m+1)$.

Combining these conditions, we obtain that $\gamma < 1/4$ and $\gamma' < 1/(4m+1)$ are sufficient conditions for the finiteness of $\mathbb{E}[\delta(G_n^{\mathsf{hyp}}, o)^4]$. □

Proof of the weak stabilization. In the following, we extend the arguments from Hiraoka et al. [48, Proposition 5.4].

For $n \geqslant 1$ we write

$$\beta_n := \dim(Z_n) - \dim(B_n) := \dim(Z(G_n^{\mathsf{hyp}})) - \dim(B(G_n^{\mathsf{hyp}}))$$

for the Betti number of G_n^{hyp}, where Z_n is the corresponding cycle space and B_n is the boundary space.

We set for $o := (0, U)$,

$$\beta_{n,o} := \dim(Z_{n,o}) - \dim(B_{n,o}) := \dim(Z(G_{n,o}^{\mathsf{hyp}})) - \dim(B(G_{n,o}^{\mathsf{hyp}})).$$

Hence, it suffices to prove the weak stabilization with respect to $\dim(Z_n)$ and $\dim(B_n)$ separately. Since the arguments are very similar, we henceforth only deal with the case $\dim(Z_n)$. We do this by showing that $\dim(Z_{n,o}) - \dim(Z_n)$ is non-decreasing and bounded in n.

For the boundedness, note that $\dim(Z_{n,o}) - \dim(Z_n) \leqslant \deg_{m,n}(o)$, where $\deg_{m,n}(o)$ is the number of m-simplices in $\mathbb{S}_n$ containing the typical $\mathcal{P}$-vertex o. This is because the m-simplices constructed from $G_{n,o}^{\mathsf{hyp}}$ can be decomposed into the set of m-simplices containing o and into the family of all m-simplices formed in G_n^{hyp} [see 48, Lemma 2.9]. To show that $\dim(Z_{n,o}) - \dim(Z_n)$ is non-decreasing, take $n_1 \leqslant n_2$, and consider the canonical map

$$Z_{n_1,o} \to Z_{n_2,o}/Z_{n_2}$$

with kernel $Z_{n_1,o} \cap Z_{n_2} \subseteq Z_{n_1}$. We claim that the kernel is equal to Z_{n_1}. Let M_n and $M_{n,o}$ denote the set of m-simplices in G_n^{hyp} and $G_{n,o}^{\mathsf{hyp}}$, respectively, and consider an m-simplex $\sigma \in M_{n_1,o} \cap M_{n_2}$ forming an m-cycle z. If $\sigma \in M_{n_1}$, then both $\sigma \in M_{n_1,o}$ and $\sigma \in M_{n_2}$. Therefore, $Z_{n_1} \subseteq Z_{n_1,o'} \cap Z_{n_2}$, and the induced map

$$Z_{n_1,o}/Z_{n_1} \to Z_{n_2,o}/Z_{n_2}$$

is injective. In particular, $\dim(Z_{n_1,o}) - \dim(Z_{n_1}) \leqslant \dim(Z_{n_2,o}) - \dim(Z_{n_2})$, which shows the assertion.

Now, we show the weak stabilization with respect to the typical $\mathcal{P}'$-vertex $o' \in \mathcal{P}'$. As before, we write

$$\beta'_n := \dim(Z_{n,o'}) - \dim(B_{n,o'}) := \dim(Z(G_{n,o'}^{\mathsf{hyp}})) - \dim(B(G_{n,o'}^{\mathsf{hyp}})),$$

and prove weak stabilization with respect to $\dim(Z_n)$.

Let M_n and $M_{n,o'}$ denote the set of m-simplices in G_n^{hyp} and $G_{n,o'}^{\mathsf{hyp}}$, respectively. Following the same arguments as above, the difference $\dim(Z_{n,o'}) - \dim(Z_n)$ is bounded

from above by the number of m-simplices $|M_{n,o'}| - |M_n|$ appearing in G_n^{hyp} due to the addition of the typical $\mathcal{P}'$-vertex o':

$$\dim(Z_{n,o'}) - \dim(Z_n) \leqslant |M_{n,o'}| - |M_n|.$$

In turn, $|M_{n,o'}| - |M_n|$ is bounded from above by the number of m-tuples of points $p \in \mathcal{P}$ in the neighborhood $\mathcal{P}(B(o'))$ of o':

$$\dim(Z_{n,o'}) - \dim(Z_n) \leqslant \binom{\mathcal{P}(B(o'))}{m} < \infty,$$

since the neighborhood $\mathcal{P}(B(o'))$ is almost surely finite.

We consider again the canonical map

$$Z_{n_1,o'} \to Z_{n_2,o'}/Z_{n_2},$$

where $n_1 \leqslant n_2$. As $Z_{n_1} \subseteq Z_{n_2}$, the kernel of the map is $Z_{n_1,o'} \cap Z_{n_2}$. If $Z_{n_1} = Z_{n_1,o'} \cap Z_{n_2}$, we can conclude the proof as above.

In contrast to the case above, however, $\dim(Z_{n,o'}) - \dim(Z_n)$ is not necessarily monotone, since $Z_{n_1,o'} \cap Z_{n_2} \neq Z_{n_1}$, i.e., there can be cycles in the kernel that are not in Z_{n_1}. To see this, consider a cycle $z \in Z_{n_1,o'} \setminus Z_{n_1}$. If z contains a simplex formed by a $\mathcal{P}'$-vertex in the increased window size n_2, but not in the window size n_1, then $z \in Z_{n_2} \setminus Z_{n_1}$. Thus, $z \notin Z_{n_1}$, but is in the kernel of the map $Z_{n_1,o'} \to Z_{n_2,o'}/Z_{n_2}$. To solve this problem, we construct a random N_2 such that for any two window sizes $n_2 \geqslant n_1 \geqslant N_2$ we have $Z_{n_1,o'} \cap Z_{n_2} = Z_{n_1}$ in the kernel of the map $Z_{n_1,o'} \to Z_{n_2,o'}/Z_{n_2}$ the sequence $(\dim(Z_{n,o'}) - \dim(Z_n))$ is monotone. Once we have shown this, we can conclude the proof as above.

To construct N_2, first observe that as $\mathcal{P}(B(o'))$ is almost surely finite, there a random $N_1 \geqslant 1$ such that for all $n \geqslant N_1$, the number of m-simplices $|M_{n,o'}| - |M_n|$ is a non-increasing sequence. As all $\mathcal{P}$-vertices in the neighborhood $B(o')$ have finite neighborhoods almost surely, there also exists $N_2 \geqslant N_1 \in \mathbb{R}$ such that for all $n \geqslant N_2$, the number of m-simplices $|M_{n,o'}| - |M_n|$ is a non-decreasing sequence, and thus constant for such n. Then, we conclude the proof as above. $\qquad\square$

C.6 Proof of Theorem C.2.5

The proof idea for Theorem C.2.5 is similar to the edge-count CLTs and stable limits obtained in Paper B. For the CLT, we use a general result on associated random variables, whereas for the stable case, we use a truncation argument and a comparison with the independent case. Besides some moment computations of the degree of a typical node, the main difficulty in the proof is to approximate the random number of nodes in the interval $[0, n]$ by a deterministic number.

We begin by proving an auxiliary result that will be used in both the normal and the stable cases. Recall the definition of the neighborhood $B(\Delta)$ of a set of points Δ as it was defined in (C.3). As before, for $u \leqslant 1$ and $\overrightarrow{\boldsymbol{p}}_m \subseteq \mathcal{P}$, we write $B(\overrightarrow{\boldsymbol{p}}_m(u))$ for the common neighborhood of $\{(0, u), p_1, \ldots, p_m\}$.

Lemma C.6.1 (Scaling of $B(\overrightarrow{\boldsymbol{p}}_m(u))$). *Let $u \leqslant 1$, $m \geqslant 1$, $0 < \gamma < 1$ and $0 < \gamma' < 1/(m+1)$. It holds that*

$$\int_{\mathbb{S}^m} |B(\overrightarrow{\boldsymbol{p}}_m(u))| \, \mathrm{d}\boldsymbol{p}_m = \frac{u^{-\gamma}}{1 - (m+1)\gamma'} \frac{(2\beta)^{m+1}}{(1-\gamma)^m}.$$

Proof. We have that

$$\int_{\mathbb{S}^m} |B(\overrightarrow{\boldsymbol{p}}_m(u))| \, \mathrm{d}\boldsymbol{p}_m = \iint_{\mathbb{S} \times \mathbb{S}^m} \mathbb{1}\{p' \in B(\overrightarrow{\boldsymbol{p}}_m(u))\} \, \mathrm{d}\boldsymbol{p}_m \, \mathrm{d}p'$$

$$= \int_{\mathbb{S}} \mathbb{1}\{(z,w) \in B(o)\} \left(\int_{\mathbb{S}} \mathbb{1}\{|z-y| \leqslant \beta v^{-\gamma} w^{-\gamma'}\} \, \mathrm{d}(y,v) \right)^m \mathrm{d}(z,w)$$

$$= \int_{\mathbb{S}} \mathbb{1}\{(z,w) \in B(o)\} \left(\frac{2\beta w^{-\gamma'}}{1-\gamma} \right)^m \mathrm{d}(z,w)$$

$$= u^{-\gamma} \int_0^1 \frac{(2\beta w^{-\gamma'})^{m+1}}{(1-\gamma)^m} \, \mathrm{d}w = \frac{u^{-\gamma}}{1 - (m+1)\gamma'} \frac{(2\beta)^{m+1}}{(1-\gamma)^m},$$

where we used the notations $p := (y,v)$ and $p' := (z,w)$. $\qquad \square$

Proof of the normal limit

The idea of the proof is to apply the CLT [107, Theorem 4.4.3] which holds for stationary sequences of identically distributed associated random variables $\boldsymbol{T} := T_1, T_2, \ldots$, and requires that $\sum_{k \geqslant 1} \mathrm{Cov}(T_1, T_k) < \infty$. Recall that the sequence of random variables $\boldsymbol{T}$ is associated if and only if $\mathrm{Cov}(f(T_1, \ldots, T_k), g(T_1, \ldots, T_k)) \geqslant 0$ for all non-decreasing functions f, g for which $\mathbb{E}[f(T_1, \ldots, T_k)]$, $\mathbb{E}[g(T_1, \ldots, T_k)]$, $\mathbb{E}[f(T_1, \ldots, T_k)g(T_1, \ldots, T_k)]$ exist [36, Definition 1.1].

Proof of Theorem C.2.5 (a). Let $\gamma < 1/2$ and define for $i \geqslant 1$,

$$T_i := \sum_{P_j \in \mathcal{P} \cap ([i-1,i] \times (0,1])} \deg(P_j).$$

Since the degree $\deg(x,u)$ is increasing in the Poisson process $\mathcal{P}'$, we conclude from the Harris-FKG inequality [66, Theorem 20.4] that the sequence $T_1, \ldots, T_k$ is associated. For $A \subseteq \mathbb{R}$ let

$$S(A) := \sum_{P_j \in \mathcal{P} \cap A \times (0,1]} \deg(P_j).$$

Then, the Mecke equation gives

$\mathrm{Var}(S(A))$

$$= \mathbb{E}\Big[\sum_{P_i \neq P_j \in \mathcal{P} \cap A} \deg(P_i) \deg(P_j) \Big] + \mathbb{E}\Big[\sum_{P_i \in \mathcal{P} \cap A} \deg(P_i)^2 \Big] - \mathbb{E}\Big[\sum_{P_i \in \mathcal{P} \cap A} \deg(P_i) \Big]^2$$

$$= \lambda^2 \iint_{(A \times (0,1])^2} \mathbb{E}[\deg(p_1) \deg(p_2)] \, \mathrm{d}p_1 \, \mathrm{d}p_2$$

$$+ \lambda \int_{A \times (0,1]} \mathbb{E}[\deg(p_1)^2] \, \mathrm{d}p_1 - \lambda^2 \Big(\int_{A \times (0,1]} \mathbb{E}[\deg(p_1)] \, \mathrm{d}p_1 \Big)^2$$

$$= \lambda |A| \int_0^1 \mathbb{E}[\deg(0,u)^2] \, \mathrm{d}u + \lambda^2 \iint_{(A \times (0,1])^2} \mathrm{Cov}(\deg(p_1), \deg(p_2)) \, \mathrm{d}p_1 \, \mathrm{d}p_2,$$

139

where the last equality holds due to translation invariance of $\deg(\,\cdot\,)$.

To bound the first integral, note that for all $u \in (0, 1]$, the random variable $\deg(0, u)$ is Poisson distributed with parameter $(2\beta\lambda' u^{-\gamma})/(1 - \gamma')$. Hence, $\mathbb{E}[\deg(0, u)^2] = \frac{2\beta\lambda'}{1-\gamma'} u^{-\gamma}(1 + \frac{2\beta\lambda'}{1-\gamma'} u^{-\gamma}) \in O(u^{-2\gamma})$. Thus, we obtain for $\gamma < 1/2$ that

$$\int_0^1 \mathbb{E}[\deg(0, u)^2]\, \mathrm{d}u < \infty.$$

Next, we deal with the second term and note that the covariance in the integrand is given by

$$\begin{aligned}
\mathrm{Cov}(\deg(p_1), \deg(p_2)) = \mathbb{E}\Big[\sum_{P' \in \mathcal{P}'} \mathbb{1}\{P' \in B(\{p_1, p_2\})\}\Big] \\
+ \mathbb{E}\Big[\sum_{P_1' \neq P_2' \in \mathcal{P}'} \mathbb{1}\{P_1' \in B(p_1), P_2' \in B(p_2)\}\Big] \\
- \mathbb{E}\Big[\sum_{P' \in \mathcal{P}'} \mathbb{1}\{P' \in B(p_1)\}\Big] \mathbb{E}\Big[\sum_{P' \in \mathcal{P}'} \mathbb{1}\{P' \in B(p_2)\}\Big] \\
= \lambda' \int_{\mathbb{S}} \mathbb{1}\{p' \in B(\{p_1, p_2\})\}\, \mathrm{d}p' = \lambda'|B(\{p_1, p_2\})|.
\end{aligned}$$

From Lemma C.6.1 with $m = 1$ and translation invariance, we obtain that

$$\int_{A \times (0,1]} \int_{\mathbb{S}} |B(\{p_1, p_2\})|\, \mathrm{d}p_1\, \mathrm{d}p_2 = \frac{1}{1 - 2\gamma'} \frac{(2\beta)^2}{1 - \gamma} \int_0^1 u^{-\gamma}\, \mathrm{d}u < \infty.$$

Hence, $\mathrm{Var}(T_1) = \mathrm{Var}(S([0, 1])) < \infty$. Similarly, we obtain that

$$\begin{aligned}
\sum_{k \geqslant 2} \mathrm{Cov}(T_1, T_k) = \mathbb{E}\Big[\sum_{\substack{P_i \in \mathcal{P} \cap [0,1] \times (0,1], \\ P_j \in \mathcal{P} \cap [1,\infty) \times (0,1]}} \deg(P_i) \deg(P_j)\Big] \\
- \mathbb{E}\Big[\sum_{P_i \in \mathcal{P} \cap [0,1] \times (0,1]} \deg(P_i)\Big] \mathbb{E}\Big[\sum_{P_j \in \mathcal{P} \cap [1,\infty) \times (0,1]} \deg(P_j)\Big] \\
\leqslant \lambda^2 \int_{[0,1] \times (0,1]} \int_{\mathbb{S}} \mathrm{Cov}(\deg(p_1), \deg(p_2))\, \mathrm{d}p_2\, \mathrm{d}p_1 \\
\leqslant \frac{\lambda^2 \lambda'}{1 - 2\gamma'} \Big(\frac{2\beta}{1 - \gamma}\Big)^2 \int_0^1 u^{-\gamma}\, \mathrm{d}u < \infty,
\end{aligned}$$

thereby showing the finiteness of $\sum_{k \geqslant 1} \mathrm{Cov}(T_1, T_k)$. $\qquad\square$

Proof of the stable limit

The idea of the proof of Theorem C.2.5 (b) is to apply [107, Theorem 4.5.2], which says the following. Let $X_i, i \geqslant 1$ be i.i.d. nonnegative random variables with $\mathbb{P}(X_1 > x) \sim Ax^{-\alpha}$ for some $\alpha \in (1, 2)$ and $A > 0$. Then $n^{-1/\alpha} \sum_{i \sim n}(X_i - \mathbb{E}[X_i])$ converges in distribution to an α-stable random variable.

Proof of Theorem C.2.5 (b). Let $u_n := n^{-b}$ for an arbitrary choice of $b \in (2/3, 1)$. We decompose S_n into

$$S_n = S_n^{\geqslant} + S_n^{\leqslant} := \sum_{P \in \mathcal{P} \cap \mathbb{S}_{n, \geqslant u_n}} \deg(P) + \sum_{P \in \mathcal{P} \cap \mathbb{S}_{n, \leqslant u_n}} \deg(P),$$

where $\mathbb{S}_{n, \geqslant u} := [0, n] \times [u, 1]$ and $\mathbb{S}_{n, \leqslant u} := [0, n] \times [0, u]$.

First, we show that $n^{-\gamma}(S_n^{\geqslant} - \mathbb{E}[S_n^{\geqslant}])$ converges to 0 in probability as $n \to \infty$. By Chebychev's inequality, this follows once we have shown that $\mathrm{Var}(S_n^{\geqslant}) \in o(n^{2\gamma})$. Note that

$$\mathrm{Var}(S_n^{\geqslant}) = \lambda \int_{\mathbb{S}_{n, \geqslant u_n}} \mathbb{E}[\deg(p)^2] \, \mathrm{d}p$$
$$+ \lambda^2 \iint_{\mathbb{S}_{n, \geqslant u_n}^2} \mathrm{Cov}(\deg(p_1), \deg(p_2)) \, \mathrm{d}p_1 \, \mathrm{d}p_2. \tag{C.6}$$

Here, by translation invariance, the first term is bounded by $(n u_n^{1-2\gamma})/(2\gamma - 1)$, which is in $o(n^{2\gamma})$ since $1 - b(1 - 2\gamma) < 2\gamma$ for all $b < 1$ and $\gamma > 1/2$. For the second term, Lemma C.6.1 gives the bound

$$2n\lambda^2 \int_{u_n}^1 \int_{\mathbb{S}_{\geqslant u}} |B(\{(0, u), (y, v)\})| \, \mathrm{d}(y, v) \, \mathrm{d}u \in O(n),$$

where $\mathbb{S}_{\geqslant u} := \mathbb{R} \times [u, 1]$. Thus, $n^{-\gamma}(S_n^{\geqslant} - \mathbb{E}[S_n^{\geqslant}]) \xrightarrow[n\uparrow\infty]{\mathbb{P}} 0$.

For $u \leqslant 1$, we set $\mu(u) := \mathbb{E}[\deg(0, u)] = (2\beta u^{-\gamma})/(1 - \gamma')$ and

$$S_n^{(1)} := \sum_{(X, U) \in \mathcal{P} \cap \mathbb{S}_{n, \leqslant u_n}} \mu(U) \qquad \text{and} \qquad S_n^{(2)} := \sum_{i \leqslant \lceil \lambda n \rceil} \mu(U_i) \, \mathbb{1}\{U_i \leqslant u_n\},$$

where $U_1, U_2, \ldots$ are i.i.d. uniforms on $(0, 1)$. We next prove that $\mathbb{E}[|S_n^{\leqslant} - S_n^{(1)}|] + \mathbb{E}[|S_n^{(1)} - S_n^{(2)}|] \in o(n^\gamma)$. For the first expectation, note that, by the Mecke equation,

$$\mathbb{E}[|S_n^{\leqslant} - S_n^{(1)}|] \leqslant n\lambda \int_0^{u_n} \mathbb{E}[|\deg(0, u) - \mu(u)|] \, \mathrm{d}u$$
$$\leqslant n\lambda \int_0^{u_n} \mathrm{Var}(\deg(0, u))^{1/2} \, \mathrm{d}u = n\lambda \int_0^{u_n} \mu(u)^{1/2} \, \mathrm{d}u,$$

Therefore, $\mathbb{E}[|S_n^{\leqslant} - S_n^{(1)}|] \in O(n u_n^{1-\gamma/2})$. Since $1 - b(1 - \gamma/2) < \gamma$, which holds for $b > 2/3$, we conclude that $n^{-\gamma} \mathbb{E}[|S_n^{\leqslant} - S_n^{(1)}|] \to 0$.

Second, we obtain a Poisson random variable N with parameter λn,

$$\mathbb{E}[|S_n^{(1)} - S_n^{(2)}|] \leqslant \mathbb{E}[|N - \lceil \lambda n \rceil|] \int_0^{u_n} \mu(u) \, \mathrm{d}u \leqslant (\mathrm{Var}(N)^{1/2} + 1) \int_0^{u_n} \mu(u) \, \mathrm{d}u.$$

Now, $\mathrm{Var}(N) = \lambda N$ and the integral above is in $O(u_n^{1-\gamma})$. Therefore, $\mathbb{E}[|S_n^{(1)} - S_n^{(2)}|] \in O(n^{1/2} u_n^{1-\gamma})$. Since $1/2 - b(1 - \gamma) < \gamma$, which holds for all b if $\gamma > 1/2$, it follows that $n^{-\gamma} \mathbb{E}[|S_n^{(1)} - S_n^{(2)}|] \to 0$.

It therefore suffices to prove that $n^{-\gamma}(S_n^{(2)} - \mathbb{E}[S_n^{(2)}])$ converges in distribution to a stable random variable. Note that by Lemma B.5.2,

$$\sum_{i \leqslant \lceil \lambda n \rceil} \mu(U_i) \, \mathbb{1}\{U_i > u_n\} \xrightarrow[n\uparrow\infty]{L^2} 0.$$

Finally, [107, Theorem 4.5.2] implies that $n^{-\gamma^{-1}} \sum_{i \leqslant \lceil \lambda n \rceil} (\mu(U_i) - \mathbb{E}[\mu(U_i)])$ converges in distribution to a γ^{-1}-stable random variable. $\qquad \square$

C.7 Proof of Theorem C.2.6

We now extend the proof of Theorem C.2.5 to the case of m-simplices. More precisely, we consider

$$S_{n,m} := \sum_{P \in \mathcal{P} \cap \mathbb{S}_n} \mathrm{d}_m(P),$$

where for $p = (x, u)$, we set

$$\mathrm{d}_m(p) := \frac{1}{m!} \sum_{(P_1, \dots, P_m) \in (\mathcal{P} \cap \mathbb{S}_{>u})_{\neq}^m} \mathbb{1}\{\mathcal{P}' \cap B(\{p, P_1, \dots, P_m\}) \neq \varnothing\}$$

is the number of m-simplices containing p.

Lemma C.7.1 (Moment computations). *Let $m \geqslant 1$. Then,*

(a) $\mathbb{E}[\mathrm{d}_m(0, u)^2] \in O(u^{-2\gamma})$.

(b) $\mathbb{E}[\mathrm{Var}(\mathrm{d}_m(0, u) \mid \mathcal{P}')] \in O(u^{1-3\gamma})$.

(c) $\int_{\mathbb{S}} |\mathbb{E}[\mathrm{Cov}(\mathrm{d}_m(0, u), \mathrm{d}_m(p) \mid \mathcal{P}')]| \, \mathrm{d}p \in O(u^{1-3\gamma})$.

(d) $\mathrm{Var}(\mathbb{E}[\mathrm{d}_m(0, u) \mid \mathcal{P}']) \in O(u^{-\gamma})$.

(e) $\int_{\mathbb{S}} |\mathrm{Cov}(\mathbb{E}[\mathrm{d}_m(0, u) \mid \mathcal{P}'], \mathbb{E}[\mathrm{d}_m(p) \mid \mathcal{P}'])| \, \mathrm{d}p \in O(u^{-\gamma})$.

We defer the technical computations to the end of this section and first explain how to conclude the proof of Theorem C.2.6 based on Lemma C.7.1.

Proof of the normal limit

For $\gamma < 1/2$, we follow the same strategy as in the proof of Theorem C.2.5 (a).

Proof of Theorem C.2.6 (a). Let

$$T_i := \sum_{P_j \in [i-1,i] \times (0,1]} \mathrm{d}_m(P_j).$$

We apply [107, Theorem 4.4.3] which holds for sequences of identically distributed associated random variables $T_1, T_2, \dots$, and need to show that $\sum_{k \geqslant 1} \mathrm{Cov}(T_1, T_k) < \infty$.

By the formula for the total variance, we have $\mathrm{Var}(T_1) = \mathbb{E}[\mathrm{Var}(T_1 \mid \mathcal{P}')] + \mathrm{Var}(\mathbb{E}[T_1 \mid \mathcal{P}'])$, where, by Lemma C.7.1 (a), (c), and translation invariance

$$\mathbb{E}[\mathrm{Var}(T_1 \mid \mathcal{P}')] = \lambda \int_{\mathbb{S}_1} \mathbb{E}[\mathrm{d}_m(p)^2] \, \mathrm{d}p$$
$$+ \lambda^2 \iint_{\mathbb{S}_1^2} \mathbb{E}[\mathrm{Cov}(\mathrm{d}_m(p_1), \mathrm{d}_m(p_2) \mid \mathcal{P}')] \, \mathrm{d}p_1 \, \mathrm{d}p_2 < \infty.$$

Moreover, by Lemma C.7.1 (e) and translation invariance,

$$\mathrm{Var}(\mathbb{E}[T_1 \mid \mathcal{P}']) = \lambda^2 \iint_{\mathbb{S}_1^2} \mathrm{Cov}(\mathbb{E}[\mathrm{d}_m(p_1) \mid \mathcal{P}'], \mathbb{E}[\mathrm{d}_m(p_2) \mid \mathcal{P}']) \, \mathrm{d}p_1 \, \mathrm{d}p_2 < \infty.$$

Analogously, we obtain that

$$\sum_{k \geqslant 2} \mathrm{Cov}(T_1, T_k) = \sum_{k \geqslant 2} \Big(\mathbb{E}[\mathrm{Cov}(T_1, T_k \mid \mathcal{P}')] + \mathrm{Cov}(\mathbb{E}[T_1 \mid \mathcal{P}'], \mathbb{E}[T_k \mid \mathcal{P}']) \Big)$$

$$= \lambda^2 \int_{\mathbb{S}_1} \int_{[1,\infty) \times (0,1]} \mathbb{E}[\mathrm{Cov}(\mathrm{d}_m(p_1), \mathrm{d}_m(p_2) \mid \mathcal{P}')] \, \mathrm{d}p_1 \, \mathrm{d}p_2$$

$$+ \lambda^2 \int_{\mathbb{S}_1} \int_{[1,\infty) \times (0,1]} \mathrm{Cov}\big(\mathbb{E}[\mathrm{d}_m(p_1) \mid \mathcal{P}'], \mathbb{E}[\mathrm{d}_m(p_2) \mid \mathcal{P}']\big) \, \mathrm{d}p_1 \, \mathrm{d}p_2 < \infty.$$

$\qquad\qquad\qquad\qquad\qquad\qquad\qquad\qquad\qquad\qquad\qquad\qquad\qquad\qquad\qquad\quad$ $\square$

Proof of the stable limit

Next, we prove Theorem C.2.6 (b).

Proof of Theorem C.2.6 (b). The idea is to proceed analogously to the proof of Theorem C.2.5 (b). We assume that $\gamma' < 1/(2m+1)$, and choose $u_n = n^{-b}$, where $b \in (2/3, 1)$, similarly to the proof of Theorem C.2.5. Then, we split $S_{n,m}$ into

$$S_{n,m} = S_{n,m}^{\geqslant} + S_{n,m}^{\leqslant} := \sum_{P_i \in \mathcal{P} \cap \mathbb{S}_{n, \geqslant u_n}} \mathrm{d}_m(P_i) + \sum_{P_i \in \mathcal{P} \cap \mathbb{S}_{n, \leqslant u_n}} \mathrm{d}_m(P_i).$$

We now show that $n^{-\gamma}(S_{n,m}^{\geqslant} - \mathbb{E}[S_{n,m}^{\geqslant}])$ converges to 0 in probability. This follows, as soon as we have proved that $\mathrm{Var}(S_{n,m}^{\geqslant}) \in o(n^{2\gamma})$. We have

$$\mathrm{Var}(S_{n,m}^{\geqslant})$$
$$= n\lambda \int_{u_n}^{1} \mathbb{E}[\mathrm{d}_m(0,u)^2] \, \mathrm{d}u + n\lambda^2 \int_{\mathbb{S}_{1, \geqslant u_n}} \int_{\mathbb{S}_{n, \geqslant u_n}} \mathrm{Cov}(\mathrm{d}_m(x,u), \mathrm{d}_m(p)) \, \mathrm{d}p \, \mathrm{d}(x,u).$$

By Lemma C.7.1 (a), (c), and translation invariance, there are constants $c_1, c_2 > 0$ such that the above is bounded by

$$c_1 n\lambda \int_{u_n}^{1} u^{-2\gamma} \, \mathrm{d}u + c_2 n\lambda^2 \int_{u_n}^{1} u^{1-3\gamma} \, \mathrm{d}u \in O(nu_n^{1-2\gamma}),$$

which is in $o(n^{2\gamma})$, since $1 - b(1 - 2\gamma) < 2\gamma$ for $\gamma > 1/2$. Thus, $n^{-\gamma}(S_{n,m}^{\geqslant} - \mathbb{E}[S_{n,m}^{\geqslant}]) \xrightarrow{\mathbb{P}} 0$. Next, we let

$$S_{n,m}^{(1)} := \sum_{(X,U) \in \mathcal{P} \cap \mathbb{S}_n} \mu_m(U), \qquad S_{n,m}^{(2)} := \sum_{i \leqslant \lceil \lambda n \rceil} \mu_m(U_i) \, \mathbb{1}\{U_i \leqslant u_n\},$$

where $\mu_m(u) := \mathbb{E}[\mathrm{d}_m(0,u)]$, and $U_1, U_2, \ldots$ are i.i.d. uniform random variables on $(0,1]$. We next prove that $\mathbb{E}[|S_{n,m}^{\leqslant} - S_{n,m}^{(1)}|] + \mathbb{E}[|S_{n,m}^{(1)} - S_{n,m}^{(2)}|] \in o(n^{\gamma})$. For the first expectation, note that by the Mecke equation,

$$\mathbb{E}[|S_{n,m}^{\leqslant} - S_{n,m}^{(1)}|] \leqslant n\lambda \int_0^{u_n} \mathbb{E}[|\mathrm{d}_m(0,u) - \mu_m(u)|] \, \mathrm{d}u \leqslant n\lambda \int_0^{u_n} \mathrm{Var}(\mathrm{d}_m(0,u))^{1/2} \, \mathrm{d}u.$$

From Lemma C.7.1 (b), (d), we have that $\mathrm{Var}(\mathrm{d}_m(0,u)) \in O(u^{1-3\gamma})$. Hence,

$$\mathbb{E}[|S_{n,m}^{\leqslant} - S_{n,m}^{(1)}|] \leqslant nu_n^{3(1-\gamma)/2} \in o(n^{\gamma}),$$

since $1 - b(3(1-\gamma)/2) < \gamma$ for $b > 2/3$. From here, we conclude the proof as in Theorem C.2.5 (b). $\qquad\qquad\qquad\qquad\qquad\qquad\qquad\qquad\qquad\qquad\qquad\qquad\quad$ $\square$

Finally, we conclude by proving Lemma C.7.1. We note that the proof of Part (b) is largely parallel to Part (c), and the proof of Part (d) is mainly parallel to Part (e). Nevertheless, to make the manuscript self-contained, we provide the details.

Proof of Lemma C.7.1. Henceforth, we use the abbreviations

$$
\begin{aligned}
\boldsymbol{p}_{i,m} &:= (p_{m-i+1}, \ldots, p_{2m-i}) \\
\overrightarrow{\boldsymbol{p}}_{i,m} &:= \{p_{m-i+1}, \ldots, p_{2m-i}\}, \\
\overrightarrow{\boldsymbol{p}}_{i,m}(u) &:= \{(0,u), p_{m-i+1}, \ldots, p_{2m-i}\}.
\end{aligned}
$$

Furthermore, to ease notation, we introduce for a set A the abbreviation $\mathcal{P}'_A := \mathcal{P}' \cap B(A)$.

Part (a). Conditioned on $\mathcal{P}'$, $\mathrm{d}_m(0,u)$ is a U-statistic. Therefore, by Reitzner and Schulte [92, Lemma 3.5] with $k_i := 1/(i!((m-i)!)^2)$,

$$
\mathbb{E}[\mathrm{d}_m(0,u)^2 \mid \mathcal{P}'] = \sum_{i=0}^{m} \lambda^{2m-i} k_i \int_{\mathbb{S}^{2m-i}_{\geqslant u}} \mathbb{P}(\mathcal{P}'_{\overrightarrow{\boldsymbol{p}}_m(u)} \neq \varnothing, \mathcal{P}'_{\overrightarrow{\boldsymbol{p}}_{i,m}(u)} \neq \varnothing \mid \mathcal{P}') \, \mathrm{d}\boldsymbol{p}_{2m-i}.
$$

Therefore,

$$
\begin{aligned}
\mathbb{E}[\mathrm{d}_m(0,u)^2] &= \sum_{i=0}^{m} \lambda^{2m-i} k_i \int_{\mathbb{S}^{2m-i}_{\geqslant u}} \mathbb{P}(\mathcal{P}'_{\overrightarrow{\boldsymbol{p}}_m(u)} \neq \varnothing, \mathcal{P}'_{\overrightarrow{\boldsymbol{p}}_{i,m}(u)} \neq \varnothing) \, \mathrm{d}\boldsymbol{p}_{2m-i} \\
&\leqslant \sum_{i=0}^{m} \lambda^{2m-i} k_i \int_{\mathbb{S}^{2m-i}_{\geqslant u}} \mathbb{P}(\mathcal{P}'_{\overrightarrow{\boldsymbol{p}}_{2m-i}(u)} \neq \varnothing) \\
&\qquad\qquad + \mathbb{P}(\mathcal{P}'_{\overrightarrow{\boldsymbol{p}}_m(u)} \neq \varnothing) \mathbb{P}(\mathcal{P}'_{\overrightarrow{\boldsymbol{p}}_{i,m}(u)} \neq \varnothing) \, \mathrm{d}\boldsymbol{p}_{2m-i},
\end{aligned}
$$

where we used that for all Borel sets $A, B \subseteq \mathbb{S}$, $\mathbb{P}(\mathcal{P}' \cap A \neq \varnothing, \mathcal{P}' \cap B \neq \varnothing) = \mathbb{P}(\mathcal{P}' \cap A \cap B \neq \varnothing) + \mathbb{P}(\mathcal{P}' \cap A \setminus B \neq \varnothing, \mathcal{P}' \cap B \setminus A \neq \varnothing)$. Next, we use that for all Borel set $A \subseteq \mathbb{R} \times (0,1]$, $\mathbb{P}(\mathcal{P}' \cap A = \varnothing) \leqslant \lambda'|A|$ and obtain that the above is bounded by

$$
\sum_{k=m}^{2m} \lambda^k \int_{\mathbb{S}^{k}_{\geqslant u}} \left(\lambda' |B(\overrightarrow{\boldsymbol{p}}_k(u))| + (\lambda')^2 |B(\overrightarrow{\boldsymbol{p}}_m(u))| |B(\{(0,u), p_{m+1}, \ldots, p_k\})| \right) \, \mathrm{d}\boldsymbol{p}_k,
$$

which is of order $O(u^{-2\gamma})$ by Lemma C.6.1.

Part (b). By Reitzner and Schulte [92, Lemma 3.5],

$$
\mathrm{Var}(\mathrm{d}_m(0,u) \mid \mathcal{P}') = \sum_{i=1}^{m} \lambda^{2m-i} k_i \int_{\mathbb{S}^{2m-i}_{\geqslant u}} \mathbb{1}\{\mathcal{P}'_{\overrightarrow{\boldsymbol{p}}_m(u)} \neq \varnothing\} \mathbb{1}\{\mathcal{P}'_{\overrightarrow{\boldsymbol{p}}_{i,m}(u)} \neq \varnothing\} \, \mathrm{d}\boldsymbol{p}_{2m-i}.
$$

Therefore,

$$
\mathbb{E}[\mathrm{Var}(\mathrm{d}_m(0,u) \mid \mathcal{P}')] = \sum_{i=1}^{m} \lambda^{2m-i} k_i \int_{\mathbb{S}^{2m-i}_{\geqslant u}} \mathbb{P}(\mathcal{P}'_{\overrightarrow{\boldsymbol{p}}_m(u)} \neq \varnothing, \mathcal{P}'_{\overrightarrow{\boldsymbol{p}}_{i,m}(u)} \neq \varnothing) \, \mathrm{d}\boldsymbol{p}_{2m-i}.
$$

Similarly to Part (a), we find that the above is bounded by

$$
\int_{\mathbb{S}^{2m-i}_{\geqslant u}} \mathbb{P}(\mathcal{P}'_{\overrightarrow{\boldsymbol{p}}\, 2m-i(u)} \neq \varnothing) + \mathbb{P}(\mathcal{P}'_{\overrightarrow{\boldsymbol{p}}\, m(u)} \neq \varnothing) \,\mathbb{P}(\mathcal{P}'_{\{(0,u),p_{m-i+1},\dots,p_{2m-i}\}} \neq \varnothing) \, \mathrm{d}\boldsymbol{p}_{2m-i}
$$

$$
\leqslant \int_{\mathbb{S}^{2m-i}_{\geqslant u}} \lambda' |B(\overrightarrow{\boldsymbol{p}}\, 2m-i(u))| + (\lambda')^2 |B(\overrightarrow{\boldsymbol{p}}\, m(u))||B(\{p_m,\dots,p_{2m-i}\})| \, \mathrm{d}\boldsymbol{p}_{2m-i},
$$

where the last inequality follows by the same argument as in Part (a). Recall that $\overrightarrow{\boldsymbol{p}}_{i,m}(u) = \{(0,u), p_{m-i+1}, \dots, p_{2m-i}\}$. Next, we apply Lemma C.6.1 to $|B(\overrightarrow{\boldsymbol{p}}\, 2m-1(u))|$, integrated with respect to $\boldsymbol{p}_{2m-1}$, and to $|B(\overrightarrow{\boldsymbol{p}}\, 1,m)|$, integrated with respect to $p_{m+1}, \dots, p_{2m-i}$. This gives

$$
\lambda^m (\lambda')^2 \Big(\sum_{i=1}^m k_i \frac{(2\beta)^{m-i+1}}{(1-\gamma)^{m-i}} \frac{1}{1-(m-i+1)\gamma'} \Big)
$$
$$
\times \int_{\mathbb{S}^m_{\geqslant u}} v_m^{-\gamma} |B(\overrightarrow{\boldsymbol{p}}\, m(u))| \, \mathrm{d}\boldsymbol{p}_m + O(u^{-\gamma}),
$$

where $p_m := (y_m, v_m)$. Moreover, for all $u \in (0,1]$,

$$
\int_{\mathbb{S}^m_{\geqslant u}} v_m^{-\gamma} |B(\overrightarrow{\boldsymbol{p}}\, m(u))| \, \mathrm{d}\boldsymbol{p}_m
$$
$$
= \int_{\mathbb{S}} \int_{\mathbb{S}^m_{\geqslant u}} v_m^{-\gamma} \, \mathbb{1}\{|z| \leqslant \beta w^{-\gamma'} u^{-\gamma}\}
$$
$$
\times \prod_{i=1}^m \mathbb{1}\{|z - y_i| \leqslant \beta w^{-\gamma'} v_i^{-\gamma}\} \, \mathrm{d}((y_1, v_1), \dots, (y_m, v_m)) \, \mathrm{d}(z, w)
$$
$$
\leqslant (2\beta)^m \int_{\mathbb{S}} \int_{(0,1]^{m-1} \times [u,1]} w^{-m\gamma'} v_1^{-\gamma} \cdots v_{m-1}^{-\gamma} v_m^{-2\gamma}
$$
$$
\times \mathbb{1}\{|z| \leqslant \beta w^{-\gamma'} u^{-\gamma}\} \, \mathrm{d}(v_1, \dots, v_m) \, \mathrm{d}(z, w)
$$
$$
= \frac{(2\beta)^{m+1}(u^{1-2\gamma} - 1)u^{-\gamma}}{(1-\gamma)^{m-1}(2\gamma - 1)} \int_0^1 w^{-(m+1)\gamma'} \, \mathrm{d}w
$$
$$
= \frac{(2\beta)^{m+1}(u^{1-2\gamma} - 1)u^{-\gamma}}{(1-\gamma)^{m-1}(2\gamma - 1)(1-(m+1)\gamma')},
$$

which shows that $\mathbb{E}[\mathrm{Var}(\mathrm{d}_m(0,u) \mid \mathcal{P}')] \in O(u^{1-3\gamma})$.

Part (c). From the polarization identity $\mathrm{Cov}(X,Y) = 1/4(\mathrm{Var}(X+Y) - \mathrm{Var}(X-Y))$ and [92, Lemma 3.5], applied to the U-statistics $\mathrm{d}_m(0,u) + \mathrm{d}_m(p)$ and $\mathrm{d}_m(0,u) - \mathrm{d}_m(p)$, we obtain that

$$
\int_{\mathbb{S}} \mathrm{Cov}(\mathrm{d}_m(0,u), \mathrm{d}_m(p) \mid \mathcal{P}') \, \mathrm{d}p
$$
$$
= \sum_{i=1}^m \lambda^{2m-i} k_i \int_{\mathbb{S}} \int_{\mathbb{S}^m_{\geqslant u} \times \mathbb{S}^{m-i}_{\geqslant v}} \mathbb{1}\{\mathcal{P}'_{\overrightarrow{\boldsymbol{p}}\, m(u)} \neq \varnothing\} \, \mathbb{1}\{\mathcal{P}'_{\{p,p_{m-i+1},\dots,p_{2m-i}\}} \neq \varnothing\} \, \mathrm{d}\boldsymbol{p}_{2m-i} \, \mathrm{d}p,
$$

where $p := (y, v)$. Therefore, analogously to Part (b),

$$\int_{\mathbb{S}} \Big| \mathbb{E}\big[\mathrm{Cov}(\mathrm{d}_m(0, u), \mathrm{d}_m(p) \mid \mathcal{P}')\big] \Big| \, \mathrm{d}p$$

$$\leqslant \sum_{i=1}^{m} \lambda^{2m-i} k_i \int_{\mathbb{S}} \int_{\mathbb{S}^m_{\geqslant u} \mathbb{S}^{m-i}_{\geqslant v}} \lambda' |B(\overrightarrow{\boldsymbol{p}}_{2m-i}(u))|$$

$$+ (\lambda')^2 |B(\overrightarrow{\boldsymbol{p}}_m(u))| |B(\{p, p_m, \ldots, p_{2m-i}\})| \, \mathrm{d}\boldsymbol{p}_{2m-i} \, \mathrm{d}p.$$

Now, we apply Lemma C.6.1 to $|B(\overrightarrow{\boldsymbol{p}}_{2m-1}(u))|$ (integrated with respect to $\boldsymbol{p}_{2m-1}$) and to $|B(\{p, p_m, \ldots, p_{2m-1}\})|$ (integrated with respect to $(p, p_{m+1}, \ldots, p_{2m-i})$). This gives

$$\lambda^m (\lambda')^2 \Big(\sum_{i=1}^{m} \frac{(2\beta)^{m-i+2}}{(1-\gamma)^{m-i+1}} \frac{k_i}{1 - (m-i+2)\gamma'} \Big) \int_{\mathbb{S}^m_{\geqslant u}} v_m^{-\gamma} |B(\overrightarrow{\boldsymbol{p}}_m(u))| \, \mathrm{d}\boldsymbol{p}_m + O(u^{-\gamma}).$$

From here, $\int_{\mathbb{S}} \mathbb{E}[\mathrm{Cov}(\mathrm{d}_m(0, u), \mathrm{d}_m(p) \mid \mathcal{P}')] \, \mathrm{d}p \in O(u^{1-3\gamma})$ follows analogously to (C.7) as asserted.

Part (d). We have that

$$\mathbb{E}[\mathrm{d}_m(0, u) \mid \mathcal{P}'] = \frac{\lambda^m}{m!} \int_{\mathbb{S}^m_{\geqslant u}} \mathbb{1}\{\mathcal{P}'_{\overrightarrow{\boldsymbol{p}}_m(u)} \neq \varnothing\} \, \mathrm{d}\boldsymbol{p}_m,$$

and therefore,

$$\mathrm{Var}(\mathbb{E}[\mathrm{d}_m(0, u) \mid \mathcal{P}']) = \frac{\lambda^{2m}}{(m!)^2} \int_{\mathbb{S}^{2m}_{\geqslant u}} \mathrm{Cov}\big(\mathbb{1}\{\mathcal{P}'_{\overrightarrow{\boldsymbol{p}}_m(u)} = \varnothing\}, \mathbb{1}\{\mathcal{P}'_{\overrightarrow{\boldsymbol{p}}_{0,m}(u)} = \varnothing\} \big) \, \mathrm{d}\boldsymbol{p}_{2m}.$$

$$\tag{C.7}$$

Now, we use that $\mathrm{Cov}(XY, XZ) = \mathbb{E}[Y] \mathbb{E}[Z] \mathrm{Var}(X)$ for independent X, Y, Z. We let

$$X := \mathbb{1}\{\mathcal{P}'_{\overrightarrow{\boldsymbol{p}}_{2m}(u)} = \varnothing\},$$
$$Y := \mathbb{1}\{\mathcal{P}' \cap (B(\overrightarrow{\boldsymbol{p}}_m(u)) \setminus B(\overrightarrow{\boldsymbol{p}}_{0,m}(u))) = \varnothing\},$$
$$Z := \mathbb{1}\{\mathcal{P}' \cap (B(\overrightarrow{\boldsymbol{p}}_{0,m}(u)) \setminus B(\overrightarrow{\boldsymbol{p}}_m(u))) = \varnothing\},$$

and deduce that

$$\mathrm{Var}(\mathbb{E}[\mathrm{d}_m(0, u) \mid \mathcal{P}'])$$

$$= \frac{\lambda^{2m}}{m!} \int_{\mathbb{S}^{2m}_{\geqslant u}} \mathbb{P}\big(\mathcal{P}'(B(\overrightarrow{\boldsymbol{p}}_m(u)) \cup B(\overrightarrow{\boldsymbol{p}}_{0,m}(u))) = 0\big) \, \mathbb{P}\big(\mathcal{P}'_{\overrightarrow{\boldsymbol{p}}_{2m}(u)} \neq \varnothing\big) \, \mathrm{d}\boldsymbol{p}_{2m}$$

$$\leqslant \frac{\lambda^{2m} \lambda'}{m!} \int_{\mathbb{S}^{2m}_{\geqslant u}} |B(\overrightarrow{\boldsymbol{p}}_{2m}(u))| \, \mathrm{d}\boldsymbol{p}_{2m},$$

which shows by Lemma C.6.1 that $\mathrm{Var}(\mathbb{E}[\mathrm{d}_m(0, u) \mid \mathcal{P}']) \in O(u^{-\gamma})$.

Part (e).   Analogously to (C.7), we find that

$$\int_{\mathbb{S}} \left| \operatorname{Cov}(\mathbb{E}[\mathrm{d}_m(0,u) \mid \mathcal{P}'], \mathbb{E}[\mathrm{d}_m(p) \mid \mathcal{P}']) \right| \mathrm{d}p$$

$$= \lambda^{2m} \int_{\mathbb{S}} \int_{\mathbb{S}_{\geqslant u}^m \times \mathbb{S}_{\geqslant v}^m} \left| \operatorname{Cov}(\mathbb{1}\{\mathcal{P}'_{\overrightarrow{\boldsymbol{p}}_m(u)} \neq \varnothing\}, \mathbb{1}\{\mathcal{P}'_{\{p\} \cup \overrightarrow{\boldsymbol{p}}_{i,m}} \neq \varnothing\}) \right| \mathrm{d}\boldsymbol{p}_{2m} \,\mathrm{d}p,$$

where $p = (y,v)$. Here, we apply the relation $\operatorname{Cov}(XY, XZ) = \mathbb{E}[Y]\,\mathbb{E}[Z]\operatorname{Var}(X)$ with

$$X := \mathbb{1}\{\mathcal{P}'_{\{p\} \cup \overrightarrow{\boldsymbol{p}}_{2m}(u)} = \varnothing\},$$
$$Y := \mathbb{1}\{\mathcal{P}' \cap (B(\overrightarrow{\boldsymbol{p}}_m(u)) \setminus B(\{p\} \cup \overrightarrow{\boldsymbol{p}}_{0,m})) = \varnothing\},$$
$$Z := \mathbb{1}\{\mathcal{P}' \cap (B(\{p\} \cup \overrightarrow{\boldsymbol{p}}_{0,m}) \setminus B(\overrightarrow{\boldsymbol{p}}_m(u))) = \varnothing\},$$

and deduce analogously to (C.8) that

$$\int_{\mathbb{S}} \left| \operatorname{Cov}(\mathbb{E}[\mathrm{d}_m(0,u) \mid \mathcal{P}'], \mathbb{E}[\mathrm{d}_m(p) \mid \mathcal{P}']) \right| \mathrm{d}p$$

$$\leqslant \lambda^{2m} \int_{\mathbb{S}} \int_{\mathbb{S}_{\geqslant u}^m \times \mathbb{S}_{\geqslant v}^m} |B(\{p\} \cup \overrightarrow{\boldsymbol{p}}_{2m}(u))| \,\mathrm{d}\boldsymbol{p}_{2m} \,\mathrm{d}p,$$

which is by Lemma C.6.1 of order $O(u^{-\gamma})$. $\qquad\square$

C.8   Simulation study

To demonstrate how the theoretical results can be applied to networks of finite size, this section presents a simulation study analyzing finite networks and Palm distributions.

To analyze the statistical properties of the model, we utilize a Monte Carlo approach: we implemented a C++ algorithm to generate several higher-order networks with identical model parameters. The simulation of a finite network consists of the following steps:

(1) We first construct a torus of dimension 1, and generate two Poisson point processes $\mathcal{P}, \mathcal{P}'$. For practical reasons, we do not keep the intensity measures λ and λ' of the Poisson point processes constant throughout the simulations, but instead generate the network samples on a torus of Lebesgue measure 1, and adjust the Poisson intensity measures accordingly to generate networks with different expected number of $\mathcal{P}$- and $\mathcal{P}'$-vertices. After generating $\mathcal{P}$ and $\mathcal{P}'$, the vertices are equipped with a mark uniformly distributed in $(0, 1]$.

(2) Then, we generate the connections between the $\mathcal{P}$- and $\mathcal{P}'$-vertices using the connection rule described in (C.2). By using periodic boundary conditions, we can treat the vertices equivalently, irrespective of their position in the torus. Note that the parameter β can be tuned to adjust the expected number of edges in the network. The expected Δ_0-degree of a point $o = (0, u)$ is given by

$$\mathbb{E}\Big[\sum_{p' \in \mathcal{P}'} \mathbb{1}\{p' \in B(o)\} \Big] = \frac{2\beta\lambda'}{(1 - \gamma)(1 - \gamma')},$$

where we followed the same arguments as in the proof of C.6.1, with $m = 0$.

(3) Finally, we construct the higher-order network on $\mathcal{P}$, where the set of m-simplices is determined according to (C.4).

The simulation of the network is computationally expensive. If we checked the connection condition for every $\mathcal{P}$- and $\mathcal{P}'$-vertex pair, our algorithm would have a time complexity of $O(\lambda\lambda')$, where λ and λ' are the intensity of the Poisson processes for the $\mathcal{P}$- and $\mathcal{P}'$-vertices, respectively. When deciding which points in $\mathcal{P}$ and $\mathcal{P}'$ are connected, we partition the space $\mathbb{S}$ into rectangles containing multiple points, similarly to the quadtree data structures [96]. This way, we can reduce the computational complexity of the simulation as

- if the furthest points of two rectangles with the highest marks connect, it is certain that all point pairs in the rectangles are connected;

- if the closest points of two rectangles with the lowest marks do not connect, it is certain that no point pairs in the rectangles are connected.

The width of the rectangles is set to be proportional to $b^{-\gamma}$ and $b^{-\gamma'}$ for the $\mathcal{P}$- and $\mathcal{P}'$-vertices, respectively, where b denotes the bottom mark of the rectangle. This results in a layout of rectangles as shown in Figure C.1.

Before generating a finite network sample, we set the model parameters to be of the same order of magnitude when fitted to the analyzed datasets. The intensity measures of the Poisson point processes are set to $\lambda = \lambda' = 100\,000$. Aligned with these parameters, the number of $\mathcal{P}$- and $\mathcal{P}'$-vertices were $100\,335$ and $93\,919$, respectively. The γ, γ' model parameters were set to $\gamma = 0.7$, $\gamma' = 0.2$. Furthermore, β was set so that the expected number of Δ_0-degrees in the infinite network limit was 3: $\beta = 3.6e - 5$.

First, we examine three degree distributions of the networks, which are analyzed in Theorem C.2.3.

- The Δ_0-degree distribution characterizes the distribution of the number of $\mathcal{P}'$-vertices connected to a typical $\mathcal{P}$-vertex.

- The Δ_1-degree distribution is the distribution of the number of $\mathcal{P}'$-vertices connected to a pair of $\mathcal{P}$-vertices.

- Finally, the distribution of the number of $\mathcal{P}$-vertices connected to a typical $\mathcal{P}'$-vertex is described by the Δ_0'-degree distribution.
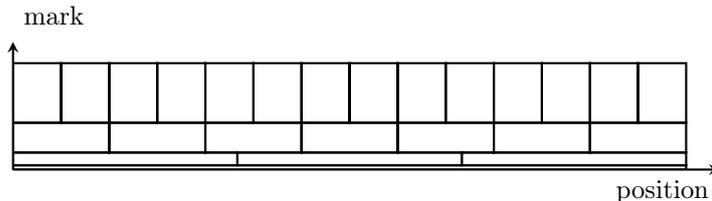
Figure C.1: Partition of $\mathbb{S}$ into rectangles
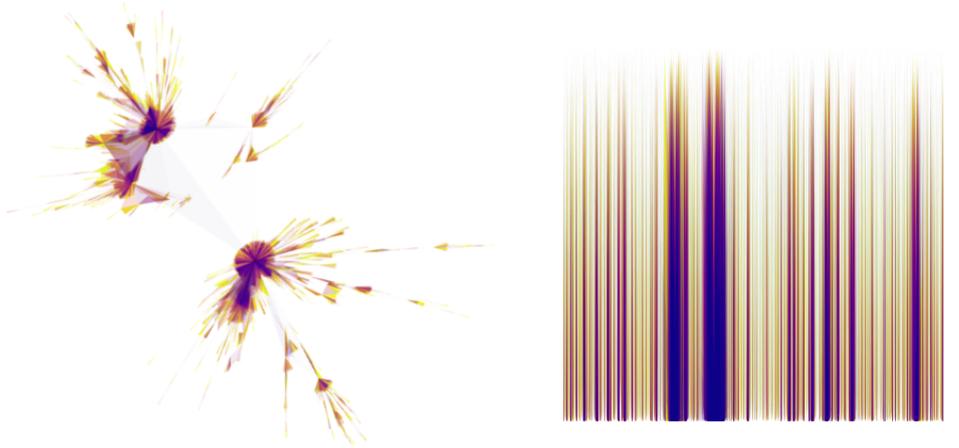
The largest component of the sample   Network sample with fixed positions

Δ_0-degree distribution Δ_1-degree distribution Δ_0'-degree distribution
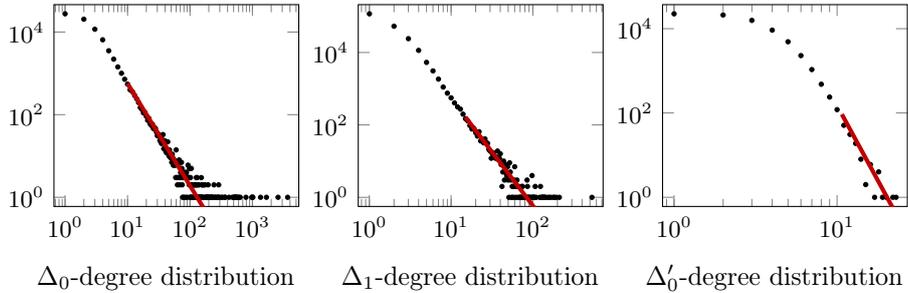
Figure C.2: Main properties of a network sample generated by our model

The main characteristics of a network generated with these parameters are shown in Figure C.2. In the top row of Figure C.2, one can see the largest component of the network (left). A polygon is drawn representing the convex hull of a set of $\mathcal{P}$-vertices whenever they form a simplex in the network. The higher number of $\mathcal{P}$-vertices forms a simplex; the darker the color of the corresponding polygon. From the largest component of the network, which contained $12\,385$ $\mathcal{P}$-vertices, one can see that the network is sparse, and that the network layout is dominated by a few dense regions corresponding to $\mathcal{P}$-vertices with high degrees.

When looking at the positions of the $\mathcal{P}$-vertices embedded in the space $\mathbb{S}$ (right), one can see that the $\mathcal{P}$-vertices form clusters that are connected by the above-mentioned heavy vertices. As illustrated in the bottom row of C.2, the various degree distributions of the $\mathcal{P}$- and $\mathcal{P}'$-vertices are all heavy-tailed, and the degree distribution of the $\mathcal{P}$-vertices is heavier than the degree distribution of the $\mathcal{P}'$-vertices, aligned with our theoretical results.

We also rely on Palm calculus to simulate typical simplices in networks devoid of finite-size effects. To do so, we first place a typical $\mathcal{P}$-vertex $(0, u)$ at the origin. Then, we simulate $\mathcal{P}'$-vertices $(y_1, v_1), \ldots, (y_n, v_n) \in B(0, u)$ in its neighborhood where $\mathcal{P}'$-vertices connect to it, where n is a Poisson distributed random variable with parameter $\lambda'|B(0, u)|$. Finally, further $\mathcal{P}$-vertices are generated by a Poisson process

of intensity λ in the union of the neighborhoods $\bigcup_i B(y_i, v_i)$ of the $\mathcal{P}'$-vertices. Each of the neighborhoods $B(y_i, v_i)$ can be split to three parts, where a connecting $\mathcal{P}$-vertex (x, w) must satisfy the below conditions:

$$
\begin{array}{lll}
\text{left tail} & w \leqslant (y_i - x)/\beta v_i^{-\gamma'} & x < y_i - \beta v_i^{-\gamma'}; \\
\text{center} & w \leqslant 1 & y_i - \beta v_i^{-\gamma'} \leqslant x \leqslant y_i + \beta v_i^{-\gamma'}; \\
\text{right tail} & w \leqslant (x - y_i)/\beta v_i^{-\gamma'} & y_i + \beta v_i^{-\gamma'} < x.
\end{array}
$$

Next, we take the union of the center parts of the neighborhoods, and generate $\mathcal{P}$-vertices in the union. Finally, we determine the dominating tail parts at every position x, and generate $\mathcal{P}$-vertices in the corresponding tail parts. Then, the simplices of the Palm distribution are those whose lowest mark $\mathcal{P}$-vertex is $(0, u)$.

With the model parameters set, the simulation framework provides an opportunity to analyze the distribution of Δ_0-degrees, Δ_1-degrees, and Δ_0'-degrees in the generated finite networks of different sizes by varying the intensities of the point processes. Specifically, to examine the finite-size effect on the distributions of the network properties of interest, we simulated 100 networks and kept the model parameters $\gamma = 0.7$, $\gamma' = 0.2$ constant, but altered the expected number λ and λ' of $\mathcal{P}$- and $\mathcal{P}'$-vertices, respectively. To examine the Palm distribution, we simulated 100 sets of 10 000 networks. In this case, the values of λ, λ' are indifferent, and we set them to $\lambda = \lambda' = 1$. Lastly, the parameter β was set so that the expected number of Δ_0-degrees in the infinite network limit was 3.

As shown in Theorem C.2.3, all the examined distributions exhibit a power-law tail in the infinite network limit. Thus, we fitted a power law distribution to the simulated values using the maximum likelihood method described by [7]. Determining the minimum value x_{min} from which the power-law distribution should be fitted is not trivial. If we use lower values of x_{min}, more data points can be considered for the fitting, resulting in a more robust fit of the power-law distribution. However, the estimated power-law exponent is more biased, as the power-law might not hold at lower values. Conversely, for higher values of x_{min}, the estimated power-law exponent has less bias, but the fit is less robust as fewer data points are considered.

The boxplots of Figure C.3 show how the fitted power-law exponents of the above-mentioned degree distributions fluctuate relative to the theoretical value derived for infinite networks in Theorem C.2.3. In the top row, we used $x_{\mathsf{min}} = 10$ for the fitting, while in the bottom row, we used $x_{\mathsf{min}} = 15$. It can be observed that the exponents in the top row fluctuate less but exhibit a higher bias, whereas the exponents in the bottom row fluctuate more but display a lower bias. This is because a set of $\mathcal{P}$-vertices form a simplex if they share a common $\mathcal{P}'$-vertex, and this more complex relationship between the $\mathcal{P}$- and $\mathcal{P}'$-vertices results in a higher variance of the estimated exponents. We can also see that the degree exponents fluctuate much more for the Δ_0'-degree distribution than for the Δ_0-degree distribution. This can be explained by the different decay rates of the neighborhoods of $\mathcal{P}$- and $\mathcal{P}'$-vertices: the power-law tails have exponents $1/\gamma = 1.43$ and $1/\gamma' = 0.5$, respectively, which results in fewer data points in the tail of the Δ_0'-degree distribution compared to the Δ_0-degree distribution. As it will be shown in Section C.9, the Δ_0- and Δ_0'-degree distributions will be of particular interest when fitting the model parameters γ and γ' to the datasets. Analyzing
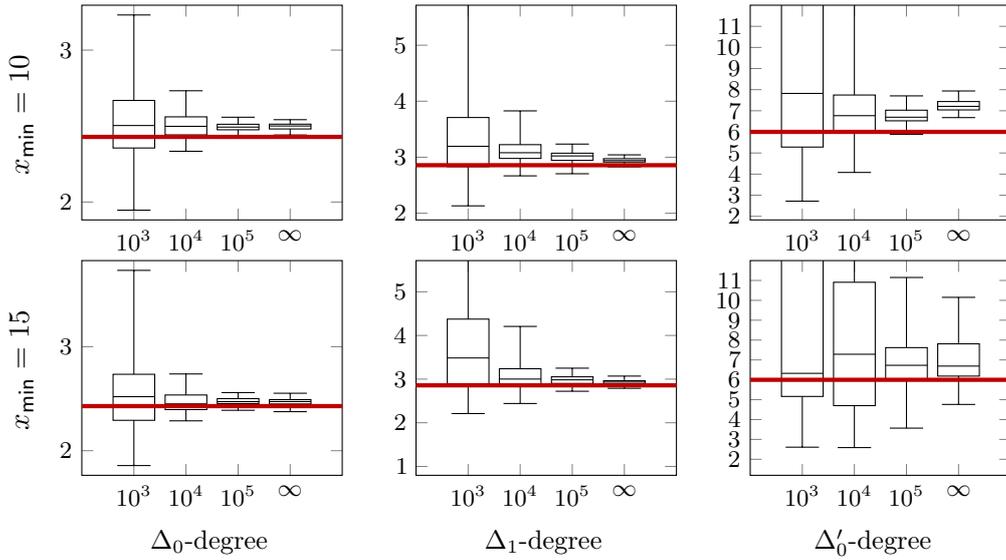
Figure C.3: Fluctuation of the degree distribution exponents for different network sizes. The top row shows the power-law exponents when estimated from values larger than $x_{\min} = 10$. In contrast, the bottom row contains boxplots for the distribution of the exponents estimated from values larger than $x_{\min} = 15$.

the boxplots of the Δ_0- and Δ_0'-degree distributions, we can see that the power-law exponents of the degree distributions are close to the theoretical values derived for infinite networks above a network size of 10 000. Considering the optimal trade-off between bias and robustness, we chose to use $x_{\min} = 10$ for the fitting in the following sections.

Next, we analyze the distributions of the first Betti number by simulating 100 networks with fixed $\lambda = \lambda' = 100\,000$ and varying γ and γ' parameters. The histograms with fitted normal distributions and the corresponding Q-Q plots are shown in Figure C.4. In alignment with Theorem C.2.4, the Q-Q plots show that the Betti number is normally distributed for parameters $\gamma < 1/4$ and $\gamma' < 1/8$. The figures for $1/4 \leqslant \gamma \leqslant 1/2$ and $\gamma' \geqslant 1/8$ suggest that the normal distribution of the first Betti number also holds for these parameter ranges. The distribution of the Betti number for $\gamma = 0.75$, however, exhibits a fat left tail. Note that the leftmost bins of the histograms for $\gamma = 0.75$ are at 0, which means that some simulated networks did not contain any loops. This behavior can be explained by the presence of low-mark $\mathcal{P}$- and/or $\mathcal{P}'$-vertices that connect to many $\mathcal{P}'$- and $\mathcal{P}$-vertices when the edge count has an infinite variance, making the loops less likely to form. This observation leads to the conjecture that the Betti numbers have α-stable distributions if $\gamma > 0.5$.

Finally, we analyze the distribution of the number of edges and triangles in the simulated networks. As before, we simulated 100 networks with fixed $\lambda = \lambda' = 100\,000$ and varying γ and γ' parameters. The distribution of the edge counts is presented in Figure C.5, where we fitted a normal distribution to the simulated values and visualized the corresponding Q-Q plots. As shown in Theorem C.2.5 in the infinite network size limit, now the Q-Q plots show for finite networks that the number of edges are normally distributed for parameters $\gamma < 1/2$ and $\gamma' < 1/3$, and that the
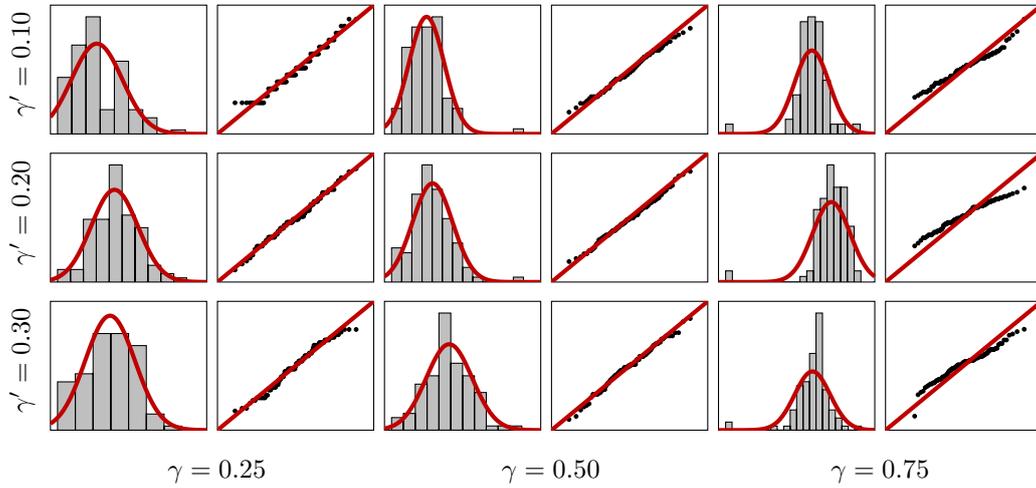
Figure C.4: Distribution of the first Betti numbers with different γ and γ' parameters
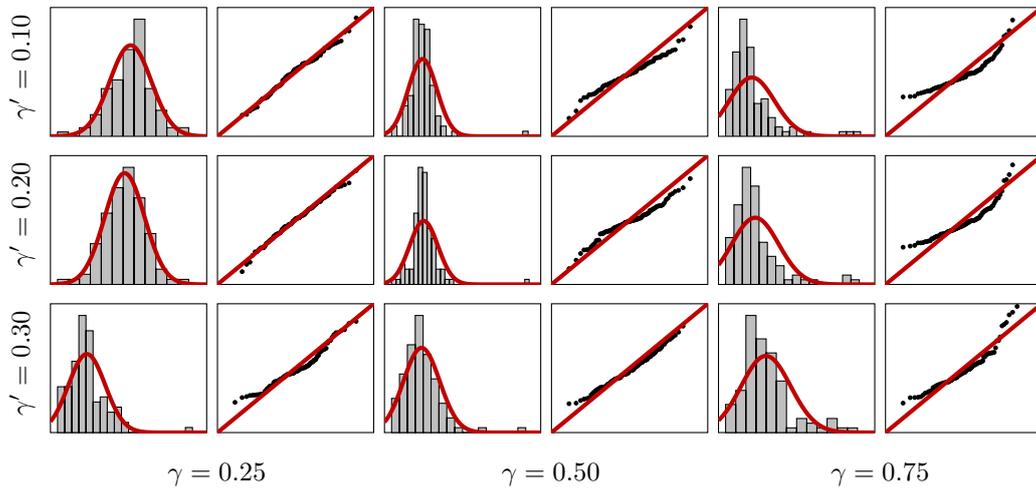
Figure C.5: Distribution of edge counts with different γ and γ' parameters. For each combination of γ and γ', we show the distribution of edge counts with the fitted normal distribution and the corresponding Q-Q plot.

number of edges have an α-stable distribution if $\gamma > 1/2$ and $\gamma' \geqslant 1/3$. For $\gamma = 1/2$, it can be inferred from the Q-Q plots that the distribution of the number of edges is close to a normal distribution. The distribution of the triangle counts together with the fitted normal distributions and the Q-Q plots are shown in Figure C.6. Again, the simulated distributions of finite networks align with Theorem C.2.6: the Q-Q plots show that the number of triangles is normally distributed for parameters $\gamma < 1/2$ and $\gamma' < 1/5$. It is also clear from the Q-Q plots of Figure C.6 that if $\gamma > 1/2$ and $\gamma' < 1/5$, the number of triangles has an α-stable distribution with $\alpha = 1/\gamma$, which was also shown for infinite networks in Theorem C.2.6. We can furthermore conjecture that the number of triangles has an α-stable distribution if $\gamma' > 1/5$ irrespective of the value of γ.
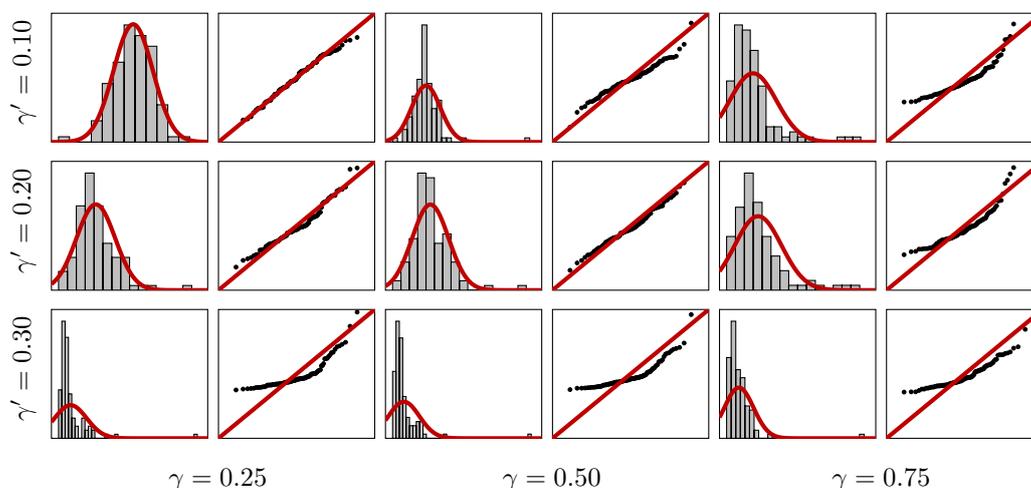
Figure C.6: Distribution of triangle counts with various γ and γ' parameters. For each combination of γ and γ', we show the distribution of triangle counts with the fitted normal distribution and the corresponding Q-Q plot.

After analyzing the degree distributions, Betti numbers, and the number of edges and triangles in the simulated networks, we can conclude that the theoretical results derived for infinite networks also hold for finite networks. We finish the simulation study by analyzing further degree distributions, which, although not of particular interest in the following sections, may be examined in a further study.

- The 0-coface degree distribution is the distribution of the number of edges incident to a $\mathcal{P}$-vertex.

- The 1-coface degree distribution is the distribution of the number of triangles incident to an edge.

As we will see in Section C.9, these degree distributions exhibit a power-law tail in the datasets we analyze.

To examine the coface degree distribution of the networks generated by the model, we calculated the coface degree distributions for the sample network described at the beginning of Section C.8. We also examined the fluctuations of the coface degree distribution exponents for different network sizes, and, as before, we simulated 100 networks

with varying $\lambda = \lambda'$ intensities and fixed $\gamma = 0.7$ and $\gamma' = 0.2$ parameters. In this case again, we used $x_{\mathsf{min}} = 10$ for the fitting and set β so that $\mathbb{E}[\Delta_0^*] = 3$. The distributions of the 0- and 1-coface degrees and the fluctuations of the exponents are shown in Figure C.7. We see that the distributions of the coface degrees are heavy-tailed, and the power-law exponents of the distributions converge above a network size of $10\,000$.

| 0-coface degree distribution | 0-coface degree exponents | 1-coface degree distribution | 1-coface degree exponents |
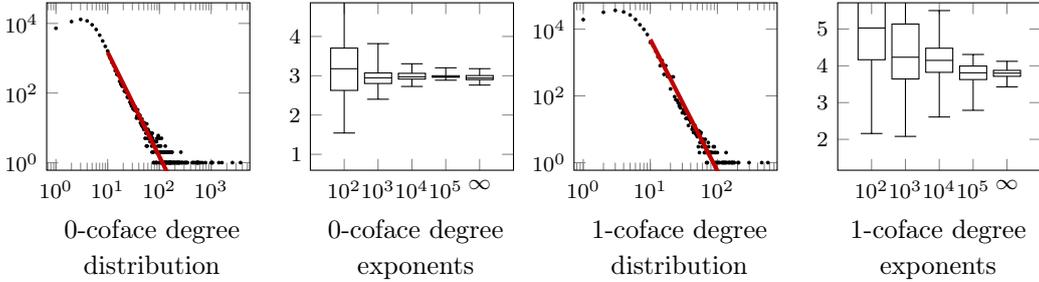
Figure C.7: Typical coface degree distributions and the fluctuation of the power-law exponents for different network sizes. The power-law exponents were estimated from values larger than $x_{\mathsf{min}} = 10$.

C.9   Analysis of collaboration networks

After the analysis of the finite-size effects in Section C.8, we now compare our model with real-world datasets. To do so, we chose to analyze coauthorship networks, where the authors are represented by $\mathcal{P}$-vertices, and a $\mathcal{P}'$-vertex represents each publication.

Using the Python wrapper for the arXiv API, we collected all documents from the arXiv preprint server that were uploaded up to 18 June 2024. Based on the label of the documents referring to their primary categories, we created four datasets for the four largest scientific fields, namely, `computer science`, `electrical engineering and systems science`, `mathematics`, and `statistics`, that we denote by `cs`, `eess`, `math`, and `stat`, respectively. In these datasets, we had access to the list of authors' names of the documents. Identifying the authors by their names, we created

- a bipartite network where the $\mathcal{P}$-vertices are the authors, and the $\mathcal{P}'$-vertices are the documents;

- a simplicial complex representing the higher-order network of the authors.

As simplicial complexes are closed under taking subcomplexes, each document with n authors is represented by $2^n - 1$-simplices in the simplicial complex. This exponential dependence of the number of simplices on the number of authors led to a disproportionate influence of documents with a high number of authors on our results. To mitigate this effect, we included documents with at most 20 authors in our analysis, thereby neglecting a proportion of 0.13% of the documents.

The main properties of the datasets are summarized in Table C.1.

Using the documents as $\mathcal{P}'$-vertices, we created a filtered simplicial complex for each dataset. We set the filtration value of a set of authors to be the number of papers they are all authors of, and used a filtration value decreasing from ∞ to 0 to

Table C.1: Main properties of the datasets

dataset	authors	documents	components	size of largest component
cs	504959	540573	23909	439375
eess	93005	85445	6061	67700
math	211757	500403	27157	163738
stat	48700	40869	4236	36094

create the filtered Dowker complex. We present the persistence diagrams computed from the filtered Dowker complex in Figure C.8. Although the datasets contain many components and loops, some of them share the same birth and death filtration values, resulting in fewer points in the persistence diagrams.

Further properties of the datasets are illustrated in Figure C.9. In the top row, we visualized the largest components of the datasets, where each document is represented by a polygon around the authors, with darker colors indicating documents with more authors. Further rows display the degree distributions of the datasets, along with the fitted power-law distributions. The degree distributions that we examine are similar to those before in Section C.8:

- The Δ_0-degree distribution is the distribution of the number of documents an author published.

- The Δ_1-degree distribution describes the distribution of the number of documents that pairs of authors wrote together.

- The distribution of the number of authors of a document is the Δ_0'-degree distribution.

We observe that all the visualized degree distributions exhibit heavy tails, and the fitted power-law distributions accurately describe the data.

To compare the datasets with our model, we first need to estimate the model parameters. The γ and γ' parameters are estimated from the exponents of the fitted power-law distributions to the Δ_0- and Δ_0'-degree distributions, respectively.

Note that the datasets do not contain isolated $\mathcal{P}$- and $\mathcal{P}'$-vertices, i.e., authors without any documents and documents without any authors. Thus, we compensate for these in our model so that the number of authors and documents in the datasets match the number of non-isolated $\mathcal{P}$- and $\mathcal{P}'$-vertices in the simulations, respectively.
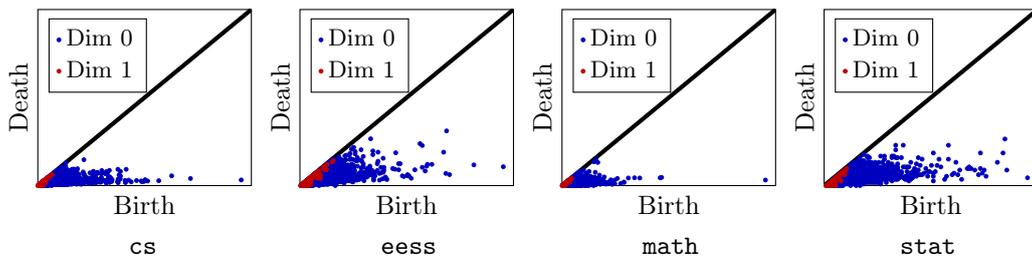
Figure C.8: Persistence diagrams of the datasets
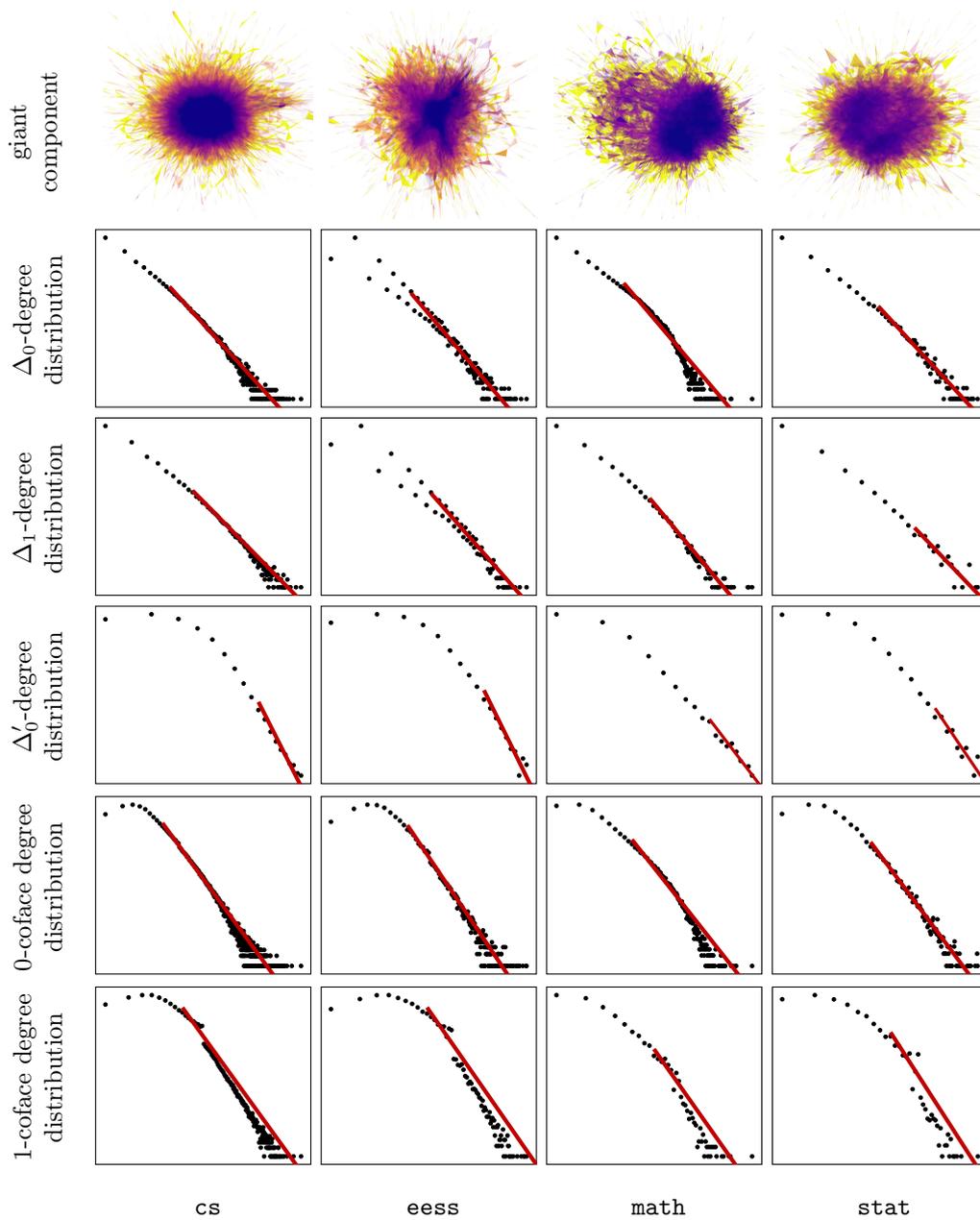
Figure C.9: Main properties of the datasets

Let $\mathcal{P}_0$ and $\mathcal{P}_0'$ be the set of isolated $\mathcal{P}$- and $\mathcal{P}'$-vertices in the simulated simplicial complex, respectively, and let $p := (x, u) \in \mathcal{P}$ and $p' := (z, w) \in \mathcal{P}'$. Then, the expected number of non-isolated $\mathcal{P}$-vertices in the simulation is given by

$$\mathbb{E}[\#(\mathcal{P} \setminus \mathcal{P}_0)] = \mathbb{E}\Big[\sum_{p \in \mathcal{P}} \mathbb{1}\{\mathcal{P}'(B(p)) \neq 0\}\Big] = \lambda \int_0^1 \mathbb{E}[\mathbb{1}\{\mathcal{P}'(B(p)) \neq 0\}] \, \mathrm{d}u$$

$$= \lambda \int_0^1 1 - \mathbb{P}(\mathcal{P}'(B(0, u)) = 0) \, \mathrm{d}u = \lambda \int_0^1 1 - \exp(-\lambda'|B(0, u)|) \, \mathrm{d}u$$

$$= \lambda \int_0^1 1 - \exp\Big(-\lambda' \int_0^1 \int_{-\beta u^{-\gamma} w^{-\gamma'}}^{\beta u^{-\gamma} w^{-\gamma'}} \mathrm{d}z \, \mathrm{d}w\Big) \, \mathrm{d}u$$

$$= \lambda\Big(1 - \int_0^1 \exp\Big(-\frac{2\beta\lambda'}{1 - \gamma'} u^{-\gamma}\Big) \, \mathrm{d}u\Big).$$

After substituting $\mu := 2\beta\lambda'/(1 - \gamma')u^{-\gamma}$, we obtain

$$\mathbb{E}[\#(\mathcal{P} \setminus \mathcal{P}_0)] = \lambda\Big(1 - \frac{1}{\gamma}\Big(\frac{1 - \gamma'}{2\beta\lambda'}\Big)^{-\frac{1}{\gamma}} \int_{\frac{2\beta\lambda'}{1-\gamma'}}^\infty \mu^{-\frac{1}{\gamma}-1} \mathrm{e}^{-\mu} \, \mathrm{d}\mu\Big)$$

$$= \lambda\Big(1 - \frac{1}{\gamma}\Big(\frac{1 - \gamma'}{2\beta\lambda'}\Big)^{-\frac{1}{\gamma}} \Gamma\Big(-\frac{1}{\gamma}, \frac{2\beta\lambda'}{1 - \gamma'}\Big)\Big),$$

where Γ denotes the upper incomplete gamma function. Following the same steps, we find that the expected number of non-isolated $\mathcal{P}'$-vertices in the simulation is given by

$$\mathbb{E}[\#(\mathcal{P}' \setminus \mathcal{P}_0')] = \lambda'\Big(1 - \frac{1}{\gamma'}\Big(\frac{1 - \gamma}{2\beta\lambda}\Big)^{-\frac{1}{\gamma'}} \Gamma\Big(-\frac{1}{\gamma'}, \frac{2\beta\lambda}{1 - \gamma}\Big)\Big).$$

Furthermore, we set the parameter β so that the expected number of edges in G^{bip} in the simulation matches the number of author–document edges in the datasets. Additionally, by the Mecke formula, we have

$$\mathbb{E}\Big[\sum_{\substack{p \in \mathcal{P} \\ p' \in \mathcal{P}'}} \mathbb{1}\{p \in B(p')\}\Big] = \int_{\mathbb{S}^2} \mathbb{P}(p \in B(p')) \, \mathrm{d}(p, p') = \frac{2\beta\lambda\lambda'}{(1 - \gamma)(1 - \gamma')}.$$

By numerically solving the above system of equations given by the expected number of non-isolated $\mathcal{P}$- and $\mathcal{P}'$-vertices, we obtain the parameter estimates shown in Table C.2.

Using these parameters, we simulated a sample network for each dataset, which is visualized in Figure C.10. While the top row contains the largest components of the datasets, the bottom row displays the $\mathcal{P}$-vertices in the space $\mathbb{S}$. In both rows, as above, each $\mathcal{P}'$-vertex is represented by a polygon around $\mathcal{P}$-vertices connecting to them with a darker color if the $\mathcal{P}'$-vertex is connected to more $\mathcal{P}$-vertices. We can see that the model networks possess a tree-like structure, dominated by a few high-degree $\mathcal{P}$-vertices.

To determine if our model can capture the higher-order structures of the datasets, we need to perform hypothesis tests on the simplex counts and the first Betti number. Although Theorem C.2.5 and our conjecture in Section C.8 show that α-stable

Table C.2: Fitted power-law exponents and the inferred model parameters

dataset	Δ_0-degree		$\mathcal{P}'$-vertex degree		β	λ	λ'
	exponent	γ	exponent	γ'			
cs	2.37	0.73	5.46	0.22	$8.19 \cdot 10^{-7}$	579719	532491
eess	2.75	0.57	5.50	0.22	$7.89 \cdot 10^{-6}$	98528	83985
math	2.44	0.69	6.51	0.18	$1.03 \cdot 10^{-6}$	231606	588628
stat	2.89	0.53	5.74	0.21	$1.13 \cdot 10^{-5}$	57488	41655

| cs | eess | math | stat |
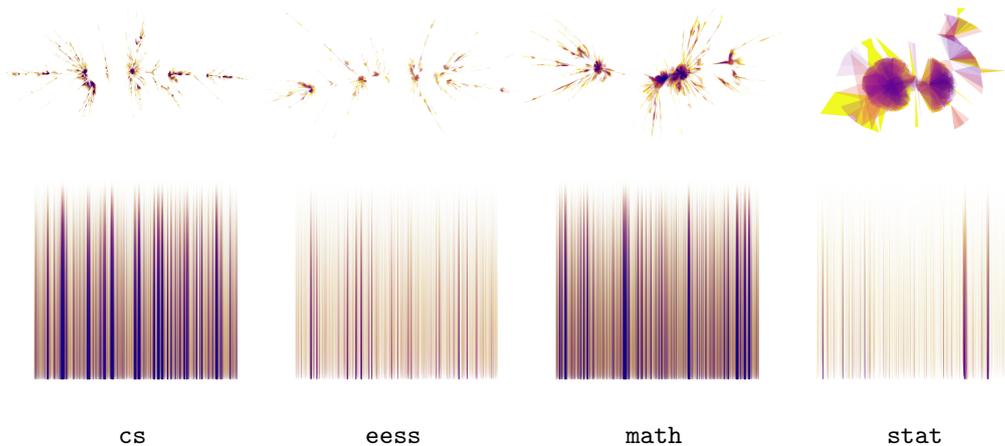
Figure C.10: The largest components of the simplicial complexes built from the datasets

distributions describe the simplex counts and the first Betti number, it is not clear how to fully specify all parameters of these distributions. Therefore, we estimated the parameters of the α-stable distributions from the simulated networks to statistically compare the datasets with those generated by the model. For each dataset, we simulated 100 networks, and fitted an α-stable distribution to the values with $\alpha = 1/\gamma$, which described the data well in all the cases.

The results of the hypothesis tests for the simplex counts and the first Betti numbers are summarized in Figure C.11, and the parameters of the fitted distributions are shown in Tables C.3, C.4, and C.5. Although the model parameters were set to ensure that the expected number of Δ_0-degrees in the simulation matches the number of author-document edges in the datasets, the hypothesis tests indicate that the higher-order structures of the datasets differ from those of the generated networks. The case of the `eess` and `math` datasets is particularly interesting, as in the case of the former, the simulated networks contain more triangles, but fewer edges, compared to the datasets. In contrast, in the case of the latter, the opposite is true. In the case of the first Betti numbers, the values of the datasets are substantially larger than for the generated networks, and all the hypothesis tests are rejected. The reason for this deviation is that the simulated networks are dominated by a few high-degree $\mathcal{P}$-vertices, resulting in a tree-like structure with a relatively small number of loops. At the same time, the datasets contain more complex structures.
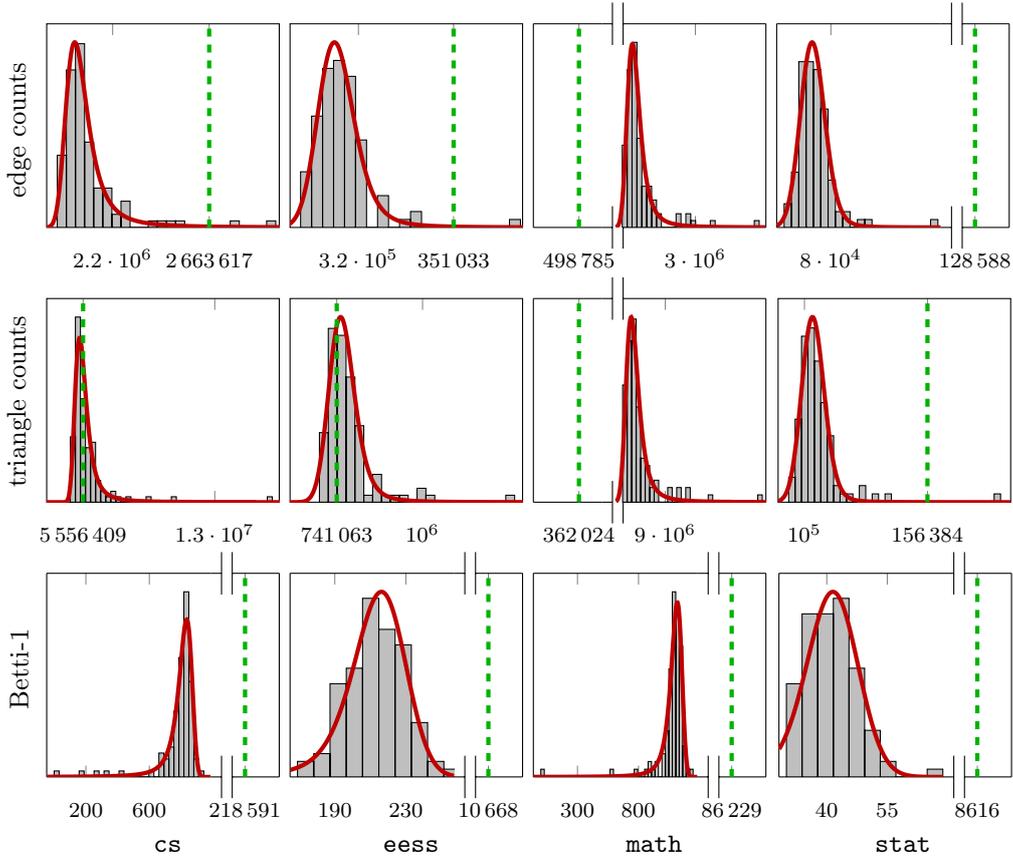
Figure C.11: Hypothesis testing of the edge counts (top), triangle counts (center), and Betti-1 (bottom) for the datasets. The model parameters were determined based on the parameters of the datasets described in Table C.2.

Table C.3: Results of the hypothesis tests for the edge counts

dataset	dataset value	$\hat{\alpha}$	$\hat{\beta}$	location	scale	p-value
cs	2663617	1.3658	1.0	2093994	43104	$2.69 \cdot 10^{-2}$
eess	351033	1.7506	1.0	314266	4331	$1.13 \cdot 10^{-2}$
math	498785	1.4415	1.0	2601637	36355	0.00
stat	128588	1.8918	1.0	77681	1201	$1.73 \cdot 10^{-4}$

Table C.4: Results of the hypothesis tests for the number of triangles

dataset	dataset value	$\hat{\alpha}$	$\hat{\beta}$	location	scale	p-value
cs	5556409	1.3658	1.0	5823007	263597	$9.13 \cdot 10^{-1}$
eess	741063	1.7506	1.0	766277	28281	$6.50 \cdot 10^{-1}$
math	362024	1.4415	1.0	6973583	187554	0.00
stat	156384	1.8918	1.0	104413	3720	$1.45 \cdot 10^{-3}$

Table C.5: Results of the hypothesis tests for the first Betti numbers

dataset	dataset value	$\hat{\alpha}$	$\hat{\beta}$	location	scale	p-value
cs	218591	1.3658	-1.0	777	33	0.00
eess	10668	1.7506	-1.0	211	11	0.00
math	86229	1.4415	-1.0	1069	35	0.00
stat	8616	1.8918	-1.0	41	5	0.00

The results of the hypothesis tests indicate that, although our model captures many properties of the datasets, it is too simplistic to accurately describe the higher-order structures of the datasets.

Disclosure statement

No potential conflict of interest was reported by the authors.

Funding

Paper D

Functional Limit Theorems for Edge Counts in Dynamic Random Connection Hypergraphs

Christian Hirsch, Benedikt Jahnel, and Péter Juhász

Abstract: We introduce a dynamic random hypergraph model constructed from a bipartite graph. In this model, both vertex sets of the bipartite graph are generated by marked Poisson point processes. Vertices of both vertex sets are equipped with marks representing their weight that influence their connection radii. Additionally, we assign the vertices of the first vertex set a birth-death process with exponential lifetimes and the vertices of the second vertex set a time instant representing the occurrence of the corresponding vertices. Connections between vertices are established based on the marks and the birth-death processes, leading to a weighted dynamic hypergraph model featuring power-law degree distributions. We analyze the edge-count process in two distinct regimes. In the case of finite fourth moments, we establish a functional central limit theorem for the normalized edge count, showing convergence to a Gaussian AR(2)-type process as the observation window increases. In the challenging case of the heavy-tailed regime with infinite variance, we prove convergence to a novel stable process that is not Lévy and not even Markov.

D.1 Introduction

Over the last 20 years, network science has evolved into a vibrant field of research, with applications in various fields, including biology, sociology, computer science, and physics. This is not surprising given the fundamental nature of the idea that many systems are essentially described by a system of nodes together with a set of links indicating which nodes interact with one another [102]. The success of network science is based on the observation that a broad variety of networks share some fundamental features, such as being scale-free (characterized by the existence of hubs) and exhibiting strong clustering.

One of the widely used models in network science is the *preferential attachment model* where nodes arrive over time and connect more likely to nodes with an already high degree [3]. However, while this model has a compelling narrative and can reproduce the scale-free property, its most basic versions lack the crucial feature of clustering. While several solutions have been proposed to address this weakness, one of the most elegant and powerful ones is the idea of embedding the components in some ambient space and making the connection probabilities distance-dependent. Then, the triangle inequality from the ambient space implies the desired clustering, and this idea led to the development of the spatial preferential attachment models [57, 58].

While spatial preferential attachment exhibits many of the qualitative features of real complex networks, they are notoriously hard to analyze from a rigorous mathematical perspective. This is because the existence of edges can only be understood by following the complex time-dynamics of the evolving networks. Due to these disadvantages, the class of *spatial inhomogeneous random graphs* or *weight-dependent random connection models* has gained popularity recently [64, 42, 41, 40]. Loosely speaking, the connection probabilities are here not driven by the actual node degrees but rather by their conditional expected values given their birth time. This is a dramatic simplification, as the edge connection event can now be determined entirely from the knowledge of the position and appearance times of the nodes involved in the pair.

Despite the success of network science, with the rise in the amount and complexity of available data, it is now apparent that in many settings, a simple network with binary interactions is insufficient, and we need to take into account *higher-order interactions*. This urgent need has been a main driver of the recent research effort in *hypergraphs* and *simplicial complexes* [10, 2, 35, 17]. For instance, in economics, several companies may simultaneously be exposed to the same risk, or in neuroscience, entire groups of neurons must fire to create an effect [91, 39]. Finally, in social sciences, a prototypical example is collaboration networks where several researchers work together on a paper [90, 20, 83].

Due to the explosion of complexities, modeling such higher-order networks is much harder than modeling binary networks. Inspired by ensembles from statistical physics, a powerful class of such models is proposed by Bianconi and Rahmede [11], but it is challenging to analyze from a rigorous mathematical perspective [37]. The generic model is the *multiparameter simplicial complex* that is a higher-order extension of the Erdős–Rényi model [100], but it lacks the scale-free property. However, as noted before, as in the case of binary networks, enforcing clustering properties can

163

be elegantly implemented by embedding nodes in an ambient space. In an earlier work, we investigated such systems when higher-order networks are given by cliques in scale-free networks (Paper B), and in Paper C, we introduced a novel spatial model called *random connection hypergraphs*, which is based on a bipartite Poisson point process.

A particular challenge in analyzing higher-order networks is that they change over time. For instance, the topology of the neuronal network changes through the process of learning, and in the case of scientific collaboration networks, PhD students enter the network when completing their first paper and leave it when they retire. There are currently highly active research streams in topological data analysis that aim to provide a toolkit for tracking the topological changes over time, e.g., vines and zigzag persistence [63, 109, 74]. The goal in this paper is to endow the random connection model from Paper C with a dynamics and to prove functional central and stable limit theorems in this setting. Here, we focus our attention on the most fundamental quantity, namely the edge count of the underlying bipartite graph.

Before we describe our results in more detail, we comment on the existing literature on functional limit results in time-varying models. The earliest investigations in this context consider higher-order networks defined on a discrete point set, such as the clique complex associated with a dynamic Erdős–Rényi graph or the multiparameter simplicial complex [101, 81]. In these works, topological quantities, such as Betti numbers and Euler characteristics, are considered. However, since the networks do not exhibit the occurrence of hubs, we only see light-tailed contributions. Therefore, the limits are Gaussian processes, or more precisely, Ornstein–Uhlenbeck processes, in the case of [101]. Additionally, a major disadvantage of these works is that the node set is entirely discrete. More recently, however, spatial models were also considered [79, 78]. Here, the dynamics are both of a movement and birth-death type, and the statistics are local in nature. However, again, since the models do not allow for the occurrence of hubs, all limits are Gaussian.

In our setting, we can go beyond this limiting behavior and prove two main results. First, a functional central limit theorem (CLT) for the normalized edge count in growing domains when the fourth moment of the degree distribution is finite. Second, a convergence of the normalized edge count to a specific stable process. While this process is not Lévy and not even Markov, we nevertheless provide a specific representation. In both limits, the main methodological challenge is to address the long-range correlations and heavy tails arising from the hub nodes. We now discuss briefly the proof ideas with further details provided in Sections D.3, D.5, D.6, and D.7 below.

We start with the setting of the finite fourth moments. Here, we proceed via the classical two steps, namely convergence of the finite-dimensional marginals and tightness. Already for the finite-dimensional marginals, the methodology from Onaran et al. [79] breaks down as our functionals are not local, and we cannot rely on the stabilization CLTs from Penrose and Yukich [89]. Hence, our approach is to use the Malliavin–Stein normal approximation from Last et al. [67], which involves delicate computations of higher-order moments. For the tightness, we essentially use the moment-based criterion from Billingsley [12]. The fourth moments are approached using cumulant computations. However, since our functional can be represented as

a difference of monotone functionals, a refinement due to Davydov [26] allows us to simplify the tightness proof.

In the case of infinite variance, we use a different approach. We distinguish between lightweight and heavyweight nodes. First, we show that the lightweight nodes are negligible. The difficulty here is that the negligibility needs to be established in the process sense, and the involved processes are not martingales. Hence, we refine our tightness computations to achieve this goal. Then, it remains to deal with the heavy nodes. Since the edge count is Poisson conditioned on the weight, it concentrates around its conditional mean. This allows us to pass from a space-time process to a classical time-varying stochastic process. While the limit process is not Lévy, the classical proof machinery for Lévy-type convergence from Resnick [93] is flexible enough to also be applicable in our more involved setting. More precisely, we first show that the edge count converges to a stable process with index $\alpha \in (1, 2)$. The proof of convergence is based on the method of moments, and tightness is shown using the method of characteristic functions. To summarize, the main contributions of our work are as follows.

(1) We propose a dynamic version of the random connection hypergraph model from Paper C where nodes are born and die over time. This model, therefore, features both higher-order interactions, spatial effects, and scale-free degree distributions.

(2) In the case of finite fourth moments of the degree distribution, we establish the convergence of the edge count to a Gaussian process of AR(2) type. Here, the mechanism of the random connection hypergraphs induces long-range dependencies that are absent in the models considered in the literature so far. This requires us to consider normal approximation techniques that differ significantly from those used in earlier works.

(3) Our work is the first to establish a functional limit theorem for the edge count in the particularly challenging case of infinite variance of the degree distribution. The process limit is a stable process that is not Lévy and not even Markov. Loosely speaking, it can be considered as a variant of a Lévy process where the noise variables have a finite lifetime.

While the focus of this paper's investigation is on the case of the edge count, we are convinced that the methods from our work will also be helpful for studying more complex functionals, such as simplex counts or Betti numbers. We leave these topics for future investigations.

The rest of the paper is organized as follows. In Section D.2, we introduce the considered model and present our main results. In Sections D.3, D.4, and D.5 we give the proofs of Propositions D.2.1, D.2.2, and D.2.3, respectively. Next, in Sections D.6 and D.7 we present the outlines of the proofs of Theorems D.2.4 and D.2.6, respectively. In the final part of the paper, we exhibit the proofs of the minor propositions and lemmas used in the main proofs presented in the previous part of the paper. In Sections D.8 we present the preliminary lemmas used frequently in the later part of the paper. Section D.9 contains the proofs of the lemmas used for Propositions D.2.1, D.2.2, and D.2.3. Section D.10 gives the proofs of the lemmas used to show Theorem D.2.4.

165

In Section D.11, we present the proofs of the lemmas used to prove Theorem D.2.6. Finally, in Section D.12 we conclude the paper by proving the lemmas presented in Section D.8.

D.2   Model and main results

In this section, we present the *dynamic random connection hypergraph model* (DRCHM) and state our main results. First, consider two independent Poisson point processes

$$\mathcal{P} \subseteq \mathbb{S} \times \mathbb{T} := (\mathbb{R} \times (0,1]) \times (\mathbb{R} \times \mathbb{R}_+) \qquad \text{and} \qquad \mathcal{P}' \subseteq \mathbb{S} \times \mathbb{R},$$

that we refer to as *vertices* and *interactions*, respectively. We will refer to the four random variables characterizing a vertex $P := (X, U, B, L) \in \mathcal{P}$ as the *position*, *weight*, *birth time*, and *lifetime* of the vertex P, respectively. Similarly, in the case of an interaction $P' := (Z, W, R) \in \mathcal{P}'$, the three real random variables denote the *position*, *weight*, and *time* of the interaction P'. If the point $P \in \mathcal{P}$ or $P' \in \mathcal{P}'$ is decorated with some indices, its coordinates (X, U, B, L) or (Z, W, R) receive the same indices as well. Whenever we refer to a nonrandom point, we will use the notations $p := (x, u, b, \ell) \in \mathbb{S} \times \mathbb{T}$ and $p' := (z, w, r) \in \mathbb{S} \times \mathbb{R}$. We emphasize that the above symbols are reserved for denoting the coordinates of vertices and interactions, and will be used throughout the remainder of the paper without further explicit definition. A pair of vertices $p \in \mathbb{S} \times \mathbb{T}$ and $p' \in \mathbb{S} \times \mathbb{R}$ is connected if and only if the following two conditions hold:

$$|x - z| \leqslant \beta u^{-\gamma} w^{-\gamma'} \qquad \text{and} \qquad b \leqslant r \leqslant b + \ell, \tag{D.1}$$

where $\beta > 0$ and $\gamma, \gamma' \in (0,1)$ are real parameters. Using this connection rule, we define the *bipartite graph* $G^{\mathsf{bip}} := G^{\mathsf{bip}}(\mathcal{P}, \mathcal{P}')$ with vertex sets $\mathcal{P}$ and $\mathcal{P}'$. In words, vertices and interactions share an edge based on the smallness of their spatial distance compared to the product of their associated weights, with small weights favoring connections, and under the constraint that the interaction time is within the lifetime of the vertex. Note that the parameter β influences the expected number of edges in G^{bip}, and, as it will be shown later, the parameters γ, γ' determine the power-law exponents of the degree distribution of the vertices and interactions. In the following, the parameter $\beta > 0$ is chosen arbitrarily. Therefore, we will not mention it explicitly throughout the presentation of the results. The connection condition (D.1) is a natural extension of the age-dependent random connection models from Gracar et al. [40, 41]. The spatial connection condition in (D.1) is visualized in Figure D.1. Additionally, Figure D.2 illustrates the temporal connection condition of the DRCHM, where the horizontal axis represents time, and the vertical axis represents position.

We assume that the Poisson point process $\mathcal{P}$ is stationary in the first and third components, the second component is uniformly distributed, and the fourth component is distributed according to $\mathbb{P}_L$, i.e., the intensity measure is given by

$$\mu(\mathrm{d}p) = \mu(\mathrm{d}x, \mathrm{d}u, \mathrm{d}b, \mathrm{d}\ell) := \mathrm{d}(x, u, b)\, \mathbb{P}_L(\mathrm{d}\ell),$$

and assume that $\mathcal{P}'$ is also stationary with intensity $\mathrm{d}(z, w, r)$.
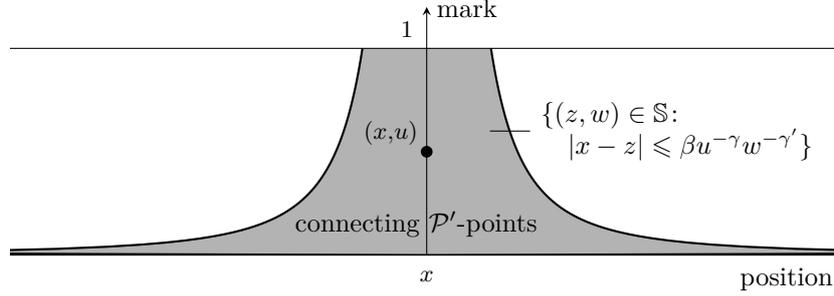
Figure D.1: The spatial connection condition of the DRCHM. The horizontal axis represents the position of a vertex $P \in \mathcal{P}$, and the vertical axis represents the mark of P. The shaded area indicates the set of points $(z, w) \in \mathbb{S}$ that connect to P based on the connection condition (D.1).
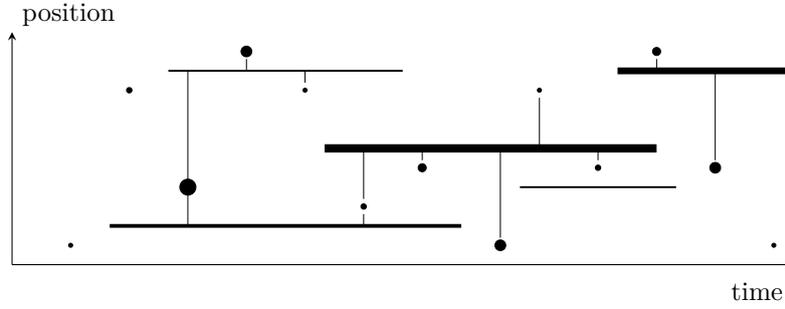
Figure D.2: The temporal connection condition of the DRCHM based on (D.1). The horizontal axis represents the time, and the vertical axis represents the position. $\mathcal{P}$-vertices are represented by intervals of different lengths and widths, where the width of the interval corresponds to the weight of the vertex. Points represent $\mathcal{P}'$-vertices, and the size of the point corresponds to the weight of the vertex. Vertical lines mark if a pair of $\mathcal{P}$- and $\mathcal{P}'$-vertices is connected.

Next, for a point $p := (x, u, b, \ell) \in \mathbb{S} \times \mathbb{T}$, we define the spatial part $p_{\mathsf{s}} := (x, u)$ and the temporal part $p_{\mathsf{t}} := (b, \ell)$ of p, together with their corresponding measures $\mathrm{d}p_{\mathsf{s}} := \mathrm{d}(x, u)$ and $\mu_{\mathsf{t}}(\mathrm{d}p_{\mathsf{t}}) := \mu_{\mathsf{t}}(\mathrm{d}(b, \ell)) = \mathrm{d}b\, \mathbb{P}_L(\mathrm{d}\ell)$, respectively. Similarly, for a point $p' := (z, w, r) \in \mathbb{S} \times \mathbb{R}$, we define its spatial part $p'_{\mathsf{s}} := (z, w)$ with the corresponding measure $\mathrm{d}p'_{\mathsf{s}} := \mathrm{d}(z, w)$.

Furthermore, we consider the *spatial neighborhood* $N_{\mathsf{s}}(p_{\mathsf{s}})$, the *temporal neighborhood* $N_{\mathsf{t}}(p_{\mathsf{t}}; t)$, and the general *neighborhood* $N(p; t)$ as

$$N_{\mathsf{s}}(p_{\mathsf{s}}) := \{(z, w) \in \mathbb{S} \colon |x - z| \leqslant \beta u^{-\gamma} w^{-\gamma'}\}$$
$$N_{\mathsf{t}}(p_{\mathsf{t}}, t) := \{r \in \mathbb{R} \colon b \leqslant r \leqslant t \leqslant b + \ell\}$$
$$N(p; t) := N_{\mathsf{s}}(p_{\mathsf{s}}) \times N_{\mathsf{t}}(p_{\mathsf{t}}; t).$$

The *degree* of p at time t is then defined as the number of interactions connecting to p at time t, i.e.,

$$\deg(p; t) := \sum_{P' \in \mathcal{P}'} \mathbb{1}\{P' \in N(p; t)\}.$$

167

Using this, we define our central quantity of interest, the *edge count* and the *normalized edge count* as

$$S_n(\,\cdot\,) := \sum_{P \in \mathcal{P} \cap (\mathbb{S}_n \times \mathbb{T})} \deg(P; \,\cdot\,) \qquad \text{and} \qquad \overline{S}_n(\,\cdot\,) := n^{-1/2}(S_n(\,\cdot\,) - \mathbb{E}[S_n(\,\cdot\,)]),$$

respectively, where $\mathbb{S}_n := [0, n] \times (0, 1]$ is an *observation window* of size n.

Our first statement is about the univariate normal limit of the edge count at a fixed time point.

Proposition D.2.1 (Univariate normal limit of edge count)**.** *Let $\gamma, \gamma' < 1/2$. Then, for all $t \in \mathbb{R}$, the normalized edge count $\overline{S}_n(t)$ converges weakly to a normal distribution, as $n \to \infty$.*

The following statement provides the limiting covariance function in the case of thin tails.

Proposition D.2.2 (Limiting covariance function of $\overline{S}_n$)**.** *Let $\gamma, \gamma' < 1/2$. Then, for all $t_1 < t_2$, the limiting covariance function of the edge count $\overline{S}_n$ is given by*

$$\lim_{n \uparrow \infty} \mathrm{Cov}\big(\overline{S}_n(t_1), \overline{S}_n(t_2)\big) = (c_1 + c_3 + c_2(2 + t_2 - t_1))\mathrm{e}^{-(t_2 - t_1)}, \tag{D.2}$$

where $c_1 = \frac{2\beta}{(1-\gamma)(1-\gamma')}$, $c_2 = \frac{(2\beta)^2}{(1-2\gamma)(1-\gamma')^2}$ and $c_3 = \frac{(2\beta)^2}{(1-\gamma)^2(1-2\gamma')}$.

The limiting covariance function is an appropriate parameterization of the Matérn covariance function [71] with smoothness parameter $\bar{\nu} = 3/2$, which is the covariance function of a continuous-time AR(2) process.

Next, we turn our attention to the multivariate normal limit of the edge counts.

Proposition D.2.3 (Multivariate normal limit of the edge count)**.** *Let $\gamma < 1/2$ and $\gamma' < 1/3$. Then, for all $k \in \mathbb{Z}_+$ and $t_1, \ldots, t_k \in \mathbb{R}$, the vector of normalized edge counts $(\overline{S}_n(t_1), \ldots, \overline{S}_n(t_k))$ converges weakly to a multivariate normal distribution, as $n \to \infty$.*

Functional limit theorems play a key role in understanding the dynamic behavior of complex random systems. In the context of dynamic higher-order networks, edge counts and their temporal evolution describe the dependencies between the heavy-tailed degree distribution and the dynamics of the vertices. Thus, establishing functional limit theorems for the edge counts provides insights into the interplay between the spatial distribution and the temporal variability of these systems. Let $X := \{X(t) : t \geqslant 0\}$ denote a Gaussian process with *AR(2)* covariance function

$$\mathrm{Cov}(X(t_1), X(t_2)) = (c_1 + c_3 + c_2(2 + |t_2 - t_1|))\mathrm{e}^{-|t_2 - t_1|},$$

where the constants are presented in Proposition D.2.2. The first main result of this paper is as follows.

Theorem D.2.4 (Functional normal limit of edge count)**.** *Let $\gamma, \gamma' < 1/4$. Then,*

$$\overline{S}_n(\,\cdot\,) \xrightarrow[n \uparrow \infty]{d} X(\,\cdot\,)$$

in the Skorokhod space $D([0, 1], \mathbb{R})$.

For the precise definition of the Skorokhod metric d_{Sk}, we refer the reader to Definition D.7.1.

Remark D.2.5. *We conjecture that Theorem D.2.4 could be proved for $\gamma \in (0, 1/2)$ instead of $\gamma \in (0, 1/4)$, using Lemma D.5.1 showing that the low-mark edge count converges to 0 in probability if $\gamma < 1/2$. We refrain from presenting the proof in this version, since this would considerably lengthen the manuscript.*

When $\gamma > 1/2$, the variance of the edge count $\overline{S}_n(t)$ diverges as $n \to \infty$ for any $t \in \mathbb{R}$. This means that a few vertices with very high degrees dominate the edge count, and the distribution of $\overline{S}_n(t)$ diverges. Thus, if $\gamma > 1/2$, we need to consider a different scaling of the edge count to obtain a nontrivial limit, and we introduce

$$\overline{S}_n(\cdot) := n^{-\gamma}(S_n(\cdot) - \mathbb{E}[S_n(\cdot)]).$$

Note that the symbol $\overline{S}_n(\cdot)$ is reused here with different scaling from the one in Theorem D.2.4. As the two scalings are used in different contexts—namely, the thin-tailed case and the heavy-tailed case—they are presented in separate sections of the paper, and we believe there is no risk of confusion. As it is shown in Theorem D.2.6 if $\gamma > 1/2$, the finite-dimensional distributions of $\overline{S}_n(\cdot)$ are heavy-tailed, and thus the limiting process is not a Gaussian process.

To state our second main result, let ν be the measure on $\mathbb{J} := [0, \infty)$ defined by $\nu([\varepsilon, \infty)) := ((2\beta)/(1 - \gamma'))^{1/\gamma}\varepsilon^{-1/\gamma}$ and let $\mathcal{P}_\infty$ denote the Poisson point process on $\mathbb{J} \times \mathbb{T}$ with intensity measure $\nu \times \mathrm{Leb} \times \mathbb{P}_L$. Note that the component $\mathbb{J}$ corresponds to the limit of the appropriately scaled size of the spatial neighborhoods of the heaviest vertices in the sense detailed in Lemma D.7.6 later. Furthermore, define

$$\begin{aligned}
S^*_\varepsilon(\cdot) &:= \sum_{(J,B,L) \in \mathcal{P}_\infty} J(\cdot - B)\, \mathbb{1}\{J \geqslant \tilde{c}\varepsilon^\gamma\}\, \mathbb{1}\{B \leqslant \cdot \leqslant B + L\} \\
\overline{S}^*_\varepsilon(\cdot) &:= S^*_\varepsilon(\cdot) - \mathbb{E}[S^*_\varepsilon(\cdot)],
\end{aligned} \tag{D.3}$$

where $\tilde{c} := 2\beta/(1 - \gamma')$ and $\mathbb{E}[S^*_\varepsilon(\cdot)] = \tilde{c}^{1/\gamma}\varepsilon^{-(1/\gamma - 1)}/(1 - \gamma)$. Then, we have the following stable limit theorem.

Theorem D.2.6 (Functional stable limit of edge count)**.** *Let $\gamma > 1/2$ and $\gamma' < 1/4$. Then, the limit $\overline{S}(\cdot) := \lim_{\varepsilon \downarrow 0} \overline{S}^*_\varepsilon(\cdot)$ exists in the Skorokhod space $D([0, 1], \mathbb{R})$, and the centered edge-count process $\overline{S}_n(\cdot)$ converges weakly to the process $\overline{S}(\cdot)$ in the Skorokhod space $D([0, 1], \mathbb{R})$.*

Remark D.2.7. *In Section D.1, we mentioned that our limiting process $\overline{S}(\cdot)$ fails to be a Lévy process or even to be Markov. After having derived a precise mathematical expression, we now elaborate on these properties in further detail.*

- *The processes $\overline{S}^*_\varepsilon(\cdot)$ are not Markov. Loosely speaking, knowing the edge count $\overline{S}^*_\varepsilon(\cdot)$ is insufficient to predict the evolution of the process. To see this, suppose that there is a single $\mathcal{P}$-vertex with 2 edges at time t. If this vertex dies, both its edges simultaneously vanish. In contrast, if there are 2 $\mathcal{P}$-vertices each with a single edge, the process evolves more smoothly. Thus, the edge count $\overline{S}^*_\varepsilon(\cdot)$ alone does not capture enough information to predict the future of the process.*

169

- *Since the processes $\overline{S}_\varepsilon^*(\,\cdot\,)$ are not Markov, they cannot be a Lévy processes either. Moreover, the increments of $\overline{S}_\varepsilon^*(\,\cdot\,)$ are not independent of each other. Consider two adjacent time intervals $[t, t+\varepsilon_1]$ and $[t+\varepsilon_1, t+\varepsilon_1+\varepsilon_2]$ for some $\varepsilon_1, \varepsilon_2 > 0$. $\mathcal{P}$-vertices alive at time $t+\varepsilon_1$ are likely to remain alive at time $t+\varepsilon_1+\varepsilon_2$ as well. Thus, the increments are not independent.*

Note that the above properties carry over to the limiting process $\overline{S}(\,\cdot\,)$ as well when taking the limit $\varepsilon \to 0$.

Before turning to the proofs, we briefly describe the main techniques used in each of the following sections.

- **Proof of Proposition D.2.1**. We prove the convergence of the normalized edge count to a Gaussian distribution using the theory of associated random variables. The key tool is a CLT for sums of associated Poisson functionals.

- **Proof of Proposition D.2.2**. With $\gamma < 1/2$, we calculate the covariance function of the normalized edge count $\overline{S}_n(t)$ by decomposing the edge count into a sum of three terms and then calculating the covariance function for each part.

- **Proof of Proposition D.2.3**. We establish the multivariate normal limit by applying the Malliavin–Stein approximation. More precisely, we bound the so-called d_3 distance of the distribution of the edge counts and the multivariate normal distribution. This is done by applying [97, Theorem 1.1], which involves the examination of cost operators.

- **Proof of Theorem D.2.4**. We show functional convergence in the Skorokhod space by decomposing the edge count into differences of monotone functionals and applying a refined tightness criterion due to Davydov [26, Theorem 2]. The main challenge of this proof is to show the refined tightness criterion required by the theorem.

- **Proof of Theorem D.2.6**. In the proof of this theorem, the main challenge is that the variance of the edge count is infinite. For infinite-variance cases, we split the edge count into contributions from light- and heavy-tailed nodes. We show the light-node contribution is negligible and the heavy-node contribution converges to a stable process that is not Markov. The proof combines conditional expectation approximations, convergence of Poisson point processes, and vague convergence of Lévy measures.

Before entering proofs, let us also introduce the *common neighborhood* of a set of m points $\boldsymbol{p}_m := (p_1, \dots, p_m) \in \mathcal{P}^m$, i.e.,

$$N_{\mathsf{s}}(\boldsymbol{p}_{\mathsf{s},m}) := \bigcap_{i=1}^m N_{\mathsf{s}}(p_{\mathsf{s},i}), \qquad N_{\mathsf{t}}(\boldsymbol{p}_{\mathsf{t},m}; t) := \bigcap_{i=1}^m N_{\mathsf{t}}(p_{\mathsf{s},i}; t), \qquad N(\boldsymbol{p}_m; t) := \bigcap_{i=1}^m N(p_i; t),$$

and the associated degree

$$\deg(\boldsymbol{p}_m; t) := \sum_{P' \in \mathcal{P}'} \mathbb{1}\{P' \in N(\boldsymbol{p}_m; t)\}.$$

Next, for Borel sets $\mathcal{X}, \mathcal{U}, \mathcal{B}, \mathcal{D} \subseteq \mathbb{R}$, we introduce the notations

$$\mathbb{S}_\mathcal{X} := \{(x,u) \in \mathbb{S} \colon x \in XX\} \quad \mathbb{S}^\mathcal{U} := \{(x,u) \in \mathbb{S} \colon u \in \mathcal{U}\} \quad \mathbb{S}_\mathcal{X}^\mathcal{U} := \mathbb{S}_\mathcal{X} \cap \mathbb{S}^\mathcal{U}$$
$$\mathbb{T}_\mathcal{B} := \{(b,\ell) \in \mathbb{T} \colon b \in \mathcal{B}\} \quad \mathbb{T}^\mathcal{D} := \{(b,\ell) \in \mathbb{T} \colon b+\ell \in \mathcal{D}\} \quad \mathbb{T}_\mathcal{B}^\mathcal{D} := \mathbb{T}_\mathcal{B} \cap \mathbb{T}^\mathcal{D}$$

and for the edge counts restricted to a Borel measurable spatial domain $\mathcal{A}$, we introduce

$$S_\mathcal{A}(t) := \sum_{P \in \mathcal{P} \cap (\mathbb{S}_\mathcal{A} \times \mathbb{T})} \deg(P; t).$$

For the coordinates of the points $\boldsymbol{p}_m \in \mathcal{P}^m$ we use the notation $\boldsymbol{x}_m$, $\boldsymbol{u}_m$, $\boldsymbol{b}_m$ and $\boldsymbol{\ell}_m$. As the Poisson point processes are stationary, we neglect the time arguments t in the notations whenever a formula contains only one time argument. We note that for readability, we maintain the uniqueness of the indices for the constants within each part of the proofs.

D.3 Proof of Proposition D.2.1

In this section, we present the proof of the univariate normal limit of the normalized edge count for a fixed time. After calculating the mean and variance of the edge count, we apply a CLT for associated random variables to show that the edge count converges to a Gaussian distribution. We begin with a lemma that gives the asymptotic behavior of the mean and variance of the edge count.

Lemma D.3.1 (Asymptotic behavior of mean and variance of $S_n(t)$)**.** *Let $t \in \mathbb{R}$ and $\gamma' \in (0,1)$. If $\gamma \in (0,1)$, then $\lim_{n \uparrow \infty} n^{-1} \mathbb{E}[S_n(t)] < \infty$. Furthermore, if $\gamma < 1/2$, then also $\lim_{n \uparrow \infty} n^{-1} \operatorname{Var}(S_n(t)) < \infty$.*

We present the proofs of this and the following statement in Section D.9. The next lemma gives the covariance of the edge counts of different spatial domains at a fixed time.

Lemma D.3.2 (Covariance of edge counts at fixed times)**.** *Let $t \in \mathbb{R}$, $\gamma, \gamma' < 1/2$, and let $\mathcal{A}_1, \mathcal{A}_2$ be two disjoint Borel sets. Then,*

$$\operatorname{Cov}(S_{\mathcal{A}_1}(t), S_{\mathcal{A}_2}(t)) \leqslant \frac{|\mathcal{A}_1|}{2(1 - 2\gamma')} \Big(\frac{2\beta}{1-\gamma} \Big)^2.$$

In particular, the right-hand side is independent of the time t and of the set $\mathcal{A}_2$.

To show the Gaussian limit, we apply the CLT for associated random variables [107, Theorem 4.4.3], which states that if $\boldsymbol{T} := T_1, T_2, \ldots$ is a sequence of associated i.i.d. random variables with $\sum_{k \geqslant 1} \operatorname{Cov}(T_1, T_k) < \infty$, then the centered and normalized sum converges to a Gaussian distribution. Let us recall that a sequence of random variables $\boldsymbol{T}$ is associated if and only if $\operatorname{Cov}(f(T_1, \ldots, T_k), g(T_1, \ldots, T_k)) \geqslant 0$ for all non-decreasing functions f, g for which $\mathbb{E}[f(T_1, \ldots, T_k)]$, $\mathbb{E}[g(T_1, \ldots, T_k)]$, and $\mathbb{E}[f(T_1, \ldots, T_k)g(T_1, \ldots, T_k)]$ exist [36, Definition 1.1]. To see this, we partition the spatial coordinates of the edges into intervals of length one and define

$$T_i := \sum_{P \in \mathcal{P} \cap (\mathbb{S}_{[i-1,i]} \times \mathbb{T})} \deg(P; t).$$

Since $\deg(P; t)$ is increasing in the Poisson process $\mathcal{P}'$, we conclude from the Harris-FKG inequality [66, Theorem 20.4] that the sequence $T_1, \ldots, T_k$ is associated. For the covariance condition, note that we have $T_i \in O(1)$ for each $i \in \mathbb{N}$ by Lemma D.3.1, where we require that $\gamma < 1/2$. By Lemma D.3.2, we have that

$$\sum_{k \geqslant 2} \mathrm{Cov}(T_1, T_k) = \mathrm{Cov}\Big(T_1, \sum_{k \geqslant 2} T_k\Big) < \infty.$$

Thus, $\sum_{k \geqslant 1} \mathrm{Cov}(T_1, T_k)$ is finite, and Proposition D.2.1 is proved.

D.4 Proof of Proposition D.2.2

The calculation of the limiting covariance function of $\overline{S}_n$ relies on a time-interval-based decomposition of the edge count. Without loss of generality, we may assume that $t_1 \leqslant t_2$. First, note that

$$\mathrm{Cov}(\overline{S}_n(t_1), \overline{S}_n(t_2)) = n^{-1} \, \mathrm{Cov}(S_n(t_1), S_n(t_2)).$$

Now, to simplify the calculations, we decompose the edge count into three parts as

$$S_n^{\mathsf{A}}(t_1, t_2) := \sum_{P \in \mathcal{P} \cap (\mathbb{S}_n \times \mathbb{T}_{\leqslant t_1}^{t_2 \leqslant})} \deg(P; t_1)$$

$$S_n^{\mathsf{B}}(t_1, t_2) := \sum_{P \in \mathcal{P} \cap (\mathbb{S}_n \times \mathbb{T}_{\leqslant t_1}^{[t_1, t_2]})} \deg(P; t_1)$$

$$S_n^{\mathsf{C}}(t_1, t_2) := \sum_{P \in \mathcal{P} \cap (\mathbb{S}_n \times \mathbb{T}_{\leqslant t_2}^{t_2 \leqslant})} \sum_{P' \in \mathcal{P}'} \mathbb{1}\{P' \in N(P; t_2)\} \, \mathbb{1}\{t_1 \leqslant R\},$$

where we abbreviate $\mathbb{T}_{\leqslant t_1}^{t_2 \leqslant} = \mathbb{T}_{(-\infty, t_1]}^{(t_2, \infty)}$, $\mathbb{T}_{\leqslant t_1}^{[t_1, t_2]} = \mathbb{T}_{(-\infty, t_1]}^{[t_1, t_2]}$ and $\mathbb{T}_{\leqslant t_2}^{t_2 \leqslant} = \mathbb{T}_{(-\infty, t_2]}^{(t_2, \infty)}$ and present a visualization in Figure D.3. With these notations, we have that

$$S_n(t_1) = S_n^{\mathsf{A}}(t_1, t_2) + S_n^{\mathsf{B}}(t_1, t_2) \qquad \text{and} \qquad S_n(t_2) = S_n^{\mathsf{A}}(t_1, t_2) + S_n^{\mathsf{C}}(t_1, t_2).$$
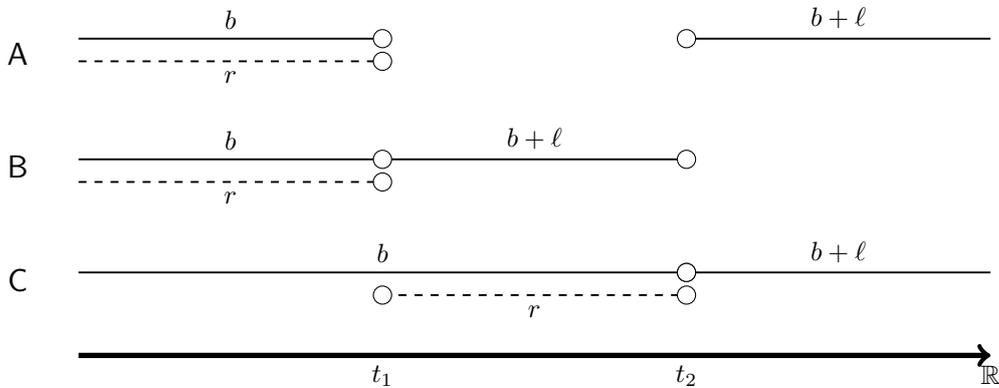
Figure D.3: Decomposition of the covariance function

Since, by the independence of the Poisson process, $\mathrm{Cov}(S_n^{\mathsf{B}}(t_1, t_2), S_n^{\mathsf{C}}(t_1, t_2)) = 0$, the covariance function is given by

$$\mathrm{Cov}(\overline{S}_n(t_1), \overline{S}_n(t_2))$$
$$= \mathrm{Var}(\overline{S}_n^{\mathsf{A}}(t_1, t_2)) + \mathrm{Cov}(\overline{S}_n^{\mathsf{A}}(t_1, t_2), \overline{S}_n^{\mathsf{B}}(t_1, t_2)) + \mathrm{Cov}(\overline{S}_n^{\mathsf{A}}(t_1, t_2), \overline{S}_n^{\mathsf{C}}(t_1, t_2)),$$

and we have the following limiting behavior.

Lemma D.4.1 (Terms of the limiting covariance function of $\overline{S}_n(t)$)**.** *Let $\gamma, \gamma' < 1/2$ and $t_1 \leqslant t_2$. Then,*

$$\lim_{n \uparrow \infty} \mathrm{Var}(\overline{S}_n^{\mathsf{A}}(t_1, t_2)) = (c_1 + 2c_2)\mathrm{e}^{-(t_2 - t_1)} + c_3 \mathrm{e}^{-2(t_2 - t_1)}$$
$$\lim_{n \uparrow \infty} \mathrm{Cov}(\overline{S}_n^{\mathsf{A}}(t_1, t_2), \overline{S}_n^{\mathsf{B}}(t_1, t_2)) = c_3\big(\mathrm{e}^{-(t_2 - t_1)} - \mathrm{e}^{-2(t_2 - t_1)}\big)$$
$$\lim_{n \uparrow \infty} \mathrm{Cov}(\overline{S}_n^{\mathsf{A}}(t_1, t_2), \overline{S}_n^{\mathsf{C}}(t_1, t_2)) = c_2(t_2 - t_1)\mathrm{e}^{-(t_2 - t_1)},$$

where $c_1 = \frac{2\beta}{(1-\gamma)(1-\gamma')}$, $c_2 = \frac{(2\beta)^2}{(1-2\gamma)(1-\gamma')^2}$ and $c_3 = \frac{(2\beta)^2}{(1-\gamma)^2(1-2\gamma')}$.

The proof of the lemma is given in Section D.9 in a slightly more complex form, since the lemma is used in a very similar scenario in the proof of Lemma D.5.5.

Finally, by summing the above terms, we have that

$$\lim_{n \uparrow \infty} \mathrm{Cov}\big(\overline{S}_n(t_1), \overline{S}_n(t_2)\big) = \big(c_1 + c_3 + c_2(2 + t_2 - t_1)\big)\mathrm{e}^{-(t_2 - t_1)},$$

which finishes the proof of Proposition D.2.2.

D.5 Proof of Proposition D.2.3

Next, we show that if $\gamma < 1/2$ and $\gamma' < 1/3$, the finite-dimensional distributions of the normalized edge count converge to a multivariate normal distribution.

To this end, we would like to apply the normal approximation result in [97, Theorem 1.1], which uses Malliavin–Stein approximation to bound the so-called d_3 distance between the distribution of Poisson functionals and the normal distribution. Applying this theorem requires controlling the error terms $E_1(n)$, $E_2(n)$, $E_3(n)$, detailed below, and establishing that they converge to zero in probability as $n \to \infty$. However, this can only be achieved under the stricter condition $\gamma < 1/3$, since it involves showing that an integral of the form $\int_0^1 u^{-3\gamma}\,\mathrm{d}u$ is finite, which diverges for $\gamma \geqslant 1/3$. To circumvent this restriction, we apply a low-mark/high-mark decomposition of the edge count S_n. We first show that the contribution from low-mark edges is negligible, and then analyze the high-mark edge count separately. This strategy enables us to establish convergence to a multivariate normal distribution under the milder condition $\gamma < 1/2$, rather than the stricter condition $\gamma < 1/3$. We begin by setting a mark $u_n := n^{-2/3}$ as a function of the window size n, and we decompose the edge count S_n to the sum of the high-mark edge count $S_n^{\geqslant}$ and the low-mark edge count $S_n^{\leqslant}$ as

$S_n(\cdot) = S_n^{\geqslant}(\cdot) + S_n^{\leqslant}(\cdot)$, with

$$S_n^{\geqslant}(\cdot) := \sum_{P \in \mathcal{P} \cap (\mathbb{S}_n^{u_n \leqslant} \times \mathbb{T})} \deg(P; \cdot) \quad \text{and}$$

$$S_n^{\leqslant}(\cdot) := \sum_{P \in \mathcal{P} \cap (\mathbb{S}_n^{\leqslant u_n} \times \mathbb{T})} \deg(P; \cdot), \tag{D.4}$$

where $\mathbb{S}_n^{\leqslant u_n} = \mathbb{S}_n^{[0,u_n)}$ and $\mathbb{S}_n^{u_n \leqslant} = \mathbb{S}_n^{[u_n,1]}$. This decomposition is illustrated in Figure D.4. The next lemma shows that the low-mark edge count $S_n^{\leqslant}$ is negligible in the sense that its normalized version

$$\overline{S}_n^{\leqslant} := n^{-1/2}\bigl(S_n^{\leqslant} - \mathbb{E}[S_n^{\leqslant}]\bigr)$$

converges to zero in probability for all times t.

Lemma D.5.1 (The low-mark edge count is negligible)**.** *Let $\gamma, \gamma' < 1/2$. Then, for any t, in probability,*

$$\overline{S}_n^{\leqslant}(t) \xrightarrow[n \uparrow \infty]{\mathbb{P}} 0.$$

Next, we apply [97, Theorem 1.1] bounding the d_3 distance between the distribution of $S_n^{\geqslant}$ and the normal distribution. The definition of the d_3 distance, a metric on the space of random vectors, is given below.

Definition D.5.2 (d_3 distance)**.** *Let $\mathcal{H}_m^{(3)}$ be the set of all C^3 functions $h \colon \mathbb{R}^m \to \mathbb{R}$ such that the absolute values of the second and third partial derivatives of h are bounded by 1 and $|h(x) - h(y)| \leqslant \|x - y\|_E$ for all $x, y \in \mathbb{R}^m$, where $\|\cdot\|_E$ denotes the Euclidean norm. Then, the d_3 distance of two m-dimensional random vectors X, Y with $\mathbb{E}[\|X\|_E], \mathbb{E}[\|Y\|_E] < \infty$ is defined by*

$$d_3(X, Y) := \sup_{h \in \mathcal{H}_m^{(3)}} \bigl|\mathbb{E}[h(X)] - \mathbb{E}[h(Y)]\bigr|.$$

Note that as convergence in d_3 distance implies convergence in distribution [34, Proposition 20.A.2], it is enough to show convergence in d_3 distance to prove Proposition D.2.3. Next, we introduce the cost operators that will be used to bound the d_3 distance.
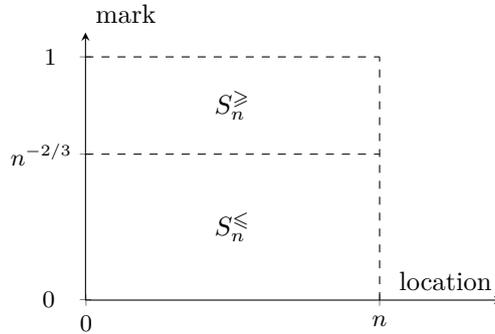
Figure D.4: Decomposition of the edge count S_n to a sum of the low-mark edge count $S_n^{\leqslant}$ and the high-mark edge count $S_n^{\geqslant}$

Definition D.5.3 (Cost operators). *For the edge count $S_n^{\geqslant}$, the add-one cost opera-tors D_p and $D_{p'}$ are defined by*

$$D_p S_n^{\geqslant}(t) := \sum_{P' \in \mathcal{P}'} \mathbb{1}\{P' \in N(p;t)\}$$

$$D_{p'} S_n^{\geqslant}(t) := \sum_{P \in \mathcal{P} \cap (\mathbb{S}_n^{u_n \leqslant} \times \mathbb{T})} \mathbb{1}\{p' \in N(P;t)\}.$$

Note that the cost operator $D_p S_n^{\geqslant}(t)$ is Poisson distributed since it counts the number of interactions in the neighborhood of p. Similarly, the cost operator $D_{p'} S_n^{\geqslant}(t)$ is also Poisson distributed, as it is the number of vertices such that $p'_\mathsf{s} \in N_\mathsf{s}(P_\mathsf{s})$ and $B \leqslant r$ on the one hand, and this restricted Poisson process is thinned with a B-dependent probability $\exp(-(t - B))$.

Turning our attention to the add-two cost operators $D^2_{p_1,p_2}$, $D^2_{p_1,p'_2}$, $D^2_{p'_1,p_2}$, *and* $D^2_{p'_1,p'_2}$, *we have*

$$D^2_{p_1,p_2} S_n^{\geqslant}(t) = S_n^{\geqslant}(t) + D_{p_1} S_n^{\geqslant}(t) + S_n^{\geqslant}(t) + D_{p_2} S_n^{\geqslant}(t) + S_n^{\geqslant}(t)$$
$$- (S_n^{\geqslant}(t) + D_{p_1} S_n^{\geqslant}(t) + S_n^{\geqslant}(t) + D_{p_2} S_n^{\geqslant}(t)) = 0$$

$$D^2_{p'_1,p'_2} S_n^{\geqslant}(t) = S_n^{\geqslant}(t) + D_{p'_1} S_n^{\geqslant}(t) + S_n^{\geqslant}(t) + D_{p'_2} S_n^{\geqslant}(t)$$
$$- (S_n^{\geqslant}(t) + D_{p'_1} S_n^{\geqslant}(t) + S_n^{\geqslant}(t) + D_{p'_2} S_n^{\geqslant}(t)) = 0$$

$$D^2_{p,p'} S_n^{\geqslant}(t) = \mathbb{1}\{p' \in N(p;t)\} + S_n^{\geqslant}(t) + D_p S_n^{\geqslant}(t) + S_n^{\geqslant}(t) + D_{p'} S_n^{\geqslant}(t)$$
$$- (S_n^{\geqslant}(t) + D_p S_n^{\geqslant}(t) + S_n^{\geqslant}(t) + D_{p'} S_n^{\geqslant}(t)) = \mathbb{1}\{p' \in N(p;t)\},$$

where we note that the add-two cost operators are much simpler than the add-one cost operators.

To apply [97, Theorem 1.1], we need to have a single Poisson process, which we obtain by merging the two Poisson processes $\mathcal{P}$ and $\mathcal{P}'$ into a single Poisson process $\widetilde{\mathcal{P}} := \mathcal{P} \sqcup \mathcal{P}'$, where $\sqcup$ denotes the disjoint union of the two Poisson processes. The point process $\widetilde{\mathcal{P}}$ is defined on the space $\mathbb{S}_n^{u_n \leqslant} \times \mathbb{T} \sqcup \mathbb{S} \times \mathbb{R}$ using appropriate marks, and its intensity measure is given by $\tilde{\mu}$. In other words, if $\tilde{p} \in \widetilde{\mathcal{P}}$, then

$$\tilde{\mu}(\mathrm{d}\tilde{p}) = \begin{cases} \mu(\mathrm{d}\tilde{p}) & \text{if } \tilde{p} \in \mathbb{S}_n^{u_n \leqslant} \times \mathbb{T} \\ \mathrm{d}\tilde{p} & \text{if } \tilde{p} \in \mathbb{S} \times \mathbb{R}. \end{cases}$$

Now, to show the multivariate convergence, we apply [97, Theorem 1.1], which we restate here for convenience.

Proposition D.5.4 (Multivariate CLT). *Let N_Σ be an m-dimensional centered multi-variate normal distribution with a positive semi-definite covariance matrix $\Sigma \in \mathbb{R}^{m \times m}$ with elements $\sigma_{i,j} \in \mathbb{R}$. Further, let $\tilde{p} \in \widetilde{\mathcal{P}}$ and let $F := (\overline{S}_n^{\geqslant}(t_1), \ldots, \overline{S}_n^{\geqslant}(t_m))$ denote an m-dimensional random vector of Poisson functionals. Then, the distance $d_3(F, N_\Sigma)$ is upper bounded by*

$$d_3(F, N_\Sigma) \leqslant \frac{m}{2} \sum_{i,j=1}^{m} |\sigma_{ij} - \mathrm{Cov}(\overline{S}_n^{\geqslant}(t_1), \overline{S}_n^{\geqslant}(t_2))| + m E_1(n) + \frac{m}{2} E_2(n) + \frac{m^2}{4} E_3(n), \quad \text{(D.5)}$$

where the terms $E_1(n), E_2(n), E_3(n)$ are defined as

$$E_1(n) := \left(\sum_{i,j=1}^{m} \int \left(\mathbb{E}\left[(D_{\tilde{p}_1,\tilde{p}_3}^2 \overline{S}_n^{\geqslant}(t_1))^2 (D_{\tilde{p}_2,\tilde{p}_3}^2 \overline{S}_n^{\geqslant}(t_1))^2 \right] \right. \right.$$

$$\left. \left. \times \mathbb{E}\left[(D_{\tilde{p}_1} \overline{S}_n^{\geqslant}(t_2))^2 (D_{\tilde{p}_2} \overline{S}_n^{\geqslant}(t_2))^2 \right] \right)^{1/2} \mathrm{d}(\tilde{p}_1, \tilde{p}_2, \tilde{p}_3) \right)^{1/2}$$

$$E_2(n) := \left(\sum_{i,j=1}^{m} \int \left(\mathbb{E}\left[(D_{\tilde{p}_1,\tilde{p}_3}^2 \overline{S}_n^{\geqslant}(t_1))^2 (D_{\tilde{p}_2,\tilde{p}_3}^2 \overline{S}_n^{\geqslant}(t_1))^2 \right] \right. \right.$$

$$\left. \left. \times \mathbb{E}\left[(D_{\tilde{p}_1,\tilde{p}_3}^2 \overline{S}_n^{\geqslant}(t_2))^2 (D_{\tilde{p}_2,\tilde{p}_3}^2 \overline{S}_n^{\geqslant}(t_2))^2 \right] \right)^{1/2} \mathrm{d}(\tilde{p}_1, \tilde{p}_2, \tilde{p}_3) \right)^{1/2}$$

$$E_3(n) := \sum_{i=1}^{m} \int \mathbb{E}\left[|D_{\tilde{p}} \overline{S}_n^{\geqslant}(t_1)|^3 \right] \mathrm{d}\tilde{p}.$$

In the above, the cost operators involving $\tilde{p}$ are defined as the number of edges of the point $\tilde{p}$, in alignment with Definition D.5.3. For notational convenience, we do not introduce further notation for the cost operators involving $\tilde{p}$.

We begin by setting the elements σ_{ij} of the covariance matrix Σ in (D.5). To do so, we show the below lemma, which is very similar to the covariance function of the total edge count introduced in Proposition D.2.2.

Lemma D.5.5 (Limiting covariance function of $\overline{S}_n^{\geqslant}$). *Let $\gamma, \gamma' < 1/2$. Then, the limiting covariance function of the edge count $\overline{S}_n^{\geqslant}$ is given by* (D.2).

Then, we see that the first term in the right-hand side of (D.5) converges to zero as $n \to \infty$. Next, we show that the error terms $E_1(n), E_2(n), E_3(n)$ converge to zero, as $n \to \infty$. This result is summarized in the following lemma, which we prove in Section D.9 by examining the cost operators $D_{\tilde{p}}$, $D_{\tilde{p}_1,\tilde{p}_3}^2$ and $D_{\tilde{p}_2,\tilde{p}_3}^2$.

Lemma D.5.6 (Bounds of error terms). *Let $\gamma < 1/2$, $\gamma' < 1/3$. Then, the error terms defined in* (D.5) *satisfy*

$$\lim_{n \uparrow \infty} (E_1(n) + E_2(n) + E_3(n)) = 0.$$

In particular, this proves Proposition D.2.3.

D.6 Proof of Theorem D.2.4

Broadly speaking, apart from the convergence of finite-dimensional distributions shown in Proposition D.2.3, we need to show that the sequence of the normalized edge counts is tight when $t \in [0,1]$. For this, we would like to apply [26, Theorem 2], which holds for non-decreasing processes. The key advantage of this theorem is that to show the moment bound for tightness, it is enough to consider time increments of size larger than a minimum n-dependent threshold, which makes the proof more manageable.

We would like to write the edge count as the difference $S_n = S_n^+ - S_n^-$ of two non-decreasing processes. To define S_n^+ and S_n^-, we first introduce the *plus* and *minus* neighborhoods of a point $p \in \mathbb{S} \times \mathbb{T}$ as

$$N^+(p;t) := N_{\mathsf{s}}(p_{\mathsf{s}}) \times N_{\mathsf{t}}^+(p_{\mathsf{t}};t) \qquad \text{and} \qquad N^-(p;t) := N_{\mathsf{s}}(p_{\mathsf{s}}) \times N_{\mathsf{t}}^-(p_{\mathsf{t}};t),$$

where

$$N_{\mathsf{t}}^+(p_{\mathsf{t}};t) := \begin{cases} \{r \in \mathbb{R} : b \leqslant r \leqslant b+\ell\} & \text{if } b+\ell \leqslant t \\ \{r \in \mathbb{R} : b \leqslant r \leqslant t\} & \text{if } b+\ell > t \end{cases}$$

$$N_{\mathsf{t}}^-(p_{\mathsf{t}};t) := \begin{cases} \{r \in \mathbb{R} : b \leqslant r \leqslant b+\ell\} & \text{if } b+\ell \leqslant t \\ \varnothing & \text{if } b+\ell > t. \end{cases}$$

Note that the spatial parts of the neighborhoods $N^+(p;t)$ and $N^-(p;t)$ are the same as the spatial part of $N(p;t)$, and the difference is only in the temporal part. Considering that $t \in [0,1]$, we also define

$$S_n^+(t) := \sum_{P \in \mathcal{P} \cap (\mathbb{S}_n \times \mathbb{T}^{0\leqslant})} \deg^+(P;t) \qquad \text{and} \qquad S_n^-(t) := \sum_{P \in \mathcal{P} \cap (\mathbb{S}_n \times \mathbb{T}^{0\leqslant})} \deg^-(P;t),$$

where

$$\deg^+(P;t) := \sum_{P' \in \mathcal{P}'} \mathbb{1}\{P' \in N^+(P;t)\} \text{ and}$$

$$\deg^-(P;t) := \sum_{P' \in \mathcal{P}'} \mathbb{1}\{P' \in N^-(P;t)\},$$

and $\mathbb{T}^{0\leqslant} := \mathbb{T}^{[0,\infty)}$ denotes the set for which the death time $b + \ell \geqslant 0$. In words, both S_n^+ and S_n^- consider only points from $\mathcal{P}$ whose lifetime $[B, B+L]$ intersects the temporal interval $[0,1]$, and $\deg^+(P)$ counts the $\mathcal{P}'$-points that

- are in the spatial neighborhood $N_{\mathsf{s}}(P_{\mathsf{s}})$ of the vertex P and

- have a birth time R in the interval $[B, (B+L) \wedge t]$, regardless of the lifetime L.

On the other hand, $\deg^-(P;t)$ considers a point P if its lifetime ends before the time t, and counts those interactions in $\mathcal{P}'$ that

- are in the spatial neighborhood $N_{\mathsf{s}}(P_{\mathsf{s}})$ of the vertex P and

- have a birth time R in the interval $[B, B+L]$, regardless of the birth time B.

We show in the following lemma that the *plus-minus decomposition* holds.

Lemma D.6.1 (Plus-minus decomposition of edge count)**.** *We have that* $S_n = S_n^+ - S_n^-$.

Since the difference of tight sequences is tight, it is enough to show that [26, Theorem 2] holds for the normalized edge counts

$$\overline{S}_n^+ := n^{-1/2}(S_n^+ - \mathbb{E}[S_n^+]) \qquad \text{and} \qquad \overline{S}_n^- := n^{-1/2}(S_n^- - \mathbb{E}[S_n^-]).$$

From now on, we will use the index $\cdot^{\pm}$ whenever a formula is valid for both $\cdot^+$ and $\cdot^-$. Unless stated otherwise, all the indices of a formula are either $+$ or $-$. For ease of reference, we summarize the statement of Davydov [26, Theorem 2] in our context.

Theorem D.6.2 (Specialized version of Davydov's theorem)**.** *Let $a_n \to 0$ be a sequence of positive numbers converging to 0, and set $t_k = ka_n$ for $k = 0, 1, \ldots, k_n$ with $k_n = \lfloor 1/a_n \rfloor$ and $t_{k_n+1} = 1$. Then, if $\overline{S}_n^\pm(\,\cdot\,)$ are non-decreasing processes defined on the interval $[0, 1]$ such that*

(1) the finite-dimensional distributions of the processes $\overline{S}_n^\pm(\,\cdot\,)$ converge to the finite-dimensional distribution of a limiting process $\overline{S}_\infty^\pm(\,\cdot\,)$,

(2) there exists some constants $\chi_1, \chi_2 > 1$ such that

$$\mathbb{E}\!\left[\left|\overline{S}_n^\pm(t) - \overline{S}_n^\pm(s)\right|^{\chi_1}\right] \in O(|t - s|^{\chi_2})$$

for all n if $|t - s| \geqslant a_n$, and

(3) for the limit of the expected increments, we have

$$\lim_{n \uparrow \infty} \max_{k \leqslant \lfloor 1/a_n \rfloor} \left|\mathbb{E}\big[\overline{S}_n^\pm(t_{k+1})\big] - \mathbb{E}\big[\overline{S}_n^\pm(t_k)\big]\right| = 0,$$

then $\overline{S}_\infty^\pm(\,\cdot\,)$ is almost surely continuous and the sequence $\overline{S}_n^\pm(\,\cdot\,)$ converges in distribution to $\overline{S}_\infty^\pm(\,\cdot\,)$.

Condition (1) of Theorem D.6.2 is fulfilled for $\overline{S}_n^\pm(\,\cdot\,)$, which is stated in the next proposition.

Proposition D.6.3 (Convergence of the finite-dimensional distributions of $\overline{S}_n^\pm$)**.** *If $\gamma < 1/2$ and $\gamma' < 1/3$, then the finite-dimensional distributions of $\overline{S}_n^\pm(\,\cdot\,)$ converge to a multivariate normal distribution.*

The following proposition shows that Condition (2) holds for $\overline{S}_n^\pm$. We set $\chi_1 := 4$, $\chi_2 := 1 + \eta$ and $a_n := n^{-1/(1+\eta)}$ for some $\eta > 0$.

Proposition D.6.4 (Tightness of the sequence $\overline{S}_n^\pm$)**.** *Let $\gamma, \gamma' < 1/4$. Then, there exists an $\eta > 0$ such that if $|t - s| \geqslant n^{-1/(1+\eta)}$, then*

$$\mathbb{E}\big[\left|\overline{S}_n^\pm(t) - \overline{S}_n^\pm(s)\right|^4\big] \in O(|t - s|^{1+\eta})$$

for all n.

Finally, we turn our attention to Condition (3). Note that the absolute value can be dropped due to the monotonicity of $S_n^\pm$. Then, the condition is fulfilled if the following lemma holds.

Lemma D.6.5 (Bound on the expectation of the increments of $\overline{S}_n^\pm(t)$)**.** *Let $t_k := kn^{1/(1+\eta)}$ for any $k \in \mathbb{N}$. Then, for all $\varepsilon > 0$,*

$$\lim_{n \uparrow \infty} \max_{k \leqslant \lfloor n^{1/(1+\eta)} \rfloor} \big(n^{-1/2}\,\mathbb{E}\big[\Delta_n^\pm(t_k, t_{k+1})\big]\big) = 0.$$

The previous propositions and lemmas establish all the conditions of Theorem D.6.2 and hence we conclude that the sequence $\overline{S}_n^\pm(t)$ is tight, and thus the functional CLT holds for the edge count $\overline{S}_n(t)$.

D.7   Proof of Theorem D.2.6

In this section, we outline the proof of the convergence of the edge count to a stable limit when $\gamma > 1/2$. We divide the proof of Theorem D.2.6 into two parts.

Before delving into the proof, recall the high-mark low-mark decomposition from (D.4) and Figure D.4, where we set $u_n = n^{-2/3}$. To promote consistency with the rest of the proof, we introduce the notation $S_n^{(1)} := S_n^{\leqslant}$ for the low-mark edge count. The normalized edge counts are defined using $n^{-\gamma}$ in place of $n^{-1/2}$ as in the case of $\gamma < 1/2$, i.e.,

$$\overline{S}_n^{\geqslant}(\,\cdot\,) := n^{-\gamma}(S_n^{\geqslant}(\,\cdot\,) - \mathbb{E}[S_n^{\geqslant}(\,\cdot\,)]) \quad \text{and} \quad \overline{S}_n^{(1)}(\,\cdot\,) := n^{-\gamma}(S_n^{(1)}(\,\cdot\,) - \mathbb{E}[S_n^{(1)}(\,\cdot\,)]).$$

Next, we define the Skorokhod metric d_{Sk} used in the proof of Theorem D.2.6.

Definition D.7.1 (Skorokhod metric)**.** *Let $f, g \in D([0,1], \mathbb{R})$. The Skorokhod metric $d_{\mathsf{Sk}}(f, g)$ is defined as*

$$d_{\mathsf{Sk}}(f, g) := \inf_\lambda \Big(\|\lambda - I\| \vee \|f \circ \lambda^{-1} - g\| \Big),$$

where the infimum is over all homeomorphisms λ from $[0,1]$ to itself, I is the identity map and $\|\cdot\|$ is the supremum norm on $[0,1]$.

The main steps of the first part of the proof of Theorem D.2.6 are as follows. In Step 1, we show that the normalized high-mark edge count is negligible, which is the following statement whose proof, together with the proofs of the remaining statements in this section, is given in Section D.11.

Proposition D.7.2 (High-mark edge count is negligible)**.** *Let $\gamma > 1/2$ and $\gamma' < 1/4$. Then,*

$$\overline{S}_n^{\geqslant}(\,\cdot\,) \xrightarrow[n\uparrow\infty]{d} 0$$

in the Skorokhod space $D([0,1], \mathbb{R})$,

In Step 2, after neglecting the high-mark edges, we approximate the low-mark edge count $S_n^{(1)}$ by a sum of conditional expectations $S_n^{(2)}$ of the neighborhoods of the points, defined as

$$S_n^{(2)}(\,\cdot\,) := \sum_{P \in \mathcal{P} \cap (\mathbb{S}_n^{\leqslant u_n} \times \mathbb{T})} \mathbb{E}\big[\deg(P; \,\cdot\,) \mid P\big]$$

$$\overline{S}_n^{(2)}(\,\cdot\,) := n^{-\gamma}\big(S_n^{(2)}(\,\cdot\,) - \mathbb{E}\big[S_n^{(2)}(\,\cdot\,)\big]\big).$$

Remark D.7.3. *We crucially note that $\overline{S}_n^{(2)}$ is devoid of the spatial correlations of the neighborhoods.*

The following proposition states that $\overline{S}_n^{(2)}$ is indeed an approximation in the sense that the difference between the two edge counts is negligible.

Proposition D.7.4 (Approximation of the low-mark edge count)**.** *Let $\gamma > 1/2$ and $\gamma' \in (0, 1)$. Then,*

$$\|\overline{S}_n^{(1)} - \overline{S}_n^{(2)}\| \xrightarrow[n\uparrow\infty]{\mathbb{P}} 0,$$

in probability.

179

This part of the proof is concluded after approximating $\overline{S}_n$ by $\overline{S}_n^{(2)}$.

In the second part of the proof, we show that the approximated low-mark edge count $\overline{S}_n^{(2)}$ converges in distribution to $\overline{S}$ as $n \to \infty$, where $\overline{S}$ is defined in the statement of Theorem D.2.6. Before presenting the remaining steps of the proof, recall the definition of the measure ν, the Poisson point process $\mathcal{P}_\infty$, and that of $\overline{S}(\,\cdot\,)$ from the statement of Theorem D.2.6. Also recall that

$$\mathbb{E}[\deg(P;t) \mid P] = |N(P;t)| = |N_{\mathsf{s}}(P_{\mathsf{s}})||N_{\mathsf{t}}(P_{\mathsf{t}};t)| = \tilde{c}U^{-\gamma}(t-B)\,\mathbb{1}\{B \leqslant t \leqslant B+L\},$$

where $\tilde{c} = 2\beta/(1-\gamma')$. Then, for all window sizes n and $\varepsilon > 0$, we define the edge count $S_{n,\varepsilon}^{(3)}$ together with its centered, normalized version as

$$S_{n,\varepsilon}^{(3)}(\,\cdot\,) := \sum_{P \in \mathcal{P} \cap (\mathbb{S}_n \times \mathbb{T})} \mathbb{E}[\deg(P;\,\cdot\,) \mid P]\,\mathbb{1}\{U \leqslant 1/(\varepsilon n)\}$$

$$\overline{S}_{n,\varepsilon}^{(3)}(\,\cdot\,) := n^{-\gamma}(S_{n,\varepsilon}^{(3)}(\,\cdot\,) - \mathbb{E}[S_{n,\varepsilon}^{(3)}(\,\cdot\,)]).$$

Furthermore, recall the definition of the edge count S_ε^* and its centered version $\overline{S}_\varepsilon^*$ from (D.3). Note that $S_{n,\varepsilon}^{(3)}$ and S_ε^* are defined on different probability spaces. The second part of the proof is divided into three steps, Steps 3, 4, and 5, which are illustrated in Figure D.5, and based on arguments presented in [93, Sections 5.5 and 7.2]. The approach is summarized as follows.

- In Step 3, we show that $\overline{S}_{n,\varepsilon}^{(3)}$ converges to $\overline{S}_n^{(2)}$ in $D([0,1],\mathbb{R})$ as $\varepsilon \to 0$ uniformly for all n. More specifically, we show that $\lim_{\varepsilon \downarrow 0} \limsup_{n \uparrow \infty} \mathbb{P}(d_{\mathsf{Sk}}(\overline{S}_{n,\varepsilon}^{(3)}, \overline{S}_n^{(2)}) > \delta) = 0$ for all $\delta > 0$. After bounding the Skorokhod distance d_{Sk} with the supremum norm, we apply the plus-minus decomposition of the edge count $S_{n,\varepsilon}^{(3)}$ to show that the supremum norm of the difference converges to zero in probability. The main idea is to decompose the edge count $S_{n,\varepsilon}^{(3)}$ into a sum of a martingale and a continuous process that can be written as a sum of integrals. Note that while other decompositions, such as the Doob–Meyer decomposition, are possible, it is unclear if they satisfy the properties we need in the proof.
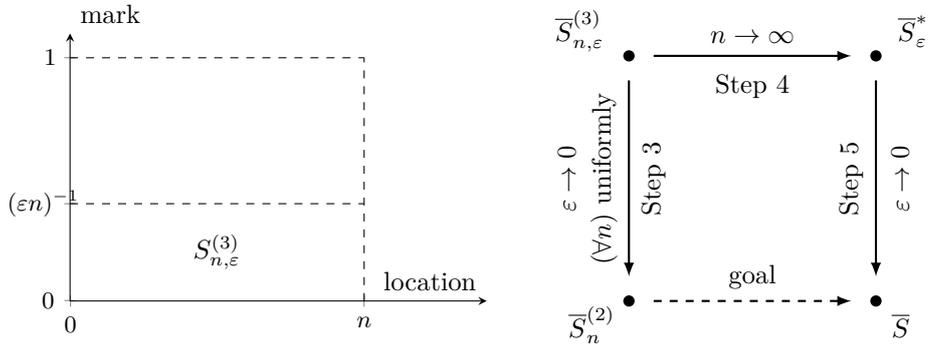
Figure D.5: Main steps of the second part of the proof of Theorem D.2.6. Step 3 shows that $\overline{S}_{n,\varepsilon}^{(3)}$ converges to $\overline{S}_n^{(2)}$ as $\varepsilon \to 0$ uniformly for all n. Step 4 shows convergence of $\overline{S}_{n,\varepsilon}^{(3)}$ to $\overline{S}_\varepsilon^*$ as $n \to \infty$. Finally, Step 5 shows that $\overline{S}_\varepsilon^*$ converges to $\overline{S}$ as $\varepsilon \to 0$.

- In Step 4, we show that the edge count $\overline{S}_{n,\varepsilon}^{(3)}$ with marks less than $(\varepsilon n)^{-1}$ converges in distribution to $\overline{S}_\varepsilon^*$ in $D([0,1], \mathbb{R})$ as $n \to \infty$. We follow the arguments in [93, Section 7.2] to show the above convergence. The main difference in our proof is that we need to show the continuity of the summation functional S_ε^* with respect to the Skorokhod metric. This is done in Proposition D.7.7, and its proof differs from the arguments in [93, Section 7.2.3].

- Finally, in Step 5, we will see that $\overline{S}_\varepsilon^* \to \overline{S}$ almost surely as $\varepsilon \to 0$ in $D([0,1], \mathbb{R})$. In this step, we follow the proof of [93, Proposition 5.7]. While the proof presented in [93, Proposition 5.7] relies on the continuous version of Kolmogorov's inequality [93, Lemma 5.3], we need to apply Lemma D.7.10, which shows that the sequence $\overline{S}_{\varepsilon_n}^*$ is Cauchy in probability with respect to the supremum norm.

Step 3. We begin with Step 3. Since the Skorokhod metric d_{Sk} on $[0,1]$ is bounded by the supremum metric, we have that

$$\lim_{\varepsilon \downarrow 0} \limsup_{n \uparrow \infty} \mathbb{P}\big(d_{\mathsf{Sk}}(\overline{S}_{n,\varepsilon}^{(3)}, \overline{S}_n^{(2)}) > \delta\big) \leqslant \lim_{\varepsilon \downarrow 0} \limsup_{n \uparrow \infty} \mathbb{P}\big(\|\overline{S}_{n,\varepsilon}^{(3)} - \overline{S}_n^{(2)}\| > \delta\big). \tag{D.6}$$

To show that the right-hand side is zero, we turn again to the *plus-minus decomposition* $S_{n,\varepsilon}^{(3)} = S_{n,\varepsilon}^{(3),+} - S_{n,\varepsilon}^{(3),-}$, i.e.,

$$S_{n,\varepsilon}^{(3),\pm}(\,\cdot\,) := \sum_{P \in \mathcal{P} \cap (\mathbb{S}_n^{\leqslant 1/(\varepsilon n)} \times \mathbb{T}^{0 \leqslant})} \mathbb{E}[\deg^\pm(P; \cdot) \mid P] = \sum_{P \in \mathcal{P} \cap (\mathbb{S}_n^{\leqslant 1/(\varepsilon n)} \times \mathbb{T}^{0 \leqslant})} |N^\pm(P; \cdot)| \text{ and}$$

$$\overline{S}_n^{(2),\pm}(\,\cdot\,) := n^{-\gamma}(S_{n,\varepsilon}^{(3),\pm}(\,\cdot\,) - \mathbb{E}[S_{n,\varepsilon}^{(3),\pm}(\,\cdot\,)]).$$

To show that the right-hand side of (D.6) is zero, we verify the convergence result for the *plus* and *minus* cases separately.

Proposition D.7.5 (Convergence of $S_{n,\varepsilon}^{(3),\pm}$ to $S_n^{(2),\pm}$)**.** *Let $\gamma > 1/2$ and $\gamma' \in (0,1)$. Then,*

$$\limsup_{n \uparrow \infty} \big\|\overline{S}_{n,\varepsilon}^{(3),\pm} - \overline{S}_n^{(2),\pm}\big\| \xrightarrow[\varepsilon \downarrow 0]{\mathbb{P}} 0$$

in probability.

This proposition is the main result of Step 3, and it shows that the edge count of the heaviest vertices approximates the total edge count.

Step 4. The proof of Step 4 begins with a lemma that shows the convergence of the scaled size $n^{-\gamma}|N_{\mathsf{s}}(P_{\mathsf{s}})|$ to a measure.

Lemma D.7.6 (Convergence to a measure)**.** *Let $\gamma > 1/2$ and $\gamma' \in (0,1)$. Then, we have that*

$$n \, \mathbb{P}(n^{-\gamma}|N_{\mathsf{s}}(P_{\mathsf{s}})| \in \,\cdot\,) \xrightarrow[n \uparrow \infty]{v} \nu(\,\cdot\,),$$

where $\xrightarrow{v}$ denotes vague convergence, and ν is the measure defined by $\nu([a,\infty)) := \tilde{c}^{1/\gamma} a^{-1/\gamma}$, i.e., the right-tail probabilities are regularly varying with tail index $-1/\gamma$.

We now turn to the total contributions of the points to $S_{n,\varepsilon}^{(3)}$. The contributions $n^{-\gamma}(|N(P;t)| - \mathbb{E}[|N(P;t)|])$ of single points to the sum $S_{n,\varepsilon}^{(3)}(t)$ are i.i.d. random variables due to the properties of the Poisson process. By Lemma D.7.6, we have that

$$\sum_{P \in \mathcal{P} \cap (\mathbb{S}_n \times \mathbb{T})} \delta_{(n^{-\gamma}|N_\mathsf{s}(P_\mathsf{s})|,B,L)} \xrightarrow[n \uparrow \infty]{d} \mathrm{PPP}(\nu \otimes \mathrm{Leb} \otimes \mathbb{P}_L),$$

where $\mathrm{PPP}(\nu \otimes \mathrm{Leb} \otimes \mathbb{P}_L)$ is a Poisson point process on $\mathbb{J} \times \mathbb{T}$ with intensity measure $\nu \otimes \mathrm{Leb} \otimes \mathbb{P}_L$. To examine the edge count $S_{n,\varepsilon}^{(3)}$, we restrict the domain of the marks $(0,1]$ to $(0, 1/(\varepsilon n)]$, which requires that $n^{-\gamma}|N_\mathsf{s}(P_\mathsf{s})| \geqslant \tilde{c}\varepsilon^\gamma$. Furthermore, we restrict the domain of the points (J, B, L) to $K := \{(J, B, L) \in \mathbb{J} \times \mathbb{T}_{\leqslant 1}^{0\leqslant}\}$, ensuring that the intervals $[B, B+L]$ intersect the interval $[0,1]$. The domain of the marks is visualized in Figure D.6. Then, we consider the summation functional

$$\sum_{(J,B,L) \in \mathcal{P}_\infty \cap ([\tilde{c}\varepsilon^\gamma, \infty) \times \mathbb{T})} \delta_{(J,B,L)} \mapsto \sum_{(J,B,L) \in \mathcal{P}_\infty} J(\,\cdot\, - B)\,\mathbb{1}\{J \geqslant \tilde{c}\varepsilon^\gamma\}\,\mathbb{1}\{B \leqslant \,\cdot\, \leqslant B + L\}.$$

(D.7)

The next result shows the continuity of the above functional. To state it, let $K_\varepsilon := \{(j, b, \ell) \in \mathbb{J} \times \mathbb{T}_{\leqslant 1}^{0\leqslant} : j \geqslant \tilde{c}\varepsilon^\gamma\}$ be the domain of the points contributing to the edge count, see again Figure D.6. As in [93], we consider K_ε to be endowed with the topology where, in the first component, we use the one-point compactification at infinity. That means, we set $\overline{\mathbb{J}} = (0, \infty]$, i.e., we compactify at the point ∞ in the first coordinate. Then, the topology of the space $\overline{K}_\varepsilon$ is the one of the space $\mathbb{J} \times \mathbb{T}_{\leqslant 1}^{0\leqslant}$ with $\mathbb{J}$ compactified at ∞ in the first coordinate. Furthermore, let $\mathbf{N}_{\mathsf{loc}}(\overline{\mathbb{J}} \times \mathbb{T})$ denote the family of point measures on locally finite subsets of $\overline{\mathbb{J}} \times \mathbb{T}$ and consider the summation functional $\chi \colon \mathbf{N}_{\mathsf{loc}}(\overline{\mathbb{J}} \times \mathbb{T}) \to D([0,1], \mathbb{R})$ defined as

$$\chi(\eta)(t) := \chi\Big(\sum_{(j,b,\ell) \in \eta} \delta_{(j,b,\ell)} \Big)(t) := \chi\Big(\sum_{(j,b,\ell) \in \eta} \delta_{(j,b,\ell)}(\,\cdot\, \cap \overline{K}_\varepsilon) \Big)(t)$$
$$:= \sum_{(j,b,\ell) \in \eta} j(t - b)\,\mathbb{1}\{j \geqslant \tilde{c}\varepsilon^\gamma\}\,\mathbb{1}\{b \leqslant t \leqslant b + \ell\}.$$

Proposition D.7.7 (Continuity of summation functional)**.** *It holds that $\chi(\eta)(t)$ is almost surely continuous with respect to the distribution of $\mathrm{PPP}(\nu \otimes \mathrm{Leb} \otimes \mathbb{P}_L)$.*
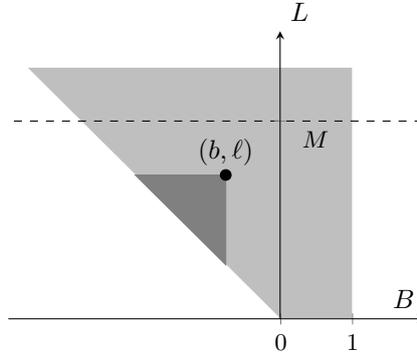
Figure D.6: Domain of the endpoints of the intervals intersecting with the time interval $[0,1]$

Note that if $j = n^{-\gamma}|N_{\mathsf{s}}(p_{\mathsf{s}})|$ for a point $p \in \mathbb{S}_n \times \mathbb{T}$ in Proposition D.7.7, then the first indicator is equivalent to $u \leqslant 1/(\varepsilon n)$. From Proposition D.7.7, we get the following convergence in $D([0,1], \mathbb{R})$,

$$n^{-\gamma} S_{n,\varepsilon}^{(3)}(\,\cdot\,) \xrightarrow[n\uparrow\infty]{d} S_{\varepsilon}^*(\,\cdot\,).$$

The following lemma shows that the expectation of the edge count S_{ε}^* is finite.

Lemma D.7.8 (Expectation of S_{ε}^*). *Let $\gamma > 1/2$. Then,*

$$\mathbb{E}\big[S_{\varepsilon}^*\big] = \frac{\tilde{c}}{1-\gamma} \varepsilon^{-(1-\gamma)}.$$

Then, for the centered and scaled edge count $\overline{S}_{n,\varepsilon}^{(3)}$, we have the convergence in $D([0,1], \mathbb{R})$,

$$\overline{S}_{n,\varepsilon}^{(3)}(\,\cdot\,) \xrightarrow[n\uparrow\infty]{d} \overline{S}_{\varepsilon}^*(\,\cdot\,).$$

Step 5. Finally, in Step 5, we show that $\overline{S}_{\varepsilon}^* \to \overline{S}$ in $D([0,1], \mathbb{R})$ as $\varepsilon \to 0$ almost surely. As a preliminary result, we first follow closely Resnick [93, Section 5.5.1] to show that almost sure convergence happens for all fixed time points $t \in [0,1]$ as $\varepsilon \to 0$.

Lemma D.7.9 (Convergence of $\overline{S}_{\varepsilon}^*(t)$ for fixed time points). *For a fixed $t \in [0,1]$, we have almost surely that*

$$\overline{S}_{\varepsilon}^*(t) \xrightarrow[\varepsilon\downarrow 0]{\text{a.s.}} \overline{S}(t).$$

Following the proof of [93, Proposition 5.7], we aim to show that the convergence is almost surely uniform. Before we do that, we need to show that the sequence $\overline{S}_{\varepsilon_n}^*$ is Cauchy in probability with respect to the supremum norm in the sense stated below.

Lemma D.7.10 ($\overline{S}_{\varepsilon_n}^*$ is Cauchy in probability). *Let $\varepsilon_k \to 0$ be a decreasing sequence as $k \to \infty$. Then,*

$$\sup_{n,m \geqslant N} \|\overline{S}_{\varepsilon_n}^* - \overline{S}_{\varepsilon_m}^*\| \xrightarrow[N\uparrow\infty]{\mathbb{P}} 0.$$

Next, in Proposition D.7.11, we present the main result of this step. We show that there exists $\overline{S}$ with almost all paths in $D([0,1], \mathbb{R})$ such that $\lim_{\varepsilon\downarrow 0}\|\overline{S}_{\varepsilon}^* - \overline{S}\| = 0$ almost surely, which is done by showing that the sequence $\overline{S}_{\varepsilon_n}^*$ is almost surely Cauchy with respect to the supremum norm on $[0,1]$.

Proposition D.7.11 ($\overline{S}_{\varepsilon_n}^*$ is Cauchy almost surely). *Let $\varepsilon_k \to 0$ be a decreasing sequence as $k \to \infty$. Then,*

$$\sup_{n,m \geqslant N} \|\overline{S}_{\varepsilon_n}^* - \overline{S}_{\varepsilon_m}^*\| \xrightarrow[N\uparrow\infty]{\text{a.s.}} 0.$$

By Proposition D.7.11, there exists $\overline{S}$ such that $\lim_{\varepsilon\downarrow 0}\|\overline{S}_{\varepsilon}^* - \overline{S}\| = 0$ almost surely. Furthermore, the limit $\overline{S}$ is in $D([0,1], \mathbb{R})$ by Resnick [93, Lemma 5.2].

D.8 Preliminary lemmas

Before presenting the proofs of the main propositions and lemmas, we collect some minor results that are used frequently in the proofs later. We begin with a lemma regarding the size of the spatial neighborhoods of points.

Lemma D.8.1 (Size of spatial neighborhoods). *Let* $\gamma, \gamma' \in (0,1)$.

(a) *For all* $p_{\mathsf{s}} \in \mathbb{S}$, *we have that*

$$|N_{\mathsf{s}}(p_{\mathsf{s}})| = \frac{2\beta}{1-\gamma'} u^{-\gamma}.$$

(b) *For all* $p_{\mathsf{s},1}, p_{\mathsf{s},2} \in \mathbb{S}$, *we have that*

$$|N_{\mathsf{s}}(p_{\mathsf{s},1}, p_{\mathsf{s},2})| \leqslant 2 \frac{(2\beta)^{1/\gamma'}}{1-\gamma'} |x_1 - x_2|^{-(1/\gamma'-1)} u_1^{-\gamma/\gamma'} u_2^{-\gamma/\gamma'}.$$

(c) *For all* $u_- \in [0,1]$, *the size of the spatial neighborhood of a point* p' *is given by*

$$\int_{\mathbb{S}^{u_- \leqslant}} \mathbb{1}\{p'_{\mathsf{s}} \in N_{\mathsf{s}}(p_{\mathsf{s}})\} \, \mathrm{d}p_{\mathsf{s}} = \frac{2\beta}{1-\gamma} w^{-\gamma'} (1 - u_-^{1-\gamma}).$$

The following lemma concerns the integrals of spatial neighborhoods.

Lemma D.8.2 (Integrals of spatial neighborhoods $N_{\mathsf{s}}(p_{\mathsf{s}})$). *We have the following.*

(a) *Let* $\gamma, \gamma' \in (0,1)$, $A \subseteq \mathbb{R}$ *a Borel set and* $\alpha \geqslant 0$. *Then, if* $\gamma < 1/\alpha$,

$$\int_{\mathbb{S}_A} |N_{\mathsf{s}}(p_{\mathsf{s}})|^\alpha \, \mathrm{d}p_{\mathsf{s}} = \left(\frac{2\beta}{1-\gamma'}\right)^\alpha \frac{|A|}{1-\alpha\gamma}.$$

If $\gamma \in (0,1)$ *and* $u_- \in (0,1]$, *then*

$$\int_{\mathbb{S}_A^{u_- \leqslant}} |N_{\mathsf{s}}(p_{\mathsf{s}})|^\alpha \, \mathrm{d}p_{\mathsf{s}} = \begin{cases} \left(\frac{2\beta}{1-\gamma'}\right)^\alpha \frac{|A|}{1-\alpha\gamma}\left(1 - u_-^{1-\alpha\gamma}\right) & \text{if } \gamma \neq 1/\alpha \\ \left(\frac{2\beta}{1-\gamma'}\right)^\alpha |A| \log(u_-^{-1}) & \text{if } \gamma = 1/\alpha. \end{cases}$$

(b) *Let* $\gamma \in (0,1)$ *and* $\gamma' < 1/m$. *Then,*

$$\frac{1}{n} \int_{\mathbb{S}_n^m} |N_{\mathsf{s}}(\boldsymbol{p}_{\mathsf{s},m})| \, \mathrm{d}\boldsymbol{p}_{\mathsf{s},m} \nearrow \frac{(2\beta)^m}{(1-\gamma)^m(1-m\gamma')} \qquad \text{as } n \to \infty,$$

where $\nearrow$ *denotes convergence from below.*

(c) Let $u_n = n^{-b}$ denote an n-dependent mark with $b \in (0,1)$. Furthermore, let $\gamma \in (0,1)$ and $\gamma' < 1/m$. Then,

$$\frac{1}{n} \int_{\left(\mathbb{S}_n^{u_n \leqslant}\right)^m} |N_{\mathsf{s}}(\boldsymbol{p}_{\mathsf{s},m})| \, \mathrm{d}\boldsymbol{p}_{\mathsf{s},m} \nearrow \frac{(2\beta)^m}{(1-\gamma)^m(1-m\gamma')} \qquad \text{as } n \to \infty.$$

(d) Let $m > 0$ be a positive integer, let $\gamma \in (0,1)$ and $\gamma' < 1/m$. Then,

$$\int_{\mathbb{S}} \left(\int_{\mathbb{S}_n} \mathbb{1}\{p_{\mathsf{s}}' \in N_{\mathsf{s}}(p_{\mathsf{s}})\} \, \mathrm{d}p_{\mathsf{s}} \right)^m \mathrm{d}p_{\mathsf{s}}' \leqslant \left(\frac{2\beta}{1-\gamma} \right)^m \frac{n}{1-m\gamma'}.$$

(e) We set $m_1, m_2, m_3 \in \{0,1,2,\ldots\}$, $\gamma < (1+(m_1 \vee m_2)+m_3)^{-1}$ and $\gamma' < (2+m_3)^{-1}$. Then,

$$\iint_{\mathbb{S}_n^2} |N_{\mathsf{s}}(p_{\mathsf{s},1})|^{m_1} |N_{\mathsf{s}}(p_{\mathsf{s},1}, p_{\mathsf{s},2})| |N_{\mathsf{s}}(p_{\mathsf{s},2})|^{m_2} |x_1 - x_2|^{m_3} \, \mathrm{d}(x_1, u_1) \, \mathrm{d}(x_2, u_2)$$

$$\leqslant c(c' + c'')n$$

$$c = \frac{(2\beta)^{2+m_1+m_2+m_3}}{(1+m_3)(1-\gamma')^{m_1+m_2}(1-(2+m_3)\gamma')}$$

$$c' = \frac{1}{(1-(1+m_1)\gamma)(1-(1+m_2+m_3)\gamma)}$$

$$c'' = \frac{1}{(1-(1+m_2)\gamma)(1-(1+m_1+m_3)\gamma)}.$$

Note that the bound is always nonnegative.

(f) We set $m_1, m_2, m_3 \in \{0,1,2,\ldots\}$, $\gamma > 1/2$, $\gamma' < (2+m_3)^{-1}$ and $u_- \in (0,1]$ a mark. Then,

$$\iint_{\left(\mathbb{S}_n^{u_- \leqslant}\right)^2} |N_{\mathsf{s}}(p_{\mathsf{s},1})|^{m_1} |N_{\mathsf{s}}((x_1, u_1), (x_2, u_2))| |N_{\mathsf{s}}((x_2, u_2))|^{m_2}$$

$$\times |x_1 - x_2|^{m_3} \, \mathrm{d}(x_1, u_1) \, \mathrm{d}(x_2, u_2)$$

$$\leqslant c \Big(|c'| u_-^{-((1+m_2+m_3)\gamma-1)_+ - ((1+m_1)\gamma-1)_+}$$

$$+ |c''| u_-^{-((1+m_1+m_3)\gamma-1)_+ - ((1+m_2)\gamma-1)_+} \Big) n,$$

where $(\,\cdot\,)_+ := \,\cdot\, \vee 0$, the constants c, c' and c'' are defined as in Part (e) of this lemma.

The next lemma is about the size of the temporal neighborhood of points.

Lemma D.8.3 (Size of temporal neighborhoods)**.** *Let $t \in \mathbb{R}$.*

(a) For all $p_{\mathsf{t}} = (b, \ell) \in \mathbb{T}$, we have that

$$|N_{\mathsf{t}}(p_{\mathsf{t}}; t)| = (t - b) \, \mathbb{1}\{b \leqslant t \leqslant b + \ell\}.$$

(b) *For all $p_{\mathsf{t}} = (b, \ell) \in \mathbb{T}$ and $r \in \mathbb{R}$, the size of the temporal neighborhood of a point p' is given by*

$$\int_{\mathbb{T}} \mathbb{1}\{r \in N_{\mathsf{t}}(p_{\mathsf{t}}; t)\} \, \mu_{\mathsf{t}}(\mathrm{d}p_{\mathsf{t}}) = \mathbb{1}\{r \leqslant t\}\mathrm{e}^{-(t-r)}.$$

The following lemma characterizes some of the temporal integrals that will be used in the proof.

Lemma D.8.4 (Integrals of temporal neighborhoods $N_{\mathsf{t}}(p_{\mathsf{t}}; t)$). *We have the following.*

(a) *For all $\alpha > 0$ we have that*

$$\int_{\mathbb{T}} |N_{\mathsf{t}}(p_{\mathsf{t}}; t)|^{\alpha} \, \mu_{\mathsf{t}}(\mathrm{d}p_{\mathsf{t}}) = \Gamma(\alpha + 1).$$

(b) *For all $t \in \mathbb{R}$, the integral of the common temporal neighborhood of the points $\boldsymbol{p}_m$ is given by*

$$\int_{\otimes_{i=1}^{m} \mathbb{T}_i} \left| \bigcap_{i=1}^{m} N_{\mathsf{t}}(p_i; t_i) \right| (\mathrm{d}\boldsymbol{b}_m \mathbb{P}_L^{\otimes m}(\mathrm{d}\boldsymbol{\ell}_m))$$
$$= \int_{\mathbb{R}} \prod_{i=1}^{m} \left(\int_{\mathbb{T}_i} \mathbb{1}\{r \in N_{\mathsf{t}}(p_{\mathsf{t}}; t)\} \, \mu_{\mathsf{t}}(\mathrm{d}p_{\mathsf{t}}) \right) \mathrm{d}r.$$

Furthermore, if $\mathbb{T}_i = \mathbb{T}$ and $t_i = t$ for all indices $i \in \{1, \ldots, m\}$, then the right-hand side equals $1/m$.

(c) *For all $\alpha_1, \alpha_2 > 0$, we have that*

$$\int_{\mathbb{T}} \int_{\mathbb{T}} |N_{\mathsf{t}}(p_{\mathsf{s},1}; t_1)|^{\alpha_1} |N_{\mathsf{t}}(p_{\mathsf{s},1}; t_1) \cap N_{\mathsf{t}}(p_{\mathsf{s},2}; t_2)| |N_{\mathsf{t}}(p_{\mathsf{s},2}; t_2)|^{\alpha_2} p_{\mathsf{s},2} \, \mu_{\mathsf{t}}(\mathrm{d}p_{\mathsf{s},1})$$
$$\leqslant \Gamma(\alpha_1 + 1)\Gamma(\alpha_2 + 2).$$

(d) *For all $\alpha > 0$, we have that*

$$\int_{\mathbb{R}} \left(\int_{\mathbb{T}} \mathbb{1}\{r \in N_{\mathsf{t}}(p_{\mathsf{t}}; t)\} \, \mu_{\mathsf{t}}(\mathrm{d}p_{\mathsf{t}}) \right)^{\alpha} \mathrm{d}r = \frac{1}{\alpha}.$$

Next, we introduce notation for the differences of temporal neighborhoods of a point p between two times $t_1 < t_2$,

$$\begin{aligned}
\delta_{t_1,t_2}(N_{\mathsf{t}}^{\pm}(p_{\mathsf{t}})) &:= N_{\mathsf{t}}^{\pm}(p_{\mathsf{t}}; t_2) \setminus N_{\mathsf{t}}^{\pm}(p_{\mathsf{t}}; t_1) \\
\delta_{t_1,t_2}(N^{\pm}(p)) &:= N^{\pm}(p; t_2) \setminus N^{\pm}(p; t_1) = N_{\mathsf{s}}(p_{\mathsf{s}}) \times \delta_{t_1,t_2}(N_{\mathsf{t}}^{\pm}(p_{\mathsf{t}}; t)).
\end{aligned} \tag{D.8}$$

Then, the size of the temporal *plus-minus neighborhoods* is given in the next lemma.

Lemma D.8.5 (Size of $N_{\mathsf{t}}^{\pm}(p_{\mathsf{t}};t)$). *Let $t, t_1, t_2 \in [0,1]$ be fixed.*

(a) The size of the temporal neighborhoods is given by

$$|N_{\mathsf{t}}^{+}(p_{\mathsf{t}};t)| = (((b+\ell)\wedge t) - b)\,\mathbb{1}\{b \leqslant t\} \qquad and \qquad |N_{\mathsf{t}}^{-}(p_{\mathsf{t}};t)| = \ell\,\mathbb{1}\{b+\ell \leqslant t\}.$$

(b) The change of the temporal neighborhood of a point p between $t_1 < t_2$ is given by

$$\left|\delta_{t_1,t_2}(N_{\mathsf{t}}^{+}(p_{\mathsf{t}};t_2))\right| = (((b+\ell)\wedge t) - (b\vee t_1))\,\mathbb{1}\{b \leqslant t_2\}\,\mathbb{1}\{t_1 \leqslant b+\ell\} \; and$$
$$\left|\delta_{t_1,t_2}(N_{\mathsf{t}}^{-}(p_{\mathsf{t}};t_2))\right| = (t_1 - b)\,\mathbb{1}\{b \leqslant t_1 \leqslant b+\ell \leqslant t_2\}.$$

(c) The size of the temporal neighborhood of a point p' is given by

$$\int_{\mathbb{T}^{0\leqslant}} \mathbb{1}\{r \in N_{\mathsf{t}}^{+}(p_{\mathsf{t}};t)\}\,\mu_{\mathsf{t}}(\mathrm{d}p_{\mathsf{t}}) = \mathbb{1}\{r \leqslant 0\}\mathrm{e}^{-(-r)} + \mathbb{1}\{0 \leqslant r \leqslant t\} \; and$$

$$\int_{\mathbb{T}^{0\leqslant}} \mathbb{1}\{r \in N_{\mathsf{t}}^{-}(p_{\mathsf{t}};t)\}\,\mu_{\mathsf{t}}(\mathrm{d}p_{\mathsf{t}})$$
$$= \mathbb{1}\{r \leqslant 0\}(\mathrm{e}^{r} - \mathrm{e}^{-(t-r)}) + \mathbb{1}\{0 \leqslant r \leqslant t\}(1 - \mathrm{e}^{-(t-r)}).$$

The next lemma is about the integrals of the temporal *plus-minus neighborhoods*.

Lemma D.8.6 (Integrals of $N_{\mathsf{t}}^{\pm}(p_{\mathsf{t}};t)$). *Let $t, t_1, t_2 \in [0,1]$ be fixed.*

(a) For all integers $m \geqslant 1$, we have that

$$\int_{\mathbb{T}^{0\leqslant}} |N_{\mathsf{t}}^{+}(p_{\mathsf{t}};t)|^{m}\,\mu_{\mathsf{t}}(\mathrm{d}p_{\mathsf{t}}) = m!(t+1) \quad and$$
$$\int_{\mathbb{T}^{0\leqslant}} |N_{\mathsf{t}}^{-}(p_{\mathsf{t}};t)|^{m}\,\mu_{\mathsf{t}}(\mathrm{d}p_{\mathsf{t}}) = m!t.$$

(b) For all $\alpha \geqslant 0$, we have that $\int_{\mathbb{T}^{0\leqslant}} |N_{\mathsf{t}}^{\pm}(p_{\mathsf{t}};t)|^{\alpha}\,\mu_{\mathsf{t}}(\mathrm{d}p_{\mathsf{t}}) \leqslant 2ct + \Gamma(\alpha+1)$, where $c := (2\alpha)^{\alpha}\mathrm{e}^{-\alpha}$.

(c) For all integers $m \geqslant 1$, we have that $\int_{\mathbb{T}^{0\leqslant}} \left|\delta_{t_1,t_2}(N_{\mathsf{t}}^{\pm}(p_{\mathsf{t}}))\right|^{m}\,\mu_{\mathsf{t}}(\mathrm{d}p_{\mathsf{t}}) \leqslant (t_2 - t_1)^{m}$.

(d) For all integers $m \geqslant 1$, we have that

$$\int_{\mathbb{R}}\left(\int_{\mathbb{T}^{0\leqslant}} \mathbb{1}\{r \in \delta_{t_1,t_2}(N_{\mathsf{t}}^{\pm}(p_{\mathsf{t}}))\}\,\mu_{\mathsf{t}}(\mathrm{d}p_{\mathsf{t}})\right)^{m}\mathrm{d}r = t_2 - t_1.$$

(e) For all integers $m \geqslant 1$, the integral of the intersection of the neighborhoods is given by

$$\iint_{(\mathbb{T}^{0\leqslant})^{m}} |N_{\mathsf{t}}^{+}(\boldsymbol{p}_{\mathsf{t},m};t)|\,\mu_{\mathsf{t}}^{\otimes m}(\mathrm{d}\boldsymbol{p}_{\mathsf{t},m})$$
$$= \int_{\mathbb{R}}\left(\int_{\mathbb{T}^{0\leqslant}} \mathbb{1}\{r \in N_{\mathsf{t}}^{\pm}(p_{\mathsf{t}};t)\}\,\mu_{\mathsf{t}}(\mathrm{d}p_{\mathsf{t}})\right)^{m}\mathrm{d}r \leqslant 1/m + t.$$

(f) For all $\alpha_1, \alpha_2 \geqslant 0$, we have that

$$\iint_{\left(\mathbb{T}_{\leqslant 1}^{0\leqslant}\right)^2} |N_{\mathsf{t}}^{\pm}(p_{\mathsf{s},1}; t_1)|^{\alpha_1} |N_{\mathsf{t}}^{\pm}(p_1; t_1) \cap N_{\mathsf{t}}^{\pm}(p_{\mathsf{s},2}; t_2)|$$
$$\times |N_{\mathsf{t}}^{\pm}(p_{\mathsf{s},2}; t_2)|^{\alpha_2} \, \mu_{\mathsf{t}}(\mathrm{d}p_{\mathsf{s},1}) \, \mu_{\mathsf{t}}(\mathrm{d}p_{\mathsf{s},2}) < \infty.$$

D.9 Proofs of the lemmas used for Propositions D.2.1, D.2.2, and D.2.3

In this section, we assume that $\gamma < 1/2$, and we do not explicitly mention this condition in the proofs.

Proofs of Lemmas D.3.1 and D.3.2

First, we present the proofs of the lemmas used in the proofs of Propositions D.2.1. The proofs are based on the application of the Mecke formula [66, Theorem 4.1] and the independence property [66, Definition 3.1 (ii)] of the Poisson process.

Proof of Lemma D.3.1. The mean of the edge count $S_n(t)$ is given by

$$\mathbb{E}[S_n(t)] = \mathbb{E}\Big[\sum_{P \in \mathcal{P} \cap (\mathbb{S}_n \times \mathbb{T})} \deg(P) \Big] = \int_{\mathbb{S}_n \times \mathbb{T}} |N(p)| \, \mu(\mathrm{d}p) = \frac{2\beta}{(1-\gamma)(1-\gamma')} n,$$

where we used the Mecke formula in the second step and Lemmas D.8.2 (a) and D.8.4 (a) with $\alpha = 1$ in the third step. Next, we calculate the variance using the Mecke formula:

$$\begin{aligned}
\mathrm{Var}(S_n(t)) &= \mathbb{E}\Big[\sum_{(P_1, P_2) \in (\mathcal{P} \cap (\mathbb{S}_n \times \mathbb{T}))^2_{\neq}} \deg(P_1) \deg(P_2) \Big] \\
&\quad - \mathbb{E}\Big[\sum_{P \in \mathcal{P} \cap (\mathbb{S}_n \times \mathbb{T})} \deg(P) \Big]^2 + \mathbb{E}\Big[\sum_{P \in \mathcal{P} \cap (\mathbb{S}_n \times \mathbb{T})} \deg(P)^2 \Big] \\
&= \int_{\mathbb{S}_n \times \mathbb{T}} \mathbb{E}[\deg(p)^2] \, \mu(\mathrm{d}p) \\
&\quad + \iint_{(\mathbb{S}_n \times \mathbb{T})^2} \mathrm{Cov}(\deg(p_1), \deg(p_2)) \, \mu(\mathrm{d}p_1) \, \mu(\mathrm{d}p_2).
\end{aligned} \tag{D.9}$$

The above formula represents the variance of a U-statistic, which was also calculated in a more general setting in [92, Lemma 3.5]. We can see that in the first step, the variance is determined by the last term, where $P = P_1 = P_2$, since the first two terms

cancel. For the first term, we have

$$
\mathbb{E}[\deg(p)^2] = \mathbb{E}\Big[\Big(\sum_{P' \in \mathcal{P}'} \mathbb{1}\{P' \in N(p)\}\Big)^2\Big]
$$

$$
= \mathbb{E}\Big[\sum_{P' \in \mathcal{P}'} \mathbb{1}\{P' \in N(p)\}\Big] + \mathbb{E}\Big[\sum_{\{P_1', P_2'\} \in (\mathcal{P}')^2_{\neq}} \mathbb{1}\{P_1' \in N(p)\}\,\mathbb{1}\{P_2' \in N(p)\}\Big]
$$

$$
= \int_{\mathbb{S}\times\mathbb{R}} \mathbb{1}\{p' \in N(p)\}\,\mathrm{d}p' + \Big(\int_{\mathbb{S}\times\mathbb{R}} \mathbb{1}\{p' \in N(p)\}\,\mathrm{d}p'\Big)^2 = |N(p)| + |N(p)|^2.
$$
(D.10)

The first term is the integral of the above expression:

$$
\lim_{n\uparrow\infty} \frac{1}{n} \int_{\mathbb{S}_n \times \mathbb{T}} \mathbb{E}[\deg(p)^2]\,\mu(\mathrm{d}p) = \sum_{k=1}^{2} \lim_{n\uparrow\infty} \frac{1}{n} \int_{\mathbb{S}_n} |N_{\mathsf{s}}(p_{\mathsf{s}})|^k\,\mathrm{d}p_{\mathsf{s}} \int_{\mathbb{T}} |N_{\mathsf{t}}(p_{\mathsf{t}})|^k\,\mu_{\mathsf{t}}(\mathrm{d}p_{\mathsf{t}})
$$

$$
= \frac{2\beta}{(1-\gamma)(1-\gamma')} + \frac{(2\beta)^2}{(1-2\gamma)(1-\gamma')^2},
$$

where we applied Lemmas D.8.2 (a) and D.8.4 (a), and it is required that $\gamma < 1/2$. For the second term, we have

$$
\mathrm{Cov}(\deg(p_1), \deg(p_2))
$$

$$
= \mathbb{E}\Big[\sum_{P' \in \mathcal{P}'} \mathbb{1}\{P' \in N(p_1, p_2)\}\Big] + \mathbb{E}\Big[\sum_{(P_1', P_2') \in \mathcal{P}'^2_{\neq}} \mathbb{1}\{P_1' \in N(p_1), P_2' \in N(p_2)\}\Big]
$$

$$
- \mathbb{E}\Big[\sum_{P' \in \mathcal{P}'} \mathbb{1}\{P' \in N(p_1)\}\Big] \mathbb{E}\Big[\sum_{P' \in \mathcal{P}'} \mathbb{1}\{P' \in N(p_2)\}\Big]
$$

$$
= \int_{\mathbb{S}\times\mathbb{R}} \mathbb{1}\{p' \in N(p_1, p_2)\}\,\mathrm{d}p' = |N(p_1, p_2)|.
$$

Note that just as in the case of the variance, the covariance is determined by the term in which $P' = P_1' = P_2'$. This insight will be used multiple times in the subsequent calculations. As $|N(p_1, p_2)|$, factorizes to the spatial and temporal parts, applying Lemmas D.8.2 (b) and D.8.4 (b) with $m = 2$, we have for the second term that

$$
\lim_{n\uparrow\infty} \frac{1}{n} \iint_{(\mathbb{S}_n \times \mathbb{T})^2} \mathrm{Cov}(\deg(p_1), \deg(p_2))\,\mu(\mathrm{d}p_1)\,\mu(\mathrm{d}p_2)
$$

$$
= \lim_{n\uparrow\infty} \frac{1}{n} \iint_{(\mathbb{S}_n \times \mathbb{T})^2} |N(p_1, p_2)|\,\mu(\mathrm{d}p_1)\,\mu(\mathrm{d}p_2) = \frac{2\beta^2}{(1-\gamma)^2(1-2\gamma')},
$$

and we require that $\gamma' < 1/2$. Combining the two terms, we have that the variance is asymptotically equal to n, more precisely,

$$
\lim_{n\uparrow\infty} \frac{1}{n} \mathrm{Var}(S_n(t)) = \frac{2\beta}{(1-\gamma)(1-\gamma')} + \frac{(2\beta)^2}{(1-2\gamma)(1-\gamma')^2} + \frac{2\beta^2}{(1-\gamma)^2(1-2\gamma')},
$$

as desired. $\qquad\square$

Proof of Lemma D.3.2. By the definition of the covariance,

$$\mathrm{Cov}(S_{A_1}(t), S_{A_2}(t)) = \mathbb{E}\Big[\sum_{\substack{P_1 \in \mathcal{P} \cap (\mathbb{S}_{A_1} \times \mathbb{T}), \\ P_2 \in \mathcal{P} \cap (\mathbb{S}_{A_2} \times \mathbb{T})}} \deg(P_1; t) \deg(P_2; t)\Big]$$

$$- \mathbb{E}\Big[\sum_{P_1 \in \mathcal{P} \cap (\mathbb{S}_{A_1} \times \mathbb{T})} \deg(P_1; t)\Big] \mathbb{E}\Big[\sum_{P_2 \in \mathcal{P} \cap (\mathbb{S}_{A_2} \times \mathbb{T})} \deg(P_2; t)\Big].$$

As A_1, A_2 are disjoint, $P_1 \neq P_2$, and thus an application of the Mecke formula yields

$$\mathrm{Cov}(S_{A_1}(t), S_{A_2}(t)) = \int_{\mathbb{S}_{A_1} \times \mathbb{T}} \int_{\mathbb{S}_{A_2} \times \mathbb{T}} \mathrm{Cov}(\deg(p_1; t), \deg(p_2; t)) \, \mathrm{d}p_2 \, \mathrm{d}p_1.$$

For the integrand, by the definition of $\deg(p)$, we have that

$$\mathrm{Cov}(\deg(p_1; t), \deg(p_2; t)) = \mathbb{E}\Big[\sum_{P' \in \mathcal{P}'} \mathbb{1}\{P' \in N(p_1, p_2; t)\}\Big]$$

$$+ \mathbb{E}\Big[\sum_{(P_1', P_2') \in (\mathcal{P}')^2_{\neq}} \mathbb{1}\{P_1' \in N(p_1; t)\} \mathbb{1}\{P_2' \in N(p_2; t)\}\Big]$$

$$- \mathbb{E}\Big[\sum_{P_1' \in \mathcal{P}'} \mathbb{1}\{P_1' \in N(p_1; t)\}\Big] \mathbb{E}\Big[\sum_{P_2' \in \mathcal{P}'} \mathbb{1}\{P_2' \in N(p_2; t)\}\Big].$$

The last two terms cancel by the independence of the Poisson process $\mathcal{P}'$, and the Mecke formula gives

$$\mathrm{Cov}(\deg(p_1; t), \deg(p_2; t)) = \int_{\mathbb{S} \times \mathbb{R}} \mathbb{1}\{p' \in N(p_1, p_2; t)\} \, \mathrm{d}p' = |N(p_1, p_2; t)|.$$

Then,

$$\mathrm{Cov}(S_{A_1}(t), S_{A_2}(t)) = \int_{\mathbb{S}_{A_1} \times \mathbb{T}} \int_{\mathbb{S}_{A_2} \times \mathbb{T}} |N(p_1, p_2; t)| \, \mathrm{d}p_2 \, \mathrm{d}p_1$$

$$\leqslant \int_{\mathbb{S}_{A_1} \times \mathbb{T}} \int_{\mathbb{S} \times \mathbb{T}} |N(p_1, p_2; t)| \, \mathrm{d}p_2 \, \mathrm{d}p_1 \leqslant \frac{|A_1|}{2(1 - 2\gamma')} \Big(\frac{2\beta}{1 - \gamma}\Big)^2,$$

where we applied Lemmas D.8.2 (b) and D.8.4 (b). $\qquad\square$

Proofs of Lemmas D.5.1, D.5.5, D.4.1, and D.5.6

Finally, we present the proofs of the lemmas used in the proof of Proposition D.2.3. In Lemma D.5.1, we show that the low-mark edge count converges to 0 in probability.

Proof of Lemma D.5.1. Our proof strategy is applying Chebyshev's inequality and bounding the variance of $S_n^{\leqslant}(t)$. Let $\delta > 0$ arbitrary. Then, applying Chebyshev's inequality yields

$$\mathbb{P}(\overline{S}_n^{\leqslant}(t) > \delta) \leqslant \delta^{-2} n^{-1} \mathrm{Var}(S_n^{\leqslant}(t)).$$

Thus, it is enough to show that $\text{Var}(S_n^{\leqslant}(t)) = o(n)$. We bound the variance by applying the Mecke formula, which, similarly to the proof of Lemma D.3.1, gives

$$\text{Var}(S_n^{\leqslant}(t)) = \int_{\mathbb{S}_n^{\leqslant u_n} \times \mathbb{T}} \mathbb{E}[\deg(p;t)^2]\, \mu(\mathrm{d}p)$$
$$+ \iint_{(\mathbb{S}_n^{\leqslant u_n} \times \mathbb{T})^2} \text{Cov}(\deg(p_1;t), \deg(p_2;t))\, \mu(\mathrm{d}p_1)\, \mu(\mathrm{d}p_2).$$

Using (D.10), we have for the first term

$$\int_{\mathbb{S}_n^{\leqslant u_n} \times \mathbb{T}} \mathbb{E}[\deg(p;t)^2]\, \mu(\mathrm{d}p) = \int_{\mathbb{S}_n^{\leqslant u_n} \times \mathbb{T}} |N(p;t)|^2 + |N(p;t)|\, \mu(\mathrm{d}p)$$
$$= c_1 n u_n^{1-2\gamma} + c_2 n u_n^{1-\gamma},$$

where $c_1 = (2\beta)^2/((1-2\gamma)(1-\gamma')^2)$ and $c_2 = 2\beta/((1-\gamma)(1-\gamma'))$. In the second step, we used Lemma D.8.4 (a) to bound the temporal part by 1 for both terms and used Lemma D.8.2 (a) twice for the spatial parts, once with $u_- = 0$ and once with $u_- = u_n$. Substituting $u_n = n^{-2/3}$, we have that the first term is of order $O(n^{1-2/3(1-2\gamma)}) \subset o(n)$, and the second term is of order $O(n^{1-2/3(1-\gamma)}) \subset o(n)$ as well.

Next, we calculate the covariance term by following the proof of Lemma D.3.1:

$$\iint_{(\mathbb{S}_n^{\leqslant u_n} \times \mathbb{T})^2} \text{Cov}(\deg(p_1;t), \deg(p_2;t))\, \mu(\mathrm{d}p_1)\, \mu(\mathrm{d}p_2)$$
$$= \iint_{(\mathbb{S}_n^{\leqslant u_n} \times \mathbb{T})^2} |N(p_1, p_2;t)|\, \mu(\mathrm{d}p_1)\, \mu(\mathrm{d}p_2).$$

We bound the temporal part by 2 using Lemma D.8.4 (b). Requiring $\gamma' < 1/2$, we bound the spatial part using Lemma D.8.2 (c) and (b). Then,

$$\iint_{(\mathbb{S}_n^{\leqslant u_n} \times \mathbb{T})^2} \text{Cov}(\deg(p_1;t), \deg(p_2;t))\, \mu(\mathrm{d}p_1)\, \mu(\mathrm{d}p_2) \leqslant c_3 n u_n^{2(1-\gamma)} + c_4 n u_n^{1-\gamma},$$

where $c_3 = 2(2\beta)^2/((1-\gamma)^2(1-2\gamma'))$ and $c_4 = 4\beta/((1-\gamma)(1-\gamma'))$. The first term is of order $O(n^{1-4/3(1-\gamma)}) \subset o(n)$, and the second term is of order $O(n^{1-2/3(1-\gamma)}) \subset o(n)$ as well. Thus, the covariance term is of order $O(n)$. $\qquad\square$

The covariance function of the high-mark edge count $\overline{S}_n^{\geqslant}$ was calculated in Lemma D.5.5, whose proof is similar to the proof of Proposition D.2.2.

Proof of Lemma D.5.5. The statement and the proof of Lemma D.5.5 are almost identical to the proof of Proposition D.2.2. The only difference is that we consider the high-mark edge count $\overline{S}_n^{\geqslant}$ instead of the total edge count $\overline{S}_n$, which entails that we need to consider $\mathbb{S}_n^{u_n \leqslant}$ in place of $\mathbb{S}$.

Using the same time interval-based decomposition of the edge count $\overline{S}_n^{\geqslant}$ as we defined in the proof of Proposition D.2.2, the covariance function can again be decomposed into three terms. Employing Lemma D.4.1 finishes the proof of Lemma D.5.5. $\qquad\square$

Next, we show the proof of the lemma used in the proofs of Proposition D.2.2 and Lemma D.5.5, which determined the terms of the limiting covariance functions of the edge counts $\overline{S}_n(t)$ and $\overline{S}_n^{\geqslant}(t)$.

Proof of Lemma D.4.1. We exhibit the terms of the covariance function of the high-mark edge count $\overline{S}_n^{\geqslant}$ when $\gamma < 1/2$. However, using Lemma D.8.2 (b) instead of Lemma D.8.2 (c), the below calculations are also valid for the limiting covariance function of the total edge count $\overline{S}_n$. As Lemma D.8.2 (b) gives a specific limit instead of an upper bound, the results of this proof are also accurate when we apply the steps for $\overline{S}_n$.

Term $\mathrm{Var}(\overline{S}_n^{\mathsf{A}}(t_1, t_2))$.   First, note that $\mathrm{Var}(\overline{S}_n^{\mathsf{A}}(t_1, t_2)) = n^{-1}\,\mathrm{Var}(S_n^{\mathsf{A}}(t_1, t_2))$. Then,

$$
\mathrm{Var}(S_n^{\mathsf{A}}(t_1, t_2)) = \int_{\mathbb{S}_n^{un\leqslant}\times\mathbb{T}_{\leqslant t_1}^{t_2\leqslant}} \mathbb{E}\big[\deg(p; t_1)^2\big]\,\mu(\mathrm{d}p)
$$
$$
+ \iint_{\big(\mathbb{S}_n^{un\leqslant}\times\mathbb{T}_{\leqslant t_1}^{t_2\leqslant}\big)^2} \mathrm{Cov}\big(\deg(p_1; t_1), \deg(p_2; t_1)\big)\,\mu(\mathrm{d}p_1)\,\mu(\mathrm{d}p_2),
$$

where, similarly to the variance term in Section D.3, we kept only the term in which the points are the same in the expansion of the variance, and used Mecke's formula. Using (D.10), we have that

$$
\int_{\mathbb{S}_n^{un\leqslant}\times\mathbb{T}_{\leqslant t_1}^{t_2\leqslant}} \mathbb{E}\big[\deg(p; t_1)^2\big]\,\mu(\mathrm{d}p) = \int_{\mathbb{S}_n^{un\leqslant}\times\mathbb{T}_{\leqslant t_1}^{t_2\leqslant}} \sum_{k=1}^{2}|N(p; t_1)|^k\,\mu(\mathrm{d}p)
$$
$$
= \sum_{k=1}^{2}\int_{\mathbb{S}_n^{un\leqslant}}|N_{\mathsf{s}}(p_{\mathsf{s}})|^k\,\mathrm{d}p_{\mathsf{s}}\int_{\mathbb{T}_{\leqslant t_1}^{t_2\leqslant}}|N_{\mathsf{t}}(p_{\mathsf{t}}; t_1)|^k\,\mu_{\mathsf{t}}(\mathrm{d}p_{\mathsf{t}})
$$
$$
= c_1 n\big(1 - u_n^{1-\gamma}\big)\int_{-\infty}^{t_1}\int_{t_2-b}^{\infty}(t_1 - b)\,\mathbb{P}_L(\mathrm{d}\ell)\,\mathrm{d}b
$$
$$
+ c_2 n\big(1 - u_n^{1-2\gamma}\big)\int_{-\infty}^{t_1}\int_{t_2-b}^{\infty}(t_1 - b)^2\,\mathbb{P}_L(\mathrm{d}\ell)\,\mathrm{d}b
$$
$$
= n\big(c_1(1 - u_n^{1-\gamma}) + 2c_2(1 - u_n^{1-2\gamma})\big)\mathrm{e}^{-(t_2-t_1)},
$$

where $c_1 = 2\beta/((1-\gamma)(1-\gamma'))$, $c_2 = (2\beta)^2/((1-2\gamma)(1-\gamma')^2)$ are positive constants. Substituting $u_n = n^{-2/3}$, we have that

$$
\lim_{n\uparrow\infty}\frac{1}{n}\int_{\mathbb{S}_n^{un\leqslant}\times\mathbb{T}_{\leqslant t_1}^{t_2\leqslant}} \mathbb{E}\big[\deg(p; t_1)^2\big]\,\mu(\mathrm{d}p) = (c_1 + 2c_2)\mathrm{e}^{-(t_2-t_1)}.
$$

The covariance term is calculated the same as in the variance calculation of the edge count $\mathrm{Cov}\big(\deg(p_1; t_1), \deg(p_2; t_1)\big) = |N(p_1, p_2; t_1)|$. After applying Lemma D.8.2 (c) and Lemma D.8.4 (b) with $m = 2$, we have that

$$
\lim_{n\uparrow\infty}\frac{1}{n}\iint_{\big(\mathbb{S}_n^{un\leqslant}\times\mathbb{T}_{\leqslant t_1}^{t_2\leqslant}\big)^2} \mathrm{Cov}\big(\deg(p_1; t_1), \deg(p_2; t_1)\big)\,\mu(\mathrm{d}p_1)\,\mu(\mathrm{d}p_2) = I_{\mathsf{s}}\times I_{\mathsf{t}}
$$
$$
I_{\mathsf{s}} := \lim_{n\uparrow\infty}\frac{1}{n}\iint_{(\mathbb{S}_n^{un\leqslant})^2}|N_{\mathsf{s}}(p_{\mathsf{s},1}, p_{\mathsf{s},2})|\,\mathrm{d}p_{\mathsf{s},1}\,\mathrm{d}p_{\mathsf{s},2} = \lim_{n\uparrow\infty}c_3\big(1 - u_n^{1-\gamma}\big)^2 = c_3
$$
$$
I_{\mathsf{t}} := \int_{\mathbb{R}}\left(\int_{\mathbb{T}_{\leqslant t_1}^{t_2\leqslant}}\mathbb{1}\{r \in N_{\mathsf{t}}(p_{\mathsf{t}}; t_1)\}\,\mu_{\mathsf{t}}(\mathrm{d}p_{\mathsf{t}})\right)^2\mathrm{d}r = \frac{1}{2}\mathrm{e}^{-2(t_2-t_1)},
$$

where $c_3 = (2\beta)^2/((1-\gamma)^2(1-2\gamma'))$ as defined in the statement of the lemma, and the application of Lemma D.8.2 (c) requires that $\gamma' < 1/2$.

Term $\mathrm{Cov}(\overline{S}_n^{\mathsf{A}}(t_1, t_2), \overline{S}_n^{\mathsf{B}}(t_1, t_2))$. First, note that

$$\mathrm{Cov}(\overline{S}_n^{\mathsf{A}}(t_1, t_2), \overline{S}_n^{\mathsf{B}}(t_1, t_2)) = n^{-1} \mathrm{Cov}(S_n^{\mathsf{A}}(t_1, t_2), S_n^{\mathsf{B}}(t_1, t_2)).$$

Then,

$$\mathrm{Cov}\big(S_n^{\mathsf{A}}(t_1, t_2), S_n^{\mathsf{B}}(t_1, t_2)\big) = \mathbb{E}\big[S_n^{\mathsf{A}}(t_1, t_2) S_n^{\mathsf{B}}(t_1, t_2)\big] - \mathbb{E}\big[S_n^{\mathsf{A}}(t_1, t_2)\big]\mathbb{E}\big[S_n^{\mathsf{B}}(t_1, t_2)\big]$$

$$= \mathbb{E}\Big[\sum_{\substack{P_1 \in \mathcal{P} \cap \big(\mathbb{S}_n^{un\leqslant} \times \mathbb{T}_{\leqslant t_1}^{t_2\leqslant}\big) \\ P_2 \in \mathcal{P} \cap \big(\mathbb{S}_n^{un\leqslant} \times \mathbb{T}_{\leqslant t_1}^{[t_1, t_2]}\big)}} \deg(\{P_1, P_2\}; t_1)\Big],$$

where we have used that $P_1 \neq P_2$ as they appear in disjoint sets. Next, we apply
Mecke's formula to the above expression, and then use Lemmas D.8.2 (c) and D.8.4 (b)
with $m = 2$ to calculate the covariance term:

$$\lim_{n\uparrow\infty} \tfrac{1}{n} \mathrm{Cov}\big(S_n^{\mathsf{A}}(t_1, t_2), S_n^{\mathsf{B}}(t_1, t_2)\big)$$

$$= \lim_{n\uparrow\infty} \frac{1}{n} \int_{\mathbb{S}_n^{un\leqslant} \times \mathbb{T}_{\leqslant t_1}^{t_2\leqslant}} \int_{\mathbb{S}_n^{un\leqslant} \times \mathbb{T}_{\leqslant t_1}^{[t_1, t_2]}} |N(p_1, p_2; t_1)| \, \mu(\mathrm{d}p_2)\, \mu(\mathrm{d}p_1) = I_{\mathsf{s}} \times I_{\mathsf{t}}$$

$$I_{\mathsf{s}} := \lim_{n\uparrow\infty} \frac{1}{n} \int_{\mathbb{S}_n^{un\leqslant}} \int_{\mathbb{S}_n^{un\leqslant}} |N_{\mathsf{s}}(p_{\mathsf{s},1}, p_{\mathsf{s},2})| \, \mathrm{d}p_{\mathsf{s},2}\, \mathrm{d}p_{\mathsf{s},1} = \lim_{n\uparrow\infty} c(1 - u_n^{1-\gamma})^2 = c_3$$

$$I_{\mathsf{t}} := \int_{\mathbb{R}} \Big(\int_{\mathbb{T}_{\leqslant t_1}^{t_2\leqslant}} \mathbb{1}\{r \in N_{\mathsf{t}}(p_{\mathsf{t}}; t_1)\} \, \mu_{\mathsf{t}}(\mathrm{d}p_{\mathsf{t}}) \int_{\mathbb{T}_{\leqslant s}^{[t_1, t_2]}} \mathbb{1}\{r \in N_{\mathsf{t}}(p_{\mathsf{t}}; t_1)\} \, \mu_{\mathsf{t}}(\mathrm{d}p_{\mathsf{t}})\Big) \, \mathrm{d}r$$

$$= \int_{-\infty}^{t_1} \mathrm{e}^{-(t_2 - r)}\big(\mathrm{e}^{-(t_1 - r)} - \mathrm{e}^{-(t_2 - r)}\big) \, \mathrm{d}r = \mathrm{e}^{-(t_2 - t_1)}\big(1 - \mathrm{e}^{-(t_2 - t_1)}\big),$$

where the finiteness of the integral I_{s} requires that $\gamma' < 1/2$, and we substituted
$u_n = n^{-2/3}$.

Term $\mathrm{Cov}(S_n^{\mathsf{A}}(t_1, t_2), S_n^{\mathsf{C}}(t_1, t_2))$. In this part of the proof, we use that the
covariance term $\mathrm{Cov}(S_n^{\mathsf{A}}(t_1, t_2), S_n^{\mathsf{C}}(t_1, t_2))$ is determined by the common $\mathcal{P}$-points,
as the $\mathcal{P}'$-points in $S_n^{\mathsf{A}}(t_1, t_2)$ and $S_n^{\mathsf{C}}(t_1, t_2)$ cannot be identical. Note that
$\mathrm{Cov}(S_n^{\mathsf{A}}(t_1, t_2), S_n^{\mathsf{C}}(t_1, t_2)) = n^{-1} \mathrm{Cov}(S_n^{\mathsf{A}}(t_1, t_2), S_n^{\mathsf{C}}(t_1, t_2))$. Then, we have

$$\mathrm{Cov}\big(S_n^{\mathsf{A}}(t_1, t_2), S_n^{\mathsf{C}}(t_1, t_2)\big) = \mathbb{E}\big[S_n^{\mathsf{A}}(t_1, t_2) S_n^{\mathsf{C}}(t_1, t_2)\big] - \mathbb{E}\big[S_n^{\mathsf{A}}(t_1, t_2)\big]\mathbb{E}\big[S_n^{\mathsf{C}}(t_1, t_2)\big]$$

$$= \mathbb{E}\Big[\sum_{P \in \mathcal{P} \cap \big(\mathbb{S}_n^{un\leqslant} \times \mathbb{T}_{\leqslant t_1}^{t_2\leqslant}\big)} \deg(P; t_1) \sum_{P' \in \mathcal{P}'} \mathbb{1}\{P' \in N(P; t_2)\} \mathbb{1}\{t_1 \leqslant R\}\Big],$$

where we have used that $P_1' \neq P_2'$ as they appear in disjoint sets. As earlier, we apply
Mecke's formula to the above expression, and, after factorizing the spatial and the

temporal parts, we use Lemma D.8.2 (a) for the spatial part:

$$\text{Cov}\big(S_n^{\mathsf{A}}(t_1,t_2), S_n^{\mathsf{C}}(t_1,t_2)\big) = \int_{\mathbb{S}_n^{u_n\leqslant}\times\mathbb{T}_{\leqslant t_1}^{t_2\leqslant}} |N(p;t_1)| \int_{\mathbb{S}\times[t_1,\infty]} \mathbb{1}\{p'\in N(p;t_2)\}\,\mathrm{d}p'\,\mu(\mathrm{d}p) = I_{\mathsf{s}}\times I_{\mathsf{t}}$$

$$I_{\mathsf{s}} := \int_{\mathbb{S}_n^{u_n\leqslant}} |N_{\mathsf{s}}(p_{\mathsf{s}})|^2\,\mathrm{d}p_{\mathsf{s}} = c_2 n\big(1-u_n^{1-2\gamma}\big)$$

$$I_{\mathsf{t}} := \int_{\mathbb{T}_{\leqslant t_1}^{t_2\leqslant}} |N_{\mathsf{t}}(p_{\mathsf{t}};t_1)| \int_{[t_1,\infty]} \mathbb{1}\{r\in N_{\mathsf{t}}(p;t_2)\}\,\mathrm{d}r\,\mu_{\mathsf{t}}(\mathrm{d}p_{\mathsf{t}})$$

$$= \int_{\mathbb{T}_{\leqslant t_1}^{t_2\leqslant}} (t_1-b)\int_{[t_1,t_2]} \mathrm{d}r\,\mu_{\mathsf{t}}(\mathrm{d}p_{\mathsf{t}})$$

$$= (t_2-t_1)\int_{-\infty}^{t_1} (t_1-b)\mathrm{e}^{-(t_2-b)}\,\mathrm{d}b = (t_2-t_1)\mathrm{e}^{-(t_2-t_1)}.$$

Then, we have that $\text{Cov}\big(S_n^{\mathsf{A}}(t_1,t_2), S_n^{\mathsf{C}}(t_1,t_2)\big) = c_2 n(t_2-t_1)\mathrm{e}^{-(t_2-t_1)}$ and thus

$$\lim_{n\uparrow\infty} \tfrac{1}{n}\,\text{Cov}\big(S_n^{\mathsf{A}}(t_1,t_2), S_n^{\mathsf{C}}(t_1,t_2)\big) = c_2(t_2-t_1)\mathrm{e}^{-(t_2-t_1)},$$

where we substituted $u_n = n^{-2/3}$. $\qquad\qquad\square$

In Lemma D.5.6, we bound the error terms to bound the d_3 distance in Proposition D.5.4. We examine the cost operators and then manipulate the error terms to show their bounds.

Proof of Lemma D.5.6. First, let us recall from the statement of Proposition D.5.4 that $\tilde{p}$ is a point of the Poisson process $\widetilde{\mathcal{P}} = \mathcal{P}\sqcup\mathcal{P}'$ with intensity measure $\tilde{\mu}$. Note that

$$D_{\tilde{p}}\overline{S}_n^{\geqslant}(t) = n^{-1/2}D_{\tilde{p}}S_n^{\geqslant}(t) \qquad\text{and}\qquad D_{\tilde{p}_1,\tilde{p}_2}^2\overline{S}_n^{\geqslant}(t) = n^{-1/2}D_{\tilde{p}_1,\tilde{p}_2}^2 S_n^{\geqslant}(t).$$

The expectations $\mathbb{E}[D_p\overline{S}_n^{\geqslant}(t)]$ and $\mathbb{E}[D_{p'}\overline{S}_n^{\geqslant}(t)]$ can be calculated by the application of Mecke's formula:

$$\mathbb{E}\big[D_p S_n^{\geqslant}(t)\big] = |N(p;t)| \qquad\text{and}\qquad \mathbb{E}\big[D_{p'}S_n^{\geqslant}(t)\big] = \int_{\mathbb{S}_n^{u_n\leqslant}\times\mathbb{T}} \mathbb{1}\{p'\in N(p;t)\}\,\mu(\mathrm{d}p).$$

In the following proof, we will need the third and fourth moments of the cost operators. As $D_p S_n^{\geqslant}(t)$ and $D_{p'}S_n^{\geqslant}(t)$ are Poisson distributed, we can express their moments using the Touchard polynomials $\tau_k(x)$ [95] defined by:

$$\tau_k(x) = \sum_{i=0}^{k}\left\{{k \atop i}\right\}x^i,$$

where the curly brackets denote the Stirling numbers of the second kind. Then, the moments of the cost operators can be upper bounded by

$$\mathbb{E}\big[D_{\tilde{p}}S_n^{\geqslant}(t)^3\big] = \tau_3\big(\mathbb{E}[D_{\tilde{p}}S_n^{\geqslant}(t)]\big) \quad\text{and}$$
$$\mathbb{E}\big[D_{\tilde{p}}S_n^{\geqslant}(t)^4\big] = \tau_4\big(\mathbb{E}[D_{\tilde{p}}S_n^{\geqslant}(t)]\big) \leqslant 16\max\big(\mathbb{E}[D_{\tilde{p}}S_n^{\geqslant}(t)]^4, 1\big).$$

(D.11)

Error term $E_1(n)$. We substitute $\overline{S}_n^{\geqslant}(t.) = n^{-1/2} S_n^{\geqslant}(t.)$ and apply the Cauchy–Schwarz inequality:

$$
E_1(n)^2 \leqslant n^{-2} \int \Big(\mathbb{E}\big[(D^2_{\tilde{p}_1,\tilde{p}_3} S_n^{\geqslant}(t_1))^4\big] \, \mathbb{E}\big[(D^2_{\tilde{p}_2,\tilde{p}_3} S_n^{\geqslant}(t_1))^4\big]
$$
$$
\times \, \mathbb{E}\big[(D_{\tilde{p}_1} S_n^{\geqslant}(t_2))^4\big] \, \mathbb{E}\big[(D_{\tilde{p}_2} S_n^{\geqslant}(t_2))^4\big] \Big)^{1/4} \tilde{\mu}(\mathrm{d}(\tilde{p}_1,\tilde{p}_2,\tilde{p}_3)).
$$

Note that the integrand is nonzero only if either $\tilde{p}_1, \tilde{p}_2 \in \mathbb{S}_n^{u_n \leqslant} \times \mathbb{T}$ and $\tilde{p}_3 \in \mathbb{S} \times \mathbb{R}$, or $\tilde{p}_1, \tilde{p}_2 \in \mathbb{S} \times \mathbb{R}$ and $\tilde{p}_3 \in \mathbb{S}_n^{u_n \leqslant} \times \mathbb{T}$, as otherwise at least one of the cost operators $D^2_{\tilde{p}_1,\tilde{p}_3}$ and $D^2_{\tilde{p}_2,\tilde{p}_3}$ is zero. In the first case, we have that

$$
E_1(n)^2 \leqslant n^{-2} \iint_{(\mathbb{S}_n^{u_n \leqslant} \times \mathbb{T})^2} \Big(\mathbb{E}\big[D_{p_1} S_n^{\geqslant}(t_2)^4\big] \, \mathbb{E}\big[D_{p_2} S_n^{\geqslant}(t_2)^4\big] \Big)^{1/4}
$$
$$
\times \, |N(p_1, p_2; t_1)| \, \mu(\mathrm{d}p_1) \, \mu(\mathrm{d}p_2).
$$

We bound the fourth moments of $D_{p_1} S_n^{\geqslant}(t_2)$ and $D_{p_2} S_n^{\geqslant}(t_2)$ using (D.11), and we extend the integral over $\mathbb{S}_n^{u_n \leqslant} \times \mathbb{T}$ to $\mathbb{S}_n \times \mathbb{T}$. Then, the integral can be upper bounded by a sum of terms of the form

$$
4 \iint_{(\mathbb{S}_n \times \mathbb{T})^2} |N(p_1; t_2)|^{m_1} |N(p_1, p_2; t_1)| |N(p_2; t_2)|^{m_2} \, \mu(\mathrm{d}p_1) \, \mu(\mathrm{d}p_2) = 4 I_{\mathsf{s}} \times I_{\mathsf{t}}
$$
$$
I_{\mathsf{s}} := \iint_{(\mathbb{S}_n)^2} |N_{\mathsf{s}}(p_{\mathsf{s},1})|^{m_1} |N_{\mathsf{s}}(p_{\mathsf{s},1}, p_{\mathsf{s},2})| |N_{\mathsf{s}}(p_{\mathsf{s},2})|^{m_2} \, \mathrm{d}p_{\mathsf{s},1} \, \mathrm{d}p_{\mathsf{s},2}
$$
$$
I_{\mathsf{t}} := \iint_{\mathbb{T}^2} |N_{\mathsf{t}}(p_{\mathsf{s},1}; t_2)|^{m_1} |N_{\mathsf{t}}(p_{\mathsf{s},1}, p_{\mathsf{s},2}; t_1)| |N_{\mathsf{t}}(p_{\mathsf{s},2}; t_2)|^{m_2} \, \mu_{\mathsf{t}}(\mathrm{d}p_{\mathsf{s},1}) \, \mu_{\mathsf{t}}(\mathrm{d}p_{\mathsf{s},2}),
$$

where $m_1, m_2 \in \{0,1\}$. For the spatial part I_{s}, we use Lemma D.8.2 (e) to see that $I_{\mathsf{s}} \in O(n)$ if $\gamma, \gamma' < 1/2$. We bound the temporal part $I_{\mathsf{t}} \leqslant 1$ using Lemma D.8.4 (c), thus $E_1(n) \in O(n^{-1/2})$.

In the second case, when $\tilde{p}_1, \tilde{p}_2 \in \mathbb{S} \times \mathbb{R}$ and $\tilde{p}_3 \in \mathbb{S}_n^{u_n \leqslant} \times \mathbb{T}$, we have that

$$
E_1(n)^2 \leqslant n^{-2} \int_{\mathbb{S}_n^{u_n \leqslant} \times \mathbb{T}} \iint_{(\mathbb{S} \times \mathbb{R})^2} \mathbb{1}\{\{p_1', p_2'\} \subseteq N(p; t_1)\}
$$
$$
\times \Big(\mathbb{E}\big[(D_{p_1'} S_n^{\geqslant}(t_2))^4\big] \, \mathbb{E}\big[(D_{p_2'} S_n^{\geqslant}(t_2))^4\big] \Big)^{1/4} \, \mathrm{d}p_1', \mathrm{d}p_2' \, \mu(\mathrm{d}p)
$$
$$
\leqslant n^{-2} \int_{\mathbb{S}_n \times \mathbb{T}} \Big(\int_{\mathbb{S} \times \mathbb{R}} \mathbb{1}\{p' \in N(p; t_1)\} \, \mathbb{E}\big[(D_{p'} S_n^{\geqslant}(t_2))^4\big]^{1/4} \, \mathrm{d}p' \Big)^2 \mu(\mathrm{d}p),
$$

where we extended the integral over $\mathbb{S}_n^{u_n \leqslant} \times \mathbb{T}$ to $\mathbb{S}_n \times \mathbb{T}$ in the last step. We use (D.11) again to bound $\mathbb{E}[D_{p'} S_n^{\geqslant}(t_2)^4]$:

$$
E_1(n)^2 \leqslant 4n^{-2} \int_{\mathbb{S}_n \times \mathbb{T}} \Big(\int_{\mathbb{S} \times \mathbb{R}} \mathbb{1}\{p' \in N(p_1; t_1)\}
$$
$$
\times \max\Big(\int_{\mathbb{S}_n \times \mathbb{T}} \mathbb{1}\{p' \in N(p_2; t_2)\} \, \mu(\mathrm{d}p_2), 1 \Big) \mathrm{d}p' \Big)^2 \mu(\mathrm{d}p_1),
$$

the integration domain of the inner integral was extended to $\mathbb{S}_n \times \mathbb{T}$ again in the last step. If the maximum is equal to one, the integral can be upper bounded by

$\int_{\mathbb{S}_n \times \mathbb{T}} |N(p; t_1)|^2 \, \mu(\mathrm{d}p) \in O(n)$ by Lemmas D.8.2 (a) and D.8.4 (a). On the other hand, if the maximum is greater than one, the integral is bounded by

$$
\int_{\mathbb{S}_n \times \mathbb{T}} \left(\int_{\mathbb{S} \times \mathbb{R}} \mathbb{1}\{p' \in N(p_1; t_1)\} \int_{\mathbb{S}_n \times \mathbb{T}} \mathbb{1}\{p' \in N(p_2; t_2)\} \, \mu(\mathrm{d}p_2) \, \mathrm{d}p' \right)^2 \mu(\mathrm{d}p_1) = I_\mathsf{s} \times I_\mathsf{t}
$$

$$
I_\mathsf{s} := \int_{\mathbb{S}_n} \left(\int_{\mathbb{S}} \mathbb{1}\{p'_\mathsf{s} \in N_\mathsf{s}(p_{\mathsf{s},1})\} \int_{\mathbb{S}_n} \mathbb{1}\{p'_\mathsf{s} \in N_\mathsf{s}(p_{\mathsf{s},2})\} \, \mathrm{d}p_{\mathsf{s},2} \, \mathrm{d}p'_\mathsf{s} \right)^2 \mathrm{d}p_{\mathsf{s},1}
$$

$$
I_\mathsf{t} := \int_{\mathbb{T}} \left(\int_{\mathbb{R}} \mathbb{1}\{r \in N_\mathsf{t}(p_{\mathsf{s},1}; t_1)\} \int_{\mathbb{T}} \mathbb{1}\{r \in N_\mathsf{t}(p_{\mathsf{s},2}; t_2)\} \, \mu_\mathsf{t}(\mathrm{d}p_{\mathsf{s},2}) \, \mathrm{d}r \right)^2 \mu_\mathsf{t}(\mathrm{d}p_{\mathsf{s},1}).
$$

We begin with the spatial part I_s:

$$
I_\mathsf{s} \leqslant \left(\frac{2\beta}{1 - \gamma} \right)^2 \int_{\mathbb{S}_n} \left(\int_{\mathbb{S}} \mathbb{1}\{p'_\mathsf{s} \in N_\mathsf{s}(p_\mathsf{s})\} w^{-\gamma'} \, \mathrm{d}p'_\mathsf{s} \right)^2 \mathrm{d}p_\mathsf{s}
$$

$$
= \frac{(2\beta)^4}{(1 - \gamma)^2 (1 - 2\gamma')^2} \int_{\mathbb{S}_n} u^{-2\gamma} \, \mathrm{d}(x, u) = \frac{(2\beta)^4 n}{(1 - \gamma)^2 (1 - 2\gamma)(1 - 2\gamma')^2} \in O(n),
$$

where we extended the innermost integral to the whole space $\mathbb{S} \times \mathbb{R}$ and applied Lemmas D.8.1 (c) and D.8.3 (b) in the first step. Next, we move on to the temporal part I_t:

$$
I_\mathsf{t} = \int_{\mathbb{T}} \left(\int_{\mathbb{R}} \mathbb{1}\{r \in N_\mathsf{t}(p_\mathsf{t}; t_1)\} \mathrm{e}^{-(t_2 - r)} \, \mathrm{d}r \right)^2 \mu_\mathsf{t}(\mathrm{d}p_\mathsf{t})
$$

$$
= \int_{\mathbb{T}} (\mathrm{e}^{-(t_2 - t_1)} - \mathrm{e}^{-(t_2 - b)})^2 \, \mathbb{1}\{b \leqslant t_1 \leqslant b + \ell\} \, \mu_\mathsf{t}(\mathrm{d}(b, \ell))
$$

$$
= \int_{-\infty}^{t_1} \int_{t_1 - b}^{\infty} (\mathrm{e}^{-(t_2 - t_1)} - \mathrm{e}^{-(t_2 - b)})^2 \, \mathbb{P}_L(\mathrm{d}\ell) \, \mathrm{d}b = \frac{1}{3} \mathrm{e}^{-(t_2 - t_1)},
$$

Thus, in both cases, we have that $E_1(n) \in O(n^{-1/2})$.

Error term $E_2(n)$. We substitute $\overline{S}_n^{\geqslant}(t.) = n^{-1/2} S_n^{\geqslant}(t.)$ and apply the Cauchy–Schwarz inequality:

$$
E_2(n)^2 \leqslant n^{-2} \int \left(\mathbb{E}\left[(D_{\tilde{p}_1, \tilde{p}_3}^2 S_n^{\geqslant}(t_1))^4 \right] \mathbb{E}\left[(D_{\tilde{p}_2, \tilde{p}_3}^2 S_n^{\geqslant}(t_1))^4 \right] \right.
$$

$$
\left. \times \mathbb{E}\left[(D_{\tilde{p}_1, \tilde{p}_3}^2 S_n^{\geqslant}(t_2))^4 \right] \mathbb{E}\left[(D_{\tilde{p}_2, \tilde{p}_3}^2 S_n^{\geqslant}(t_2))^4 \right] \right)^{1/4} \tilde{\mu}(\mathrm{d}(\tilde{p}_1, \tilde{p}_2, \tilde{p}_3)).
$$

As in the case of E_1, the integrand is nonzero only if either $\tilde{p}_1, \tilde{p}_2 \in \mathbb{S}_n^{u_n \leqslant} \times \mathbb{T}$ and $\tilde{p}_3 \in \mathbb{S} \times \mathbb{R}$, or if $\tilde{p}_1, \tilde{p}_2 \in \mathbb{S} \times \mathbb{R}$ and $\tilde{p}_3 \in \mathbb{S}_n^{u_n \leqslant} \times \mathbb{T}$. In the first case,

$$
E_2(n)^2
$$

$$
\leqslant n^{-2} \int_{(\mathbb{S}_n^{u_n \leqslant} \times \mathbb{T})^2} \int_{\mathbb{S} \times \mathbb{R}} \mathbb{1}\{p' \in N(p_1, p_2; t_1)\} \, \mathbb{1}\{p' \in N(p_1, p_2; t_2)\} \, \mathrm{d}p' \, \mu^{\otimes 2}(\mathrm{d}(p_1, p_2))
$$

$$
\leqslant n^{-2} \iint_{\mathbb{S}_n^2} |N_\mathsf{s}(p_{\mathsf{s},1}, p_{\mathsf{s},2})| \, \mathrm{d}p_{\mathsf{s},2} \, \mathrm{d}p_{\mathsf{s},1} \iint_{\mathbb{T}^2} |N_\mathsf{t}(p_{\mathsf{s},1}, p_{\mathsf{s},2}; t_1)| \, \mu_\mathsf{t}(\mathrm{d}p_{\mathsf{s},1}) \, \mu_\mathsf{t}(\mathrm{d}p_{\mathsf{s},2}),
$$

where we extended the integration domain from $\mathbb{S}_n^{u_n \leqslant} \times \mathbb{T}$ to $\mathbb{S}_n \times \mathbb{T}$, and we used that $|N_{\mathsf{t}}(p_{\mathsf{s},1}, p_{\mathsf{s},2}; t_1) \cap N_{\mathsf{t}}(p_{\mathsf{s},1}, p_{\mathsf{s},2}; t_2)| \leqslant |N_{\mathsf{t}}(p_{\mathsf{s},1}, p_{\mathsf{s},2}; t_1)|$. To upper bound the spatial and the temporal parts, we use Lemmas D.8.2 (c) and D.8.4 (b) with $m = 2$, respectively:

$$E_2(n)^2 \leqslant \frac{2\beta^2}{(1-\gamma)^2(1-2\gamma')} n^{-1},$$

and thus $E_2(n) \in O(n^{-1/2})$.

In the second case, when $\tilde{p}_1, \tilde{p}_2 \in \mathbb{S} \times \mathbb{R}$ and $\tilde{p}_3 \in \mathbb{S}_n^{u_n \leqslant} \times \mathbb{T}$, we have that

$$
\begin{aligned}
E_2(n)^2 &\leqslant n^{-2} \int_{\mathbb{S}_n^{u_n \leqslant} \times \mathbb{T}} \iint_{(\mathbb{S} \times \mathbb{R})^2} \mathbb{1}\{p_1' \in N(p; t_1) \cap N(p; t_2)\} \\
&\qquad\qquad\qquad\qquad \times \mathbb{1}\{p_2' \in N(p; t_1) \cap N(p; t_2)\}\, \mathrm{d}(p_1', p_2')\, \mu(\mathrm{d}p) \\
&\leqslant n^{-2} \int_{\mathbb{S}_n \times \mathbb{T}} |N(p; t_1) \cap N(p; t_2)|^2\, \mu(\mathrm{d}p) \\
&\leqslant n^{-2} \int_{\mathbb{S}_n \times \mathbb{T}} |N(p; t_1)|^2\, \mu(\mathrm{d}p) \leqslant \frac{2(2\beta)^2 n^{-1}}{(1-2\gamma)(1-\gamma')^2} \in O(n^{-1}),
\end{aligned}
$$

where we used Lemma D.8.2 (a) with $\alpha = 2$, $A = [0, n]$ and $u_- = 0$. Thus, in both cases, we have that $E_2(n) \in O(n^{-1/2})$.

Error term $E_3(n)$.   If $p := \tilde{p} \in \mathbb{S}_n^{u_n \leqslant} \times \mathbb{T}$, then

$$
\begin{aligned}
E_3(n) &= n^{-3/2} \int_{\mathbb{S}_n^{u_n \leqslant} \times \mathbb{T}} \mathbb{E}\big[(D_p S_n^{\geqslant}(t))^3\big]\, \mu(\mathrm{d}p) \\
&= n^{-3/2} \int_{\mathbb{S}_n^{u_n \leqslant} \times \mathbb{T}} |N(p; t)|^3 + 3|N(p; t)|^2 + |N(p; t)|\, \mu(\mathrm{d}p),
\end{aligned}
$$

where we expressed the third moment of the cost operator with the third Touchard polynomial. Next, we apply Lemma D.8.4 (a) for the temporal parts to show that they can be bounded by $\Gamma(4)$:

$$E_3(n) \leqslant \Gamma(4) n^{-3/2} \int_{\mathbb{S}_n^{u_n \leqslant}} |N_{\mathsf{s}}(p_{\mathsf{s}})|^3 + 3|N_{\mathsf{s}}(p_{\mathsf{s}})|^2 + |N_{\mathsf{s}}(p_{\mathsf{s}})|\, \mathrm{d}p_{\mathsf{s}}.$$

For the second and third terms, we extend the integration domain from $\mathbb{S}_n^{u_n \leqslant}$ to $\mathbb{S}_n$, and apply Lemma D.8.2 (a) with $A = [0, n]$ and $u_- = 0$, requiring that $\gamma < 1/2$, to show that their orders are $O(n^{-1/2})$. For the first term, we apply Lemma D.8.2 (a) to get

$$
\int_{\mathbb{S}_n^{u_n \leqslant}} |N(p; t)|^3\, \mathrm{d}(x, u) = \begin{cases} \left(\frac{2\beta}{1-\gamma'}\right)^3 \frac{n}{1-3\gamma}(1 - u_n^{1-3\gamma}) & \text{if } \gamma \neq 1/3 \\ \left(\frac{2\beta}{1-\gamma'}\right)^3 n \log(u_n^{-1}) & \text{if } \gamma = 1/3, \end{cases}
$$

which is positive regardless of the value of $\gamma \in (0, 1/2)$, since when the constant $\gamma > 1/3$, then $(1 - u_n^{1-3\gamma}) < 0$ as well. Substituting $u_n = n^{-2/3}$, we have that the order of the integral is $o(n^{3/2})$, thus $E_3(n) \to 0$ as $n \to \infty$.

If $p' := \tilde{p} \in \mathbb{S} \times \mathbb{R}$, then

$$E_3(n) = n^{-3/2} \int_{\mathbb{S} \times \mathbb{R}} \mathbb{E}\big[(D_{p'} S_n^{\geqslant}(t))^3\big] \, \mathrm{d}p'$$

$$= n^{-3/2} \int_{\mathbb{S} \times \mathbb{R}} \mathbb{E}\big[D_{p'} S_n^{\geqslant}(t)\big]^3 + 3\,\mathbb{E}\big[D_{p'} S_n^{\geqslant}(t)\big]^2 + \mathbb{E}\big[D_{p'} S_n^{\geqslant}(t)\big] \, \mathrm{d}p'.$$

To see that $\lim_{n \uparrow \infty} E_3(n) = 0$, it is enough to show that $\int_{\mathbb{S} \times \mathbb{R}} \mathbb{E}[D_{p'} S_n^{\geqslant}(t)]^m \, \mathrm{d}p' \in O(n)$ where $m \in \{1, 2, 3\}$. Thus, factorizing the integral as usual into the spatial and the temporal parts,

$$\int_{\mathbb{S} \times \mathbb{R}} \mathbb{E}\big[D_{p'} S_n^{\geqslant}(t)\big]^m \, \mathrm{d}p' = \int_{\mathbb{S} \times \mathbb{R}} \left(\int_{\mathbb{S}_n^{un\leqslant} \times \mathbb{T}} \mathbb{1}\{p' \in N(p;t)\} \, \mu(\mathrm{d}p) \right)^m \mathrm{d}p' = I_{\mathsf{s}} \times I_{\mathsf{t}}$$

$$I_{\mathsf{s}} := \int_{\mathbb{S}} \left(\int_{\mathbb{S}_n^{un\leqslant}} \mathbb{1}\{p'_{\mathsf{s}} \in N_{\mathsf{s}}(p_{\mathsf{s}})\} \, \mathrm{d}p_{\mathsf{s}} \right)^m \mathrm{d}p'_{\mathsf{s}} \in O(n)$$

$$I_{\mathsf{t}} := \int_{\mathbb{R}} \left(\int_{\mathbb{T}} \mathbb{1}\{r \in N_{\mathsf{t}}(p_{\mathsf{t}};t)\} \, \mu_{\mathsf{t}}(\mathrm{d}p_{\mathsf{t}}) \right)^m \mathrm{d}r = \frac{1}{m},$$

where, after extending the integration domain from $\mathbb{S}_n^{un\leqslant}$ to $\mathbb{S}_n$, we applied Lemma D.8.2 (d) to the spatial part, and we used Lemma D.8.4 (d) for the temporal part. Thus, we have that $\lim_{n \uparrow \infty} E_3(n) = 0$. $\qquad \square$

D.10 Proofs of the lemmas used to prove Theorem D.2.4

This section presents the proofs of the lemmas used in the proof of Theorem D.2.4. In the proof of Theorem D.2.4, we introduced the *plus-minus decomposition* at the beginning of Section D.6 to decompose S_n to the difference of two monotone increasing functions. The first proof shows that the difference of the *plus* and *minus* parts of the edge count is indeed the total edge count.

Proof of Lemma D.6.1. We have that

$$S_n^+(t) - S_n^-(t)$$

$$= \sum_{P \in \mathcal{P} \cap (\mathbb{S}_n \times \mathbb{T}^{0\leqslant})} \sum_{P' \in \mathcal{P}'} \mathbb{1}\{P' \in N^+(P;t)\} - \sum_{P \in \mathcal{P} \cap (\mathbb{S}_n \times \mathbb{T}^{0\leqslant})} \sum_{P' \in \mathcal{P}'} \mathbb{1}\{P' \in N^-(P;t)\}$$

$$= \sum_{P \in \mathcal{P} \cap (\mathbb{S}_n \times \mathbb{T}^{0\leqslant})} \sum_{P' \in \mathcal{P}'} \mathbb{1}\{P'_{\mathsf{s}} \in N_{\mathsf{s}}(P_{\mathsf{s}})\}$$

$$\times \left(\mathbb{1}\{0 \leqslant B + L\} \mathbb{1}\{B \leqslant R \leqslant (B+L) \wedge t\} - \mathbb{1}\{B \leqslant R \leqslant B + L \leqslant t\} \right)$$

$$= \sum_{P \in \mathcal{P} \cap (\mathbb{S}_n \times \mathbb{T}^{0\leqslant})} \sum_{P' \in \mathcal{P}'} \mathbb{1}\{P'_{\mathsf{s}} \in N_{\mathsf{s}}(P_{\mathsf{s}})\} \mathbb{1}\{R \in N_{\mathsf{t}}(P_{\mathsf{t}};t)\} = S_n(t),$$

as desired. $\qquad \square$

We continue by showing that the conditions of Theorem D.6.2 hold for the processes $\overline{S}_n^{\pm}(\,\cdot\,)$. The details follow after an overview of the proof of the conditions. Condition (1) of Davydov's theorem is about the convergence of the finite-dimensional distributions of $\overline{S}_n^{\pm}$, which we show in the following proof.

Proof of Proposition D.6.3. To show Condition (1), we follow the same arguments for $\overline{S}_n^{\pm}(t)$ as in Section D.5 for $S_n(t)$, i.e., we employ [97, Theorem 1.1]. Following the same steps, we first show that the limiting covariance function of $\overline{S}_n^{\pm}(t)$ is bounded.

Lemma D.10.1 (Covariance function of $\overline{S}_n^{\pm}(t)$)**.** *Let $\gamma, \gamma' < 1/2$ and $0 \leqslant s \leqslant t \leqslant 1$. Then the limit $\lim_{n\uparrow\infty} \mathrm{Cov}(\overline{S}_n^{\pm}(s), \overline{S}_n^{\pm}(t)) < \infty$, exists.*

The proof of Lemma D.10.1 and all proofs of subsequent lemmas in this section are given in Section D.10. The next step is to bound the error terms $E_1(n)$, $E_2(n)$, $E_3(n)$. As in the proof of Lemma D.5.6, the cost operators $D_p S_n^{\pm}(t)$, $D_{p'} S_n^{\pm}(t)$ and $D_{p,p'}^2 S_n^{\pm}(t)$ are given by

$$D_p S_n^{\pm}(t) := \sum_{P' \in \mathcal{P}'} \mathbb{1}\{P' \in N^{\pm}(p;t)\}$$

$$D_{p'} S_n^{\pm}(t) := \sum_{P \in \mathcal{P} \cap (\mathbb{S}_n \times \mathbb{T})} \mathbb{1}\{p' \in N^{\pm}(P;t)\}$$

$$D_{p,p'}^2 S_n^{\pm}(t) := \mathbb{1}\{p' \in N^{\pm}(p;t)\},$$

where $D_p S_n^{\pm}(t)$ and $D_{p'} S_n^{\pm}(t)$ are Poisson distributed, and $D_{p,p'}^2 S_n^{\pm}(t)$ is deterministic.

Lemma D.10.2 (Bounds of the error terms for $\overline{S}_n^{\pm}(t)$)**.** *Let $\gamma < 1/2$, $\gamma' < 1/3$. Then, the error terms defined in* (D.5) *with $\overline{S}_n^{\pm}$ in place of $\overline{S}_n$ satisfy $\lim_{n\uparrow\infty}(E_1(n) + E_2(n) + E_3(n)) = 0$.*

This shows that each finite-dimensional distribution of $\overline{S}_n^{\pm}$ converges to a multivariate normal distribution. $\qquad\square$

Condition (2) of Davydov's theorem is about the tightness of the processes $\overline{S}_n^{\pm}(\,\cdot\,)$, which is shown next.

Proof of Proposition D.6.4. We have that

$$\mathbb{E}\big[(\overline{S}_n^{\pm}(t) - \overline{S}_n^{\pm}(s))^4\big] = n^{-2}\,\mathbb{E}\big[(\Delta_n^{\pm}(s,t) - \mathbb{E}[\Delta_n^{\pm}(s,t)])^4\big],$$

where we wrote $\Delta_n^{\pm}(s,t) := S_n^{\pm}(t) - S_n^{\pm}(s)$, which is nonnegative for $s \leqslant t$. The fourth moment can be expressed with the fourth cumulant κ_4 [84, Appendix B] as

$$\mathbb{E}\big[(\Delta_n^{\pm}(s,t) - \mathbb{E}[\Delta_n^{\pm}(s,t)])^4\big] = \kappa_4(\Delta_n^{\pm}(s,t)) + 3\,\mathrm{Var}(\Delta_n^{\pm}(s,t))^2.$$

Beginning with the variance term, we have the following.

Lemma D.10.3 (Variance of $\Delta_n^{\pm}(s,t)$)**.** *Let $\gamma, \gamma' < 1/2$, then, we have $\mathrm{Var}(\Delta_n^{\pm}(s,t)) \in O(n(t-s))$.*

Next, we show for the cumulant term that $|\kappa_4(\Delta_n^{\pm}(s,t))| \in O(n(t-s)) \subseteq O(n^2(t-s)^{1+\eta})$ for all $s, t \in (0,1)$ if $t - s \geqslant a_n$.

Lemma D.10.4 (Order of the cumulant term $\kappa_4(\Delta_n^{\pm}(s,t))$)**.** *Let $\gamma, \gamma' < 1/4$. We have for $0 \leqslant s < t \leqslant 1$ the orders of the cumulant term $\kappa_4(\Delta_n^{\pm}(s,t)) \in O(n(t-s))$.*

Before presenting the proof of Lemma D.10.4 in Section D.10, we provide a rough outline here.

We follow the arguments in [22, Lemma C.3] and partition the window $[0, n]$ into n disjoint intervals $\{[i-1, i] \colon i \in \{1, \dots, n\}\}$ of size 1, and write $\mathbb{V}_i \coloneqq \mathbb{S}_{[i-1,i]}$. For $t \in [0, 1]$, analogously to the definition of $S_n^\pm(t)$, we write $V_i^\pm(t)$ for the number of edges whose $\mathcal{P}$-*endpoint* is in $\mathbb{V}_i$, i.e.,

$$V_i^\pm(t) \coloneqq \sum_{P \in \mathcal{P} \cap (\mathbb{V}_i \times \mathbb{T}^{0 \leqslant})} \deg^\pm(P; t) \qquad \text{and} \qquad S_n^\pm(t) = \sum_{i=1}^n V_i^\pm(t).$$

Note that the mappings $t \mapsto V_i^\pm(t)$ are monotone. Furthermore, we write

$$\Delta_{i,n}^\pm(s, t) \coloneqq V_i^\pm(t) - V_i^\pm(s) \qquad \text{and} \qquad \Delta_n^\pm(s, t) = \sum_{i=1}^n \Delta_{i,n}^\pm(s, t)$$

to denote the change of $V_i^\pm(t)$ in the time interval $[s, t]$. Then, using the multilinearity of the cumulant,

$$
\begin{aligned}
|\kappa_4(\Delta_n^\pm(s, t))| &= \Big| \sum_{i,j,k,\ell=1}^n c_{i,j,k,\ell} \kappa_4(\Delta_{i,n}^\pm(s,t), \Delta_{j,n}^\pm(s,t), \Delta_{k,n}^\pm(s,t), \Delta_{\ell,n}^\pm(s,t)) \Big| \\
&\leqslant c_1 \sum_{i,j,k,\ell=1}^n |\kappa_4(\Delta_{i,n}^\pm(s,t), \Delta_{j,n}^\pm(s,t), \Delta_{k,n}^\pm(s,t), \Delta_{\ell,n}^\pm(s,t))|,
\end{aligned}
$$

where $c_{i,j,k,\ell} > 0$ are coefficients depending only on which of the indices i, j, k, ℓ are equal, $c_1 \coloneqq \max(\{c_{i,j,k,\ell}\})$, $\kappa_4(\Delta_{i,n}^\pm(s,t), \Delta_{j,n}^\pm(s,t), \Delta_{k,n}^\pm(s,t), \Delta_{\ell,n}^\pm(s,t))$ denotes the joint fourth-order cumulant, and we used the triangle inequality in the last step. From now on, we drop the arguments (s, t) for brevity. Let $\{\pi_1, \pi_2\} \preceq \{i, j, k, \ell\}$ denote a partition of the set $\{i, j, k, \ell\}$, and define

$$\rho(i, j, k, \ell) \coloneqq \max_{\{\pi_1, \pi_2\} \preceq \{i,j,k,\ell\}} \big(\mathrm{dist}(\boldsymbol{V}_{\pi_1}, \boldsymbol{V}_{\pi_2}) \big), \tag{D.12}$$

where $\boldsymbol{V}_\pi \coloneqq \{\mathbb{V}_a \colon a \in \pi\}$. Then,

$$|\kappa_4(\Delta_n^\pm)| = c_1 \sum_{m=0}^n \sum_{\substack{i,j,k,\ell \\ \rho(i,j,k,\ell)=m}}^n |\kappa_4(\Delta_{i,n}^\pm, \Delta_{j,n}^\pm, \Delta_{k,n}^\pm, \Delta_{\ell,n}^\pm)|.$$

Next, we distinguish three cases.

Case (1) In the first case, all the blocks are the same: $\rho(i, j, k, \ell) = 0$, and thus $\mathbb{V}_i = \mathbb{V}_j = \mathbb{V}_k = \mathbb{V}_\ell$.

Case (2) In the second case, not all the blocks are identical. Three of them are relatively close to each other, while the fourth is separated from the rest: $\rho(i, j, k, \ell) = \mathrm{dist}(\mathbb{V}_i, \{\mathbb{V}_j, \mathbb{V}_k, \mathbb{V}_\ell\}) > 0$ and $\mathrm{diam}(\{\mathbb{V}_j, \mathbb{V}_k, \mathbb{V}_\ell\}) \leqslant \rho(i, j, k, \ell) + 1$.

Case (3) In the third case, there are two pairs of blocks, with the blocks within each pair being close, but the pairs themselves relatively far apart: $\rho(i,j,k,\ell) = \mathrm{dist}(\{\mathbb{V}_i, \mathbb{V}_k\}, \{\mathbb{V}_j, \mathbb{V}_\ell\}) > 0$ and $\mathrm{dist}(\mathbb{V}_i, \mathbb{V}_j) \vee \mathrm{dist}(\mathbb{V}_k, \mathbb{V}_\ell) \leqslant \rho(i,j,k,\ell)$,

where the term $+1$ in Case (2) is due to the size of the blocks. Even though Case (2) and Case (3) are not mutually exclusive, we treat them separately for clarity. The remainder of the proof is devoted to showing that in all three cases, $\kappa_4(\Delta_n^\pm(s,t)) \in O(n(t-s))$, with all the details provided in the proof of Lemma D.10.4 below.

Then, by Lemma D.10.4, since $t - s > n^{-1/(1+\eta)}$, we have in all cases that $\kappa_4(\Delta_n^\pm(s,t)) \in O(n(t-s)) \subseteq O(n^2(t-s)^{1+\eta})$. □

Finally, we show that Condition (3) of Theorem D.6.2 holds, which is about the convergence of the expected increments $\mathbb{E}[\Delta_n^\pm(t_k, t_{k+1})]$.

Proof of Lemma D.6.5. Note that for some constant $c > 0$, we can bound

$$\mathbb{E}[\Delta_n^\pm(t_k, t_{k+1})] = \int_{\mathbb{S}_n \times \mathbb{T}^{0\leqslant}} |\delta_{t_k, t_{k+1}}(N^\pm(p))| \, \mathrm{d}p \leqslant cn(t_{k+1} - t_k),$$

as the integral factors into the product of the spatial and the temporal parts, and the spatial part is bounded by Lemma D.8.2 (a) with $u_- = 0$, and the temporal part is bounded by Lemma D.8.6 (b). Now, setting $t_k := kn^{-1/(1+\eta)}$, we have $\mathbb{E}[\Delta_n^\pm(t_k, t_{k+1})] \leqslant cn^{1-1/(1+\eta)}$, which is independent of k. Finally, setting $\eta < 1$ gives

$$\max_{k \leqslant \lfloor n^{1/(1+\eta)} \rfloor} \left(n^{-1/2} \mathbb{E}[\Delta_n^\pm(t_k, t_{k+1})]\right) \in O(n^{1/2 - 1/(1+\eta)}) \subset o(1),$$

as desired. □

Since the proofs of the Lemmas D.10.1 and D.10.2 are very similar to the proofs of the corresponding lemmas used in the proof of Proposition D.5.4, we postpone their proofs to Appendix D.A.

Next, we present the bounds of the variance and cumulant terms that were required by Condition (2) of Theorem D.6.2 to show the tightness of the sequence of random variables $\overline{S}_n^\pm$. While bounding the variance term $\mathrm{Var}(\Delta_n^\pm(s,t))$ is relatively straightforward after the application of the Poincaré inequality, bounding the cumulant term $\kappa_4 \Delta_n^\pm(s,t)$ requires a more careful analysis.

Proof of Lemma D.10.3. First, note that $D_p(\Delta_n^\pm(s,t))$ does not depend on the point process $\mathcal{P}$, and $D_{p'}(\Delta_n^\pm(s,t))$ does not depend on the point process $\mathcal{P}'$. We bound the variance term using the Poincaré inequality [66, Theorem 18.7]:

$$\mathrm{Var}(\Delta_n^\pm(s,t)) \leqslant \int_{\mathbb{S}_n \times \mathbb{T}^{0\leqslant}} \mathbb{E}[D_p(\Delta_n^\pm(s,t))^2] \, \mu(\mathrm{d}p) + \int_{\mathbb{S}_n \times \mathbb{R}} \mathbb{E}[D_{p'}(\Delta_n^\pm(s,t))^2] \, \mathrm{d}p'.$$
(D.13)

We consider the first term first. Note that

$$D_p(\Delta_n^\pm(s,t)) = D_p(S_n^\pm(t)) - D_p(S_n^\pm(s))$$

is the number of $\mathcal{P}'$-points connecting to p in the time interval $[s, t]$ in both of the *plus* and *minus* cases. Thus, $D_p(\Delta_n^\pm(s, t))$ is Poisson distributed with mean

$$\mathbb{E}[D_p(\Delta_n^\pm(s,t))] = \mathbb{E}\Big[\sum_{P' \in \mathcal{P}'} \big(\mathbb{1}\{P' \in \delta_{s,t}(N^\pm(p))\}\big)\Big] = |\delta_{s,t}(N^\pm(p))|. \qquad \text{(D.14)}$$

Let us recall the definition of $\delta_{s,t}(N^\pm(p))$ from (D.8). Then, we integrate the second moment of this random variable over $\mathbb{S}_n \times \mathbb{T}^{0\leqslant}$:

$$\int_{\mathbb{S}_n \times \mathbb{T}^{0\leqslant}} \mathbb{E}\big[D_p(\Delta_n^\pm(s,t))^2\big]\,\mu(\mathrm{d}p)$$

$$= \int_{\mathbb{S}_n \times \mathbb{T}^{0\leqslant}} \mathbb{E}\big[D_p(\Delta_n^\pm(s,t))\big] + \mathbb{E}\big[D_p(\Delta_n^\pm(s,t))\big]^2 \,\mu(\mathrm{d}p) \qquad \text{(D.15)}$$

$$= \int_{\mathbb{S}_n \times \mathbb{T}^{0\leqslant}} \big|\delta_{s,t}(N^\pm(p))\big| + \big|\delta_{s,t}(N^\pm(p))\big|^2 \,\mu(\mathrm{d}p).$$

As $|\delta_{s,t}(N^\pm(p))| = |N_{\mathsf{s}}(p_{\mathsf{s}})||\delta_{s,t}(N_{\mathsf{t}}^\pm(p_{\mathsf{t}}))|$, applying Lemmas D.8.2 (a) and D.8.6 (c) yields

$$\int_{\mathbb{S}_n \times \mathbb{T}^{0\leqslant}} \mathbb{E}\big[D_p(\Delta_n^\pm(s,t))^2\big]\,\mu(\mathrm{d}p) \in O(n(t-s)).$$

Note that $D_{p'}(\Delta_n^\pm(s,t))$ is also a Poisson distributed random variable with mean

$$\mathbb{E}[D_{p'}(\Delta_n^\pm(s,t))] = \mathbb{E}\Big[\sum_{P \in \mathcal{P} \cap (\mathbb{S}_n \times \mathbb{T}^{0\leqslant})} \mathbb{1}\{p' \in \delta_{s,t}(N^\pm(P))\}\Big]$$

$$= \int_{\mathbb{S}_n \times \mathbb{T}^{0\leqslant}} \mathbb{1}\{p' \in \delta_{s,t}(N^\pm(p))\}\,\mu(\mathrm{d}p). \qquad \text{(D.16)}$$

Then, following a similar calculation to (D.15), since $\mathbb{E}[D_{p'}(\Delta_n^\pm(s,t))^2] = \mathbb{E}[D_{p'}(\Delta_n^\pm(s,t))]^2 + \mathbb{E}[D_{p'}(\Delta_n^\pm(s,t))]$, we have

$$\int_{\mathbb{S} \times \mathbb{R}} \mathbb{E}\big[D_{p'}(\Delta_n^\pm(s,t))^2\big]\,\mathrm{d}p'$$

$$= \sum_{m=1}^{2} \int_{\mathbb{S} \times \mathbb{R}} \Big(\int_{\mathbb{S}_n \times \mathbb{T}^{0\leqslant}} \mathbb{1}\{p' \in \delta_{s,t}(N^\pm(p))\}\,\mu(\mathrm{d}p)\Big)^m \,\mathrm{d}p'. \qquad \text{(D.17)}$$

Both integrals can be factored into a spatial and a temporal part. For the spatial parts,

$$\int_{\mathbb{S}} \Big(\int_{\mathbb{S}_n} \mathbb{1}\{p'_{\mathsf{s}} \in N_{\mathsf{s}}(p_{\mathsf{s}})\}\,\mu(\mathrm{d}p)\Big)^m \,\mathrm{d}p'_{\mathsf{s}} \in O(n),$$

by Lemma D.8.2 (d), and for the temporal parts,

$$\int_{\mathbb{R}} \Big(\int_{\mathbb{T}^{0\leqslant}} \mathbb{1}\{r \in \delta_{s,t}(N_{\mathsf{t}}^\pm(p_{\mathsf{t}}))\}\,\mu_{\mathsf{t}}(\mathrm{d}p_{\mathsf{t}})\Big)^m \,\mathrm{d}r \in O(t-s),$$

by Lemma D.8.4 (d). Thus, $\int_{\mathbb{S}_n \times \mathbb{R}} \mathbb{E}\big[D_{p'}(\Delta_n^\pm(s,t))^2\big]\,\mathrm{d}p' \in O(n(t-s))$, where we require again that $\gamma' < 1/2$. Then, $\mathrm{Var}(\Delta_n^\pm(s,t))^2 \in O(n^2(t-s)^{1+\eta})$, as desired. $\qquad \square$

To bound the cumulant term in the three cases introduced in Section D.10, we employ [84, Proposition 3.2.1] to rewrite the fourth cumulant $\kappa_4(\Delta_n^{\pm})$ in a form that is easier to bound.

Proof of Lemma D.10.4. In the following, we show the proof for the three cases of the lemma.

Case (1). We begin with Case (1). In this case, $i = j = k = \ell$, and using the definition [84, Proposition 3.2.1] of the fourth cumulant $\kappa_4(\Delta_{i,n}^{\pm})$, we have that

$$\kappa_4(\Delta_{i,n}^{\pm}) = \sum_{M_1^{(1)},\ldots,M_q^{(1)}} c_{M_1^{(1)},\ldots,M_q^{(1)}} \prod_{b=1}^{q} \mathbb{E}\left[(\Delta_{i,n}^{\pm})^{|M_b^{(1)}|}\right] \quad \text{with}$$

$$c_{M_1^{(1)},\ldots,M_q^{(1)}} := (-1)^{q-1}(q-1)!,$$

(D.18)

where $\{M_1^{(1)},\ldots,M_q^{(1)}\} \preceq \{i,i,i,i\}$ denotes a partition of the multiset $\{i,i,i,i\}$ and $|c_{M_1^{(1)},\ldots,M_q^{(1)}}| < \infty$ are coefficients depending on the number of groups q of the partition $M_1^{(1)},\ldots,M_q^{(1)}$. Then, taking absolute values and applying the triangle inequality, we have the following upper bound:

$$|\kappa_4(\Delta_{i,n}^{\pm})| \leqslant c_2 \sum_{M_1^{(1)},\ldots,M_q^{(1)}} \prod_{b=1}^{q} \mathbb{E}\left[(\Delta_{1,n}^{\pm})^{|M_b^{(1)}|}\right]$$

$$\leqslant c_2 \sum_{M_1^{(1)},\ldots,M_q^{(1)}} \prod_{b=1}^{q} \mathbb{E}\left[(\Delta_{1,n}^{\pm})^{4}\right]^{|M_b^{(1)}|/4} \leqslant c_3 \mathbb{E}[(\Delta_{1,n}^{\pm})^{4}],$$

(D.19)

where $c_2 := \max(\{|c_{M_1^{(1)},\ldots,M_q^{(1)}}|\})$, and in the first step we used stationarity of the Poisson processes $\mathcal{P},\mathcal{P}'$, and that $\Delta_{1,n}^{\pm} \geqslant 0$. In the third step, recognizing that $|M_b^{(1)}| \in \{1,\ldots,4\}$, we applied Jensen's inequality, and finally, we used that $\sum_{b=1}^{q}|M_b^{(1)}| = 4$ with a large enough constant $c_3 := \sum_{M_1^{(1)},\ldots,M_q^{(1)}} c_2$.

Lemma D.10.5 (Bound on the fourth moment of $\Delta_{1,n}^{\pm}$). *Let $\gamma < 1/4$. Then, we have that*

$$\mathbb{E}[(\Delta_{1,n}^{\pm})^{4}] \in O(t-s).$$

Then, we have that in Case (1),

$$|\kappa_4(\Delta_n^{\pm}(s,t))| \leqslant c_1 c_3 \sum_{i=1}^{n} \mathbb{E}[(\Delta_{1,n}^{\pm})^{4}] \in O(n(t-s)).$$

Case (2). For Case (2), we employ [4, Lemma 5.1] to decompose the cumulant into a sum of products, where the terms involve covariances and moments. Our strategy is to bound the moments by a constant, and then bound the covariances using the common neighborhood of the points. Let us denote the blocks of a partition of the

indices $\{j, k, \ell\}$ by $M_1^{(2)}, \ldots, M_q^{(2)}$, and let $|c_{M_1^{(2)}, \ldots, M_q^{(2)}}| < \infty$ be coefficients depending on the partition $M_1^{(2)}, \ldots, M_q^{(2)}$ of the indices $\{j, k, \ell\}$. Then, we have that

$$
\begin{aligned}
&|\kappa_4(\Delta_{i,n}^\pm, \Delta_{j,n}^\pm, \Delta_{k,n}^\pm, \Delta_{\ell,n}^\pm)| \\
&\quad = \Big| \sum_{M_1^{(2)}, \ldots, M_q^{(2)}} c_{M_1^{(2)}, \ldots, M_q^{(2)}} \operatorname{Cov}\Big(\Delta_{i,n}^\pm, \prod_{m \in M_1^{(2)}} \Delta_{m,n}^\pm\Big) \prod_{b=2}^q \mathbb{E}\Big[\prod_{m \in M_b^{(2)}} \Delta_{m,n}^\pm \Big] \Big| \\
&\quad \leqslant c_4 \sum_{M_1^{(2)}, \ldots, M_q^{(2)}} \Big| \operatorname{Cov}\Big(\Delta_{i,n}^\pm, \prod_{m \in M_1^{(2)}} \Delta_{m,n}^\pm\Big) \Big| \prod_{b=2}^q \mathbb{E}\Big[\prod_{m \in M_b^{(2)}} \Delta_{m,n}^\pm \Big],
\end{aligned}
\tag{D.20}
$$

where we used the triangle inequality in the second step, set $c_4 := \max(\{|c_{M_1^{(2)}, \ldots, M_q^{(2)}}|\})$, and dropped the absolute values on the second term as $\Delta_{m,n}^\pm \geqslant 0$. Note that $|M_b^{(2)}| \leqslant 2$ as $M_1^{(2)}$ contains at least one of $\{j, k, \ell\}$. To upper bound the product, we apply Hölder's inequality:

$$
\begin{aligned}
\prod_{b=2}^q \mathbb{E}\Big[\prod_{m \in M_b^{(2)}} \Delta_{m,n}^\pm \Big] &\leqslant \prod_{b=2}^q \prod_{m \in M_b^{(2)}} \mathbb{E}\big[(\Delta_{m,n}^\pm)^{|M_b^{(2)}|} \big]^{1/|M_b^{(2)}|} = \prod_{b=2}^q \mathbb{E}\big[(\Delta_{1,n}^\pm)^{|M_b^{(2)}|} \big] \\
&\leqslant \prod_{b=2}^q \mathbb{E}\big[(\Delta_{1,n}^\pm)^2 \big]^{|M_b^{(2)}|/2} \leqslant \mathbb{E}\big[(\Delta_{1,n}^\pm)^2 \big]^{1/2 \sum_{b=2}^q |M_b^{(2)}|},
\end{aligned}
\tag{D.21}
$$

where we used that $\{\Delta_{m,n}^\pm\}$ are identically distributed in the second step, and employed Jensen's inequality in the third step as $|M_b^{(2)}| \in \{1, 2\}$. As we saw in Case (1), $\mathbb{E}[|\Delta_{1,n}^\pm|^2] \leqslant \mathbb{E}[|\Delta_{1,n}^\pm|^4]^{1/2} < \infty$ by the Cauchy–Schwarz inequality, thus the product in (D.21) is finite. Next, we need to bound the covariance term in (D.20). With this, so far, we have that

$$
|\kappa_4(\Delta_n^\pm(s, t))| \leqslant c_5 \sum_{a=0}^{n-1} \sum_{\substack{i,j,k,\ell \\ \rho(i,j,k,\ell)=a}} \sum_{M_1^{(2)}, \ldots, M_q^{(2)}} \Big| \operatorname{Cov}\Big(\Delta_{i,n}^\pm, \prod_{m \in M_1^{(2)}} \Delta_{m,n}^\pm\Big) \Big|,
\tag{D.22}
$$

where $c_5 > 0$ is a finite constant bounding c_4 and the sum of the product terms. Next, we bound the covariance term. Note that $|M_1^{(2)}| \in \{1, 2, 3\}$. As each of these terms is similar, we only consider the case $|M_1^{(2)}| = 3$.

Lemma D.10.6 (Bound on the covariance term). *Let $\gamma < 1/3$. Then, we have that*

$$
|\operatorname{Cov}(\Delta_{i,n}^\pm, \Delta_{j,n}^\pm \Delta_{k,n}^\pm \Delta_{\ell,n}^\pm)| \leqslant \sum_{\substack{P_1 \in \mathcal{P} \cap (\mathbb{V}_i \cap \mathbb{T}^{0 \leqslant}), P_2 \in \mathcal{P} \cap (\mathbb{V}_j \cap \mathbb{T}^{0 \leqslant}) \\ P_3 \in \mathcal{P} \cap (\mathbb{V}_k \cap \mathbb{T}^{0 \leqslant}), P_4 \in \mathcal{P} \cap (\mathbb{V}_\ell \cap \mathbb{T}^{0 \leqslant})}} A(\boldsymbol{P}_4, \boldsymbol{\sigma}_4),
$$

where $\boldsymbol{P}_4 := \{P_1, P_2, P_3, P_4\}$, $\boldsymbol{\sigma}_4 := \{\sigma_1, \sigma_2, \sigma_3, \sigma_4\} \subseteq \{s, t\}$, and

$$
A(\boldsymbol{P}_4, \boldsymbol{\sigma}_4) := |N^\pm(P_1; \sigma_1) \cap N^\pm(P_2; \sigma_2)|(|N^\pm(P_3; \sigma_3)| + 2)(|N^\pm(P_4; \sigma_4)| + 2).
$$

Then, we have the following bound for $|\kappa_4(\Delta_n^\pm(s,t))|$:

$$|\kappa_4(\Delta_n^\pm(s,t))| \leqslant c_6 \, \mathbb{E}\Bigg[\sum_{a=0}^{n-1} \sum_{\substack{i,j,k,\ell \\ \rho(i,j,k,\ell)=a}} \sum_{\substack{P_1\in\mathcal{P}\cap(\mathbb{V}_i\cap\mathbb{T}^{0\leqslant}),P_2\in\mathcal{P}\cap(\mathbb{V}_j\cap\mathbb{T}^{0\leqslant}) \\ P_3\in\mathcal{P}\cap(\mathbb{V}_k\cap\mathbb{T}^{0\leqslant}),P_4\in\mathcal{P}\cap(\mathbb{V}_\ell\cap\mathbb{T}^{0\leqslant})}} A(\boldsymbol{P}_4,\boldsymbol{\sigma}_4)\Bigg]$$

with a large enough constant $c_6 > 0$. We distinguish several cases depending on which of the points P_2, P_3, P_4 are identical, and we apply the Mecke formula to each of these cases. The integrals with respect to p_3, p_4 factor, and we combine the sum over the blocks and the integral over a block to a single integral. Using $|j-k| \vee |j-\ell| \leqslant a$, we obtain the following bounds for the factors:

$$\int_{\mathbb{S}_{[j-a,j+a+1]}\times\mathbb{T}^{0\leqslant}} |N^\pm(p_3,\sigma_3)|^{m_k} \, \mu(\mathrm{d}p_3) \leqslant c_7 a$$

$$\int_{\mathbb{S}_{[j-a,j+a+1]}\times\mathbb{T}^{0\leqslant}} |N^\pm(p_4,\sigma_4)|^{m_\ell} \, \mu(\mathrm{d}p_4) \leqslant c_7 a,$$

with some large enough constant $c_7 > 0$, where the exponents $m_k, m_\ell \in \{0,1,2\}$ depend on the term we are looking at and on the case $P_3 = P_4$. We used Lemmas D.8.2 (a) with $u_- = 0$ and D.8.6 (b). Let us set $m_a \in \{0,1,2\}$ to be the number of points in $\{P_3, P_4\}$ that appear in the term we consider, and we examine the integral with respect to p_2. Then, combining again the integral within the block $\mathbb{V}_j$ and the sum of the blocks with respect to $a \leqslant |i-j| \leqslant |x_1-x_2|+1$ into a single integral, we have bounds of the form

$$|\kappa_4(\Delta_n^\pm(s,t))|$$

$$\leqslant c_8 \sum_{i=1}^n \int_{\mathbb{V}_i\times\mathbb{T}^{0\leqslant}} \sum_{a=0}^{n-1} \int_{\mathbb{V}_j\times\mathbb{T}^{0\leqslant}} |N^\pm(p_1,\sigma_1)|^{m_1} |N^\pm(p_1,\sigma_1)\cap N^\pm(p_2,\sigma_2)|$$

$$\times\, |N^\pm(p_2,\sigma_2)|^{m_2} a^{m_a} \, \mu(\mathrm{d}p_2)\,\mu(\mathrm{d}p_1)$$

$$\leqslant 2^{m_a+1} c_8 \int_{\mathbb{S}_n\times\mathbb{T}^{0\leqslant}} \int_{\mathbb{S}_n\times\mathbb{T}^{0\leqslant}} |N^\pm(p_1,\sigma_1)|^{m_1} |N^\pm(p_1,\sigma_1)\cap N^\pm(p_2,\sigma_2)|$$

$$\times\, |N^\pm(p_2,\sigma_2)|^{m_2}(|x_1-x_2|^{m_a}+1) \, \mu(\mathrm{d}p_2)\,\mu(\mathrm{d}p_1),$$
$$\tag{D.23}$$

where the exponents $m_1 = 0$ and $m_2 \in \{0,1,2\}$ depend on the term we are looking at and on the number of the points in P_3, P_4 that are identical to P_2. Even though $m_1 = 0$ in (D.23), this formula is referenced later in Case (3), where m_1 can be 1. Note also that $m_2 + m_a \leqslant 2$. Then, using Lemma D.8.2 (e), we have that the spatial part is $O(n)$. The maximum values of the exponents in the application of Lemma D.8.2 (e) are summarized in Table D.1 for each case, where we used that the expressions are symmetric in the indices $3, 4$. Noting that we consider only $\mathcal{P}$-vertices whose lifetime intersects the interval $[0,1]$, the temporal part is bounded by a constant using Lemma D.8.6 (f). Then, $|\kappa_4(\Delta_n^\pm)(s,t)| \in O(n)$. If $|M_1^{(2)}| < 3$, the same calculation can be followed with possibly different exponents m_j, m_k, m_ℓ, m_a.

Case (3). We calculate Case (3) similarly. Let $M_1^{(3)}, \ldots, M_{q_1}^{(3)}$ be the groups of the partition of $\{i,j\}$, and $M_{q_1+1}^{(3)}, \ldots, M_{q_1+q_2}^{(3)}$ be the groups of the partition of $\{k,\ell\}$, with

$q_1, q_2 \in \{1, 2\}$. Applying [4, Lemma 5.1] yields

$$|\kappa_4(\Delta_{i,n}^\pm, \Delta_{j,n}^\pm, \Delta_{k,n}^\pm, \Delta_{\ell,n}^\pm)| = \Bigg| \sum_{M_1^{(3)}, \ldots, M_{q_1+q_2}^{(3)}} c_{M_1^{(3)}, \ldots, M_{q_1+q_2}^{(3)}}$$

$$\times \mathrm{Cov}\Big(\prod_{m_1 \in M_1} \Delta_{m_1,n}^\pm, \prod_{m_{q+1} \in M_{q+1}} \Delta_{m_{q+1},n}^\pm \Big) \mathbb{E}[\Delta_{m_2,n}^\pm]\,\mathbb{E}[\Delta_{m_{q+2},n}^\pm] \Bigg|.$$

After the application of the triangle inequality, we bound the product of the expectations by a constant in the same way as in Case (2), which requires no constraint on γ in this case. Then, we only need to show a bound for the covariance term. As all partitions of the set $\{i, j\}$ and $\{k, \ell\}$ are considered similar, we consider only the case when $q_1 = q_2 = 2$. Then, the covariance term is bounded by $|\mathrm{Cov}(\Delta_{i,n}^\pm \Delta_{j,n}^\pm, \Delta_{k,n}^\pm \Delta_{\ell,n}^\pm)| \leqslant |\mathbb{E}[\mathrm{Cov}(\Delta_{i,n}^\pm \Delta_{j,n}^\pm, \Delta_{k,n}^\pm \Delta_{\ell,n}^\pm \mid \mathcal{P})]|$, where we used the independence property of the Poisson process $\mathcal{P}$ to see that $\mathrm{Cov}(\mathbb{E}[\Delta_{i,n}^\pm \Delta_{j,n}^\pm | \mathcal{P}], \mathbb{E}[\Delta_{k,n}^\pm \Delta_{\ell,n}^\pm | \mathcal{P}]) = 0$. Using bilinearity and the triangle inequality again,

$$\big|\mathbb{E}[\mathrm{Cov}(\Delta_{i,n}^\pm \Delta_{j,n}^\pm, \Delta_{k,n}^\pm \Delta_{\ell,n}^\pm \mid \mathcal{P})]\big|$$

$$\leqslant \sum_{\substack{\sigma_1, \sigma_2, \sigma_3, \sigma_4 \in \{s,t\} \\ P_1 \in \mathcal{P} \cap (\mathbb{V}_i \times \mathbb{T}^{0\leqslant}), P_3 \in \mathcal{P} \cap (\mathbb{V}_j \times \mathbb{T}^{0\leqslant}) \\ P_2 \in \mathcal{P} \cap (\mathbb{V}_k \times \mathbb{T}^{0\leqslant}), P_4 \in \mathcal{P} \cap (\mathbb{V}_\ell \times \mathbb{T}^{0\leqslant})}} \left| \mathrm{Cov}\left(\begin{array}{c} \deg^\pm(P_1; \sigma_1)\deg^\pm(P_3; \sigma_3), \\ \deg^\pm(P_2; \sigma_2)\deg^\pm(P_4; \sigma_4) \end{array} \,\middle|\, \mathcal{P} \right) \right|.$$

Note the indices of the points P_1, P_2, P_3, P_4 in the covariance term. We set them so that P_1, P_2 are the points corresponding to the indices i, k, respectively. This is because we would like to use the common neighborhood of the points P_1, P_2 to bound the covariance term, so that we can reuse the calculations from Case (2). Expanding one of the individual covariance terms as in Case (2), we have that

$$\left| \mathrm{Cov}\big(\deg^\pm(P_1; \sigma_1) \deg^\pm(P_2; \sigma_2), \deg^\pm(P_3; \sigma_3) \deg^\pm(P_4; \sigma_4) \mid \mathcal{P} \big) \right|$$

$$= \mathbb{E}\Big[\sum_{\substack{\{P_1', P_2', P_3', P_4'\} \in (\mathcal{P}')^4 \\ \{P_1', P_3'\} \cap \{P_2', P_4'\} \neq \varnothing}} \mathbb{1}\{P_1' \in N^\pm(P_1; \sigma_1)\}\, \mathbb{1}\{P_3' \in N^\pm(P_3; \sigma_3)\}$$

$$\times \mathbb{1}\{P_2' \in N^\pm(P_2; \sigma_2)\}\, \mathbb{1}\{P_4' \in N^\pm(P_4; \sigma_4)\} \,\Big|\, \mathcal{P} \Big]$$

$$= \mathbb{E}\Big[\sum_{\{P_1', P_3', P_4'\} \in (\mathcal{P}')^3} \mathbb{1}\{P_1' \in N^\pm(P_1; \sigma_1) \cap N^\pm(P_2; \sigma_2)\}$$

$$\times \mathbb{1}\{P_3' \in N^\pm(P_3; \sigma_3)\}\, \mathbb{1}\{P_4' \in N^\pm(P_4; \sigma_4)\} \,\Big|\, \mathcal{P} \Big],$$

where in the last step we used that the formula above is symmetric in the indices i, j and k, ℓ, thus we assume that $P_1' = P_2'$. Apart from a change of indices, this expression is identical to the one in (D.30) in Case (2). Although the application of the Mecke formula for the sum over the points P_1, P_2, P_3, P_4 results in cases $P_1 = P_3 \neq P_2 = P_4$, $P_1 = P_3 \neq P_2 \neq P_4$, $P_1 \neq P_3 \neq P_2 = P_4$, $P_1 \neq P_3 \neq P_2 \neq P_4$, all of these terms can be upper bounded with the same calculations as in Case (2). The only difference is the

possible values of the exponents m_1, m_2, m_3, m_4, m_a. In this case, $m_1 = 1$ whenever $P_1 = P_3$ and $P'_1 \neq P'_3$.

We summarized the maximum values of the exponents in the application of Lemma D.8.2 (e) in Table D.1. □

For Case (1), we bound the fourth moment of $\Delta_n^\pm(s, t)$ in the following proof.

Proof of Lemma D.10.5. Let us introduce the notation

$$\delta_{s,t}^\pm(P) := \deg^\pm(P; t) - \deg^\pm(P; s) = \sum_{P' \in \mathcal{P}'} \mathbb{1}\{P' \in N^\pm(P; t) \setminus N^\pm(P; s)\}.$$

Then,

$$\Delta_{1,n}^\pm = V_1^\pm(t) - V_1^\pm(s) = \sum_{P \in \mathcal{P} \cap (\mathbb{V}_1 \times \mathbb{T}^{0 \leqslant})} \delta_{s,t}^\pm(P),$$

and we expand the fourth moment $\mathbb{E}[(\Delta_{1,n}^\pm)^4]$ as follows:

$$\mathbb{E}[(\Delta_{1,n}^\pm)^4] = \mathbb{E}\Big[\Big(\sum_{P \in \mathcal{P} \cap (\mathbb{V}_1 \times \mathbb{T}^{0 \leqslant})} \delta_{s,t}^\pm(P)\Big)^4\Big] = c_1 \mathbb{E}\Big[\sum_{\boldsymbol{P}_4 \in \mathcal{P}_{\neq}^4 \cap (\mathbb{V}_1 \times \mathbb{T}^{0 \leqslant})^4} \prod_{i \leqslant 4} \delta_{s,t}^\pm(P_1)\Big]$$

$$+ c_2 \mathbb{E}\Big[\sum_{\boldsymbol{P}_3 \in \mathcal{P}_{\neq}^3 \cap (\mathbb{V}_1 \times \mathbb{T}^{0 \leqslant})^3} \delta_{s,t}^\pm(P_1)^2 \delta_{s,t}^\pm(P_2) \delta_{s,t}^\pm(P_3)\Big]$$

$$+ c_3 \mathbb{E}\Big[\sum_{\boldsymbol{P}_2 \in \mathcal{P}_{\neq}^2 \cap (\mathbb{V}_1 \times \mathbb{T}^{0 \leqslant})^2} \delta_{s,t}^\pm(P_1)^2 \delta_{s,t}^\pm(P_2)^2\Big]$$

$$+ c_4 \mathbb{E}\Big[\sum_{\boldsymbol{P}_2 \in \mathcal{P}_{\neq}^2 \cap (\mathbb{V}_1 \times \mathbb{T}^{0 \leqslant})^2} \delta_{s,t}^\pm(P_1)^3 \delta_{s,t}^\pm(P_2)\Big] + c_5 \mathbb{E}\Big[\sum_{P \in \mathcal{P} \cap \mathbb{V}_1 \times \mathbb{T}^{0 \leqslant}} \delta_{s,t}^\pm(P)^4\Big],$$

$$\tag{D.24}$$

Table D.1: Maximum values of the exponents. We put the identical points into the same set for each case.

Case (2)					
identical $\mathcal{P}$-points	m_1	m_2	m_3	m_4	m_a
$\{P_1\}, \{P_2, P_3, P_4\}$	0	2	–	–	0
$\{P_1\}, \{P_2\}, \{P_3, P_4\}$	0	0	2	–	1
$\{P_1\}, \{P_2, P_3\}, \{P_4\}$	0	1	–	1	1
$\{P_1\}, \{P_2\}, \{P_3\}, \{P_4\}$	0	0	1	1	2

Case (3)					
identical $\mathcal{P}$-points	m_1	m_2	m_3	m_4	m_a
$\{P_1, P_3\}, \{P_2, P_4\}$	1	1	–	–	0
$\{P_1, P_3\}, \{P_2\}, \{P_4\}$	1	0	–	1	1
$\{P_1\}, \{P_3\}, \{P_2, P_4\}$	0	1	1	–	1
$\{P_1\}, \{P_3\}, \{P_2\}, \{P_4\}$	0	0	1	1	2

where $\boldsymbol{P}_m := (P_1, \ldots, P_m)$, $\{c_i : i \in \{4, \ldots, 8\}\} \subseteq (0, \infty)$ are real constants, and we dropped the arguments t for brevity. The application of the Mecke formula to the above expression yields

$$
\begin{aligned}
\mathbb{E}&[(\Delta_{1,n}^{\pm})^4] \\
&= c_1 \int_{(\mathbb{V}_1 \times \mathbb{T}^{0 \leqslant})^4} \mathbb{E}\Big[\prod_{i \leqslant 4} \delta_{s,t}^{\pm}(p_1)\Big] \, \mathrm{d}\boldsymbol{p}_4 + c_2 \int_{(\mathbb{V}_1 \times \mathbb{T}^{0 \leqslant})^3} \mathbb{E}[\delta_{s,t}^{\pm}(p_1)^2 \delta_{s,t}^{\pm}(p_2) \delta_{s,t}^{\pm}(p_3)] \, \mathrm{d}\boldsymbol{p}_3 \\
&\quad + c_3 \int_{(\mathbb{V}_1 \times \mathbb{T}^{0 \leqslant})^2} \mathbb{E}[\delta_{s,t}^{\pm}(p_1)^2 \delta_{s,t}^{\pm}(p_2)^2] \, \mathrm{d}\boldsymbol{p}_2 + c_4 \int_{(\mathbb{V}_1 \times \mathbb{T}^{0 \leqslant})^2} \mathbb{E}[\delta_{s,t}^{\pm}(p_1)^3 \delta_{s,t}^{\pm}(p_2)] \, \mathrm{d}\boldsymbol{p}_2 \\
&\quad + c_5 \int_{\mathbb{V}_1 \times \mathbb{T}^{0 \leqslant}} \mathbb{E}[\delta_{s,t}^{\pm}(p)^4] \, \mathrm{d}p,
\end{aligned}
$$
(D.25)

where $\boldsymbol{p}_m := (p_1, \ldots, p_m)$. Each of the expectations in the integrands above can be written in the form $\mathbb{E}[\prod_{q=1}^{Q} \delta_{s,t}^{\pm}(p_q)^{m_q}]$, where $Q \in \{1, \ldots, 4\}$ is the number of terms in the products and $m_q \in \{1, \ldots, 4\}$ denote the exponents where $\sum_{q=1}^{Q} m_q = 4$. Then, we bound the terms using Hölder's inequality as follows:

$$
\mathbb{E}\Big[\prod_{q=1}^{Q} \delta_{s,t}^{\pm}(p_q)^{m_q}\Big] \leqslant \prod_{q=1}^{Q} \mathbb{E}[\delta_{s,t}^{\pm}(p_q)^4]^{m_q/4}.
$$
(D.26)

Recalling the definition of $\delta_{s,t}^{\pm}(p_q)$, to apply Mecke's formula to its fourth moment

$$
\mathbb{E}[\delta_{s,t}^{\pm}(p_q)^4] = \mathbb{E}\Big[\Big(\sum_{P' \in \mathcal{P}'} \mathbb{1}\{P' \in N^{\pm}(p_q; t) \setminus N^{\pm}(p_q; s)\}\Big)^4\Big],
$$

we need to examine which of the four points in $P' \in \mathcal{P}'$ are equal. To do so, we generate all the partitions of the four points $P_1', \ldots, P_4'$ consisting of Q' groups, so that the points in the same group are considered to be equal. Then, apart from combinatorial symmetries, we arrive again at five different partition types of the four points that we also used to distinguish the points in $\mathcal{P}$ above. In each case, Mecke's formula leads to $|\delta_{s,t}(N^{\pm}(p_q; t))|^{Q'}$, where $Q' \in \{1, \ldots, 4\}$ denotes the number of groups in the partition, i.e., the number of distinct points in $\{P_1', \ldots, P_4'\}$. Then,

$$
\begin{aligned}
\mathbb{E}[\delta_{s,t}^{\pm}(p_q)^4] \leqslant c_6 \Big(&|\delta_{s,t}(N^{\pm}(p_q))| + |\delta_{s,t}(N^{\pm}(p_q))|^2 \\
&+ |\delta_{s,t}(N^{\pm}(p_q))|^3 + |\delta_{s,t}(N^{\pm}(p_q))|^4\Big)
\end{aligned}
$$
(D.27)

with some large enough constant $c_6 > 0$. Substituting the above expressions to the formula (D.26), the integrals in (D.25) can be bounded by

$$
\begin{aligned}
\int_{\mathbb{V}_1 \times \mathbb{T}^{0 \leqslant}} |\delta_{s,t}(N^{\pm}(p))|^m \, \mu(\mathrm{d}p) &= \int_{\mathbb{V}_1} |N_{\mathsf{s}}(p_{\mathsf{s}})|^m \, \mathrm{d}p_{\mathsf{s}} \int_{\mathbb{T}^{0 \leqslant}} |\delta_{s,t}(N_{\mathsf{t}}^{\pm}(p_{\mathsf{t}}))|^m \, \mu_{\mathsf{t}}(\mathrm{d}p_{\mathsf{t}}) \\
&\in O((t-s)^m),
\end{aligned}
$$

where $m \in \{1, 2, 3, 4\}$, and we applied Lemmas D.8.2 (a) and D.8.6 (c). $\qquad \square$

For Case (2), we bound the covariance term appearing in (D.20).

Proof of Lemma D.10.6. First, note that

$$
\begin{aligned}
\left|\operatorname{Cov}(\Delta_{i,n}^{\pm}, \Delta_{j,n}^{\pm}\Delta_{k,n}^{\pm}\Delta_{\ell,n}^{\pm})\right| &\leqslant \left|\operatorname{Cov}\left(\mathbb{E}[\Delta_{i,n}^{\pm} \mid \mathcal{P}], \mathbb{E}[\Delta_{j,n}^{\pm}\Delta_{k,n}^{\pm}\Delta_{\ell,n}^{\pm} \mid \mathcal{P}]\right)\right| \\
&\quad + \left|\mathbb{E}\left[\operatorname{Cov}(\Delta_{i,n}^{\pm}, \Delta_{j,n}^{\pm}\Delta_{k,n}^{\pm}\Delta_{\ell,n}^{\pm} \mid \mathcal{P})\right]\right| \\
&= \left|\mathbb{E}\left[\operatorname{Cov}(\Delta_{i,n}^{\pm}, \Delta_{j,n}^{\pm}\Delta_{k,n}^{\pm}\Delta_{\ell,n}^{\pm} \mid \mathcal{P})\right]\right|,
\end{aligned}
\tag{D.28}
$$

where in the last step we used that the conditional expectations $\mathbb{E}[\Delta_{i,n}^{\pm} \mid \mathcal{P}]$ and $\mathbb{E}[\Delta_{j,n}^{\pm}\Delta_{k,n}^{\pm}\Delta_{\ell,n}^{\pm} \mid \mathcal{P}]$ are independent by the independence property of the Poisson process $\mathcal{P}$ since $\mathbb{V}_i \notin \{\mathbb{V}_j, \mathbb{V}_k, \mathbb{V}_\ell\}$. Recalling the definition of $\Delta_{i,n}^{\pm}, \Delta_{j,n}^{\pm}, \Delta_{k,n}^{\pm}, \Delta_{\ell,n}^{\pm}$, let us upper bound the covariance using bilinearity:

$$
\begin{aligned}
&\left|\operatorname{Cov}(\Delta_{i,n}^{\pm}, \Delta_{j,n}^{\pm}\Delta_{k,n}^{\pm}\Delta_{\ell,n}^{\pm} \mid \mathcal{P})\right| \\
&\qquad\leqslant \left|\sum_{\sigma_1,\sigma_2,\sigma_3,\sigma_4 \in \{s,t\}} \operatorname{Cov}(V_i^{\pm}(\sigma_1), V_j^{\pm}(\sigma_2)V_k^{\pm}(\sigma_3)V_\ell^{\pm}(\sigma_4) \mid \mathcal{P})\right| \\
&\qquad\leqslant \sum_{\substack{\sigma_1,\sigma_2,\sigma_3,\sigma_4 \in \{s,t\} \\ P_1 \in \mathcal{P} \cap (\mathbb{V}_i \cap \mathbb{T}^{0\leqslant}), P_2 \in \mathcal{P} \cap (\mathbb{V}_j \cap \mathbb{T}^{0\leqslant}) \\ P_3 \in \mathcal{P} \cap (\mathbb{V}_k \cap \mathbb{T}^{0\leqslant}), P_4 \in \mathcal{P} \cap (\mathbb{V}_\ell \cap \mathbb{T}^{0\leqslant})}} \left|\operatorname{Cov}\left(\begin{array}{c} \deg^{\pm}(P_1;\sigma_1), \\ \deg^{\pm}(P_2;\sigma_2)\deg^{\pm}(P_3;\sigma_3)\deg^{\pm}(P_4;\sigma_4) \end{array} \,\middle|\, \mathcal{P}\right)\right|.
\end{aligned}
\tag{D.29}
$$

Expanding one of the covariance terms in the sum, we recognize that it is non-zero only if $P_1' \in \{P_2', P_3', P_4'\}$:

$$
\begin{aligned}
&\left|\operatorname{Cov}\left(\deg^{\pm}(P_1;\sigma_1), \deg^{\pm}(P_2;\sigma_2)\deg^{\pm}(P_3;\sigma_3)\deg^{\pm}(P_4;\sigma_4) \mid \mathcal{P}\right)\right| \\
&\quad= \mathbb{E}\Bigg[\sum_{\substack{\{P_1',P_2',P_3',P_4'\} \in (\mathcal{P}')^4 \\ P_1' \in \{P_2',P_3',P_4'\}}} \mathbb{1}\{P_1' \in N^{\pm}(P_1;\sigma_1)\}\,\mathbb{1}\{P_2' \in N^{\pm}(P_2;\sigma_2)\} \\
&\hspace{5cm} \times \mathbb{1}\{P_3' \in N^{\pm}(P_3;\sigma_3)\}\,\mathbb{1}\{P_4' \in N^{\pm}(P_4;\sigma_4)\} \,\Big|\, \mathcal{P}\Bigg] \\
&\quad= \mathbb{E}\Bigg[\sum_{\{P_1',P_3',P_4'\} \in (\mathcal{P}')^3} \mathbb{1}\{P_1' \in N^{\pm}(P_1;\sigma_1) \cap N^{\pm}(P_2;\sigma_2)\} \\
&\hspace{5cm} \times \mathbb{1}\{P_3' \in N^{\pm}(P_3;\sigma_3)\}\,\mathbb{1}\{P_4' \in N^{\pm}(P_4;\sigma_4)\} \,\Big|\, \mathcal{P}\Bigg],
\end{aligned}
\tag{D.30}
$$

where in the last step we assumed without loss of generality that $P_1' = P_2'$, as the formula above is symmetric in the indices j, k, ℓ. We need to distinguish several cases depending on which of the points P_1', P_3', P_4' are identical: $P_1' \neq P_3' \neq P_4'$, $P_1' = P_3' \neq P_4'$, $P_1' = P_4' \neq P_3'$, $P_1' \neq P_3' = P_4'$ and $P_1' = P_3' = P_4'$. Decomposing the covariance

accordingly, we have that

$$
\begin{aligned}
&\Big|\mathrm{Cov}\big(\deg^{\pm}(P_1;\sigma_1), \deg^{\pm}(P_2;\sigma_2)\deg^{\pm}(P_3;\sigma_3)\deg^{\pm}(P_4;\sigma_4) \mid \mathcal{P}\big)\Big| \\
&\quad= c_1 \prod_{i\in\{3,4\}} \mathbb{E}[\deg^{\pm}(P_i;\sigma_i) \mid \mathcal{P}]\, \mathbb{E}\Big[\sum_{P'\in\mathcal{P}} \mathbb{1}\Big\{P' \in \bigcap_{i\in\{1,2\}} N^{\pm}(P_i;\sigma_i)\Big\} \,\Big|\, \mathcal{P}\Big] \\
&\qquad+ c_2\, \mathbb{E}[\deg^{\pm}(P_4;\sigma_4) \mid \mathcal{P}]\, \mathbb{E}\Big[\sum_{P'\in\mathcal{P}'} \mathbb{1}\Big\{P' \in \bigcap_{i\in\{1,2,3\}} N^{\pm}(P_i;\sigma_i)\Big\} \,\Big|\, \mathcal{P}\Big] \\
&\qquad+ c_3\, \mathbb{E}[\deg^{\pm}(P_3;\sigma_3) \mid \mathcal{P}]\, \mathbb{E}\Big[\sum_{P'\in\mathcal{P}'} \mathbb{1}\Big\{P' \in \bigcap_{i=\{1,2,4\}} N^{\pm}(P_i;\sigma_i)\Big\} \,\Big|\, \mathcal{P}\Big] \\
&\qquad+ c_4\, \mathbb{E}\Big[\sum_{P'\in\mathcal{P}'} \mathbb{1}\Big\{P' \in \bigcap_{i\in\{1,2\}} N^{\pm}(P_i;\sigma_i)\Big\} \,\Big|\, \mathcal{P}\Big] \mathbb{E}\Big[\sum_{P'\in\mathcal{P}'} \mathbb{1}\Big\{P' \in \bigcap_{i\in\{3,4\}} N^{\pm}(P_i;\sigma_i)\Big\} \,\Big|\, \mathcal{P}\Big] \\
&\qquad+ c_5\, \mathbb{E}\Big[\sum_{P'\in\mathcal{P}'} \mathbb{1}\Big\{P' \in \bigcap_{i\in\{1,2,3,4\}} N^{\pm}(P_i;\sigma_i)\Big\} \,\Big|\, \mathcal{P}\Big],
\end{aligned}
\tag{D.31}
$$

where $c_1,\dots,c_5 > 0$ are some coefficients. Next, we apply the Mecke formula to the above expression:

$$
\begin{aligned}
&\Big|\mathrm{Cov}\big(\deg^{\pm}(P_1;\sigma_1), \deg^{\pm}(P_2;\sigma_2)\deg^{\pm}(P_3;\sigma_3)\deg^{\pm}(P_4;\sigma_4) \mid \mathcal{P}\big)\Big| \\
&\quad= |N^{\pm}(P_1;\sigma_1) \cap N^{\pm}(P_2;\sigma_2)||N^{\pm}(P_3;\sigma_3)||N^{\pm}(P_4;\sigma_4)| \\
&\qquad+ |N^{\pm}(P_1;\sigma_1) \cap N^{\pm}(P_2;\sigma_2)||N^{\pm}(P_3;\sigma_3) \cap N^{\pm}(P_4;\sigma_4)| \\
&\qquad+ |N^{\pm}(P_1;\sigma_1) \cap N^{\pm}(P_2;\sigma_2) \cap N^{\pm}(P_3;\sigma_3)||N^{\pm}(P_4;\sigma_4)| \\
&\qquad+ |N^{\pm}(P_1;\sigma_1) \cap N^{\pm}(P_2;\sigma_2) \cap N^{\pm}(P_4;\sigma_4)||N^{\pm}(P_3;\sigma_3)| \\
&\qquad+ |N^{\pm}(P_1;\sigma_1) \cap N^{\pm}(P_2;\sigma_2) \cap N^{\pm}(P_3;\sigma_3) \cap N^{\pm}(P_4;\sigma_4)| \\
&\quad\leqslant |N^{\pm}(P_1;\sigma_1) \cap N^{\pm}(P_2;\sigma_2)|(|N^{\pm}(P_3;\sigma_3)| + 2)(|N^{\pm}(P_4;\sigma_4)| + 2) \\
&\quad=: A(\boldsymbol{P}_4, \boldsymbol{\sigma}_4),
\end{aligned}
\tag{D.32}
$$

where we bounded by neglecting some intersecting sets, and set $\boldsymbol{P}_4 := (P_1, P_2, P_3, P_4)$, $\boldsymbol{\sigma}_4 := (\sigma_1, \sigma_2, \sigma_3, \sigma_4)$. $\qquad\square$

D.11 Proofs of the propositions and lemmas used to prove Theorem D.2.6

In this section, we first show the main propositions that were used in the proof of Theorem D.2.6.

Proofs of the propositions and lemmas used in Steps 1 and 2 of the proof of Theorem D.2.6

We begin with proving that the high-mark edge count $\overline{S}_n^{\geqslant}$ is negligible compared to the total edge count $\overline{S}_n$, which Step 1 of the proof required. The proof strategy is the

same as in the proof of Theorem D.2.4 above, and we show convergence of $\overline{S}_n^{\geqslant}$ to 0 in the Skorokhod topology using the plus-minus decomposition.

Proof of Proposition D.7.2. We apply again [26, Theorem 2] to the *plus-minus decomposition* of $S_n^{\geqslant}(t)$, and verify the three conditions of the theorem. We first define

$$S_n^{\geqslant,+}(t) := \sum_{P \in \mathcal{P} \cap (\mathbb{S}_n^{un\leqslant} \times \mathbb{T}^{0\leqslant})} \deg^+(P;t) \quad \text{and}$$

$$S_n^{\geqslant,-}(t) := \sum_{P \in \mathcal{P} \cap (\mathbb{S}_n^{un\leqslant} \times \mathbb{T}^{0\leqslant})} \deg^-(P;t),$$

and we use the notation $S_n^{\geqslant,\pm}(t)$ whenever we refer to both $S_n^{\geqslant,+}(t)$ and $S_n^{\geqslant,-}(t)$ together.

For Condition (1), we would like to show that for all $t_1, \ldots, t_m \in [0,1]$ and $\varepsilon_2 > 0$,

$$\lim_{n\uparrow\infty} \mathbb{P}\Big(\big\|(\overline{S}_n^{\geqslant,\pm}(t_1), \ldots, \overline{S}_n^{\geqslant,\pm}(t_m))\big\|_\infty > \varepsilon_2\Big)$$
$$= \lim_{n\uparrow\infty} \mathbb{P}\Big(\max_{i\in\{1,\ldots,m\}}(\overline{S}_n^{\geqslant,\pm}(t_i)) > \varepsilon_2\Big) = 0.$$

We bound the probability of the maximum by the sum of the probabilities of the individual events, and then apply Chebyshev's inequality:

$$\mathbb{P}\Big(\max_{1\leqslant i\leqslant m}(\overline{S}_n^{\geqslant,\pm}(t_i)) > \varepsilon_2\Big) \leqslant \sum_{i=1}^m \mathbb{P}\Big(\overline{S}_n^{\geqslant,\pm}(t_i) > \varepsilon_2\Big) \leqslant \frac{mn^{-2\gamma}}{\varepsilon_2^2} \operatorname{Var}(S_n^{\geqslant,\pm}(t)).$$

Thus, we need to show the following lemma.

Lemma D.11.1 (Variance of the high-mark edge count $S_n^{\geqslant,\pm}(t)$)**.** *If $\gamma > 1/2$ and $\gamma' < 1/2$, then*

$$\operatorname{Var}(S_n^{\geqslant,\pm}(t)) \in o(n^{2\gamma}).$$

Then, the finite-dimensional distributions of $\overline{S}_n^{\geqslant}$ converge to 0.

To verify Condition (2), we follow closely the arguments in the proof of Theorem D.2.4 for $\overline{S}_n^{\geqslant,\pm}$ in place of $\overline{S}_n^{\pm}$. This time, we set $\chi_1 := 4$, $\chi_2 := 1 + \eta$ with $\eta = 1/3$, and $a_n := n^{-1/2}$ also differs from the thin-tailed case. We define $\Delta_n^{\geqslant,\pm}(s,t) := S_n^{\geqslant,\pm}(t) - S_n^{\geqslant,\pm}(s)$, and we would like to show that if $t - s > n^{-1/2}$, then

$$\mathbb{E}\big[(\Delta_n^{\geqslant,\pm}(s,t) - \mathbb{E}[\Delta_n^{\geqslant,\pm}(s,t)])^4\big] = \kappa_4(\Delta_n^{\geqslant,\pm}(s,t)) + 3\operatorname{Var}(\Delta_n^{\geqslant,\pm}(s,t))^2$$
$$\in O(n^{4\gamma}(t-s)^{1+\eta}).$$

We state the following lemma to bound the variance term.

Lemma D.11.2 (Variance of the change of high-mark edge count $\Delta_n^{\geqslant,\pm}(s,t)$)**.** *If $\gamma > 1/2$ and $\gamma' < 1/2$, then*

$$\operatorname{Var}(\Delta_n^{\geqslant,\pm}(s,t)) \in O(n^{2\gamma}(t-s)^{(1+\eta)/2}).$$

Then, $\mathrm{Var}(\Delta_n^{\geqslant,\pm}(s,t))^2 \in O(n^{4\gamma}(t-s)^{1+\eta})$. Turning our attention to the fourth cumulant, we would like to show that $\kappa_4(\Delta_n^{\geqslant,\pm}(s,t)) \in O(n^{4\gamma}(t-s)^{1+\eta})$ whenever $t - s > n^{-1/2}$. We begin by partitioning the domain $\mathbb{S}_n^{u_n\leqslant}$ to n disjoint blocks $\mathbb{V}_i^{u_n\leqslant} := \mathbb{S}_{[i-1,i]}^{u_n\leqslant}$ ($i \in \{1,\ldots,n\}$), and we introduce

$$V_i^{\geqslant,\pm}(t) := \sum_{P\in\mathcal{P}\cap(\mathbb{V}_i^{u_n\leqslant}\times\mathbb{T}^{0\leqslant})} \deg^\pm(P;t), \qquad S_n^{\geqslant,\pm}(t) = \sum_{i=1}^n V_i^{\geqslant,\pm}(t),$$

$$\Delta_{i,n}^{\geqslant,\pm}(s,t) := V_i^{\geqslant,\pm}(t) - V_i^{\geqslant,\pm}(s), \qquad \Delta_n^{\geqslant,\pm}(s,t) = \sum_{i=1}^n \Delta_{i,n}^{\geqslant,\pm}(s,t),$$

which are again monotone functions of t. The multilinearity of the cumulant will lead to

$$\left|\kappa_4(\Delta_n^{\geqslant,\pm})\right| \leqslant c_1 \sum_{i,j,k,\ell=1}^n \left|\kappa_4(\Delta_{i,n}^{\geqslant,\pm}, \Delta_{j,n}^{\geqslant,\pm}, \Delta_{k,n}^{\geqslant,\pm}, \Delta_{\ell,n}^{\geqslant,\pm})\right|,$$

with some constant $c_1 > 0$, and we dropped the arguments (s,t) for brevity. We partition the indices again and define $\rho^\geqslant(i,j,k,\ell)$ as in (D.12) with the blocks $\{\mathbb{V}_i^{u_n\leqslant}, \mathbb{V}_j^{u_n\leqslant}, \mathbb{V}_k^{u_n\leqslant}, \mathbb{V}_\ell^{u_n\leqslant}\}$ in place of $\{\mathbb{V}_i, \mathbb{V}_j, \mathbb{V}_k, \mathbb{V}_\ell\}$. Then, we distinguish three cases based on the distance of the blocks $\mathbb{V}_i^{u_n\leqslant}, \mathbb{V}_j^{u_n\leqslant}, \mathbb{V}_k^{u_n\leqslant}, \mathbb{V}_\ell^{u_n\leqslant}$ the same way as in the proof of Theorem D.2.4, which we treat separately.

Case ($1^\geqslant$) $\rho^\geqslant(i,j,k,\ell) = 0$, i.e., $i = j = k = \ell$;

Case ($2^\geqslant$) $\rho^\geqslant(i,j,k,\ell) = \mathrm{dist}(\mathbb{V}_i^{u_n\leqslant}, \{\mathbb{V}_j^{u_n\leqslant}, \mathbb{V}_k^{u_n\leqslant}, \mathbb{V}_\ell^{u_n\leqslant}\}) > 0$,
and $\mathrm{diam}(\{\mathbb{V}_j^{u_n\leqslant}, \mathbb{V}_k^{u_n\leqslant}, \mathbb{V}_\ell^{u_n\leqslant}\}) \leqslant \rho^\geqslant(i,j,k,\ell) + 1$;

Case ($3^\geqslant$) $\rho^\geqslant(i,j,k,\ell) = \mathrm{dist}(\{\mathbb{V}_i^{u_n\leqslant}, \mathbb{V}_k^{u_n\leqslant}\}, \{\mathbb{V}_j^{u_n\leqslant}, \mathbb{V}_\ell^{u_n\leqslant}\}) > 0$,
and $\mathrm{dist}(\mathbb{V}_i^{u_n\leqslant}, \mathbb{V}_j^{u_n\leqslant}) \vee \mathrm{dist}(\mathbb{V}_k^{u_n\leqslant}, \mathbb{V}_\ell^{u_n\leqslant}) \leqslant \rho^\geqslant(i,j,k,\ell)$.

The following lemma summarizes the orders of the cumulant term $|\kappa_4(\Delta_n^{\geqslant,\pm}(s,t))|$.

Lemma D.11.3 (Order of the cumulant term $|\kappa_4(\Delta_n^{\geqslant,\pm}(s,t))|$). *Let $\gamma > 1/2$ and $\gamma' < 1/4$. We have for $0 \leqslant s < t \leqslant 1$ the orders of the cumulant term $|\kappa_4(\Delta_n^{\geqslant,\pm}(s,t))| \in O(n^{4\gamma}(t-s)^{1+\eta})$ in the three cases Case ($1^\geqslant$), Case ($2^\geqslant$), and Case ($3^\geqslant$).*

Thus, considering all the three cases $|\kappa_4(\Delta_n^{\geqslant,\pm}(s,t))| \in O(n^{4\gamma}(t-s)^{1+\eta})$ if $t-s > n^{-1/2}$.
 Finally, Condition (3) is fulfilled if the following lemma holds.

Lemma D.11.4 (Bound on the expectation of the increments of $\overline{S}_n^\pm(t)$). *Let $t_k := kn^{1/(1+\eta)}$, and let $\gamma > 1/2$ and $\gamma' \in (0,1)$. Then, for all $\varepsilon > 0$,*

$$\lim_{n\uparrow\infty} \max_{k\leqslant\lfloor n^{1/2}\rfloor} \left\{ n^{-\gamma} \mathbb{E}\left[\Delta_n^{\geqslant,\pm}(t_k, t_{k+1})\right] \right\} = 0.$$

We conclude that if $n \to \infty$, we can approximate $\overline{S}_n(t)$ by the edge count of the low-mark vertices $\overline{S}_n^{(1)}(t)$ for all $t \in [0,1]$. $\qquad\square$

The proofs of the lemmas used to show that the finite-dimensional distributions of the high-mark edge count $\overline{S}_n^{\geqslant}$ converge to 0 are similar to the proofs of the lemmas in the proof of Theorem D.2.4. Thus, we shift the proofs of the lemmas to Appendix D.B.

Next, we show that we can approximate the low-mark edges by applying Chebyshev's inequality, which was the goal of Step 2 of the proof. We aim to bound the difference of the low-mark edge count $\overline{S}_n^{(1)}$ and its approximation $\overline{S}_n^{(2)}$ by bounding the supremum of the difference.

Proof of Proposition D.7.4. Note that $\|\overline{S}_n^{(1)} - \overline{S}_n^{(2)}\| = n^{-\gamma}\|S_n^{(1)} - S_n^{(2)}\|$. We define and bound the error term E as follows:

$$
\begin{aligned}
E &:= \mathbb{P}\Big(n^{-\gamma}\|S_n^{(1)} - S_n^{(2)}\| \geqslant \varepsilon_4\Big)\\
&\leqslant \mathbb{P}\Big(\sup_{t\in[0,1]} \sum_{P\in\mathcal{P}\cap\mathbb{S}_n^{\leqslant u_n}\times\mathbb{T}} \Big|\deg(P;t) - \mathbb{E}\big[\deg(P;t)\,\big|\,\mathcal{P}\big]\Big| \geqslant \varepsilon_4 n^{\gamma}\Big)\\
&\leqslant \varepsilon_4^{-1} n^{-\gamma}\, \mathbb{E}\Big[\sup_{t\in[0,1]} \sum_{P\in\mathcal{P}\cap\mathbb{S}_n^{\leqslant u_n}\times\mathbb{T}} \Big|\deg(P;t) - \mathbb{E}\big[\deg(P;t)\,\big|\,\mathcal{P}\big]\Big|\Big],
\end{aligned}
$$

where we used Markov's inequality. We now upper bound the supremum of the sum by the sum of the suprema, and apply the Mecke formula to obtain:

$$
\begin{aligned}
E &\leqslant \varepsilon_4^{-1} n^{-\gamma} \int_{\mathbb{S}_n^{\leqslant u_n}\times\mathbb{T}} \mathbb{E}\Big[\sup_{t\in[0,1]}\Big|\deg(p;t) - \mathbb{E}\big[\deg(p;t)\big]\Big|\Big]\, \mu(\mathrm{d}p)\\
&\leqslant \varepsilon_4^{-1} n^{-\gamma} \int_{\mathbb{S}_n^{\leqslant u_n}\times\mathbb{T}} \mathbb{E}\Big[\Big(\sup_{t\in[0,1]}\Big|\deg(p;t) - \mathbb{E}\big[\deg(p;t)\big]\Big|\Big)^2\Big]^{1/2} \mu(\mathrm{d}p),
\end{aligned}
$$

where we applied Jensen's inequality to the expectation inside the integral in the last step. Note that if $b > 1$ or $b+\ell < 0$, then $\deg(p;t) = 0$, and thus the supremum is zero. Therefore, we can assume that $b \leqslant 1$ and $b+\ell \geqslant 0$, and we restrict the supremum to the interval $[0\vee b, 1\wedge(b+\ell)]$:

$$
E \leqslant \varepsilon_4^{-1} n^{-\gamma} \int_{\mathbb{S}_n^{\leqslant u_n}\times\mathbb{T}_{\leqslant 1}^{0\leqslant}} \mathbb{E}\Big[\Big(\sup_{t\in[0\vee b,1\wedge(b+\ell)]}\Big|\deg(p;t) - \mathbb{E}\big[\deg(p;t)\big]\Big|\Big)^2\Big]^{1/2} \mu(\mathrm{d}p).
$$

Since the process $\deg(p;t) - \mathbb{E}[\deg(p;t)]$ is a martingale, the application of Doob's inequality [62, Theorem 1.3.8 (iv)] yields

$$
E \leqslant 2\varepsilon_4^{-1} n^{-\gamma} \int_{\mathbb{S}_n^{\leqslant u_n}\times\mathbb{T}_{\leqslant 1}^{0\leqslant}} \mathbb{E}\Big[\big(\deg(p;1\wedge(b+\ell)) - \mathbb{E}\big[\deg(p;1\wedge(b+\ell))\big]\big)^2\Big]^{1/2} \mu(\mathrm{d}p).
$$

As $\deg(p;1\wedge(b+\ell))$ is Poisson distributed with expectation $\mathbb{E}[\deg(p;1\wedge(b+\ell))\,|\,p]$, we have

$$
E \leqslant 2\varepsilon_4^{-1} n^{-\gamma} \int_{\mathbb{S}_n^{\leqslant u_n}\times\mathbb{T}_{\leqslant 1}^{0\leqslant}} \Big(\mathbb{E}\big[\deg(p;1\wedge(b+\ell))\big]\Big)^{1/2} \mu(\mathrm{d}p).
$$

Noting that $\mathbb{E}[\deg(p;1\wedge(b+\ell))\,|\,p] = |N(p;1\wedge(b+\ell))|$, we calculate the integral:

$$
E \leqslant 2\varepsilon_4^{-1} n^{-\gamma} \int_{\mathbb{S}_n^{\leqslant u_n}} |N_{\mathsf{s}}(p_{\mathsf{s}})|^{1/2}\, \mathrm{d}(x,u) \int_{\mathbb{T}_{\leqslant 1}^{0\leqslant}} |N_{\mathsf{t}}(p_{\mathsf{t}};1\wedge(b+\ell))|^{1/2}\, \mu_{\mathsf{t}}(\mathrm{d}p_{\mathsf{t}}).
$$

We apply Lemma D.8.2 (a) to the spatial integral:

$$\int_{\mathbb{S}_n^{\leqslant u_n}} |N_{\mathsf{s}}(p_{\mathsf{s}})|^{1/2} \, \mathrm{d}p_{\mathsf{s}} = \Big(\frac{2\beta}{1-\gamma'}\Big)^{1/2} \frac{2}{1-\gamma/2} n u_n^{1-\gamma/2} \in O(n^{(1+\gamma)/3}),$$

where, in the last step, we do not need to impose any constraints on γ, and we used that $u_n = n^{-2/3}$. The temporal integral can be calculated as follows:

$$\int_{\mathbb{T}_{\leqslant 1}^{0\leqslant}} |N_{\mathsf{t}}(p_{\mathsf{t}}; 1 \wedge (b+\ell))|^{1/2} \, \mu_{\mathsf{t}}(\mathrm{d}p_{\mathsf{t}})$$

$$= \int_{\mathbb{T}_{\leqslant 1}^{0\leqslant}} \big((1 \wedge (b+\ell)) - b\big)^{1/2} \mathbb{1}\{b \leqslant 1 \wedge (b+\ell) \leqslant b+\ell\} \, \mu_{\mathsf{t}}(\mathrm{d}(b,\ell))$$

$$= \int_{\mathbb{T}_{\leqslant 1}^{0\leqslant}} \big((1-b) \wedge \ell\big)^{1/2} \mu_{\mathsf{t}}(\mathrm{d}(b,\ell)) = \int_0^\infty \int_\ell^{1-\ell} \ell^{1/2} \, \mathrm{d}b + \int_{1-\ell}^1 (1-b)^{1/2} \, \mathrm{d}b \, \mathbb{P}_L(\mathrm{d}\ell)$$

$$\leqslant \int_0^\infty \int_\ell^1 \ell^{1/2} \, \mathrm{d}b \, \mathbb{P}_L(\mathrm{d}\ell) = \int_0^\infty (1+\ell)\ell^{1/2} \, \mathbb{P}_L(\mathrm{d}\ell) = \Gamma(3/2) + \Gamma(5/2),$$

where we used that the indicator does not affect the integral in the second step, and split the integration domain with respect to b to $[\ell, 1-\ell]$ and $b \in [1-\ell, 1]$ in the third step. Combining the spatial and temporal integrals, we obtain

$$E \leqslant \frac{4}{\varepsilon_4(1-\gamma/2)} \Big(\Gamma\Big(\frac{3}{2}\Big) + \Gamma\Big(\frac{5}{2}\Big)\Big) \Big(\frac{2\beta}{1-\gamma'}\Big)^{1/2} n^{-(2\gamma-1)/3} \in o(1),$$

as desired. $\qquad\square$

Proofs of propositions and lemmas used in Steps 3, 4, and 5 of the proof of Theorem D.2.6

In Step 3, we introduced the edge count $S_{n,\varepsilon}^{(3)}$ to represent the edges of vertices with marks less than $1/(n\varepsilon)$. The following proof show that its plus-minus decomposition $S_{n,\varepsilon}^{(3),\pm}$ converges to $S_n^{(2),\pm}(\,\cdot\,)$ as $\varepsilon \to 0$ uniformly for all n. This is done by bounding the supremum norm of the difference of the two edge counts. For the minus part, we recognize that the difference is the supremum of a martingale, and we apply Doob's inequality to bound the difference. For the plus part, we write the $\overline{S}_{n,\varepsilon}^{(3),+}(t)$ as a sum of the integrals of the neighborhoods to bound the supremum.

Proof of Proposition D.7.5. We prove the two cases separately.

Minus case. We consider the *minus case* first. For a point $(X, U, B, L) \in \mathcal{P}$, we introduce the notation $D := B + L$ for the death coordinate. The birth coordinates $\{B_i\}$ constitute a Poisson point process with intensity measure Leb. Since $\{L_i\}$ is also a Poisson point process with intensity measure $\mathbb{P}_L$, by the displacement theorem [66, Exercise 5.1], $\{D_i\}$ is also a Poisson point process on $\mathbb{R}$ with intensity measure $\mathrm{Leb} * \mathbb{P}_L = \mathrm{Leb}$. The set of points (D_i, L_i) is a $\mathrm{PPP}(\mathrm{Leb} \otimes \mathbb{P}_L)$, and we transform the point process $\mathcal{P}$ into a point process $\mathcal{P}_-$ on $\mathbb{S} \times \mathbb{T}$ with intensity measure $\mathrm{Leb} \otimes \mathbb{P}_L$ by replacing the coordinates $\{B_i\}$ with $\{D_i\}$. Note that the total intensity measure of the

point process $\mathcal{P}_-$ is given μ as it was defined in Section D.2. Using Lemmas D.8.1 (a) and D.8.5 (a), $|N^-(P;t)| = \tilde{c} U^{-\gamma} L \, \mathbb{1}\{D \leqslant t\}$. Then, we have

$$S_{n,\varepsilon}^{(3),-}(t) = \tilde{c} \sum_{P \in \mathcal{P}_- \cap (\mathbb{S}_n \times \mathbb{T})} U^{-\gamma} L \, \mathbb{1}\{U \leqslant 1/(\varepsilon n)\} \, \mathbb{1}\{D \in [0,t]\}.$$

We proceed similarly to Step 2:

$$E_1^- := \lim_{\varepsilon \downarrow 0} \limsup_{n \uparrow \infty} \mathbb{P}\Big(\sup_{t \in [0,1]} \Big| S_{n,\varepsilon}^{(3),-}(t) - S_n^{(2),-}(t) - \mathbb{E}[S_{n,\varepsilon}^{(3),-}(t) - S_n^{(2),-}(t)] \Big| > n^\gamma \delta \Big)$$

$$= \lim_{\varepsilon \downarrow 0} \limsup_{n \uparrow \infty} \mathbb{P}\Big(\sup_{t \in [0,1]} \Big| \sum_{P \in \mathcal{P} \cap (\mathbb{S}_n^{1/(\varepsilon n) \leqslant} \times \mathbb{T}^{0 \leqslant})} |N^-(P;t)|$$

$$- \mathbb{E}\Big[\sum_{P \in \mathcal{P} \cap (\mathbb{S}_n^{1/(\varepsilon n) \leqslant} \times \mathbb{T}^{0 \leqslant})} |N^-(P;t)| \Big] \Big| > n^\gamma \delta \Big),$$

where only the high-mark vertices are considered in the sums. The expectation is calculated using the Mecke formula:

$$\mathbb{E}\Big[\sum_{P \in \mathcal{P}_- \cap (\mathbb{S}_n \times \mathbb{T})} U^{-\gamma} L \, \mathbb{1}\{U \geqslant 1/(\varepsilon n)\} \, \mathbb{1}\{D \in [0,t]\} \Big]$$

$$= \int_{\mathbb{S}_n \times \mathbb{T}} u^{-\gamma} \ell \, \mathbb{1}\{u \geqslant 1/(\varepsilon n)\} \, \mathbb{1}\{w \in [0,t]\} \, \mathrm{d}x \, \mathrm{d}u \, \mathrm{d}b \, \mathbb{P}_L(\mathrm{d}\ell)$$

$$= \int_0^n \int_{1/(\varepsilon n)}^1 \int_0^t \int_0^\infty u^{-\gamma} \ell \, \mathbb{P}_L(\mathrm{d}\ell) \, \mathrm{d}w \, \mathrm{d}u \, \mathrm{d}x = \frac{\tilde{c} n t}{1 - \gamma} \big(1 - (\varepsilon n)^{-(1-\gamma)} \big).$$

Using the above, we write

$$M_n(t) := \sum_{P \in \mathcal{P}_- \cap (\mathbb{S}_n \times \mathbb{T})} U^{-\gamma} L \, \mathbb{1}\{U \geqslant 1/(\varepsilon n)\} \, \mathbb{1}\{D \in [0,t]\} - \frac{nt}{1-\gamma} \big(1 - (\varepsilon n)^{-(1-\gamma)} \big),$$

$$E_1^- \leqslant \lim_{\varepsilon \downarrow 0} \limsup_{n \uparrow \infty} \mathbb{P}\Big(\sup_{t \in [0,1]} |M_n(t)| > \tilde{c}^{-1} n^\gamma \delta \Big),$$

where only the high-mark vertices are considered in $M_n(t)$. Note that $M_n(t)$ is a martingale, since the points are independent. To see this, let us introduce $(\mathcal{F}_t)_{t \geqslant 0}$ for the filtration generated by the points in $\mathcal{P}_-$ up to time t, and let $s, t \in [0,1]$ be two time points such that $s \leqslant t$. Then, the expectation of the increments conditioned on the sigma-algebra $\mathcal{F}_s$ is given by

$$\mathbb{E}\big[M_n(t) - M_n(s) \mid \mathcal{F}_s \big] = \mathbb{E}\Big[\sum_{P \in \mathcal{P}_- \cap (\mathbb{S}_n \times \mathbb{T})} U^{-\gamma} L \, \mathbb{1}\{U \geqslant 1/(\varepsilon n)\} \, \mathbb{1}\{D \in [s,t]\} \,\Big|\, \mathcal{F}_s \Big]$$

$$- \frac{n(t-s)}{1-\gamma} \big(1 - (\varepsilon n)^{-(1-\gamma)} \big) = 0,$$

where in the last step we recognized that the expectation is zero, since the points are independent. This shows that $M_n(t)$ is a martingale with respect to the filtration $\mathcal{F}_t$

generated by the points in $\mathcal{P}_-$ up to time t. Then, Doob's martingale inequality gives that

$$E_1^- \leqslant \lim_{\varepsilon\downarrow 0} \limsup_{n\uparrow\infty} \tilde{c} n^{-\gamma} \delta^{-1} \mathbb{E}\Big[\Big| \sum_{P\in\mathcal{P}_-\cap(\mathbb{S}_n\times\mathbb{T})} U^{-\gamma}L\,\mathbb{1}\{U \geqslant 1/(\varepsilon n)\}\,\mathbb{1}\{D\in[0,1]\}$$
$$- \frac{n}{1-\gamma}\big(1-(\varepsilon n)^{-(1-\gamma)}\big)\Big|\Big].$$

The expectation contains the absolute difference of a random variable and its expectation; thus, Jensen's inequality gives that

$$E_1^- \leqslant \lim_{\varepsilon\downarrow 0} \limsup_{n\uparrow\infty} \tilde{c} n^{-\gamma} \delta^{-1} \operatorname{Var}\Big(\sum_{P\in\mathcal{P}_-\cap(\mathbb{S}_n\times\mathbb{T})} U^{-\gamma}L\,\mathbb{1}\{U \geqslant 1/(\varepsilon n)\}\,\mathbb{1}\{D\in[0,1]\}\Big)^{1/2}.$$

We calculate the variance similarly to (D.9). Then, since $D = B + L$, the Mecke formula gives

$$\operatorname{Var}\Big(\sum_{P\in\mathcal{P}_-\cap(\mathbb{S}_n\times\mathbb{T})} U^{-\gamma}L\,\mathbb{1}\{U \geqslant 1/(\varepsilon n)\}\,\mathbb{1}\{B+L\in[0,1]\}\Big)$$
$$= \int_{\mathbb{S}_n^{1/(\varepsilon n)\leqslant}\times\mathbb{T}} u^{-2\gamma}\ell^2\,\mathbb{1}\{b+\ell\in[0,1]\}\,\mathrm{d}x\,\mathrm{d}u\,\mathrm{d}b\,\mathbb{P}_L(\mathrm{d}\ell) \tag{D.33}$$
$$= n\int_{1/(\varepsilon n)\wedge 1}^{1} u^{-2\gamma}\,\mathrm{d}u \int_0^\infty \ell^2\,\mathbb{P}_L(\mathrm{d}\ell) = \frac{2n}{2\gamma-1}\big((\varepsilon n\vee 1)^{2\gamma-1}-1\big),$$

where, in the first step, we used that the covariance part of the expression for two distinct points is zero. Then, the bound for E_1^- becomes

$$E_1^- \leqslant c_1 \lim_{\varepsilon\downarrow 0} \limsup_{n\uparrow\infty} n^{-\gamma}\Big(n\big((\varepsilon n\vee 1)^{2\gamma-1}-1\big)\Big)^{1/2}$$
$$= c_1 \lim_{\varepsilon\downarrow 0} \limsup_{n\uparrow\infty}\Big((\varepsilon\vee 1/n)^{2\gamma-1}-n^{-(2\gamma-1)}\Big)^{1/2} = c_1 \lim_{\varepsilon\downarrow 0} \varepsilon^{\gamma-1/2} = 0,$$

where $c_1 = \tilde{c}\delta^{-1}(2/(2\gamma-1))^{1/2}$, since $\gamma > 1/2$.

Plus case. Next, we consider the *plus case*. As for the *minus case*, we define

$$E_1^+ := \lim_{\varepsilon\downarrow 0} \limsup_{n\uparrow\infty} \mathbb{P}(\|\overline{S}_{n,\varepsilon}^{(3),+} - \overline{S}_n^{(2),+}\| > \delta).$$

First, we examine the edge count $\overline{S}_{n,\varepsilon}^{(3),+}(\,\cdot\,) = n^{-\gamma}(S_{n,\varepsilon}^{(3),+}(\,\cdot\,) - \mathbb{E}[S_{n,\varepsilon}^{(3),+}(\,\cdot\,)])$. Noting that

$$|N_{\mathsf{t}}^+(P_{\mathsf{t}};t)| = \big(((B+L)\wedge t)-B\big)\mathbb{1}\{B\leqslant t\} \quad \text{and}$$
$$\frac{\mathrm{d}}{\mathrm{d}t}|N_{\mathsf{t}}^+(P_{\mathsf{t}};t)| = \mathbb{1}\{t\in[B,B+L]\},$$

we see that $S_{n,\varepsilon}^{(3),+}(t)$ is a continuous, monotone increasing function of t, which we write as an integral over the interval $[0,t]$ as follows:

$$S_{n,\varepsilon}^{(3),+}(t) = \sum_{P\in\mathcal{P}\cap(\mathbb{S}_n^{\leqslant 1/(\varepsilon n)}\times\mathbb{T}^{0\leqslant})} |N^+(P;t)|$$
$$= S_{n,\varepsilon}^{(3),+}(0) + \int_0^t \sum_{P\in\mathcal{P}\cap(\mathbb{S}_n^{\leqslant 1/(\varepsilon n)}\times\mathbb{T}^{0\leqslant})} \frac{\mathrm{d}}{\mathrm{d}t'}|N^+(P;t')|\,\mathrm{d}t'.$$

We define the edge count $H_{n,\varepsilon}(t)$ that considers the vertices with higher marks than $1/(\varepsilon n)$:

$$H_{n,\varepsilon}(t) := \sum_{P \in \mathcal{P} \cap (\mathbb{S}_n^{1/(\varepsilon n) \leqslant} \times \mathbb{T}^{0 \leqslant})} \frac{\mathrm{d}}{\mathrm{d}t} |N^+(P; t)|, \tag{D.34}$$

where we note that the interval of allowed marks $[1/(\varepsilon n), 1]$ is the complement of $[0, 1/(\varepsilon n)]$ taken into account in the edge count $S_{n,\varepsilon}^{(3),+}(t)$. Then,

$$E_1^+ = \lim_{\varepsilon \downarrow 0} \limsup_{n \uparrow \infty} \mathbb{P}\Big(\sup_{t \in [0,1]} \Big| \overline{S}_{n,\varepsilon}^{(3),+}(0) - \overline{S}_n^{(2),+}(0) + \int_0^t H_{n,\varepsilon}(t') - \mathbb{E}[H_{n,\varepsilon}(t')] \, \mathrm{d}t' \Big| > n^\gamma \delta \Big).$$

The application of the triangle inequality and the union bound gives

$$E_1^+ \leqslant \lim_{\varepsilon \downarrow 0} \limsup_{n \uparrow \infty} \Big(\mathbb{P}\Big(|\overline{S}_{n,\varepsilon}^{(3),+}(0) - \overline{S}_n^{(2),+}(0)| > n^\gamma \delta/2 \Big)$$

$$+ \mathbb{P}\Big(\sup_{t \in [0,1]} \Big| \int_0^t H_{n,\varepsilon}(t') - \mathbb{E}[H_{n,\varepsilon}(t')] \, \mathrm{d}t' \Big| > n^\gamma \delta/2 \Big) \Big).$$

We apply Chebyshev's inequality to the first term:

$$\mathbb{P}\Big(|\overline{S}_{n,\varepsilon}^{(3),+}(0) - \overline{S}_n^{(2),+}(0)| > n^\gamma \delta/2 \Big) \leqslant 4\delta^{-2} n^{-2\gamma} \operatorname{Var}\big(S_{n,\varepsilon}^{(3),+}(0) - S_n^{(2),+}(0) \big)$$

$$= 4\delta^{-2} n^{-2\gamma} \mathbb{E}\Big[\sum_{P \in \mathcal{P} \cap (\mathbb{S}_n^{1/(\varepsilon n) \leqslant} \times \mathbb{T}^{0 \leqslant})} |N^+(P; 0)|^2 \Big]$$

$$= 4\delta^{-2} n^{-2\gamma} \int_{\mathbb{S}_n^{1/(\varepsilon n) \leqslant} \times \mathbb{T}^{0 \leqslant}} |N^+(p; 0)|^2 \, \mu(\mathrm{d}p)$$

$$= \frac{8\tilde{c}^2 \delta^{-2}}{2\gamma - 1} n^{-(2\gamma-1)} \big(((\varepsilon n)^{2\gamma-1} \vee 1) - 1 \big)$$

where we used that the covariance part of the expression for two distinct points is zero in the second step, and applied Lemmas D.8.2 (a) and D.8.6 (a) for the spatial and the temporal parts, respectively, in the third step. Then, for the first term, we have

$$\lim_{\varepsilon \downarrow 0} \limsup_{n \uparrow \infty} \mathbb{P}\Big(|\overline{S}_{n,\varepsilon}^{(3),+}(0) - \overline{S}_n^{(2),+}(0)| > n^\gamma \delta/2 \Big) = \frac{8\tilde{c}^2 \delta^{-2}}{2\gamma - 1} \lim_{\varepsilon \downarrow 0} \varepsilon^{2\gamma-1} = 0.$$

Next, we consider the second term. We apply the triangle inequality to push the absolute value inside the integral, and then we use that $\sup_{t \in [0,1]} \int_0^t |\cdot| \, \mathrm{d}\tilde{t} \leqslant \int_0^1 |\cdot| \, \mathrm{d}t$:

$$\mathbb{P}\Big(\sup_{t \in [0,1]} \int_0^t |H_{n,\varepsilon}(t') - \mathbb{E}[H_{n,\varepsilon}(t')]| \, \mathrm{d}t' > n^\gamma \delta/2 \Big)$$

$$\leqslant \mathbb{P}\Big(\int_0^1 |H_{n,\varepsilon}(t') - \mathbb{E}[H_{n,\varepsilon}(t')]| \, \mathrm{d}t' > n^\gamma \delta/2 \Big)$$

$$\leqslant 2\delta^{-1} n^{-\gamma} \int_0^1 \mathbb{E}\Big[|H_{n,\varepsilon}(t') - \mathbb{E}[H_{n,\varepsilon}(t')]| \Big] \, \mathrm{d}t'$$

$$\leqslant 2\delta^{-1} n^{-\gamma} \int_0^1 \operatorname{Var}\big(H_{n,\varepsilon}(t') \big)^{1/2} \, \mathrm{d}t',$$

where we applied Markov's inequality in the first step and Jensen's inequality in the second step. The variance is calculated using Lemmas D.8.2 (a) and D.8.6 (a) as above:

$$\mathrm{Var}\big(H_{n,\varepsilon}(t')\big) = \int_{\mathbb{S}_n^{1/(\varepsilon n)\leqslant} \times \mathbb{T}^{0\leqslant}} |N^+(p;t')|^2\, \mu(\mathrm{d}p) = \frac{2\tilde{c}^2}{2\gamma-1} n\big(((\varepsilon n)^{2\gamma-1}\vee 1)-1\big)(t'+1).$$

Then, we have

$$\lim_{\varepsilon\downarrow 0}\limsup_{n\uparrow\infty}\mathbb{P}\Big(\sup_{t\in[0,1]}\int_0^t |H_{n,\varepsilon}(t') - \mathbb{E}[H_{n,\varepsilon}(t')]|\,\mathrm{d}t' > n^\gamma\delta/2\Big)$$

$$\leqslant \lim_{\varepsilon\downarrow 0}\limsup_{n\uparrow\infty}\Big(c_2 n^{-(\gamma-1/2)}\big(((\varepsilon n)^{2\gamma-1}\vee 1)-1\big)^{1/2}\int_0^1 (t'+1)^{1/2}\,\mathrm{d}t'\Big)$$

$$= c_3\lim_{\varepsilon\downarrow 0}\big(\varepsilon^{\gamma-1/2}\big) = 0,$$

where $c_2 = 2\tilde{c}\delta^{-1}(2/(2\gamma-1))^{1/2}$ and $c_3 = c_2(4\sqrt{2}-1)/3$. Thus, we have shown that $E_1^+ = 0$, and thus $E_1 = 0$. $\qquad\square$

In the following, we present the results required for Steps 4 and 5 in the proof of Theorem D.2.6.

In the next proof, we show that $n\,\mathbb{P}(n^{-\gamma}|N_{\mathsf{s}}(P_{\mathsf{s}})| \in [\,\cdot\,,\infty))$ converges to a measure in the vague topology as $n\to\infty$.

Proof of Lemma D.7.6. First, for $a > 0$, we have

$$\lim_{n\uparrow\infty} n\,\mathbb{P}\big(n^{-\gamma}|N_{\mathsf{s}}(P_{\mathsf{s}})| \geqslant a\big) = \lim_{n\uparrow\infty} n\,\mathbb{P}\big(\tilde{c}n^{-\gamma}U^{-\gamma} \geqslant a\big) = \lim_{n\uparrow\infty} n\,\mathbb{P}\big(U \leqslant (an^\gamma/\tilde{c})^{-1/\gamma}\big)$$

$$= \lim_{n\uparrow\infty} n\big(an^\gamma/\tilde{c}\big)^{-1/\gamma} = \tilde{c}^{1/\gamma}a^{-1/\gamma} =: \nu([a,\infty)),$$

where we applied Lemma D.8.1 (a). Note that $\nu(\cdot)$ is totally skewed to the right, since $\nu((-\infty, 0]) = 0$. $\qquad\square$

Remark D.11.5. *The measure ν is a Lévy measure, since it is non-negative, $\nu(\cdot) = 0$ for any set of Lebesgue measure zero, and*

$$\int_0^1 |a|^2\nu(\mathrm{d}a) = 2\tilde{c}^{1/\gamma}\int_0^1 aa^{-1/\gamma}\,\mathrm{d}a = \frac{2\tilde{c}^{1/\gamma}\gamma}{2\gamma-1} < \infty \quad and$$

$$\int_1^\infty \mathrm{d}\nu = \nu([1,\infty)) = \tilde{c}^{1/\gamma} < \infty,$$

where we used that $\gamma > 1/2$ for the finiteness of the first integral.

In (D.7), we defined the summation functional, which was used to define $S_\varepsilon^*(\cdot)$. To show convergence of $S_{n,\varepsilon}^{(3)}(\cdot)$ to $S_\varepsilon^*(\cdot)$, we need to show that the summation functional is continuous with respect to the Skorokhod metric d_{Sk}. As the proof is similar to the proof of the continuity of the summation functional in [93, Section 7.2.3], we present the proof in Appendix D.C.

In the last part of Step 4, we show that the expectation of $S_\varepsilon^*(\cdot)$ is finite.

Proof of Lemma D.7.8. Applying the Mecke formula to the expectation of S^*_ε, we have

$$\mathbb{E}[S^*_\varepsilon(t)] = \mathbb{E}\Big[\sum_{(J,B,L)\in\mathcal{P}_\infty} J(t-B)\,\mathbb{1}\{J \geqslant \tilde{c}\varepsilon^\gamma\}\,\mathbb{1}\{B \leqslant t \leqslant B+L\}\Big]$$

$$= \int_{\tilde{c}\varepsilon^\gamma}^\infty j\,\nu(\mathrm{d}j)\int_{\mathbb{T}^{t\leqslant}_{\leqslant t}}(t-b)\,\mu_{\mathsf{t}}(\mathrm{d}(b,\ell)),$$

where we used the fact that J is independent of (B,L), and ν is the intensity measure of J. The first integral can be calculated using the definition of ν as follows:

$$\int_{\tilde{c}\varepsilon^\gamma}^\infty j\,\nu(\mathrm{d}j) = \frac{\tilde{c}^{1/\gamma}}{\gamma}\int_{\tilde{c}\varepsilon^\gamma}^\infty j^{-1/\gamma}\,\mathrm{d}j = \frac{\tilde{c}}{1-\gamma}\varepsilon^{-(1-\gamma)}.$$

The temporal integral is the integral of the size of the temporal neighborhood at time t; thus, the application of Lemma D.8.4 (a) gives that the second integral is equal to 1, which concludes the proof. $\qquad\square$

Step 5 is about showing the convergence of $\overline{S}^*_\varepsilon(\,\cdot\,)$ to $\overline{S}(\,\cdot\,)$ as $\varepsilon \to 0$. We claimed that the edge count $\overline{S}^*_\varepsilon(t)$ converges to $\overline{S}(t)$ for a fixed time point t, which is shown in the following proof, following the arguments presented in [93, Section 5.5.1].

Proof of Lemma D.7.9. Let us define the strictly decreasing sequence of $\varepsilon_i \to 0$ such that $1 = \varepsilon_0 > \varepsilon_1 > \varepsilon_2 > \cdots$, and let $I_{i+1} := [\varepsilon_{i+1}, \varepsilon_i]$. We also define the edge count where the jump size is restricted to the interval I_{i+1} as

$$S^*_{I_{i+1}}(t) := \sum_{(J,B,L)\in\mathcal{P}_\infty} J(t-B)\,\mathbb{1}\{J \in I_{i+1}\}\,\mathbb{1}\{B \leqslant t \leqslant B+L\}$$

$$\overline{S}^*_{I_{i+1}}(t) := S^*_{I_{i+1}}(t) - \mathbb{E}[S^*_{I_{i+1}}(t)].$$

The expectation is calculated using the Mecke formula:

$$\mathbb{E}[S^*_{I_{i+1}}(t)] = \int_{I_{i+1}} j\,\nu(\mathrm{d}j)\int_{-\infty}^t (t-b)\int_{t-b}^\infty \mathbb{P}_L(\mathrm{d}\ell)\,\mathrm{d}b = c_1\big(\varepsilon_{i+1}^{-(1/\gamma-1)} - \varepsilon_i^{-(1/\gamma-1)}\big),$$

where we used the definition of the intensity measure ν, and $c_1 := \tilde{c}^{1/\gamma}/(1-\gamma)$. Note that the variance of the edge count $S^*_{I_{i+1}}(t)$ is given by

$$\mathrm{Var}(S^*_{I_{i+1}}(t)) = \int_{I_{i+1}} j^2\nu(\mathrm{d}j)\int_{-\infty}^t (t-b)^2\int_{t-b}^\infty \mathbb{P}_L(\mathrm{d}\ell)\,\mathrm{d}b = \frac{2\tilde{c}^{1/\gamma}}{2\gamma-1}\big(\varepsilon_i^{2-1/\gamma} - \varepsilon_{i+1}^{2-1/\gamma}\big),$$

where we used the fact that the points are independent. Then, again by independence, $\sum_{i=0}^\infty \mathrm{Var}(S^*_{I_{i+1}}(t)) = 2\tilde{c}^{1/\gamma}/(2\gamma-1) < \infty$, since $\varepsilon_0 = 1$ and $\gamma > 1/2$. By the Kolmogorov convergence criterion [61, Lemma 5.16], we have that $\sum_{i=0}^\infty \overline{S}^*_{I_{i+1}}(t)$ converges

almost surely, and

$$\sum_{i=0}^{\infty} \overline{S}^*_{I_{i+1}}(t) = \sum_{i=0}^{\infty} \Bigg(\sum_{(J,B,L) \in \mathcal{P}_{\infty}} J(t-B)\,\mathbb{1}\{J \in I_{i+1}\}\,\mathbb{1}\{B \leqslant t \leqslant B+L\}$$

$$- c_1 \Big(\varepsilon_{i+1}^{-(1/\gamma-1)} - \varepsilon_i^{-(1/\gamma-1)} \Big) \Bigg)$$

$$= \lim_{\varepsilon \downarrow 0} \Bigg(\sum_{(J,B,L) \in \mathcal{P}_{\infty}} J(t-B)\,\mathbb{1}\{J \in [\varepsilon, 1]\}\,\mathbb{1}\{B \leqslant t \leqslant B+L\}$$

$$- c_1 \big(\varepsilon^{-(1/\gamma-1)} - 1 \big) \Bigg).$$

Next, for large jumps, we set

$$S_0^*(t) := \sum_{(J,B,L) \in \mathcal{P}_{\infty}} J(t-B)\,\mathbb{1}\{J \geqslant 1\}\,\mathbb{1}\{B \leqslant t \leqslant B+L\}$$

$$\mathbb{E}\big[S_0^*(t)\big] = c_1 < \infty,$$

where we used similar arguments as above to calculate the expectation. Since the expectation is finite, the sum is almost surely finite. Defining the centered version, we then have $\overline{S}_0^*(t) := S_0^*(t) - \mathbb{E}[S_0^*(t)]$. Using the above, for a fixed time point t, we have

$$\overline{S}(t) = \lim_{\varepsilon \downarrow 0} \overline{S}_\varepsilon^*(t) = \overline{S}_0^*(t) + \sum_{i=0}^{\infty} \overline{S}^*_{I_{i+1}}(t)$$

$$= \lim_{\varepsilon \downarrow 0} \Bigg(\sum_{(J,B,L) \in \mathcal{P}_{\infty}} J(t-B)\,\mathbb{1}\{J \geqslant \varepsilon\}\,\mathbb{1}\{B \leqslant t \leqslant B+L\} - c_1 \varepsilon^{-(1/\gamma-1)} \Bigg),$$

which converges almost surely. $\qquad\square$

Finally, the proofs showing that $\overline{S}_{\varepsilon_n}^*$ is Cauchy in probability and almost surely with respect to the uniform convergence is postponed to Appendix D.C, since the proof of the Cauchy property in probability is very similar to the arguments presented in Step 3. The proof of the Cauchy property almost surely follows the same approach as the proof of Property 2 in [93, Proposition 5.7].

D.12 Proofs of the minor lemmas

Finally, we present the proofs of the minor lemmas stated at the beginning of this section.

Proof of Lemma D.8.1. Here, we calculate the size of the spatial neighborhoods of points.

Part (a). The size of the spatial neighborhood of a point $p_{\mathsf{s}} := (x, u) \in \mathbb{S}$ is given by

$$|N_{\mathsf{s}}(p_{\mathsf{s}})| = \int_{\mathbb{S}} \mathbb{1}\{p_{\mathsf{s}}' \in N(p_{\mathsf{s}})\}\,\mathrm{d}p_{\mathsf{s}}' = \int_{\mathbb{S}} \mathbb{1}\{|z - x| \leqslant \beta u^{-\gamma} w^{-\gamma'}\}\,\mathrm{d}(z, w) = \frac{2\beta}{1 - \gamma'} u^{-\gamma},$$

where we used the notation $p' := (z, w, r)$ as usual.

Part (b). We write the size of the common spatial neighborhood of points p_1 and p_2 as an integral:

$$|N_{\mathsf{s}}(p_{\mathsf{s},1}, p_{\mathsf{s},2})| = \int_{\mathbb{S}} \mathbb{1}\{|x_1 - z| \leqslant \beta u_1^{-\gamma} w^{-\gamma'}\} \, \mathbb{1}\{|x_2 - z| \leqslant \beta u_2^{-\gamma} w^{-\gamma'}\} \, \mathrm{d}(z, w).$$

Next, we introduce $\rho := |x_1 - x_2| \leqslant |x_1 - z| + |x_2 - z|$, where we used the triangle inequality. We assume that $|x_1 - z| \geqslant \rho/2$. As the bound is symmetric in the indices $1, 2$, we have the same bound in the case $|x_2 - z| \geqslant \rho/2$. Then,

$$|N_{\mathsf{s}}(p_{\mathsf{s},1}, p_{\mathsf{s},2})| \leqslant \int_{\mathbb{S}} \mathbb{1}\{\rho/2 \leqslant \beta u_1^{-\gamma} w^{-\gamma'}\} \, \mathbb{1}\{|x_2 - z| \leqslant \beta u_2^{-\gamma} w^{-\gamma'}\} \, \mathrm{d}(z, w).$$

The first indicator represents an upper bound on w:

$$\rho/2 \leqslant \beta u_1^{-\gamma} w^{-\gamma'} \qquad \Longleftrightarrow \qquad w \leqslant (2\beta)^{1/\gamma'} \rho^{-1/\gamma'} u_1^{-\gamma/\gamma'} =: r(\rho, u_1).$$

Using these, we integrate with respect to z and the integral can be bounded as

$$|N_{\mathsf{s}}(p_{\mathsf{s},1}, p_{\mathsf{s},2})| \leqslant 2\beta u_2^{-\gamma} \int_0^{r(\rho, u_1)} w^{-\gamma'} \, \mathrm{d}w = \frac{2\beta}{1 - \gamma'} u_2^{-\gamma} r(\rho, u_1)^{1-\gamma'}$$

$$= \frac{(2\beta)^{1/\gamma'}}{1 - \gamma'} \rho^{-(1/\gamma' - 1)} u_1^{-(1/\gamma' - 1)\gamma} u_2^{-\gamma} \leqslant \frac{(2\beta)^{1/\gamma'}}{1 - \gamma'} \rho^{-(1/\gamma' - 1)} u_1^{-\gamma/\gamma'} u_2^{-\gamma/\gamma'}.$$

Thus, we obtain the desired bound.

Part (c). The size of the neighborhood of a point $p_{\mathsf{s}}' := (z, w) \in \mathbb{S}$ is given by

$$\int_{\mathbb{S}^{u-\leqslant}} \mathbb{1}\{p_{\mathsf{s}}' \in N_{\mathsf{s}}(p_{\mathsf{s}})\} \, \mathrm{d}p_{\mathsf{s}} = \int_{\mathbb{S}^{u-\leqslant}} \mathbb{1}\{|x - z| \leqslant \beta u^{-\gamma} w^{-\gamma'}\} \, \mathrm{d}(x, u)$$

$$= 2\beta w^{-\gamma'} \int_{u_-}^1 u^{-\gamma} \, \mathrm{d}u = \frac{2\beta}{1 - \gamma} w^{-\gamma'} (1 - u_-^{1-\gamma}),$$

as desired. $\qquad\qquad\square$

Proof of Lemma D.8.2. We calculate the integrals one by one.

Part (a). The integral is calculated as follows:

$$\int_{\mathbb{S}_A^{u-\leqslant}} |N_{\mathsf{s}}(p_{\mathsf{s}})|^\alpha \, \mathrm{d}p_{\mathsf{s}} = \left(\frac{2\beta}{1 - \gamma'}\right)^\alpha \int_{\mathbb{S}_A^{u-\leqslant}} u^{-\alpha\gamma} \, \mathrm{d}(x, u)$$

$$= \begin{cases} \left(\frac{2\beta}{1-\gamma'}\right)^\alpha \frac{|A|}{1-\alpha\gamma}\left(1 - u_-^{1-\alpha\gamma}\right) & \text{if } \gamma \neq 1/\alpha \\ \left(\frac{2\beta}{1-\gamma'}\right)^\alpha |A| \log(u_-^{-1}) & \text{if } \gamma = 1/\alpha. \end{cases}$$

If $u_- = 0$, then the integral with respect to u requires that $\gamma < 1/\alpha$.

Part (b). If $m = 1$, we apply Lemma D.8.2 (a) to see that the lower and upper bounds match. Thus, we assume that $m > 1$. Then,

$$
\begin{aligned}
I &:= \int_{\mathbb{S}_n^m} |N_{\mathsf{s}}(\boldsymbol{p}_{\mathsf{s},m})| \, \mathrm{d}\boldsymbol{p}_{\mathsf{s},m} \\
&= \int_{\mathbb{S}_n} \int_{\mathbb{S}} \mathbb{1}\{p_{\mathsf{s}}' \in N_{\mathsf{s}}(p_{\mathsf{s},1})\} \left(\int_{\mathbb{S}_n} \mathbb{1}\{p_{\mathsf{s}}' \in N_{\mathsf{s}}(p_{\mathsf{s}})\} \, \mathrm{d}p_{\mathsf{s}} \right)^{m-1} \mathrm{d}p_{\mathsf{s}}' \, \mathrm{d}p_{\mathsf{s},1}.
\end{aligned}
\tag{D.35}
$$

To show an upper bound I_{upper}, the inner integral can be bounded using Lemma D.8.1 (c) after extending the integration domain from $\mathbb{S}_n$ to $\mathbb{S}$:

$$
\begin{aligned}
I \leqslant I_{\mathsf{upper}} &= \int_{\mathbb{S}_n} \int_{\mathbb{S}} \mathbb{1}\{p_{\mathsf{s}}' \in N_{\mathsf{s}}(p_{\mathsf{s},1})\} \left(\int_{\mathbb{S}} \mathbb{1}\{p_{\mathsf{s}}' \in N_{\mathsf{s}}(p_{\mathsf{s}})\} \, \mathrm{d}p_{\mathsf{s}} \right)^{m-1} \mathrm{d}p_{\mathsf{s}}' \, \mathrm{d}p_{\mathsf{s},1} \\
&= c_1^{m-1} \int_{\mathbb{S}_n} \int_{\mathbb{S}} w^{-(m-1)\gamma'} \mathbb{1}\{|x_1 - z| \leqslant \beta u_1^{-\gamma} w^{-\gamma'}\} \, \mathrm{d}(z, w) \, \mathrm{d}(x_1, u_1) \quad \text{(D.36)} \\
&= 2\beta c_1^{m-1} \int_{\mathbb{S}_n} u_1^{-\gamma} \int_0^1 w^{-m\gamma'} \, \mathrm{d}w \, \mathrm{d}(x_1, u_1) = \frac{c_1^m}{1 - m\gamma'} n,
\end{aligned}
$$

where $c_1 := 2\beta/(1 - \gamma)$. Then, $\limsup_{n \uparrow \infty} I/n \leqslant \lim_{n \uparrow \infty} I_{\mathsf{upper}}/n$, which gives the upper bound

$$
\limsup_{n \uparrow \infty} \frac{1}{n} \int_{\mathbb{S}_n^m} |N_{\mathsf{s}}(\boldsymbol{p}_{\mathsf{s},m})| \, \mathrm{d}\boldsymbol{p}_{\mathsf{s},m} \leqslant \frac{(2\beta)^m}{(1 - \gamma)^m (1 - m\gamma')},
$$

as mentioned in the lemma. For the lower bound, let us set the error term $E > 0$ such that $I = I_{\mathsf{upper}} - E$. We would like to show that $\lim_{n \uparrow \infty} E/n = 0$ since then $\lim_{n \uparrow \infty} I/n = \lim_{n \uparrow \infty} I_{\mathsf{upper}}/n - \lim_{n \uparrow \infty} E/n = \lim_{n \uparrow \infty} I_{\mathsf{upper}}/n$. In I_{upper}, let us assume without loss of generality that $p_1 \in \boldsymbol{p}_m$ is the point which is furthest from the point p', i.e., $|x_1 - z| \geqslant \max_{i \in \{2, \dots, m\}} |x_i - z|$. Then, due to symmetry,

$$
\begin{aligned}
I = m \int_{\mathbb{S}_n} \int_{\mathbb{S}} \mathbb{1}\{(z, w) \in N_{\mathsf{s}}(x_1, u_1)\} \Bigg(\int_{\mathbb{S}} \mathbb{1}\{(z, w) \in N_{\mathsf{s}}(x, u)\} \\
\times \mathbb{1}\{|x - z| \leqslant |x_1 - z|\} \, \mathrm{d}(x, u) \Bigg)^{m-1} \mathrm{d}(z, w) \, \mathrm{d}(x_1, u_1) - E,
\end{aligned}
$$

and the lower bound matches the upper bound. Note that $E \neq 0$ only if there is at least one point $p_* \in \boldsymbol{p}_m \setminus \{p_1\}$ for which $x_* \notin [0, n]$. Then,

$$
\begin{aligned}
\frac{E}{m} &\leqslant \int_{\mathbb{S}_n} \int_{\mathbb{S}} \int_{\mathbb{S}_{[0,n]^C}} \mathbb{1}\{(z, w) \in N_{\mathsf{s}}((x_1, u_1), (x_*, u_*))\} \mathbb{1}\{|x_* - z| \leqslant |x_1 - z|\} \, \mathrm{d}(x_*, u_*) \\
&\quad \times \left(\int_{\mathbb{S}_n} \mathbb{1}\{(z, w) \in N_{\mathsf{s}}(p_{\mathsf{s}})\} \, \mathrm{d}p_{\mathsf{s}} \right)^{m-2} \mathrm{d}(z, w) \, \mathrm{d}(x_1, u_1) \\
&\leqslant \int_{\mathbb{S}_n} \int_{\mathbb{S}} \int_{\mathbb{S}_{[0,n]^C}} \mathbb{1}\{(z, w) \in N_{\mathsf{s}}((x_1, u_1), (x_*, u_*))\} \mathbb{1}\{|x_* - z| \leqslant |x_1 - z|\} \, \mathrm{d}(x_*, u_*) \\
&\quad \times c_1^{m-2} w^{-(m-2)\gamma'} \, \mathrm{d}(z, w) \, \mathrm{d}(x_1, u_1),
\end{aligned}
$$

where we used again the fact that the inner integral can be bounded by Lemma D.8.1 (c) after extending the integration domain from $\mathbb{S}_n$ to $\mathbb{S}$. We distinguish two cases depending on whether the position x_1 of the point p_1 is close to the boundary of the window $[0, n]$. More precisely, with $\varepsilon \in (0, 1/2)$, we consider the cases

Case (A) $(x_1, u_1) \in \mathbb{S}_{[0,\varepsilon n] \cup [(1-\varepsilon)n, n]} =: S_A$;

Case (B) $(x_1, u_1) \in \mathbb{S}_{(\varepsilon n, (1-\varepsilon)n)} =: S_B$.

In Case (A), we bound the error term E similarly to the case of the upper bound above as follows:

$$\frac{E}{m} \leqslant c_1^{m-1} \int_{\mathbb{S}_A} \int_{\mathbb{S}} w^{-(m-1)\gamma'} \, \mathbb{1}\{(z,w) \in N_{\mathsf{s}}(p_{\mathsf{s},1})\} \, \mathrm{d}(z,w) \, \mathrm{d}p_{\mathsf{s},1}$$

$$= \frac{2\beta c_1^{m-1}}{1 - (m-1)\gamma'} \int_{\mathbb{S}_A} u_1^{-\gamma} \, \mathrm{d}(x_1, u_1) = \frac{2c_1^m}{1 - (m-1)\gamma'} \, \varepsilon n \in O(n),$$

For Case (B), we have

$$\frac{E}{m} \leqslant c_1^{m-2} \int_{\mathbb{S}_B} \int_{\mathbb{S}} w^{-(m-2)\gamma'} \int_{\mathbb{S}_{[0,n]^C}} \mathbb{1}\Big\{(z,w) \in N_{\mathsf{s}}((x_1,u_1), (x_*, u_*))\Big\}$$

$$\times \mathbb{1}\Big\{|x_* - z| \leqslant |x_1 - z|\Big\} \, \mathrm{d}(x_*, u_*) \, \mathrm{d}(z,w) \, \mathrm{d}(x_1, u_1).$$

As $|x_1 - x_*| \geqslant \varepsilon n$, the triangle inequality gives

$$\varepsilon n/2 \leqslant |x_1 - x_*|/2 \leqslant (|x_1 - z| + |x_* - z|)/2 \leqslant |x_1 - z|.$$

Extending the integration domain of the integral with respect to p_* from $\mathbb{S}_{[0,n]^C}$ to $\mathbb{S}$, we have

$$\frac{E}{m} \leqslant c_1^{m-1} \int_{\mathbb{S}_B} \int_{\mathbb{S}} w^{-(m-1)\gamma'} \, \mathbb{1}\Big\{(z,w) \in N_{\mathsf{s}}((x_1,u_1))\Big\}$$

$$\times \mathbb{1}\Big\{\varepsilon n/2 \leqslant |x_1 - z|\Big\} \, \mathrm{d}(z,w) \, \mathrm{d}(x_1, u_1)$$

$$= c_1^{m-1} \int_{\mathbb{S}_B} \int_{\mathbb{S}} w^{-(m-1)\gamma'} \, \mathbb{1}\Big\{\varepsilon n/2 \leqslant |z - x_1| \leqslant \beta u_1^{-\gamma} w^{-\gamma'}\Big\} \, \mathrm{d}(z,w) \, \mathrm{d}(x_1, u_1)$$

$$= c_1^{m-1} \int_{\mathbb{S}_B} \int_0^1 w^{-(m-1)\gamma'} \big(2\beta u_1^{-\gamma} w^{-\gamma'} - \varepsilon n\big)_+ \, \mathrm{d}w \, \mathrm{d}(x_1, u_1).$$

The integrand is non-zero only if $w \leqslant (2\beta u_1^{-\gamma}/(\varepsilon n))^{1/\gamma'} \wedge 1 =: r_n(u_1)$. Then, neglecting the term $-\varepsilon n$, we have

$$\frac{E}{m} \leqslant 2\beta c_1^{m-1} \int_{\mathbb{S}_B} u_1^{-\gamma} \int_0^{r_n(u_1)} w^{-m\gamma'} \, \mathrm{d}w \, \mathrm{d}(x_1, u_1)$$

$$= \frac{2\beta c_1^{m-1}}{1 - m\gamma'} \int_{\mathbb{S}_B} u_1^{-\gamma} r_n(u_1)^{1-m\gamma'} \, \mathrm{d}(x_1, u_1) \leqslant c_2 n \int_0^1 u_1^{-\gamma} r_n(u_1)^{1-m\gamma'} \, \mathrm{d}u_1,$$

(D.37)

where $c_2 = (2\beta)^m/((1-\gamma)^{m-1}(1-m\gamma'))$ is a positive constant if $\gamma' < 1/m$, we integrated with respect to x_1, and substituted c_1. Let us examine when $r_n(u_1) \leqslant 1$:

$$\Big(\frac{2\beta}{\varepsilon n}u_1^{-\gamma}\Big)^{1/\gamma'} \leqslant 1 \qquad \Longleftrightarrow \qquad u_1 \geqslant \Big(\frac{2\beta}{\varepsilon n}\Big)^{1/\gamma}.$$

Then,

$$\frac{E}{m} \leqslant c_2 n\Big(\int_0^{\big(\frac{2\beta}{\varepsilon n}\big)^{1/\gamma}} u_1^{-\gamma}\,\mathrm{d}u_1 + \Big(\frac{2\beta}{\varepsilon n}\Big)^{1/\gamma'-m}\int_{\big(\frac{2\beta}{\varepsilon n}\big)^{1/\gamma}}^1 u_1^{-(1/\gamma'-m+1)\gamma}\,\mathrm{d}u_1\Big).$$

For the first integral,

$$\int_0^{\big(\frac{2\beta}{\varepsilon n}\big)^{1/\gamma}} u_1^{-\gamma}\,\mathrm{d}u_1 = \frac{1}{1-\gamma}\Big(\frac{2\beta}{\varepsilon n}\Big)^{1/\gamma-1} \in o(n).$$

For the second integral,

$$\Big(\frac{2\beta}{\varepsilon n}\Big)^{1/\gamma'-m}\int_{\big(\frac{2\beta}{\varepsilon n}\big)^{1/\gamma}}^1 u_1^{-(1/\gamma'-m+1)\gamma}\,\mathrm{d}u_1$$

$$= \begin{cases} c_3\Big(\big(\frac{2\beta}{\varepsilon n}\big)^{1/\gamma'-m} - \big(\frac{2\beta}{\varepsilon n}\big)^{1/\gamma-1}\Big) & \text{if } 1/\gamma' - 1/\gamma \neq m-1 \\ -\frac{1}{\gamma}\big(\frac{2\beta}{\varepsilon n}\big)^{1/\gamma'-m}\log\big(\frac{2\beta}{\varepsilon n}\big) & \text{if } 1/\gamma' - 1/\gamma = m-1, \end{cases}$$

where $c_3 = (1-(1/\gamma'-m+1)\gamma)^{-1} \in \mathbb{R}$, which is of order $o(n)$. Then, $\limsup_{n\uparrow\infty} E/n = 0$ for all $\varepsilon > 0$.

Part (c). We begin this proof by following the same steps as in Part (b) through (D.35)–(D.36), and we arrive at the following bound:

$$\int_{(\mathbb{S}_n^{u_n\leqslant})^m} |N_{\mathsf{s}}(\boldsymbol{p}_{\mathsf{s},m})|\,\mathrm{d}\boldsymbol{p}_{\mathsf{s},m} \leqslant \frac{c_{u_n}^m}{1-m\gamma'}\,n,$$

where $c_{u_n} = 2\beta(1-u_n^{1-\gamma})/(1-\gamma)$, which shows the upper bound since $\lim_{n\uparrow\infty} u_n^{1-\gamma} = 0$.

For the lower bound, we follow the same arguments from Part (b) with $\mathbb{S}^{u_n\leqslant}$, c_{u_n} in place of $\mathbb{S}.$, c_1, respectively. Then, for Case (A), we arrive at the bound

$$\frac{E}{m} \leqslant \frac{2c_{u_n}^m}{1-(m-1)\gamma'}\,\varepsilon n \in O(n).$$

For Case (B), following the steps in Part (b) until (D.37), we have

$$\frac{E}{m} \leqslant c_2(1-u_n^{1-\gamma})^{m-1}n\int_{u_n}^1 u_1^{-\gamma}r_n(u_1)^{1-m\gamma'}\,\mathrm{d}u_1,$$

where $c_2 := (2\beta)^m/((1-\gamma)^{m-1}(1-m\gamma'))$, and we substituted c_{u_n}. Deviating from the proof of the previous part, we bound $r_n(u_1) \leqslant (2\beta u_1^{-\gamma}/(\varepsilon n))^{1/\gamma'}$ by neglecting the $\wedge 1$ part. Then,

$$\frac{E}{m} \leqslant c_2(1-u_n^{1-\gamma})^{m-1}n(\varepsilon n)^{-(1/\gamma'-m)}\int_{u_n}^1 u_1^{-(1/\gamma'-m+1)\gamma}\,\mathrm{d}u_1,$$

where $c_3 := (2\beta)^{1/\gamma'-m}c_2 > 0$. The integral can be bounded as follows:

$$\int_{u_n}^1 u_1^{-(1/\gamma'-m+1)\gamma} \, \mathrm{d}u_1 \leqslant \begin{cases} |c_4|u_n^{-((1/\gamma'-m+1)\gamma-1)_+} & \text{if } 1/\gamma' - 1/\gamma \neq m - 1 \\ \log(u_n^{-1}) & \text{if } 1/\gamma' - 1/\gamma = m - 1, \end{cases}$$

where $c_4 := (1 - (1/\gamma' - m + 1)\gamma)^{-1}$. Then, if $1/\gamma' - 1/\gamma \neq m - 1$, we have

$$\limsup_{n\uparrow\infty} \frac{E}{nm} \leqslant c_3|c_4|\varepsilon^{-(1/\gamma'-m)} \limsup_{n\uparrow\infty} \left(n^{-(1/\gamma'-m)}u_n^{-((1/\gamma'-m+1)\gamma-1)_+}\right).$$

If the exponent of u_n is 0, $\limsup_{n\uparrow\infty} E/n = 0$ for all $\varepsilon > 0$ since $\gamma' < 1/m$. If the exponent of u_n is negative, as $u_n > c_5 n^{-1}$ for some constant $c_5 > 0$, we apply the following bound:

$$\limsup_{n\uparrow\infty} \frac{E}{nm} \leqslant c_3|c_4|c_6\varepsilon^{-(1/\gamma'-m)} \limsup_{n\uparrow\infty} \left(n^{-(1/\gamma'-m+1)(1-\gamma)}\right) = 0,$$

where $c_6 := c_5^{1-(1/\gamma'-m+1)\gamma} > 0$. On the other hand, if $1/\gamma' - 1/\gamma = m - 1$, then

$$\limsup_{n\uparrow\infty} \frac{E}{nm} \leqslant c_3\varepsilon^{-(1/\gamma'-m)} \limsup_{n\uparrow\infty} \left(n^{-(1/\gamma'-m)} \log(u_n^{-1})\right)$$
$$\leqslant c_3\varepsilon^{-(1/\gamma'-m)} \lim_{n\uparrow\infty} \left(n^{-(1/\gamma'-m)} \log(c_5^{-1}n)\right) = 0,$$

where we used that $u_n > c_5 n^{-1}$ for large n. Thus, $\lim_{\varepsilon\downarrow 0} \limsup_{n\uparrow\infty} E/n = 0$ in both cases A and B, and the lower bound matches the upper bound in the limit as $n \to \infty$.

Part (d). We have that

$$\int_{\mathbb{S}} \left(\int_{\mathbb{S}_n^{u-\leqslant}} \mathbb{1}\{p_{\mathsf{s}}' \in N_{\mathsf{s}}(p_{\mathsf{s}})\} \, \mathrm{d}p_{\mathsf{s}}\right)^m \mathrm{d}p_{\mathsf{s}}' = \int_{\mathbb{S}} \int_{\left(\mathbb{S}_n^{u-\leqslant}\right)^m} \prod_{i=1}^m \mathbb{1}\{p_{\mathsf{s}}' \in N_{\mathsf{s}}(p_{\mathsf{s},i})\} \, \mathrm{d}\boldsymbol{p}_{\mathsf{s},m} \, \mathrm{d}p_{\mathsf{s}}'$$
$$= \int_{\left(\mathbb{S}_n^{u-\leqslant}\right)^m} \int_{\mathbb{S}} \mathbb{1}\{p_{\mathsf{s}}' \in N_{\mathsf{s}}(\boldsymbol{p}_{\mathsf{s},m})\} \, \mathrm{d}p_{\mathsf{s}}' \, \mathrm{d}\boldsymbol{p}_{\mathsf{s},m} = \int_{\left(\mathbb{S}_n^{u-\leqslant}\right)^m} |N_{\mathsf{s}}(\boldsymbol{p}_{\mathsf{s},m})| \, \mathrm{d}\boldsymbol{p}_{\mathsf{s},m},$$

where we used Fubini's theorem to switch the order of integration, and $\boldsymbol{p}_m := (p_1, \ldots, p_m)$. This expression can be bounded using Lemma D.8.2 (c) as follows:

$$\int_{\left(\mathbb{S}_n^{u-\leqslant}\right)^m} |N_{\mathsf{s}}(\boldsymbol{p}_{\mathsf{s},m})| \, \mathrm{d}\boldsymbol{p}_{\mathsf{s},m} \leqslant \left(\frac{2\beta}{1-\gamma}\right)^m \frac{n}{1-m\gamma'},$$

where we used that $1 - u_-^{1-\gamma} < 1$.

Part (e). We write the common neighborhood as an integral, and then use Fubini's theorem. Then, using Lemma D.8.1 (a) to calculate $|N_{\mathsf{s}}(p_{\mathsf{s},1})|$ and $|N_{\mathsf{s}}(p_{\mathsf{s},2})|$, we have

that

$$I := \iint_{\mathbb{S}_n^2} |N_{\mathsf{s}}((x_1, u_1))|^{m_1} |N_{\mathsf{s}}((x_1, u_1), (x_2, u_2))|$$

$$\times |N_{\mathsf{s}}((x_2, u_2))|^{m_2} |x_1 - x_2|^{m_3} \, \mathrm{d}(x_1, u_1) \, \mathrm{d}(x_2, u_2)$$

$$= c_1 \iint_{\mathbb{S}_n^2} u_1^{-m_1\gamma} u_2^{-m_2\gamma} |N_{\mathsf{s}}((x_1, u_1), (x_2, u_2))| |x_1 - x_2|^{m_3} \, \mathrm{d}(x_1, u_1) \, \mathrm{d}(x_2, u_2)$$

$$= c_1 \int_{\mathbb{S}_n} u_1^{-m_1\gamma} \int_{\mathbb{S}} \mathbb{1}\{p_{\mathsf{s}}' \in N_{\mathsf{s}}((x_1, u_1))\}$$

$$\times \int_{\mathbb{S}_n} \mathbb{1}\{p_{\mathsf{s}}' \in N_{\mathsf{s}}((x_2, u_2))\} u_2^{-m_2\gamma} |x_1 - x_2|^{m_3} \, \mathrm{d}(x_2, u_2) \, \mathrm{d}p_{\mathsf{s}}' \, \mathrm{d}(x_1, u_1),$$

where $c_1 := (2\beta/(1 - \gamma'))^{m_1+m_2}$, and we require that $\gamma < (m_1 \vee m_2)^{-1}$ to apply Lemma D.8.1 (a). Focusing on the inner integral, we use the triangle inequality $|x_1 - x_2|^{m_3} \leqslant (|x_1 - z| + |x_2 - z|)^{m_3}$:

$$I_{\mathsf{inner}} := \int_{\mathbb{S}_n} \mathbb{1}\{p_{\mathsf{s}}' \in N_{\mathsf{s}}((x_2, u_2))\} u_2^{-m_2\gamma} |x_1 - x_2|^{m_3} \, \mathrm{d}(x_2, u_2)$$

$$\leqslant 2^{m_3} \int_{\mathbb{S}} \mathbb{1}\{|z - x_2| \leqslant \beta u_2^{-\gamma} w^{-\gamma'}\} u_2^{-m_2\gamma} (|z - x_2|^{m_3} + |z - x_1|^{m_3}) \, \mathrm{d}(x_2, u_2)$$

$$= 2^{1+m_3} \int_0^1 u_2^{-m_2\gamma} \int_0^{\beta u_2^{-\gamma} w^{-\gamma'}} (x_2')^{m_3} + |z - x_1|^{m_3} \, \mathrm{d}x_2 \, \mathrm{d}u_2$$

$$= c_2 w^{-(1+m_3)\gamma'} \int_0^1 u_2^{-(1+m_2+m_3)\gamma} \, \mathrm{d}u_2$$

$$+ 2^{1+m_3} \beta w^{-\gamma'} |z - x_1|^{m_3} \int_0^1 u_2^{-(1+m_2)\gamma} \, \mathrm{d}u_2$$

$$= c_3 w^{-(1+m_3)\gamma'} \left(1 - u_-^{1-(1+m_2+m_3)\gamma}\right) + c_4 w^{-\gamma'} |z - x_1|^{m_3},$$

where $c_2 := (2\beta)^{1+m_3}/(1 + m_3)$, $c_3 := c_2/(1 - (1 + m_2 + m_3)\gamma)$, $c_4 := 2^{1+m_3}\beta/(1 - (1 + m_2)\gamma)$, we extended the integration domain from $\mathbb{S}_n$ to $\mathbb{S}$, and substituted for $x_2' := |z - x_2|$. Furthermore, if $u_- = 0$, then we require $\gamma < (1 + m_2 + m_3)^{-1}$ for the finiteness of the integral with respect to u_2. Then,

$$I \leqslant c_1 \int_{\mathbb{S}_n} u_1^{-m_1\gamma} \int_{\mathbb{S}} \mathbb{1}\{(z, w) \in N_{\mathsf{s}}((x_1, u_1))\}$$

$$\times \left(c_3 w^{-(1+m_3)\gamma'} + c_4 w^{-\gamma'} |z - x_1|^{m_3}\right) \mathrm{d}(z, w) \, \mathrm{d}(x_1, u_1)$$

$$= 2c_1 \int_{\mathbb{S}_n} u_1^{-m_1\gamma} \int_0^1 \int_0^{\beta u_1^{-\gamma} w^{-\gamma'}} \left(c_3 w^{-(1+m_3)\gamma'} + c_4 w^{-\gamma'} (z')^{m_3}\right) \mathrm{d}z' \, \mathrm{d}w \, \mathrm{d}(x_1, u_1)$$

$$= \int_0^1 w^{-(2+m_3)\gamma'} \, \mathrm{d}w \Big(c_5 \int_{\mathbb{S}_n} u_1^{-(1+m_1)\gamma} \, \mathrm{d}(x_1, u_1)$$

$$+ c_6 \int_{\mathbb{S}_n} u_1^{-(1+m_1+m_3)\gamma} \, \mathrm{d}(x_1, u_1)\Big) = c(c' + c'')n,$$

where we substituted for $z' := |z - x_1|$ in the first step, and $c_5 := 2\beta c_1 c_3$, $c_6 := (2\beta^{1+m_3} c_1 c_4)/(1 + m_3)$, $c_7 := c_5/((1 - (1 + m_1)\gamma)(1 - (2 + m_3)\gamma'))$, $c_8 := c_6/((1 - (1 +$

$m_1 + m_3)\gamma)(1 - (2 + m_3)\gamma'))$. Moreover, the finiteness of the integral with respect to w requires $\gamma' < 1/(2 + m_3)$, and if $u_- = 0$, then the integral with respect to u_1 is finite if $\gamma < 1/(1 + m_1 + m_3)$. All in all, we require $\gamma < 1/(1 + (m_1 \vee m_2) + m_3)$ and $\gamma' < 1/(2 + m_3)$.

Part (f). In this part, we follow the same strategy as in the previous part, but we consider the case where we have a minimum mark $u_- > 0$. Writing the common neighborhood as an integral, the application of Fubini's theorem and Lemma D.8.1 (a) yields

$$
I := \iint_{\left(\mathbb{S}_n^{u_-\leqslant}\right)^2} |N_{\mathsf{s}}((x_1, u_1))|^{m_1} |N_{\mathsf{s}}((x_1, u_1), (x_2, u_2))| |N_{\mathsf{s}}((x_2, u_2))|^{m_2}
$$
$$
\times |x_1 - x_2|^{m_3} \,\mathrm{d}(x_1, u_1)\,\mathrm{d}(x_2, u_2)
$$
$$
= c_1 \int_{\mathbb{S}_n^{u_-\leqslant}} u_1^{-m_1\gamma} \int_{\mathbb{S}} \mathbb{1}\{p_{\mathsf{s}}' \in N_{\mathsf{s}}((x_1, u_1))\}
$$
$$
\times \int_{\mathbb{S}_n^{u_-\leqslant}} \mathbb{1}\{p_{\mathsf{s}}' \in N_{\mathsf{s}}((x_2, u_2))\} u_2^{-m_2\gamma} |x_1 - x_2|^{m_3} \,\mathrm{d}(x_2, u_2)\,\mathrm{d}p_{\mathsf{s}}'\,\mathrm{d}(x_1, u_1),
$$

where $c_1 := (2\beta/(1 - \gamma'))^{m_1 + m_2}$. For the inner integral, the triangle inequality gives:

$$
I_{\text{inner}} := \int_{\mathbb{S}_n^{u_-\leqslant}} \mathbb{1}\{p_{\mathsf{s}}' \in N_{\mathsf{s}}((x_2, u_2))\} u_2^{-m_2\gamma} |x_1 - x_2|^{m_3} \,\mathrm{d}(x_2, u_2)
$$
$$
= c_2 w^{-(1+m_3)\gamma'} \int_{u_-}^1 u_2^{-(1+m_2+m_3)\gamma} \,\mathrm{d}u_2
$$
$$
+ 2^{1+m_3} \beta w^{-\gamma'} |z - x_1|^{m_3} \int_{u_-}^1 u_2^{-(1+m_2)\gamma} \,\mathrm{d}u_2
$$
$$
\leqslant |c_3| w^{-(1+m_3)\gamma'} u_-^{-((1+m_2+m_3)\gamma - 1)+} + |c_4| w^{-\gamma'} |z - x_1|^{m_3} u_-^{-((1+m_2)\gamma - 1)+},
$$

where we followed the same steps as in the previous part, and set $c_2 := (2\beta)^{1+m_3}/(1 + m_3)$, $c_3 := c_2/(1 - (1 + m_2 + m_3)\gamma)$ and $c_4 := (2\beta c_3)/(1 - (1 + m_2)\gamma)$. Note that we do not require any bounds on γ for the finiteness of the integrals. Then,

$$
I \leqslant c_1 \int_{\mathbb{S}_n^{u_-\leqslant}} u_1^{-m_1\gamma} \int_{\mathbb{S}} \mathbb{1}\{(z, w) \in N_{\mathsf{s}}((x_1, u_1))\} \Big(|c_3| w^{-(1+m_3)\gamma'} u_-^{-((1+m_2+m_3)\gamma - 1)+}
$$
$$
+ |c_4| w^{-\gamma'} |z - x_1|^{m_3} u_-^{-((1+m_2)\gamma - 1)+} \Big) \,\mathrm{d}(z, w)\,\mathrm{d}(x_1, u_1)
$$
$$
= 2c_1 \int_{\mathbb{S}_n^{u_-\leqslant}} u_1^{-m_1\gamma} \int_0^1 \int_0^{\beta u_1^{-\gamma} w^{-\gamma'}} \Big(|c_3| w^{-(1+m_3)\gamma'} u_-^{-((1+m_2+m_3)\gamma - 1)+}
$$
$$
+ |c_4| w^{-\gamma'} (z')^{m_3} u_-^{-((1+m_2)\gamma - 1)+} \Big) \,\mathrm{d}z'\,\mathrm{d}w\,\mathrm{d}(x_1, u_1)
$$
$$
= \int_0^1 w^{-(2+m_3)\gamma'} \,\mathrm{d}w \Big(c_5 u_-^{-((1+m_2+m_3)\gamma - 1)+} \int_{\mathbb{S}_n^{u_-\leqslant}} u_1^{-(1+m_1)\gamma} \,\mathrm{d}(x_1, u_1)
$$
$$
+ c_6 u_-^{-((1+m_2)\gamma - 1)+} \int_{\mathbb{S}_n^{u_-\leqslant}} u_1^{-(1+m_1+m_3)\gamma} \,\mathrm{d}(x_1, u_1) \Big)
$$
$$
\leqslant c \Big(|c'| u_-^{-((1+m_2+m_3)\gamma - 1)+ - ((1+m_1)\gamma - 1)+} + |c''| u_-^{-((1+m_2)\gamma - 1)+ - ((1+m_1+m_3)\gamma - 1)+} \Big) n,
$$

where we substituted for $z' := |z - x_1|$ in the first step, and $c_5 := 2\beta c_1 |c_3|$, $c_6 := (2\beta^{1+m_3} c_1 |c_4|)/(1+m_3)$, $c_7 := c_5/((1 - (1+m_1)\gamma)(1 - (2+m_3)\gamma'))$, $c_8 := c_6/((1 - (1 + m_1 + m_3)\gamma)(1 - (2 + m_3)\gamma'))$, and the constants c, c', c'' are specified in the statement of Lemma D.8.2 (e). We also used that $\gamma \notin \{(1 + m_2 + m_3)^{-1}, (1 + m_1 + m_3)^{-1}\}$ since $\gamma > 1/2$. $\qquad\square$

Proof of Lemma D.8.3. Here, we calculate the size of the temporal neighborhoods of points.

Part (a). The size of the temporal neighborhood of a point $p_t = (b, \ell) \in \mathbb{T}$ is given by

$$|N_t(p_t; t)| = \int_{\mathbb{R}} \mathbb{1}\{b \leqslant r \leqslant t \leqslant b + \ell\} \, dr = \mathbb{1}\{b \leqslant t \leqslant b + \ell\}(t - b).$$

Part (b). The size of the neighborhood of a point $r \in \mathbb{R}$ is given by

$$\int_{\mathbb{T}} \mathbb{1}\{r \in N_t(p_t; t)\} \, \mu_t(dp_t) = \int_{\mathbb{T}} \mathbb{1}\{b \leqslant r \leqslant t \leqslant b + \ell\} \, \mu_t(d(b, \ell))$$
$$= \mathbb{1}\{r \leqslant t\} \int_{-\infty}^{r} \int_{t-b}^{\infty} \mathbb{P}_L(d\ell) \, db = \mathbb{1}\{r \leqslant t\} \int_{-\infty}^{r} e^{-(t-b)} \, db = \mathbb{1}\{r \leqslant t\} e^{-(t-r)},$$

as required. $\qquad\square$

Proof of Lemma D.8.4. In this proof, we calculate the integrals one by one using Fubini's theorem.

Part (a). The integral is given by

$$\int_{\mathbb{T}} |N_t(p_t)|^\alpha \, \mu_t(dp_t) = \int_{\mathbb{T}} (t - b)^\alpha \, \mathbb{1}\{b \leqslant t \leqslant b + \ell\} \, \mu_t(d(b, \ell))$$
$$= \int_{-\infty}^{t} (t - b)^\alpha e^{t-b} \, db = \Gamma(\alpha + 1).$$

Part (b). We have that

$$\int_{\otimes_{i=1}^{m} \mathbb{T}_i} \Big| \bigcap_{i=1}^{m} N_t(p_{s,i}; t_i) \Big| \, dp_{t,m} = \int_{\mathbb{R}} \Big(\prod_{i=1}^{m} \int_{\mathbb{T}_i} \mathbb{1}\{r \in N_t(p_t; t_i)\} \, \mu_t(dp_t) \Big) \, dr.$$

If $\mathbb{T}_i = \mathbb{T}$ and $t_i = t$ for all indices $i \in \{1, \dots, m\}$, then

$$\int_{\otimes_{i=1}^{m} \mathbb{T}_i} |N_t(p_{t,m}; t)| \, dp_{t,m} = \int_{\mathbb{R}} \Big(\int_{\mathbb{T}} \mathbb{1}\{r \in N_t(p_t; t)\} \, \mu_t(dp_t) \Big)^m \, dr$$
$$= \int_{\mathbb{R}} \Big(\int_{\mathbb{T}} \mathbb{1}\{b \leqslant r \leqslant t \leqslant b + \ell\} \, \mu_t(d(b, \ell)) \Big)^m \, dr = \int_{-\infty}^{t} e^{-m(t-r)} \, dr = \frac{1}{m}.$$

Part (c). We bound the integral using Lemma D.8.3 (a) as follows:

$$\int_{\mathbb{T}} \int_{\mathbb{T}} |N_{\mathsf{t}}(p_{\mathsf{s},1}; t_1)|^{\alpha_1} |N_{\mathsf{t}}(p_{\mathsf{s},1}; t_1) \cap N_{\mathsf{t}}(p_{\mathsf{s},2}; t_2)| |N_{\mathsf{t}}(p_{\mathsf{s},2}; t_2)|^{\alpha_2} \, \mu_{\mathsf{t}}(\mathrm{d}p_{\mathsf{s},2}) \, \mu_{\mathsf{t}}(\mathrm{d}p_{\mathsf{s},1})$$

$$\leqslant \int_{\mathbb{T}} |N_{\mathsf{t}}(p_{\mathsf{s},1}; t_1)|^{\alpha_1} \, \mu_{\mathsf{t}}(\mathrm{d}p_{\mathsf{s},1}) \int_{\mathbb{T}} |N_{\mathsf{t}}(p_{\mathsf{s},2}; t_2)|^{\alpha_2+1} \, \mu_{\mathsf{t}}(\mathrm{d}p_{\mathsf{s},2}) \leqslant \Gamma(\alpha_1+1)\Gamma(\alpha_2+2),$$

where we used Part (a) of this lemma in the second step.

Part (d). We use Lemma D.8.3 (b) to calculate the integral:

$$\int_{\mathbb{R}} \left(\int_{\mathbb{T}} \mathbb{1}\{p' \in N(p; t)\} \, \mu(\mathrm{d}p) \right)^{\alpha} \mathrm{d}p' = \int_{-\infty}^{t} \mathrm{e}^{-\alpha(t-r)} \, \mathrm{d}r = \frac{1}{\alpha},$$

as required. □

Proof of Lemma D.8.5. **Part (a).** Part (a) of the lemma is trivial.
Part (b). For the *plus case*, we have

$$\left| \delta_{t_1,t_2}(N_{\mathsf{t}}^+(p_{\mathsf{t}})) \right| = |N_{\mathsf{t}}^+(p_{\mathsf{t}}; t_2)| - |N_{\mathsf{t}}^+(p_{\mathsf{t}}; t_1)|$$

$$= \int_{\mathbb{R}} \mathbb{1}\{b \leqslant r \leqslant (b+\ell) \wedge t_2\} - \mathbb{1}\{b \leqslant r \leqslant (b+\ell) \wedge t_1\} \, \mathrm{d}r$$

$$= \int_{\mathbb{R}} \mathbb{1}\{b \vee t_1 \leqslant r \leqslant (b+\ell) \wedge t_2\} \, \mathrm{d}r$$

$$= (((b+\ell) \wedge t) - (b \vee t_1)) \, \mathbb{1}\{b \leqslant t_2\} \, \mathbb{1}\{t_1 \leqslant b+\ell\}.$$

In the *minus case*,

$$\left| \delta_{t_1,t_2}(N_{\mathsf{t}}^-(p_{\mathsf{t}})) \right| = |N_{\mathsf{t}}^-(p_{\mathsf{t}}; t_2)| - |N_{\mathsf{t}}^-(p_{\mathsf{t}}; t_1)|$$

$$= \int_{\mathbb{R}} \mathbb{1}\{b \leqslant r \leqslant b+\ell \leqslant t_2\} - \mathbb{1}\{b \leqslant r \leqslant b+\ell \leqslant t_1\} \, \mathrm{d}r$$

$$= \int_{\mathbb{R}} \mathbb{1}\{b \leqslant r \leqslant t_1 \leqslant b+\ell \leqslant t_2\} \, \mathrm{d}r$$

$$= (t_1 - b) \, \mathbb{1}\{b \leqslant t_1 \leqslant b+\ell \leqslant t_2\}.$$

Part (c). For the *plus case*, we have

$$\int_{\mathbb{T}^{0\leqslant}} \mathbb{1}\{r \in N_{\mathsf{t}}^+(p_{\mathsf{t}}; t)\} \, \mu_{\mathsf{t}}(\mathrm{d}p_{\mathsf{t}}) = \int_{\mathbb{T}^{0\leqslant}} \mathbb{1}\{b \leqslant r \leqslant (b+\ell) \wedge t\} \, \mu_{\mathsf{t}}(\mathrm{d}(b,\ell))$$

$$= \mathbb{1}\{r \leqslant 0\} \int_{-\infty}^{r} \int_{-b}^{\infty} \mathbb{P}_L(\mathrm{d}\ell) \, \mathrm{d}b + \mathbb{1}\{0 \leqslant r \leqslant t\} \int_{-\infty}^{r} \int_{r-b}^{\infty} \mathbb{P}_L(\mathrm{d}\ell) \, \mathrm{d}b$$

$$= \mathbb{1}\{r \leqslant 0\} \mathrm{e}^r + \mathbb{1}\{0 \leqslant r \leqslant t\}.$$

For the *minus case*,

$$\int_{\mathbb{T}^{0\leqslant}} \mathbb{1}\{r \in N_{\mathsf{t}}^-(p_{\mathsf{t}}; t)\} \, \mu_{\mathsf{t}}(\mathrm{d}p_{\mathsf{t}}) = \int_{\mathbb{T}^{0\leqslant}} \mathbb{1}\{b \leqslant r \leqslant (b+\ell) \wedge t\} \, \mu_{\mathsf{t}}(\mathrm{d}(b,\ell))$$

$$= \mathbb{1}\{r \leqslant 0\} \int_{-\infty}^{r} \int_{-b}^{t-b} \mathbb{P}_L(\mathrm{d}\ell) \, \mathrm{d}b + \mathbb{1}\{0 \leqslant r \leqslant t\} \int_{-\infty}^{r} \int_{r-b}^{t-b} \mathbb{P}_L(\mathrm{d}\ell) \, \mathrm{d}b$$

$$= \mathbb{1}\{r \leqslant 0\}(\mathrm{e}^r - \mathrm{e}^{-(t-r)}) + \mathbb{1}\{0 \leqslant r \leqslant t\}(1 - \mathrm{e}^{-(t-r)}),$$

as required. □

Proof of Lemma D.8.6. Here we show the integrals of the *plus-minus* temporal neighborhoods.

Part (a). For the *plus case*, we have

$$\int_{\mathbb{T}^{0\leqslant}} |N_{\mathsf{t}}^+(p_{\mathsf{t}};t)|^m \, \mu_{\mathsf{t}}(\mathrm{d}p_{\mathsf{t}}) = \int_{\mathbb{T}_{\leqslant t}^{0\leqslant}} (((b+\ell)\wedge t) - b)^m \, \mu_{\mathsf{t}}(\mathrm{d}(b,\ell))$$

$$= \int_{-\infty}^0 \int_{-b}^{t-b} \ell^m \, \mathbb{P}_L(\mathrm{d}\ell) \, \mathrm{d}b + \int_0^t \int_0^{t-b} \ell^m \, \mathbb{P}_L(\mathrm{d}\ell) \, \mathrm{d}b$$

$$+ \int_{-\infty}^t \int_{t-b}^\infty (t-b)^m \, \mathbb{P}_L(\mathrm{d}\ell) \, \mathrm{d}b.$$

Note that

$$\frac{\mathrm{d}}{\mathrm{d}\ell}\left(-\mathrm{e}^{-\ell} m! \sum_{i=0}^m \frac{\ell^i}{i!}\right) = \ell^m \mathrm{e}^{-\ell}.$$

Then,

$$\int_{\mathbb{T}^{0\leqslant}} |N_{\mathsf{t}}^+(p_{\mathsf{t}};t)|^m \, \mu_{\mathsf{t}}(\mathrm{d}p_{\mathsf{t}}) = \int_{-\infty}^0 m!\left(\mathrm{e}^b \sum_{i=0}^m \frac{(-b)^i}{i!} - \mathrm{e}^{-(t-b)} \sum_{i=0}^m \frac{(t-b)^i}{i!}\right) \mathrm{d}b$$

$$+ \int_0^t m!\left(1 - \mathrm{e}^{-(t-b)} \sum_{i=0}^m \frac{(t-b)^i}{i!}\right) \mathrm{d}b + \int_{-\infty}^t (t-b)^m \mathrm{e}^{-(t-b)} \, \mathrm{d}b$$

$$= \sum_{i=0}^m \frac{m!}{i!}\left(\int_{-\infty}^0 (-b)^i \mathrm{e}^b \, \mathrm{d}b - \int_{-\infty}^t (t-b)^i \mathrm{e}^{-(t-b)} \, \mathrm{d}b\right) + m!(t+1) = m!(t+1),$$

where we applied the dominated convergence theorem with $\exp(-(t-b))$ and $\exp(b)$ as the dominating functions to interchange the integral and the summation, and recognized the Gamma functions. For the *minus case*, we use the same argument to obtain

$$\int_{\mathbb{T}^{0\leqslant}} |N_{\mathsf{t}}^-(p_{\mathsf{t}};t)|^m \, \mu_{\mathsf{t}}(\mathrm{d}p_{\mathsf{t}}) = \int_{\mathbb{T}^{[0,t]}} \ell^m \, \mu_{\mathsf{t}}(\mathrm{d}(b,\ell))$$

$$= \int_{-\infty}^0 \int_{-b}^{t-b} \ell^m \, \mathbb{P}_L(\mathrm{d}\ell) \, \mathrm{d}b + \int_0^t \int_0^{t-b} \ell^m \, \mathbb{P}_L(\mathrm{d}\ell) \, \mathrm{d}b = m!t.$$

Part (b). For the *plus case*, we have

$$\int_{\mathbb{T}^{0\leqslant}} |N_{\mathsf{t}}^+(p_{\mathsf{t}};t)|^\alpha \, \mu_{\mathsf{t}}(\mathrm{d}p_{\mathsf{t}}) = \int_{\mathbb{T}_{\leqslant t}^{0\leqslant}} (((b+\ell)\wedge t) - b)^\alpha \, \mu_{\mathsf{t}}(\mathrm{d}(b,\ell))$$

$$= \int_{-\infty}^0 \int_{-b}^{t-b} \ell^\alpha \, \mathbb{P}_L(\mathrm{d}\ell) \, \mathrm{d}b + \int_0^t \int_0^{t-b} \ell^\alpha \, \mathbb{P}_L(\mathrm{d}\ell) \, \mathrm{d}b + \int_{-\infty}^t \int_{t-b}^\infty (t-b)^\alpha \, \mathbb{P}_L(\mathrm{d}\ell) \, \mathrm{d}b$$

$$\leqslant 2c \int_{-\infty}^0 \mathrm{e}^b - \mathrm{e}^{-(t-b)} \, \mathrm{d}b + 2c \int_0^t 1 - \mathrm{e}^{-(t-b)} \, \mathrm{d}b + \int_{-\infty}^t (t-b)^\alpha \mathrm{e}^{-(t-b)} \, \mathrm{d}b$$

$$= 2ct + \Gamma(\alpha+1),$$

where we used that $\ell^\alpha \mathrm{e}^{-\ell} \leqslant c\mathrm{e}^{-\ell/2}$ with $c := (2\alpha)^\alpha \mathrm{e}^{-\alpha}$, and substituted for $t - b$ in the last term. In the *minus case*, we use the same argument as above to obtain

$$\int_{\mathbb{T}^{0\leqslant}} |N_{\mathsf{t}}^-(p_{\mathsf{t}};t)|^\alpha \, \mu_{\mathsf{t}}(\mathrm{d}p_{\mathsf{t}}) = \int_{\mathbb{T}^{[0,t]}} \ell^\alpha \, \mu_{\mathsf{t}}(\mathrm{d}(b,\ell))$$
$$= \int_{-\infty}^0 \int_{-b}^{t-b} \ell^\alpha \, \mathbb{P}_L(\mathrm{d}\ell) \, \mathrm{d}b + \int_0^t \int_0^{t-b} \ell^\alpha \, \mathbb{P}_L(\mathrm{d}\ell) \, \mathrm{d}b \leqslant 2ct.$$

Part (c). First, using Lemma D.8.5 (b), we calculate the integral in the *plus case*:

$$\int_{\mathbb{T}_{\leqslant t_2}^{t_1 \leqslant}} |\delta_{t_1,t_2}(N_{\mathsf{t}}^+(p_{\mathsf{t}}))|^m \, \mu_{\mathsf{t}}(\mathrm{d}p_{\mathsf{t}}) = \int_{\mathbb{T}_{\leqslant t_2}^{t_1 \leqslant}} (((b+\ell) \wedge t_2) - (b \vee t_1))^m \, \mu_{\mathsf{t}}(\mathrm{d}(b,\ell))$$
$$= \int_{-\infty}^{t_1} \int_{t_1-b}^{t_2-b} (b+\ell-t_1)^m \, \mathbb{P}_L(\mathrm{d}\ell) \, \mathrm{d}b + \int_{-\infty}^{t_1} \int_{t_2-b}^\infty (t_2-t_1)^m \, \mathbb{P}_L(\mathrm{d}\ell) \, \mathrm{d}b$$
$$+ \int_{t_1}^{t_2} \int_0^{t_2-b} \ell^m \, \mathbb{P}_L(\mathrm{d}\ell) \, \mathrm{d}b + \int_{t_1}^{t_2} \int_{t_2-b}^\infty (t_2-b)^m \, \mathbb{P}_L(\mathrm{d}\ell) \, \mathrm{d}b.$$

We treat each term individually. For the first integral, we substitute $a := b + \ell - t_1$:

$$\int_{-\infty}^{t_1} \int_{t_1-b}^{t_2-b} (b+\ell-t_1)^m \, \mathbb{P}_L(\mathrm{d}\ell) \, \mathrm{d}b = \int_{-\infty}^{t_1} \mathrm{e}^{-(t_1-b)} \int_0^{t_2-t_1} a^m \mathrm{e}^{-a} \, \mathrm{d}a \, \mathrm{d}b$$
$$\leqslant c_1(t_2-t_1) \in O(t_2-t_1),$$

where we used that $a^m \mathrm{e}^{-a} \leqslant c_1$ is bounded in the second step. For the second integral, we have

$$\int_{-\infty}^{t_1} \int_{t_2-b}^\infty (t_2-t_1)^m \, \mathbb{P}_L(\mathrm{d}\ell) \, \mathrm{d}b = (t_2-t_1)^m \mathrm{e}^{-(t_2-t_1)} \in O(t_2-t_1),$$

where, in the last step, we used that $t_2 - t_1 \leqslant 1$. For the third term, we have

$$\int_{t_1}^{t_2} \int_0^{t_2-b} \ell^m \, \mathbb{P}_L(\mathrm{d}\ell) \, \mathrm{d}b \leqslant \Gamma(m+1)(t_2-t_1) \in O(t_2-t_1),$$

where we extended the integration domain from $[0, t_2 - b]$ to $[0, \infty)$. For the last integral,

$$\int_{t_1}^{t_2} \int_{t_2-b}^\infty (t_2-b)^m \, \mathbb{P}_L(\mathrm{d}\ell) \, \mathrm{d}b = \int_{t_1}^{t_2} (t_2-b)^m \mathrm{e}^{-(t_2-b)} \, \mathrm{d}b$$
$$= \int_0^{t_2-t_1} a^m \mathrm{e}^{-a} \, \mathrm{d}a \in O(t_2-t_1),$$

where we used the substitution $a := t_2 - b$ in the second step, and used that the integrand is bounded in the last step. Then, each of the terms is in $O(t_2 - t_1)$, which completes the proof for the *plus case*.

For the *minus case*,

$$\int_{\mathbb{T}^{0\leqslant}} |\delta_{t_1,t_2}(N_{\mathsf{t}}^-(p_{\mathsf{t}}))|^m \, \mu_{\mathsf{t}}(\mathrm{d}p_{\mathsf{t}}) = \int_{\mathbb{T}_{\leqslant t_1}^{[t_1,t_2]}} (t_1 - b)^m \, \mu_{\mathsf{t}}(\mathrm{d}(b,\ell))$$

$$= \int_{-\infty}^{t_1} (t_1 - b)^m \big(\mathrm{e}^{-(t_1-b)} - \mathrm{e}^{-(t_2-b)} \big) \, \mathrm{d}b$$

$$= \big(1 - \mathrm{e}^{-(t_2-t_1)}\big) \int_0^\infty a^m \mathrm{e}^{-a} \, \mathrm{d}a$$

$$= \Gamma(m+1)\big(1 - \mathrm{e}^{-(t_2-t_1)}\big) \in O(t_2 - t_1),$$

where we substituted $a := t_1 - b$ in the third step. Thus,

$$\int_{\mathbb{T}^{0\leqslant}} |\delta_{t_1,t_2}(N_{\mathsf{t}}^\pm(p_{\mathsf{t}}))|^m \, \mu_{\mathsf{t}}(\mathrm{d}p_{\mathsf{t}}) \leqslant (t_2 - t_1)^m.$$

Part (d). For the *plus case*,

$$\int_{\mathbb{R}} \bigg(\int_{\mathbb{T}^{0\leqslant}} \mathbb{1}\{r \in \delta_{t_1,t_2}(N_{\mathsf{t}}^+(p_{\mathsf{t}}))\} \, \mu_{\mathsf{t}}(\mathrm{d}p_{\mathsf{t}}) \bigg)^m \mathrm{d}r$$

$$= \int_{\mathbb{R}} \bigg(\int_{\mathbb{T}_{\leqslant t_2}^{t_1\leqslant}} \mathbb{1}\{b \vee t_1 \leqslant r \leqslant (b+\ell) \wedge t_2\} \, \mu_{\mathsf{t}}(\mathrm{d}(b,\ell)) \bigg)^m \mathrm{d}r$$

$$= \int_{\mathbb{R}} \mathbb{1}\{t_1 \leqslant r \leqslant t_2\} \bigg(\int_{\mathbb{T}} \mathbb{1}\{b \leqslant r \leqslant b+\ell\} \, \mu_{\mathsf{t}}(\mathrm{d}(b,\ell)) \bigg)^m \mathrm{d}r \in O(t_2 - t_1),$$

since the inner integral is equal to 1 since

$$\int_{\mathbb{T}} \mathbb{1}\{b \leqslant r \leqslant b+\ell\} \, \mu_{\mathsf{t}}(\mathrm{d}(b,\ell)) = \int_{-\infty}^t \int_{t-b}^\infty \mathbb{P}_L(\mathrm{d}\ell) \, \mathrm{d}b = \int_{-\infty}^t \mathrm{e}^{-(t-b)} \, \mathrm{d}b = 1.$$

For the *minus case*, we have

$$\int_{\mathbb{R}} \bigg(\int_{\mathbb{T}^{0\leqslant}} \mathbb{1}\{r \in \delta_{t_1,t_2}(N_{\mathsf{t}}^-(p_{\mathsf{t}}))\} \, \mu_{\mathsf{t}}(\mathrm{d}p_{\mathsf{t}}) \bigg)^\alpha \mathrm{d}r = \int_{-\infty}^{t_1} \bigg(\int_{\mathbb{T}_{\leqslant r}^{[t_1,t_2]}} \mu_{\mathsf{t}}(\mathrm{d}p_{\mathsf{t}}) \bigg)^\alpha \mathrm{d}r$$

$$= \int_{-\infty}^{t_1} \big(\mathrm{e}^{-(t_1-r)} - \mathrm{e}^{-(t_2-r)} \big)^\alpha \, \mathrm{d}r = \big(\mathrm{e}^{-t_1} - \mathrm{e}^{-t_2} \big)^\alpha \int_{-\infty}^{t_1} \mathrm{e}^{\alpha r} \, \mathrm{d}r$$

$$= \frac{1}{\alpha} \big(1 - \mathrm{e}^{-(t_2-t_1)}\big)^\alpha \in O(t_2 - t_1).$$

Part (e). Note that by independence of the points p_i and their neighborhoods $N_{\mathsf{t}}^\pm(p_{\mathsf{s},i}; t)$, Fubini's theorem gives

$$\iint_{(\mathbb{T}^{0\leqslant})^m} |N_{\mathsf{t}}^\pm(\boldsymbol{p}_{\mathsf{t},m}; t)| \, \mathrm{d}\boldsymbol{p}_{\mathsf{t},m} = \int_{\mathbb{R}} \bigg(\int_{\mathbb{T}^{0\leqslant}} \mathbb{1}\{r \in N_{\mathsf{t}}^\pm(p_{\mathsf{t}}; t)\} \, \mu_{\mathsf{t}}(\mathrm{d}p_{\mathsf{t}}) \bigg)^m \mathrm{d}r.$$

For the *plus case*, using Lemma D.8.5 (c), we have:

$$\int_{\mathbb{R}} \left(\int_{\mathbb{T}^{0\leqslant}} \mathbb{1}\{r \in N_{\mathsf{t}}^+(p_{\mathsf{t}}; t)\} \, \mu_{\mathsf{t}}(\mathrm{d}p_{\mathsf{t}}) \right)^m \mathrm{d}r$$

$$= \int_{\mathbb{R}} \left(\int_{\mathbb{T}^{0\leqslant}} \mathbb{1}\{b \leqslant r \leqslant (b+\ell) \wedge t\} \, \mu_{\mathsf{t}}(\mathrm{d}(b,\ell)) \right)^m \mathrm{d}r$$

$$= \int_{\mathbb{R}} \left(\mathbb{1}\{r \leqslant 0\} \int_{-\infty}^r \int_{-b}^\infty \mathbb{P}_L(\mathrm{d}\ell) \, \mathrm{d}b + \mathbb{1}\{0 \leqslant r \leqslant t\} \int_{-\infty}^r \int_{r-b}^\infty \mathbb{P}_L(\mathrm{d}\ell) \, \mathrm{d}b \right)^m \mathrm{d}r$$

$$= \int_{-\infty}^0 \mathrm{e}^{mr} \, \mathrm{d}r + \int_0^t \mathrm{d}r = \frac{1}{m} + t.$$

For the *minus case*, we have

$$\int_{\mathbb{R}} \left(\int_{\mathbb{T}^{0\leqslant}} \mathbb{1}\{r \in N_{\mathsf{t}}^-(p_{\mathsf{t}}; t)\} \, \mu_{\mathsf{t}}(\mathrm{d}p_{\mathsf{t}}) \right)^m \mathrm{d}r \leqslant \int_{\mathbb{R}} \left(\int_{\mathbb{T}^{0\leqslant}} \mathbb{1}\{r \in N_{\mathsf{t}}^+(p_{\mathsf{t}}; t)\} \, \mu_{\mathsf{t}}(\mathrm{d}p_{\mathsf{t}}) \right)^m \mathrm{d}r.$$

Part (f). For the *plus case*, we have

$$\iint_{(\mathbb{T}_{\leqslant 1}^{0\leqslant})^2} |N_{\mathsf{t}}^\pm(p_{\mathsf{s},1}; t_1)|^{\alpha_1} |N_{\mathsf{t}}^\pm(p_{\mathsf{s},1}; t_1) \cap N_{\mathsf{t}}^\pm(p_{\mathsf{s},2}; t_2)| |N_{\mathsf{t}}^\pm(p_{\mathsf{s},2}; t_2)|^{\alpha_2} \, \mu_{\mathsf{t}}(\mathrm{d}p_{\mathsf{s},1}) \, \mu_{\mathsf{t}}(\mathrm{d}p_{\mathsf{s},2})$$

$$\leqslant \int_{\mathbb{T}_{\leqslant 1}^{0\leqslant}} \int_{\mathbb{T}^{0\leqslant}} |N_{\mathsf{t}}^\pm(p_{\mathsf{s},2}; t_2)|^{\alpha_2+1} \, \mu_{\mathsf{t}}(\mathrm{d}p_{\mathsf{s},1}) \, \mu_{\mathsf{t}}(\mathrm{d}p_{\mathsf{s},2}) \leqslant c \int_{\mathbb{T}_{\leqslant 1}^{0\leqslant}} \mu_{\mathsf{t}}(\mathrm{d}p_{\mathsf{t}})$$

$$= c \int_{-\infty}^0 \int_{-b}^\infty \mathbb{P}_L(\mathrm{d}\ell) \, \mathrm{d}b + c \int_0^1 \int_0^\infty \mathbb{P}_L(\mathrm{d}\ell) \, \mathrm{d}b = 2c < \infty$$

with some constant $c > 0$, and we used Lemma D.8.6 (b) in the second step for the integral with respect to $p_{\mathsf{s},2}$. $\qquad\square$

D.A Proofs of Lemmas D.10.1 and D.10.2

The following two lemmas were necessary to apply Proposition D.5.4 to show the finite-dimensional convergence of the plus and minus parts. Here, we follow the same approach as in the proof of Proposition D.5.4 and use the time interval-based decomposition of the edge counts to calculate the limiting covariance functions of $\overline{S}_n^\pm$.

Proof of Lemma D.10.1. The proof follows the same steps as the proof of Proposition D.2.2. Note that

$$\mathrm{Cov}(\overline{S}_n^\pm(s), \overline{S}_n^\pm(t)) = \tfrac{1}{n} \, \mathrm{Cov}(S_n^\pm(s), S_n^\pm(t)).$$

For the covariance functions of $\overline{S}_n^\pm(t)$, we assume that $0 \leqslant s \leqslant t \leqslant 1$, and decompose them based on

$$S_n^+(s) = S_n^{\mathsf{A}+}(s) \qquad S_n^+(t) = S_n^{\mathsf{A}+}(s) + S_n^{\mathsf{B}+}(s,t) + S_n^{\mathsf{C}+}(s,t)$$

$$S_n^-(s) = S_n^{\mathsf{A}-}(s) \qquad S_n^-(t) = S_n^{\mathsf{A}-}(s) + S_n^{\mathsf{B}-}(s,t) + S_n^{\mathsf{C}-}(s,t),$$

where

$$S_n^{\mathsf{A}+}(s) := \sum_{P \in \mathcal{P} \cap (\mathbb{S}_n \times \mathbb{T}^{0 \leqslant})} \sum_{P' \in \mathcal{P}'} \mathbb{1}\{P' \in N^+(P; s)\}$$

$$S_n^{\mathsf{B}+}(s,t) := \sum_{P \in \mathcal{P} \cap (\mathbb{S}_n \times \mathbb{T}^{0 \leqslant}_{\leqslant s})} \sum_{P' \in \mathcal{P}'} \mathbb{1}\{P' \in N^+(P; t)\}\, \mathbb{1}\{s \leqslant R\}$$

$$S_n^{\mathsf{C}+}(s,t) := \sum_{P \in \mathcal{P} \cap (\mathbb{S}_n \times \mathbb{T}_{[s,t]})} \sum_{P' \in \mathcal{P}'} \mathbb{1}\{P' \in N^+(P; t)\}$$

for the *plus case* and

$$S_n^{\mathsf{A}-}(s) := \sum_{P \in \mathcal{P} \cap (\mathbb{S}_n \times \mathbb{T}^{[0,s]})} \sum_{P' \in \mathcal{P}'} \mathbb{1}\{P' \in N^-(P; s)\}$$

$$S_n^{\mathsf{B}-}(s,t) := \sum_{P \in \mathcal{P} \cap (\mathbb{S}_n \times \mathbb{T}^{[s,t]})} \sum_{P' \in \mathcal{P}'} \mathbb{1}\{P' \in N^-(P; t)\}\, \mathbb{1}\{R \leqslant s\} \qquad \text{(D.38)}$$

$$S_n^{\mathsf{C}-}(s,t) := \sum_{P \in \mathcal{P} \cap (\mathbb{S}_n \times \mathbb{T}^{[s,t]})} \sum_{P' \in \mathcal{P}'} \mathbb{1}\{P' \in N^-(P; t)\}\, \mathbb{1}\{s \leqslant R\}$$

for the *minus case*. These decompositions of the edge counts are visualized in Figure D.7. With these notations, the covariance functions are given as follows:

$$\begin{aligned}
\mathrm{Cov}(S_n^+(s), S_n^+(t)) &= \mathrm{Var}(S_n^{\mathsf{A}+}(s)) + \mathrm{Cov}(S_n^{\mathsf{A}+}(s), S_n^{\mathsf{B}+}(s,t)) \\
\mathrm{Cov}(S_n^-(s), S_n^-(t)) &= \mathrm{Var}(S_n^{\mathsf{A}-}(s)) + \mathrm{Cov}(S_n^{\mathsf{A}-}(s), S_n^{\mathsf{B}-}(s,t)),
\end{aligned} \qquad \text{(D.39)}$$
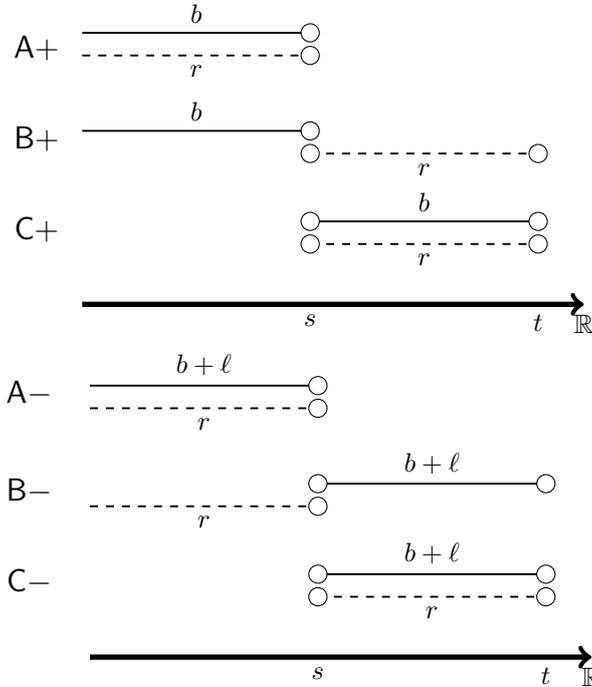
Figure D.7: Decomposition of the edge count functions $S_n^{\pm}(s)$ and $S_n^{\pm}(t)$. We require that $b \leqslant r \leqslant b + \ell$.

as $\mathrm{Cov}(S_n^{\mathsf{A}+}(s), S_n^{\mathsf{C}+}(s,t)) = \mathrm{Cov}(S_n^{\mathsf{A}-}(s), S_n^{\mathsf{C}-}(s,t)) = 0$ due to the independence property of the Poisson processes $\mathcal{P}$ and $\mathcal{P}'$.

Covariance function of $S_n^+(t)$. We begin with the *plus case*. The variance term in (D.39) is

$$\mathrm{Var}(S_n^{\mathsf{A}+}(s)) = \mathbb{E}\Big[\sum_{P \in \mathcal{P} \cap \mathbb{S}_n \times \mathbb{T}^{0\leqslant}} \deg^+(P;s)^2\Big] = \int_{\mathbb{S}_n \times \mathbb{T}^{0\leqslant}} \mathbb{E}\big[\deg^+(p;s)^2\big]\,\mu(\mathrm{d}p)$$
$$+ \iint_{(\mathbb{S}_n \times \mathbb{T}^{0\leqslant})^2} \mathrm{Cov}\big(\deg^+(p_1;s), \deg^+(p_2;s)\big)\,\mu(\mathrm{d}p_1)\,\mu(\mathrm{d}p_2).$$

Using the same calculations as in the proof of Lemma D.3.1, we see that $\mathbb{E}[\deg^+(p;s)^2] = |N^+(p;s)| + |N^+(p;s)|^2$, which leads to

$$\lim_{n\uparrow\infty} \frac{1}{n} \int_{\mathbb{S}_n \times \mathbb{T}^{0\leqslant}} \mathbb{E}\big[\deg^+(p;s)^2\big]\,\mu(\mathrm{d}p)$$
$$= \sum_{k=1}^{2} \lim_{n\uparrow\infty} \frac{1}{n} \int_{\mathbb{S}_n} |N_{\mathsf{s}}(p_{\mathsf{s}})|^k\,\mathrm{d}p_{\mathsf{s}} \int_{\mathbb{T}^{0\leqslant}} |N_{\mathsf{t}}^+(p_{\mathsf{t}};s)|^k\,\mu_{\mathsf{t}}(\mathrm{d}p_{\mathsf{t}}) = \sum_{k=1}^{2} \Big(\frac{2\beta}{1-\gamma'}\Big)^k \frac{k!(s+1)}{1-k\gamma},$$

where in the last step we used Lemma D.8.2 (a) for the spatial part and Lemma D.8.6 (a) for the temporal part. Following again the same calculations as in Lemma D.3.1, we get $\mathrm{Cov}(\deg^+(p_1;s), \deg^+(p_2;s)) = |N^+(p_1,p_2;s)|$. Using this result, we factorize the second integral:

$$\lim_{n\uparrow\infty} \frac{1}{n} \iint_{(\mathbb{S}_n \times \mathbb{T}^{0\leqslant})^2} |N^+(p_1,p_2;s)|\,\mu(\mathrm{d}p_1)\,\mu(\mathrm{d}p_2)$$
$$= \lim_{n\uparrow\infty} \frac{1}{n} \iint_{\mathbb{S}_n^2} |N_{\mathsf{s}}(p_{\mathsf{s},1}, p_{\mathsf{s},2})|\,\mathrm{d}p_{\mathsf{s},1}\,\mathrm{d}p_{\mathsf{s},2}$$
$$\times \iint_{(\mathbb{T}^{0\leqslant})^2} |N_{\mathsf{t}}^+(p_{\mathsf{s},1}, p_{\mathsf{s},2};s)|\,\mu_{\mathsf{t}}(\mathrm{d}p_{\mathsf{s},1})\,\mu_{\mathsf{t}}(\mathrm{d}p_{\mathsf{s},2}) < \infty,$$

where we used Lemma D.8.2 (b) with $m = 2$ for the spatial part and Lemma D.8.6 (e) for the temporal part. Similarly to the proof of Proposition D.2.2, the covariance term $\mathrm{Cov}(S_n^{\mathsf{A}+}(s), S_n^{\mathsf{B}+}(s,t))$ is determined by the common $\mathcal{P}$-points of $S_n^{\mathsf{A}+}(s)$ and $S_n^{\mathsf{B}+}(s,t)$:

$$\lim_{n\uparrow\infty} \frac{1}{n} \mathrm{Cov}(S_n^{\mathsf{A}+}(s), S_n^{\mathsf{B}+}(s,t))$$
$$= \lim_{n\uparrow\infty} \frac{1}{n} \int_{\mathbb{S}_n \times \mathbb{T}_{\leqslant s}^{0\leqslant}} |N^+(p;s)| \int_{\mathbb{S} \times [s,t]} \mathbb{1}\{p' \in N^+(p;t)\}\,\mathrm{d}p'\,\mu(\mathrm{d}p) = I_{\mathsf{s}} \times I_{\mathsf{t}},$$

where

$$I_{\mathsf{s}} := \lim_{n\uparrow\infty} \frac{1}{n} \int_{\mathbb{S}_n} |N_{\mathsf{s}}(p_{\mathsf{s}})|^2\,\mathrm{d}p_{\mathsf{s}}$$
$$I_{\mathsf{t}} := \int_{\mathbb{T}_{\leqslant s}^{0\leqslant}} |N_{\mathsf{t}}^+(p_{\mathsf{t}};s)| \int_{[s,t]} \mathbb{1}\{r \in N_{\mathsf{t}}^+(p_{\mathsf{t}};t)\}\,\mathrm{d}r\,\mu_{\mathsf{t}}(\mathrm{d}p_{\mathsf{t}}),$$

and we used that the $\mathcal{P}'$-points connecting to the point p cannot be identical due to the disjoint sets to which the $\mathcal{P}'$-points belong. By Lemma D.8.2 (a), we see that $I_{\mathsf{s}} < \infty$. Using Lemma D.8.6 (b), we see that I_{t} is bounded:

$$I_{\mathsf{t}} \leqslant (t - s) \int_{\mathbb{T}^{0\leqslant}} |N_{\mathsf{t}}^+(p_{\mathsf{t}}; s)| \, \mu_{\mathsf{t}}(\mathrm{d}p_{\mathsf{t}}) < \infty.$$

Thus, for some finite constant $c_+ > 0$, $\lim_{n\uparrow\infty} \mathrm{Cov}(\overline{S}_n^+(s), \overline{S}_n^+(t)) = c_+$.

Covariance function of $S_n^-(t)$. Let us recall the notations in (D.38). The variance term in (D.39) is

$$\mathrm{Var}(S_n^{\mathsf{A}-}(s)) = \mathbb{E}\Big[\sum_{P \in \mathcal{P} \cap \mathbb{S}_n \times \mathbb{T}^{[0,s]}} \deg^-(P; s)^2 \Big] = \int_{\mathbb{S}_n \times \mathbb{T}^{[0,s]}} \mathbb{E}\big[\deg^-(p; s)^2\big] \, \mu(\mathrm{d}p)$$

$$+ \iint_{\left(\mathbb{S}_n \times \mathbb{T}^{[0,s]}\right)^2} \mathrm{Cov}\big(\deg^-(p_1; s), \deg^-(p_2; s)\big) \, \mu(\mathrm{d}p_1) \, \mu(\mathrm{d}p_2).$$

Using the same calculations as in Lemma D.3.1, we have $\mathbb{E}\big[\deg^-(p; s)^2\big] = |N^-(p; s)| + |N^-(p; s)|^2$, thus

$$\lim_{n\uparrow\infty} \frac{1}{n} \int_{\mathbb{S}_n \times \mathbb{T}^{[0,s]}} \mathbb{E}\big[\deg^-(p; s)^2\big] \, \mu(\mathrm{d}p)$$

$$= \sum_{k=1}^{2} \lim_{n\uparrow\infty} \frac{1}{n} \int_{\mathbb{S}_n} |N_{\mathsf{s}}(p_{\mathsf{s}})|^k \, \mathrm{d}p_{\mathsf{s}} \int_{\mathbb{T}^{0\leqslant}} |N_{\mathsf{t}}^-(p_{\mathsf{t}}; s)|^k \, \mu_{\mathsf{t}}(\mathrm{d}p_{\mathsf{t}}) < \infty,$$

where in the last step we used Lemma D.8.2 (a) for the spatial part and Lemma D.8.6 (b) for the temporal part, and we require that $\gamma < 1/2$. As $\mathrm{Cov}(\deg^-(p_1; s), \deg^-(p_2; s)) = |N^-(p_1, p_2; s)|$, factorizing the second integral, and the application of Lemma D.8.2 (b) with $m = 2$ for the spatial part and Lemma D.8.6 (e) for the temporal part leads to

$$\lim_{n\uparrow\infty} \frac{1}{n} \iint_{\left(\mathbb{S}_n \times \mathbb{T}^{[0,s]}\right)^2} |N^-(p_1, p_2; s)| \, \mu(\mathrm{d}p_1) \, \mu(\mathrm{d}p_2) < \infty,$$

where we require again that $\gamma' < 1/2$. The covariance term $\mathrm{Cov}(S_n^{\mathsf{A}-}(s), S_n^{\mathsf{B}-}(s, t))$ is determined by the common $\mathcal{P}'$-points of $S_n^{\mathsf{A}-}(s)$ and $S_n^{\mathsf{B}-}(s, t)$:

$$\lim_{n\uparrow\infty} \frac{1}{n} \mathrm{Cov}(S_n^{\mathsf{A}-}(s), S_n^{\mathsf{B}-}(s, t)) = \lim_{n\uparrow\infty} \frac{1}{n} \int_{\mathbb{S}_n \times \mathbb{T}^{[0,s]}} \int_{\mathbb{S}_n \times \mathbb{T}^{[s,t]}} \int_{\mathbb{S} \times \mathbb{R}} \mathbb{1}\{p' \in N^-(p_1; s)\}$$

$$\times \mathbb{1}\{p' \in N^-(p_2; s)\} \, \mathrm{d}p' \, \mu(\mathrm{d}p_1) \, \mu(\mathrm{d}p_2) = I_{\mathsf{s}} \times I_{\mathsf{t}}$$

$$I_{\mathsf{s}} := \lim_{n\uparrow\infty} \frac{1}{n} \int_{\mathbb{S}_n^2} |N_{\mathsf{s}}(p_{\mathsf{s},1}, p_{\mathsf{s},2})| \, \mathrm{d}p_{\mathsf{s},1} \, \mathrm{d}p_{\mathsf{s},2}$$

$$I_{\mathsf{t}} := \int_{\mathbb{T}^{[0,s]}} \int_{\mathbb{T}^{[s,t]}} |N_{\mathsf{t}}^-(p_{\mathsf{s},1}, p_{\mathsf{s},2}; s)| \, \mu_{\mathsf{t}}(\mathrm{d}p_{\mathsf{s},2}) \, \mu_{\mathsf{t}}(\mathrm{d}p_{\mathsf{s},1}),$$

where we used that the $\mathcal{P}$-points connecting to the point p' cannot be identical due to the disjoint sets the $\mathcal{P}$-points belong to. By Lemma D.8.2 (b), $I_{\mathsf{s}} < \infty$ if $\gamma' < 1/2$. The temporal integral I_{t} is bounded by Lemma D.8.6 (e):

$$I_{\mathsf{t}} \leqslant \iint_{\left(\mathbb{T}^{0\leqslant}\right)^2} |N_{\mathsf{t}}^-(p_{\mathsf{s},1}, p_{\mathsf{s},2}; s)| \, \mu_{\mathsf{t}}(\mathrm{d}p_{\mathsf{s},1}) \, \mu_{\mathsf{t}}(\mathrm{d}p_{\mathsf{s},2}) < \infty.$$

Thus, for some constant $c_- > 0$, the limiting covariance function of $\overline{S}_n^-(t)$ is given by $\lim_{n\uparrow\infty} \mathrm{Cov}(\overline{S}_n^-(s), \overline{S}_n^-(t)) = c_-$, as desired. $\qquad\square$

Proof of Lemma D.10.2. The proof follows the same steps as the proof of Lemma D.5.6, and we calculate only the parts that differ from the previous calculations. As the spatial parts of the integrals are identical, we only need to show that the temporal integrals are finite.

Error term $E_1(n)$. In case of the error term $E_1(n)$, if $\tilde{p}_1, \tilde{p}_2 \in \mathbb{S}_n \times \mathbb{T}^{0\leqslant}$ and $\tilde{p}_3 \in \mathbb{S} \times \mathbb{R}$, we have

$$\int_{\mathbb{T}^{0\leqslant}} |N_{\mathsf{t}}^{\pm}(p_{\mathsf{t}};t)|^{m_1} \, \mu_{\mathsf{t}}(\mathrm{d}p_{\mathsf{t}}) \int_{\mathbb{T}^{0\leqslant}} |N_{\mathsf{t}}^{\pm}(p_{\mathsf{t}};t)|^{m_2+1} \, \mu_{\mathsf{t}}(\mathrm{d}p_{\mathsf{t}}) < \infty$$

due to Lemma D.8.6 (b). If $\tilde{p}_1, \tilde{p}_2 \in \mathbb{S} \times \mathbb{R}$ and $\tilde{p}_3 \in \mathbb{S}_n \times \mathbb{T}^{0\leqslant}$, then the argument in the proof of Lemma D.5.6 applies, if we show first that

$$\int_{\mathbb{T}^{0\leqslant}} |N_{\mathsf{t}}^{\pm}(p_{\mathsf{t}};t)|^2 \, \mu_{\mathsf{t}}(\mathrm{d}p_{\mathsf{t}}) < \infty, \tag{D.40}$$

which holds due to Lemma D.8.6 (b), and second that

$$\int_{\mathbb{T}^{0\leqslant}} \left(\int_{\mathbb{R}} \mathbb{1}\{r \in N_{\mathsf{t}}^{\pm}(p_{\mathsf{s},1};s)\} \int_{\mathbb{T}^{0\leqslant}} \mathbb{1}\{r \in N_{\mathsf{t}}^{\pm}(p_{\mathsf{s},2};t)\} \, \mu_{\mathsf{t}}(\mathrm{d}p_{\mathsf{s},2}) \, \mathrm{d}r \right)^2 \mu_{\mathsf{t}}(\mathrm{d}p_{\mathsf{s},1}) < \infty.$$

As the inner integral is a finite constant due to Lemma D.8.6 (b), the expression reduces to (D.40), which is finite.

Error term $E_2(n)$. Next, we turn our attention to the error term $E_2(n)$. Following along the same lines as in the proof of Lemma D.5.6, we need to show that

$$\iint_{(\mathbb{T}^{0\leqslant})^2} |N_{\mathsf{t}}^{\pm}(p_{\mathsf{s},1}, p_{\mathsf{s},2}; s)| \, \mu_{\mathsf{t}}(\mathrm{d}p_{\mathsf{s},1}) \, \mu_{\mathsf{t}}(\mathrm{d}p_{\mathsf{s},2}) < \infty,$$

which follows from Lemma D.8.6 (e), and that (D.40) holds.

Error term $E_3(n)$. For the error term $E_3(n)$,

$$\int_{\mathbb{T}^{0\leqslant}} |N_{\mathsf{t}}^{\pm}(p_{\mathsf{t}};t)|^m \, \mu_{\mathsf{t}}(\mathrm{d}p_{\mathsf{t}}) < \infty$$

$$\int_{\mathbb{R}} \left(\int_{\mathbb{T}^{0\leqslant}} \mathbb{1}\{r \in N_{\mathsf{t}}^+(p_{\mathsf{t}};t)\} \, \mu_{\mathsf{t}}(\mathrm{d}p_{\mathsf{t}}) \right)^m \mathrm{d}r < \infty$$

by Lemmas D.8.6 (b) and D.8.6 (e), respectively. $\qquad\square$

D.B   Proofs of Lemmas D.11.1, D.11.2, and D.11.3 used in Section D.11

The following proofs verify the lemmas used to show that the finite-dimensional distributions of the high-mark edge count $\overline{S}_n^{\geqslant}$ converge to 0. The ideas are similar to the proof of Theorem D.2.4.

Proof of Lemma D.11.1. After the application of Mecke's formula, similarly to (D.9), we have

$$\operatorname{Var}(S_n^{\geqslant,\pm}(t)) = \int_{\mathbb{S}_n^{u_n\leqslant}\times\mathbb{T}^{0\leqslant}} \mathbb{E}[\deg^{\pm}(p;t)^2]\,\mu(\mathrm{d}p)$$
$$+ \iint_{(\mathbb{S}_n^{u_n\leqslant}\times\mathbb{T}^{0\leqslant})^2} \operatorname{Cov}(\deg^{\pm}(p_1;t),\deg^{\pm}(p_2;t))\,\mu(\mathrm{d}p_1)\,\mu(\mathrm{d}p_2).$$

Using (D.10), we have for the first term

$$\int_{\mathbb{S}_n^{u_n\leqslant}\times\mathbb{T}^{0\leqslant}} \mathbb{E}[\deg^{\pm}(p;t)^2]\,\mu(\mathrm{d}p) = \int_{\mathbb{S}_n^{u_n\leqslant}\times\mathbb{T}^{0\leqslant}} |N^{\pm}(p;t)| + |N^{\pm}(p;t)|^2\,\mu(\mathrm{d}p)$$
$$= n\big(c_1(t)(1-u_n^{1-\gamma}) + c_2(t)(u_n^{-(2\gamma-1)}-1)\big),$$

where $\gamma > 1/2$, $c_1(t), c_2(t) > 0$ are t-dependent constants, and we used Lemmas D.8.2 (a) and D.8.6 (a) for the spatial and temporal parts respectively. For a large enough n, the terms above can be bounded by $c_2(t)nu_n^{2\gamma-1}$. As $u_n = n^{-2/3}$ the first term is in $O(n^{1+2/3(2\gamma-1)}) \subset o(n^{2\gamma})$. Next, we calculate the covariance term by following again the steps in the proof of Lemma D.3.1:

$$\iint_{(\mathbb{S}_n^{u_n\leqslant}\times\mathbb{T}^{0\leqslant})^2} \operatorname{Cov}(\deg^{\pm}(p_1;t),\deg^{\pm}(p_2;t))\,\mu(\mathrm{d}p_1)\,\mu(\mathrm{d}p_2)$$
$$= \iint_{(\mathbb{S}_n^{u_n\leqslant}\times\mathbb{T}^{0\leqslant})^2} |N^{\pm}(p_1,p_2;t)|\,\mu(\mathrm{d}p_1)\,\mu(\mathrm{d}p_2).$$

Requiring $\gamma' < 1/2$, we bound the spatial part using Lemma D.8.2 (c) and the temporal part by $t + 1/2$ using Lemma D.8.6 (e). Thus, the covariance term is of order $O(n) \subseteq o(n^{2\gamma})$. □

Proof of Lemma D.11.2. As in (D.13), we bound the variance term using the Poincaré inequality [66, Theorem 18.7], and following (D.14), we recognize again that $D_p(\Delta_n^{\geqslant,\pm}(s,t))$ is Poisson distributed with mean $\mathbb{E}[D_p(\Delta_n^{\geqslant,\pm}(s,t))] = |N^{\pm}(p;t) \setminus N^{\pm}(p;s)|$. We apply the same steps as in (D.15), and then by the application of Lemmas D.8.2 (a) and D.8.6 (c), we obtain

$$\int_{\mathbb{S}_n^{u_n\leqslant}\times\mathbb{T}^{0\leqslant}} |N^{\pm}(p;t)\setminus N^{\pm}(p;s)| + |N^{\pm}(p;t)\setminus N^{\pm}(p;s)|^2\,\mu(\mathrm{d}p)$$
$$\leqslant n(t-s)\big(c_1(1-u_n^{1-\gamma}) + c_2(u_n^{-(2\gamma-1)}-1)\big),$$

where $c_1, c_2 > 0$ are positive constants, and as $u_n > 0$, the bound is valid for $\gamma \in (1/2, 1)$.

To show that the above integral is in $O(n^{2\gamma}(t-s)^{(1+\eta)/2})$, we check the order of each term:

$$n(t-s) \in O(n^{2\gamma}(t-s)^{(1+\eta)/2}) \qquad \Longleftrightarrow \qquad (t-s)^{(1-\eta)/2} \in O(n^{2\gamma-1})$$

$$n(t-s)u_n^{1-\gamma} \in O(n^{2\gamma}(t-s)^{(1+\eta)/2}) \qquad \Longleftrightarrow \qquad (t-s)^{(1-\eta)/2} \in O(n^{(4\gamma-1)/3})$$

$$n(t-s)u_n^{-(2\gamma-1)} \in O(n^{2\gamma}(t-s)^{(1+\eta)/2}) \qquad \Longleftrightarrow \qquad (t-s)^{(1-\eta)/2} \in O(n^{(2\gamma-1)/3})$$

as $\eta = 1/3$, $u_n = n^{-2/3}$. Similarly to (D.16), the cost operator $D_{p'}(\Delta_n^{\geqslant,\pm}(s,t))$ is also Poisson distributed with mean

$$\mathbb{E}[D_{p'}(\Delta_n^{\geqslant,\pm}(s,t))] = \int_{\mathbb{S}_n^{u_n\leqslant}\times\mathbb{T}^{0\leqslant}} \mathbb{1}\{p' \in N^\pm(p;t) \setminus N^\pm(p;s)\}\,\mu(\mathrm{d}p).$$

Next, we follow along (D.17) and Lemmas D.8.2 (d) and D.8.6 (d) yield

$$\int_{\mathbb{S}\times\mathbb{R}} \mathbb{E}\big[D_{p'}(\Delta_n^{\geqslant,\pm}(s,t))\big] + \mathbb{E}\big[D_{p'}(\Delta_n^{\geqslant,\pm}(s,t))\big]^2 \,\mathrm{d}p' \in O(n(t-s)),$$

where we used Lemmas D.8.2 (d) and D.8.6 (e) to bound the spatial and temporal parts, respectively. $\qquad\square$

To show Condition (2) of Theorem D.6.2 for the high-mark edge count $\overline{S}_n^{\geqslant}$, we need to bound the cumulant term $\kappa_4(\Delta_n^{\geqslant,\pm}(s,t))$, which is done in the following proof.

Proof of Lemma D.11.3. The proof is similar to the proof of Lemma D.10.4 for the thin-tailed case. In this proof, we follow the same steps.

Case ($1^{\geqslant}$). In Case ($1^{\geqslant}$), as in (D.18), we write the cumulant term $\kappa_4(\Delta_n^{\geqslant,\pm}(s,t))$ using [84, Proposition 3.2.1]. Then, following the steps of (D.19), taking absolute values, applying triangle and Jensen's inequalities leads to $|\kappa_4(\Delta_{1,n}^{\geqslant,\pm}(s,t))| \leqslant c_1 n\,\mathbb{E}\big[(V_1^\pm(t) - V_1^\pm(s))^4\big]$ with some $c_1 > 0$. Following the fourth moment calculations through (D.24)–(D.27) with $\mathbb{V}_i^{u_n\leqslant}$ and $\Delta_n^{\geqslant,\pm}$ in place of $\mathbb{V}_i$ and $\Delta_n^\pm$, respectively, we obtain that $\mathbb{E}[(\Delta_{1,n}^{\geqslant,\pm})^4]$ can be bounded by sums of products of integrals of the form

$$\int_{\mathbb{V}_i^{u_n\leqslant}\times\mathbb{T}^{0\leqslant}} |\delta_{s,t}(N^\pm(p))|^m\,\mu(\mathrm{d}p) \leqslant c_3 u_n^{-(m\gamma-1)+}(t-s)^m \qquad m \in \{1,2,3,4\},$$

which was bounded using Lemmas D.8.2 (a) and D.8.6 (c) without imposing any constraints on the parameter $\gamma \in (1/2, 1)$. This, in turn, leads to the bounds

$$\mathbb{E}[(\Delta_{1,n}^{\geqslant,\pm})^4] \leqslant \sum_{H_1\ldots,H_Q} \prod_{q=1}^{Q} c_q u_n^{-(m_q\gamma-1)+}(t-s)^{m_q} \qquad \text{and} \qquad \sum_{q=1}^{Q} m_q \leqslant 4,$$

where the sum is over all partitions $\{H_1\ldots,H_Q\} \preceq \{1,\ldots,4\}$ of the indices $\{1,\ldots,4\}$ into Q groups, $c_q > 0$, and m_q is the number of factors in the qth group. The number of factors in the terms are denoted by $Q \in \{1,\ldots,4\}$ and $m_q \in \{1,\ldots,4\}$ for all

indices $q \in \{1, \ldots, Q\}$. Expanding the product, we obtain a similar bound regardless of the value of $Q \leqslant 4$:

$$\mathbb{E}[(\Delta_{1,n}^{\geqslant,\pm})^4] \leqslant \sum_{H_1 \ldots, H_Q} \prod_{q=1}^{4} \left((t-s)^{m_q}\right)$$

$$\times \left(c_4 + c_5 \sum_{q \leqslant 4} u_n^{-(m_q\gamma - 1)_+} + c_6 \sum_{q_1 < q_2 \leqslant 4} u_n^{-((m_{q_1} + m_{q_2})\gamma - 2)_+}\right.$$

$$\left. + c_7 \sum_{q_1 < q_2 < q_3 \leqslant 4} u_n^{-((m_{q_1} + m_{q_2} + m_{q_3})\gamma - 3)_+} + c_8 u_n^{-(\sum_{q=1}^{4} m_q\gamma - 4)_+}\right),$$

where $c_4, \ldots, c_8 > 0$ are positive constants. As $\sum_{q=1}^{Q} m_q \leqslant 4$, each of the terms involving u_n can be bounded by $c_9 u_n^{-(4\gamma - 1)}(t - s)$ with some constant $c_9 > 0$. For n blocks, we need to show that

$$n u_n^{-(4\gamma-1)}(t-s) \in O(n^{4\gamma}(t-s)^{1+\eta}) \quad \Longleftrightarrow \quad n u_n^{-(4\gamma-1)} \in O(n^{4\gamma}(t-s)^{\eta}).$$

Since $t - s > n^{-1/2}$ and $\gamma \in (1/2, 1)$, setting $\eta = 1/3$ and $u_n = n^{-2/3}$ yields $n^{1+2/3(4\gamma-1)} \in O(n^{4\gamma-1/6})$.

Case ($3^{\geqslant}$). In Case ($3^{\geqslant}$), we follow the same steps as in the proof of Lemma D.10.4 to conclude that $|\kappa_4(\Delta_n^{\geqslant,\pm}(s,t))| \in O(n^{2/3(3\gamma-1)})$ if $\gamma' < 1/4$, without any constraints on parameter γ. The orders of the terms T_{prod} and T_{cov} are presented in Table D.2.

Case ($2^{\geqslant}$). In Case ($2^{\geqslant}$), we introduce the notations

$$T_{\mathsf{prod}} := \prod_{b=2}^{q} \mathbb{E}\left[\prod_{m \in M_b^{(2)}} \Delta_{m,n}^{\geqslant,\pm}\right] \quad \text{and} \quad T_{\mathsf{cov}} := \left|\mathrm{Cov}\left(\Delta_{i,n}^{\geqslant,\pm}, \prod_{m \in M_1^{(2)}} \Delta_{m,n}^{\geqslant,\pm}\right)\right|$$

for the product and the covariance terms, respectively, and bound the cumulant $|\kappa_4(\Delta_{i,n}^{\geqslant,\pm}, \Delta_{j,n}^{\geqslant,\pm}, \Delta_{k,n}^{\geqslant,\pm}, \Delta_{\ell,n}^{\geqslant,\pm})|$ as in (D.20) by $|\kappa_4(\Delta_{i,n}^{\geqslant,\pm}, \Delta_{j,n}^{\geqslant,\pm}, \Delta_{k,n}^{\geqslant,\pm}, \Delta_{\ell,n}^{\geqslant,\pm})| \leqslant c_{10} \sum_{M_1^{(2)}, \ldots, M_q^{(2)}} T_{\mathsf{prod}} T_{\mathsf{cov}}$. To ease understanding, we expanded the formula for each partition of $\{i, j, k, \ell\}$ in Table D.2. We bound $\mathbb{E}[\Delta_{k,n}^{\geqslant,\pm} \Delta_{\ell,n}^{\geqslant,\pm}]$ using Cauchy–Schwarz inequality:

$$\mathbb{E}[\Delta_{k,n}^{\geqslant,\pm} \Delta_{\ell,n}^{\geqslant,\pm}] \leqslant \mathbb{E}[(\Delta_{k,n}^{\geqslant,\pm})^2]^{1/2} \mathbb{E}[(\Delta_{\ell,n}^{\geqslant,\pm})^2]^{1/2} = \mathbb{E}[(\Delta_{1,n}^{\geqslant,\pm})^2] \leqslant \mathbb{E}[V_1^{\geqslant,\pm}(t)^2],$$

where we used that $\Delta_{k,n}^{\geqslant,\pm}$ and $\Delta_{\ell,n}^{\geqslant,\pm}$ are identically distributed in the second step, and that $V_i^{\geqslant,\pm}(t)$ is monotone in the second step. Following the calculations of Case ($1^{\geqslant}$) for the second moment, we have

$$\mathbb{E}[(V_i^{\geqslant,\pm})^2] \leqslant \prod_{q=1}^{Q} c_q u_n^{-(m_q\gamma-1)_+} \qquad \sum_{q=1}^{Q} m_q \leqslant 2,$$

where $Q \in \{1, 2\}$ and $m_q \in \{1, 2\}$ for all indices $q \in \{1, \ldots Q\}$. If $Q = 2$, then

$$\mathbb{E}[(V_i^{\geqslant,\pm})^2] \leqslant c_{11}\left(1 + \sum_{q \leqslant 2} u_n^{-(m_q\gamma-1)_+} + \sum_{q_1 < q_2 \leqslant 2} u_n^{-((m_{q_1} + m_{q_2})\gamma - 2)_+}\right),$$

Table D.2: Possible partitions of the indices $\{i, j, k, \ell\}$ in Case $(2^{\geqslant})$ and Case $(3^{\geqslant})$

Case $(2^{\geqslant})$		
partition	T_{prod}	order
$\{i\}, \{j, k, \ell\}$	1	$O(1)$
$\{i\}, \{j\}, \{k, \ell\}$	$\mathbb{E}[\Delta_{k,n}^{\geqslant,\pm} \Delta_{\ell,n}^{\geqslant,\pm}]$	$O(n^{2/3(2\gamma-1)})$
$\{i\}, \{j, k\}, \{\ell\}$	$\mathbb{E}[\Delta_{\ell,n}^{\geqslant,\pm}]$	$O(1)$
$\{i\}, \{j\}, \{k\}, \{\ell\}$	$\mathbb{E}[\Delta_{k,n}^{\geqslant,\pm}] \, \mathbb{E}[\Delta_{\ell,n}^{\geqslant,\pm}]$	$O(1)$
partition	T_{cov}	order
$\{i\}, \{j, k, \ell\}$	$\big|\mathrm{Cov}(\Delta_{i,n}^{\geqslant,\pm}, \Delta_{j,n}^{\geqslant,\pm} \Delta_{k,n}^{\geqslant,\pm} \Delta_{\ell,n}^{\geqslant,\pm})\big|$	$O(n^{2/3(3\gamma-1)})$
$\{i\}, \{j\}, \{k, \ell\}$	$\big|\mathrm{Cov}(\Delta_{i,n}^{\geqslant,\pm}, \Delta_{j,n}^{\geqslant,\pm})\big|$	$O(1)$
$\{i\}, \{j, k\}, \{\ell\}$	$\big|\mathrm{Cov}(\Delta_{i,n}^{\geqslant,\pm}, \Delta_{j,n}^{\geqslant,\pm} \Delta_{k,n}^{\geqslant,\pm})\big|$	$O(n^{2/3(2\gamma-1)})$
$\{i\}, \{j\}, \{k\}, \{\ell\}$	$\big|\mathrm{Cov}(\Delta_{i,n}^{\geqslant,\pm}, \Delta_{j,n}^{\geqslant,\pm})\big|$	$O(1)$
Case $(3^{\geqslant})$		
partition	T_{prod}	order
$\{i, j\}, \{k, \ell\}$	1	$O(1)$
$\{i, j\}, \{k\}, \{\ell\}$	$\mathbb{E}[\Delta_{\ell,n}^{\geqslant,\pm}]$	$O(1)$
$\{i\}, \{j\}, \{k, \ell\}$	$\mathbb{E}[\Delta_{i,n}^{\geqslant,\pm}]$	$O(1)$
$\{i\}, \{j\}, \{k\}, \{\ell\}$	$\mathbb{E}[\Delta_{i,n}^{\geqslant,\pm}] \, \mathbb{E}[\Delta_{\ell,n}^{\geqslant,\pm}]$	$O(1)$
partition	T_{cov}	order
$\{i, j\}, \{k, \ell\}$	$\big|\mathrm{Cov}(\Delta_{i,n}^{\geqslant,\pm} \Delta_{j,n}^{\geqslant,\pm}, \Delta_{k,n}^{\geqslant,\pm} \Delta_{\ell,n}^{\geqslant,\pm})\big|$	$O(n^{2/3(3\gamma-1)})$
$\{i, j\}, \{k\}, \{\ell\}$	$\big|\mathrm{Cov}(\Delta_{i,n}^{\geqslant,\pm} \Delta_{j,n}^{\geqslant,\pm}, \Delta_{k,n}^{\geqslant,\pm})\big|$	$O(n^{2/3(3\gamma-1)})$
$\{i\}, \{j\}, \{k, \ell\}$	$\big|\mathrm{Cov}(\Delta_{j,n}^{\geqslant,\pm}, \Delta_{k,n}^{\geqslant,\pm} \Delta_{\ell,n}^{\geqslant,\pm})\big|$	$O(n^{2/3(3\gamma-1)})$
$\{i\}, \{j\}, \{k\}, \{\ell\}$	$\big|\mathrm{Cov}(\Delta_{j,n}^{\geqslant,\pm}, \Delta_{k,n}^{\geqslant,\pm})\big|$	$O(1)$

with some constant $c_{11} > 0$. We bound again each term in the parentheses involving u_n by $c_{12} u_n^{-(2\gamma-1)} \in O(n^{2/3(2\gamma-1)})$ with some constant $c_{12} > 0$, where $u_n = n^{-2/3}$. For the first moments $\mathbb{E}[(V_i^{\geqslant,\pm})]$, it is easy to see that they are elements of $O(1)$. We move on to the covariance term $|\mathrm{Cov}(\Delta_{i,n}^{\geqslant,\pm}, \Delta_{j,n}^{\geqslant,\pm} \Delta_{k,n}^{\geqslant,\pm} \Delta_{\ell,n}^{\geqslant,\pm})|$ in the case $|M_1^{(2)}| = 3$. Note that in this case, the product term is of order $O(1)$. We apply again (D.28):

$$\big|\mathrm{Cov}(\Delta_{i,n}^{\geqslant,\pm}, \Delta_{j,n}^{\geqslant,\pm} \Delta_{k,n}^{\geqslant,\pm} \Delta_{\ell,n}^{\geqslant,\pm})\big| = \big|\mathbb{E}[\mathrm{Cov}(\Delta_{i,n}^{\geqslant,\pm}, \Delta_{j,n}^{\geqslant,\pm} \Delta_{k,n}^{\geqslant,\pm} \Delta_{\ell,n}^{\geqslant,\pm} \mid \mathcal{P})]\big|,$$

and we bound the conditional covariance using bilinearity as in (D.29), where we use $\mathbb{V}_i^{u_n \leqslant}, \mathbb{V}_j^{u_n \leqslant}, \mathbb{V}_k^{u_n \leqslant}, \mathbb{V}_\ell^{u_n \leqslant}$ in place of $\mathbb{V}_i, \mathbb{V}_j, \mathbb{V}_k, \mathbb{V}_\ell$ for the domains of the points P_1, P_2, P_3, P_4, respectively. The arguments for (D.30)–(D.32) can be applied without any changes, and we obtain the bound

$$\big|\kappa_4(\Delta_n^{\geqslant,\pm}(s,t))\big| \leqslant c_{13} \, \mathbb{E}\Bigg[\sum_{\substack{a=0}}^{n-1} \sum_{\substack{i,j,k,\ell \\ \rho^{\geqslant}(i,j,k,\ell)=a}} \sum_{\substack{P_1 \in \mathcal{P} \cap (\mathbb{V}_i^{u_n \leqslant} \cap \mathbb{T}^{0\leqslant}), P_2 \in \mathcal{P} \cap (\mathbb{V}_j^{u_n \leqslant} \cap \mathbb{T}^{0\leqslant}) \\ P_3 \in \mathcal{P} \cap (\mathbb{V}_k^{u_n \leqslant} \cap \mathbb{T}^{0\leqslant}), P_4 \in \mathcal{P} \cap (\mathbb{V}_\ell^{u_n \leqslant} \cap \mathbb{T}^{0\leqslant})}} A(\boldsymbol{P}_4, \boldsymbol{\sigma}_4)\Bigg].$$

Depending on which of the points P_2, P_3, P_4 are identical, we apply the Mecke formula to all the cases. The integrals with respect to p_3, p_4 factor again leading to factors

with bounds

$$\int_{\mathbb{S}^{u_n\leqslant}_{[j-a,j+a+1]}\times\mathbb{T}^{0\leqslant}} |N^\pm(p_3,\sigma_3)|^{m_3}\,\mu(\mathrm{d}p) \leqslant c_{14}au_n^{-(m_3\gamma-1)_+} \qquad m_3\in\{0,1,2\}$$

$$\int_{\mathbb{S}^{u_n\leqslant}_{[j-a,j+a+1]}\times\mathbb{T}^{0\leqslant}} |N^\pm(p_4,\sigma_4)|^{m_4}\,\mu(\mathrm{d}p) \leqslant c_{14}au_n^{-(m_4\gamma-1)_+} \qquad m_4\in\{0,1,2\},$$

with some constant $c_{14}\in\mathbb{R}$, where we used Lemmas D.8.2 (a) and D.8.6 (b) with $u_-=u_n>0$, which requires no constraint on $\gamma\in(1/2,1)$. For the integral with respect to p_2, similarly to (D.23), the following bound holds:

$$\big|\kappa_4(\Delta_n^{\geqslant,\pm}(s,t))\big| \leqslant c_{15}\prod_{q\in\{3,4\}} u_n^{-(m_q\gamma-1)_+}$$

$$\times \int_{\mathbb{S}_n^{u_n\leqslant}\times\mathbb{T}^{0\leqslant}}\int_{\mathbb{S}_n^{u_n\leqslant}\times\mathbb{T}^{0\leqslant}} |N^\pm(p_1,\sigma_1)|^{m_1}|N^\pm(p_1,\sigma_1)\cap N^\pm(p_2,\sigma_2)|$$

$$\times |N^\pm(p_2,\sigma_2)|^{m_2}(|x_1-x_2|^{m_a}+1)\,\mu(\mathrm{d}p_2)\,\mu(\mathrm{d}p_1),$$

where $m_1=0$ and $\sum_{q=1}^{m_a}m_q\leqslant 2$, $m_a\in\{0,1,2\}$. The temporal part can be bounded with Lemma D.8.6 (f), and the spatial part is bounded by Lemma D.8.2 (f) with $u_-=u_n$. Then,

$$\big|\kappa_4(\Delta_n^{\geqslant,\pm}(s,t))\big| \leqslant c_{16}n\prod_{q\in\{3,4\}} u_n^{-(m_q\gamma-1)_+}\Big(u_n^{-((1+m_2+m_a)\gamma-1)_+-((1+m_1)\gamma-1)_+}$$

$$+ u_n^{-((1+m_1+m_a)\gamma-1)_+-((1+m_2)\gamma-1)_+}\Big),$$

where $c_{16}>0$ is a large enough constant. To bound each term in the expansion of the product above, we would like to find the most negative exponent of u_n. The exponent $-(m_q\gamma-1)_+$ is nonzero only if $m_q\geqslant 2$. Looking into Table D.1, this happens only if $P_3=P_4$, in which case $m_1=m_2=0$ and $m_a=1$. Then, the exponent of u_n can be bounded by $-2(2\gamma-1)$. Otherwise, $-(m_q\gamma-1)_+=0$, and then $m_1+m_2+m_a\leqslant 2$. In these cases, we bound the exponent of u_n by $-(3\gamma-1)$. Then, as $u_n=n^{-2/3}$, $T_{\mathsf{cov}}\in O(n^{2/3(3\gamma-1)})$, and thus $T_{\mathsf{prod}}T_{\mathsf{cov}}\in O(n^{2/3(3\gamma-1)})$ since $\mathbb{E}[\Delta_{k,n}^{\geqslant,\pm}\Delta_{\ell,n}^{\geqslant,\pm}]$ can only appear in T_{prod} if $M_1^{(2)}=\{j\}$. If we look at the partition $\{j\}$, $\{k,\ell\}$ of the indices j,k,ℓ, then the product term is or order $O(n^{2/3(2\gamma-1)})$, and all the exponents $m_1=m_2=m_3=m_4=m_a=0$ in the covariance term. Then, the covariance term is of order $O(1)$, and $T_{\mathsf{prod}}T_{\mathsf{cov}}\in O(n^{2/3(2\gamma-1)})$. Following the same train of thought, we arrive at the orders of the terms T_{prod} and T_{cov} as in Table D.2. Thus, we conclude that

$$\big|\kappa_4(\Delta_n^{\geqslant,\pm}(s,t))\big| = c_{16}nT_{\mathsf{prod}}T_{\mathsf{cov}}\in O(n^{2\gamma+1/3}),$$

as desired. □

Finally, Condition (3) of Theorem D.6.2 is about the convergence of the expected increments $\mathbb{E}\big[\Delta_n^{\geqslant,\pm}(t_k,t_{k+1})\big]$, which in proved next.

Proof of Lemma D.11.4. Following the same argument as in the proof of Lemma D.6.5, the expectation $\mathbb{E}[S_n^{\geqslant,\pm}(t)]\leqslant\mathbb{E}[S_n^\pm(t)]$ can be bounded identically by Lemmas D.8.2 (a)

and D.8.6 (a) for $\gamma \in (0,1)$. As $t_k = kn^{-1/2}$, $\mathbb{E}[\Delta_n^{\geqslant,\pm}(t_k, t_{k+1})] \in O(n^{1/2})$, and thus for $\gamma > 1/2$,

$$\max_{k \leqslant \lfloor n^{1/2} \rfloor} \left(n^{-\gamma} \, \mathbb{E}[\Delta_n^{\geqslant,\pm}(t_k, t_{k+1})] \right) \in O(n^{-(\gamma-1/2)}) \subset o(1),$$

as required. $\qquad\square$

D.C   Proofs of Propositions D.7.7, D.7.11, and Lemma D.7.10 used in the proof of Section D.7

Proposition D.7.7 stated that the summation functional $\chi(\eta)(t)$ is almost surely continuous with respect to the Skorokhod metric d_{Sk}. In the proof of Proposition D.7.7, we follow the argument of Resnick [93, Section 7.2.3]. Our proof is slightly more involved since we have to deal with vertices having potentially large lifetimes, and we need to restrict the domain of the summation functional χ to a compact set K. In the first step, we show that if two point measures are close, then the number of points in a compact set are almost surely identical. In the second step, we show that as the points of the point measures are close, the respective functions that the summation functional maps these measures are also close with respect to the Skorokhod metric d_{Sk}.

Proof of Proposition D.7.7. Let $\eta \in \mathbf{N}_{\mathsf{loc}}(K)$ denote a point measure on the domain K. Let us define $M := M(\eta) := \max_{(j_i,b_i,\ell_i)\in\eta} \ell_i + 1$, and set $\overline{K}_{\varepsilon,M} := \{(j,b,\ell) \in \overline{K}_\varepsilon : \ell \leqslant M\}$, such that $\eta(\cdot) = \eta(\cdot \cap \overline{K}_{\varepsilon,M})$. We define a subset $\Lambda_{\varepsilon,M}$ of point measures as follows:

$$
\begin{aligned}
\Lambda_{\varepsilon,M} := \big\{ \eta \in \mathbf{N}_{\mathsf{loc}}(\overline{K}_{\varepsilon,M}) : \ & \eta(\overline{K}_{\varepsilon,M}) < \infty, \ \eta(\partial\overline{K}_{\varepsilon,M}) = 0, \\
& \eta(\{(j,b,\ell) \in \overline{K}_{\varepsilon,M} : b = 0\}) = 0, \\
& \eta(\{(j_i,b_i,\ell_i) \in \overline{K}_{\varepsilon,M} : \exists j \neq i : b_i = b_j\}) = 0, \\
& \eta(\{(j_i,b_i,\ell_i) \in \overline{K}_{\varepsilon,M} : \exists j \neq i : b_i + \ell_i = b_j + \ell_j\}) = 0, \\
& \eta(\{(j_i,b_i,\ell_i) \in \overline{K}_{\varepsilon,M} : \exists j : b_i = b_j + \ell_j\}) = 0 \big\}.
\end{aligned}
$$

We now follow two steps:

(1) first, we show that $\mathcal{P}_\infty \in \Lambda_{M(\mathcal{P}_\infty)}$ almost surely;

(2) then, we show that the functional χ is continuous on $\Lambda_{\varepsilon,M}$.

$\mathcal{P}_\infty \in \Lambda_{M(\mathcal{P}_\infty)}$ almost surely.   Since the expected number of points $\mathbb{E}[\mathcal{P}_\infty(\overline{K}_\varepsilon)]$ is finite, the number of points $\mathcal{P}_\infty(\overline{K}_\varepsilon)$ in the domain $\overline{K}_\varepsilon$ is almost surely finite. Then, $M(\mathcal{P}_\infty) < \infty$ almost surely, and then $\overline{K}_{\varepsilon,M(\mathcal{P}_\infty)}$ is almost surely compact containing all the points contributing to $S_{n,\varepsilon}^{(3)}(\cdot)$. Recall that in the dimension $\overline{\overline{\mathbb{J}}}$, the set $\overline{K}_{\varepsilon,M}$ is compactified at ∞. We check each condition in the definition of $\Lambda_{\varepsilon,M}$ to show that $\mathbb{P}(\eta \cap \overline{K}_{\varepsilon,M} \in \Lambda_{\varepsilon,M}) = 1$. The coordinates J_i of the points $(J_i, B_i, L_i) \in \mathcal{P}_\infty$ are i.i.d.

random variables with distribution $\varepsilon\nu([\tilde{c}\varepsilon^\gamma, \infty) \cap \cdot)$. Furthermore, (B_i, L_i) are also i.i.d. with joint distribution

$$\mathbb{P}(B_i \leqslant b, L_i \leqslant \ell)$$
$$= \begin{cases} \dfrac{1}{2}\displaystyle\int_{-\ell}^{b}\int_{-b'}^{\ell} \mathbb{P}_L(\mathrm{d}\ell')\,\mathrm{d}b' = \dfrac{1}{2}(\mathrm{e}^b - (1+b+\ell)\mathrm{e}^{-\ell}) & \text{if } b \in [-\ell, 0] \\[2ex] \dfrac{1}{2}\displaystyle\int_{-\ell}^{0}\int_{-b'}^{\ell} \mathbb{P}_L(\mathrm{d}\ell')\,\mathrm{d}b' + \dfrac{1}{2}\displaystyle\int_{0}^{b}\int_{0}^{\ell} \mathbb{P}_L(\mathrm{d}\ell')\,\mathrm{d}b' \\[2ex] \qquad = \dfrac{1}{2}(1 + b - (1+b+\ell)\mathrm{e}^{-\ell}) & \text{if } b \in [0,1]. \end{cases}$$

Note that at $b = 0$, both parts of the distribution are equal, and thus the distribution of the points (J_i, B_i, L_i) is continuous without any atoms.

- The first condition states that the total number of points we consider is finite. This holds almost surely since the expected number of points $\nu([\tilde{c}\varepsilon^\gamma, \infty))c_1 = \varepsilon c_1$ in the domain $\overline{K}_{\varepsilon,M}$ is finite, for some constant $c_1 > 0$.

- The second and third conditions require that no points can be born or die at the boundaries of the time interval $[0, 1]$, and no points can have a lifetime of exactly M. As the distribution of the points is continuous, the second and third conditions hold almost surely as well, since the corresponding sets have measure 0.

- The last three conditions require that all points are born and die at different times, which holds almost surely since the distributions of the coordinates B_i, L_i are continuous:

$$\mathbb{P}\left(\bigcup_{i<j}\{B_i = B_j\}\right) \leqslant \sum_{i<j}\mathbb{P}(\{B_i = B_j\}) = 0,$$

which can also be applied to the final two conditions.

Thus, $\mathbb{P}(\mathcal{P}_\infty \in \Lambda_{\varepsilon,M}) = 1$.

χ is continuous on $\Lambda_{\varepsilon,M}$. Next, we show that if $\eta \in \Lambda_{\varepsilon,M}$, then χ is continuous at η, i.e., if $\eta_n \xrightarrow{v} \eta$ is a converging sequence of point measures in the vague topology, then $\chi(\eta_n) \to \chi(\eta)$ in $D([0,1], \mathbb{R})$. Note that $\eta_n \xrightarrow{v} \eta$ if and only if for all continuous functions f with compact support $|\int f\,\mathrm{d}\eta_n - \int f\,\mathrm{d}\eta| \to 0$. Also note that the function $a \mapsto \nu([a, \infty))$ from $(0, \infty)$ to $(0, \infty)$ is continuous by Lemma D.7.6. Thus, the restriction of the jumps using the indicator $\mathbb{1}\{J \geqslant \tilde{c}\varepsilon^\gamma\}$ is almost surely continuous. Consider two point measures $\eta_1, \eta_2 \in \Lambda_{\varepsilon,M}$. We would like to show that if η_1, η_2 are close to each other, then the summation functionals $\chi(\eta_1)$, $\chi(\eta_2)$ are close in the Skorokhod space $D([0,1], \mathbb{R})$. Note that $\overline{K}_{\varepsilon,M}$ is compact, and $\eta \in \Lambda_{\varepsilon,M}$ almost surely. We label the $k \in \mathbb{N}$ number of points $(j_i, b_i, \ell_i) \in \mathrm{supp}(\eta)$ such that $\eta(\cdot) = \sum_{i=1}^{k}\delta_{(J_i, B_i, L_i)}(\cdot)$ and $B_1 < \cdots < B_k$, which is possible since $\eta \in \Lambda_{\varepsilon,M}$. Next, we show that there

exists an index $n_0 \in \mathbb{N}$ such that for all $n \geqslant n_0$, there exists a labeling of the points $(j_i^{(n)}, b_i^{(n)}, \ell_i^{(n)}) \in \eta_n$ such that

$$\eta_n(\,\cdot \cap \overline{K}_{\varepsilon,M}) = \sum_{i=1}^{k} \delta_{(j_i^{(n)}, b_i^{(n)}, \ell_i^{(n)})}(\,\cdot\,) \qquad \text{and} \qquad (j_i^{(n)}, b_i^{(n)}, \ell_i^{(n)}) \to (j_i, b_i, \ell_i),$$

for all indices $i \in \{1, \ldots, k\}$. We pick a $\delta > 0$ small enough such that $G_\delta(P) \cap G_\delta(P') = \varnothing$ for all distinct pair of points $P \neq P'$ in η and $G_\delta(P) \subseteq \overline{K}_{\varepsilon,M}$, where $G_\delta(P)$ is the ball of radius δ around a point $P \in \eta$. For a large enough n, we have that $(P_i^{(n)}) \in G_\delta(P_i)$ for all $i \in \{1, \ldots, k\}$. Then, by Resnick [93, Theorem 3.2], $\eta_n(G_\delta(P_i)) \to \eta(G_\delta(P_i))$ for all indices i. Since η_n, η are integer valued, $\eta_n(G_\delta(P_i)) = \eta(G_\delta(P_i))$ for $n \geqslant n_0$ with some large enough n_0. Thus, the total number of points k in the set $\overline{K}_{\varepsilon,M}$ is the same for all measures $\{\eta_n\}$ and η if $n \geqslant n_0$, and there is a possible labeling of the temporal coordinates $T := \left(\{0,1\} \cup \bigcap_{i=1}^{k} \{b_i, b_i + \ell_i\} \cap [0,1]\right)$ such that $0 = \tau_1 < \cdots < \tau_{k'} = 1$, where τ_i is the ith smallest element in the set T, and the number of elements in the set T is k'. We denote by $\tau_i^{(n)}$ the corresponding elements of the set $T^{(n)} := \left(\{0,1\} \cup \bigcap_{i=1}^{k} \{b_i^{(n)}, b_i^{(n)} + \ell_i^{(n)}\} \cap [0,1]\right)$.

Next, we define a sequence of homeomorphisms $\lambda_n \colon [0,1] \to [0,1]$ by $\lambda_n(\tau_i^{(n)}) := \tau_i$ for all $i \in \{1, \ldots, k'\}$, and $\lambda_n(\,\cdot\,)$ is defined by linear interpolation between these points. Note that the domain of λ_n was chosen so that it is defined for all time instants $\{b_i\} \cup \{b_i + \ell_i\}$, $i \in \{1, \ldots, k'\}$. The graph of the homeomorphism λ_n is shown in Figure D.8. The next lemma bounds the Skorokhod distance $d_{\mathsf{Sk}}(\chi(\eta_n), \chi(\eta))$ of the functionals $\chi(\eta_n)$ and $\chi(\eta)$, which was defined in Definition D.7.1.

Lemma D.C.1 (Skorokhod distance between $\chi(\eta_n)$ and $\chi(\eta)$). *The Skorokhod distance between $\chi(\eta_n)$ and $\chi(\eta)$ is bounded by*

$$d_{\mathsf{Sk}}(\chi(\eta_n), \chi(\eta)) \leqslant (ck + 3)\delta,$$

where c is a constant depending on the distribution of the points in η.
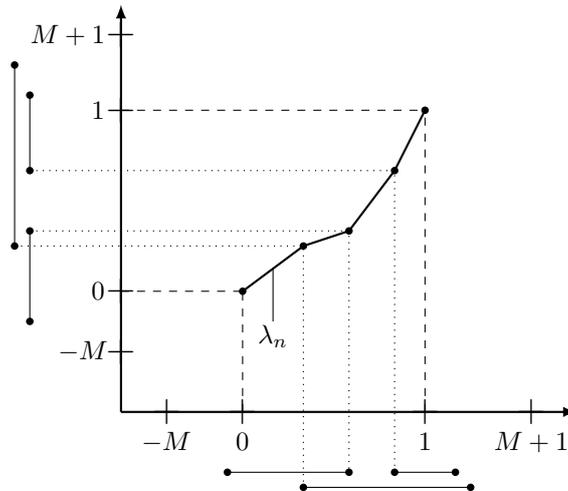
Figure D.8: Graph of the temporal transformation λ_n

Thus, by Lemma D.C.1, $\chi_{\eta_n} \to \chi(\eta)$ in $D([0,1], \mathbb{R})$ almost surely. $\qquad\square$

In the next proof, we bound the Skorokhod distance $d_{\mathsf{Sk}}(\chi(\eta_n), \chi(\eta))$ of the functionals $\chi(\eta_n)$ and $\chi(\eta)$ used in the proof of Proposition D.7.7.

Proof of Lemma D.C.1. The Skorokhod distance can be bounded by

$$d_{\mathsf{Sk}}(\chi(\eta_n), \chi(\eta)) \leqslant \|\lambda_n - I\| \vee \|\chi(\eta_n) \circ \lambda_n^{-1} - \chi(\eta)\|.$$

For the first term, we have

$$
\begin{aligned}
\|\lambda_n - I\| &= \sup_{i \in \{1,\ldots,k'\}} \sup_{s \in [\tau_i^{(n)}, \tau_{i+1}^{(n)}]} |\lambda_n(s) - s| \\
&= \sup_{i \in \{1,\ldots,k'\}} \sup_{s \in [\tau_i^{(n)}, \tau_{i+1}^{(n)}]} \left| \tau_i + \frac{\tau_{i+1} - \tau_i}{\tau_{i+1}^{(n)} - \tau_i^{(n)}} (s - \tau_i^{(n)}) - s \right| \\
&= \sup_{i \in \{1,\ldots,k'\}} \sup_{s \in [\tau_i^{(n)}, \tau_{i+1}^{(n)}]} \left| \tau_i - \tau_i^{(n)} + \left(\frac{\tau_{i+1} - \tau_i}{\tau_{i+1}^{(n)} - \tau_i^{(n)}} - 1 \right)(s - \tau_i^{(n)}) \right|.
\end{aligned}
$$

Next, we apply the triangle inequality, and use that $s - \tau_i^{(n)} \leqslant \tau_{i+1}^{(n)} - \tau_i^{(n)}$:

$$\|\lambda_n - I\| \leqslant \sup_{i \in \{1,\ldots,k'\}} \left(|\tau_i - \tau_i^{(n)}| + \left| \frac{\tau_{i+1} - \tau_i}{\tau_{i+1}^{(n)} - \tau_i^{(n)}} - 1 \right| (\tau_{i+1}^{(n)} - \tau_i^{(n)}) \right) \leqslant 3\delta.$$

For the second term,

$$
\begin{aligned}
&\|\chi(\eta_n) \circ \lambda_n^{-1} - \chi(\eta)\| \\
&= \Big\| \sum_{(j^{(n)}, b^{(n)}, \ell^{(n)}) \in \eta_n} j^{(n)}(\lambda_n^{-1}(t) - b^{(n)}) \mathbb{1}\{j^{(n)} \geqslant \tilde{c}\varepsilon^\gamma\} \mathbb{1}\{b^{(n)} \leqslant \lambda_n^{-1}(t) \leqslant b^{(n)} + \ell^{(n)}\} \\
&\qquad - \sum_{(j, b, \ell) \in \eta} j(t - b) \mathbb{1}\{j \geqslant \tilde{c}\varepsilon^\gamma\} \mathbb{1}\{b \leqslant t \leqslant b + \ell\} \Big\| \\
&= \Big\| \sum_{i=1}^{k} \Big(j_i^{(n)}(\lambda_n^{-1}(t) - b_i^{(n)}) \mathbb{1}\{b_i^{(n)} \leqslant \lambda_n^{-1}(t) \leqslant b_i^{(n)} + \ell_i^{(n)}\} \\
&\qquad\qquad\qquad - j_i(t - b_i) \mathbb{1}\{b_i \leqslant t \leqslant b_i + \ell_i\} \Big) \Big\|.
\end{aligned}
$$

Using the identity $abc - a'b'c' = (a - a')bc + a'(b - b')c + a'b'(c - c')$ for the above expression, we have

$$
\begin{aligned}
&\|\chi(\eta_n) \circ \lambda_n^{-1} - \chi(\eta)\| \\
&= \sup_{t \in [0,1]} \Big| \sum_{i=1}^{k} (j_i^{(n)} - j_i)(\lambda_n^{-1}(t) - b_i^{(n)}) \mathbb{1}\{b_i^{(n)} \leqslant \lambda_n^{-1}(t) \leqslant b_i^{(n)} + \ell_i^{(n)}\} \\
&\quad + j_i \Big((\lambda_n^{-1}(t) - b_i^{(n)}) - (t - b_i) \Big) \mathbb{1}\{b_i \leqslant t \leqslant b_i + \ell_i\} \\
&\quad + j_i(t - b_i) \Big(\mathbb{1}\{b_i^{(n)} \leqslant \lambda_n^{-1}(t) \leqslant b_i^{(n)} + \ell_i^{(n)}\} - \mathbb{1}\{b_i \leqslant t \leqslant b_i + \ell_i\} \Big) \Big|.
\end{aligned}
$$

Next, we apply the triangle inequality and examine the three terms separately. For the first term, $\lambda_n^{-1}(t)b_i^{(n)} < \infty$ whenever the indicator is 1, and $|j_i^{(n)} - j_i| < \delta$. In the second term, $j_i < \infty$ almost surely, thus we set $c_1 := \sup_{i\in\{1,\dots,k\}} j_i < \infty$. Then, $|(\lambda_n^{-1}(t) - b_i^{(n)}) - (t - b_i)| = |\lambda_n^{-1}(t) - t - (b_i^{(n)} - b_i)| \leqslant |\lambda_n^{-1}(t) - t| - |b_i^{(n)} - b_i|$. We have seen that $|\lambda_n^{-1}(t) - t| \leqslant 3\delta$ above, and $|b_i^{(n)} - b_i| \leqslant \delta$ by assumption for all indices i, thus the second term is bounded by $4c_1\delta$. In the last term, $j_i(t - b_i) < \infty$, and we need to show that the indicators are the same.

- Note that $b_i^{(n)} < 0$ if and only if $b_i < 0$. If $b_i < 0$, then $\mathbb{1}\{b_i^{(n)} \leqslant \lambda_n^{-1}(t)\} = \mathbb{1}\{b_i \leqslant t\} = 1$. Otherwise, $\mathbb{1}\{b_i^{(n)} \leqslant \lambda_n^{-1}(t)\} = \mathbb{1}\{\lambda_n(b_i^{(n)}) \leqslant t\} = \mathbb{1}\{b_i \leqslant t\}$.

- Similarly, $b_i^{(n)} + \ell_i^{(n)} > 1$ if and only if $b_i + \ell_i > 1$. If $b_i + \ell_i > 1$, then $\mathbb{1}\{\lambda_n^{-1}(t) \leqslant b_i^{(n)} + \ell_i^{(n)}\} = \mathbb{1}\{t \leqslant b_i + \ell_i\} = 1$. Otherwise, $\mathbb{1}\{\lambda_n^{-1}(t) \leqslant b_i^{(n)} + \ell_i^{(n)}\} = \mathbb{1}\{t \leqslant \lambda_n(b_i^{(n)} + \ell_i^{(n)})\} = \mathbb{1}\{t \leqslant b_i + \ell_i\}$.

Then, the indicators are the same, and the last term is also 0. Then,

$$\|\chi(\eta_n) \circ \lambda_n^{-1} - \chi(\eta)\| = \sup_{t\in[0,1]} \sum_{i=1}^{k} c_2\delta = c_2 k\delta$$

for some constant $c_2 > 0$. Considering the above two terms, we have

$$\inf_\lambda \Big(\|\lambda - I\| \vee \|\chi(\eta_n) \circ \lambda^{-1} - \chi(\eta)\| \Big) \leqslant (c_2 k + 3)\delta,$$

as required. $\qquad\square$

The following proofs show that the sequence $\overline{S}^*_{\varepsilon_n}$ is Cauchy in probability and almost surely with respect to the supremum norm, and we follow a similar approach to what was done in Step 3.

Proof of Lemma D.7.10. To ease notations, we set $\varepsilon'_n := \tilde{c}\varepsilon_n^\gamma$ for all indices $n \geqslant 0$. Furthermore, without loss of generality, we assume that $n \leqslant m$. Then, similarly to Step 2, we write

$$E := \lim_{N\uparrow\infty} \sup_{N\leqslant n\leqslant m} \mathbb{P}\Big(\Big\| \sum_{(J,B,L)\in\mathcal{P}_\infty} J(t - B)\,\mathbb{1}\{J \in [\varepsilon'_m, \varepsilon'_n]\}\,\mathbb{1}\{B \leqslant t \leqslant B + L\}$$
$$- c\big((\varepsilon'_m)^{-(1/\gamma-1)} - (\varepsilon'_n)^{-(1/\gamma-1)}\big)\Big\| \geqslant 2\delta \Big),$$

where $c := \tilde{c}^{1/\gamma}/(1 - \gamma)$. We use the usual *plus-minus decomposition* again with the notation

$$\overline{S}^{*,+}_\varepsilon(t) := \sum_{(J,B,L)\in\mathcal{P}_\infty} J(((B + L) \wedge t) - B)\,\mathbb{1}\{J \geqslant \varepsilon'\}\,\mathbb{1}\{B \leqslant t\}\,\mathbb{1}\{B + L \geqslant 0\}$$
$$- c(\varepsilon')^{-(1/\gamma-1)}(t + 1)$$
$$\overline{S}^{*,-}_\varepsilon(t) := \sum_{(J,B,L)\in\mathcal{P}_\infty} JL\,\mathbb{1}\{J \geqslant \varepsilon'\}\,\mathbb{1}\{B + L \in [0,t]\} - c(\varepsilon')^{-(1/\gamma-1)},$$

where we applied Lemma D.8.6 (a) to calculate the expectations. Then, we have that $\overline{S}^*_\varepsilon = \overline{S}^{*,+}_\varepsilon - \overline{S}^{*,-}_\varepsilon$, and the triangle inequality gives $E \leqslant E^+ + E^-$, where

$$E^+ := \lim_{N\uparrow\infty} \sup_{N\leqslant n\leqslant m} \mathbb{P}\Big(\big\| \overline{S}^{*,+}_{\varepsilon_n} - \overline{S}^{*,+}_{\varepsilon_m} \big\| \geqslant \delta \Big) \quad \text{and}$$

$$E^- := \lim_{N\uparrow\infty} \sup_{N\leqslant n\leqslant m} \mathbb{P}\Big(\big\| \overline{S}^{*,-}_{\varepsilon_n} - \overline{S}^{*,-}_{\varepsilon_m} \big\| \geqslant \delta \Big).$$

Similarly to Step 3, $\|\overline{S}^{*,-}_{\varepsilon_n} - \overline{S}^{*,-}_{\varepsilon_m}\|$ in the term E^- is a martingale since $\overline{S}^{*,-}_{\varepsilon_n}$ is a sum of independent random variables, and the expectation is equal to zero by the independence of the points $(J, B, L) \in \mathcal{P}_\infty$ in the definition of $\overline{S}^{*,-}_{\varepsilon_n}$. Then, by Doob's martingale inequality, we have

$$E^- \leqslant \lim_{N\uparrow\infty} \sup_{N\leqslant n\leqslant m} \delta^{-1} \mathbb{E}\Big[\big| \overline{S}^{*,-}_{\varepsilon_n}(1) - \overline{S}^{*,-}_{\varepsilon_m}(1) \big| \Big]$$

$$\leqslant \lim_{N\uparrow\infty} \sup_{N\leqslant n\leqslant m} \delta^{-1} \operatorname{Var}\Big(\sum_{(J,B,L)\in\mathcal{P}_\infty} JL\, \mathbb{1}\{J \in [\varepsilon'_m, \varepsilon'_n]\} \, \mathbb{1}\{B + L \in [0,1]\} \Big)^{1/2},$$

where we applied the Cauchy–Schwarz inequality in the second step. The variance is calculated using the independence of the points, and then Mecke's formula gives

$$\operatorname{Var}\Big(\sum_{(J,B,L)\in\mathcal{P}_\infty} JL\, \mathbb{1}\{J \in [\varepsilon'_m, \varepsilon'_n]\} \, \mathbb{1}\{B + L \leqslant 1\} \Big) = \int_{\mathbb{T}^{[0,1]}} \int_{\varepsilon'_m}^{\varepsilon'_n} j^2 \ell^2 \nu(\mathrm{d}j)\, \mu_{\mathsf{t}}(\mathrm{d}(b, \ell))$$

$$= \int_{\varepsilon'_m}^{\varepsilon'_n} j^2 \nu(\mathrm{d}j) = \frac{2\tilde{c}^{1/\gamma}\gamma}{2\gamma - 1}\big((\varepsilon'_n)^{2-1/\gamma} - (\varepsilon'_m)^{2-1/\gamma} \big),$$

where, in the second step, we used that the temporal part of the integral is 2 by Part (a). Note that the variance is similar to the variance given in the proof of Lemma D.7.9. Then, $E^- = 0$ since $\gamma > 1/2$. For the E^+ term, we have

$$E^+ = \lim_{N\uparrow\infty} \sup_{N\leqslant n\leqslant m} \mathbb{P}\Big(\sup_{t\in[0,1]} \Big| \sum_{(J,B,L)\in\mathcal{P}_\infty} J(t - B)\, \mathbb{1}\{J \in [\varepsilon'_m, \varepsilon'_n]\}$$

$$\times \mathbb{1}\{B \leqslant t\}\, \mathbb{1}\{B + L \geqslant 0\}$$

$$- c\big((\varepsilon'_m)^{-(1/\gamma-1)} - (\varepsilon'_n)^{-(1/\gamma-1)} \big)(t + 1) \Big| \geqslant \delta \Big)$$

We use the same strategy as in Step 3, and similarly to the Definition (D.34), we introduce $H'_{\varepsilon'_m, \varepsilon'_n}(t)$ and write the edge count as an integral:

$$H'_{\varepsilon'_m, \varepsilon'_n}(t) := \sum_{(J,B,L)\in\mathcal{P}_\infty} J\, \mathbb{1}\{J \in [\varepsilon'_m, \varepsilon'_n]\}\, \mathbb{1}\{t \in [B, B + L]\}\, \mathbb{1}\{B + L \geqslant 0\}$$

$$\overline{S}^{*,+}_\varepsilon(t) = \overline{S}^{*,+}_\varepsilon(0) + \int_0^t H'_{\varepsilon'_m, \varepsilon'_n}(t') - \mathbb{E}[H'_{\varepsilon'_m, \varepsilon'_n}(t')]\, \mathrm{d}t',$$

for and $0 < \varepsilon_m \leqslant \varepsilon_n$. Then, following Step 3, we apply the triangle inequality twice to bound E^+:

$$
E^+ = \lim_{N \uparrow \infty} \sup_{N \leqslant n \leqslant m} \mathbb{P}\Big(\sup_{t \in [0,1]} \Big| \overline{S}^*_{\varepsilon'_m}(0) - \overline{S}^*_{\varepsilon'_n}(0)
$$
$$
+ \int_0^t H'_{\varepsilon'_m, \varepsilon'_n}(t') - \mathbb{E}[H'_{\varepsilon'_m, \varepsilon'_n}(t')] \, \mathrm{d}t' \Big| \geqslant \delta \Big)
$$
$$
\leqslant \lim_{N \uparrow \infty} \sup_{N \leqslant n \leqslant m} \Big(\mathbb{P}\Big(\Big| \overline{S}^*_{\varepsilon'_m}(0) - \overline{S}^*_{\varepsilon'_n}(0) \Big| \geqslant \delta/2 \Big)
$$
$$
+ \mathbb{P}\Big(\int_0^1 \Big| H'_{\varepsilon'_m, \varepsilon'_n}(t') - \mathbb{E}[H'_{\varepsilon'_m, \varepsilon'_n}(t')] \Big| \, \mathrm{d}t' \geqslant \delta/2 \Big) \Big),
$$

where, we used that $\sup_{t \in [0,1]} \int_0^t |\cdot| \leqslant \int_0^1 |\cdot|$. For the first term, Chebyshev's inequality yields

$$
\mathbb{P}\Big(|\overline{S}^*_{\varepsilon_m}(0) - \overline{S}^*_{\varepsilon_n}(0)| \geqslant \delta/2 \Big) \leqslant 4\delta^{-2} \operatorname{Var}\big(S^*_{\varepsilon_m}(0) - S^*_{\varepsilon_n}(0) \big)
$$
$$
= 4\delta^{-2} \int_{\mathbb{T}^{0 \leqslant}_{\leqslant 0}} \int_{\varepsilon'_m}^{\varepsilon'_n} j^2 b^2 \nu(\mathrm{d}j) \, \mu_t(\mathrm{d}(b,\ell)) = \frac{16 \tilde{c}^{1/\gamma} \gamma \delta^{-2}}{2\gamma - 1} \big((\varepsilon'_n)^{2-1/\gamma} - (\varepsilon'_m)^{2-1/\gamma} \big),
$$

where we applied the Mecke formula to calculate the variance in the second step, and in the last step we used that the integral of the temporal part is 2 by Lemma D.8.6 (a). This term converges to 0 as $n, m \to 0$ since $\gamma > 1/2$. For the second term, we follow again the same arguments as in Step 3, and first we apply Markov's and then Jensen's inequality:

$$
\mathbb{P}\Big(\int_0^1 \Big| H'_{\varepsilon'_m, \varepsilon'_n}(t') - \mathbb{E}[H'_{\varepsilon'_m, \varepsilon'_n}(t')] \Big| \, \mathrm{d}t' \geqslant \delta/2 \Big)
$$
$$
\leqslant 2\delta^{-1} \mathbb{E}\Big[\int_0^1 \Big| H'_{\varepsilon'_m, \varepsilon'_n}(t') - \mathbb{E}[H'_{\varepsilon'_m, \varepsilon'_n}(t')] \Big| \, \mathrm{d}t' \Big]
$$
$$
\leqslant 2\delta^{-1} \int_0^1 \operatorname{Var}(H'_{\varepsilon'_m, \varepsilon'_n}(t'))^{1/2} \, \mathrm{d}t'.
$$

We calculate the variance using Mecke's formula:

$$
\operatorname{Var}(H'_{\varepsilon'_m, \varepsilon'_n}(t')) = \int_{\mathbb{T}^{0 \leqslant}} \int_{\varepsilon'_m}^{\varepsilon'_n} j^2 \, \mathbb{1}\{b \leqslant t \leqslant b + \ell\} \, \nu(\mathrm{d}j) \, \mu_t(\mathrm{d}(b,\ell))
$$
$$
= \frac{2\tilde{c}^{1/\gamma} \gamma}{2\gamma - 1} \big((\varepsilon'_n)^{2-1/\gamma} - (\varepsilon'_m)^{2-1/\gamma} \big)(t' + 1),
$$

where the temporal integral is $t' + 1$ by Part (a). Then,

$$
\mathbb{P}\Big(\int_0^1 \Big| H'_{\varepsilon'_m, \varepsilon'_n}(t') - \mathbb{E}[H'_{\varepsilon'_m, \varepsilon'_n}(t')] \Big| \, \mathrm{d}t' \geqslant \delta/2 \Big)
$$
$$
\leqslant \frac{4}{3} \delta^{-1} \Big(\frac{2\tilde{c}^{1/\gamma} \gamma}{2\gamma - 1} \big((\varepsilon'_n)^{2-1/\gamma} - (\varepsilon'_m)^{2-1/\gamma} \big) \Big)^{1/2} (2^{3/2} - 1),
$$

which converges to 0 as $n, m \to \infty$ since $\gamma > 1/2$. $\qquad \square$

In the next proof showing the Cauchy property almost surely, we follow the approach of the proof of Property 2 in [93, Proposition 5.7].

Proof of Proposition D.7.11. Let $\widetilde{\Lambda}$ be a set with $\mathbb{P}(\widetilde{\Lambda}) = 1$ such that if $\omega \in \widetilde{\Lambda}$, then the sequence $\{\overline{S}^*_{\varepsilon_k}(\,\cdot\,, \omega), k \geqslant 1\}$ is Cauchy with respect to the uniform convergence on $[0, 1]$. We prove the Cauchy property by showing $\sup_{m,n \geqslant N} \|\overline{S}^*_{\varepsilon_m} - \overline{S}^*_{\varepsilon_n}\| \to 0$ almost surely as $N \to \infty$. Since the supremum is non-increasing in N, it is enough to show that it converges to 0 in probability [93, Equation (5.45)]. Then, with $\delta' := \delta/4$, we have

$$
\lim_{N\uparrow\infty} \mathbb{P}\Big(\sup_{m,n \geqslant N} \|\overline{S}^*_{\varepsilon_m} - \overline{S}^*_{\varepsilon_n}\| \geqslant \delta\Big) = \lim_{N\uparrow\infty} \lim_{M\uparrow\infty} \mathbb{P}\Big(\sup_{m,n \in \{N,\dots,M\}} \|\overline{S}^*_{\varepsilon_m} - \overline{S}^*_{\varepsilon_n}\| \geqslant \delta\Big)
$$

$$
\leqslant \lim_{N\uparrow\infty} \lim_{M\uparrow\infty} \mathbb{P}\Big(\sup_{n \in \{N,\dots,M\}} \|\overline{S}^*_{\varepsilon_n} - \overline{S}^*_{\varepsilon_N}\| \geqslant 2\delta'\Big),
$$

where in the last step we used that by the triangle inequality,

$$
\|\overline{S}^*_{\varepsilon_m} - \overline{S}^*_{\varepsilon_n}\| \leqslant \|\overline{S}^*_{\varepsilon_m} - \overline{S}^*_{\varepsilon_N}\| + \|\overline{S}^*_{\varepsilon_N} - \overline{S}^*_{\varepsilon_n}\|,
$$

but then

$$
\sup_{m,n \in \{N,\dots,M\}} \|\overline{S}^*_{\varepsilon_m} - \overline{S}^*_{\varepsilon_n}\| \leqslant 2 \sup_{n \in \{N,\dots,M\}} \|\overline{S}^*_{\varepsilon_n} - \overline{S}^*_{\varepsilon_N}\|.
$$

Again, by the triangle inequality, we have that

$$
\|\overline{S}^*_{\varepsilon_M} - \overline{S}^*_{\varepsilon_N}\| \geqslant \|\overline{S}^*_{\varepsilon_i} - \overline{S}^*_{\varepsilon_N}\| - \|\overline{S}^*_{\varepsilon_M} - \overline{S}^*_{\varepsilon_i}\|,
$$

which implies that

$$
\Big\{\|\overline{S}^*_{\varepsilon_i} - \overline{S}^*_{\varepsilon_N}\| > 2\delta', \|\overline{S}^*_{\varepsilon_M} - \overline{S}^*_{\varepsilon_i}\| \leqslant \delta'\Big\} \subseteq \Big\{\|\overline{S}^*_{\varepsilon_M} - \overline{S}^*_{\varepsilon_N}\| > \delta'\Big\} \qquad \text{for all } i,
$$

and then

$$
\bigcup_{i=N+1}^{M} \Big\{\max_{k \in \{N,\dots,i-1\}}\big(\|\overline{S}^*_{\varepsilon_k} - \overline{S}^*_{\varepsilon_N}\|\big) \leqslant 2\delta', \|\overline{S}^*_{\varepsilon_i} - \overline{S}^*_{\varepsilon_N}\| > 2\delta', \|\overline{S}^*_{\varepsilon_M} - \overline{S}^*_{\varepsilon_i}\| \leqslant \delta'\Big\}
$$

$$
\subseteq \Big\{\|\overline{S}^*_{\varepsilon_M} - \overline{S}^*_{\varepsilon_N}\| > \delta'\Big\}.
$$

Note that the union is a disjoint union, since for all $k \in \{N\dots, i-1\}$, $\overline{S}^*_{\varepsilon_k}$ is within a distance of $2\delta'$ from $\overline{S}^*_{\varepsilon_N}$, and $\overline{S}^*_{\varepsilon_i}$ is further from $\overline{S}^*_{\varepsilon_N}$ than δ'. Thus, we have

$$
\mathbb{P}\Big(\|\overline{S}^*_{\varepsilon_M} - \overline{S}^*_{\varepsilon_N}\| > \delta'\Big)
$$

$$
\geqslant \sum_{i=N+1}^{M} \mathbb{P}\Big(\max_{k \in \{N,\dots,i-1\}}\big(\|\overline{S}^*_{\varepsilon_k} - \overline{S}^*_{\varepsilon_N}\|\big) \leqslant 2\delta',
$$

$$
\|\overline{S}^*_{\varepsilon_i} - \overline{S}^*_{\varepsilon_N}\| > 2\delta', \|\overline{S}^*_{\varepsilon_M} - \overline{S}^*_{\varepsilon_i}\| \leqslant \delta'\Big)
$$

$$
= \sum_{i=N+1}^{M} \mathbb{P}\Big(\max_{k \in \{N,\dots,i-1\}}\big(\|\overline{S}^*_{\varepsilon_k} - \overline{S}^*_{\varepsilon_N}\|\big) \leqslant 2\delta', \|\overline{S}^*_{\varepsilon_i} - \overline{S}^*_{\varepsilon_N}\| > 2\delta'\Big)
$$

$$
\times \mathbb{P}\Big(\|\overline{S}^*_{\varepsilon_M} - \overline{S}^*_{\varepsilon_i}\| \leqslant \delta'\Big),
$$

where in the last step we used the independence of the points whose jumps are in $[\varepsilon_i, \varepsilon_N]$ and those whose jumps are between $[\varepsilon_M, \varepsilon_i]$. Then, for the last term, we have $\mathbb{P}(\|\overline{S}^*_{\varepsilon_M} - \overline{S}^*_{\varepsilon_i}\| \leqslant \delta') \to 1$ as $N \to \infty$, where we applied Lemma D.7.10. Now, we choose $N \geqslant N_0$ large enough such that $\mathbb{P}(\max_{i \in \{N,\dots,M\}}(\|\overline{S}^*_{\varepsilon_M} - \overline{S}^*_{\varepsilon_i}\|) \leqslant \delta') \geqslant 1/2$. Then, continuing the lower bound for $\mathbb{P}(\|\overline{S}^*_{\varepsilon_M} - \overline{S}^*_{\varepsilon_N} > \delta'\|)$, we have

$$
2\,\mathbb{P}(\|\overline{S}^*_{\varepsilon_M} - \overline{S}^*_{\varepsilon_N}\| > \delta')
$$
$$
\geqslant \sum_{i=N+1}^{M} \mathbb{P}\left(\max_{k \in \{N,\dots,i-1\}}\left(\|\overline{S}^*_{\varepsilon_k} - \overline{S}^*_{\varepsilon_N}\|\right) \leqslant 2\delta', \|\overline{S}^*_{\varepsilon_i} - \overline{S}^*_{\varepsilon_N}\| > 2\delta' \right)
$$
$$
= \mathbb{P}\left(\max_{n \in \{N+1,\dots,M\}}\left(\|\overline{S}^*_{\varepsilon_n} - \overline{S}^*_{\varepsilon_N}\|\right) > 2\delta' \right).
$$

The second application of Lemma D.7.10 gives that $\lim_{N\uparrow\infty} \lim_{M\uparrow\infty} 2\,\mathbb{P}(\|\overline{S}^*_{\varepsilon_M} - \overline{S}^*_{\varepsilon_N}\| > \delta') = 0$. Then, $\lim_{N\uparrow\infty} \lim_{M\uparrow\infty} \mathbb{P}(\sup_{m,n \in \{N,\dots,M\}} \|\overline{S}^*_{\varepsilon_m} - \overline{S}^*_{\varepsilon_n}\| \geqslant \delta) = 0$. $\qquad\square$

Acknowledgement

Errata

In this section, the corrections made to the included papers are summarized.

- The notation in the included papers has been unified to match the notation used in the thesis. This includes changes to symbols, abbreviations, and other notational elements.

- The formatting of the included papers has been adjusted to match the overall style of the thesis. This includes changes to the layout, numbering of the sections, theorems and figures, font size and type, line spacing, margins, line breaks in the formulas, and other formatting elements to ensure consistency throughout the document.

- Typographical and grammatical errors in the included papers have been corrected including commas, spacing, and capitalization.

- References of the included papers have been updated to the latest versions. Furthermore, the references of all the papers are now listed collectively in the bibliography at the end of the thesis. References of the included papers to each other are replaced with the corresponding chapter numbers in the thesis.

- For references to equations, the word "Equation" is removed to match the notation used in the thesis.

- Date formats have been standardized to the format "31 October 2025".

- The thousand separators are changed from , to space.

The below list contains the individual corrections that could affect understanding, including mathematical mistakes, wrong references, misprints in formulas, or misleading wording. Furthermore, in several places minor typographical corrections have been made, and the wording has been refined to enhance clarity and readability; these changes do not affect the mathematical content or meaning and are not listed individually.

Paper A

- In the model section, the display describing the regular variation of the profile function φ is changed from

$$\lim_{r\uparrow\infty} \varphi(tr)/\varphi(r) = t^{\alpha} \qquad \text{for all } t > 0$$

253

to

$$\lim_{r\uparrow\infty} \varphi(tr)/\varphi(r) = t^{-\alpha} \qquad \text{for all } t > 0.$$

- In Section A.4, the display

$$\deg_f(\boldsymbol{x}) := \sum_{\boldsymbol{y}\in\widetilde{\mathcal{P}}_s\,:\,\boldsymbol{y}\leftrightarrow\boldsymbol{x}} f(|B_{x-y}(o)|, W_x, W_y).$$

is changed to

$$\deg_f(\boldsymbol{x}) := \sum_{\boldsymbol{y}\in\widetilde{\mathcal{P}}_s\,:\,\boldsymbol{y}\leftrightarrow\boldsymbol{x}} f(|B_{|x-y|}(o)|, W_x, W_y).$$

Paper B

- In mathematical formulas, the notation for distinct elements a_1, a_2 of a set A is changed from "$a_1, a_2 \in A$ distinct" to "$a_1, a_2 \in A_{\neq}^2$".

- In the entire paper, the mark space was changed from $[0, 1]$ to $(0, 1]$.

- In Section B.2 at the definition of the degree distribution $d_{m,m'}(k)$, "generalized vertex-degree distribution" is changed to "generalized simplex-degree distribution".

- Below the definition of the distribution $d_{m,m'}(k)$, the text "the distribution of the number of m'-simplices incident to o" should read "the distribution of the number of m'-simplices incident to Δ_m^*".

- The title of Theorem B.2.1 is changed from "Power law for the typical vertex & edge degree" to "Power law for the typical simplex degree".

- In Theorem B.2.1, the expression $m' \geqslant m \geqslant 0$ is changed to $m' > m \geqslant 0$.

- In Theorem B.2.2, the sentence "Then, $\mathrm{Var}(\beta_{n,q})^{-1/2}(\beta_{n,q} - \mathbb{E}[\beta_{n,q}])$ converges in distribution to a standard normal distribution." is changed to "Then, $n^{-1/2}(\beta_{n,q} - \mathbb{E}[\beta_{n,q}])$ converges in distribution to a normal distribution.".

- In Section B.3, the display

$$B_k := B_k' \times [0, \beta'k]^m := \big(\prod_{j\leqslant m+1} [(j/(Mmk))^{1/\gamma}, ((j+1)/(Mmk))^{1/\gamma}]\big) \times [0, \beta'k]^m$$

is changed to

$$B_k := [0, \beta'k]^m \times B_k' \qquad \text{with} \qquad B_k' := \prod_{j=0}^{m}\Big[\Big(\frac{j}{Mmk}\Big)^{1/\gamma}, \Big(\frac{j+1}{Mmk}\Big)^{1/\gamma}\Big].$$

- In Section B.3, three occurrences of the notation b' are changed to β'.

- At the end of Section B.3, the text "implies that $\mathbb{P}(\mathcal{P}(C_k) \geqslant k) \to 1$ as $k \to \infty$" is changed to "implies that $\mathbb{P}(\mathcal{P}(B_k) \geqslant k) \to 1$ as $k \to \infty$"

- In Section B.3, the text "the higher-order degree of the typical vertex, $o = (0, U)$" is changed to "the higher-order degree of the typical simplex Δ_m^*".

- In Equation (B.3), the symbol Δ_m is changed to Δ_m^*.

- In Section B.5, in the first display about the edge count S_n is changed from

$$S_n = \sum_{i \leqslant n} T_i := \sum_{i \leqslant n} \sum_{P_j \in [i-1,i] \times [0,1]} D_{\mathsf{in}}(P_j)$$

to

$$S_n = \sum_{i \leqslant n} T_i := \sum_{i \leqslant n} \sum_{P_j \in \mathcal{P} \cap ([i-1,i] \times (0,1])} D_{\mathsf{in}}(P_j).$$

- In three cases, the notation for the point in the origin with mark u was incorrectly written $(u, 0)$, which should be $(0, u)$. This is corrected in the tick label of Figure B.3, and in the enumeration listing the steps of the simulation of a single network in Section B.7.

Paper C

- In the entire paper, the mark space was changed from $[0, 1]$ to $(0, 1]$.

Paper D

- In the entire paper, the mark space was changed from $[0, 1]$ to $(0, 1]$.

- In Section D.2, the connection rule between two vertices in the bipartite graph G^{bip} is changed from " A pair of vertices $P \in \mathcal{P}$ and $P' \in \mathcal{P}'$ are connected in the *bipartite graph* $G^{\mathsf{bip}} := G^{\mathsf{bip}}(\mathcal{P}, \mathcal{P}')$ if and only if the following two conditions hold:
$$|X - Z| \leqslant \beta U^{-\gamma} W^{-\gamma'} \qquad \text{and} \qquad B \leqslant R \leqslant B + L,$$
where $\beta > 0$ and $\gamma, \gamma' \in (0, 1)$ are real parameters. " to " A pair of vertices $p := (x, u, b, \ell) \in \mathbb{S} \times \mathbb{T}$ and $p' := (z, w, r) \in \mathbb{S} \times \mathbb{R}$ is connected if and only if the following two conditions hold:

$$|x - z| \leqslant \beta u^{-\gamma} w^{-\gamma'} \qquad \text{and} \qquad b \leqslant r \leqslant b + \ell,$$

where $\beta > 0$ and $\gamma, \gamma' \in (0, 1)$ are real parameters. Using this connection rule, we define the *bipartite graph* $G^{\mathsf{bip}} := G^{\mathsf{bip}}(\mathcal{P}, \mathcal{P}')$ with vertex sets $\mathcal{P}$ and $\mathcal{P}'$. "

- In Section D.2, the text " This means that a few vertices with very high degrees dominate the edge count, leading to a heavy-tailed distribution. Thus, if $\gamma > 1/2$, the limiting process is not a Gaussian process. " is changed to " This means that a few vertices with very high degrees dominate the edge count, and the distribution of $\overline{S}_n(t)$ diverges. Thus, if $\gamma > 1/2$, we need to consider a different scaling of the edge count to obtain a nontrivial limit, and we introduce

$$\overline{S}_n(\cdot) := n^{-\gamma}(S_n(\cdot) - \mathbb{E}[S_n(\cdot)]).$$

Note that the symbol $\overline{S}_n(\,\cdot\,)$ is reused here with different scaling from the one in Theorem D.2.4. As the two scalings are used in different contexts, namely the thin-tailed case and the heavy-tailed case, they are used in separate sections of the paper, and we believe that there is no risk of confusion. As it is shown in Theorem D.2.6 if $\gamma > 1/2$, the finite-dimensional distributions of $\overline{S}_n(\,\cdot\,)$ are heavy-tailed, and thus the limiting process is not a Gaussian process. ".

- In Section D.2, at the definition of the spatial and temporal parts of points, the text "$p := (x, u, b, \ell) \in \mathcal{P}$, we define the spatial part" is changed to "$p := (x, u, b, \ell) \in \mathbb{S} \times \mathbb{T}$, we define the spatial part". Similarly, the text "for a point $p' := (z, w, r) \in \mathcal{P}'$, we define its spatial part" is changed to "for a point $p' := (z, w, r) \in \mathbb{S} \times \mathbb{R}$, we define its spatial part".

- In the proof of Lemma D.10.1, the last sentence of the proof is changed from "Thus, for some constant $c_- > 0$, the covariance function of $\overline{S}_n^-(t)$ is given by" to "Thus, for some constant $c_- > 0$, the limiting covariance function of $\overline{S}_n^-(t)$ is given by".

- In Section D.11, the text "In the next proof, we show that the size of the spatial neighborhoods of the points converges to a measure, which is done by showing convergence to a distribution function." is changed to "In the next proof, we show that $n\,\mathbb{P}(n^{-\gamma}|N_{\mathsf{s}}(P_{\mathsf{s}})| \in [\,\cdot\,, \infty))$ converges to a measure in the vague topology as $n \to \infty$.".

List of Figures

List of Tables

References

[1] arXiv Preprint Server. `https://arxiv.org/`, 2023. Accessed: 4 August 2023.

[2] F. Baccini, F. Geraci, and G. Bianconi. Weighted simplicial complexes and their representation power of higher-order network data and topology. *Phys. Rev. E*, 106(3):034319, 2022.

[3] A.-L. Barabási and R. Albert. Emergence of scaling in random networks. *Science*, 286(5439):509–512, 1999.

[4] Y. Baryshnikov and J. E. Yukich. Gaussian limits for random measures in geometric probability. *Ann. Appl. Probab.*, 15(1A):213–253, 2005.

[5] B. Basrak, D. Krizmanić, and J. Segers. A functional limit theorem for dependent sequences with infinite variance stable limits. *Ann. Probab.*, 40(5):2008–2033, 2012.

[6] F. Battiston, G. Cencetti, I. Iacopini, V. Latora, M. Lucas, A. Patania, J. Young, and G. Petri. Networks beyond pairwise interactions: structure and dynamics. *Phys. Rep.*, 874:1–92, 2020.

[7] H. Bauke. Parameter estimation for power-law distributions by maximum likelihood methods. *Eur. Phys. J. B*, 58:167–173, 2007.

[8] G. Bennett. Probability inequalities for the sum of independent random variables. *J. Amer. Statist. Assoc.*, 57(297):33–45, 1961.

[9] C. Berge. *Graphs and Hypergraphs.* Elsevier Science, New York, 1973.

[10] G. Bianconi. *Higher-Order Networks.* Cambridge University Press, Cambridge, 2021.

[11] G. Bianconi and C. Rahmede. Network geometry with flavor: from complexity to quantum geometry. *Phys. Rev. E*, 93(3):032315, 15, 2016.

[12] P. Billingsley. *Convergence of Probability Measures.* John Wiley & Sons, New York, 1999.

[13] N. H. Bingham, C. M. Goldie, and J. L. Teugels. *Regular Variation.* Cambridge University Press, Cambridge, 1989.

[14] B. H. Bloom. Space/time trade-offs in hash coding with allowable errors. *ACM Commun.*, 13(7):422–426, 1970.

[15] Gudhi Editorial Board. Gudhi – Geometry Understanding in Higher Dimensions. `https://gudhi.inria.fr/`, 2023. Version 3.9.0.

[16] O. Bobrowski, M. Schulte, and D. Yogeshwaran. Poisson process approximation under stabilization and Palm coupling. *Ann. H. Lebesgue*, 5:1489–1534, 2022.

[17] J.-D. Boissonnat, F. Chazal, and M. Yvinec. *Geometric and Topological Inference.* Cambridge University Press, Cambridge, 2018.

[18] M. Brun and N. Blaser. Sparse Dowker nerves. *J. Appl. Comput. Topol.*, 3(1-2): 1–28, 2019.

[19] M. Brun, C. Hirsch, P. Juhász, and M. Otto. Random connection hypergraphs. *arXiv preprint arXiv:2407.16334v2*, 2025.

[20] C. J. Carstens and K. J. Horadam. Persistent homology of collaboration networks. *Math. Probl. Eng.*, pages Art. ID 815035, 7, 2013.

[21] K. Choi. On medians of Gamma distributions and equations of Ramanujan. *Proc. Amer. Math. Soc.*, 121(1):245–251, 1994.

[22] A. Cipriani, C. Hirsch, and M. Vittorietti. Topology-based goodness-of-fit tests for sliced spatial data. *Comput. Statist. Data Anal.*, 179:107655, 2023.

[23] A. Clauset, C. R. Shalizi, and M. E. J. Newman. Power-law distributions in empirical data. *SIAM Rev.*, 51(4):661–703, 2009.

[24] O. T. Courtney and G. Bianconi. Generalized network structures: The configuration model and the canonical ensemble of simplicial complexes. *Phys. Rev. E*, 93:062311, 2016.

[25] J. A. Davis and S. Leinhardt. The structure of positive interpersonal relations in small groups. In E. Buzila and B. Holzer, editors, *Schlüsselwerke der Netzwerkforschung*, pages 141–145. Springer, Wiesbaden, 1967.

[26] Y. Davydov. Weak convergence of discontinuous processes to continuous ones. In I. A. Ibragimov and A. Y. Zaitsev, editors, *Probability Theory and Mathematical Statistics*, pages 15–18. Gordon and Breach, Amsterdam, 1996.

[27] L. Decreusefond, M. Schulte, and C. Thäle. Functional Poisson approximation in Kantorovich-Rubinstein distance with applications to U-statistics and stochastic geometry. *Ann. Probab.*, 44:2147–2197, 2016.

[28] M. Deijfen, R. van der Hofstad, and G. Hooghiemstra. Scale-free percolation. *Ann. Inst. Henri Poincaré Probab. Stat.*, 49(3):817–838, 2013.

[29] P. Deprez and M. V. Wüthrich. Scale-free percolation in continuum space. *Commun. Math. Stat.*, 7(3):269–308, 2019.

[30] S. Dereich and P. Mörters. Random networks with sublinear preferential attachment: degree evolutions. *Electron. J. Probab.*, 14:no. 43, 1222–1267, 2009.

[31] S. Dereich and P. Mörters. Random networks with sublinear preferential attachment: the giant component. *Ann. Probab.*, 41(1):329–384, 2013.

[32] D. Dereudre and M. D. Penrose. On the critical threshold for AB percolation. *J. Appl. Probab.*, 55(4):1228–1237, 2018.

[33] T. K. Dey and Y. Wang. *Computational Topology for Data Analysis.* Cambridge University Press, Cambridge, 2021.

[34] R. Douc, E. Moulines, P. Priouret, and P. Soulier. *Markov Chains.* Springer, Cham, 2018.

[35] H. Edelsbrunner and J. Harer. *Computational Topology: An Introduction.* American Mathematical Society, Providence, 2010.

[36] J. D. Esary, F. Proschan, and D. W. Walkup. Association of random variables, with applications. *Ann. Math. Statist.*, 38(5):1466–1474, 1967.

[37] N. Fountoulakis, T. Iyer, C. Mailler, and H. Sulzbach. Dynamical models for random simplicial complexes. *Ann. Appl. Probab.*, 32(4):2860–2913, 2022.

[38] M. Franceschetti, M. D. Penrose, and T. Rosoman. Strict inequalities of critical values in continuum percolation. *J. Stat. Phys.*, 142(3):460–486, 2011.

[39] C. Giusti, E. Pastalkova, C. Curto, and V. Itskov. Clique topology reveals intrinsic geometric structure in neural correlations. *Proc. Natl. Acad. Sci. USA*, 112(44):13455–13460, 2015.

[40] P. Gracar, A. Grauer, L. Lüchtrath, and P. Mörters. The age-dependent random connection model. *Queueing Syst.*, 93(3-4):309–331, 2019.

[41] P. Gracar, L. Lüchtrath, and P. Mörters. Percolation phase transition in weight-dependent random connection models. *Adv. in Appl. Probab.*, 53(4):1090–1114, 2021.

[42] P. Gracar, M. Heydenreich, C. Mönch, and P. Mörters. Recurrence versus transience for weight-dependent random connection models. *Electron. J. Probab.*, 27:Paper No. 60, 31, 2022.

[43] M. Haenggi. *Stochastic Geometry for Wireless Networks.* Cambridge University Press, Cambridge, 2012.

[44] A. A. Hagberg, D. A. Schult, and P. J. Swart. Exploring network structure, dynamics, and function using NetworkX. In *Proceedings of the 7th Python in Science Conference*, pages 11–15, 2008.

[45] C. R. Harris, K. J. Millman, S. J. van der Walt, R. Gommers, P. Virtanen, D. Cournapeau, E. Wieser, J. Taylor, S. Berg, N. J. Smith, R. Kern, M. Picus, S. Hoyer, M. H. van Kerkwijk, M. Brett, A. Haldane, J. F. del Río, M. Wiebe, P. Peterson, P. Gérard-Marchant, K. Sheppard, T. Reddy, W. Weckesser, H. Abbasi, C. Gohlke, and T. E. Oliphant. Array programming with NumPy. *Nature*, 585(7825):357–362, 2020.

[46] L. Heinrich and W. Wolf. On the convergence of U-statistics with stable limit distribution. *J. Multivariate Anal.*, 44(2):266–278, 1993.

[47] H. Hinnant. Combinations – A C++ implementation of combination generation. `https://github.com/HowardHinnant/combinations`, 2011. Accessed: 2025-02-16.

[48] Y. Hiraoka, T. Shirai, and K. D. Trinh. Limit theorems for persistence diagrams. *Ann. Appl. Probab.*, 28(5):2740–2780, 2018.

[49] C. Hirsch and P. Juhász. On the topology of higher-order age-dependent random connection models. *Methodol. Comput. Appl. Probab.*, 27(2):Paper No. 44, 41, 2025.

[50] C. Hirsch and P. Juhász. Network simulator. `https://github.com/shepherd92/network_simulator`, 2025.

[51] C. Hirsch, B. Jahnel, S. K. Jhawar, and P. Juhász. Poisson approximation of fixed-degree nodes in weighted random connection models. *Stochastic Process. Appl.*, 183:104593, 2025.

[52] C. Hirsch, B. Jahnel, and P. Juhász. Functional limit theorems for edge counts in dynamic random connection hypergraphs. *arXiv preprint arXiv:2507.16270*, 2025.

[53] P. W. Holland and S. Leinhardt. Local structure in social networks. *Sociol. Methodol.*, 7:1–45, 1976.

[54] J. D. Hunter. Matplotlib: A 2D graphics environment. *Computing in Science & Engineering*, 9(3):90–95, 2007.

[55] S. K. Iyer and S. K. Jhawar. Poisson approximation and connectivity in a scale-free random connection model. *Electron. J. Probab.*, 26:Paper No. 86, 23, 2021.

[56] S. K. Iyer and D. Yogeshwaran. Percolation and connectivity in AB random geometric graphs. *Adv. in Appl. Probab.*, 44(1):21–41, 2012.

[57] E. Jacob and P. Mörters. Spatial preferential attachment networks: power laws and clustering coefficients. *Ann. Appl. Probab.*, 25(2):632–662, 2015.

[58] E. Jacob and P. Mörters. Robustness of scale-free spatial networks. *Ann. Probab.*, 45(3):1680–1722, 2017.

[59] B. Jahnel and W. König. *Probabilistic Methods in Telecommunications*. Birkhäuser, Cham, 2020.

[60] W. Jakob, J. Rhinelander, and D. Moldovan. pybind11 – Seamless Operability between C++11 and Python. `https://github.com/pybind/pybind11`, 2017. Version 2.10.0.

[61] O. Kallenberg. *Random Measures, Theory and Applications*. Springer, Cham, 2017.

[62] I. Karatzas and S. E. Shreve. *Brownian Motion and Stochastic Calculus*. Springer, New York, 1991.

[63] W. Kim and F. Mémoli. Extracting persistent clusters in dynamic data via Möbius inversion. *Discrete Comput. Geom.*, 71(4):1276–1342, 2024.

[64] J. Komjáthy and B. Lodewijks. Explosion in weighted hyperbolic random graphs and geometric inhomogeneous random graphs. *Stochastic Process. Appl.*, 130(3): 1309–1367, 2020.

[65] R. Lambiotte, M. Rosvall, and I. Scholtes. From networks to optimal higher-order models of complex systems. *Nature Physics*, 15(4):313–320, 2019.

[66] G. Last and M. D. Penrose. *Lectures on the Poisson Process*. Cambridge University Press, Cambridge, 2016.

[67] G. Last, G. Peccati, and M. Schulte. Normal approximation on Poisson spaces: Mehler's formula, second order Poincaré inequalities and stabilization. *Probab. Theory Related Fields*, 165:667–723, 2016.

[68] G. Last, F. Nestmann, and M. Schulte. The random connection model and functions of edge-marked Poisson processes: second order properties and normal approximation. *Ann. Appl. Probab.*, 31(1):128–168, 2021.

[69] G. Last, G. Peccati, and D. Yogeshwaran. Phase transitions and noise sensitivity on the Poisson space via stopping sets and decision trees. *Random Structures Algorithms*, 63(2):457–511, 2023.

[70] L. Lüchtrath. *Percolation in weight-dependent random connection models*. PhD thesis, Universität zu Köln, 2022.

[71] B. Matérn. *Spatial Variation*. Springer, Berlin, 1986.

[72] R. Meester and R. Roy. *Continuum Percolation*. Cambridge University Press, Cambridge, 1996.

[73] J. R. Munkres, S. G. Krantz, and H. R. Parks. *Elements of Algebraic Topology*. CRC press, New York, 2nd edition, 2025.

[74] A. Myers, D. Muñoz, F. A. Khasawneh, and E. Munch. Temporal network analysis using zigzag persistence. *EPJ Data Sci.*, 12(1):6, 2023.

[75] M. E. J. Newman. The structure and function of complex networks. *SIAM Review*, 45(2):167–256, 2003.

[76] M. E. J. Newman. Properties of highly clustered networks. *Phys. Rev. E*, 68(2): 026121, 2003.

[77] J. P. Nolan. Maximum likelihood estimation and diagnostics for stable distributions. In O. E. Barndorff-Nielsen, S. I. Resnick, and T. Mikosch, editors, *Lévy Processes*, pages 379–400. Birkhäuser, Boston, 2001.

[78] E. Onaran, O. Bobrowski, and R. J. Adler. Functional central limit theorems for local statistics of spatial birth–death processes in the thermodynamic regime. *Ann. Appl. Probab.*, 33(5):3958–3986, 2023.

[79] E. Onaran, O. Bobrowski, and R. J. Adler. Functional limit theorems for local functionals of dynamic point processes. *arXiv preprint arXiv:2310.17775*, 2023.

[80] T. Owada and C. Hirsch. Limit theorems under heavy-tailed scenario in the age dependent random connection models. *arXiv preprint arXiv:2409.05226*, 2024.

[81] T. Owada, G. Samorodnitsky, and G. Thoppe. Limit theorems for topological invariants of the dynamic multi-parameter simplicial complex. *Stochastic Process. Appl.*, 138:56–95, 2021.

[82] D. Pabst. Betti numbers in the random connection model for higher-dimensional simplicial complexes and the Boolean model. *arXiv preprint arXiv:2506.13429*, 2025.

[83] A. Patania, G. Petri, and F. Vaccarino. The shape of collaborations. *EPJ Data Science*, 6(1):1–16, 2017.

[84] G. Peccati and M. S. Taqqu. *Wiener Chaos: Moments, Cumulants and Diagrams.* Springer, Milan, 2011.

[85] M. D. Penrose. On a continuum percolation model. *Adv. in Appl. Probab.*, 23 (3):536–556, 1991.

[86] M. D. Penrose. *Random Geometric Graphs.* Oxford University Press, Oxford, 2003.

[87] M. D. Penrose. Continuum AB percolation and AB random geometric graphs. *J. Appl. Probab.*, 51A:333–344, 2014.

[88] M. D. Penrose. Inhomogeneous random graphs, isolated vertices, and Poisson approximation. *J. Appl. Probab.*, 55(1):112–136, 2018.

[89] M. D. Penrose and J. E. Yukich. Central limit theorems for some graphs in computational geometry. *Ann. Appl. Probab.*, 11(4):1005–1041, 2001.

[90] G. Petri, M. Scolamiero, I. Donato, and F. Vaccarino. Topological strata of weighted complex networks. *PLoS One*, 8(6):1–8, 2013.

[91] G. Petri, P. Expert, F. Turkheimer, R. Carhart-Harris, D. Nutt, P. J. Hellyer, and F. Vaccarino. Homological scaffolds of brain functional networks. *J. Roy. Soc. Interface*, 11(101):20140873, 2014.

[92] M. Reitzner and M. Schulte. Central limit theorems for *U*-statistics of Poisson point processes. *Ann. Prob.*, 41(6):3879–3909, 2013.

[93] S. I Resnick. *Heavy-Tail Phenomena: Probabilistic and Statistical Modeling.* Springer, New York, 2007.

[94] S. I. Resnick. *Extreme Values, Regular Variation and Point Processes.* Springer, New York, 2008.

[95] J. Riordan. Moment recurrence relations for binomial, Poisson and hypergeometric frequency distributions. *Ann. Math. Stat.*, 8(2):103–111, 1937.

[96] H. Samet. An overview of quadtrees, octrees, and related hierarchical data structures. In R. A. Earnshaw, editor, *Theoretical Foundations of Computer Graphics and CAD*, pages 51–68, Berlin, 1988. Springer.

[97] M. Schulte and J. E. Yukich. Multivariate second order Poincaré inequalities for Poisson functionals. *Electron. J. Probab.*, 24:Paper No. 130, 42, 2019.

[98] C. Siu, G. Samorodnitsky, C. L. Yu, and R. He. Asymptotics of the expected Betti numbers of preferential attachment clique complexes. *Adv. in Appl. Probab.*, 57:1–29, 2025.

[99] C. Stegehuis and L. Weedage. Degree distributions in AB geometric graphs. *Phys. A*, 586:Paper No. 126460, 12, 2022.

[100] T. Temčinas, V. Nanda, and G. Reinert. Goodness-of-fit via count statistics in dense random simplicial complexes. *Found. Data Sci.*, 2025. Early Access.

[101] G. C. Thoppe, D. Yogeshwaran, and R. J. Adler. On the evolution of topology in dynamic clique complexes. *Adv. Appl. Probab.*, 48(4):989–1014, 2016.

[102] R. van der Hofstad. *Random Graphs and Complex Networks. Vol. 1.* Cambridge University Press, Cambridge, 2017.

[103] R. van der Hofstad, P. van der Hoorn, N. Litvak, and C. Stegehuis. Limit theorems for assortativity and clustering in null models for scale-free networks. *Adv. in Appl. Probab.*, 52(4):1035–1084, 2020.

[104] R. van der Hofstad, P. van der Hoorn, and N. Maitra. Scaling of the clustering function in spatial inhomogeneous random graphs. *J. Stat. Phys.*, 190(6):110, 2023.

[105] P. Virtanen, R. Gommers, T. E. Oliphant, M. Haberland, T. Reddy, D. Cournapeau, E. Burovski, P. Peterson, W. Weckesser, J. Bright, S. J. van der Walt, M. Brett, J. Wilson, K. J. Millman, N. Mayorov, A. R. J. Nelson, E. Jones, R. Kern, E. Larson, C. J. Carey, İ. Polat, Y. Feng, E. W. Moore, J. VanderPlas,

D. Laxalde, J. Perktold, R. Cimrman, I. Henriksen, E. A. Quintero, C. R. Harris, A. M. Archibald, A. H. Ribeiro, F. Pedregosa, P. van Mulbregt, and SciPy 1.0 Contributors. SciPy 1.0: Fundamental Algorithms for Scientific Computing in Python. *Nature Methods*, 17:261–272, 2020.

[106] S. Wasserman and P. Pattison. Logit models and logistic regressions for social networks: I. An introduction to Markov graphs and *p. Psychometrika*, 61(3): 401–425, 1996.

[107] W. Whitt. *Stochastic-Process Limits.* Springer-Verlag, New York, 2002.

[108] J. Xu, T. L. Wickramarathne, and N. V. Chawla. Representing higher-order dependencies in networks. *Sci. Adv.*, 2(5):e1600028, 2016.

[109] J. Yoo, E. Y. Kim, Y. M. Ahn, and J. C. Ye. Topological persistence vineyard for dynamic functional brain connectivity during resting and gaming stages. *J. Neurosci. Methods*, 267:1–13, 2016.